



**A University of Sussex DPhil thesis**

Available online via Sussex Research Online:

<http://eprints.sussex.ac.uk/>

This thesis is protected by copyright which belongs to the author.

This thesis cannot be reproduced or quoted extensively from without first obtaining permission in writing from the Author

The content must not be changed in any way or sold commercially in any format or medium without the formal permission of the Author

When referring to this work, full bibliographic details including the author, title, awarding institution and date of the thesis must be given

Please visit Sussex Research Online for more information and further details

**Deubiquitinating Enzymes and  
Post-Replication Repair in  
*Schizosaccharomyces pombe***

A Thesis Submitted to the University  
of Sussex for the Degree of Doctor of  
Philosophy

by  
Rosalind Mary Holmes

August 2009

I hereby declare that this thesis has not, whether in the same or a different form, been submitted to this or any other University for a degree. The work described herein is my own, except where otherwise stated.

Rosalind Mary Holmes

August 2009

**UNIVERSITY OF SUSSEX**  
**ROSALIND MARY HOLMES**  
**DPHIL BIOCHEMISTRY**

**DEUBIQUITINATING ENZYMES AND POST-REPLICATION REPAIR**  
**IN *SCHIZOSACCHAROMYCES POMBE***

**SUMMARY**

DNA damage is chronic, inevitable and extensive. Damage caused by UV irradiation can cause bulky DNA lesions that block replication forks. Post-replication repair (PRR) is a DNA damage tolerance mechanism, which enables the replication machinery to bypass DNA lesions. The PRR machinery is thought to be recruited by ubiquitination of the sliding clamp, PCNA. In human cells, the USP/UBP superfamily deubiquitinating enzyme (DUB) USP1 has been shown to remove ubiquitin from PCNA and hence acts as a PRR modulator.

However, little is understood about the deubiquitination of PCNA or its regulation in yeast. The purpose of this study was to characterise the role of DUBs in yeast PRR. 24 DUBs were found to be encoded in the genome of *Schizosaccharomyces pombe*. No clear USP1 orthologue was found. A DUB deletion library was created and screened. A double mutant wherein two paralogous DUBs were deleted, *ubp21Δ ubp22Δ*, was found to exhibit sensitivity to UVC and increased PCNA ubiquitination. The *ubp21Δ ubp22Δ* strain was also found to be sensitive to a variety of DNA damaging agents and some spindle poisons. The double delete was epistatic with a mutant strain in which PCNA cannot be ubiquitinated. However, the genetic relationship with the enzymes that ubiquitinate PCNA was not so clear and a reduction in PCNA ubiquitination was not detected when either Ubp21 or Ubp22 was exogenously expressed.

Ubp21 and Ubp22 also contain a meprin and TRAF homology (MATH) domain and a conserved DWGF motif in the MATH domain was found to be important for Ubp22 function. The human orthologue, HAUSP<sup>USP7</sup>, stabilises the tumour suppressor p53 and is a highly characterised DUb. The *Saccharomyces cerevisiae* orthologue is Ubp15, but when this gene was deleted, only modest spindle poison sensitivity was detected. Determination of the precise functions of Ubp21 and Ubp22 in PRR requires further investigation.

## Acknowledgements

I would like to thank Alan Lehmann, Tony Carr and Eva Hoffmann for their help, ideas and unreserved support during my time at Sussex, giving me such an interesting project and the freedom to take it down my own path. I would also like to acknowledge the members of the Genome Damage and Stability Centre, past and present, for their contributions, big and small, to help and inspire this project. Additional thanks should be given to Felicity Watts, Kay Hofmann, Norbert Käufer, Dieter Wolf, Edgar Hartsuiker, Ken Sawin, Eva Hoffmann, Jessica Downs, Olaf Nielsen, and Tokayoshi Kuno for their generous and prompt supply of materials and information.

Outside of the University, it is important for me to thank Jon Markham, friends and family for the unwavering emotional support that I could not have survived without. Particularly important is the continued support of my boyfriend Tom Baker, without whom writing in Germany, managing it around my new career and duly submitting would have been so much harder. Furthermore, I would like to mention Jackie Whitford and George – the former made such a great and uncomplicated landlady and the latter a great companion on late-evening, post lab work, stress-busting, South Downs jogging sessions. More recently, I would like to acknowledge my new colleagues, Patrick Marollé and Uwe Hirsch, for their support during the writing-up phase, which helped enable this thesis be the quality it should.

## Table of Contents

Section number	Title	Starting page number
	Title Page	1
	Declaration	2
	Summary	3
	Acknowledgements	5
	Table of Contents	6
	List of Figures	11
	List of Tables	21
	Abbreviations	22
	Nomenclature	27
	<b>Chapter 1: Introduction</b>	28
1.1	The Function and Stability of DNA	28
1.2	The Cell Cycle and its Checkpoints	28
1.3	DNA Replication	30
1.4	DNA Damage and Mutagenesis	32
1.5	Cellular Responses to DNA Damage	33
1.6	Excision Repair	34
1.7	Homologous Recombination	36
1.8	Fanconi's Anaemia	39
1.9	p53	40
1.10	The Importance of Understanding the DNA Damage Response: Carcinogenesis and Ageing	41
1.11	An Introduction to Post-Replication Repair	42
1.12	Xeroderma Pigmentosum Variant	43
1.13	DNA Polymerases and Translesion Synthesis	44
1.14	The Template Switch Mechanism	45
1.15	PCNA: Functions and Binding Partners	46
1.16	Post-Translational Modification of Proteins by Ubiquitination	48
1.17	Ubiquitin-like Proteins and Non-Degradative Functions of the Ubiquitin Superfold	50
1.18	Post-Replication Repair in <i>S. cerevisiae</i>	52
1.19	Post-Replication Repair in Higher Eukaryotes	54
1.20	The Utilisation of <i>Schizosaccharomyces pombe</i> as a Model Organism	58
1.21	Post-Replication Repair in <i>S. pombe</i>	59
1.22	An Introduction to Deubiquitinating Enzymes	60
1.23	Superfamilies of Deubiquitinating Enzymes	61
1.24	Cysteine Protease Superfamilies of	63

	Deubiquitinating Enzymes	
1.25	JAMM Superfamily Deubiquitinating Enzymes	68
1.26	Deubiquitinating Enzymes Encoded within the Human Genome	70
1.27	Deubiquitinating Enzymes in Post-Replication Repair	71
1.28	An Introduction to This Study	73
	<b>Chapter 2: Materials and Methods</b>	74
2.1	Chemicals and Buffers	74
2.2	Routine Bacterial and DNA Methods	75
2.2.1	<i>E. coli</i> Culture	75
2.2.2	Plasmid Transformation of DH5 $\alpha$	75
2.2.3	Creation of <i>E. coli</i> Glycerol Stocks	75
2.2.4	Plasmid DNA Preparation	76
2.2.5	DNA Enzymatic Reactions	76
2.2.6	Agarose Gel Electrophoresis	76
2.2.7	DNA Extraction from Agarose Gels	77
2.2.8	Purification of Polymerase Chain Reactions	77
2.2.9	Oligonucleotide Preparation	77
2.2.10	DNA Sequencing	78
2.2.11	DH5 $\alpha$ Colony Polymerase Chain Reaction	78
2.2.12	Gateway System "LR" Clonase Reaction	78
2.2.13	Site-Directed Mutagenesis	79
2.2.14	BL21 <i>E. coli</i> Transformation	79
2.3	Routine Protein Methods	80
2.3.1	Expression and Native Purification of <i>S. pombe</i> His <sub>6</sub> - <sup>Sp</sup> PCNA for Antibody Production	80
2.3.2	Protein Quantitation	80
2.3.3	SDS-PAGE Analysis	81
2.3.4	Coomassie Staining of Gels	81
2.3.5	Semi-Dry Western Blotting	81
2.3.6	Immunodetection	82
2.3.7	Affinity Purification of Antibodies	82
2.4	<i>Schizosaccharomyces pombe</i> Methods	83
2.4.1	<i>S. pombe</i> Culture	83
2.4.2	Generation of Transforming DNA for DUB Gene Disruptions	84
2.4.3	Transformation using Lithium Acetate	85
2.4.4	Creation of Glycerol Stocks	86
2.4.5	Isolation of Haploids from Heterozygous Diploids	86
2.4.6	Isolation of Genomic DNA	86
2.4.7	DUB Gene Disruption Verification by PCR	87
2.4.8	DUB Gene Disruption Verification by Southern Analysis	88
2.4.9	DNA Damage of <i>S. pombe</i> Deletion Strain	90



2.4.10	HU Block and Release	91
2.4.11	Fluorescence Activated Cell Sorting (FACS)	91
2.4.12	Fluorescence Microscopy	91
2.4.13	Trichloroacetic Acid (TCA) Extraction	92
2.4.14	Drop Test Colony Forming Assay	93
2.4.15	UV Survival Colony Forming Assay	93
2.4.16	Spot Test Colony Forming Assay	94
2.4.17	DUb Expression	95
2.5.	<i>Saccharomyces cerevisiae</i> Methods	96
2.6	Computational Methods	96
2.6.1	Thesis Production	96
2.6.2	Useful Websites	96
	<b>Chapter 3: Identification and Disruption of Deubiquitinating Enzyme Genes in <i>S. pombe</i></b>	99
3.1	Introduction	99
3.2	Evidence for <sup>Sp</sup> PCNA Deubiquitination in <i>S. pombe</i>	99
3.3	Identification of Deubiquitinating Enzyme Genes in <i>S. pombe</i>	101
3.4	USP/UBP <i>S. pombe</i> DUBs Containing a DUSP Domain	101
3.5	<i>S. pombe</i> USP/UBP DUBs Containing a UBP-type Zinc Finger Domain	104
3.6	<i>S. pombe</i> USP/UBP DUBs Containing Ubiquitin-like Domains	109
3.7	Other <i>S. pombe</i> UBP/USP DUBs	112
3.8	<i>S. pombe</i> UCH DUBs	119
3.9	<i>S. pombe</i> PPPDE DUBs	120
3.10	<i>S. pombe</i> OTU DUBs	121
3.11	<i>S. pombe</i> JAMM DUBs	123
3.12	Summary of <i>S. pombe</i> DUBs	124
3.13	Exclusion of <i>S. pombe</i> DUB Genes from this Study	125
3.14	Assembly of a <i>S. pombe</i> DUB Deletion Library	126
3.15	Disruption of <i>S. pombe</i> DUB Genes by Integration of the Nourseothricin-Resistance Gene	127
3.16	Verification of Disrupted <i>S. pombe</i> DUB Genes by Polymerase Chain Reaction and Sequencing	127
3.17	Verification of Disrupted <i>S. pombe</i> DUB Genes by Southern Analysis	128
3.18	Verification of <i>S. pombe</i> DUB Gene Disrupted Strains Obtained from Collaborators	129
3.19	Sporulation of <i>S. pombe</i> Diploids Obtained from Bioneer	129
3.20	Conclusions	130

	<b>Chapter 4: Screening of Deubiquitinating Enzyme Gene Disrupted <i>S. pombe</i> Strains</b>	131
4.1	Introduction	131
4.2	Screen for Sensitivity to UVC Radiation	132
4.3	Screen for an Increase in <sup>Sp</sup> PCNA Ubiquitination	134
4.4	<i>ubp16<sup>+</sup></i> Deleted <i>S. pombe</i> Cells	140
4.5	Discussion	143
	<b>Chapter 5: Characterisation of <i>S. pombe</i> Strains Deficient in <sup>Sp</sup>Ubp21 and/or <sup>Sp</sup>Ubp22</b>	145
5.1	Introduction	145
5.2	Screening Results for the Strains <i>ubp21Δ::ura4</i> , <i>ubp22Δ::ura4</i> and <i>ubp21Δ::ura4 ubp22Δ::ura4</i>	145
5.3	Previous Studies, Homology and Domains of <sup>Sp</sup> Ubp21 and <sup>Sp</sup> Ubp22	148
5.4	Meprin and Tumour Necrosis Factor Receptor Associated Factor (MATH) Domain	150
5.5	Other MATH Domain Containing Proteins	151
5.6	The Human Meprin and Tumour Necrosis Factor Receptor Associated Factor (MATH) Domain Deubiquitinating Enzyme	153
5.7	MATH Domain Containing DUBs in Other Species	159
5.8	Structure of the Catalytic Core of <sup>Hs</sup> HAUSP <sup>USP7</sup>	160
5.9	Structure of the MATH Domain of <sup>Hs</sup> HAUSP <sup>USP7</sup>	166
5.10	Further Investigation of the Phenotypes of <i>S. pombe</i> Strains Deficient in MATH Domain DUBs	167
5.11	Sensitivity of <i>S. pombe</i> Strains Deficient in MATH Domain DUBs to Variety of Genotoxic Agents and Other Stresses	172
5.12	Discussion	178
	<b>Chapter 6: <i>S. cerevisiae</i> Deubiquitinating Enzymes and the MATH Domain-Containing DUB <sup>Sc</sup>Ubp15</b>	180
6.1	Introduction	180
6.2	Deubiquitinating Enzymes in <i>S. cerevisiae</i>	181
6.3	<sup>Sc</sup> Ubp15	182
6.4	Verification of the <i>ubp15Δ::kan</i> and <i>rad5Δ::kan</i> Strains	183
6.5	Phenotypes of <i>ubp15Δ::kan</i> Cells	184
6.6	Discussion	184

	<b>Chapter 7: Expression of <sup>Sp</sup>Ubp21 and <sup>Sp</sup>Ubp22</b>	186
7.1	Introduction	186
7.2	Construction of Gateway System-Based Plasmids for the Expression of <sup>Sp</sup> Ubp21 and <sup>Sp</sup> Ubp22	186
7.3	Exogenous Expression of <sup>Sp</sup> Ubp21 and <sup>Sp</sup> Ubp22 in Wild-Type Cells	187
7.4	Expression of <sup>Sp</sup> Ubp21 and <sup>Sp</sup> Ubp22 in <i>ubp21Δ::kan ubp22Δ::nat1</i> Cells	189
7.5	An Important DWGF Motif in the MATH domain	190
7.6	Structure of Prediction of <sup>Sp</sup> Ubp21 and <sup>Sp</sup> Ubp22	192
7.7	Discussion	192
	<b>Chapter 8: Epistasis Analysis</b>	194
8.1	Introduction	194
8.2	Creation of Strains	194
8.3	Epistasis with <i>pcn1-K164R</i> , <i>rad8Δ</i> and <i>rhp18Δ</i>	195
8.4	Mutation Frequency Analysis	197
8.5	Discussion	197
	<b>Chapter 9: Discussion</b>	199
9.1	Introduction	199
9.2	Deubiquitination of <sup>Sp</sup> PCNA and Functions of <sup>Sp</sup> Ubp21 and <sup>Sp</sup> Ubp22	199
9.3	<i>S. cerevisiae</i> <sup>Sc</sup> PCNA Deubiquitination	201
9.4	<sup>Hs</sup> HAUSP <sup>USP7</sup> , <sup>Hs</sup> USP1 and <sup>Hs</sup> UAF1 <sup>WDR48</sup>	202
9.5	Functions of the MATH Domain	204
9.6	<sup>Sp</sup> PCNA Deubiquitination in <i>S. Pombe</i>	205
9.7	A Role of <sup>Sp</sup> Ubp21 and <sup>Sp</sup> Ubp22 in the Spindle Checkpoint	206
9.8	Final Conclusions	206
	<b>Chapter 10: Bibliography</b>	207

## List of Figures

Figure	Title	Preceding Page Number
<b>Chapter 1: Introduction</b>		
1.1	Summary of the Mammalian Cell Cycle and its Checkpoints.	28
1.2	The Semi-Discontinuous Model of DNA Replication: Leading and Lagging Strand DNA Synthesis.	30
1.3	Core Components of the Replication Factory.	31
1.4	DNA Damage and its Consequences.	33
1.5	Nucleotide Excision Repair (NER).	35
1.6	A Summary of Homologous Recombination (HR) Pathways.	36
1.7	The “Chicken Foot” Model – Homologous Recombination at Replication Forks.	38
1.8	Summary of p53 Activation and the Resultant Downstream Effects.	41
1.9	Structure of PCNA in Cartoon Format.	47
1.10	Structures of Ubiquitin (light blue) and SUMO-1 (light green)	50
1.11	Post-replication Repair in <i>S. cerevisiae</i> .	53
1.12	Function of <sup>Hs</sup> USP1 in the Deubiquitination of <sup>Hs</sup> PCNA.	72
<b>Chapter 2: Materials and Methods</b>		
<b>Chapter 3: Identification and Disruption of Deubiquitinating Enzyme Genes in <i>S. pombe</i></b>		
3.1	Persistence of <sup>Sp</sup> PCNA Ubiquitination after UVC Irradiation in wild-type and <i>pcn1-K164R</i> cells.	99
3.2	Alignment of Otu1 DUBs in Three Eukaryotic Species.	122
3.3	Alignment of Otu2 DUBs in Three Eukaryotic Species.	123
3.4	Alignment of AMSH DUBs in <i>S. pombe</i> and <i>H. sapiens</i> .	124
3.5	DUB Gene Deletion-Insertion Approach Using the <i>nat1</i> Integration.	127
3.6	PCR Primer Positions for Checking <i>dub</i> Knockout Status.	127
3.7	PCR Amplification of the <i>ubp13</i> , <i>ubp7</i> , <i>ubp22</i> , and <i>ubp16</i> Loci Utilising Primers that Anneal to Flanking DNA and the <i>nat1</i> marker.	128
3.8	PCR Amplification of the <i>ubp8</i> , <i>ubp14</i> , and <i>ubp11</i> Loci Utilising Primers that Anneal to Flanking DNA and the <i>nat1</i> marker.	128
3.9	PCR Amplification of the <i>ubp4</i> , <i>ubp9</i> , <i>uch2</i> , and <i>amsh</i>	128

	Loci Utilising Primers that Anneal to Flanking DNA and the <i>nat1</i> marker.	
3.10	Verification of <i>ubp13Δ::nat1</i> Genotype via Southern Analysis.	128
3.11	Verification of <i>ubp7Δ::nat1</i> Genotype via Southern Analysis.	128
3.12	Verification of <i>ubp22Δ::nat1</i> Genotype via Southern Analysis.	128
3.13	PCR Amplification of the <i>ubp1</i> and <i>ubp12</i> Loci Utilising Primers that Anneal to Flanking DNA.	129
3.14	PCR Amplification of the <i>ubp2</i> , <i>ubp3</i> , and <i>uch1</i> Loci Utilising Primers that Anneal to Flanking DNA.	129
3.15	PCR Amplification of the <i>otu1</i> and <i>otu2</i> Loci Utilising Primers that Anneal to Flanking DNA.	129
3.16	PCR Amplification of the <i>ubp21</i> and <i>ubp22</i> Loci Utilising Primers that Anneal to Flanking DNA.	129
3.17	PCR Amplification of the <i>lub1</i> , <i>hag1</i> and <i>ubp6</i> Loci Utilising Primers that Anneal to Flanking DNA.	130
3.18	PCR Amplification of the <i>ubp10</i> and <i>ubp21</i> Loci Utilising Primers that Anneal to Flanking DNA.	130
<b>Chapter 4: Screening of Deubiquitinating Enzyme Gene Disrupted <i>S. pombe</i> Strains</b>		
4.1	Drop Test Assays Measuring the Relative Sensitivities of <i>S. pombe</i> Strains wild-type, <i>otu1Δ</i> , <i>otu2Δ</i> , <i>otu1Δ otu2Δ</i> , <i>ubp1Δ</i> , <i>ubp2Δ</i> and <i>pcn1-K164R</i> to Different Doses of UVC.	132
4.2	Drop Test Assays Measuring the Relative Sensitivities of <i>S. pombe</i> Strains wild-type, <i>ubp3Δ</i> , <i>ubp12Δ</i> , <i>ubp1Δ ubp12Δ</i> , <i>ubp10Δ</i> , <i>uch1Δ</i> and <i>pcn1-K164R</i> to Different Doses of UVC.	132
4.3	Drop Test Assays Measuring the Relative Sensitivities of <i>S. pombe</i> Strains wild-type, <i>lub1-1</i> , <i>lub1Δ</i> , <i>hag1Δ</i> , <i>ubp6Δ</i> , and <i>pcn1-K164R</i> to Different Doses of UVC.	132
4.4	Drop Test Assays Measuring the Relative Sensitivities of <i>S. pombe</i> Strains wild-type, <i>ubp11Δ</i> , <i>ubp14Δ</i> , <i>amshΔ</i> , and <i>pcn1-K164R</i> to Different Doses of UVC.	132
4.5	Drop Test Assays Measuring the Relative Sensitivities of <i>S. pombe</i> Strains wild-type, <i>ubp13Δ</i> , <i>ubp7Δ</i> , <i>ubp8Δ</i> , and <i>pcn1-K164R</i> to Different Doses of UVC.	132
4.6	Drop Test Assays Measuring the Relative Sensitivities of <i>S. pombe</i> Strains wild-type, <i>uch2Δ</i> , <i>ubp4Δ</i> , <i>ubp9Δ</i> , and <i>pcn1-K164R</i> to Different Doses of UVC.	132
4.7	Colony Forming Assay Measuring the Percentage Survival Following UVC Irradiation.	132
4.8	Colony Forming Assay Measuring the Percentage	132

	Survival Following UVC Irradiation.	
4.9	Colony Forming Assay Measuring the Percentage Survival Following UVC Irradiation.	132
4.10	Colony Forming Assay Measuring the Percentage Survival Following UVC Irradiation.	132
4.11	Colony Forming Assay Measuring the Percentage Survival Following UVC Irradiation.	132
4.12	Levels of <sup>32</sup> P-PCNA Ubiquitination in the <i>S. pombe</i> Strains wild-type, <i>pcn1-K164R</i> , <i>otu1Δ</i> , <i>otu1Δ</i> , <i>otu1Δ otu2Δ</i> , <i>ubp1Δ</i> , <i>ubp3Δ</i> , <i>ubp12Δ</i> , <i>ubp1Δ ubp12Δ</i> and <i>uch1Δ</i> Without Treatment (-) or Following 50 mM Hydroxyurea Treatment (+).	134
4.13	Levels of <sup>32</sup> P-PCNA Ubiquitination in the <i>S. pombe</i> Strains wild-type, <i>pcn1-K164R</i> , and <i>ubp2Δ</i> Without Treatment (-) or Following 50 mM Hydroxyurea (+).	134
4.14	Levels of <sup>32</sup> P-PCNA Ubiquitination in the <i>S. pombe</i> Strains wild-type, <i>pcn1-K164R</i> , <i>otu1Δ</i> , <i>otu1Δ</i> , <i>otu1Δ otu2Δ</i> , <i>ubp1Δ</i> , <i>ubp2Δ</i> , <i>ubp3Δ</i> , <i>ubp12Δ</i> , <i>ubp1Δ ubp12Δ</i> and <i>uch1Δ</i> Following Mock Treatment (A) or 100 Jm <sup>-2</sup> UVC (B).	135
4.15	Levels of <sup>32</sup> P-PCNA Ubiquitination in the <i>S. pombe</i> Strains wild-type, <i>ubp10Δ</i> and <i>pcn1-K164R</i> Without Treatment (-) or Following 10 mM Hydroxyurea (+).	135
4.16	Levels of <sup>32</sup> P-PCNA Ubiquitination in the <i>S. pombe</i> Strains wild-type, <i>ubp8Δ</i> , <i>ubp14Δ</i> and <i>pcn1-K164R</i> Without Treatment (-) or Following 10 mM Hydroxyurea Treatment (+).	135
4.17	Levels of <sup>32</sup> P-PCNA Ubiquitination in the <i>S. pombe</i> Strains wild-type, <i>ubp4Δ</i> , <i>ubp7Δ</i> , <i>ubp8Δ</i> , <i>ubp11Δ</i> , <i>ubp13Δ</i> , <i>ubp14Δ</i> and <i>pcn1-K164R</i> Following Mock Treatment (-) or UVC Treatment (+).	137
4.18	Levels of <sup>32</sup> P-PCNA Ubiquitination in the <i>S. pombe</i> Strains wild-type, <i>amshΔ</i> , <i>lub1Δ</i> , <i>lub1-1</i> , <i>hag1Δ</i> , <i>ubp6Δ</i> , <i>uch2Δ</i> and <i>pcn1-K164R</i> Following Mock Treatment (-) or UVC Treatment (+).	137
4.19	Levels of <sup>32</sup> P-PCNA Ubiquitination in Wild-type <i>S. pombe</i> Cells During the Cell Cycle.	137
4.20	Levels of <sup>32</sup> P-PCNA Ubiquitination Prior to and Following Cell Cycle Block in S-phase in wild-type <i>S. pombe</i> cells.	138
4.21	Cell Cytology Following Cell Cycle Block in S-phase in Wild-type <i>S. pombe</i> Cells.	138
4.22	Levels of <sup>32</sup> P-PCNA Ubiquitination Following Cell Cycle Block in S-phase in the <i>S. pombe</i> Strains Wild-type, <i>ubp13Δ::nat1</i> , <i>ubp8Δ::nat1</i> , and <i>pcn1-K164R</i> .	139

4.23	Levels of <sup>Sp</sup> PCNA Ubiquitination Following Cell Cycle Block in S-phase in the <i>S. pombe</i> Strains wild-type, <i>lub1-1</i> , <i>lub1Δ::kan</i> , <i>hag1Δ::kan</i> , <i>ubp6Δ::kan</i> and <i>pcn1-K164R</i> .	139
4.24	Levels of <sup>Sp</sup> PCNA Ubiquitination Prior to and Following Cell Cycle Block in S-phase in the <i>S. pombe</i> Strains wild-type, <i>amshΔ::nat1</i> , and <i>pcn1-K164R</i> .	139
4.25	Levels of <sup>Sp</sup> PCNA Ubiquitination Prior to and Following Cell Cycle Block in S-phase in the <i>S. pombe</i> Strains wild-type, <i>ubp3Δ::ura4</i> , and <i>pcn1-K164R</i> .	139
4.26	Drop Test Assays Measuring the Relative Sensitivities of <i>S. pombe</i> Strains wild-type, <i>ubp16Δ::kan</i> , <i>ubp16Δ::nat1</i> , and <i>pcn1-K164R</i> to Different Doses of UVC.	140
4.27	Levels of <sup>Sp</sup> PCNA Ubiquitination Prior to and Following Cell Cycle Block in S-phase in the <i>S. pombe</i> Strains wild-type, <i>ubp16Δ::kan</i> , <i>ubp16Δ::nat1</i> , and <i>pcn1-K164R</i> .	140
4.28	PCR Amplification of the <i>ubp16</i> Locus Utilising Primers that Anneal to Flanking DNA.	141
4.29	Digestion of PCR Products Obtained from Amplification of the <i>ubp16</i> Locus.	141
4.30	Drop Test Assays Measuring the Relative Sensitivities to Different Doses of UVC of Different <i>S. pombe</i> <i>ubp16Δ::nat1</i> Haploid Clones Compared to wild-type, <i>ubp16Δ::nat1</i> Diploid and <i>pcn1-K164R</i> .	143
4.31	Drop Test Assays Measuring the Relative Sensitivities to Different Doses of UVC of Different <i>S. pombe</i> <i>ubp16Δ::nat1</i> Haploid Clones Compared to wild-type, <i>ubp16Δ::nat1</i> Diploid and <i>pcn1-K164R</i> .	143
4.32	Colony Forming Assay Measuring the Percentage Survival Following UVC Irradiation.	143
4.33	Colony Forming Assay Measuring the Percentage Survival Following UVC Irradiation.	143
4.34	PCR Amplification of the <i>ubp16</i> Locus Utilising Primers that Anneal to Flanking DNA.	143
<b>Chapter 5: Characterisation of <i>S. pombe</i> Strains Deficient in <sup>Sp</sup>Ubp21 and/or <sup>Sp</sup>Ubp22</b>		
5.1	Drop Test Assays Measuring the Relative Sensitivities of <i>S. pombe</i> Strains wild-type, <i>ubp21Δ</i> , <i>ubp22Δ</i> , <i>ubp21Δ ubp22Δ</i> , and <i>pcn1-K164R</i> to Different Doses of UVC.	145
5.2	Levels of <sup>Sp</sup> PCNA Ubiquitination in the <i>S. pombe</i>	146

	Strains wild-type, <i>ubp21Δ::ura4</i> , <i>ubp22Δ::ura4</i> , <i>ubp21Δ::ura4 ubp22Δ::ura4</i> and <i>pcn1-K164R</i> Without Treatment (-) or Following Hydroxyurea Treatment (+).	
5.3	Levels of <sup>Sp</sup> PCNA Ubiquitination Prior to and Following Cell Cycle Block in S-phase in the <i>S. pombe</i> Strains wild-type, <i>ubp21Δ::ura4</i> , <i>ubp22Δ::ura4</i> , <i>ubp21Δ::ura4 ubp22Δ::ura4</i> , and <i>pcn1-K164R</i> .	146
5.4	Domain Structures of the <i>S. pombe</i> DUBs (A) <sup>Sp</sup> Ubp21 and (B) <sup>Sp</sup> Ubp22.	149
5.5	EBI-CLUSTALW Alignment of the Amino Acid Sequence <i>S. pombe</i> DUBs <sup>Sp</sup> Ubp22 and <sup>Sp</sup> Ubp21.	149
5.6	EBI-CLUSTALW Alignment of the Amino Acid Sequence <i>S. pombe</i> DUBs <sup>Sp</sup> Ubp22 and <sup>Sp</sup> Ubp21.	149
5.7	Oligomerisation of a and b Subunits to Form Rat Meprins.	151
5.8	EBI-CLUSTALW Alignment of the Amino Acid Sequence <sup>Sp</sup> Ubp22 and <sup>Sp</sup> Ubp21 with <sup>Hs</sup> HAUSP <sup>USP7</sup> .	153
5.9	EBI-CLUSTALW Alignment of the Amino Acid Sequence <sup>Sp</sup> Ubp22 and <sup>Sp</sup> Ubp21 with <sup>Hs</sup> HAUSP <sup>USP7</sup> .	153
5.10	Association of <sup>Hs</sup> MDM2 with <sup>Hs</sup> DAXX, <sup>Hs</sup> HAUSP <sup>USP7</sup> and <sup>Hs</sup> MDMX to induce <sup>Hs</sup> MDM2 destabilisation of <sup>Hs</sup> p53.	155
5.11	Crystal Structure of <sup>Hs</sup> HAUSP <sup>USP7</sup> Catalytic Core.	160
5.12	Ubiquitin binding by DUBs.	163
5.13	Crystal Structure of the MATH domain of <sup>Hs</sup> HAUSP <sup>USP7</sup> in Complex with a <sup>Hs</sup> p53 Peptide.	166
5.14	Colony Forming Assay Measuring the Percentage Survival Following UVC Irradiation.	167
5.15	Growth Curve Comparing Mid-log Growth Rates Between Strains.	168
5.16	Growth Curve Comparing Recovery of Strains Following Release From Stationary Phase.	168
5.17	Drop Test Assays Measuring the Relative Sensitivities of <i>S. pombe</i> Strains wild-type, <i>ubp13Δ</i> , <i>ubp7Δ</i> , <i>ubp22Δ</i> , <i>ubp8Δ</i> , and <i>pcn1-K164R</i> to Different Doses of UVC.	168
5.18	Levels of <sup>Sp</sup> PCNA Ubiquitination Following Cell Cycle Block in S-phase in the <i>S. pombe</i> Strains Wild-type, <i>ubp13Δ::nat1</i> , <i>ubp22Δ::nat1</i> , <i>ubp8Δ::nat1</i> , and <i>pcn1-K164R</i> .	169
5.19	Drop Test Assays Measuring the Relative Sensitivities to Different Doses of UVC of Different <i>S. pombe</i> <i>ubp22Δ::nat1</i> Clones Compared to wild-type, <i>ubp22Δ::ura4</i> and <i>pcn1-K164R</i> .	169



5.20	PCR Amplification of the <i>ubp22</i> Locus Utilising Primers that Anneal to Flanking DNA and Genomic DNA from the <i>S. pombe</i> Strains wild-type, and <i>ubp22Δ::hph</i> .	170
5.21	Colony Forming Assay Measuring the Percentage Survival Following UVC Irradiation.	170
5.22	Colony Forming Assay Measuring the Percentage Survival Following UVC Irradiation.	170
5.23	Levels of <sup>32</sup> P-PCNA Ubiquitination in the <i>S. pombe</i> Strains wild-type, <i>ubp21Δ::ura4 ubp22Δ::ura4</i> and <i>pcn1-K164R</i> Following Mock (-) or UVC Treatment (+).	171
5.24	Levels of <sup>32</sup> P-PCNA Ubiquitination in the <i>S. pombe</i> Strains wild-type, <i>ubp21Δ::ura4 ubp22Δ::ura4</i> and <i>pcn1-K164R</i> Following Mock (-) or UVC Treatment (+).	171
5.25	Levels of <sup>32</sup> P-PCNA Ubiquitination Following Cell Cycle Block in S-phase in the <i>S. pombe</i> Strains wild-type and <i>ubp21Δ::ura4, ubp22Δ::ura4</i> .	171
5.26	DNA Content Analysis Following Cell Cycle Block in S-phase in the <i>S. pombe</i> Strains wild-type and <i>ubp21Δ::ura4 ubp22Δ::ura4</i> .	171
5.27	Growth Analysis on Agar Containing 4-Nitroquinoline-1-oxide (4NQO) of the <i>S. pombe</i> Strains wild-type, <i>ubp21Δ::ura4, ubp22Δ::ura4, ubp21Δ::ura4 ubp22Δ::ura4</i> and <i>pcn1-K164R</i> .	172
5.28	Growth Analysis on Agar Containing Dimethylsulfoxide (DMSO) of the <i>S. pombe</i> Strains wild-type, <i>ubp21Δ::ura4, ubp22Δ::ura4, ubp21Δ::ura4 ubp22Δ::ura4</i> and <i>pcn1-K164R</i> .	173
5.29	Temperature Sensitivity of Strains <i>ubp21Δ, ubp22Δ</i> and <i>ubp21Δ ubp22Δ</i> .	173
5.30	Growth Analysis on Agar Containing Hydroxyurea (HU) of the <i>S. pombe</i> Strains wild-type, <i>ubp21Δ::ura4, ubp22Δ::ura4, ubp21Δ::ura4 ubp22Δ::ura4</i> and <i>pcn1-K164R</i> .	173
5.31	Growth Analysis on Agar Containing Methyl Methanesulfonate (MMS) of the <i>S. pombe</i> Strains wild-type, <i>ubp21Δ::ura4, ubp22Δ::ura4, ubp21Δ::ura4 ubp22Δ::ura4</i> and <i>pcn1-K164R</i> .	173
5.32	Growth Analysis on Agar Containing Camptothecin (CPT) of the <i>S. pombe</i> Strains wild-type, <i>ubp21Δ::ura4, ubp22Δ::ura4, ubp21Δ::ura4 ubp22Δ::ura4</i> and <i>pcn1-K164R</i> .	174
5.33	Growth Analysis on Agar Containing cisplatin ( <i>cisPt</i> )	174

	of the <i>S. pombe</i> Strains wild-type, <i>ubp21Δ::ura4</i> , <i>ubp22Δ::ura4</i> , <i>ubp21Δ::ura4 ubp22Δ::ura4</i> and <i>pcn1-K164R</i> .	
5.34	Growth Analysis on Agar Containing Dimethylformamide (DMF) of the <i>S. pombe</i> Strains wild-type, <i>ubp21Δ::ura4</i> , <i>ubp22Δ::ura4</i> , <i>ubp21Δ::ura4 ubp22Δ::ura4</i> and <i>pcn1-K164R</i> .	175
5.35	Growth Analysis on Agar Containing Hydrogen Peroxide (H <sub>2</sub> O <sub>2</sub> ) of the <i>S. pombe</i> Strains wild-type, <i>ubp21Δ::ura4</i> , <i>ubp22Δ::ura4</i> , <i>ubp21Δ::ura4 ubp22Δ::ura4</i> and <i>pcn1-K164R</i> .	175
5.36	Growth Analysis on Agar Containing Bleomycin (Bleo) of the <i>S. pombe</i> Strains wild-type, <i>ubp21Δ::ura4</i> , <i>ubp22Δ::ura4</i> , <i>ubp21Δ::ura4 ubp22Δ::ura4</i> and <i>pcn1-K164R</i> .	176
5.37	Growth Analysis on Agar Containing Phleomycin (Phleo) of the <i>S. pombe</i> Strains wild-type, <i>ubp21Δ::ura4</i> , <i>ubp22Δ::ura4</i> , <i>ubp21Δ::ura4 ubp22Δ::ura4</i> and <i>pcn1-K164R</i> .	176
5.38	Growth Analysis Following g Irradiation of the <i>S. pombe</i> Strains wild-type, <i>ubp21Δ::ura4</i> , <i>ubp22Δ::ura4</i> , <i>ubp21Δ::ura4 ubp22Δ::ura4</i> and <i>pcn1-K164R</i> .	176
5.39	Growth Analysis on Agar Containing Thiabendazole (TBZ) of the <i>S. pombe</i> Strains wild-type, <i>ubp21Δ::ura4</i> , <i>ubp22Δ::ura4</i> , <i>ubp21Δ::ura4 ubp22Δ::ura4</i> and <i>pcn1-K164R</i> .	177
5.40	Growth Analysis on Agar Containing Carbendazim (CBZ) of the <i>S. pombe</i> Strains wild-type, <i>ubp21Δ::ura4</i> , <i>ubp22Δ::ura4</i> , <i>ubp21Δ::ura4 ubp22Δ::ura4</i> and <i>pcn1-K164R</i> .	177
5.41	Growth Analysis on Agar Containing 4-Nitroquinoline-1-oxide (4NQO) of the <i>S. pombe</i> Strains wild-type, <i>ubp21Δ::ura4</i> , <i>ubp22Δ::ura4</i> , <i>ubp21Δ::ura4 ubp22Δ::ura4</i> and <i>pcn1-K164R</i> .	177
5.42	Growth Analysis on Agar Containing Dimethylsulfoxide (DMSO) of the <i>S. pombe</i> Strains wild-type, <i>ubp21Δ::ura4</i> , <i>ubp22Δ::ura4</i> , <i>ubp21Δ::ura4 ubp22Δ::ura4</i> and <i>pcn1-K164R</i> .	177
5.43	Growth Analysis on Agar Containing cisplatin ( <i>cisPt</i> ) of the <i>S. pombe</i> Strains wild-type, <i>ubp21Δ::ura4</i> , <i>ubp22Δ::ura4</i> , <i>ubp21Δ::ura4 ubp22Δ::ura4</i> and <i>pcn1-K164R</i> .	177
5.44	Growth Analysis on Agar Containing Dimethylformamide (DMF) of the <i>S. pombe</i> Strains wild-type, <i>ubp21Δ::ura4</i> , <i>ubp22Δ::ura4</i> , <i>ubp21Δ::ura4</i>	177

	<i>ubp22Δ::ura4</i> and <i>pcn1-K164R</i> .	
5.45	Growth Analysis on Agar Containing Bleomycin (Bleo) of the <i>S. pombe</i> Strains wild-type, <i>ubp21Δ::ura4</i> , <i>ubp22Δ::ura4</i> , <i>ubp21Δ::ura4 ubp22Δ::ura4</i> and <i>pcn1-K164R</i> .	177
5.46	Growth Analysis on Agar Containing Phleomycin (Phleo) of the <i>S. pombe</i> Strains wild-type, <i>ubp21Δ::ura4</i> , <i>ubp22Δ::ura4</i> , <i>ubp21Δ::ura4 ubp22Δ::ura4</i> and <i>pcn1-K164R</i> .	177
5.47	Growth Analysis on Agar Containing Carbendazim (CBZ) of the <i>S. pombe</i> Strains wild-type, <i>ubp21Δ::ura4</i> , <i>ubp22Δ::ura4</i> , <i>ubp21Δ::ura4 ubp22Δ::ura4</i> and <i>pcn1-K164R</i> .	177
<b>Chapter 6: <i>S. cerevisiae</i> Deubiquitinating Enzymes and the MATH Domain-Containing DUB <sup>Sc</sup>Ubp15</b>		
6.1	EBI-CLUSTALW Alignment of the Amino Acid Sequence <sup>Sp</sup> Ubp21, <sup>Sp</sup> Ubp22, <sup>Sc</sup> Ubp15 and <sup>Hs</sup> HAUSP <sup>USP7</sup> .	183
6.2	EBI-CLUSTALW Alignment of the Amino Acid Sequence <sup>Sp</sup> Ubp21, <sup>Sp</sup> Ubp22, <sup>Sc</sup> Ubp15 and <sup>Hs</sup> HAUSP <sup>USP7</sup> .	183
6.3	EBI-CLUSTALW Alignment of the Amino Acid Sequence <sup>Sp</sup> Ubp21, <sup>Sp</sup> Ubp22, <sup>Sc</sup> Ubp15 and <sup>Hs</sup> HAUSP <sup>USP7</sup> .	183
6.4	PCR Amplification of the <i>rad5</i> and <i>ubp15</i> Loci Utilising Primers that Anneal to Flanking DNA and Genomic DNA.	183
6.5	Drop Test Assays Measuring the Relative Sensitivities of <i>S. cerevisiae</i> Strains wild-type, <i>ubp15Δ</i> and <i>rad5Δ</i> to Different Doses of UVC.	184
6.6	Growth Analysis on Agar Containing Hydrogen Peroxide of the <i>S. cerevisiae</i> Strains wild-type, <i>ubp15Δ</i> and <i>rad5Δ</i> .	184
6.7	Growth Analysis on Agar Containing Phleomycin of the <i>S. cerevisiae</i> Strains wild-type, <i>ubp15Δ</i> and <i>rad5Δ</i> .	184
6.8	Growth Analysis on Agar Containing Hydrogen Peroxide of the <i>S. cerevisiae</i> Strains wild-type, <i>ubp15Δ::kan</i> and <i>rad5Δ::kan</i> .	184
6.9	Growth Analysis on Agar Containing Thiabendazole (TBZ) of the <i>S. cerevisiae</i> Strains wild-type, <i>ubp15Δ</i> and <i>rad5Δ</i> .	184
6.10	Growth Analysis on Agar Containing Thiabendazole of the <i>S. cerevisiae</i> Strains wild-type, <i>ubp15Δ::kan</i>	184

	and <i>rad5Δ::kan</i> .	
<b>Chapter 7: Expression of <sup>Sp</sup>Ubp21 and <sup>Sp</sup>Ubp22</b>		
7.1	Exogenously Expressed <sup>Sp</sup> Ubp21 and <sup>Sp</sup> Ubp22 Protein Constructs.	187
7.2	<sup>Sp</sup> PCNA Ubiquitination Following Exogenous Expression of <sup>Sp</sup> Ubp21.	187
7.3	<sup>Sp</sup> PCNA Ubiquitination Following Exogenous Expression of <sup>Sp</sup> Ubp22.	188
7.4	Status of Ubiquitinated Species of Cellular Proteins Following the Exogenous Expression of <sup>Sp</sup> Ubp22.	188
7.5	PCR Amplification of the <i>ubp21</i> and <i>ubp22</i> Loci Utilising Primers that Anneal to Flanking DNA and Genomic DNA.	188
7.6	<i>ubp21Δ::kan ubp22Δ::nat1</i> Cells have the Same Sensitivity to UVC as <i>ubp21Δ::ura4 ubp22Δ::ura4</i> Cells.	189
7.7	<i>ubp21Δ::kan ubp22Δ::nat1</i> Cells are Temperature Sensitive.	189
7.8	Rescue of UVC sensitivity by the Exogenous Expression of <sup>Sp</sup> Ubp21 Protein Constructs in <i>ubp21Δ::kan ubp22Δ::nat1</i> Cells.	189
7.9	Rescue of UVC sensitivity by the Exogenous Expression of <sup>Sp</sup> Ubp22 Protein Constructs in <i>ubp21Δ::kan ubp22Δ::nat1</i> Cells.	189
7.10	Alignment of the MATH Domain in MATH-USP/UBP DUBs from 23 Different Species.	190
7.11	Structure of the MATH Domain of <sup>Hs</sup> HAUSP <sup>USP7</sup> in Complex with an <sup>Hs</sup> MDM2 peptide.	190
7.12	Rescue of UV Sensitivity of Double Delete Via Exogenous Expression of <sup>Sp</sup> Ubp22-DWGF-AAAA.	191
7.13	EBI-CLUSTALW Alignment of the Amino Acid Sequence <sup>Sp</sup> Ubp21, <sup>Sp</sup> Ubp22, <sup>Sc</sup> Ubp15 and <sup>Hs</sup> HAUSP <sup>USP7</sup> .	192
7.14	Secondary Structure Prediction of the Potential PIP Boxes of <sup>Sp</sup> Ubp21 and <sup>Sp</sup> Ubp22 Using the PHYRE Program.	192
<b>Chapter 8: Epistasis Analysis</b>		
8.1	PCR Amplification of the <i>pcn1</i> , <i>rad8</i> and <i>rhp18</i> Loci Utilising <i>ura4</i> Gene Primers, and Genomic DNA.	195
8.2	PCR Amplification of the <i>ubp21</i> Locus Utilising Primers that Anneal to Flanking DNA and Genomic DNA.	195
8.3	PCR Amplification of the <i>ubp21</i> Locus Utilising Primers that Anneal to Flanking DNA and Genomic DNA.	195

8.4	UV Epistasis Analysis with <i>pcn1-K164R</i> .	195
8.5	UV Epistasis Analysis with <i>rad8Δ</i> .	195
8.6	UV Epistasis Analysis with <i>rhp18Δ</i> .	196
<b>Chapter 9: Discussion</b>		

## List of Tables

Table	Title	Preceding Page Number
<b>Chapter 1: Introduction</b>		
1.1	Superfamilies of Deubiquitinating enzymes and their Peptidase Domains.	63
<b>Chapter 2: Materials and Methods</b>		
2.1	SDS-PAGE Gel Preparation.	81
2.2	Immunodetection Methods.	82
2.3	PCR Cycling Conditions for Amplification of Transforming DNA.	84
2.4	Genotoxic Agent Stocks and Diluents.	94
<b>Chapter 3: Identification and Disruption of Deubiquitinating Enzyme Genes in <i>S. pombe</i></b>		
3.1	DUBs in Three Species	101
3.2	DUBs in <i>S. pombe</i> .	101
3.3	DUBs in <i>S. pombe</i> .	101
3.4	DUBs in <i>S. pombe</i> .	101
<b>Chapter 5: Characterisation of <i>S. pombe</i> Strains Deficient in <sup>Sp</sup>Ubp21 and/or <sup>Sp</sup>Ubp22</b>		
5.1	Sensitivity of <i>ubp21Δ::ura4 ubp22Δ::ura4</i> and <i>pcn1-K164R</i> To Genotoxins	178
<b>Chapter 6: <i>S. cerevisiae</i> Deubiquitinating Enzymes and the MATH Domain-Containing DUB <sup>Sc</sup>Ubp15</b>		
6.1	DUBs in <i>S. cerevisiae</i> .	181
6.2	DUBs in <i>S. cerevisiae</i> .	181
6.3	DUBs in <i>S. cerevisiae</i> .	181

## Abbreviations

Abbreviation	Meaning
4NQO	4-nitroquinoline <i>N</i> -oxide
6-4PP	6-4 photoproduct
A	adenine
AD	Alzheimer's disease
Ade	adenine
AMPS	ammonium persulfate
AMSH	associated molecule of the SH3 domain of signal transducing adapter molecule (STAM)
A-T	ataxia-telangiectasia
ATM	ataxia-telangiectasia mutated
ATR	ATM-related
BER	base excision repair
BIR	break-induced replication
BRCA1	breast cancer 1
BRCA2	breast cancer 2
BRCT	BRCA1 C-terminal domain
C	cytosine
CBZ	carbendazim
CDK	cyclin-dependent kinase
CHK1	checkpoint 1
CHK2	checkpoint 2
CIP	cyclin-dependent kinase inhibitor protein
<i>cis</i> platin	<i>cis</i> -diammineplatinum(II) dichloride
CPD	cyclobutane pyrimidine dimer
CPT	camptothecin
CS	Cockayne syndrome
CSN	constitutive photomorphogenic gene 9 (COP9) signalosome
dCTP	deoxyribocytidine triphosphate
DHJ	double Holliday junction
DJD	double Holliday junction dissolution
DMF	dimethylformamide
DMSO	dimethylsulfoxide
DNA	deoxyribonucleic acid
DNA-PK	DNA protein kinase
dNTP	deoxyribonucleotide
DSB	double strand break
DSBR	double strand break repair
dsDNA	double-stranded DNA

DTT	dithiothreitol
DUb	deubiquitinating enzyme
DUB	deubiquitinating enzyme
DUF	domain of unknown function
DUSP	domain present in ubiquitin-specific proteases
<i>E. coli</i>	<i>Escherichia coli</i>
E1	ubiquitin activating enzyme
E2	ubiquitin conjugating enzyme
E3	ubiquitin-protein ligase
<i>Ec</i>	<i>Escherichia coli</i>
EDTA	ethylenediaminetetraacetic acid
EGFR	epidermal growth factor receptor
FA	Fanconi's anaemia
FANCD2	Fanconi's anaemia complementation group protein D2
FANCI	Fanconi's anaemia complementation group protein I
G	guanine
G1	gap/growth phase 1
G2	gap/growth phase 2
GGR	global genome repair
Gly	glycine
HAUSP	Herpes virus-associated ubiquitin-specific protease
HECT	homologous to the E6-AP carboxy-terminus
HEPES	4-(2-hydroxyethyl)-1-piperazineethanesulfonic acid
HIRAN	HIP116 Rad5 N-terminal domain
HJ	Holliday junction
HR	homologous recombination
HU	hydroxyurea
INK	cyclin-dependent kinase inhibitor
IPTG	isopropyl- $\beta$ -D-thiogalactopyranoside
IR	ionising radiation
ISG15	interferon-stimulated gene-15 (ubiquitin cross-reactive protein [UCRP])
JAMM	Jab1/Pad1/MPN/Mov34 domain metalloenzyme
kan	kanamycin
kb	kilobases
kDa	kilodaltons
KOD	DNA Polymerase isolated from the extreme thermophile <i>Thermococcus</i>



	<i>kodakaraensis</i>
Leu	leucine
LOH	loss of heterozygosity
M phase	mitosis
MAPK	mitogen-activated protein kinase
MATH	meprin and tumour necrosis factor receptor-associated factor homology
MCM	mini-chromosome maintenance
MJD	Machado-Joseph/Jakob disease protein/Josephin domain protease
MMC	mitomycin C
MMR	mismatch repair
MMS	methylmethane sulfonate
mRNA	messenger ribonucleic acid
MVB	multi-vesicular body
NAT	nourseothricin
<i>nat1</i>	nourseothricin-resistance gene
NBS	Nijmegen breakage syndrome
NEDD8	neuronal-precursor-cell-expressed developmentally downregulated protein-8
NER	nucleotide excision repair
NHEJ	non-homologous end joining
OTU	ovarian tumour-like protease
PAN	poly(A)-specific ribonuclease complex
PARP	poly-(ADP-ribose) polymerase
PBST	phosphate buffered saline plus tween surfactant
PCNA	proliferating cell nuclear antigen
PCR	polymerase chain reaction
PD	Parkinson's disease
PEG	polyethylene glycol
PEST	motif rich in proline, glutamate, serine and threonine residues
PIP box	PCNA-interacting protein motif
PML	promyelocytic leukaemia protein
Pol $\eta$	DNA polymerase $\eta$ (eta)
Pol $\iota$	DNA polymerase $\iota$ (iota)
Pol $\zeta$	DNA polymerase $\zeta$ (zeta)
Pol $\kappa$	DNA polymerase $\kappa$ (kappa)
Pol $\delta$	DNA polymerase $\delta$ (delta)
Pol $\epsilon$	DNA polymerase $\epsilon$ (epsilon)
PolIV	DNA polymerase IV
Pol $\beta$	DNA polymerase $\beta$ (beta)
PPPDE	permuted papain fold peptidases of dsDNA viruses and eukaryotes

PRR	post-replication repair
PVDF	polyvinylidene fluoride
QSP	Quantité suffisante pour
RAD	radiation
RF	replication fork
RFC	replication factor C
Rhp	rad-homologue in <i>S. pombe</i>
RING	really interesting new gene
RNA	ribonucleic acid
RPA	replication protein A
S phase	DNA synthesis phase
<i>S. cerevisiae</i>	<i>Saccharomyces cerevisiae</i>
<i>S. pombe</i>	<i>Schizosaccharomyces pombe</i>
SAP	SAF-A/B, Acinus, Pias domain
SBM	signal transducing adapter molecule (STAM)-binding motif
<i>Sc</i>	<i>Saccharomyces cerevisiae</i>
SCF	Skp1-Cullin-F-box
SDS	sodium dodecyl sulfate
SDSA	synthesis-dependent strand annealing
SDS-PAGE	sodium dodecylsulfate polyacrylamide gel electrophoresis
SIM	SUMO interaction motif
SMC	structural maintenance of chromosomes
<i>Sp</i>	<i>Schizosaccharomyces pombe</i>
ssDNA	single-stranded DNA
STAM	signal transducing adapter molecule
SUMO	small ubiquitin-like modifier
T	thymine
TBZ	2-[4-thiazoyl]benzimidazole
TCR	transcription coupled repair
TEMED	N,N,N',N'-tetramethylethylenediamine
TF	transcription factor
TLS	translesion synthesis
Top1	topoisomerase 1
TRAF	tumour necrosis factor receptor associated factor
tris	tris(hydroxymethyl)aminomethane
TTD	trichothiodystrophy
Ub	ubiquitin
UBA	ubiquitin-associated domain
UBL	ubiquitin-like protein
UBM	ubiquitin-binding motif
UBZ3	ubiquitin-binding zinc finger 3
UBZ4	ubiquitin-binding zinc finger 4

UCH	ubiquitin C-terminal hydrolase
UDS	unscheduled DNA synthesis
UEV	ubiquitin-enzyme variant
UIM	ubiquitin-interacting motif
UPS	ubiquitin proteasome system
Ura	uracil
<i>ura4</i>	Gene encoding dihydroorotase (involved in the <i>de novo</i> biosynthesis of pyrimidines)
USP	ubiquitin-specific protease
USP/UBP	ubiquitin-specific protease superfamily
USPV	inactive ubiquitin-specific protease variant
UV	ultra-violet
UVC	UV of wavelength 280 nm –100 nm.
UVDE	UV-dependent exonuclease
UVDR	UV damage repair
wt	wild-type
Xgal	5-bromo-4-chloro-3-indolyl- $\beta$ -D-galactosidase
XP	xeroderma pigmentosum
XP-V	xeroderma pigmentosum variant

## Nomenclature

### Protein names

With the exception of the first half of the introduction, mammalian protein names are written in the format of *Species*PROTEIN<sup>Alias</sup> and yeast protein names in the format *Species*Protein<sup>Alias</sup>. This format was found to be the most concise, and also clear when the literature is highly divided with regard to protein names. This nomenclature does not apply to viral proteins. Alias names, where given, may be capitalised or in lowercase depending upon literature conventions.

### Gene names

Mammalian gene names are written in capital letters and italicised.

Yeast gene names are written in lowercase in italics e.g. *ubp21*. A plus sign next to the gene name emphasises that it is an unmutated, wild-type version of the gene. *ubp21Δ* indicates a null mutant of *ubp21*, in other words, the *ubp21* gene has been deleted, as indicated by the greek letter “Δ”. *ubp21Δ::nat1* indicates a strain wherein the *ubp21* gene has been deleted and replaced with the nourseothricin-resistance gene, *nat1* – this strain is able to grow in the presence of nourseothricin. Whereas, *pcn1-K164R::ura4* indicates a strain where the *pcn1* has not been deleted, but merely modified. This modification results in the mutation of lysine-164 to an arginine in the translated protein. This mutation is marked (“::”) with the *ura4* gene – this strain is able to grow in the absence of uracil. *lub1-1* means *lub1* mutant number 1, and indicates that the *lub1* gene is present, but a mutation exists in the open reading frame of this gene.

## **Chapter 1: Introduction**

### **1.1. The Function of DNA**

It can be argued that life has evolved entirely for its ability to continue life. That is, life has evolved to survive, reproduce, and aid the survival of its offspring. Millions of years of selection for exceptional efficiency in these processes is neatly stored in the blueprint of an organism – its genome. Deoxyribonucleic acid (DNA) is the polymer within which the genetic information of the genome is stored. Efficient and accurate duplication of DNA is key to the production and survival of daughter cells. Hence, it can be concluded that the cellular processes involved in DNA duplication, repair and maintenance are of fundamental importance to the survival of the species.

### **1.2. The Cell Cycle and its Checkpoints**

The process undertaken by cells to grow, duplicate their cellular contents and subsequently divide into two daughter cells is known as the cell division cycle, or simply, cell cycle. This is due to the repeating pattern observed: following completion of one cycle of growth and division, a new cell results, which subsequently grows and divides in its own right. As biochemical research to date has outlined, the intracellular environment is very complicated, hence it follows that the preparation for and subsequent division of a cell into two daughter cells is also an incredibly complex procedure. As explained above, it is fundamental for survival that cell duplication must be highly controlled and co-ordinated.

The fundamentals of the cell cycle are reviewed in chapter 21 of Lodish *et al.*, 2004. Figure 1.1 depicts the different phases of the mammalian cell cycle and their respective temporal control systems, known as the cell cycle checkpoints. In growth or gap phase 1 (G1), the diploid cell contains two copies of each

chromosome – a maternal and a paternal copy. At this stage, a chromosome is more commonly referred to as a chromatid, which is made up of one double strand of DNA. During synthesis or S-phase, each chromatid is duplicated resulting in an identical copy, known as its sister chromatid. Following gap or growth phase 2 (G2), the cell enters mitosis (M), which is a very complicated and tightly regulated phase wherein the mother cell splits into two daughter cells. Of particular importance is the separation of each pair of sisters such that each sister is accurately segregated into one daughter cell. During metaphase, the chromatid pairs line up across the centre of the cell, and during anaphase, one sister chromatid is pulled to one pole, and the other sister to the opposite pole. The molecular motors that effect this process are associated with the spindle microtubules. Subsequently, the cytoplasm is divided into two (cytokinesis) and the nuclear envelope then reforms around the segregated chromatids.

The cell cycle is driven by complexes made up of a cyclin and a cyclin-dependent kinase (CDK). The association of a particular cyclin with a particular CDK affects the kinase activity of the CDK, which in turn effects cell cycle progression. Still referring to mammalian cells, G1 is driven by cyclinD-CDK4 and cyclinD-CDK6, S-phase entry by cyclinE-CDK2, progression through S-phase by cyclinA-CDK2, and G2 and M by cyclinA-CDK1 and cyclinB-CDK1. Levels of these complexes are tightly controlled by phosphorylation, which alters binding affinity, inhibition by CDK inhibitory proteins (CIPs and INKs), and degradation. As summarised in Figure 1.1, the cell cycle is controlled at important phases by checkpoints. There are four main types of checkpoint. DNA damage checkpoints prevent progression when genome integrity is found to be compromised (reviewed in Sancar *et al.*, 2004). For example, lesions on the DNA can interfere with genome duplication during S-phase, so p21<sup>CIP</sup> is activated to inhibit cyclin A and E and halt the cell cycle at this point. Cyclins A and B are sensitive to the inhibitory effect of proteins activated following the detection of unreplicated DNA prior to mitosis. Furthermore, the cell halts mitosis if incorrect assembly of the spindles or aberrant chromosome segregation occurs. It is much less catastrophic for the cell if these problems are

rectified before further progression. For example, both daughter cells may not have sufficient genetic information to survive if they are provided with an aberrant number of chromatids following cell division. However, despite these checkpoint mechanisms, of particular interest to this study is how the cell copes with DNA damage encountered during DNA replication.

### **1.3. DNA Replication**

DNA replication occurs during S-phase of the cell cycle. Here the entire genome of the cell is duplicated. Replication occurs at many different parts of the genome simultaneously – initiating from specific DNA origins upon which replication factories, made from colocalised replication machineries, form. At the heart of the factory is the DNA polymerase, an enzyme that covalently links DNA monomers in a specified order to create a polymeric copy of the parental template genome. Eukaryotic DNA polymerases are reviewed in detail in Hubscher *et al.*, 2002.

In addition to the DNA polymerase, a plethora of other proteins are required for the functioning of an effective replication factory. This is not just due to the importance of the procedure, but also a result of the format in which cellular DNA exists. A single strand of DNA has directionality, and the double helix is formed by the annealing of a second DNA strand with a complementary monomeric sequence of opposite polarity. That is a 5' to 3' single strand of DNA anneals to single-stranded DNA (ssDNA) that is complementary in a 3' to 5' direction. However, a daughter strand of DNA can only be polymerised in one direction. This has led to the semi-discontinuous model of DNA replication, which is shown in Figure 1.2. Here, one strand, known as the leading strand, is synthesised continuously. However, for the strand that runs in the opposite direction, the lagging strand, new DNA must be synthesised in discrete segments. The daughter DNA segments, known as Okazaki fragments, are then joined up later.

Another important aspect of DNA replication is the inability of the DNA polymerase to synthesise DNA *de novo*. That is, when provided with naked, ssDNA and monomers for the production of a complementary strand, the DNA polymerase is unable to produce double-stranded DNA (dsDNA). The DNA polymerase can only extend a 3' end – in other words, the polymerase requires a primer to get started. In leading strand synthesis, only one primer is needed, but lagging strand synthesis requires multiple priming events. To do this, the cell employs an RNA polymerase called a primase, which is capable of synthesising *de novo*. The DNA polymerase extends the RNA primers with DNA, and later the short stretches of RNA are replaced with DNA.

Other core components of the replication factory include proteins for: separating the double helix (helicase), preventing reformation of the double helix and protecting the single strands (replication protein A, RPA), tethering the DNA polymerase to its template (clamp), loading the clamp (clamp loader), and ligating the Okazaki fragments (ligase). The positions of some of these core proteins are shown in Figure 1.3. For simplicity, the figure is based on replication in the eubacterium *Escherichia coli* and is adapted from Langston and O'Donnell, 2006, but as explained in the accompanying review, the model is equally relevant to eukaryotic DNA replication. The core components of the replication factory are reviewed in Johnson and O'Donnell, 2005. In addition to these key proteins, each are associated with a variety of other proteinaceous cofactors that aid and direct their function and assembly in the replication factory. Furthermore, when the replication machinery encounters problems, for example a damaged template that the DNA polymerase does not recognise, other important proteins associate with the factory to resolve the issue. Therefore, the replication factory is a complex and dynamic machine.

There are two fundamental characteristics of DNA replication: fidelity and speed. Firstly, the DNA polymerase itself has evolved to be highly accurate – the active site of the DNA polymerase is very stringent. Only when a template monomer fits



perfectly is a complementary monomer inserted into the nascent, daughter strand. Factors most relevant to DNA replication fidelity are reviewed in Kunkel, 2004. Secondly, the DNA polymerase associates tightly with the doughnut-shaped sliding clamp protein to confer high speed replication. Prior to DNA polymerisation, a clamp loader cofactor loads the sliding clamp onto the ssDNA such that the strand passes through the hole in the centre of the doughnut. Binding of the polymerase to this sliding clamp confers high processivity to the polymerase – it dissociates from its template with low frequency due to mechanical association.

This sliding clamp is conserved across all three domains of life, which implies fundamental importance to cells. In *E. coli* it is known as the  $\beta$ -clamp, and in archaea and eukaryotes, it is known as proliferating cell nuclear antigen, now subsequently referred to as PCNA. Eukaryotic PCNA is the subject of this thesis and so will be discussed extensively later in this introduction and in subsequent chapters. To further introduce and justify this study, the relevance of PCNA to genome integrity and research interest will be outlined in the following sections.

#### **1.4. DNA Damage**

A fundamental factor in cell survival is its ability to withstand and repair insult to the genetic information. DNA damage is chronic, inevitable and extensive. Not only does DNA damage disrupt DNA replication, but persisting damage can result in DNA mutation, that is, a heritable change to the genetic information. Accumulation of mutations in the genome results in carcinogenesis and ageing (reviewed in Hoeijmakers, 2001b).

DNA damage results from both exogenous and endogenous sources (for example, see Hillis, 1996, Lindahl, 1993; Halliwell and Aruoma, 1991). Deliberate or accidental exposure to chemicals, such as those found in smoke, chemotherapy drugs, and plant toxins, causes DNA damage. Radiation, particularly ultra-violet (UV) light and ionising radiation from radon in rocks, x-rays, radioactive decay,

cosmic rays and  $\gamma$  sources, induce reactions within DNA resulting in lesions. Free radicals, such as reactive oxygen species that result from normal intracellular metabolism, are also able to react with DNA. Furthermore, DNA replication is not 100% accurate, hence replication errors are also an important endogenous source of mutation. Moreover, in the manipulation of their hosts, viral infection can cause DNA damage. Typical sources, effects and consequences of different types of DNA damage are summarised in Figure 1.4.

The type and extent of damage caused depends on the source, its intensity and the format in which the DNA exists at the time. For example, benzo[a]pyrene, a bulky chemical constituent of cigarette smoke, typically reacts with the base component of a DNA monomer, whereas bifunctional chemicals may induce the formation of a covalent bond between two different DNA strands – known as an interstrand crosslink.

## **1.5. Cellular Responses to DNA Damage**

As alluded to in Figure 1.4, a plethora of responses to genetic insult have evolved in cells, which fall into two main categories – manipulation of the cell cycle and processing of the damage. The latter includes damage repair processes (reviewed in Friedberg, 2003; Lindahl and Wood, 1999; Hoeijmakers, 2001a; Friedberg *et al.*, 2004). Repair is carried out by simple, direct reversal of the lesion, or by excising the damage and filling in the gap. Which bonds are broken, and the means by which the correct bonds are formed, i.e. the pathway utilised, is dependent upon the type of lesion, where it occurs and its extent, along with temporal factors, such as when during the cell cycle the damage occurs and when it is detected. For example, sometimes only the damaged portion is removed and replaced, such as in a pathway called base excision repair, alternatively the lesion plus surrounding undamaged regions will also be removed and replaced, such as in nucleotide excision repair. Furthermore, there are differences in how healthy DNA is restored. When only one strand is affected, the opposite, undamaged strand can be used as

a template to fill in the missing information. However, when both strands are locally affected, the sister chromatid or homologous chromosome may be utilised if there is one available at the time. This decision is important as it may result in loss of heterozygosity, which may have lethal consequences in the longer term.

Therefore, the choice of pathway utilised for the type of damage, where it occurs, and when is critical for the cell. Some pathways carry high risks, which may outweigh the benefits if used at the wrong cell cycle phase. Furthermore, some repair processes are simple and quick, and others are complex and lengthy. A focus of this study is a type of DNA damage tolerance pathway wherein the lesions, typically those that have occurred during S-phase, are directed down a pathway that provides a quick fix that is less disruptive to DNA replication. The tolerated damage can then be repaired more thoroughly once replication is complete. Before DNA damage tolerance is discussed more extensively, exemplary DNA repair mechanisms will be outlined.

## **1.6. Excision Repair**

Base excision and nucleotide excision repair, commonly known as BER and NER respectively, involve breaking the sugar-phosphate backbone of the DNA, removing the damaged section and then filling in the gap (reviewed in Friedberg *et al.*, 2006; Sancar, 1996). In short patch mode, the former involves the extraction of a single, damaged base via the cleavage of the glycosidic bond between the sugar and base moieties. This process is catalysed by a glycosylase (reviewed in Friedberg *et al.*, 2006; Seeberg *et al.*, 1995). The resultant abasic site is then recognised by an endonuclease, which hydrolyses the sugar-phosphate backbone leaving what is referred to as a single-strand DNA break (SSB). This type of lesion is subsequently bound by DNA polymerase  $\beta$  (Pol $\beta$ ), which is capable of inserting the correct nucleotide across the gap and removing the 5'-terminal deoxyribose. Long patch BER occurs when Pol $\beta$ -dependent activity alone is insufficient, so a variety of other enzymes are recruited to extend the gap, whereupon Pol $\delta$ , Pol $\epsilon$  or

Pol $\beta$  are utilised to polymerise across the gap using undamaged monomers, all in a PCNA-dependent manner (reviewed in Almeida and Sobol, 2007).

NER is typically employed when the secondary structure of the double helix is distorted as a result of the lesion – a stretch of around 25 to 35 nucleotides is typically excised (reviewed in Friedberg, 2001; Wood, 1997; Costa *et al.*, 2003; Mitchell *et al.*, 2003). This process involves a cascade where different proteins detect the damage, and then recruit other proteins to instigate unwinding, excision, and removal of the damaged section, polymerisation of replacement, healthy DNA, and ligation to the sugar-phosphate backbone. This process is summarised in Figure 1.5, which is taken from Friedberg, 2001.

NER has been particularly well characterised due to the existence of the condition xeroderma pigmentosum, which results when any one of the 7 proteins fundamental to NER, XPA to XPG, are mutant. XP patients have been found to demonstrate a markedly increased likelihood of developing sunlight-induced skin cancer. It can be concluded, therefore, that NER is very important in the repair of DNA damage caused by UV. The molecular mechanism of NER is classified into two pathways: transcription-coupled repair (TCR) and global genome repair (GGR). The former, as its name suggests, is linked to transcription and has been found to rapidly repair damage on the transcribed strand of active genes. Hence, it can be concluded that TCR acts to help prevent DNA damage from disrupting the action of RNA polymerases (reviewed in van Hoffen *et al.*, 2003). GGR seems to have a more general role in the cell by acting on lesions that occur in non-specific locations in the genome. Later in this study, an eighth classification of XP, known as XP variant (XP-V), which is not linked to NER, will be discussed.

## 1.7. Homologous Recombination

Non-homologous end joining (NHEJ) and homologous recombination (HR) are two processes well characterised for their involvement in repairing double strand breaks (DSBs), and are commonly known as DSB repair (DSBR) pathways (reviewed in Friedberg *et al.*, 2006; Karran, 2000; Pastink *et al.*, 2001). DSBs can arise as a result of exposure to ionising radiation, specific chemicals, and blocked replication forks. NHEJ is generally thought to be the more prevalent DSBR pathway in mammalian cells and involves the direct ligation of the two pairs of ends. This pathway is reviewed in Barnes, 2001 and Doherty and Jackson, 2001, but will not be discussed further in this study.

HR is an error-free mechanism of repair that requires a sister chromatid or homologous chromosome for use as a template. HR has been reviewed frequently (Liu and West, 2004, San Filippo *et al.*, 2008; West, 2003; and Symington, 2002) and repair of DSB by HR is summarised in Figure 1.6. Upon detection of a DSB, nucleases perform a resection resulting in ssDNA overhangs. RAD51 has high affinity for ssDNA, and if RAD51 coats the ssDNA in this scenario (to form a RAD51 nucleoprotein filament) then it is able to induce strand invasion into complementary dsDNA. For this reason, HR activity cannot occur when a sister chromatid or homologous chromosome is absent, for example during S-phase, mitosis or G1 in haploid cells. How the RAD51 nucleoprotein filament is able to detect complementary DNA is not well understood. However, RAD52, which is not mentioned in Figure 1.6, has been found to be important for both nucleoprotein filament assembly and strand invasion (West, 2003), although this is a contentious point in the research community. The effect of strand invasion is that the DNA replication machinery is able to utilise the hydrogen-bonded complementary strand of the template to direct dNTP insertion and hence synthesise healthy DNA across the break. As Figure 1.6 depicts, there are many possible routes for the pathway to take depending upon which protein sets bind the DSB.

An important intermediate is a cruciform structure known as a Holliday junction, named after Robin Holliday who proposed a model in 1964, following work with smut fungi and budding yeast, to show how linked genes on the same chromosome could segregate away from each other (Liu and West, 2004; Stahl, 1994). Due to the intertwined nature of the DNA strands, it is only possible to exit from a Holliday junction by nucleolytic cleavage of the DNA, untangling of two complementary pairs of dsDNA and resealing of the nicks. In the classical pathway, disassembly of the Holliday junction is known as resolution, and is typically catalysed by a resolvase protein, the paradigm of which is *E. coli* RuvC. In Figure 1.6, MUS81 is an example of a eukaryotic resolvase (reviewed in Whitby, 2004; Heyer, 2004). The Holliday junction can also be branch migrated – ‘slid’ along to a different portion of the genome. RecQ-superfamily helicases, for example mammalian BLM, which is mutant in Bloom’s syndrome, have been ascribed such a role. In double Holliday junction dissolution, BLM is thought to branch migrate two Holliday junctions such that they become in close proximity. A topoisomerase enzyme, which functions to cleave DNA such to reduce torsional stress due to supercoiling of the helix, topoisomerase III in this case, can then cleave and hence dissolve the Holliday junctions.

The orientation of resolution cleavage can result in what is referred to as either a ‘crossover’ or a ‘non-crossover’ product. In the latter case, the damaged DNA is repaired and the two **original** pairs of dsDNA are restored after cleavage and separation. However, in the former situation, the pairs of dsDNA are hybrids of the original pairs. Using Figure 1.6 as an example, when a crossover has occurred, each new pair of dsDNA is half red and half blue. Crossovers, as you might expect from swapping one end of a homologous chromosome with the end of its partner, can have devastating consequences for the cell. Hence, crossovers are associated with gross chromosomal rearrangements and genome instability. Loss of heterozygosity (LOH) occurs when a cell, already deficient in one normal copy of a gene, is deprived of the second normal copy. LOH is closely associated with

oncogenesis. Therefore, crossovers are not normally associated with untransformed somatic cells.

Important links between HR and breast cancer have been made. The genes encoding two tumour suppressor proteins, breast cancer 1 (BRCA1) and breast cancer 2 (BRCA2), have been found to be mutant in many familial breast and ovarian tumours. Cells from these tumours show genome instability – that is, large-scale rearrangements of their chromosomes and evidence of truncated chromosomes. BRCA2, a huge protein of 3418 residues – a fact that has severely impaired research into this protein, binds RAD51 and mediates the loading of RAD51 onto RPA-coated ssDNA (reviewed in San Filippo *et al.*, 2008). BRCA1, which is also a large protein, but approximately half the length of BRCA2, is an ubiquitin-protein ligase enzyme and will be discussed in the subsequent section on Fanconi anaemia.

The recombinational pathways synthesis-dependent strand annealing (SDSA), which is also mentioned in Figure 1.6, and break-induced replication (BIR), are reviewed in Haber *et al.*, 2004. HR has also been found to be employed in a wide variety of scenarios other than following a DSB, for example, SSBs and stalled replication forks can be repaired by recombination. A pathway for repair at a stalled replication fork is shown in Figure 1.7, which is adapted from Oakley and Hickson, 2002. In this model, the replication machinery encounters localised DNA damage on the leading strand template, which, if the helicase is not blocked by the lesion, causes leading and lagging strand replication to become uncoupled – lagging strand synthesis can continue. This uncoupling is thought to induce fork regression and formation of a ‘chicken foot’ structure. The motor proteins that effect this regression are not known in eukaryotes, but a helicase called RecG has been identified in *E. coli* as a likely candidate (McGlynn and Lloyd, 2002a). This pathway, as shown in Figure 1.7, is thought to be RAD51-independent as no strand invasion or homology search is required. Also, it is an example of DNA damage tolerance, as the lesion has not been removed – it has been bypassed.

The replication fork has been prevented from collapsing and the lesion can be removed later, by NER for example. However, the chicken foot is thought to be pathological in yeast and an intermediate that may simply be a consequence of fork blockage (discussed in Atkinson and McGlynn, 2009).

Also, the ssDNA ahead of the lesion due to continuation of lagging strand synthesis, can be a target for RAD51 and processed by more classical HR pathways. Alternatively, the ssDNA can act as a substrate for nucleases, resulting in a SSB or asymmetric DSB, which can also be processed by HR, for example by BIR. Li and Heyer, 2008, Atkinson and McGlynn, 2009, and McGlynn and Lloyd, 2002b are reviews of the pathways thought to be important for restarting stalled or broken replication forks.

## **1.8. Fanconi's Anaemia**

The condition Fanconi's anaemia (FA) is associated with a deficiency in a cellular pathway that repairs DNA crosslinks (reviewed in Jacquemont and Taniguchi, 2007). Crosslinks may occur between different strands of DNA, inter-strand crosslinks, or when a covalent bond is formed between different atoms from the same strand, an intra-strand crosslink. As you would expect, this damage blocks DNA replication and anaphase. Common crosslinking agents include *cis*platin, mitomycin C and nitrogen mustards, and unsurprisingly, FA cells are hypersensitive to these agents. There are 13 genetic complementation groups associated with FA, known as FA-A, -B, -C, -D1, -D2, -E, -F, -G, -I, -J, -L, -M, and -N. The protein products of eight of the responsible genes, FANCA, FANCB, FANCC, FANCE, FANCF, FANCG, FANCL and FANCM, are required to form a core complex with the capability of catalysing the ligation of the small modifying protein known as ubiquitin onto substrates. Enzymes with this catalytic activity are known as ubiquitin-protein ligases, or more commonly, E3s. Ubiquitin and E3s will be discussed more extensively below. FANCL is a RING finger protein and in collaboration with the FA core complex, modifies FANCD2 with one ubiquitin,



which causes it, with further aid from the core complex, to localise into nuclear foci with other DNA repair proteins – particularly those also involved in HR, for example BRCA1 and BRCA2 (which turned out to be the same gene as FANCD1). It is thought that the result of this cascade is RAD51-mediated DNA repair by HR. The gene linked to the FA-I complementation group was the most recent to be discovered (Dorsman *et al.*, 2007) and also in 2007, the FANCI protein was identified and found to be a FANCD2 paralogue (Smogorzewska *et al.*, 2007). In the latter study, the authors concluded that FANCI and FANCD2 form a complex, which is necessary for FANCD2 to become localised into damage-induced foci. Furthermore, FANCI is also mono-ubiquitinated, and this is dependent upon the presence of FANCA and an intact ubiquitination site on FANCD2. Interestingly, phosphorylation of FANCD2 and FANCI are also important precedents for the ubiquitination of these proteins, and this appears to be carried out by kinases involved in damage response signalling. Mono-ubiquitination of FA pathway proteins has been recently reviewed (Alpi and Patel, 2009).

## **1.9. p53**

A transcription factor called p53 is a central integration point for detection of DNA damage (reviewed in Riley *et al.*, 2008). A variety of signalling pathways exist to detect and co-ordinate responses to DNA damage. Ataxia telangiectasia mutated (ATM), ATM and Rad3-related (ATR), DNA-dependent protein kinase (DNA-PK), checkpoint 1 (CHK1) and checkpoint 2 (CHK2) are all kinases activated by DNA damage. For example, ssDNA, such as that resultant from NER or from replication fork stall at a lesion, is thought to activate ATR, whereas DNA-PK and ATM are particularly important in the alerting the cell to DSBs. Prompted by this damage, these kinases phosphorylate p53 directly and indirectly, which initiates other types of modification of p53, such as methylation and acetylation. This results in p53 stabilisation that allows binding to specific p53-responsive DNA response elements that control the expression of genes that control tumour suppression. The downstream effect of p53 stabilisation is the arrest of the proliferation of aberrant

cells by induction of senescence or programmed cell death. This pathway is summarised in Figure 1.8.

The p53 protein, which is sometimes referred to as TP53, is encoded by a gene also called p53. In modulating the expression of particular genes important in preventing cancer, the p53 protein acts as a tumour suppressor (reviewed in Riley *et al.*, 2008). In fact, p53 is commonly known as the “guardian of the genome”, due to the fact that its function has been abrogated in all known cancers, either due to mutation of p53, or via bypass of the p53 pathway altogether. An entire family of p53-like genes also exists, of which p63 and p73 are members (reviewed in Bourdon, 2007). Furthermore, p53 family genes each encode multiple different protein isoforms – the p53 gene encodes nine different isoforms. Moreover, p53 is mutant in Li-Fraumeni syndrome, which results in a dramatically increased risk of a wide variety of malignancies, which often strike at an early age. p53 also binds PCNA (Moldovan *et al.*, 2007).

### **1.10. The Importance of Understanding the DNA Damage Response: Carcinogenesis and Ageing**

As alluded to already, deficiencies in responses to DNA damage correlate with an increase in carcinogenesis and premature ageing. Hence, the study of DNA repair processes can be justified in many ways, which will be explained here in no particular order. Whilst the number of patients with inherited deficiencies in DNA repair pathways is relatively small, the exciting promise of gene therapy cures for these patients warrants research into the functional significance of their deficiency at the molecular level and the impact genetic intervention would play in this context. Secondly, cancer is an age-related condition – the repeated exposure to carcinogens over time causes and affects carcinogenesis. There are many steps that lead to a carcinogenic cell and the majority of these steps can result from unrepaired damage. It is important to understand this transformation in order to prevent cancer in the healthy population. Thirdly, recent evidence suggests that

reactions to DNA damage and ageing are inextricably linked – replication stress is thought to promote ageing (see, for example, Burhans and Weinberger, 2007), and of course there is massive public interest in delaying this. Finally, the DNA of cancer cells can be specifically targeted with DNA damaging agents, such as in chemotherapy. Whilst the vast majority of cells in the human body are in senescence, transformed cells are growing and dividing actively. This fact has been utilised for decades in order to kill malignant cells during the treatment of cancer patients. DNA repair pathways have been successfully used as targets for cancer therapy (reviewed in Helleday *et al.*, 2008).

The fundamentals of DNA damage and cellular responses have now been outlined from basic principles. Furthermore, the importance of research into damage tolerance and repair has been emphasised. Now, a more detailed introduction to the biochemistry of post-replication repair and deubiquitinating enzymes will follow.

### **1.11. An Introduction to Post-Replication Repair**

Post-replication repair (PRR) relates to processes that enable DNA damage to be tolerated by cells. UV irradiation of DNA typically induces adjacent DNA bases to react with each other. The principal, resulting chemical products when two pyrimidine bases are involved are cyclobutane pyrimidine dimers (CPDs) or, less commonly, a 6-4 photoproduct (6-4PP). It was found that when DNA containing these lesions is replicated, gaps form in the daughter strand opposite each lesion (Rupp and Howard-Flanders, 1968; Lehmann, 1972). From experiments in *E. coli*, it was hypothesised that a “post-replication repair” mechanism, that is, repair occurring after the replication fork has moved on, was responsible for the filling of these gaps i.e. the conversion from low molecular weight DNA (with gaps) to high molecular weight DNA (gaps filled; see Rupp and Howard-Flanders, 1968, which is reviewed in Bridges, 2005). It was also demonstrated in *E. coli* that PRR involved a HR mechanism between daughter DNA strands to restore the high-molecular weight DNA (Rupp and Howard-Flanders, 1968). In mammalian cells however, it

was also shown that the gaps opposite the CPDs are filled in by newly synthesised DNA, as opposed to DNA obtained from elsewhere such as occurs in HR (Lehmann, 1972). Interestingly, it was later discovered that dimer-free DNA is not likely to result from this gap-filling mechanism (Ganesan, 1974).

### **1.12. Xeroderma Pigmentosum Variant**

XP is a rare autosomal recessive disease and its name refers to the mottled, dry skin characteristic of XP patients. For a review see Gratchev *et al.*, 2003. It is a very rare disease – an incidence of 2.3 cases per million live births in Western Europe has been calculated (Kleijer *et al.*, 2008), and a higher frequency has been reported in Japan (Takebe *et al.*, 1987). XP patients have a 2000-fold higher risk of developing skin cancer than the normal population (Kraemer *et al.*, 1987). Other phenotypes include photophobia and other ocular pathologies, immunological skin abnormalities, premature ageing, neurological problems and premature death.

In the early 1970s, patients were identified with XP symptoms but no defect in unscheduled DNA synthesis (UDS), which measures the amount  $^3\text{H}$ -thymidine incorporation in non-S-phase cells and correlates with the level of DNA repair by NER. This new form of XP was designated xeroderma pigmentosum variant, XP-V, and one fifth of XP patients fall into this category (Gratchev *et al.*, 2003). However, it was not until 1999 that DNA polymerase  $\eta$  (Pol $\eta$ ), the protein encoded by the gene that is mutant in XP-V, was finally identified (Masutani *et al.*, 1999).

In a seminal paper in 1975, it was found that subsequent to the UV-irradiation of XP-V cells, “the time taken for the newly synthesised DNA to attain a high molecular weight similar to that in unirradiated controls is much longer than in normal cells” (Lehmann *et al.*, 1975). Hence it was concluded that XP-V cells are deficient in PRR and therefore this pathway is fundamentally important in the prevention of UV-induced carcinogenesis.

The current model for PRR is thus: lesions can be dealt with via two distinct pathways, a principally error-prone mechanism known as translesion synthesis (TLS), which can be error-free and error-prone, and an error-free mechanism referred to as a “template switch”.

### 1.13. DNA Polymerases and Translesion Synthesis

Pol $\eta$  functions in the former pathway and is known as a specialised polymerase. Specialised polymerases are reviewed in Friedberg *et al.*, 2002; Goodman, 2002; Prakash *et al.*, 2005, and are named as such because they perform different, specialised functions compared to the high-fidelity replicative polymerases, such as DNA polymerases  $\alpha$  (Pol $\alpha$ ),  $\delta$  (Pol $\delta$ ), and  $\epsilon$  (Pol $\epsilon$ ) found in eukaryotes. There are nine specialised polymerases in human cells: DNA polymerases  $\beta$ ,  $\zeta$ ,  $\kappa$ ,  $\eta$ ,  $\iota$ ,  $\lambda$ ,  $\mu$ ,  $\theta$ , and Rev1 (Friedberg *et al.*, 2002). DNA polymerases can also be classified into seven distinct families, A, B, C, D, X, Y, and RT, based on sequence homology. The specialised polymerases Pol $\eta$ , Pol $\iota$ , Pol $\kappa$  and Rev1 are members of the Y-family of DNA polymerases. There are six sub-classifications of Y-family polymerases (Ohmori *et al.*, 2001). The UmuC Gram-positive and UmuC Gram-negative groups relate to bacterial Y-family polymerases. The Rad30A group comprises Pol $\eta$ ; the Rad30B group, Pol $\iota$ ; the Rev1 group, Rev1; and the DinB group, Pol $\kappa$ . DNA polymerase  $\zeta$  consists of a heterodimer comprising a B-family polymerase subunit, Rev3, and a cofactor protein called Rev7. The B-family also comprises Pol $\alpha$ , Pol $\delta$  and Pol $\epsilon$ , so as expected Rev3 has a greater fidelity than Y-family polymerases, however it is missing the proofreading exonuclease domain found in these aforementioned replicative polymerases.

Pol $\eta$ , Pol $\iota$ , Rev1, Pol $\kappa$  and Pol $\zeta$  have all been found to function in TLS. These Y-family polymerases are characterised in that they comprise a more open active site, which can accommodate a damaged base. This structure has two important consequences, (1) these polymerases are able to bypass sites of DNA damage where a normal, replicative polymerase would stall, and (2) they have low-fidelity.

The TLS pathway is referred to as error-prone due to the latter. In the TLS model, the replicative polymerase encounters a damaged base and stalls, there is a “polymerase switch” to a TLS polymerase, which tries to bypass the damage, and then a switch back to the highly processive and accurate replicative polymerase occurs. However, Pol $\eta$  is actually very effective at inserting two consecutive adenine nucleotides, -A-A-, in the daughter strand opposite a -T-T- CPD, hence effectively bypassing this lesion (Johnson *et al.*, 1999). For this reason, Pol $\eta$ -mediated TLS is often referred to as an error-free sub-pathway of TLS.

Recent research effort has tried to differentiate the functions of the different specialised polymerases (Lehmann, 2006) and how the polymerase switch occurs (Fischhaber and Friedberg, 2005). Rev1 is able to insert a dCTP, i.e. a “-C-“, opposite a template “-G-“ or abasic site. Rev1 has been found to interact with Pol $\eta$ , Pol $\iota$ , Pol $\kappa$ , and Rev7, and has been proposed to have a role in gap-filling during G2-M in *S. cerevisiae* (Waters and Walker, 2006) and to recruit Pol $\zeta$  to stalled replication forks and DSBs (reviewed in Kolas and Durocher, 2006). Furthermore, Pol $\kappa$  cannot carry out TLS past UV-induced dimers *in vitro* and has been found to function in NER (Ogi and Lehmann, 2006).

### 1.14. The Template Switch Mechanism

Very little is known about the template switch sub-pathway of PRR, however epistasis analysis in *S. cerevisiae* has revealed that it is error-free (Prakash, 1981; Xiao *et al.*, 2000). A template switch mechanism was actually first suggested in 1976 (Higgins *et al.*, 1976). The authors proposed that a chicken-foot structure could be formed in order to bypass damage encountered by replication forks (Figure 1.7), hence this was a “replication repair” mechanism rather than a **post**-replication repair mechanism. However, recent evidence using electron microscopy with *S. cerevisiae* suggests that these four-way structures are rare *in vivo* (Lopes *et al.*, 2006). Alternatively, HR machinery may be used in PRR gap-filling after the fork has moved on following its stall and reinitiation (reviewed in Friedberg, 2005).

Key work in *E. coli* has led to a plausible hypothesis for the reinitiation of replication on the leading strand beyond a blocked fork (Heller and Marians, 2006), the prior deficiency of such a model has always inhibited research progress in this area. In this model, the replicative helicase recruits multiple primase proteins to reprime both the leading and lagging strands.

Taken together, there appears to be a role for PRR proteins to carry out TLS and/or recruit HR machinery in order to repair stalled replication forks, as well as in a truly post-replicative sense i.e. gap filling (Friedberg, 2005). In the latter mode, it is thought that the cell first tries to gap-fill using TLS, whereas persistent gaps are filled by a HR mechanism (discussed in Lehmann and Fuchs, 2006).

Whilst the general principles of PRR are conserved in all three domains of life: archaea, eubacteria, and eukaryotes, differences exist between domains, and within domains. For example, DinB is absent from *S. cerevisiae* but found in other yeasts and Rad30B group polymerases are only found in higher eukaryotes.

The modification of PCNA has been shown to be fundamental for PRR. Modulation of the biochemistry of the binding surfaces of PCNA, in particular by covalent modifications in eukaryotes, has been shown to be pivotal in PRR pathway decisions. The functions and binding partners of PCNA will now be discussed in greater detail.

### **1.15. PCNA: Functions and Binding Partners**

PCNA is the doughnut-shaped sliding clamp that encircles DNA and confers high-processivity to bound DNA polymerases. Said sliding clamp in eukaryotes is actually a homotrimer of PCNA subunits that form a ring, which is loaded onto DNA in eukaryotes by the clamp-loader replication factor C (RFC). As previously discussed, PCNA is fundamentally important for ensuring processive DNA

synthesis, either during DNA replication or during many of the repair events that require polymerase activity.

However, PCNA binds a variety of proteins other than polymerases and has been proposed to function as a sliding “toolbelt” that provides a binding platform for proteins requiring access to DNA (reviewed in Warbrick, 2000, Maga and Hubscher, 2003). The functions and binding partners of PCNA have been particularly eloquently reviewed in detail in Moldovan *et al.*, 2007. For example, PCNA binds chromatin licensing and DNA replication factor 1 (Cdt1), which is important for correct replication origin firing (reviewed in Green, 2006). The wide variety of processes that PCNA is involved in is best illustrated by the variety of proteins that PCNA binds to: topoisomerases, endonucleases, DNA ligases, helicases, mismatch repair enzymes, BER enzymes, NER enzymes, histone and chromatin remodelers, poly-(ADP-ribose) polymerase (PARP), DNA methyltransferases, protein kinases e.g. CDK2, cell cycle regulators e.g. cyclin D1 and p21<sup>CIP</sup>, sister-chromatid cohesion proteins, apoptotic factors, plus a variety of enzymes involved in post-replication repair and modification of proteins with ubiquitin and SUMO that will be discussed in the second half of this chapter (Moldovan *et al.*, 2007).

Known PCNA binding proteins contain a PCNA-interacting protein motif or PIP box. At the primary sequence level, this loosely comprises KAxQxxψxxθθ, wherein x is any residue, ψ is L, M or I, and θ is F or Y (Xu *et al.*, 2001). The motif must also be found within an unstructured area of the PCNA-interacting protein in order to be a *bona fide* PIP box (Shell *et al.*, 2007). For the PIP box sequences of a wide variety of PCNA interacting proteins, see supplementary figure S1 of Moldovan *et al.*, 2007.

Each PCNA subunit comprises two globular domains connected by what is normally referred to as an interdomain connecting loop. Structure ‘A’ in Figure 1.9 was solved in Gulbis *et al.*, 1996, and here shows each subunit in a different



colour. The structure is angled such that the division between the two domains can be clearly distinguished in the light purple subunit. The interdomain connecting loop is the unstructured portion on the outer surface of each subunit. The inner surface of the homotrimer comprises positively charged  $\alpha$ -helices that interact with DNA. The remainder of each subunit forms  $\beta$ -sheets. The homotrimer has two distinct faces. The 'C' face (Figure 1.9, D), so-called because this is the side from which the C-terminus of each PCNA subunit protrudes, facing towards the 3' end of the DNA i.e. forwards. RFC and the DNA polymerases bind the C face, and so PCNA is dragged along behind during DNA replication.

Structural studies have shown that the PIP box of a PCNA interacting protein slots into a hydrophobic pocket underneath the interdomain connecting loop of one subunit. Only one PIP box can dock into this pocket, so interacting proteins must compete for one of the three docking sites on the PCNA homotrimer.

Post-translational modifications of PCNA modulate the binding interfaces – of particular relevance to PRR is the modification of lysine residues in PCNA. Each human PCNA polypeptide is 261 amino acids long and contains 11 lysine residues. PCNA is ubiquitinated on lysine 164 (Figure 1.9, B) and modified with small ubiquitin-like modifier (SUMO) on lysine-164 and on lysine-127 (Figure 1.9, C).

In order to further understand the roles of ubiquitination of PRR proteins and the functions of deubiquitinating enzymes, the following sections will introduce post-translation modification of proteins, ubiquitin fold containing proteins and ubiquitination.

## **1.16. Post-Translational Modification of Proteins by Ubiquitination**

Following their synthesis, cellular proteins have been found to be covalently modified by a wide variety of modifiers. Proteins can be acetylated,

phosphorylated, biotinylated, hydroxylated, palmitoylated, farnesylated, and sulfated, to name but a few. Here we will discuss protein ubiquitination.

The Nobel prize for chemistry in 2004 was won by Aaron Ciechanover, Avram Herskho, and Irwin Rose for their discovery of ubiquitin-mediated protein degradation (reviewed in Ciechanover, 2005 and Wilkinson, 2005). Ubiquitin is a small protein of only 76 amino acids that can be covalently attached to target proteins. Poly-ubiquitination of target proteins was found to induce their degradation, which is carried out by a large proteinaceous peptidase complex called the proteasome. In other words, the poly-ubiquitin tag is a death signal for the ubiquitinated protein. The ubiquitin-proteasome system is reviewed in Hochstrasser, 1996 and Voges *et al.*, 1999.

Post-translational modification of substrate proteins by ubiquitin requires a minimum of two enzymes, an E1 (ubiquitin-activating enzyme) and an E2 (ubiquitin conjugating enzyme). An E3 (ubiquitin-protein ligase) is also typically utilised. Ubiquitin is reversibly, covalently bonded to a target protein by the formation of an isopeptide bond between the C-terminal glycine-76 residue of ubiquitin, and the  $\epsilon$ -amino group on the side-chain of a lysine residue on the target. The E1 prepares the  $\alpha$ -carboxyl group of glycine-76 on ubiquitin in an ATP-dependent step. This activation step results in an E1–ubiquitin conjugate. The E2 specifically recognises this conjugate, and ubiquitin is transferred to the E2 by transthioylation. The ubiquitin can then be transferred from the E2 to the target protein, and this is typically catalysed by an E3. E3s exist in two forms, HECT domain E3s become covalently bonded to the ubiquitin prior to its transferral to the target, and really interesting new gene (RING) finger E3s do not. The latter simply speeds up the process. E3s are thought to provide the most target specificity to the ubiquitination reaction. Furthermore, another enzyme class exists called the E4s, which are thought to be involved in chain elongation. Deubiquitinating enzymes catalyse the removal of ubiquitin from modified targets (discussed later).

Target proteins may be mono-ubiquitinated, in other words, modified by one ubiquitin tag. This single ubiquitin may be extended to form a poly-ubiquitin chain. Alternatively, a target may be ubiquitinated on multiple sites, which is known as multi-ubiquitination, and this can be multiple single ubiquitin tags or multiple poly-ubiquitin chains.

To direct a target to the proteasome for degradation, the poly-ubiquitin chain was found to be in a specific configuration. Following mono-ubiquitination of a target lysine, an ubiquitin chain is formed by bonding a second ubiquitin to a lysine residue on the first, followed by a third ubiquitin bonded to a lysine on the second, and so on as required. There are seven lysines in ubiquitin, lysine-6, -11, -27, -29, -33, -48, and -63. These lysines are highlighted in pink in Figure 1.10, which is based on a structure solved in Vijay-Kumar *et al.*, 1987. In order to direct the target to the proteasome, the mono-ubiquitin is extended with a lysine-48-linked poly-ubiquitin chain. The position of lysine-48 is also shown in Figure 1.10, and lysine-48-linked poly-ubiquitin chains form a compact chain. However, a different lysine on ubiquitin can be selected and this results in a different chain conformation that activates non-degradative pathways.

### **1.17. Ubiquitin-like Proteins and Non-Degradative Functions of the Ubiquitin Superfold**

Ubiquitin has been coined Darwin's phosphate (Welchman *et al.*, 2005). Phosphorylation is a very common type of post-translational modification and involves the addition of a single phosphate group onto a target, and quite often the target is phosphorylated in multiple places. Attachment with members of the ubiquitin system, on the other hand, is a more complex and "evolved" form of modification (Welchman *et al.*, 2005). As alluded to already, mono-, multi- and poly-ubiquitination can occur. Furthermore, the poly-ubiquitination can occur in different configurations depending upon the lysine residue of ubiquitin that the chain is extended from, and chains with mixed linkages can occur (reviewed in

Ikeda and Dikic, 2008). These non-canonical ubiquitin modifications activate non-degradative pathways. For example, as described above mono-ubiquitination of FANCD2 and FANCI induces colocalisation with DSB repair proteins; also AMP-activated protein kinase-related protein kinases are inhibited by modification with lysine-29/lysine-33-linked mixed poly-ubiquitin chains (Al-Hakim *et al.*, 2008).

Additionally, a variety of other ubiquitin-like proteins exist, one of which has been found to be involved in PRR. Known ubiquitin-like proteins (UBLs) include: small ubiquitin-like modifier (SUMO), ubiquitin cross-reactive protein (UCRP, also known as interferon-stimulated gene-15 [ISG15]), ubiquitin-related modifier-1 (URM1), neuronal-precursor-cell-expressed developmentally downregulated protein-8 (NEDD8, but called Rub1 in *S. cerevisiae*), human leukocyte antigen F associated (FAT10), autophagy-8 (ATG8) and -12 (ATG12), Fugu ubiquitin-like protein (FUB1), MUB (membrane-anchored UBL), ubiquitin fold-modifier-1 (UFM1) and ubiquitin-like protein-5 (UBL5, which is also known as homologous to ubiquitin-1 [Hub1]). UBLs are reviewed in Welchman *et al.*, 2005, Kerscher *et al.*, 2006, and Grabbe and Dikic, 2009b. Whilst these proteins share only modest primary sequence identity with ubiquitin, they are closely related three-dimensionally. They all comprise an ubiquitin fold (often called an ubiquitin-like domain and sometimes an ubiquitin fold) – in fact, FAT10 and UCRP contain two. This compact globular  $\beta$ -grasp fold is found in ubiquitin, UBLs, and proteins that comprise an ubiquitin-like domain. For example the *S. cerevisiae* spindle pole body duplication protein, Dsk2, and NER protein, Rad23, both contain N-terminal ubiquitin-like domains (Welchman *et al.*, 2005).

There are three SUMO proteins in *H. sapiens*, SUMO-1, -2, and -3. SUMO-1 is also known as Sentrin, suppressor of *MIF2* mutations-3 (Smt3) and as Pmt3. A comparison of the structure of SUMO-1 and ubiquitin can be found in Figure 1.10 (the structure of SUMO-1 shown was elucidated in Bayer *et al.*, 1998). Despite sharing only 18% sequence identity and being over a third larger, SUMO folds to form the  $\beta$ -grasp domain found in ubiquitin. Modification of targets by SUMO is

known as sumoylation, which has been found to be important in a wide variety of cellular processes (reviewed in Zhao, 2007) such as transcription inhibition, the migration of the promyelocytic leukaemia protein (PML) into nuclear bodies, and genome stability (reviewed in Watts *et al.*, 2007). SUMO has its own specific set of E1, E2 and E3 enzymes, as well as desumoylating enzymes (reviewed in Johnson, 2004), and poly-SUMO chains can sometimes form (Vertegaal, 2007).

PCNA ubiquitination and sumoylation influence the PRR pathway in a way that is independent of proteasomal degradation.

### 1.18. Post-Replication Repair in *S. cerevisiae*

Key aspects of the molecular mechanisms of PRR in eukaryotes were first elucidated in the baker's yeast *S. cerevisiae*. (For brevity and clarity hereon, protein names will be preceded by a two-letter prefix indicating the species from which it originates). In *S. cerevisiae*, <sup>Sc</sup>PCNA was shown to be ubiquitinated in response to treatment with the damaging agent methyl methanesulfonate (MMS). This reaction was shown to be carried out by the E2 <sup>Sc</sup>Rad6 and the E3 <sup>Sc</sup>Rad18 (Maga and Hubscher, 2003). These enzymes were found to catalyse the mono-ubiquitination of <sup>Sc</sup>PCNA on lysine-164 (Hoege *et al.*, 2002), which is thought to activate the TLS branch of PRR.

There are two Y-family polymerases in *S. cerevisiae*, <sup>Sc</sup>Rad30 (Rad30A group), <sup>Sc</sup>Rev1 (Rev1 group), plus the B-family polymerase, <sup>Sc</sup>Rev3 and its partner <sup>Sc</sup>Rev7. The mechanism for this activation is thought to be thus: upon encountering a lesion, PCNA is mono-ubiquitinated, which leads to a switch from the normal, replicative DNA polymerase to the TLS DNA polymerase (Friedberg *et al.*, 2005).

Alternatively, the mono-ubiquitination can be extended by a second set of enzymes, the <sup>Sc</sup>Ubc13-<sup>Sc</sup>Mms2 E2 heterodimer and the E3 <sup>Sc</sup>Rad5, to create a lysine-63-linked poly-ubiquitin chain (Hoege *et al.*, 2002). <sup>Sc</sup>Ubc13 confers the E2

activity and <sup>Sc</sup>Mms2 is a cofactor containing a domain known as an ubiquitin-enzyme variant (UEV), which is thought to be the product of an E2 pseudogene. <sup>Sc</sup>Mms2 has a similar structure to <sup>Sc</sup>Ubc13, but lacks the catalytic cysteine residue. This non-canonical, lysine-63-linked form of chain is thought to activate the template switch pathway proposed to use HR machinery to carry out the error-free method of lesion bypass. It has also been suggested that the HR proteins, such as <sup>Sc</sup>Rad51, <sup>Sc</sup>Rad52, <sup>Sc</sup>Rad54 and <sup>Sc</sup>Rad55, are involved (Pfander *et al.*, 2005). Furthermore, a lysine-63-linked poly-ubiquitin chain has been found to adopt a more extended structure wherein, unlike ubiquitin in lysine-48-linked chains, there are no inter-ubiquitin interactions (Varadan *et al.*, 2004, Tenno *et al.*, 2004). Hence it is plausible that currently unidentified proteins with ubiquitin-binding domains capable of binding lysine-63-linked chains specifically can then recruit HR machinery to the stalled fork or gap.

In the aforementioned, seminal paper by the Jentsch group in 2002 it was also shown that <sup>Sc</sup>PCNA is sumoylated on lysine-164, and to a lesser extent, lysine-127 (Hoege *et al.*, 2002, and reviewed in Matunis, 2002). <sup>Sc</sup>PCNA is sumoylated in undamaged cells during S-phase and this modification was proposed to antagonise PRR by sequestering lysine-164 from ubiquitin modification. A DNA helicase called <sup>Sc</sup>Srs2 with 5' to 3' polarity that is known to be involved in HR had already been implicated in the template switch portion of PRR (Ulrich, 2001). In further papers by the Jentsch and Ulrich groups in 2005, <sup>Sc</sup>Srs2 was found to bind SUMO-modified <sup>Sc</sup>PCNA (Pfander *et al.*, 2005, Papouli *et al.*, 2005). <sup>Sc</sup>Srs2 was proposed to inhibit HR induced by poly-ubiquitination of <sup>Sc</sup>PCNA by disrupting <sup>Sc</sup>Rad51 nucleoprotein filaments (Veaute *et al.*, 2003, Krejci *et al.*, 2003). Systems where modification of the same site by ubiquitin or SUMO that result in different sometimes opposing downstream effects are known in the literature (reviewed in Ulrich, 2005). The modifications of <sup>Sc</sup>PCNA are summarised in Figure 1.11 (Hoege *et al.*, 2002).

It has also been proposed that lysine-63-linked poly-ubiquitin chains on PCNA may simply sequester lysine-164 from activating normal replication or TLS, when in un-

modified and mono-ubiquitinated form, respectively (Hofmann, 2009). This hypothesis primarily comes from (1) the complex domain architecture of *Sc*Rad5 and its homologues in other organisms, and (2) work of the Prakash group in 2007 who found a role for *Sc*Rad5 in replication fork regression (Blastyak *et al.*, 2007). *Sc*Rad5 comprises a HIRAN (HIP116 Rad5 N-terminal) domain, the seven motifs (I, Ia, II, III, IV, V and VI) that make up a classical helicase domain, and a RING finger domain in the gap between the last few helicase motifs. The HIRAN domain is thought to bind DNA particularly in the context of damage or stalled replication forks (Iyer *et al.*, 2006). Therefore, perhaps the lysine-63-linked poly-ubiquitination of *Sc*PCNA promoted by the RING finger halts the activation of other pathways, in turn allowing *Sc*Rad5 to unwind the DNA helix, regress the fork, and generate the chicken-foot structure such as that seen in the template switch model shown in Figure 1.7. However, the function of the lysine-63-linked poly-ubiquitin as an inert chain in this way is merely speculation.

### 1.19. Post-Replication Repair in Higher Eukaryotes

The literature reports that PRR occurs in a similar way in higher eukaryotes compared to budding yeast (reviewed in Lee and Myung, 2008; Lehmann *et al.*, 2007; Ulrich, 2009).

Recent research using human cells has provided information about the damage that activates PRR. Specific types of DNA damage have been found to cause *Hs*PCNA ubiquitination, particularly those that result in replication fork stall (Niimi *et al.*, 2008). The hypothesis is that this results in ssDNA, which activates PRR. Knockdown with small interfering RNA (siRNA) targeted to the gene encoding *Hs*RPA resulted in a reduction in *Hs*PCNA ubiquitination (Niimi *et al.*, 2008) and this agrees with evidence from mouse cells (Bi *et al.*, 2006) and *S. cerevisiae* (Davies *et al.*, 2008).

There are two E2s, *Hs*RAD6A and *Hs*RAD6B, and one E3, *Hs*RAD18, thought to be involved in *Hs*PCNA mono-ubiquitination on lysine-164 in human cells. *Hs*RAD18 is 495 residues long and contains five distinct binding domains: a RING finger that confers the E3 activity, a C2H2 zinc-finger, a SAP (SAF-A/B, Acinus, Pias) domain, a *Hs*RAD6-binding domain, and a *Hs*Pol $\eta$ -binding domain. In addition to *Hs*Pol $\eta$ , *Hs*RAD18 binds forked and ssDNA, *Hs*RAD6B, ubiquitin and *Hs*RPA, and is therefore thought to be a particularly fundamental control point in the activation of PRR (Notenboom *et al.*, 2007, Tsuji *et al.*, 2008). Evidence from *S. cerevisiae* corroborates this (Huttner and Ulrich, 2008). The *Hs*Pol $\eta$ –*Hs*RAD18 interaction is thought to act as a guide to bring *Hs*Pol $\eta$  to mono-ubiquitinated *Hs*PCNA (Watanabe *et al.*, 2004). Moreover, *Hs*RAD18 is capable of auto-ubiquitination, which is dependent upon *Hs*RAD6 and is thought to function to control the subcellular localisation of *Hs*RAD18 (Miyase *et al.*, 2005).

There are five known TLS polymerases in human cells: *Hs*Pol $\eta$  (RAD30A group), *Hs*Pol $\iota$  (RAD30B group), *Hs*Pol $\zeta$  (B-family), *Hs*Rev1, and *Hs*Pol $\kappa$  (DinB group). *Hs*Pol $\eta$ , *Hs*Pol $\iota$ , *Hs*Rev1 and *Hs*Pol $\kappa$  have been shown to bind mono-ubiquitinated *Hs*PCNA via novel ubiquitin-binding domains (Kannouche *et al.*, 2004; Watanabe *et al.*, 2004; Bienko *et al.*, 2005; Plosky *et al.*, 2006; Guo *et al.*, 2009). The accepted thinking is that mono-ubiquitination of *Hs*PCNA increases its affinity for Y-family polymerases and induces a switch from a replicative to a TLS polymerase. Due to the homotrimeric nature of the PCNA doughnut, it is possible that the replicative polymerase binds a non-ubiquitinated subunit of *Hs*PCNA, and one or more TLS polymerases bind ubiquitinated *Hs*PCNA subunits. Hence, the “sliding toolbelt” model of the sliding clamp. A TLS polymerase is employed until the lesion is bypassed. It is not known whether or how specific TLS polymerases are selected for particular lesions. There is a theory proposed by Errol Friedberg that each TLS polymerase has cognate lesion(s), which it is able to bypass more accurately than non-cognate types, although this is not accepted in the majority of the research community.



Recent work clearly shows that <sup>Hs</sup>PCNA mono-ubiquitination persists for some time following damage and repair of the damage (Niimi *et al.*, 2008). In this study, a new model was proposed wherein each fork-blocking lesion results in an ubiquitinated <sup>Hs</sup>PCNA molecule retained at that site. In other words, the replication machinery stalls, <sup>Hs</sup>PCNA is mono-ubiquitinated, the replication fork is reloaded beyond the lesion using non-ubiquitinated <sup>Hs</sup>PCNA and processive replication continues until the next lesion, whereupon the cycle repeats. The TLS machinery loads at each mono-ubiquitinated <sup>Hs</sup>PCNA behind the fork to fill in the gaps.

In human cells, recent, prominent work has finally provided substantiation that <sup>Hs</sup>PCNA is poly-ubiquitinated, albeit at very low levels compared to yeast. Two <sup>Sc</sup>Rad5 homologues have now been identified in human cells – <sup>Hs</sup>SHPRH (Motegi *et al.*, 2006, Unk *et al.*, 2006) and <sup>Hs</sup>HLTF (Motegi *et al.*, 2008) and there is evidence that lysine-63-linked poly-ubiquitination of <sup>Hs</sup>PCNA is linked to the error-free pathway – particularly due to its dependence upon the presence of <sup>Hs</sup>UBC13 (Chiu *et al.*, 2006). By domain architecture, <sup>Hs</sup>HLTF demonstrates the most similarity to <sup>Sc</sup>Rad5 in that it contains also the N-terminal HIRAN domain, and the seven helicase motifs with a zinc-finger before the final few C-terminal helicase motifs. <sup>Hs</sup>SHPRH on the other hand is more dissimilar in this respect. Immediately following helicase motif I lies a linker histone domain, and a PHD-finger domain is found just before motif Ia. A PHD-finger is thought to be involved in chromatin-mediated transcriptional regulation processes, and is reminiscent of a RING finger (Aasland *et al.*, 1995). A more divergent RING finger domain, compared to <sup>Sc</sup>Rad5 and <sup>Hs</sup>HLTF, is also found at the C-terminus of <sup>Hs</sup>SHPRH. Although, there seems to be disagreement in the literature as to whether helicase motif IV comes after (Unk *et al.*, 2006) or before (Motegi *et al.*, 2006, Motegi *et al.*, 2008) the RING finger in all three proteins. <sup>Hs</sup>SHPRH is also approximately 50% longer than <sup>Sc</sup>Rad5 and <sup>Hs</sup>HLTF.

There are also findings to suggest that <sup>Hs</sup>MMS2 is not the only UEV protein that can be used for poly-ubiquitination of <sup>Hs</sup>PCNA. There are four UEV loci in human

cells and there appeared to be little difference in poly-ubiquitination of <sup>Hs</sup>PCNA with or without siRNA-mediated depletion of only <sup>Hs</sup>MMS2 (Brun *et al.*, 2008).

No <sup>Hs</sup>PCNA sumoylation has been reported in human cells, although there is evidence in chicken cells and *Xenopus laevis* extracts (Arakawa *et al.*, 2006, Goehler *et al.*, 2008). However, the consequence of this modification on PRR has not been elucidated in these organisms, and no evidence for helicase involvement has been found. Therefore, it is plausible that this PRR antagonisation system is limited to *S. cerevisiae* (Ulrich, 2009).

According to the polymerase switch model, once PRR has occurred, processive replication surely must be restored. TLS polymerases have poor fidelity on undamaged DNA, low processivity and excessive HR also has dangerous consequences for the cell. How such a switch is effected is not known. A potential mechanism was proposed in light of evidence that each TLS polymerase comprises a novel ubiquitin-binding domain and that the TLS polymerase itself is mono-ubiquitinated in undamaged cells (Bienko *et al.*, 2005).

<sup>Hs</sup>Pol $\eta$  comprises one C-terminal ubiquitin-binding zinc finger 3 (UBZ3) domain, which is a C2H2 zinc-finger. <sup>Hs</sup>Pol $\kappa$  contains an ubiquitin-binding zinc finger 4 (UBZ4) domain, which is a C2HC zinc-finger. Interestingly, this domain is also found in <sup>Hs</sup>RAD18, and has been postulated to bind to mono-ubiquitinated <sup>Hs</sup>PCNA to block the extension to a poly-ubiquitin chain (Hofmann, 2009), thus inhibiting the template switch reaction. <sup>Hs</sup>Pol $\iota$  and <sup>Hs</sup>REV1 each contain an ubiquitin-binding motif, or UBM domain. These new ubiquitin-binding domains seem to be found in proteins with roles in the nucleus, particularly DNA damage responses (reviewed in Hofmann, 2009).

The mechanism proposed by Bienko *et al.* is thus: polymerase mono-ubiquitination is thought to induce a conformational change within the polymerase enabling it to bind its own covalently attached ubiquitin via its ubiquitin-binding domain. This

intra-molecular interaction out-competes the inter-molecular interaction of the TLS polymerase with mono-ubiquitinated <sup>Hs</sup>PCNA (Bienko *et al.*, 2005).

However, the obvious model for activation of a switch back to normal replication is the deubiquitination of <sup>Hs</sup>PCNA. A deubiquitinating enzyme called <sup>Hs</sup>USP1 has been found to remove the mono-ubiquitination from <sup>Hs</sup>PCNA in human cells (Huang *et al.*, 2006). This enzyme will be discussed extensively later in this chapter.

The fission yeast *Schizosaccharomyces pombe* was utilised as a model organism to study potential deubiquitinating enzymes that can act on <sup>Sp</sup>PCNA. Before deubiquitinating enzymes and their roles in PRR are discussed in detail, the reason why *S. pombe* was used will be outlined.

## **1.20. The Utilisation of *Schizosaccharomyces pombe* as a Model Organism**

Yeast are unicellular, eukaryotic micro-organisms of the fungi kingdom that can be cultured rapidly and easily in the lab. They offer a stripped down model system for the understanding of fundamental cellular processes, which can be directly applicable to more complicated, higher eukaryotes such as humans. *S. pombe* was the first species of fission yeast discovered, which as their name suggests, propagate by linear elongation and binary, medial fission (Sipiczki, 2000). *S. pombe*'s distant relative, *S. cerevisiae*, has been the yeast of choice due to its use for thousands of years in brewing and baking. The combination of popular use with the fact that baker's yeast is generally more easily manipulated in the laboratory, has resulted in a more solid foundation of understanding of molecular processes in this organism. However, *S. pombe* is more comparable to humans from certain physiological perspectives, such as in the biochemistry of the cell cycle (Nurse, 2002). *S. pombe* cells are rod-shaped and much larger than the small, round cells of *S. cerevisiae*. When blocked in cell cycle progression, the cells become progressively elongated, which can be recognisable by the naked eye and very

easily by light microscope. Upon medial fission, *S. pombe* produce two daughter cells of equal sizes. Baker's yeast, on the other hand, divide by budding and do not demonstrate such an identifiable phenotype when blocked in the cell cycle. Sir Paul Nurse won the 2001 Nobel Prize in physiology and medicine, in combination with Tim Hunt and Lee Hartwell, for his ground-breaking work on the cell cycle using *S. pombe*. The full genome sequence of *S. pombe* was published in 2002 by the Sanger Institute in Cambridge, UK (Wood *et al.*, 2002). A particularly germane advantage is the study of PRR is easier because the ubiquitination of PCNA occurs to a greater extent in *S. pombe* than in *S. cerevisiae*. Ubiquitinated forms of <sup>Sp</sup>PCNA can be detected using anti-<sup>Sp</sup>PCNA antibodies on whole cell extracts from fission yeast, rather than perform an  $\alpha$ -<sup>Sc</sup>PCNA immunoprecipitation as is necessary with baker's yeast (compare Frampton *et al.*, 2006 with Hoege *et al.*, 2002). Certainly, information about cellular biochemistry provided by both species of yeast provides, in combination, a powerful tool for biomedical research.

### 1.21. Post-Replication Repair in *S. pombe*

In accordance with its distantly related cousin *S. cerevisiae*, *S. pombe* PRR utilises a similar system using orthologous genes. Lysine-164 of <sup>Sp</sup>PCNA was found to be mono-ubiquitinated by <sup>Sp</sup>Rhp6 (E2) and <sup>Sp</sup>Rhp18 (E3, Frampton *et al.*, 2006), where "Rhp" stands for Rad homologue in *S. pombe*. The proposed template switch is effected by lysine-63-linked poly-ubiquitination of <sup>Sp</sup>PCNA by extending the mono-ubiquitin on lysine-164 via the <sup>Sp</sup>Ubc13-<sup>Sp</sup>Mms2 (E2 heterodimer) and the E3 <sup>Sp</sup>Rad8 (Frampton *et al.*, 2006). There are three Y-family polymerases in *S. pombe*, <sup>Sp</sup>Eso1 (Rad30A group of Y family polymerases), <sup>Sp</sup>Rev1 (Rev1 group), and <sup>Sp</sup>DinB (DinB group), as well as the B-family heterodimer, <sup>Sp</sup>Rev3-<sup>Sp</sup>Rev7, which forms the homologue of <sup>Hs</sup>Pol $\zeta$ . A <sup>Hs</sup>SUMO-1 homologue exists in *S. pombe*, which is known as <sup>Sp</sup>Pmt3, <sup>Sp</sup>Ubl2 or <sup>Sp</sup>Smt3 (the nomenclature used hereafter: <sup>Sp</sup>Pmt3<sup>Ubl2/Smt3</sup>). However, no <sup>Sp</sup>PCNA sumoylation has been detected in *S. pombe* (Frampton *et al.*, 2006) and PRR in fission yeast is little studied.

Deubiquitination of PCNA in either budding or fission yeast has not been demonstrated. However, as alluded to already, deubiquitination of <sup>Hs</sup>PCNA by <sup>Hs</sup>USP1 has been reported in human cells (Huang *et al.*, 2006). Due to the pertinence of this protein to this project, before the work with <sup>Hs</sup>USP1 is discussed deubiquitinating enzymes will be introduced properly first.

## 1.22. An Introduction to Deubiquitinating Enzymes

Deubiquitinating enzymes, deubiquitinating peptidases, deubiquitinating isopeptidases, deubiquitinases, ubiquitin proteases, ubiquitin hydrolases, ubiquitin-protein hydrolases, ubiquitin isopeptidases, DUBs, or DUBs, are enzymes able to catalyse the removal of ubiquitin from ubiquitinated molecules. A key review of these enzymes is that written in 2004 by Amerik and Hochstrasser (Amerik and Hochstrasser, 2004). However, a review of DUBs in the Annual Review of Biochemistry has been published this year, which was authored in part by Keith D. Wilkinson of the Emory University School of Medicine, Atlanta, USA, who has made extensive contributions to the understanding of DUB function in his career (Reyes-Turcu *et al.*, 2009). DUBs and their functions have been reviewed: Johnston and Burrows, 2006; Rytönen and Holden, 2007; Lindner, 2007; Wing, 2003; Song and Rape, 2008; Chung and Baek, 1999; Ha and Kim, 2008; Kim *et al.*, 2003; and Nijman *et al.*, 2005b. DUBs function most commonly in either the removal of mono-ubiquitin from a modified cellular substrate, or the depolymerisation of a poly-ubiquitin chain into a shorter chain and/or individual ubiquitin monomers. In general, DUBs hydrolyse the covalent bond between the carboxy-terminus of the glycine-76 of an ubiquitin superfold, and the  $\epsilon$ -amino group of a lysine side-chain on the modified target.

DUBs are predominantly cysteine proteases, where the thiol group of the cysteine side chain within the active site performs a nucleophilic attack on the amide (or isopeptide) bond (Amerik and Hochstrasser, 2004). However, other known DUBs are metalloenzymes that are thought to utilise  $\text{Zn}^{2+}$  to activate water into a

nucleophilic hydroxyl. DUBs have four main functions in the cell: (1) They process inactive ubiquitin precursors as a quality control mechanism. Ubiquitin in most organisms is synthesised as fusions to ribosomal proteins, as head-to-tail repeats, and with other additional amino acids. Hence, DUBs provide a pool of useable ubiquitin. (2) They cleave ubiquitin–protein conjugates by removing ubiquitin from proteins inappropriately or mistakenly ubiquitinated. Alternatively the ubiquitination was appropriate, and the subsequent deubiquitination changes the binding partners of the previously ubiquitinated protein, which has downstream signalling effects. Also, a DUB may revert a poly-ubiquitinated protein into a mono-ubiquitinated version. (3) DUBs maintain a sufficient pool of free ubiquitin in the cell by disassembling poly-ubiquitin chains. For example, a poly-ubiquitinated protein can be deubiquitinated by breaking the bond between the target protein and the first ubiquitin, which results in an unattached polyubiquitin chain. (4) DUBs also keep the 26S proteasome free from inhibitory ubiquitin chains. Only deubiquitinated and unfolded proteins can be cleaved by the proteasome. The proteasome lid subunits have deubiquitinating and unfolding functions (Amerik and Hochstrasser, 2004).

### **1.23. Superfamilies of Deubiquitinating Enzymes**

The proteinaceous fold that confers deubiquitinating activity is thought to have evolved in three independent ways: from a papain fold, from a metal-dependent deaminase fold, and from a retroviral aspartyl protease fold (Iyer *et al.*, 2004). The papain-like domain, which has cysteine protease activity, confers the canonical, most highly characterised deubiquitinating activity, and has been highly expanded in eukaryotic organisms. DUBs containing DUB activity derived from the metal-dependent deaminase fold, known as JAMM domain metalloenzymes (defined below), are less abundant, but have attained significant interest of late due to their important roles as essential proteasome subunits, and in endocytosis. The superfamilies of papain-like DUBs and the JAMM domain superfamily will be

discussed more extensively below. First, the aspartyl protease fold will be briefly discussed for completeness.

A bioinformatical analysis, carried out by the group of Eugene Koonin at the National Center for Biotechnology Information, National Institute of Health in Bethesda, USA, predicted that a domain derived from retroviral aspartyl proteases may confer deubiquitinating activity (Krylov and Koonin, 2001). The protein DNA damage-inducible 1 ( $^{Sc}Ddi1^{Vsm1}$ ), as its name suggests, was originally found to be upregulated in *S. cerevisiae* in response to genotoxic stress (Liu and Xiao, 1997), and has been shown to interact with ubiquitinated Pds1 and inhibit its proteasome-dependent degradation (Bertolaet *et al.*, 2001).  $^{Sc}Pds1$  is a checkpoint protein that is important for cell cycle arrest following detection of DNA damage during S-phase or incorrectly formed spindles during mitosis. Whilst no known orthologues of  $^{Sc}Pds1$  are known, all eukaryotes contain a highly-conserved  $^{Sc}Ddi1^{Vsm1}$  orthologue (Sirkis *et al.*, 2006).  $^{Sc}Ddi1^{Vsm1}$  contains three domains, an N-terminal weakly ubiquitin-like domain, the aspartyl protease domain and a C-terminal ubiquitin-binding domain known as an ubiquitin-associated domain (UBA). Two human orthologues exist, called  $^{Hs}DDI1$  and  $^{Hs}DDI2$ , which do not contain the UBA domain, and there is an orthologue in *S. pombe* called  $^{Sp}Mud1$ , which does not contain the N-terminal ubiquitin-like domain. Furthermore, the aspartyl protease domain is found in  $^{Hs}NIX1$ -like proteins, which are only found in mammals – there are three of this class in humans,  $^{Hs}NIX1$ ,  $^{Hs}NRIP1$  and  $^{Hs}NRIP2$ . Other proteins containing this aspartyl protease domain are found in bacteria and viruses (Krylov and Koonin, 2001). Whilst bioinformatics specialists suggest that this domain may confer deubiquitinating activity, significant research on  $^{Sc}Ddi1^{Vsm1}$  and its orthologues has been carried out since Eugene Koonin's prediction in 2001, and no studies have reported any *bona fide* ubiquitin protease function. Whilst the crystal structure of the aspartyl protease domain of *S. cerevisiae*  $^{Sc}Ddi1^{Vsm1}$  could not rule out deubiquitinating activity (Sirkis *et al.*, 2006), a recent study that determined the functional importance of the different domains in  $^{Sc}Ddi1^{Vsm1}$ , still referred to the protein as a “ubiquitin receptor” (Gabriely *et al.*, 2008). Hence, whilst

this class of aspartyl protease may later be shown to possess deubiquitinating activity, they will not be discussed further.

The six superfamilies of eukaryotic DUBs known in the literature will be considered in this thesis and these superfamilies are summarised in Table 1.1. All superfamilies are from the papain-like evolutionary tree, with the exception of the JAMM superfamily, which is derived from a metal-dependent deaminase fold.

#### **1.24. Cysteine Protease Superfamilies of Deubiquitinating Enzymes**

The catalytic triad of a cysteine protease is made up of cysteine, histidine, and aspartate side-chains in close three-dimensional proximity. The delocalised electrons of the aspartate side-chain polarise the pyrazole ring of a histidine side-chain. The deprotonated nitrogen atom in the pyrazole ring then accepts a proton from the thiol group of the cysteine. In DUBs, the resulting nucleophilic sulfur reacts with the amide bond formed between the amino group of the lysine side-chain of the target protein and the carboxy-terminus of ubiquitin. The sulfur attacks the carbonyl carbon and the electrons of the amide bond are accepted by the electrophilic pyrazole of the histidine. At this stage, the target protein is released, and the DUB cysteine and ubiquitin carboxy-terminus form an intermediate. The intermediate is stabilised by additional residues that hydrogen bond with the oxyanion – that is, the oxyanion is stabilised by an oxyanion hole, typically created by proteins in glutamine, glutamate, or asparagine residues and the catalytic cysteine (Nijman *et al.*, 2005b). Hydrolysis of the DUB—ubiquitin bond by the lone pair of the oxygen atom of water restores free DUB and free ubiquitin, hence completing the reaction.

USP/UBP superfamily DUBs, the ubiquitin-specific proteases, which is by far the largest superfamily, all contain the C19 peptidase domain of clan CA of cysteine-type peptidases. In general, USP/UBP family DUBs from mammals are most



commonly named numerically utilising a USP prefix e.g. USP1, and those from yeast almost always use a UBP prefix. USP/UBP DUBs have been found to be involved in DNA damage response processes. For example, *Hs*USP28 has been implicated in regulating the levels of p53-binding protein 1 (*Hs*53BP1), *Hs*Claspin and mediator of DNA damage checkpoint 1 (*Hs*Mdc1), which are involved in transducing the presence of DSBs to the cell (Zhang *et al.*, 2006). Furthermore, *Hs*USP11 has been shown to be involved in a pathway involving *Hs*BRCA2 function in response to damage caused by the crosslinking agent mitomycin C (Schoenfeld *et al.*, 2004). Moreover, *Hs*USP1 has been found to be involved in both the FA and PRR pathways, and these data will be discussed later.

It is interesting to note that five *Hs*USP DUBs, *Hs*USP16, *Hs*USP30, *Hs*USP39, *Hs*USP45 and *Hs*USP52 were found to be missing catalytic residues (Nijman *et al.*, 2005b). The authors propose that as they are merely missing the catalytic aspartate, *Hs*USP16 and *Hs*USP30 likely utilise a different side-chain for catalysis. However, they suggest that the remainder, particularly *Hs*USP39, are inactive USP variants (USPVs) that are only able to bind ubiquitin, analogous to the UEV proteins thought to arise from E2 pseudogenes (Nijman *et al.*, 2005b).

The ubiquitin C-terminal hydrolase (UCH) superfamily of DUBs is one of the smallest superfamilies. Members contain the C12 peptidase domain of clan CA of cysteine-type peptidases. They were the first superfamily of DUBs to be characterised (Nijman *et al.*, 2005b) and were originally identified as small proteins that were able to hydrolyse short amides and esters from the carboxy-terminus of ubiquitin (Amerik and Hochstrasser, 2004). Structural work showed that the active site of this superfamily is very similar to that of the USP/UBP superfamily. However, an active site crossover loop was also discovered, through which DUB substrates must pass through in order to access the active site cysteine. The diameter of the loop is only about 15 Å, which is thought to be the reason why most UCH DUBs only seem able to cleave small molecules from ubiquitin (Amerik and Hochstrasser, 2004). An important member of this family includes *Hs*UCH-L1, which

is expressed in neurons and has been linked to Alzheimer's and Parkinson's diseases. This DUB is very interesting because it has also been found to have ATP-independent E3 activity dependent upon homo-dimerisation, and the ability to stabilise mono-ubiquitin, which is dependent upon its catalytic cysteine (reviewed in Setsuie and Wada, 2007). Another UCH DUB called <sup>Hs</sup>BRCA1-associated protein 1 (<sup>Hs</sup>BAP1) has been shown to bind the RING finger of <sup>Hs</sup>BRCA1 to inhibit the E3 activity of the <sup>Hs</sup>BRCA1/<sup>Hs</sup>BARD1 complex, hence modulating the role of this protein in DNA repair (Nishikawa *et al.*, 2009). It is interesting that <sup>Hs</sup>BRCA1 can also be associated with a JAMM superfamily (discussed in the next section) DUB called BRCA1/BRCA2-containing complex protein 36 or <sup>Hs</sup>BRCC36 (Dong *et al.*, 2003), and that the USP/UBP DUB <sup>Hs</sup>USP11 presumably also functions in the vicinity.

It is worth noting here that the literature occasionally denotes C12 peptidases as ubiquitin C-terminal hydrolase (UCH) family 1 and C19 peptidases as UCH family 2. Although USP/UBP superfamily DUBs may for this reason be denoted as containing a UCH domain, for example within the ExPASy, UniProt and Pfam databases, I do not know of an example where a UCH superfamily DUB has been described as containing a USP or UBP domain.

The ovarian tumour protease (OTU) superfamily of DUBs was identified bioinformatically in 2000 using the *OTU* gene, which is involved in oocyte maturation in *Drosophila*, as a query (Makarova *et al.*, 2000). Characterised OTU DUBs include <sup>Hs</sup>DUBA, <sup>Hs</sup>A20, <sup>Hs</sup>Otubain-1 and -2, and <sup>Hs</sup>Cezanne. There is a particular bias for the involvement of OTU DUBs in the inhibition of cytokine inflammatory signalling cascades. For example, <sup>Hs</sup>Cezanne has been shown to deubiquitinate the signalling adaptor receptor-interacting protein 1, <sup>Hs</sup>RIP1, which effects a negative feedback loop that inhibits nuclear factor-κB (<sup>Hs</sup>NF-κB) activation (Enesa *et al.*, 2008). <sup>Hs</sup>DUBA has been found to deubiquitinate lysine-63-linked chains from tumour necrosis factor receptor associated factor 3 (<sup>Hs</sup>TRAF3), which affects <sup>Hs</sup>TRAF3 interactions and in turn results in the inhibition of type 1 interferon

(Kayagaki *et al.*, 2007). Furthermore, in addition to its OTU domain, <sup>Hs</sup>A20 also comprises seven zinc finger domains within its carboxy-terminus that fold up to form a domain with E3 activity. The result of <sup>Hs</sup>A20 function is deubiquitination of lysine-63-linked chains from <sup>Hs</sup>TRAF2, <sup>Hs</sup>TRAF6 and <sup>Hs</sup>RIP1, and subsequent replacement with lysine-48-linked chains (reviewed in Coornaert *et al.*, 2009).

Machado-Joseph disease aka Machado-Jakob disease aka Josephin protein domain proteases aka MJDs form one of the smallest DUB superfamilies. Machado-Joseph disease is also known as spinocerebellar ataxia type 3, and is caused by expanded poly-glutamine tracts in <sup>Hs</sup>Ataxin-3, and results in neurodegeneration. MJD DUBs comprise a Josephin domain that imparts the DUB activity. <sup>Hs</sup>Ataxin-3 is by far the most studied member of the superfamily. <sup>Hs</sup>Ataxin-3 can bind poly-ubiquitin chains via its ubiquitin interaction motifs (UIMs), and cleave the ubiquitin–target amide bond via its amino-terminal Josephin domain. Interestingly, <sup>Hs</sup>Ataxin-3 was found able to bind lysine-63- and lysine-48-linked chains, but seemed particularly efficient at cleaving lysine-63-amide bonds in mixed linked chains (Winborn *et al.*, 2008). <sup>Hs</sup>Ataxin-3 is thought to be involved in the ubiquitin-proteasome pathway.

The permutated papain fold peptidases of dsDNA viruses and eukaryotes (PPPDE) superfamily, is a small, entirely putative superfamily of DUBs predicted by bioinformatics analyses carried out by a collaboration of the groups of Eugene Koonin and L. Aravind in Bethesda, USA (Iyer *et al.*, 2004). No members of this family have been experimentally confirmed as having *bona fide* DUB activity. Please note that the PPPDE domain is also commonly referred to as a DUF862 domain (domain of unknown function), for example in the Pfam, ExPASy and EMBL databases.

In the aforementioned paper, PPPDE DUBs were classified by similarity into three major families: eukaryotic family 1, eukaryotic family 2, and a more divergent viral family, which will not be discussed further. The viral counterparts of fungal family 2

PPPDE DUBs are also classified into eukaryotic family 2. No PPPDE DUBs were found in eubacteria or archaea. Eukaryotic family 1 consists of PPPDE DUBs from a variety of eukaryotes including plants, vertebrates and fungi, and contains one human protein known as *Hs*FAM152B. Eukaryotic family 2 also contains proteins from various eukaryotes, which include plants, vertebrates and fungi, as well as fungal dsDNA viruses. Whereas *Arabidopsis thaliana* contains 7 paralogous family 2 PPPDE DUBs, most eukaryotes contain one or two DUBs from this family, and there is one orthologue in humans, *Hs*PNAS4<sup>FAM152A</sup>, and one in *S. pombe*, *Sp*Hag1<sup>Mug67</sup>. The authors of this study noted that there are distinct differences between residues near the catalytic site in family 1 and family 2 PPPDE DUBs, which indicates that they may differ in target specificity. Furthermore, they argue that all PPPDE DUBs are likely to deubiquitinate conserved targets, particularly family 1 members, which points towards targets relating to the cell cycle and genome manipulation, such as DNA replication. However, Iyer *et al* also point out that some organisms do not contain any PPPDE DUBs suggesting redundancy with other non-PPPDE superfamily DUBs (Iyer *et al.*, 2004).

This study actually identified both the PPPDE superfamily of predicted DUBs, but also the weak suppressor of *Sc*Smt3 (*Sc*Wss1)-like metalloprotease (WLM) superfamily of putative desumoylating enzymes, which are found in plants, fungi, *Trypanosoma* and *Plasmodium* (Iyer *et al.*, 2004). *Sc*Smt3 is the *S. cerevisiae* SUMO-1 orthologue and a link between *Sc*Wss1 and PRR has been demonstrated – *Sc*Wss1 was found to physically interact with the replication fork stabiliser *Sc*Tof1 and demonstrated genetic additivity with a variety of PRR components (O'Neill *et al.*, 2004). Interestingly, there are two WLM members in *S. pombe*, SPAC521.02 and SPCC1442.07c (Iyer *et al.*, 2004), and the *Sc*Tof1 orthologue is *Sp*Swi1, however these proteins do not fall within the remit of this study and so will not be discussed further.

## 1.25. JAMM Superfamily Deubiquitinating Enzymes

Jab1/Mov34/Mpr1, Pad1 N-terminal + (MPN+) (JAMM) domain superfamily of DUBs is found in a variety of cellular proteins, some of which have ubiquitin and ubiquitin-like isopeptidase activity. The JAMM superfamily is of medium size – with reference to mammals, it contains more members than the UCH, MJD and PPPDE superfamilies, but less than USP/UBP. <sup>Hs</sup>RPN11<sup>POH1</sup>, <sup>Hs</sup>AMSH and <sup>Hs</sup>CSN5<sup>RRI1/JAB1</sup> are the most studied enzymes of the JAMM superfamily. <sup>Hs</sup>RPN11 (regulatory particle non-ATPase 11), also known as <sup>Hs</sup>POH1, is a 19S proteasome lid component thought to remove ubiquitin from lysine-48-linked poly-ubiquitinated substrates committed for proteasomal degradation, and thus acts in ubiquitin recycling. <sup>Hs</sup>AMSH (associated molecule of the SH3 domain of signal transducing adapter molecule [STAM]) is a DUB involved in the control of targeting membrane proteins for transport to the lysosome in endosomal vesicles (reviewed in Clague and Urbé, 2006). <sup>Hs</sup>CSN5 (constitutive photomorphogenic gene 9 [COP9] signalosome 5), also known as <sup>Hs</sup>RRI1 and <sup>Hs</sup>JAB1, is thought to be the catalytic component of the COP9 signalosome (reviewed in Schwechheimer, 2004). <sup>Sp</sup>Csn5 has been shown to deneddylate Cullin 1 (<sup>Sp</sup>Cul1), a subunit of Skp1-Cullin-F-box (SCF) ubiquitin-protein ligases (Lyapina *et al.*, 2001; Zhou *et al.*, 2001; Cope *et al.*, 2002).

During 2002, the JAMM superfamily received significant attention due to three important publications (reviewed in Hochstrasser, 2002, and Wilkinson, 2002). In September 2002, a seminal bioinformatics study, included within a paper discussing this domain, from a collaboration between the groups of Glickman and Hofmann (Maytal-Kivity *et al.*, 2002). In this study, four main types of proteins were studied, proteasome lid components, CSN components, translation elongation factors type 3, and <sup>Hs</sup>AMSH orthologues, all of which are known to contain the domain most commonly known as Jab1, MPN or Mov34. An alignment of the amino acid sequences of these proteins enabled classification into two distinct

groups: MPN+ or 'plain' MPN. In addition to the core MPN residues, the MPN+ group members, which includes *Hs*RPN11<sup>POH1</sup>, *Hs*AMSH and *Hs*CSN5<sup>RRI1/JAB1</sup> and their respective orthologues from selected eukaryotes, contain a further five specifically conserved residues within the motif, all of which have polar chemistry. The MPN domain of *Hs*RPN8, *Hs*eIF3f, *Hs*eIF3h and *Hs*CSN6, and their respective orthologues, contained, at the most, one of the extra conserved residues, so were classified as containing a plain MPN domain. MPN+ members were also found in archaea and eubacteria (Maytal-Kivity *et al.*, 2002). An independent study also found antecedents in prokaryotes and bacteriophage (Iyer, Burroughs and Aravind, 2006).

The term JAMM is mainly used to refer to proteins classified as MPN+ by this study. Having said this, plain MPN proteins are frequently referred to as JAMM DUBs in the literature. Interestingly, recent evidence suggests that the plain MPN domain is a DUB pseudogene in that it can bind ubiquitin, but has lost its catalytic activity (Bellare *et al.*, 2006) and hence this domain features in more comprehensive reviews of ubiquitin-binding motifs (Hurley *et al.*, 2006).

The crystal structure of an MPN+ JAMM domain, from a protein from the archaeon *Archaeoglobus fulgidus* was solved in 2003 (Tran *et al.*, 2003). The function of this protein, known as AF2198, is not known. The structure revealed a fold very similar to that of cytidine deaminase, a member of the metal-dependent hydrolase superfamily, which binds zinc. The Zn<sup>2+</sup> ion is utilised to activate water, forming a hydroxide ion that reacts with the carbon at the 4 position of the base of cytidine. The result of this nucleophilic attack is an amino group on this carbon becomes substituted with an oxygen atom from the water molecule forming a ketone moiety – hence the base of a cytosine nucleoside is converted into a uracil. The significance of this structure was revealed when it was found that the five MPN+ residues of AF2198 were found to co-ordinate the Zn<sup>2+</sup> ion (Tran *et al.*, 2003).

In the Glickman and Hofmann 2002 paper, the bioinformatics study was combined with biochemistry using  $^{Hs}RPN11^{POH1}$ , a component of the 19S proteasome lid that is involved in removing poly-ubiquitin chains from proteins committed for proteasome-mediated degradation (Maytal-Kivity *et al.*, 2002). Mutation of MPN+ residues in  $^{Hs}RPN11^{POH1}$  resulted in an accumulation of poly-ubiquitinated proteins (Maytal-Kivity *et al.*, 2002). The following week, Yao and Cohen's *Nature* paper demonstrated that the deubiquitination activity of *S. cerevisiae*  $^{Sc}Rpn11$  was dependent upon  $Zn^{2+}$  and single mutations of three MPN+ residues resulted in lethality (Yao and Cohen, 2002) –  $^{Sc}Rpn11$  is essential in *S. cerevisiae*. The following month the groups of Eugene Koonin, Raymond Deshaies, and collaborators published two papers in *Science*. One confirmed Yao and Cohen's findings with  $^{Sc}Rpn11$  and proposed that the function of the proteasome lid is to effect tight coupling between lid DUB action to remove ubiquitin from ubiquitinated substrates and the degradation of deubiquitinated substrates mediated by the proteasome itself (Verma *et al.*, 2002). The other paper described the importance of the JAMM motif in CSN function (Cope *et al.*, 2002). Metal chelators allowed CSN assembly, but abrogated  $^{Sc}Csn5^{Rri1/Jab1}$  function in the removal of Nedd8 from  $^{Sc}Cul1$ , and similar conclusions could be drawn about Csn5 function in *S. pombe* and *D. melanogaster* (Cope *et al.*, 2002).

More recently, the structure of the human MPN+ JAMM domain DUB,  $^{Hs}AMSH-LP$ , has been solved (Sato *et al.*, 2008).  $^{Hs}AMSH-LP$  and its paralogue,  $^{Hs}AMSH$ , as well as its *S. pombe* orthologue,  $^{Sp}Amsh$ , will be discussed further in Chapter 3.

## 1.26. Deubiquitinating Enzymes Encoded within the Human Genome

According to a recent review, there are 95 DUBs in human cells, and 58 are UBP/USP superfamily DUBs, 4 are UCH DUBs, 5 are MJD DUBs, 14 are OTU DUBs and 14 are JAMM DUBs (Nijman *et al.*, 2005b). However, this review, whilst very informative, can be misleading. Firstly, two UBP/USP superfamily DUBs were

found to be absent from this study, <sup>Hs</sup>USP27<sup>USP22L</sup> and <sup>Hs</sup>USPL1. Furthermore, the aspartyl proteases and, more importantly, the PPPDE superfamily are not even mentioned in this review. As described above, there are two human PPPDE members, <sup>Hs</sup>PNAS4<sup>FAM152A</sup> and <sup>Hs</sup>FAM152B, that were identified in the Koonin and Aravind study (Iyer *et al.*, 2004). Moreover, when the JAMM superfamily was analysed, proteins containing a plain MPN domain as well as those with an MPN+ were included in the Nijman *et al.* review. Only half of the 14 cited appear to be *bona fide* MPN+.

### 1.27. Deubiquitinating Enzymes in Post-Replication Repair

<sup>Hs</sup>USP1 is a 785 amino acid DUB of the USP/UBP superfamily. Close orthologues can be found in *Xenopus laevis*, *Mus musculus*, *Rattus norvegicus*, *Danio rerio* (zebrafish), and *Gallus gallus*. <sup>Hs</sup>USP1 has been found to only contain the USP/UBP catalytic domain – the section comprising the first 75 residues that are not part of this domain is only highly conserved in DUBs of the aforementioned species. However, buried in the catalytic domain is an ubiquitin fold (Huang *et al.*, 2006), which is a common structural element in USP/UBP DUBs (Zhu *et al.*, 2007). <sup>Hs</sup>USP1 is localised in the nucleus, expressed highly during S-phase, and can be ubiquitinated and degraded by the proteasome (Nijman *et al.*, 2005a). It is also thought to be phosphorylated by <sup>Hs</sup>ATM or <sup>Hs</sup>ATR on serine-42 (Matsuoka *et al.*, 2007).

In 2005, the function of <sup>Hs</sup>USP1 in FA was studied by a collaboration between the Bernards laboratory and the D'Andrea laboratory. <sup>Hs</sup>USP1 was found to deubiquitinate FANCD2 (Nijman *et al.*, 2005a). As described in section 1.8 above, this has the effect of preventing FANCD2 from localising in DNA repair foci and thus aid crosslink repair. In fact, it was shown that knockdown of <sup>Hs</sup>USP1 had the effect of reducing the number of chromosomal aberrations compared to control cells (Nijman *et al.*, 2005a). However, recent work in murine cells has shown that knocking out *USP1* resulted in an FA phenotype and increased levels of mono-



ubiquitinated <sup>Mm</sup>FANCD2, and that a double knockout of *USP1* and *FANCD2* demonstrated a more severe phenotype (Kim *et al.*, 2009). This implies that <sup>Mm</sup>USP1 function in the FA pathway is complex in this organism. It is not known whether the findings in mice can also be attributed to the FA pathway in other organisms.

In 2006, D'Andrea's laboratory and collaborators showed that <sup>Hs</sup>USP1 deubiquitinates <sup>Hs</sup>PCNA (Huang *et al.*, 2006). Knockdown of <sup>Hs</sup>USP1 levels resulted in an increase in mono-ubiquitinated <sup>Hs</sup>PCNA, and overexpression of wildtype <sup>Hs</sup>USP1 reduced mono-ubiquitinated <sup>Hs</sup>PCNA levels whereas a mutant <sup>Hs</sup>USP1 in which the catalytic cysteine had been mutated to a serine could not. Interestingly, UV irradiation induced cleavage of the <sup>Hs</sup>USP1 protein into two discrete parts. This cleavage was dependent upon the catalytic activity of <sup>Hs</sup>USP1. The cleavage was found to occur carboxy-terminal to two consecutive glycine residues. Mutation of the di-glycines to di-alanines inhibited autocleavage. Furthermore, the authors also showed that knockdown of <sup>Hs</sup>USP1 resulted in an increased mutation frequency compared to control siRNA. The authors conclude that the role of <sup>Hs</sup>USP1 is to maintain low levels of mono-ubiquitinated <sup>Hs</sup>PCNA in unchallenged cells to prevent error-prone PRR. However, in the presence of UV damage, <sup>Hs</sup>USP1 autocleaves and is degraded by the proteasome, activating PRR. More specifically, they propose that "in the presence of UV damage, USP1 switches its substrate target from ubiquitinated PCNA to its own C-terminal Gly-Gly motif, resulting in an increase in mono-ubiquitinated PCNA levels and TLS" (Huang *et al.*, 2006). This work is reviewed in Friedberg, 2006 and Ulrich, 2006. Figure 1.12, which is adapted from Ulrich, 2006, summarises the pathway.

There is also preliminary evidence to suggest that <sup>Hs</sup>USP1 can remove poly-ubiquitin chains from <sup>Hs</sup>PCNA – <sup>Hs</sup>USP1 knockdown resulted in an increase in the intensity of bands of higher molecular weight than mono-ubiquitinated <sup>Hs</sup>PCNA (Motegi *et al.*, 2008). However, this effect may be indirect.

## 1.28. An Introduction to This Study

The aim of this study is to investigate the roles of DUBs in *S. pombe* PRR. Is there a <sup>Hs</sup>USP1 orthologue in yeast? Or does a different DUB deubiquitinate <sup>Sp</sup>PCNA, and if so, which one performs this task?

This project is divided into five main parts. Firstly, DUBs encoded within the *S. pombe* genome will be identified. The literature surrounding each DUB (and/or its orthologues in humans and budding yeast) will be discussed, its superfamily and likely importance in the cell outlined, if known. Here, its potential for involvement in PRR or <sup>Sp</sup>PCNA deubiquitination will also be summarised. This first part corresponds to Chapter 3. Secondly, the assembly of an *S. pombe* DUB deletion library will be discussed, along with how this library was screened and the results (Chapter 4). In the third part, the literature surrounding the positive hit resulting from the screen will be summarised, along with the rationale behind the decision to investigate the role of these proteins in PRR further (Chapter 5). In the fourth section, the function of these proteins in *S. pombe* will be investigated further (Chapters 5, 7 and 8), along with the identification of, introduction to, and investigation into the role of the likely *S. cerevisiae* counterparts (Chapter 6). In the fifth and final section (Chapter 9), the significance of these data will be discussed.

## Chapter 2: Materials and Methods

Many of the methods described below are taken or adapted from Sambrook *et al.*, 1989.

### 2.1. Chemicals and Buffers

Materials were typically obtained from Sigma and were of the highest purity available unless otherwise stated.

**10x Blue Juice:** 0.25% bromophenol blue, 0.25% xylene cyanol, 30% glycerol, water.

**Coomassie Stain:** 450 ml methanol, 100 ml glacial acetic acid, 1 g Coomassie blue, water qsp 1 l.

**Destain Solution:** 10% methanol, 10% acetic acid, water.

**10x Gel Running Buffer (GRB):** 30 g tris base, 144 g glycine, 10 g SDS, water qsp 1 l.

**Elution Buffer (EB):** 10 mM tris, pH 8.5, water.

**3x Laemmli Buffer:** 2 ml glycerol, 1.5 ml  $\beta$ -mercaptoethanol, 4.5 ml 20% SDS, 1.875 ml 1 M tris HCl pH 6.8, 125  $\mu$ l 1% bromophenol blue.

**Phosphate Buffered Saline (PBS):** 8 g NaCl, 0.3 g KCl, 1.44 g  $\text{Na}_2\text{HPO}_4$ , 0.24 g  $\text{KH}_2\text{PO}_4$ , pH 7.4 (using HCl), water qsp 1 l.

**Ponceau S Stain:** 1 g Ponceau S, 15 g trichloroacetic acid, 15 g sulphosalicylic acid, water qsp 500 ml.

**TE Buffer:** 10 mM tris HCl pH 8.0, 1 mM EDTA pH 8.0, water.

**TAE (50x):** 242 g tris base, 57.1 ml glacial acetic acid, 100 ml 0.5 M  $\text{Na}_2$  EDTA (pH 8.0), water qsp 1 l.

**TBE (5x):** 54 g tris base, 27.5 g boric acid, 20 ml 0.5 M EDTA pH8.0, water qsp 1 l.

**Semi-Dry Transfer Buffer:** 5.82 g tris base, 2.93 g glycine, 1.875 ml 20% SDS, 200 ml ethanol, water qsp 1 l.

**Antibody Elution Solution:** 800 µl 1M glycine pH 2.3, water qsp 4 ml.

**Antibody Storage Buffer:** 1 ml 1M KCl, 200 µl 1M HEPES pH 7.7, water qsp 2 ml.

## **2.2. Routine Bacterial and DNA Methods**

### **2.2.1. *E. coli* Culture**

*E. coli* cells grow optimally in liquid culture in LB broth at 37 °C with agitation and on standard Luria Bertani (LB) agar plates in a plate incubator at the same temperature, hence all culture was performed using these conditions unless otherwise stated. Cell density was measured as absorbance at 600 nm using a spectrophotometer.

### **2.2.2. Plasmid Transformation of DH5α**

Competent DH5α *E. coli* cells were thawed on ice for 30 min and added to 0.5-2 µl (typically 400 to 1600 ng) of cooled plasmid or ligated DNA in buffer “EB” (as supplied in Qiagen kits). The *E. coli*-DNA mixture was incubated on ice for 30 minutes, heat shocked at 42°C for 30 seconds and incubated on ice for a further 2 minutes. Pre-warmed LB broth (250-500 µl) was added and the cells were incubated at 37 °C with agitation for 1 h to allow for the expression of the antibiotic resistance gene. The cells were then plated onto LB agar plus the relevant antibiotic and grown overnight 37°C.

### **2.2.3. Creation of *E. coli* Glycerol Stocks**

700 µl of late log *E. coli* culture in LB broth was added to 300 µl of 50% glycerol in a screw topped tube and stored at –80°C.

#### **2.2.4. Plasmid DNA Preparation**

A single DH5 $\alpha$  colony was picked and used to inoculate 5 ml of LB broth plus relevant antibiotic and grown for approximately 5 h during the day. In the evening, this was added to 100 ml of fresh LB broth plus appropriate antibiotic and grown overnight. The following morning, plasmid DNA was isolated using a QIAfilter® Midiprep kit (Qiagen) according to the manufacturer's instructions, with the final DNA pellet resuspended in up to 200  $\mu$ l of EB. The quantity of plasmid DNA prepared was elucidated by analysing a 1  $\mu$ l sample in 99  $\mu$ l of water using a spectrophotometer at 260 nm. Typically between 500 and 1000 ng/ $\mu$ l of DNA was isolated. For smaller quantities of plasmid DNA, a QIAprep® Miniprep kit (Qiagen) was utilised. In this case, 2 ml of LB plus pertinent antibiotic was inoculated with a single colony and grown overnight. Plasmid DNA was then isolated according to the manufacturer's instructions. DNA was typically eluted in 30  $\mu$ l EB, which was typically ~200 ng/ $\mu$ l.

#### **2.2.5. DNA Enzymatic Reactions**

Restriction digests, dephosphorylations and ligations were performed according to the manufacturers instructions with the buffers supplied. Restriction endonucleases, Antarctic phosphatase and Quick T4 DNA ligase were from New England Biolabs (NEB), and calf intestinal alkaline phosphatase was from Invitrogen.

#### **2.2.6. Agarose Gel Electrophoresis**

DNA from restriction digests or polymerase chain reaction (PCR) was fractionated using a 0.8–1.5% (w/v) agarose gel in 1x TAE or 1x TBE depending on

requirements. Ethidium bromide was added to the gel to a final concentration of 0.5 µg/ml. Blue juice was used as a loading buffer to a final dilution of 2x and “1 kb Plus” molecular weight marker (Invitrogen) was used as a DNA ladder. DNA samples were run at 120-130 V until the desired fractionation was achieved. Gels were visualized with a UV transilluminator and photographed. DNA bands required for further cloning were quickly cut out of the gel using a scalpel blade. Where ligation of DNA extracted from agarose gels had failed previously, the DNA for extraction was shielded from UV damage using aluminium foil and then relevant part of the gel excised using DNA (5% of the total DNA) in flanking lanes as a guide.

### **2.2.7. DNA Extraction from Agarose Gels**

DNA fragments were excised and purified from agarose gels using QIAquick gel extraction kit (Qiagen) according to the manufacturer's instructions, with the DNA eluted into typically 30 µl of EB buffer.

### **2.2.8. Purification of Polymerase Chain Reactions**

PCR products were purified from PCR reaction components using a PCR purification kit (Qiagen) according to the manufacturer's instructions. Typically the DNA was eluted into 30-50 µl of EB buffer.

### **2.2.9. Oligonucleotide Preparation**

Standard oligonucleotides were designed and obtained from the Invitrogen custom primer synthesis service. Without exception, primers were dissolved in TE to 100 pM and diluted 1/10 or 1/100 as necessary.

### 2.2.10. DNA Sequencing

Plasmid DNA or PCR reaction products were sent for sequencing at GATC Biotech, according to their instructions. Plasmid DNA was sent diluted in water at a concentration of 30-100 ng/μl and PCR products 10-50 ng/μl.

### 2.2.11. DH5α Colony Polymerase Chain Reaction

Correct plasmids transformed into DH5α were identified using colony PCR. A single colony of DH5α was added to 20 μl of EB and vortexed. Half of this mixture was then boiled for 10 minutes and then incubated on ice. *Taq* DNA polymerase (NEB) or KOD HotStart DNA polymerase (Novagen), primers for amplifying the appropriate gene and appropriate remaining PCR reagents were then added to a final volume of 50 μl and the PCR carried out according to the manufacturer's instructions. Completed reactions were then analyzed by agarose gel electrophoresis.

### 2.2.12. Gateway System “LR” Clonase Reaction

DUb genes incorporated into pDONR201 entry vector were purchased from RIKEN Bioresource Center, Japan (Matsuyama *et al.*, 2006). Genes were shuttled between Gateway System (Invitrogen) compatible vectors using the site-specific recombinase, Clonase II (Invitrogen). The pDUAL destination vectors were prepped using DB3.1 competent cells (Invitrogen), which are resistant to the *ccdB* gene (Ken Sawin; Matsuyama *et al.*, 2004). To set up this reaction, 50 ng of pDONR201-*dub* plasmid, 75 ng of pDUAL destination vector and TE buffer to a total of 4 μl was added to a 1.5 ml microfuge tube, which was then vortexed briefly. The LR Clonase II (Invitrogen) enzyme was thawed on ice for two minutes, vortexed briefly and 1 μl was added to the DNA mix. Mixed and spun down reactions were then incubated overnight in a 25 °C plate incubator. The following

day, the reactions were incubated with 0.5 µl of proteinase K solution (Invitrogen) for 10 minutes in a 37 °C water bath to terminate the reaction. The reaction was then transformed into DH5α as described above. The pDUAL destination vectors contained the ampicillin-resistance gene and *ura4* marker.

### 2.2.13. Site-Directed Mutagenesis

Site-directed mutagenesis was carried out using the QuikChange® II XL Site-Directed Mutagenesis Kit (Stratagene) according to the manufacturer's instructions. These instructions were carried out with high stringency, except the total reaction mixture was halved. Primers designed using the QuikChange® primer design program (see section 2.6.2 for website link) were found to be more reliable than without. For the DWGF-AAAA mutation described in Chapter 7, the mutation was carried out in two steps. Furthermore, an elongation time of 20 min for each cycle was typically used. Initially, the supplied XL10-Gold® ultracompetent cells were utilised, but it was found that DH5α cells prepared in-house resulted in significantly higher frequency of success.

### 2.2.14. BL21 *E. coli* Transformation

Competent BL21 (DE3, Stratagene) *E. coli* expression strain cells, β-mercaptoethanol and transformation tubes were pre-cooled on ice. Then 50 µl of cells were mixed with 0.85 µl of β-mercaptoethanol and incubated on ice for a further 10 minutes, with periodic mixing by flicking the tube. After the addition of 1 µl of plasmid DNA, the mixture was incubated on ice for another 30 minutes. The mixture was then heat shocked at 42°C for exactly 45 seconds, and then chilled on ice for 2 minutes. Then 400 µl of pre-warmed LB broth was added, the tube incubated at 37°C for 1 h and 100 µl spread onto LB agar plates with the appropriate antibiotic at 37°C overnight.



## 2.3. Routine Protein Methods

### 2.3.1. Expression and Native Purification of *S. pombe* His<sub>6</sub>-<sup>Sp</sup>PCNA for Antibody Production

*S. pombe pcn1*<sup>+</sup> was subcloned into pET16b (Novagen) from pREP41HA via *Bam*HI and *Nde*I sites and the correctly ligated plasmids checked by colony PCR using primers complementary to the *pcn1*<sup>+</sup> gene and pET16b plasmid and sequencing. Hence, 1 µl of a pET16b-*pcn1*<sup>+</sup> plasmid Midiprep was used to transform competent BL21 (DE3) cells and a single colony was picked and used to inoculate 5 ml of LB Amp broth, which was cultured overnight. In the morning, this was added to 1 l of fresh LB Amp broth in a 2 l flask and cultured to mid-log phase. At this point, 1 ml was removed, harvested by centrifugation and resuspended in Laemmli buffer to 0.01A<sub>600</sub>/µl for use as an uninduced control for SDS-PAGE analysis. The remaining culture was induced with isopropyl-β-D-galactopyranoside (IPTG) at 50 mM and incubated at 30 °C for 4 h. The culture was then harvested by centrifugation and resuspended in native lysis buffer and lysozyme to 1 mg/ml. After thorough sonication, the supernatant was spun multiple times until completely clear, whereupon Ni-NTA slurry (Qiagen) was added and used according to the manufacturers instructions. Purified <sup>Sp</sup>PCNA was eluted using 250 mM imidazole and samples analysed by SDS-PAGE, Western blotting and immunodetection. Adequately pure elutions were then pooled and quantified, before sending 2 mg to Eurogentec for injection into two rabbits as part of an immunisation program. Unfortunately, the resultant antibodies were not able to detect ubiquitinated <sup>Sp</sup>PCNA despite affinity purification.

### 2.3.2. Protein Quantitation

BioRad protein assay dye reagent concentrate was diluted 1 in 5 and 1 ml added to 6 µl of protein. The absorbance at 600 nm was determined using a

spectrophotometer and the concentration estimated using a standard curve from known concentrations of bovine serum albumin.

### **2.3.3. SDS-PAGE Analysis**

10% SDS-PAGE protein gels were run using either the BioRad protean mini gel system (up to 15 lanes) or the Scie-Plas TV200 system (up to 36 lanes) in 1x GRB. Table 2.1 depicts typical recipes for the resolving and stacking gel. Gels were run for about 1.5 h at 100-200V. To calibrate the molecular weight of fractionated proteins, NEB broad-range prestained protein markers were run on the gel. <sup>Sp</sup>PCNA typically runs in the region of the 32.5 kDa marker and a 10% resolving gel was utilised. In order to resolve ubiquitinated <sup>Sp</sup>PCNA multiplet bands, a longer SDS-PAGE gel system (28 cm plates) was utilised, which was of an unknown brand. In this case, gels were run at 240 V for 4-5 h and ColorPlus prestained markers (NEB) were also used to aid differentiation of marker bands.

### **2.3.4. Coomassie Staining of Gels**

Gels were stained in Coomassie stain for 40 min with agitation, and immediately destained using 3x 10 minute washes of destain solution until the contrast was sufficient. The gel was then dried in cling film onto blotting paper using a gel drier.

### **2.3.5. Semi-Dry Western Blotting**

The SDS-PAGE gel, two sheets of extra thick blotting paper and Hybond C-extra supported nitrocellulose membrane (Amersham) of the same size were soaked in semi-dry transfer buffer. Later unsupported nitrocellulose membrane, Hybond ECL (Amersham), was utilised as it provides much greater band resolution. One side of the membrane was marked with a pencil and placed on the anode side of the gel to mark the protein-bound face of the membrane. These were then placed on the semi-dry transfer apparatus (BioRad) as a paper–gel–membrane–paper sandwich

from top to bottom, air bubbles were rolled out with a glass test tube and the cathode lid secured on top. A voltage of between 15-20 V for 30-40 minutes was applied depending upon the size of the gel. Transfer and loading was checked by staining the blot with Ponceau S for 5 minutes, rinsing off in water and photographing. The remaining stain was removed by washing a plurality of times, typically four times, in PBST.

### **2.3.6. Immunodetection**

Western blots were immunodetected as outlined in Table 2.2. After the final wash in PBS, the bound antibodies were detected by the addition of enhanced chemiluminescence (ECL) Western Lighting kit (PerkinElmer) reagents at a 1:1 ratio for 1 min with agitation. Excess ECL reagent was then blotted off with tissue and the blot wrapped in cling film. However, it was later found that sandwiching the blot with two pieces of transparent over-head projector film provided a clearer image as it was free from creases. The blot was then exposed to light-sensitive hyperfilm (Amersham) in the dark room and developed using a mechanical developer.

### **2.3.7. Affinity Purification of Antibodies**

Pure  $^{Sp}$ PCNA (see 2.3.1 above) was run on a 10% SDS-PAGE gel, transferred onto Hybond ECL and stained with Ponceau S in order to identify the  $^{Sp}$ PCNA band. This band was cut out and into small squares and the stain was washed off using 0.1% PBST three times. The antigen squares were incubated in 5% milk 0.1% PBST for 30 minutes and then the excess milk was washed off using PBS. A tube was then prepared containing 5 ml  $\alpha$ - $^{Sp}$ PCNA antibody serum plus 500  $\mu$ l PBS and the antigen squares. This mixture was incubated overnight at 4°C on a roller. Subsequently, the antigen squares were removed from the serum using tweezers and put them into a clean 1.5 ml Eppendorf tube. The antigen squares were washed via the addition of 1 ml PBS, vortexing for 10 s and then removing

the PBS. This process was repeated four times. Then, four clean 1.5 ml Eppendorfs each containing 100  $\mu$ l 1.5M Tris pH 8.8 and 220  $\mu$ l antibody storage buffer was prepared. This neutralises and buffers the antibodies following elution. 1 ml of elution solution was then added to the antigen squares, which was vortexed for 10 s. The elution solution was removed and pipetted directly into one of the prepared Eppendorfs. This was repeated three times. The pooled elutions were added to a Sartorius Vivaspin 6 column with a 32 kDa molecular weight cut-off and spun in a Heraeus benchtop centrifuge at 3000 g for 20 min at 4°C. The flow-through was emptied from the lower chamber. Then, 300 ml of 2 mg/ml BSA in PBS was added to the upper chamber and then the upper chamber filled to the top (6 ml mark) with PBS. The BSA helps to stop the antibody from sticking to the membrane. Spin in the Heraus benchtop centrifuge at 3000 g for 20 min at 4°C. The purified antibody was then removed from the upper chamber, NaN<sub>3</sub> added to 0.025% to inhibit microbe growth, aliquotted and stored at -80°C.

## **2.4. *Schizosaccharomyces pombe* Methods**

Particularly helpful resources for *S. pombe* culture and experimentation was the Nurse laboratory manual (see section 2.6 below for a link to a copy of this) and the “Basic Methods for Fission Yeast” review by Susan Forsburg (Forsburg and Rhind, 2006).

### **2.4.1. *S. pombe* Culture**

*S. pombe* cells were grown in liquid culture in complete media, YEP (yeast extract, peptone, and nutritional supplements) in sterile glass tubes at 30 °C with light agitation and on YEA plates in a plate incubator at the same temperature, hence all culture was performed using these conditions unless otherwise stated. However, it is important to note here that a shift from YEP to YE (without peptone) occurred within my research institute approximately half-way through this project. Peptone

helps to prevent cells from clumping together (particularly seen in certain mutants), which makes them difficult to count or perform fluorescence activated cell sorting (FACS) analysis on. No difference in cell growth or experimental outcomes was found following the switch from YEP to YE.

Cell density of liquid culture was measured by counting the number of cells in a set volume using a haemocytometer. Simultaneously, the culture was checked for phenotype, cell cycle progression and infection by foreign microbes.

#### **2.4.2. Generation of Transforming DNA for DUB Gene Disruptions**

The disruptions were performed by integrating DNA containing the *nat1* gene, which encodes resistance to nourseothricin (NAT), in place of the DUB gene (Hentges *et al.*, 2005). Hence, cells with successfully disrupted DUB genes were selected for by plating on YEA containing NAT. The knockout strategy utilised has previously been described (Baehler *et al.*, 1998). Long primers were designed with approximately 20 bp homology to the *nat1* gene at the 3' end and 80 bp to the flanking regions outside the relevant DUB gene at the 5' end. The resultant PCR product consisted, therefore, of the entire *nat1* gene with 80 bp of homology to the flanking sequences of the DUB gene at either end. The strategy is also depicted in Figure 3.5.

The amplification was initially performed using PicoMaxx high-fidelity PCR system (Stratagene) according to the manufacturer's instructions. Later in the study, it was found that KOD HotStart (Novagen) was a much faster, higher fidelity and more reliable PCR polymerase for this purpose. To synthesise enough DNA for the highly inefficient transformation, 16 x 50 µl PCR reactions were set up. Due to the long, bulky primers utilised, two-stage cycling conditions were used to aid primer annealing and hence successful amplification (Table 2.3). In the first stage, a low annealing temperature increased the likelihood of primers annealing successfully. In the second stage, a higher, more stringent annealing temperature was used to

amplify only PCR products where the primers had annealed to the correct site of the plasmid.

Reactions were then pooled, a small aliquot checked by agarose gel electrophoresis and cleaned up by phenol-chloroform extraction and ethanol precipitation, finally resuspending in 10 µl of 1x TE. The quantity of DNA was elucidated by analysing a 1 µl sample in 99 µl of water using a spectrophotometer at 260 nm. Typically 30-100 µg of transformable DNA was generated.

### **2.4.3. Transformation using Lithium Acetate**

After growth overnight in YE, approximately  $1 \times 10^8$  wild type 501 cells at mid-log phase were harvested by centrifugation at 2500 rpm for five minutes. The cells were washed once with 1 ml of 1x LiAc/TE and resuspended in 100 µl of the same buffer and added to transforming DNA (9 µl) plus 2 µl of salmon sperm carrier DNA. After ten minutes incubation at room temperature, 260 µl of 40% PEG in 1x LiAc/TE was added and the mixture incubated for 1 h at 30 °C with gentle agitation. Subsequently, 43 µl of dimethyl sulfoxide (DMSO) was added and the cells were heat shocked at 42 °C for five minutes and spun down. After washing with 1 ml of water, the cells were resuspended in 500 µl of water and plated onto YEA plates, which were incubated at 30 °C. After 18 h, the yeast were replica plated onto YEA NAT agar to select for NAT-resistant cells. After three days at 30°C, large colonies were restreaked onto fresh YEA NAT plates. Resultant single colonies were grown in YEP NAT broth until late log from which glycerol stocks were taken for long-term storage at -80 °C and genomic DNA isolated for PCR analysis.

#### 2.4.4. Creation of Glycerol Stocks

800  $\mu$ l of late log *S. pombe* culture in YE plus appropriate selection was added to 500  $\mu$ l of 80% glycerol plus 300  $\mu$ l of YE in a screw topped tube and stored at  $-80^{\circ}\text{C}$ .

#### 2.4.5. Isolation of Haploids from Heterozygous Diploids

The pON177 plasmid, which carries the  $h^{-}$  mating type information (*mat1-M*) required to sporulate  $h^{+}/h^{+}$  heterozygous diploids, was a gift from Olaf Nielsen and has already been described (Styrkarsdottir *et al.*, 1993). This plasmid was transformed into a diploid strain and positive *ura4+* clones were spread onto agar extremely low in nitrogen for 2 days at  $25^{\circ}\text{C}$  to induce sporulation. The presence of tetrads was then verified using the light microscope. An enzyme called helicase, which comes from the juice of the snail *Helix pomatia* was used to digest the ascus wall. 1 ml of water was inoculated with a loopful of cells from the plate, 20  $\mu$ l of a 1 in 10 dilution of helicase was added and the mixture incubated overnight at  $25^{\circ}\text{C}$  in a plate incubator. The following day, the haploid spores were plated out onto media containing the appropriate supplements. Correctly disrupted haploids were verified by PCR and sequencing.

#### 2.4.6. Isolation of Genomic DNA

1 ml of late log cells was harvested by centrifugation at 13 krpm for 2 minutes and the cells lysed and the genomic DNA isolated using the Wizard Genomic DNA purification kit (Promega) according to the manufacturers instructions, except using 20 mg/ml Zymolyase®-20T ( $\beta$ -1,3-glucan laminaripentanolhydrolase from Seikagaku Corporation) to digest the cell wall. However, it was later found that using a small amount of neat zymolyase powder resulted in more efficient cell wall digestion. Cell wall digestion was deemed complete by the observation of very high

proportion of “ghost” *S. pombe* cells that lacked a cell wall under the light microscope. Isolated DNA was resuspended in 50 µl of the supplied DNA rehydration solution and allowed to rehydrate overnight at 4°C. The quantity of DNA was elucidated by analysing a 1 µl sample in 99 µl of water in a suitable cuvette using a spectrophotometer at 260 nm.

#### **2.4.7. DUB Gene Disruption Verification by PCR**

A quick, preliminary screen for genomic DNA containing a disrupted DUB gene was devised utilising a Multiplex PCR kit (Qiagen) according to the manufacturer’s instructions. Primers were designed to anneal to sequences flanking either side of the DUB gene as well as within the *nat1* gene. For correctly disrupted DUB genes, this favours the amplification of two short products of typically 400–700 bp depending upon the DUB gene in question.

The disrupted DUB gene in genomic DNA that resulted in correctly amplified integration sites by multiplex were then analysed in detail by PCR using HotStarTaq (Qiagen) according to the manufacturers instructions. Later in the study, it was found that KOD HotStart (Novagen) was a much faster, higher fidelity and more reliable PCR polymerase for this purpose. Cycles that can correctly amplify the ~2 kb successfully disrupted gene were utilised as well as cycles that can amplify the wild type gene (2-4.6 kb, depending upon the DUB in question), using flanking (“checkKO”) primers on potentially disrupted genomic DNA or wild type genomic DNA, respectively. This strategy is illustrated in Chapter 3, Figure 3.6. All PCR reactions were checked by agarose gel electrophoresis. Following the identification of a correctly-sized product, the PCR reaction was repeated on a larger scale and the purified product sent for sequencing using appropriate primers, including a negative control primer designed to anneal to the wild-type DUB gene.



#### **2.4.8. DUB Gene Disruption Verification by Southern Analysis**

Chromosomal DNA was prepared on a large scale – 100 ml of YE late-log culture was harvested by centrifugation and resuspended in 5 ml of resuspension buffer (20 mM citrate-phosphate buffer pH 5.6, 1.2 M sorbitol, 40 mM EDTA) plus zymolyase. The cells were incubated for 1 h or until the cells were lysed. The cells were then harvested at 5 krpm for 5 min using a benchtop centrifuge (Heraeus) and the pellet resuspended in 10 ml of 5x TE pH 7.5 and one tenth of the subsequent volume of 10% SDS to disrupt the cell membrane. Then 3.7 ml of 5M potassium acetate was added and the lysate put on ice for 30 min. The lysate was then centrifuged at 4600 rpm for 10 min and the supernatant decanted into 2 volumes of ethanol and incubated at room temperature for 5 min. Following centrifugation at 4600 rpm for 10 mins, the pellet was washed with 70% ethanol. The resulting pellet of nucleic acids was then redissolved in 3 ml of 5x TE pH 7.5 and RNase (Sigma) was added to a concentration of 20 µg/ml. To digest the RNA, the solution was incubated at 37°C for 2 h. The remaining genomic DNA was then further purified from contaminants with 4x phenol extractions and 2x chloroform extractions using phase-lock tubes (Eppendorf). A final ethanol precipitation was then carried out and the DNA resuspended in water at 37°C.

The chromosomal DNA was digested overnight with appropriate enzymes according to the availability of restriction sites in the vicinity of the locus to be checked. Digestion and DNA concentration was checked on a mini agarose gel before running overnight at 60-70 V on a large 1% agarose gel with markers and digested wild-type control genomic DNA. A picture of the gel was taken using the transilluminator and then gel then cut to size. The gel was then washed for 20 min in denaturing solution (1.5 M NaCl, 0.5 M NaOH) to denature the DNA double helix and then 20 min in neutralising solution (1 M tris pH 7.5, 1.5 M NaCl). The DNA was transferred onto a GeneScreen nylon membrane by capillary action. A plastic tray was filled with 10x saline-sodium citrate (SSC) buffer and the agarose gel

placed onto a Whatmann paper bridge pre-soaked in 10x SSC, which dipped into the tray solution at either end. The nylon blotting membrane was placed onto the gel, followed by one piece of Whatmann paper. These layers above the gel were pre-soaked in 10x SSC and rolled carefully to remove air bubbles. A piece of dry Whatmann paper, 2 stacks of green paper towels and finally a heavy weight were then placed onto. The Southern blotting was carried out overnight at room temperature. The following morning, the DNA was crosslinked to the membrane by irradiating both sides with UV (Stratalinker). Southern blots were left at 4°C wrapped in cling film and Whatman paper and sandwiched between glass plates prior to detection.

A 400-600 bp probe template was generated by designing primers that annealed to flanking regions of the gene to be verified and performing PCR. The template DNA was purified from the PCR components and diluted to 2.5–25 ng/μl in 45 μl TE, boiled for 5 min to denature and then cooled on ice for 5 min. Then, 5 μl of  $\alpha^{32}\text{P}$  dCTP (GE Healthcare) and the 45 μl DNA was added to a tube containing the Klenow reaction mix (Ready-To-Go DNA Labelling Beads, Amersham) and mixed in by pipetting. The mixture was incubated at 37°C for 10 min. The reaction was stopped using 5 μl of 0.2 M EDTA, the probe purified with a Sephadex G-50 column (Roche) and then boiled (5 min) and cooled on ice (5 min). The Southern blot was prehybridised in 30 ml hybridisation solution (1.5 ml 10% SDS, 20x SSC, 100x Denhardt's reagent, water qsp 1 l) at 65°C for 1 h, whereupon the probe was added to 15 ml fresh, pre-heated hybridisation solution. Hybridisation took place overnight in a hybridisation tube with gentle agitation (wheel) in the hybridisation oven (65°C). The hybridisation solution was discarded appropriately and the membrane washed twice for 30 min at 65°C using half the hybridisation tube full of washing solution (5 ml 20x SSC, 10 ml 10% SDS, water qsp 1 l). The membrane was then air dried on Whatmann paper for 10 min and wrapped in cling film. The counts per minute were measured with the Geiger counter and the pattern of hybridization was visualised by overnight exposure to X-ray film by autoradiography.

#### 2.4.9. DNA Damage of *S. pombe* Deletion Strains

For HU experiments, a single colony from a plated *dubΔ* strain (along with wild-type “501” and *pcn1-K164R* as controls) was used to inoculate 4 ml of YE media and grown for approximately 8-10 h, then diluted to  $5 \times 10^4$  cells/ml in 10 ml of YE and incubated overnight. The following morning, the cells were diluted to between  $1 \times 10^6$  and  $1 \times 10^7$  cells/ml (mid-log phase) in 5 ml YE in duplicate and treated (or left untreated) with 50 mM HU for 3 h at 30 °C. It was later decided to reduce the amount of HU to 10 mM due to reports from colleagues that some cells were unable to recover from incubation in 50 mM HU.  $1 \times 10^7 - 1 \times 10^8$  cells were harvested and prepared for analysis by trichloroacetic acid (TCA) extraction.

UV damage experiments were performed as above, except between  $5 \times 10^6$  and  $1 \times 10^8$  mid-log cells were transferred to a 0.45  $\mu\text{m}$  PVDF membrane with a 47 mm diameter (Millipore) in duplicate using a vacuum pump. The cells were irradiated with typically 50 or 100  $\text{J/m}^2$  UVC (254 nm, dose rate  $\sim 0.54 \text{ Jm}^{-2}\text{s}^{-1}$ ) and resuspended in 10 ml of YE for 30 minutes at 30°C. Mock treatment for control samples involved transferring the cells onto the membrane, but not irradiating with UV.

The approximate two-dimensional area of a wild-type haploid *S. pombe* cell is between 36 and 75  $\text{mm}^2$  and of the PVDF membrane is 1735  $\text{mm}^2$ . These quantities were found to be limiting – if too many cells were transferred to one membrane, cells may shield each other and hence receive different UV doses. Whilst multiple membranes could be used per sample when more than  $1 \times 10^8$  cells were required, the cells would dry out if left on the membrane for too long. Therefore, a different method was devised and employed when irradiating significantly more cells. In this situation, a liquid culture of cells was spun down and spread onto a large (20 cm) YEA agar plate using a spreader and spreading wheel. Then, the plate was irradiated, 10 ml of YE was added to the plate, the cells were

resuspended using a spreader, and decanted into a culture tube. Mock treatment for control samples involved transferring the cells onto the agar plate, but not irradiating it with UV.

#### **2.4.10. HU Block and Release**

Cells were grown in 10 ml YE to mid-log phase and normalised to the same concentration (typically  $\sim 6 \times 10^6$  cells/ml). 1 M hydroxyurea was made up fresh in water and added to the cultures to 10 mM. After 2.5-3 hours growth in HU, the cells were spun down gently (2 krpm), the media discarded, the pellet washed, and 10 ml fresh YE added. 1 ml samples were taken at various time points following release from HU, typically every 15, 30 or 60 min. Sometimes a sample was also taken prior to the addition of HU and before HU was washed out. Samples were spun down, washed, frozen in liquid nitrogen in TCA extracted.

#### **2.4.11. Fluorescence Activated Cell Sorting (FACS)**

Cells for FACS analysis were spun down, the media removed, washed once in water and 1 ml of 4°C 70% ethanol added and stored at 4°C until ready for analysis. At that stage, the cells were washed in ethanol and then resuspended in 500  $\mu$ l 50 mM sodium citrate pH 7.0 and 50  $\mu$ l of 10 mg/ml RNase A was added. RNA was digested for 3 h at 37°C. To 200  $\mu$ l of cells, 10  $\mu$ l of 500  $\mu$ g/ml propidium iodide, and 1 ml of FACS buffer was added to special FACS tubes. A FACSCaliber (BD Biosciences) machine was used to measure the DNA content of the cells.

#### **2.4.12. Fluorescence Microscopy**

Cells were prepared for microscopy by fixing in methanol. The cells were then placed on glass microscope slide and the methanol allowed to evaporate. A solution containing 1  $\mu$ g/ml 4',6-diamidino-2-phenylindole (DAPI), 50  $\mu$ g/ml calcofluor, 1 mg/ml p-phenylenediamine (anti-fade), and 50% glycerol. DAPI binds

strongly to DNA and is excited by UV light and emits as a blue colour. Calcofluor binds chitin and cellulose and is used for visualised septating cells, which is seen as a bright white bar.

#### **2.4.13. Trichloroacetic Acid (TCA) Extraction**

Whole cell extracts were prepared using TCA. This technique adequately preserved the ubiquitinated forms of <sup>Sp</sup>PCNA.  $1 \times 10^7 - 2 \times 10^8$  cells were harvested by centrifugation at 4.5 krpm for 10 min in 15 ml falcon tubes and the supernatant discarded. The cell pellet was then resuspended in 1 ml water and transferred to 2 ml screw-top ribolyser tubes. The washed cells were then spun down for 10 min at 13.5 krpm in a microfuge and the supernatant discarded. The cell pellet was then snap frozen in liquid nitrogen and stored at  $-80^\circ\text{C}$ . To complete the extraction, the tubes were transferred from the  $-80^\circ\text{C}$  freezer to liquid nitrogen and then batches of eight tubes maximum were transferred to ice. Immediately, one microfuge tube lid full of glass beads (acid washed, Sigma) and 200  $\mu\text{l}$  of 20% TCA was added. Ensuring the lids were tightly closed and the cells were kept at  $4^\circ\text{C}$  at all times, the tubes were then vortexed for one second (Vortex Genie 2, full speed), bead-beaten for 2 x 30 seconds in the ribolyser at 6.5 krpm and then vortexed again as before. Each tube was then placed upside-down in a metal tube rack (for safety) and the base pierced using a clean, sharp needle. The lysed cell contents were recovered by spinning through the hole at 4.6 krpm for 10 min at  $4^\circ\text{C}$  into a clean 1.5 ml screw-top microfuge tube containing 400  $\mu\text{l}$  of 5% TCA using a 15 ml falcon tube with the base cut off as a support. The ribolyser tubes containing only glass beads were discarded. The precipitated protein was then spun down for 20-30 min at 13 krpm at  $4^\circ\text{C}$ . The supernatant was completely removed and the protein resuspended in a volume of Laemmli buffer proportional to the number of cells originally harvested. The tubes were stored at room temperature (RT) for up to a few hours, or  $-20^\circ\text{C}$  for longer periods, prior to fractionation by SDS-PAGE and analysis by Western blotting and immunodetection.

#### 2.4.14. Drop Test Colony Forming Assay

A high throughput “drop test” assay for measuring sensitivity of mutant strains to UV radiation was devised. This method has been previously used in assays for sensitivity of mutant strains to MMS treatment in *S. cerevisiae* (Xiao *et al.*, 2000) and *S. pombe* (Memisoglu and Samson, 2000). It involves the creation of a linear array of cells of one particular strain down an agar plate, where the cells are at approximately uniform concentration along the extent of the array. To do this, suitable agar was poured into 12 cm x 12 cm square, sterile petri dishes and dried in a laminar flow hood. Each dried plate was then set at a ~45° angle. Mid-log cells were normalised to  $4 \times 10^6$  cells/ml in YE and 45  $\mu$ l was pipetted onto a labelled point at the top of the angled plate. The cells would flow down the agar at a constant speed. The liquid media was then allowed to dry off. Different strains could be added to the same plate – about 9 different arrays could be created on one square plate before there was a risk of arrays cross-contaminating. To create a UV dose gradient, the agar was subsequently irradiated in lateral strips, for example a 0-200  $\text{Jm}^{-2}$  gradient was created in 40  $\text{Jm}^{-2}$  increments. To irradiate in strips, 6 dish lids were cut into different sizes, such that that difference between each lid size was approximately constant. Using the flow rate of the UVC source, the number of seconds required to deliver the incremental dose, in this example 40  $\text{Jm}^{-2}$ , was calculated and every 40  $\text{Jm}^{-2}$  timed, the previous lid was replaced by a slightly smaller lid. The lowest section of each plate was not exposed to any UV. Cell death due to unrepaired UV damage was measured qualitatively by the density of colonies compared to controls. An entirely unirradiated agar plate was also utilised as a further control.

#### 2.4.15. UV Survival Colony Forming Assay

Mid-log cells originating from a single colony were grown to a suitable concentration in YE and serially diluted such that when 100  $\mu$ l was spread on a

plate, 100-200 cells would survive. For example, for wild-type cells the concentrations used were as follows: 0 and 40 J/m<sup>2</sup>: 2 x 10<sup>3</sup> cells/ml; 60 J/m<sup>2</sup>: 2 x 10<sup>3</sup> cells/ml; 100 J/m<sup>2</sup>: 1 x 10<sup>4</sup> cells/ml. YEA plates were prepared beforehand and dried in a laminar flow hood. The cells were then spread on the plates and in at least triplicate i.e. in one experiment there was at least three identical plates for each strain at each dose. Spreading using glass beads was tried, but it was found that it was necessary for the plates to be over-dried in order to prevent the glass beads from retaining too many cells once they were discarded after being used to spread the cells. The optimum spreading means was found to be a wedge-shaped spreader and a rotating wheel. The cells were allowed a minimum amount of time on the plates before irradiation, which was carried out by placing an individual plate into the UVC box. Plates were irradiated one at a time. Following irradiation, the cells were incubated at 30°C. Following an appropriate growth period, the number of colonies on each plate was counted.

#### **2.4.16. Spot Test Colony Forming Assay**

Mid-log cells originating from a single colony were grown to ~1 x 10<sup>7</sup> cells/ml concentration in YE, 1 x 10<sup>7</sup> cells were spun down and resuspended in 240 µl, which was added to the first well in a 96 well plate. Cells for each strain were then diluted serially 1 in 6 across each row of the 96 well plate. Plates containing specific concentrations of various DNA damaging agents were prepared earlier the same day (the stock concentrations and diluents for these agents are shown in Table 2.4). The agar was cooled to 50°C before adding the genotoxin in order to prevent heat damage to it. The plates were then dried in a laminar flow hood or fume hood, depending upon the toxicity of the genotoxin. Various spotting techniques were tried e.g. a “frogger” was used, which comprises 96 metal rods. Following sterilisation using a flame, the frogger was simply dipped into the 96 well plate and the cells applied to the agar. This method was found to be less reliable and the plate was prone to becoming host to contaminant microbes, especially when highly toxic chemicals e.g. MMS, cisplatin etc required the use of a fume

hood throughout. Most reliable was an electronic repeating multi-channel pipette – 4  $\mu$ l from each well was added to the plate to make each spot. It was found that it was important to mix the cells in each well regularly or else the cells would sink to the bottom of the well. The plates were allowed to dry in the hood, put in a plastic bag for safety, and then allowed to grow in the plate incubator until photographed.

#### 2.4.17. DUB Expression

DUBs were expressed by cloning the gene into an *S. pombe* compatible Gateway system destination vector of the pDUAL series, such that expression was controlled by the *nmt1* promoter. This promoter is repressed by the addition of thiamine into growth media although repression is not 100% efficient and low-levels of protein will be expressed in the presence of thiamine. Also, complete recovery from repression i.e. removal of thiamine, requires 18-24 h. pDUAL-*dub* constructs were transformed into *S. pombe* cells and plated onto minimal agar lacking uracil in order to select for *ura4<sup>+</sup>* cells comprising the plasmid. For each transformation, half the cells were plated onto plates also comprising 15  $\mu$ M thiamine and maintained in/on +thiamine –uracil media at all times. The remaining half were plated/maintained on/in –uracil media. When processing the blot resultant from running the samples from *SpUbp21/SpUbp22* expression experiments, the blot was first probed with  $\alpha$ -*Sp*PCNA antibodies. Following detection, the blot was washed once in 1% sodium azide in 0.1% PBST to denature the horseradish peroxidase (HRP) enzyme, then ten times in 0.1% PBST, then cut longitudinally at the 62.5 kDa marker, and reblocked. The high molecular weight section of the blot was probed with  $\alpha$ -FLAG to detect the tagged DUBs and the lower portion with  $\alpha$ -tubulin. In order to optimise loading, either the Ponceau S stained blot or the tubulin bands were quantified using Adobe Photoshop and the loading recalculated.



## **2.5. *Saccharomyces cerevisiae* Methods**

*S. cerevisiae* was used in Chapter 6 and the *S. pombe* methods above were utilised unless otherwise specified. Standard YPD-based media, which comprises yeast extract, peptone and dextrose, was utilised. All strains were a kind gift from Eva Hofmann, but originated from the European Saccharoymces Cerevisiae Archive for Functional Analysis (EUROSCARF; see website link below; Brachmann *et al.*, 1998). All strains were based on wild type “BY405” and the deleted genes were replaced by the *kanMX4* cassette. The mutant strains were found to be able to grow on media containing G418, whereas the wild-type strain could not. Deletions were verified by isolating genomic DNA and amplifying the relevant locus, which was then sequenced. Also prior to counting with a haemocytometer, the cells were sonicated briefly.

## **2.6. Computational Methods**

### **2.6.1. Thesis Production**

This thesis was created using Microsoft Word, Microsoft PowerPoint and Microsoft Excel on a Windows XP operating system.

### **2.6.2. Useful Websites**

#### **Literature searching:**

<http://www.ncbi.nlm.nih.gov/sites/entrez>

#### ***S. pombe* genome annotations:**

<http://www.genedb.org/genedb/pombe/>

***S. pombe* information:**

<http://www-rcf.usc.edu/~forsburg/index.html>

[http://www.ebi.ac.uk/2can/genomes/eukaryotes/Schizosaccharomyces\\_pombe.htm](http://www.ebi.ac.uk/2can/genomes/eukaryotes/Schizosaccharomyces_pombe.htm)

<http://www.biotwiki.org/twiki/bin/view>

**Paul Nurse laboratory manual:**

<http://www.biotwiki.org/bin/view/Pombe/NurseLabManual>

***S. pombe* genome BLAST software:**

<http://www.genedb.org/genedb/pombe/blast.jsp>

**RIKEN Chemical Genetics Laboratory:**

<http://www.riken.jp/SPD/index.html>

***S. cerevisiae* genome annotations:**

<http://www.yeastgenome.org/>

<http://www.genedb.org/genedb/cerevisiae/>

***S. cerevisiae* EUROSCARF project:**

<http://web.uni-frankfurt.de/fb15/mikro/euroscarf/index.html>

**Genome annotations:**

<http://www.uniprot.org/>

<http://www.genecards.org/index.shtml>

**Protein structure information:**

<http://www.rcsb.org/pdb/home/home.do>

**Protein domain information:**

<http://pfam.sanger.ac.uk/>

**Protein structure analysis:**

[http://www.umass.edu/microbio/chime/pe\\_beta/pe/protexpl/frntdoo2.htm](http://www.umass.edu/microbio/chime/pe_beta/pe/protexpl/frntdoo2.htm)

**Protein structure prediction:**

<http://www.sbg.bio.ic.ac.uk/phyre/>

**Alignments:**

<http://www.ebi.ac.uk/Tools/clustalw2/index.html>

**BLASTs:**

<http://www.ebi.ac.uk/Tools/psiblast/>

**Molecular biology:**

<http://tools.neb.com/NEBcutter2/index.php>

**Primer design:**

[http://frodo.wi.mit.edu/cgi-bin/primer3/primer3\\_www\\_slow.cgi](http://frodo.wi.mit.edu/cgi-bin/primer3/primer3_www_slow.cgi)

<http://www.stratagene.com/qcprimerdesign>

**Primer properties analysis:**

<http://eu.idtdna.com/analyzer/Applications/OligoAnalyzer/Default.aspx>

**Reverse complementation tool:**

[http://www.bioinformatics.org/sms/rev\\_comp.html](http://www.bioinformatics.org/sms/rev_comp.html)

**DNA sequencing:**

<http://www.gatc-biotech.com/en/index.html>

**Translation tool:**

<http://us.expasy.org/tools/dna.html>

## Chapter 3: Identification and Disruption of Deubiquitinating Enzyme Genes in *S. pombe*

### 3.1. Introduction

There are many open questions with regard to the mechanism and employment of PRR. This study concentrates on an investigation of the role of deubiquitination in PRR. The species of fission yeast, *S. pombe*, was utilised. The main aim of this project is to identify a DUB enzyme capable of removing ubiquitin or ubiquitin chains from <sup>Sp</sup>PCNA. This chapter discusses, firstly, evidence for ubiquitination and subsequent deubiquitination of <sup>Sp</sup>PCNA. Secondly, DUB genes were identified in the *S. pombe* genome and the literature searched for roles of the encoded enzymes. Thirdly, the assembly of a DUB deletion library is explained.

### 3.2. Evidence for PCNA Deubiquitination in *S. pombe*

<sup>Sp</sup>PCNA ubiquitination has already been described (Frampton *et al.*, 2006). Figure 3.1 depicts the cycle of appearance, persistence and subsequent disappearance of ubiquitinated species of <sup>Sp</sup>PCNA following UVC irradiation. In this experiment, asynchronous wild-type *S. pombe* cells were grown to mid-log phase, irradiated with 100 J/m<sup>2</sup> of UVC, and then allowed to recover. Samples were taken at the time points indicated. Each sample was TCA extracted and the whole cell extracts were fractionated by SDS-PAGE. Western blotting was then performed and the blot probed with an anti-<sup>Sp</sup>PCNA antibody, which was a kind gift from Dr. Felicity Watts.

Following 100 J/m<sup>2</sup> UVC, ubiquitinated forms of <sup>Sp</sup>PCNA are apparent after 1 h. A single subunit of <sup>Sp</sup>PCNA, which is encoded by the *pcn1+* gene, is 260 amino acids long or 28.9 kDa. On a denaturing gel, a <sup>Sp</sup>PCNA monomer runs at around the 32.5 kDa marker. Two controls were also employed in this experiment, mock-irradiated

wild-type cells (not treated, NT), and a strain called *pcn1-K164R* (also a kind gift from Dr. Felicity Watts) where the ubiquitinated lysine of <sup>Sp</sup>PCNA (lysine-164) has been mutated to an arginine. Low levels of ubiquitinated <sup>Sp</sup>PCNA are seen in the mock treated, wild-type samples – it has previously been shown that <sup>Sp</sup>PCNA is ubiquitinated at low levels every S-phase in unchallenged cells (Frampton *et al.*, 2006). No ubiquitinated forms of <sup>Sp</sup>PCNA are seen in the *pcn1-K164R* strain following UVC irradiation.

This experiment shows that following a high dose of UVC, ubiquitination of <sup>Sp</sup>PCNA persists for many hours. Persistence of <sup>Sp</sup>PCNA ubiquitination correlated with increased cell length (data not shown) implying the cells were blocked in G2 repairing the damage – the cells were at their longest 11 h after irradiation. The following morning, a final sample was taken (24 h after irradiation), no <sup>Sp</sup>PCNA ubiquitination was found, the cells had returned to normal cytology and were actively growing. Following lower doses of UVC, un-ubiquitinated <sup>Sp</sup>PCNA was restored more quickly (data not shown).

It is thought that <sup>Sp</sup>PCNA is ubiquitinated in response to the occurrence of ssDNA following to replication fork blockage due to, for example, polymerase-blocking lesions resulting from UV irradiation. It is hypothesised that <sup>Sp</sup>PCNA is deubiquitinated once cells have recovered from this crisis in order to prevent untimely PRR.

Whilst there are other explanations for the disappearance of ubiquitinated forms of <sup>Sp</sup>PCNA, proteasomal degradation for example, it is important to understand whether DUBs play a role in PRR in lower eukaryotes as has been shown for <sup>Hs</sup>USP1 in human cells.

### 3.3. Identification of Deubiquitinating Enzyme Genes in *S. pombe*

*S. pombe* DUB genes were identified by database searching DUB catalytic and additional protein domain names and aliases. Table 3.1-4 depicts all the *S. pombe* DUBs experimentally considered in this study. The Table is arranged such that the DUBs are divided according to superfamily – the relevant rows are shaded in different colours, and the large UBP/USP superfamily is further divided according to any extra, well-known domains.

The subsequent sections will summarise the literature surrounding each identified *S. pombe* DUB. Orthologues in humans and *S. cerevisiae* will be identified and their functions discussed, particularly when there is little or no information on the *S. pombe* version. The information provided is biased towards potential functions of additional domains, roles in carcinogenesis, and type of poly-ubiquitin chain disassembled. Alignments between orthologues were also performed in most cases, but only those alignments are shown herein where orthology has not previously been shown before.

### 3.4. USP/UBP *S. pombe* DUBs Containing a DUSP Domain

<sup>Sp</sup>Ubp1 and <sup>Sp</sup>Ubp12 share 32% sequence identity at the amino acid level, and are likely paralogous. In addition to the UBP/USP domain that confers catalytic function, <sup>Sp</sup>Ubp1 and <sup>Sp</sup>Ubp12 also contain an N-terminal DUSP (domain present in ubiquitin-specific proteases) domain, which, as its name suggests, is common in USP/UBP DUBs. The function of this domain, which is typically around 120 residues in length, is not known. However, functions for DUSP domain-containing DUBs have been ascribed.

Seven human UBP/USP superfamily DUBs contain this domain (de Jong *et al.*, 2006). <sup>Hs</sup>USP15, <sup>Hs</sup>USP4<sup>UNP</sup> and <sup>Hs</sup>USP11 all contain a DUSP domain N-terminal

to the catalytic domain, are a similar length, and are the likely orthologues of *Sp*Ubp1 and *Sp*Ubp12 (Kay Hofmann, personal communication). The DUSP domain of *Hs*USP15 has been solved, which revealed a novel  $\alpha/\beta$  tripod structure, known as an AB3 fold, and the authors propose that it is involved in mediating protein-protein interactions or direct substrate recognition (de Jong *et al.*, 2006).

A functional role of *Sp*Ubp12 was ascribed in 2003 by the Wolf group (Zhou *et al.*, 2003). The COP9 (constitutive photomorphogenic gene 9) -signalosome (CSN) is a multi-subunit complex with deneddylating activity. Cullins are a family of proteins important for the formation of Skp1-Cullin-F-box (SCF) complexes, which function as E3s. Deneddylation of cullins is inactivating because neddylated cullins have an enhanced affinity for E2s (Kawakami *et al.*, 2001), hence the CSN functions to downregulate the E3 activity of SCF complexes. E3s able to ligate lysine-48-linked poly-ubiquitin chains are known to control their activity by auto-ubiquitination, which directs them for proteasome-mediated degradation. The Wolf group proposed that the CSN recruits *Sp*Ubp12 to F-box proteins for deubiquitination, which prevents degradation by their E3 neighbours, and hence, the CSN functions as a stabiliser of SCF assembly (Zhou *et al.*, 2003; Wee *et al.*, 2005). Furthermore, *Hs*USP15 was found to co-purify with the human CSN, and the ability of exogenously expressed *Hs*USP15 to stabilise *Hs*RBX1, an SCF component containing the RING domain that confers the E3 activity to the SCF, was dependent upon a zinc finger domain found in the UBP/USP domain (Hetfeld *et al.*, 2005).

The authors found that many other UBP/USP DUBs also comprised this zinc finger integrated into the catalytic domain (Hetfeld *et al.*, 2005). The same domain in the same position was found in another UBP/USP DUB called *Hs*HAUSP<sup>USP7</sup> (Herpes-associated ubiquitin-specific protease), but this was found to be “circularly permuted” and had lost its capacity to bind zinc (Krishna and Grishin, 2004; Hetfeld *et al.*, 2005). However, the authors noted that the circularly permuted version was also found in other UBP/USP DUBs (Hetfeld *et al.*, 2005).

The DUSP domain DUB <sup>Hs</sup>USP11, as mentioned in the Introduction, interacts with and, when overexpressed, can deubiquitinate <sup>Hs</sup>BRCA2 (Schoenfeld *et al.*, 2004). In this study, they also showed, as a control, that <sup>Hs</sup>USP11 cannot deubiquitinate mono-ubiquitinated <sup>Hs</sup>FANCD2. <sup>Hs</sup>USP11 was found to be important in cellular survival following MMC treatment – knockdown of <sup>Hs</sup>USP11 resulted in sensitivity to MMC. However, the authors also found that MMC treatment up-regulated the poly-ubiquitination of <sup>Hs</sup>BRCA2, which caused its degradation, in a <sup>Hs</sup>USP11-independent manner. It was concluded that the “USP11 prosurvival functions, although shown to be BRCA2 dependent, appear to be mediated through a USP11 substrate other than BRCA2” (Schoenfeld *et al.*, 2004).

Furthermore, levels of the alpha subunit of IκB kinase (<sup>Hs</sup>IKKα) and <sup>Hs</sup>p53 are controlled by <sup>Hs</sup>USP11 (Yamaguchi *et al.*, 2007a). In this study, it was shown that <sup>Hs</sup>USP11 knockdown resulted in decreased <sup>Hs</sup>IKKα mRNA levels as measured by the real-time polymerase chain reaction (RT-PCR) technique. The mechanism of this transcriptional control is not known (Yamaguchi *et al.*, 2007a). It had been previously shown that <sup>Hs</sup>IKKα forms part of a pathway that stabilises and activates <sup>Hs</sup>p53 in response to reactive oxygen species (Yamaguchi *et al.*, 2007b). <sup>Hs</sup>USP11 also affects <sup>Hs</sup>p53 levels – it was demonstrated that <sup>Hs</sup>USP11 knockdown also resulted in reduced <sup>Hs</sup>p53 levels, whereas <sup>Hs</sup>p53 mRNA levels were unaffected (Yamaguchi *et al.*, 2007a).

The remaining <sup>Sp</sup>Ubp1 and <sup>Sp</sup>Ubp12 orthologue in humans, <sup>Hs</sup>USP4<sup>UNP</sup>, has been found to have altered levels in lung cancer cells (Gray *et al.*, 1995; Frederick *et al.*, 1998). It has additionally been shown to interact with the important tumour suppressor protein <sup>Hs</sup>pRB (DeSalle *et al.*, 2001). <sup>Hs</sup>USP4<sup>UNP</sup> comprises both a nuclear export signal and a nuclear localisation signal, and has been shown to have nucleo-cytoplasmic shuttling properties (Soboleva *et al.*, 2005).

<sup>Hs</sup>USP4<sup>UNP</sup> targets have also been identified. Tripartite motif containing protein 21, <sup>Hs</sup>TRIM21<sup>Ro52</sup>, is a ribonucleoprotein particle with unknown function, and it has



been shown to interact with and be deubiquitinated by  $HsUSP4^{UNP}$  (Wada *et al.*, 2006).  $HsTRIM21^{Ro52}$  comprises the tripartite RING-B-box-Coiled coil (RBCC) domain (this domain is also discussed in Chapter 5, section 5.5) and hence is an E3. The same group also showed in 2006 that  $HsTRIM21^{Ro52}$  ubiquitinates  $HsUSP4^{UNP}$  and that  $HsUSP4^{UNP}$  can auto-deubiquitinate (Wada and Kamitani, 2006).

### 3.5. *S. pombe* USP/UBP DUBs Containing a UBP-type Zinc Finger Domain

There are four UBP/USP DUBs in *S. pombe*,  $SpUbp7$ ,  $SpUbp8$ ,  $SpUbp10$  and  $SpUbp14^{Ucp2}$ , that contain a UBP-type zinc finger domain, which is simply a zinc finger as found in many UBP/USP DUBs. It is not the same as the zinc finger found in the catalytic domain mentioned in section 3.3 above. The UBP-type zinc finger domain is also found in the human DUBs  $HsUSP3$ ,  $HsUSP5^{IsoT1}$  (and the likely paralogous  $HsUSP13^{IsoT2}$ ),  $HsUSP16$  (and the likely paralogous  $HsUSP45$ ),  $HsUSP20^{VDU2}$  (and the likely paralogous  $HsUSP33^{VDU1}$ ),  $HsUSP22^{USP3L}$  (and the likely paralogous  $HsUSP27$  and  $HsUSP51$ ), and  $HsUSP44$  (and the likely paralogous  $HsUSP49$ ; Kay Hofmann, personal communication; Bonnet *et al.*, 2008). This domain is also found in  $HsUSP39^{SNUT2}$ , which is involved in spliceosome formation.

The UBP-type zinc finger domain is also found in some non-DUB proteins, for example the cytoplasmic deacetylase,  $HsHDAC6$ , and BRCA1-associated protein 2 ( $HsBRAP2$ ). The latter is a RING E3 and there is an uncharacterised orthologue in *S. pombe* (gene identifier: SPAC16E8.13). The UBP-type zinc finger domain is also known as a BUZ domain (binder of ubiquitin zinc-finger) domain, a DAUP (deacetylase and ubiquitin-specific protease) domain, and a PAZ (polyubiquitin-associated zinc-finger) domain.

The likely human orthologues of  $SpUbp14^{Ucp2}$  are  $HsUSP5^{IsoT1}$  and  $HsUSP13^{IsoT2}$  (Kay Hofmann, personal communication).  $HsUSP5^{IsoT1}$ , which is also known as

*Hs*IsopeptidaseT, has been well characterised and has been found to deubiquitinate unattached poly-ubiquitin chains. The likely *S. cerevisiae* orthologue of these DUBs is *Sc*Ubp14, which appears to have the same function as *Hs*USP5<sup>IsoT1</sup> (Kay Hofmann, personal communication; Amerik *et al.*, 1997). Deletion of *Sc*Ubp14 leads to the accumulation of free poly-ubiquitin chains and inhibition of the proteasome (Amerik *et al.*, 1997). *Hs*USP5<sup>IsoT1</sup> and *Sc*Ubp14 each comprise an N-terminal UBP-type zinc finger domain, followed by the catalytic domain, which features two integrated ubiquitin-associated (UBA) domains. The crystal structure of the N-terminal UBP-type zinc finger domain has been solved alone and in complex with ubiquitin, which revealed that it binds the unanchored C-terminus of ubiquitin, and binds ubiquitin with high affinity compared to other ubiquitin binding domains (Reyes-Turcu *et al.*, 2006).

Furthermore, Reyes-Turcu *et al* showed that the ubiquitin binding in the UBP-type zinc finger domain activated deubiquitinating catalysis by the UBP/USP domain. UBP-type zinc finger domain residues important for this were those that co-ordinate Zn<sup>2+</sup> and those that interact with ubiquitin (Reyes-Turcu *et al.*, 2006).

More recently, the same group has investigated the role of the UBA domains in *Hs*USP5<sup>IsoT1</sup> function (Reyes-Turcu *et al.*, 2008). This work showed that the UBA domains interact with the distal ubiquitins in linear and lysine-48-linked poly-ubiquitin chains. In other words, when binding to a free poly-ubiquitin chain, the UBP-type zinc finger domain interacts with the proximal ubiquitin (ubiquitin-1), the catalytic domain interacts with ubiquitin-2, and the UBA domains interact with ubiquitin-3 and ubiquitin-4 (Reyes-Turcu *et al.*, 2008).

The structure of the UBP-type zinc finger domain of *Hs*USP33<sup>VDU1</sup> has also been solved (Allen and Bycroft, 2007). There appears to be no *S. pombe* orthologue of *Hs*USP33<sup>VDU</sup> and the paralogous *Hs*USP20<sup>VDU2</sup>. These DUBs comprise an N-terminal UBP-type zinc finger domain, followed by a central USP/UBP catalytic domain, and two C-terminal DUSP domains. It is pertinent to note here that

$^{Hs}USP33^{VDU1}$  was utilised as negative control in the paper that linked  $^{Hs}USP1$  to deubiquitination of  $^{Hs}PCNA$ , that is,  $^{Hs}USP33^{VDU1}$  could not deubiquitinate  $^{Hs}PCNA$  (Huang *et al.*, 2006).

The structure of the UBP-type zinc finger domain of  $^{Hs}USP33^{VDU1}$  differed slightly from that of  $^{Hs}USP5^{IsoT1}$  and the domain was not found to bind ubiquitin (Allen and Bycroft, 2007). This was found to be intriguing by Bonnet *et al* because the ubiquitin-binding pocket and many ubiquitin-binding residues found to be important in the  $^{Hs}USP5^{IsoT1}$  UBP-type zinc finger were conserved. So, Bonnet *et al* investigated the matter further by bioinformatically comparing the sequence of  $^{Hs}USP5^{IsoT1}$  and  $^{Hs}USP33^{VDU1}$  in addition to the UBP-type zinc finger domain of other proteins. They found a crucial ubiquitin-binding aspartate and arginine were serine and glutamate residues in  $^{Hs}USP33^{VDU1}$ . This would be incompatible with ubiquitin-binding. From this analysis, they were able to draw conclusions about the ubiquitin-binding capacity of UBP-type zinc finger domains in other DUBs. In particular, they concluded that the UBP-type zinc finger domain of  $^{Hs}USP16^{UBP-M}$ ,  $^{Hs}USP44$ ,  $^{Hs}USP45$ , and  $^{Hs}USP49$  **can** interact with ubiquitin, whereas that of  $^{Sc}Ubp8$ ,  $^{Hs}USP22$ , and  $^{Hs}USP20$  **cannot**. Also, the authors imply it is unlikely that  $^{Hs}USP13^{IsoT2}$  and  $^{Hs}USP39$  are able to bind ubiquitin (Bonnet *et al.*, 2008).

Interestingly,  $^{Sp}Ubp14^{Ucp2}$  comprises **two** N-terminal UBP-type zinc finger domains, followed by the catalytic domain that also contains two UBA domains. The functional significance of two N-terminal UBP-type zinc finger domains is not known, and it would be interesting to see whether both domains are able to bind ubiquitin and the effect of ubiquitin-binding to one or both of the domains on catalytic activity. Only three other species, *Aspergillus niger*, *Aspergillus oryzae*, *Chaetomium globosum* (soil fungus), have  $^{Sp}Ubp14^{Ucp2}$ -like DUBs encoded within their genome with two N-terminal UBP-type zinc finger domains followed by a catalytic domain that also contains two UBA domains. No work on  $^{Sp}Ubp14^{Ucp2}$  itself has been published to date.

$Hs$ USP13<sup>IsoT2</sup> shows 55% identity at the protein level with  $Hs$ USP5<sup>IsoT1</sup> and comprises the same domain structure (Timms *et al.*, 1998). However, despite the extensive characterisation of its paralogue,  $Hs$ USP13<sup>IsoT2</sup> is much less studied. Interestingly, a study showed that  $Hs$ USP13<sup>IsoT2</sup> is expressed highly in the ovary and testes, whereas  $Hs$ USP5<sup>IsoT1</sup> is highly expressed in brain cells and was not detected in the ovary (Timms *et al.*, 1998). Also, both  $Hs$ USP5<sup>IsoT1</sup> and  $Hs$ USP13<sup>IsoT2</sup> have been shown to be able to react with a suicide substrate of the  $Hs$ ISG15<sup>UCRP</sup> ubiquitin-like protein (Catic *et al.*, 2007). In this study  $Hs$ USP2 and  $Hs$ USP14 were also identified, in addition to the  $Hs$ ISG15<sup>UCRP</sup>-specific protein  $Hs$ USP18.

The likely human orthologues of  $Sp$ Ubp7 are  $Hs$ USP16<sup>UBP-M</sup> and  $Hs$ USP45 (Kay Hofmann, personal communication). A cellular function of  $Hs$ USP45 has not been described in the literature. However, the UBP-type zinc finger of  $Hs$ USP16<sup>UBP-M</sup> has also been shown to bind the C-terminus of unanchored ubiquitin and the authors conclude that the function of the UBP-type zinc finger is as a sensor for free ubiquitin in the cell (Pai *et al.*, 2007). Based on the above studies, it seems likely that the UBP-type zinc finger of  $Sp$ Ubp7 is also able to bind ubiquitin. So far,  $Hs$ USP16<sup>UBP-M</sup> has been found to comprise only the UBP-type zinc finger and catalytic domains.  $Hs$ USP16<sup>UBP-M</sup> deubiquitinates mono-ubiquitinated histone H2A (but not H2B), which is important for mitotic chromosome condensation and caspase-induced apoptosis (Mimnaugh *et al.*, 2001; Joo *et al.*, 2007).  $Hs$ USP16<sup>UBP-M</sup> is regulated by phosphorylation – the phosphorylated form is active, and siRNA knockdown results in cell cycle delay (Joo *et al.*, 2007).

It has been proposed that structural and sequence similarities between  $Hs$ USP27,  $Hs$ USP16<sup>UBP-M</sup> and  $Hs$ USP3 suggest similar activating functions for the UBP-type zinc finger in these proteins (Bonnet *et al.*, 2008). The authors suggest that this domain in  $Hs$ USP16<sup>UBP-M</sup> and  $Hs$ USP3 functions as a free ubiquitin pool sensor, that is, their targets are only deubiquitinated when free ubiquitin levels are high enough – for example during particularly cell cycle phases (Bonnet *et al.*, 2008). Congruent to  $Hs$ USP16<sup>UBP-M</sup>,  $Hs$ USP3 also deubiquitinates mono-ubiquitinated H2A, but also

H2B. It has also been shown that depletion of <sup>Hs</sup>USP3 causes S-phase delay, accumulation of DNA breaks in unchallenged cells as measured by comet assay, and checkpoint activation. Furthermore, <sup>Hs</sup>USP3 accumulates in  $\gamma$ H2AX foci (Nicassio *et al.*, 2007). No additional domains, other than the catalytic and UBP-type zinc finger domains, have been ascribed to <sup>Hs</sup>USP3, and there is no likely orthologue of this enzyme in *S. pombe*. However, it would be interesting to see whether <sup>Sp</sup>Ubp7 is able to undertake the functions of both <sup>Hs</sup>USP16<sup>UBP-M</sup> and <sup>Hs</sup>USP3, i.e. deubiquitinate histones in *S. pombe*, and whether <sup>Sp</sup>Ubp7 has any other roles in the DNA damage response. Furthermore, there is no <sup>Sp</sup>Ubp7 orthologue in *S. cerevisiae*. H2A is not ubiquitinated in *S. cerevisiae* (Weake and Workman, 2008; Osley, 2006). No work on <sup>Sp</sup>Ubp7 has been published so far.

The likely orthologues of <sup>Sp</sup>Ubp8 are <sup>Sc</sup>Ubp8, <sup>Hs</sup>USP22, <sup>Hs</sup>USP27 and <sup>Hs</sup>USP51 (Kay Hofmann, personal communication). However, <sup>Hs</sup>USP27 and <sup>Hs</sup>USP51, whilst very similar to <sup>Hs</sup>USP22, are encoded by intronless genes and hence have questionable functionality (Bonnet *et al.*, 2008). The Bonnet *et al* study also suggested that <sup>Sc</sup>Ubp8 and <sup>Hs</sup>USP22 cannot bind ubiquitin in their UBP-type zinc finger, which implies the same for <sup>Sp</sup>Ubp8.

<sup>Sc</sup>Ubp8 and <sup>Hs</sup>USP22 are components of the Spt-Ada-Gcn5-acetyl transferase (SAGA) transcriptional co-activator complex, which links gene transcription with chromatin modifications (reviewed in Baker and Grant, 2007; Pijnappel and Timmers, 2008). <sup>Hs</sup>USP22 and <sup>Sc</sup>Ubp8 have been shown to deubiquitinate mono-ubiquitinated H2B (Zhang *et al.*, 2008c; Henry *et al.*, 2003), and <sup>Hs</sup>USP22 has been shown to also deubiquitinate mono-ubiquitinated H2A (Zhang *et al.*, 2008b). Interestingly, the <sup>Sc</sup>PCNA ubiquitinase <sup>Sc</sup>Rad6 is also the E2 that catalyses H2B mono-ubiquitination, but in combination with a different E3 (reviewed in Game and Chernikova, 2009). The same function has been ascribed to <sup>Sp</sup>Rhp6 (Zofall and Grewal, 2007). No work on <sup>Sp</sup>Ubp8 has been published.

*Hs*USP39<sup>SNUT2</sup> also comprises an N-terminal UBP-type zinc finger, although the catalytic domain is inactive (Makarova *et al.*, 2001; van Leuken *et al.*, 2008). *Hs*USP39<sup>SNUT2</sup> is involved in spliceosome maturation. The likely orthologues of *Hs*USP39<sup>SNUT2</sup> are *sn*RNP (*s*mall *n*uclear *r*ibonucleoprotein *p*article) *a*ssembly-*d*efective protein 1 (*Sc*Sad1) and *Sp*Ubp10 (Makarova *et al.*, 2001; Kay Hofmann, personal communication). *Sc*Sad1 has also been implicated in spliceosome maturation, and is essential in *S. cerevisiae* (Lygerou *et al.*, 1999). *Sc*Sad1 was found to be involved in the *de novo* assembly of one of the particles required for splicing, and in splicing itself (Lygerou *et al.*, 1999). It is important to note here that *Sc*Sad1 is a different protein from *Sc*Rad53<sup>Sad1</sup> (gene identifier: YPL153C). However, *Hs*USP39<sup>SNUT2</sup> has also been found to be necessary for spindle checkpoint maintenance and for cytokinesis (van Leuken *et al.*, 2008). The authors found a dramatic reduction in the mRNA levels of *Hs*AuroraB when *Hs*USP39<sup>SNUT2</sup> was knocked down, and they suggested that *Hs*USP39<sup>SNUT2</sup> has a role in splicing of *Hs*Aurora B mRNA and maybe the mRNA of other spindle checkpoint proteins (van Leuken *et al.*, 2008). There no publications studying *Sp*Ubp10 in the literature. Also, *Sp*Ubp10 is not an alias for the spindle pole body protein, *Sp*Sad1 (SPBC16H5.01c).

### 3.6. *S. pombe* USP/UBP DUBs Containing Ubiquitin-like Domains

*Sp*Ubp6 comprises an N-terminal ubiquitin-like domain. The *S. cerevisiae* and *H. sapiens* orthologues, *Sc*Ubp6 and *Hs*USP14, respectively, have been well characterised due to their important role in the ubiquitin-proteasome system (UPS; reviewed in Reyes-Turcu *et al.*, 2009; Reyes-Turcu and Wilkinson, 2009). Before entering the 20S proteolytic proteasome cylinder, proteins to be degraded must be deubiquitinated and unfolded by the lid portion of the 19S regulatory particle that associates with the 20S proteasome. Hence, the lid comprises subunits with DUB activity. Additionally, free DUBs associate with the proteasome to aid deubiquitination. The resulting free ubiquitin is recycled by the cell. *Sc*Ubp6 and its human counterpart *Hs*USP14 are the latter – free, proteasome-associated DUBs. The N-terminal ubiquitin fold of *Sc*Ubp6 and *Hs*USP14 is used to dock with the

proteasome lid, and this docking strongly stimulates the DUB activity (Leggett *et al.*, 2002; Hu *et al.*, 2005). In other words, the proteasome acts as a cofactor to these DUBs. It has also been shown that <sup>Hs</sup>USP14 trims poly-ubiquitin chains from the distal end (Hu *et al.*, 2005; Reyes-Turcu and Wilkinson, 2009).

<sup>Sc</sup>Ubp6 deletion results in reduced cellular pools of free ubiquitin and severely impinges upon growth in stress conditions (Leggett *et al.*, 2002). Congruent to this, <sup>Mm</sup>USP14 mutation resulted in reduced ubiquitin levels in mouse brain and ataxia (Wilson *et al.*, 2002; Crimmins *et al.*, 2006).

<sup>Sp</sup>Ubp6 has been studied during a research project on proteasome-associated fission yeast DUBs (Stone *et al.*, 2004). Most <sup>Sp</sup>Ubp6 was found to be bound to 26S proteasome, and to co-operate with different proteasome subunits to those found in humans and budding yeast. However, unlike <sup>Sc</sup>Ubp6 (Leggett *et al.*, 2002), <sup>Sp</sup>Ubp6 seems to have more of a structural role rather than functioning as the principal proteasome-associated DUB as is found in budding yeast (Stone *et al.*, 2004).

An important, recent bioinformatics study identified ubiquitin-like domains in numerous UBP/USP DUBs (Zhu *et al.*, 2007). In fact, the authors concluded that “[this] domain can be regarded as the most frequently occurring domain in the human USP family, after the characteristic protease core domain”. An N-terminal ubiquitin fold was found inbetween the DUSP and catalytic domains of <sup>Hs</sup>USP4<sup>UNP</sup>, <sup>Hs</sup>USP11, <sup>Hs</sup>USP15 (orthologous to <sup>Sp</sup>Ubp1 and <sup>Sp</sup>Ubp12) and <sup>Hs</sup>USP32 (Zhu *et al.*, 2007). An ubiquitin fold was also found embedded in the catalytic core (within the zinc finger) of these four DUBs, and also in <sup>Hs</sup>USP6, <sup>Hs</sup>USP19, <sup>Hs</sup>USP21, and <sup>Hs</sup>USP43. One N-terminal ubiquitin fold was found in each of <sup>Hs</sup>USP9X<sup>FAFX</sup>, <sup>Hs</sup>USP9Y<sup>FAFY</sup>, <sup>Hs</sup>USP24, <sup>Hs</sup>USP34, and <sup>Hs</sup>USP47. Finally, multiple C-terminal ubiquitin folds were found in <sup>Hs</sup>USP47, <sup>Hs</sup>USP40 and also <sup>Hs</sup>HAUSP<sup>USP7</sup>, which is the human orthologue of <sup>Sp</sup>Ubp21 and <sup>Sp</sup>Ubp22.

The authors of this study discuss the functional significance of the ubiquitin fold in UBP/USP superfamily DUBs. They propose two main roles: firstly, to modulate the deubiquitination of targets, and secondly, for binding to cofactors (Zhu *et al.*, 2007). With respect to the first role, they suggest that the domain may function to auto-inhibit DUB function by competing directly with ubiquitinated targets. They also propose that when integrated into the catalytic domain, the ubiquitin fold modulates the specificity of the DUB toward particular types of ubiquitination. They note that work with *Hs*USP15 showed that the cysteine residue that co-ordinated zinc in the catalytic domain abrogated poly-ubiquitin chain deubiquitination but not the deubiquitination of a ubiquitin-GFP fusion (Hetfeld *et al.*, 2005; Zhu *et al.*, 2007). Zhu *et al* imply that the ubiquitin fold that nests in the middle of the zinc finger likely has a role in target specificity as well – presumably guilt by association. With regard to the latter role, they suggest that the ubiquitin-like domain in a DUB may be used to dock with the proteasome akin to *Sc*Ubp6/*Hs*USP14. They further propose, due to the discovery of an ubiquitin fold in the N-terminus of *Hs*USP15, that the mechanism by which *Hs*USP15 associates with the CSN may be analogous to the docking of *Sc*Ubp6/*Hs*USP14 with the proteasome (Zhu *et al.*, 2007).

*Sp*Ubp21 and *Sp*Ubp22 both comprise an N-terminal meprin and tumour necrosis factor receptor associated factor (MATH) domain, in addition to a UBP/USP catalytic domain with a circularly permuted zinc finger. Published work on *Sp*Ubp21 and *Sp*Ubp22 links them to pre-mRNA splicing (Richert *et al.*, 2002). The human orthologue of these DUBs is the highly characterised *Hs*HAUSP<sup>USP7</sup>, which has a role in responses to DNA damage (reviewed in Brooks and Gu, 2006). In addition – as alluded to briefly above – four ubiquitin-like domains were found in the C-terminus of *Hs*HAUSP<sup>USP7</sup> (Zhu *et al.*, 2007). Furthermore, Zhu *et al* mention the existence of other ubiquitin-like domains within *Hs*HAUSP<sup>USP7</sup> that were not reported in the study due to scores below the significance threshold. *Sp*Ubp21, *Sp*Ubp22 and orthologues will be discussed extensively from Chapter 5 onwards.



### 3.7. Other *S. pombe* UBP/USP DUBs

*Sp*Ubp13 is the likely orthologue of *Sc*Pan2 and *Hs*USP52 (Kay Hofmann, personal communication). No work characterising *Sp*Ubp13 has been published. *Sp*Ubp13, *Sc*Pan2, and *Hs*USP52 share very similar domain structures – no domains have been identified within the N-terminus, but their C-termini each comprise a UBP/USP catalytic domain followed by an exonuclease domain, which is found in ribonucleases and replicative DNA polymerases. *Sc*Pan2 and *Hs*USP52 have both found to have roles in mRNA poly(A) tail editing (Boeck *et al.*, 1996).

However, more recently, a link between *Sc*Pan2 and the DNA damage response has been reported (Hammet *et al.*, 2002). DNA-damage Un-inducible 1 (*Sc*Dun1) is a serine/threonine protein kinase activated by DNA damage. It is important in the DNA damage response because it transcriptionally upregulates genes whose protein products are important in the response. Hammet *et al* showed that *Sc*Dun1 collaborates with the PAN to stabilise *rad5* mRNA, and that this was an important post-transcriptional mechanism action for DNA damage checkpoint effectors (Hammet *et al.*, 2002).

*Sp*Ubp11 comprises the UBP/USP catalytic motif from residues 36 to 341, plus a predicted transmembrane helix between residues 20 and 39. *Sc*Ubp1 is the likely orthologue of *Sp*Ubp11, despite the former being double the size of the latter (Kay Hofmann, personal communication). *Sc*Ubp1 comprises the UBP/USP catalytic motif from residues 98 to 735, plus a predicted transmembrane helix between residues 34 and 51. No work characterising *Sp*Ubp11 has been published, however *Sc*Ubp1 has been implicated in endocytosis (Schmitz *et al.*, 2005). In this study, they found that two independent myc-tagged forms of *Sc*Ubp1 were expressed from an integrated *ubp1-13myc* gene: a membrane-anchored form (*Sc*mUbp1) and a soluble version (*Sc*sUbp1). They found that *Sc*mUbp1 behaved like an integral membrane protein, and was most likely localised to the ER. The majority of

<sup>Sc</sup>Ubp1 was found in the soluble fraction, but a small triton-resistant fraction was also likely localised to membrane rafts or a large protein complex.

Overexpression of <sup>Sc</sup>Ubp1 stabilised the ATP-binding cassette (ABC) transporter <sup>Sc</sup>Ste6 (Schmitz *et al.*, 2005). <sup>Sc</sup>Ste6 is a multi-membrane spanning protein, is the yeast orthologue of <sup>Hs</sup>P-glycoprotein (encoded by the multi-drug resistance 1 [*MDR1*] gene) and transports the *S. cerevisiae* mating pheromone  $\alpha$ -factor (Raymond *et al.*, 1992). When degraded, <sup>Sc</sup>Ste6 is ubiquitinated and carried to the vacuole by the multi-vesicular body (MVB) system. Hence, the authors propose that <sup>Sc</sup>Ubp1 regulates this (Schmitz *et al.*, 2005).

No clear orthologue of either <sup>Sc</sup>Ubp1 or <sup>Sp</sup>Ubp11 is present in humans (Kay Hofmann, personal communication). However, evidence has been put forward suggesting that the human orthologue of <sup>Sc</sup>Ubp1, which is not identified, processes <sup>Hs</sup>ISG15<sup>UCRP</sup> precursors (Potter *et al.*, 1999). The authors purified the <sup>Hs</sup>ISG15<sup>UCRP</sup> precursor processing enzyme and sequenced a fragment of it, which was found to have “significant” homology with only <sup>Sc</sup>Ubp1 and a putative E3 called <sup>Hs</sup>RNF144A. However, there is no <sup>Hs</sup>ISG15<sup>UCRP</sup> ubiquitin-like protein in yeast and <sup>Sc</sup>Ubp1 cannot process <sup>Hs</sup>ISG15<sup>UCRP</sup> precursors *in vitro* (Potter *et al.*, 1999).

Aside of their catalytic motifs, five DUBs in *S. pombe*, <sup>Sp</sup>Ubp2, <sup>Sp</sup>Ubp3, <sup>Sp</sup>Ubp4, <sup>Sp</sup>Ubp9, <sup>Sp</sup>Ubp16, contain no other domains that are clearly defined in databases. However, research of the literature indicates that other domains are present in the budding yeast and human counterparts of some of these DUBs.

With 1141 amino acids (130.2 kDa), <sup>Sp</sup>Ubp2 is the largest DUB in *S. pombe*. <sup>Sp</sup>Ubp2 is the likely orthologue of <sup>Sc</sup>Ubp2, <sup>Hs</sup>USP25 and <sup>Hs</sup>USP28 (Kay Hofmann, personal communication). <sup>Sc</sup>Ubp2 is slightly larger at 1272 residues and shares significant homology with <sup>Sp</sup>Ubp2, and the UBP/USP catalytic domain occupies the entire C-terminal half of these proteins. <sup>Hs</sup>USP28 and <sup>Hs</sup>USP25 are slightly smaller than <sup>Sp</sup>Ubp2. Unlike <sup>Sp</sup>Ubp2 and <sup>Sc</sup>Ubp2, the catalytic domain takes a central

position in the primary sequence of *Hs*USP28 and *Hs*USP25. However, *Hs*USP25 and *Hs*USP28 share homology in their C-termini. The Pfam database also states that *Hs*USP25 comprises two ubiquitin-interacting motifs (UIM domains) in its amino-terminus.

*Sc*Rsp5 is an essential HECT E3 with pleiotropic functions. For example, it regulates fatty acid biosynthesis pathway components (Kaliszewski and Zoladek, 2008), and has been shown to ubiquitinate an RNA polymerase II subunit, directing it for proteasome-mediated degradation (Huibregtse *et al.*, 1997). *Sc*Ubp2, in combination with the UBA domain containing cofactor *Sc*Rup1, regulates *Sc*Rsp5 activity. Furthermore, *Sc*Rsp5 assembles lysine-63-linked poly-ubiquitin chains and *Sc*Ubp2–*Sc*Rup1 can disassemble them (Kee *et al.*, 2005). In another study, a *rsp5-1* mutant was found to be sensitive to hydroxyurea (HU), an agent that stalls replication forks (Lu *et al.*, 2008). HU inhibits ribonucleotide reductase (RNR) – the enzyme that converts ribonucleotides into deoxyribonucleotides for use by DNA polymerases. The authors explain this phenotype with evidence that *Sc*Rsp5 ubiquitinates the RNR subunit *Sc*Rnr2 (Lu *et al.*, 2008). The *Sc*Rsp5–*Sc*Ubp2–*Sc*Rup1 E3–DUB complex is involved in MVB pathway, and has been shown to control the endocytosis of an uracil permease called *Sc*Fur4 (Lam *et al.*, 2009).

As alluded to in Chapter 1, *Hs*USP28 has a role in signalling the presence of DNA damage. *Hs*USP28 interacts with *Hs*53BP1, *Hs*Claspin and *Hs*Mdc1, which react to the presence of DSBs, particularly caused by IR, in the genome and transduce the signal to checkpoint kinases (Zhang *et al.*, 2006). The function of this interaction is thought to protect these important proteins from unscheduled direction to the proteasome (Zhang *et al.*, 2006). The yeast orthologues of *Hs*53BP1 are *Sc*Rad9 and *Sp*Crb2<sup>Rhp9</sup>, and of *Hs*Claspin are *Sc*Mrc1 and *Sp*Mrc1. *Hs*USP28 has also been shown to be phosphorylated by the checkpoint kinases *Hs*ATM and *Hs*ATR (Matsuoka *et al.*, 2007), the yeast equivalents of which are known as *Sc*Tel1 and *Sp*Tel1, and *Sc*Mec1 and *Sp*Rad3, respectively.

<sup>Hs</sup>c-MYC is a transcription factor involved in promoting cell cycle progression. Following DNA damage, levels of <sup>Hs</sup>c-MYC reduce in the cell, which correlates with the responses to genetic insult that halt the cell cycle to allow repair. F-box WD repeat-containing protein 7 (<sup>Hs</sup>FBW7) is an F-box protein that forms a SCF E3 which ubiquitinates <sup>Hs</sup>c-MYC causing it to be degraded. <sup>Hs</sup>FBW7 is the substrate recognition portion of its SCF E3. <sup>Hs</sup>USP28 deubiquitinates nucleolar <sup>Hs</sup>c-MYC in the nucleolus by binding to the isoform of <sup>Hs</sup>FBW7 that is expressed in the nucleolus, <sup>Hs</sup>FBW7 $\alpha$  (Popov *et al.*, 2007). Hence, <sup>Hs</sup>USP28 stabilises <sup>Hs</sup>c-MYC by antagonising the <sup>Hs</sup>c-MYC–<sup>Hs</sup>FBW7 $\alpha$  interaction. <sup>Hs</sup>USP28 has also been shown to be a proto-oncogene – it is upregulated in colon and breast cancer cells (Popov *et al.*, 2007).

Little work has been published on <sup>Hs</sup>USP25 and its cellular function is not known. However, the UIM domains of <sup>Hs</sup>USP25 have recently shown to be sumoylated by multiple SUMO modifiers (Meulmeester *et al.*, 2008). In this interesting study, the authors state that the domain structure (from N- to C-termini) of <sup>Hs</sup>USP25 is as follows: UBA; UIM-1; UIM-2; UBP/USP; predicted coiled-coil domain. It was shown that <sup>Hs</sup>USP25 is able to efficiently hydrolyse both lysine-48-linked and lysine-63-linked tetra-ubiquitin. Furthermore, the UIM domains but not the UBA domain, were found to be important for efficient poly-ubiquitin chain hydrolysis, of either linkage. The authors found that <sup>Hs</sup>USP25 interacts more efficiently with SUMO-3 than SUMO-1, and a SUMO interaction motif (SIM) was found in UIM-1. Moreover, sumoylation of <sup>Hs</sup>USP25 was found to be dependent upon its SIM, and sumoylation of <sup>Hs</sup>USP25 by SUMO-3 is 2-3x more efficient than with SUMO-1. The sites of sumoylation were found to be lysine-99 and -141, which are within UIM-1 and next to UIM-2, respectively, and these sites do not fall within the canonical  $\psi$ KxE context known for sites of sumoylation. Taken together, the authors predicted that sumoylation of the UIM would negatively affect the DUB activity of <sup>Hs</sup>USP25, and this was found to be true with regard to tetra-ubiquitin. Hence, the authors conclude that sumoylation of <sup>Hs</sup>USP25 acts to control its DUB activity on poly-ubiquitin chains (Meulmeester *et al.*, 2008).

No investigations into *Sp*Ubp3 function have been published. The likely orthologues of this DUB are *Sc*Ubp3<sup>BIm3</sup> and *Hs*USP10 (Kay Hofmann, personal communication). *Sc*Ubp3<sup>BIm3</sup> is a 912 amino acid protein wherein the catalytic domain occupies the C-terminal half of the protein. Its function in autophagy has been investigated. *Sc*Ubp3<sup>BIm3</sup> binds its cofactor brefeldin A sensitivity 5 (*Sc*Bre5) – brefeldin A is a lactone-based antibiotic that inhibits GTPase proteins involved in particular autophagy pathways. The interaction between *Sc*Ubp3<sup>BIm3</sup> and *Sc*Bre5 was first shown to be important in stabilising *Sc*Sec23, which is important in the transport between the ER and the Golgi apparatus, from proteasomal degradation (Cohen *et al.*, 2003a). The *Sc*Ubp3<sup>BIm3</sup>–*Sc*Bre5 complex has also been shown to be important in NHEJ in response to a DSB-inducing agent called phleomycin (Bilsland *et al.*, 2007). Indeed, *Sc*Ubp3<sup>BIm3</sup> was originally identified because mutants were sensitive to the similar DSB-causing agent bleomycin (Moore, 1991). A crystal structure of the *Sc*Ubp3<sup>BIm3</sup>–*Sc*Bre5 complex has confirmed that it is the nuclear transport factor 2 (NTF2)-like domain of *Sc*Bre5 mediated the interaction with *Sc*Ubp3<sup>BIm3</sup> and that *Sc*Ubp3<sup>BIm3</sup> residues 208 to 211 were particularly important for this – mutation of these residues severely abrogated *Sc*Sec23 deubiquitination (Li *et al.*, 2007). Interestingly, the Pfam database suggests that the N-terminus of *Sc*Ubp3<sup>BIm3</sup> resembles the N-terminus of *Hs*USP21. *Sc*Ubp3<sup>BIm3</sup> has also been implicated in inhibiting silencing of transcription at silent mating type loci and telomeres (Moazed and Johnson, 1996).

*Hs*USP10 has not been well characterised. *Hs*USP10 is a 798 amino acid protein where, like *Sc*Ubp3<sup>BIm3</sup>, the catalytic domain occupies the C-terminal half of the protein. However, a poly(A)-binding protein (PABP)-interacting motif 2 (PAM2) has been found between residues 78 and 95 in the N-terminus of *Hs*USP10 (Albrecht and Lengauer, 2004). The function of this domain is not known, but it is particularly found in eukaryotic proteins that are involved in RNA metabolism processes (Albrecht and Lengauer, 2004).

The N-terminus of *Hs*USP10 has been shown to interact with *Hs*RAS GTPase activating protein (*Hs*RAS-GAP) SH3 domain binding protein 1 (*Hs*G3BP1), which was found to inhibit the DUB activity of *Hs*USP10 (Soncini *et al.*, 2001). *Hs*G3BP is thought to be important in *Hs*RAS signalling when *Hs*RAS is in its active conformation (Parker *et al.*, 1996). Residues 52 to 280 of *Hs*USP10 mediated the interaction with *Hs*G3BP1, but the molecular basis for the inhibition of *Hs*USP10 is not known (Soncini *et al.*, 2001). Interestingly, the human orthologues of *Sc*Bre5 are thought to be *Hs*G3BP1 and *Hs*G3BP2, and *Hs*USP10 has also been shown to interact with the latter (Cohen *et al.*, 2003b). Despite the inhibitory effect of *Hs*G3BP1 on *Hs*USP10, it has been proposed that *Hs*USP10 acts in an evolutionary conserved way to *Sc*Ubp3<sup>Bim3</sup> in regulating transport between the Golgi apparatus and the ER (Cohen *et al.*, 2003b).

The rhodanese domain is a sulfur-binding motif that has sulfurtransferase activity. Three UBP/USP DUBs in *S. cerevisiae*, *Sc*Doa4<sup>Ubp4</sup>, *Sc*Ubp5, and *Sc*Ubp7, possess this additional domain, whereas it is not represented in *S. pombe*. Having said this, bioinformatics suggest that *Sp*Ubp4 is the true orthologue despite the fact that it has lost its rhodanese domain (Kay Hofmann, personal communication). A human orthologue also exists, *Hs*USP8<sup>UBPY</sup> (Kay Hofmann, personal communication), which is important in the inhibition of endocytotic internalisation of EGFRs (Mizuno *et al.*, 2005). The crystal structure of the rhodanese domain of *Hs*USP8<sup>UBPY</sup> in combination with an E3 called neuregulin receptor degradation protein-1 (*Hs*NRDP1) has been solved (Avvakumov *et al.*, 2006). *Hs*USP8<sup>UBPY</sup> also harbours a microtubule interaction and transport (MIT) domain, as does the JAMM domain DUB *Hs*AMSH (Row *et al.*, 2007), which is discussed below. Both *Hs*USP8<sup>UBPY</sup> and *Hs*AMSH, compete for the same binding site on *Hs*STAM via their respective SBMs (*Hs*STAM-binding motifs), which has been investigated by a collaboration between the Urbé, Clague and Prior laboratories (Row *et al.*, 2006). *Sp*Ubp4 is significantly shorter than its human and budding yeast counterparts and an alignment suggests that there is no MIT domain present (data not shown). There are no *Sp*Ubp4 studies published in the literature.

The *S. cerevisiae* and *H. sapiens* orthologues of *SpUbp9* are *ScUbp9* and *ScUbp13*, and *HsUSP12<sup>UBH1</sup>* and *HsUSP46* (Kay Hofmann, personal communication). The orthology of *ScUbp9* and *ScUbp13* with *HsUSP12<sup>UBH1</sup>* has also been demonstrated independently (Hansen-Hagge *et al.*, 1998). The *S. cerevisiae* orthologues are ~750 residues, *SpUbp9* is 583 residues, and the human orthologues are ~370 residues. No cellular function has been ascribed to any of these proteins.

*SpUbp16* has no clear *S. cerevisiae* orthologues, but is orthologous to *HsUSP17*, *HsUSP36* and *HsUSP42* (Kay Hofmann, personal communication). *HsUSP17* is encoded by one member of a family of *USP17*-like genes that share over 95% homology (Burrows *et al.*, 2005). The *USP17* gene is found in a highly polymorphic, megasatellite repeat found on chromosomes 4 and 8, and the copy number varies between 20 and ~100. Thirteen *HsUSP17*-like proteins have been identified *HsUSP17A-J* and *HsDUB1-3* (Burrows *et al.*, 2005). Recently, the localisation of *HsRAS* has been shown to be controlled by the deubiquitinating activity of *HsUSP17* (Burrows *et al.*, 2009). Other DUBs in this family have been shown to be involved in cytokine signalling. For example, cells overexpressing *HsDUB-1* became blocked in G1 (Zhu *et al.*, 1996a), and *HsDUB-1* mRNA was shown to be induced by the cytokines interleukin-3 and -5 (Zhu *et al.*, 1996b).

Little is known about the other *SpUbp16* orthologues *HsUSP36* and *HsUSP42*. *HsUSP36* has been shown to be important in regulating the nucleolus (Endo *et al.*, 2009). *HsUSP42* has been implicated in acute myeloid leukemia (AML). The runt-related transcription factor 1 (*HsRUNX1<sup>AML1</sup>*) is important for normal haematopoiesis and is known to be mutant in various leukaemias (reviewed in Wang *et al.*, 2009). A study has shown that a mutation found in AML involves the fusion of *HsRUNX1<sup>AML1</sup>* with *HsUSP42* (Paulsson *et al.*, 2006).

### 3.8. *S. pombe* UCH DUBs

Two UCH DUBs are encoded in the *S. pombe* genome, *Sp*Uch1 and *Sp*Uch2 (Li *et al.*, 2000). The larger, latter DUB has a C-terminal extension in addition to the catalytic domain and hence is the orthologue of the proteasome-associated *Hs*UCH37<sup>UCH-L5</sup> (Li *et al.*, 2000). It has been shown that whilst a *uch2*Δ strain was found to be viable, *Sp*Uch2 was responsible for the majority of DUB activity at the proteasome (Li *et al.*, 2000; Stone *et al.*, 2004). Stone *et al.* concluded that, *in vivo*, other DUB enzymes compensate for the lack of *Sp*Uch2. This was found to be different to budding yeast, which has no *Hs*UCH37<sup>UCH-L5</sup> orthologue, where it has been shown that *Sc*Ubp6 confers the majority of proteasomal DUB activity (Leggett *et al.*, 2002). It has also recently been shown that *Hs*UCH37<sup>UCH-L5</sup> is a component of the INO80 chromatin remodelling complex and that this complex and the proteasome may act in concert to modulate DNA repair and transcription (Yao *et al.*, 2008b).

*Sp*Uch1 appears more similar to *Sc*Yuh1, *Hs*UCH-L1 and *Hs*UCH-L3 (Johnston *et al.*, 1997; Li *et al.*, 2000). *Hs*UCH-L3 *Hs*UCH-L1 is exclusively expressed in neurons (Wilson *et al.*, 1988), and has been found to be mutant in Parkinson's disease (PD) and altered in Alzheimer's disease (AD; reviewed in Setsuie and Wada, 2007).

In summary, increased amounts of oxidatively modified *Hs*UCH-L1 has been found in the brains of PD and AD patients, and decreased levels of soluble *Hs*UCH-L1 correlate with increased neurofibrillary tangles, within which *Hs*UCH-L1 is known to be present, have been found in AD. A toxic gain of function mutation, whereby isoleucine-93 is mutated to methionine in *Hs*UCH-L1, has been found in German family with PD. This mutation was shown to reduce the DUB activity by nearly half and caused the protein to be found in more cellular aggregates (Setsuie and Wada, 2007).



Interestingly, E3 functionality has also been ascribed to homo-dimerised <sup>Hs</sup>UCH-L1 (Liu *et al.*, 2002). Furthermore, a S18Y polymorphism is responsible for a reduced risk for PD and is dependent upon the E3 activity – <sup>Hs</sup>UCH-L1 with the S18Y mutation were less likely to form dimers compared to wild-type (Liu *et al.*, 2002).

A control mechanism for <sup>Hs</sup>UCH-L1 has been reported whereby lysines near the active site of <sup>Hs</sup>UCH-L1 are mono-ubiquitinated, which inhibits ubiquitin binding (Meray and Lansbury, 2007). The modification can be removed by auto-deubiquitination (Meray and Lansbury, 2007).

The remaining *H. sapiens*, and important BRCA1-associated, UCH DUB, <sup>Hs</sup>BAP1, is not thought to be orthologous to either <sup>Sp</sup>Uch1 or <sup>Sp</sup>Uch2.

### 3.9. *S. pombe* PPPDE DUBs

There is one PPPDE superfamily DUB known in *S. pombe* called <sup>Sp</sup>Hag1<sup>Mug67</sup>, which is the smallest DUB in *S. pombe* at only 201 amino acids (21.9 kDa). <sup>Sp</sup>Hag1<sup>Mug67</sup> is the orthologue of <sup>Hs</sup>PNAS4<sup>FAM152A</sup>, which was originally identified as a pro-apoptotic protein in the human acute PML cell line NB4 (Iyer *et al.*, 2004). It has been reported that the gene encoding <sup>Hs</sup>PNAS4<sup>FAM152A</sup> is activated early in response DNA damage (Zhang *et al.*, 2008a). There have been reports that it is important in development, and recent work using the zebrafish orthologue have confirmed this (Yao *et al.*, 2008a). Both <sup>Sp</sup>Hag1<sup>Mug67</sup> and <sup>Hs</sup>PNAS4<sup>FAM152A</sup> are very small and consist almost entirely of the papain-like PPPDE fold.

It is important to mention here that the *S. pombe* protein <sup>Sp</sup>Lub1 was also included in this study. With the benefit of hindsight, this inclusion was in error. Confusion in the literature implied that <sup>Sp</sup>Lub1, which has the orthologues <sup>Hs</sup>PLAP<sup>PLAA</sup> and <sup>Sc</sup>Ufd3<sup>Doa1</sup>, was a divergent PPPDE member. This was later found to be not the case.

In the study that identified the PPPDE superfamily, certain PPPDE eukaryotic family 1 members from fungi were found to have the PPPDE domain fused to a N-terminal thioredoxin domain followed by an uncharacterised C-terminal domain (Iyer *et al.*, 2004). The authors searched for other proteins that contained this domain and found the proteins human phospholipase A2-activating protein ( $Hs\_PLAP^{PLAA}$ ),  $Sc\_Ufd3^{Doa1}$  and  $Sp\_Lub1$ , and named it a PUL domain. These three proteins contain an N-terminal WD40  $\beta$ -propeller domain, an  $Hs\_PLAP^{PLAA}$  family ubiquitin binding (PFU) domain, followed by the C-terminal PUL domain. They do not contain the PPPDE papain-like motif that confers DUB activity to the true PPPDE members  $Sp\_Hag1$ ,  $Hs\_PNAS4^{FAM152A}$  and  $Hs\_FAM152B$ . Proteins with a conserved (WD40)<sub>n</sub>—PFU—PUL structure are found in most eukaryotes, although the number of WD40 repeats (n) varies. Work in *S. cerevisiae* revealed that the PFU and PUL domains of  $Sc\_Ufd3^{Doa1}$  were required for the formation of a ternary complex with  $Sc\_Cdc48^{p97/VCP}$  (discussed below) and ubiquitin, and the PFU and PUL domains were purported to be novel ubiquitin-binding motifs (Mullally *et al.*, 2006).  $Sc\_Ufd3^{Doa1}$  was originally found to be associated with the ubiquitin-fusion degradation pathway, and when  $Sc\_Ufd3^{Doa1}$  is absent, a depletion in cellular mono- and poly-ubiquitin results (Johnson *et al.*, 1995).

### 3.10. *S. pombe* OTU DUBs

No work on either  $Sp\_Otu1$  or  $Sp\_Otu2$  has been published.  $Sc\_Otu1$ , the *S. cerevisiae* orthologue of the former, however, has been found to interact with  $Sc\_Cdc48^{p97/VCP}$  and be involved in the OLE pathway of fatty acid biosynthesis (reviewed in Jentsch and Rumpf, 2006).  $Sc\_Cdc48^{p97/VCP}$  is a chaperone-like protein that binds and escorts poly-ubiquitinated proteins to the proteasome for degradation, particularly in the ER-associated protein degradation (ERAD) pathway.  $Sc\_Cdc48^{p97/VCP}$  is a barrel-shaped, hexameric, AAA ATPase (reviewed in Halawani and Latterich, 2006).  $Sc\_Ufd3^{Doa1}$  has been shown to interact with  $Sc\_Cdc48^{p97/VCP}$  and  $Sc\_Otu1$ , and  $Sc\_Ufd3^{Doa1}$  inhibits the function of  $Sc\_Cdc48^{p97/VCP}$  – it acts as a negative regulator of protein degradation (Rumpf and Jentsch, 2006). The same study showed that

*Sc*Otu1 was able to deubiquitinate lysine-48-linked poly-ubiquitin chains and interacts with *Sc*Cdc48<sup>p97/VCP</sup> via its N-terminus, which is alleged to comprise an UBX-like domain (Rumpf and Jentsch, 2006; Messick *et al.*, 2008). The UBX domain has been said to be similar to the UBA domain and an important binding module in the ERAD pathway (reviewed in Grabbe and Dikic, 2009a; Buchberger *et al.*, 2001). The UBX domain actually comprises an ubiquitin fold. *Sc*Otu1 has also been found to contain a C2H2 zinc finger at its C-terminus (Bohm *et al.*, 1997).

Figure 3.2 depicts an alignment between *Sc*Otu1 and its orthologues in *S. pombe*, *Sp*Otu1, and *H. sapiens*, *Hs*OTU1<sup>YOD1</sup>, which share about 30% identity with each other. This alignment is included here because no mention of the orthology between these DUBs was found in the literature. The cysteine and histidine residues in the C2H2 zinc finger are completely conserved between these organisms. Only weak homology was found at the N-terminus – the UBX domain is thought to occupy the first 86 residues of *Sc*Otu1 (Messick *et al.*, 2008).

The crystal structure of the C-terminus (residues 87 to 301) of *Sc*Otu1 has also recently been solved (Messick *et al.*, 2008), which, as expected, was found to be analogous to the crystal structure of its fellow OTU DUB *Hs*Otubain 2 (Nanao *et al.*, 2004). This study also showed that *Sc*Otu1 had very little activity on lysine-63 and -29-linked poly-ubiquitin chains and preferred to bind lysine-48-linked poly-ubiquitin chains over mono-ubiquitin.

*Sp*Otu2 and *Sc*Otu2 share 31% sequence identity, no work on either has been published. No mention of the human counterpart of these DUBs was found in the literature. A PSI-BLAST using the amino acid sequence of *Sc*Otu2 as a query revealed the closest human homologues to be *Hs*OTUD6B and *Hs*OTUD6A, which had E-values of  $4e^{-35}$  and  $3e^{-24}$  (very high significance), respectively, and share 56% identity with each other. Between the yeast and human proteins, *Sp*Otu2 and *Hs*OTUD6B were most similar with an identity of 32%, and *Sc*Otu2 and *Hs*OTUD6A were least similar at 25% identity. An alignment between with these four DUBs is

shown in Figure 3.3. Cellular roles for these DUBs have not been ascribed, although *Sc*Otu2 has been identified as a weak interactor of ribosomal complexes (Fleischer *et al.*, 2006).

### 3.11. *S. pombe* JAMM DUBs

Seven JAMM domain-containing proteins were found in *S. pombe*, two proteasome lid subunit DUBs, *Sp*Rpn11<sup>Pad1</sup> and *Sp*Rpn8; two translation elongation factors *Sp*eIF3f and *Sp*eIF3h; the CSN component *Sp*Csn5; and *Sp*Amsh<sup>Sst2</sup>. Like in *S. cerevisiae*, there is no known *Hs*CSN6 orthologue in *S. pombe*. According to the Hofmann and Glickman study, *Sp*Rpn11<sup>Pad1</sup>, *Sp*Csn5 and *Sp*Amsh<sup>Sst2</sup> contain the Zn<sup>2+</sup> co-ordinating MPN+ residues, whereas *Sp*Rpn8, *Sp*eIF3f and *Sp*eIF3h do not (Maytal-Kivity *et al.*, 2002). From the structural study outlined in Chapter 1, it is unlikely that the latter proteins function as active DUBs (Tran *et al.*, 2003).

An *Hs*AMSH paralogue called *Hs*AMSH-LP also exists – these proteins share 56% amino acid sequence identity (Kikuchi *et al.*, 2003). However, *Hs*AMSH-LP was found to be unable to interact with *Hs*STAM – the authors concluded that this was because a key residue in its SBM was a threonine, whereas it is a lysine in *Hs*AMSH. The consensus for interactions with *Hs*STAM, as exists in the SBM of *Hs*AMSH and *Hs*USP8<sup>UBPY</sup>, has been shown to be Px(V/I)(D/N)RxxKP (Kato *et al.*, 2000). Like *Hs*AMSH (McCullough *et al.*, 2004), *Hs*AMSH-LP has also been shown to be active on lysine-63-linked poly-ubiquitin chains (Nakamura *et al.*, 2006). Furthermore, a crystal structure of *Hs*AMSH-LP in complex with lysine-63-linked di-ubiquitin has been solved (Sato *et al.*, 2008).

*Sp*Amsh<sup>Sst2</sup> has been shown, congruent to its human counterpart, to function in the MVB pathway (Iwaki *et al.*, 2007). The authors found 31% identity between *Sp*Amsh<sup>Sst2</sup> and *Hs*AMSH at the amino acid level, but did not find the correct SBM required for *Hs*AMSH to interact with its substrate *Hs*STAM. An alignment shows that the SBM of *Sp*Amsh<sup>Sst2</sup> reads PxYTRxxEP (Figure 3.4). The *S. pombe* orthologue of

<sup>Hs</sup>STAM is <sup>Sp</sup>Hse1 (Iwaki *et al.*, 2007). Figure 3.4 also shows that <sup>Sp</sup>Amsh<sup>Sst2</sup> only contains two of the key residues found to be conserved in MIT domain-containing proteins (Row *et al.*, 2007), and the bi-partite nuclear localisation signal (NLS) and clathrin-binding site (CBS) are also not conserved (Kikuchi *et al.*, 2003; Nakamura *et al.*, 2006). However, the crystal structure of <sup>Hs</sup>AMSH-LP revealed two important inserts into the catalytic domain, which were thought to confer the specificity of this JAMM DUB to lysine-63-linked poly-ubiquitin chains, were said to be conserved in the *S. pombe* protein (Sato *et al.*, 2008). The inserts are boxed in Figure 3.4.

The seventh JAMM domain protein found in *S. pombe* is <sup>Sp</sup>Ssp42<sup>Cwf6/Prp8</sup>, which contains a further seven different domains. In the Hofmann and Glickman study, the Prp8 kinases also featured in their analyses as a more divergent class of JAMM domain-containing proteins. Some of the MPN+ residues were also conserved and Hofmann and Glickman could not decide whether to classify them as MPN+ or plain MPN. However, a study of *S. cerevisiae* suggests that Zn<sup>2+</sup> co-ordination by the JAMM domain in <sup>Sc</sup>Prp8 is not necessary for function, and attempts to demonstrate deubiquitinating activity were not successful (Bellare *et al.*, 2006). Whilst <sup>Sp</sup>Ssp42<sup>Cwf6/Prp8</sup> contains three out of the five MPN+ residues – <sup>Sc</sup>Prp8 only contains one – the upstream glutamate residue, thought to be involved in water de-protonation in the catalytic cascade, is conserved as a glutamine in all eukaryotic Prp8 orthologues aligned in the Hofmann and Glickman study, which includes <sup>Sp</sup>Ssp42<sup>Cwf6/Prp8</sup> (Maytal-Kivity *et al.*, 2002). It is worth noting here that the *S. pombe* protein <sup>Sp</sup>Cdc28<sup>Prp8</sup>, which is a DEAH-box RNA helicase involved in pre-mRNA splicing and cell cycle control, is not a Prp8-like kinase and does not contain a JAMM domain.

### 3.12. Summary of *S. pombe* DUBs

All superfamilies of DUBs are represented in *S. pombe*, with the exception of the MJD superfamily. However, the above review revealed that very little is known

about *S. pombe* DUBs. No DUBs have been implicated in PRR and no <sup>Hs</sup>USP1 orthologue was elucidated.

However, in almost all cases, a function has been assigned for a *S. cerevisiae* or *H. sapiens* orthologue. Out of these orthologues, none have been implicated directly in PRR, however some have involvement in DNA repair or responses to DNA damage. Furthermore, some have the ability to disassemble lysine-63-linked poly-ubiquitin chains. Specifically, <sup>Sc</sup>Ubp2 (Kee *et al.*, 2005), <sup>Hs</sup>AMSH (McCullough *et al.*, 2004; McCullough *et al.*, 2006), and <sup>Hs</sup>AMSH-LP (Nakamura *et al.*, 2006; Sato *et al.*, 2008) have been shown to have activity on this variety of chain.

### 3.13. Exclusion of *S. pombe* DUB Genes from this Study

Using bioinformatics and a literature review of *S. pombe* DUBs summarised above, the DUBs targeted in this study were chosen. The reasons for the choices were to create an optimal balance between the breadth of the screen and ability to follow up screen results. In other words, given the finite time frame of this research project, if too many proteins were targeted – even those that are unlikely to have functional ubiquitin isopeptidase activity – there may not be time to investigate the role of positive hits, i.e. candidate PCNA deubiquitinases, in PRR.

With regard to the UBP/USP, UCH, and OTU superfamily DUBs, all known members of these superfamilies in *S. pombe* were included. The likely non-functional UBP/USP superfamily DUB <sup>Sp</sup>Ubp13<sup>Pan2</sup>, was included because of a tenuous link to PRR. A study using *S. cerevisiae* showed that the levels of <sup>Sc</sup>Rad5 were higher in a *dun1Δ pan2Δ* double mutant, than in wild-type cells (Hammet *et al.*, 2002).

Of the JAMM domain DUBs, only <sup>Sp</sup>Amsh<sup>Sst2</sup> was included in this project. Many of the proteasome lid components are essential in baker's yeast (Giaever *et al.*, 2002) and are highly conserved between *S. cerevisiae* and *S. pombe* at the amino acid

level, hence it is highly likely that *rpn11Δ* *S. pombe* strains would not be viable. Hence, *Sp*Rpn11 was excluded from this project. Whilst, *Sp*Uch2 is also a proteasome lid component, it was decided to study this DUB because the null mutant was already known to be viable (Li *et al.*, 2000; Stone *et al.*, 2004), and due to the tenuous link to DNA repair mentioned above (Yao *et al.*, 2008b).

Whilst its MPN+ motif is very similar to that of the DUB *Sc*Rpn11, the *S. pombe* MPN+ protein *Sp*Csn5 has been shown to possess deneddylating activity (Cope *et al.*, 2002). Whilst a wide variety of functions for the CSN have been ascribed (reviewed in Schwechheimer, 2004), *S. pombe csn5Δ* cells have previously been investigated from a DNA damage response perspective in my laboratory and no interesting phenotypes have been noted (Mundt *et al.*, 2002). Therefore, *Sp*Csn5 was not included in this project.

Moreover, none of the ubiquitin-like proteases known to be encoded in the *S. pombe* genome, e.g. *Sp*Ulp1, a SUMO protease (Taylor *et al.*, 2002), and *Sp*Nep1, a deneddylase (Zhou and Watts, 2005), were included in this project.

As a result of these decisions, 22 *S. pombe* DUBs were included in this study. These proteins are listed in Tables 3.1 to 3.3, which detail important information for each DUB in addition to marking those DUBs that are not included in this project and those that are unlikely to be functional.

### 3.14. Assembly of a *S. pombe* DUB Deletion Library

It was planned to find PRR involved DUBs by using reverse genetics. The hypothesis was that a strain deficient in a DUB involved in PRR may show increased *Sp*PCNA ubiquitination, and may show sensitivity to UV due to upregulated, error-prone PRR. As a result, it was decided to assemble of a *S. pombe* DUB deletion library. Therefore, *S. pombe* strains singly deleted for each of the 22 selected DUB enzymes were collected. The strains were either created by

replacing the DUB gene with the gene that encodes nourseothricin-resistance, *nat1*, or obtained from collaborators. In the latter case, some double deletes were also added to the library.

### **3.15. Disruption of *S. pombe* DUB Genes by Integration of the Nourseothricin-Resistance Gene**

The wild-type haploid h<sup>-</sup> *S. pombe* strain “501” was transformed with DNA designed to disrupt *ubp7<sup>+</sup>*, *ubp8<sup>+</sup>*, *ubp11<sup>+</sup>*, *ubp13<sup>+</sup>*, *ubp14<sup>+</sup>*, *ubp16<sup>+</sup>*, *uch2<sup>+</sup>* or *ubp22<sup>+</sup>* genes by the integration of a gene encoding nourseothricin resistance (*nat1*). The *nat1* gene encodes nourseothricin acetyltransferase. The antibiotic nourseothricin (hereafter NAT) inhibits eukaryotic translation, and is produced naturally by certain bacteria. NAT acetyltransferase mono-acetylates NAT, which is inactivating. The construction of the *nat1* antibiotic cassette for use with *S. pombe* has been described (Hentges *et al.*, 2005).

Figure 3.5 depicts the strategy for amplification of an approximately 1200 bp PCR product containing the *nat1* gene flanked by 80 bp sequences with homology to the flanking chromosomal regions of the DUB gene to be disrupted. The strategy has previously been described (Baehler *et al.*, 1998).

### **3.16. Verification of Disrupted *S. pombe* DUB Genes by Polymerase Chain Reaction and Sequencing**

Correct disruption of DUB genes was verified by PCR at the DUB gene locus using isolated genomic DNA (gDNA) of each NAT-resistant strain. gDNA was isolated on a small scale, and primers were designed to anneal to flanking DNA of each DUB gene, in addition to oligonucleotides complementary to the *nat1* gene. The PCR strategy is depicted in Figure 3.6.



Figure 3.7 shows the successful verification results for strains *ubp13Δ::nat1*, *ubp7Δ::nat1*, *ubp22Δ::nat1*, and *ubp16Δ::nat1*. For each DUB, lanes from left to right, the first lane shows a multiplex PCR using all four primers described in Figure 3.6 in one reaction. A correctly disrupted strain revealed a distinctive pair of bands with 100-200 bp size difference. The multiplex PCR kit (Qiagen®) was found to be very quick and reliable. The second and third lanes show the products amplified using primers a and b on gDNA from disrupted and wild-type strains, respectively. With a congruent lane arrangement, Figure 3.8 shows the successful verification results for strains *ubp8Δ::nat1*, *ubp14Δ::nat1*, and *ubp11Δ::nat1* and Figure 3.9 for strains *ubp4Δ::nat1*, *ubp9Δ::nat1*, *uch2Δ::nat1*, and *amshΔ::nat1*.

Correctly sized PCR products resultant from an a+b reaction on gDNA from a NAT-resistant strain were also sent for sequencing. A primer with homology to the undisrupted DUB gene was also tested.

### 3.17. Verification of Disrupted *S. pombe* DUB Genes by Southern Analysis

In order to completely verify the disruption of DUB genes, gDNA was examined by Southern analysis. Disrupted haploids were grown on a large scale and chromosomal DNA was isolated and digested with selected restriction endonucleases, which was then run on an agarose gel and a Southern blot was performed. In all cases, wild-type genomic DNA was used digested with the same enzymes and used as a control. Blots were probed with radioactively-labelled DNA designed to specifically hybridise to chromosomal regions flanking a DUB gene.

Figures 3.10, 3.11 and 3.12 show the successfully verified knockout strains *ubp13Δ::nat1*, *ubp7Δ::nat1* and *ubp22Δ::nat1*, respectively. In each figure, part A shows the digestion strategy and the complementary site to which the probe was designed to hybridise. In part B, the results of the Southern analysis are shown – correctly-sized fragments of DNA resulted.

It was planned to also check for integration of the *nat1* gene into other loci. The blots probed with the gene flanking probe were to be stripped and re-probed with a probe complementary to a portion of the *nat1* gene. Despite repeated attempts, this proved to be unsuccessful, and unfortunately no further time for Southern analysis was available. It was decided that verification by PCR and sequencing was sufficient for this project.

### **3.18. Verification of *S. pombe* DUB Gene Disrupted Strains Obtained from Collaborators**

Strains disrupted for the DUB genes *ubp1*, *ubp2*, *ubp3*, *ubp12*, *otu1*, *otu2*, and *uch1* by integration of the *ura4* gene were kind gifts from Dieter Wolf. The strain *ubp12Δ::ura4* has been previously described (Zhou *et al.*, 2003; Wee *et al.*, 2005). Figures 3.13, 3.14 and 3.15 depict the successful verification of the deletion of the aforementioned DUB genes by PCR using a and b primers. These strains were also checked for independence from uracil for growth.

The strains *ubp21Δ::ura4*, *ubp22Δ::ura4* and a double delete resulting from a cross of these strains were obtained from Norbert Käufer, and have been previously described (Richert *et al.*, 2002). The *ubp21* and *ubp22* loci of these strains were also checked by PCR (Figure 3.16) and sequencing.

### **3.19. Sporulation of *S. pombe* Diploids Obtained from Bioneer**

For the following DUB genes: *ubp6<sup>+</sup>*, *ubp10<sup>+</sup>*, *ubp21<sup>+</sup>*, *lub1<sup>+</sup>* and *hag1<sup>+</sup>* disrupted strains were purchased from Bioneer in the form of *h<sup>+</sup>/h<sup>+</sup>* heterozygous, kanamycin-resistance gene (*kan*) disrupted diploids. Transformation of a plasmid called pON177, which contains the *h<sup>-</sup>* mating type information, was performed to allow sporulation. Resulting haploids were isolated by selection with the addition of

geneticin to growth media. Figures 3.17 to 3.18 depict the products from PCR using a and b primers.

### 3.20. Conclusions

With the exception of the MJD superfamily, the genome of *S. pombe* encodes 24 DUB enzymes. None of these DUBs nor orthologues in humans or budding yeast have been shown to be involved in PRR. It was decided to concentrate on 22 DUBs in this study via the exclusion of the deneddylase *Sp*Csn5 and the proteasome subunit *Sp*Rpn11<sup>Pad1</sup>.

The strategy for discovering PRR involved DUBs was via analysing the effects of DUB deficiency. It was hypothesised that increased *Sp*PCNA ubiquitination and/or UV sensitivity may result when a PRR DUB was not present in the cell. Hence a DUB deletion library was assembled. DUBs were disrupted or deletion strains collected from collaborators. All strains were successfully verified.

## Chapter 4: Screening of Deubiquitinating Enzyme Gene Disrupted *S. pombe* Strains

### 4.1. Introduction

Once a library of *S. pombe* strains containing single disruptions of selected DUB genes was assembled, a strategy for screening each of these strains for involvement in PRR, specifically the deubiquitination of  $^{Sp}$ PCNA, was developed. At this particular point in the project, there were significant concerns about redundancy among deubiquitinating enzymes. It was thought likely that multiple DUBs may be able to remove ubiquitin from  $^{Sp}$ PCNA; hence no phenotype may be observed when one DUB is removed from the cell because a second compensates. Hence, there was a high-throughput emphasis on these screening experiments with the expectation that double and triple deletes would be required. Every singly deleted strain was tested for sensitivity to UV as well as an increased level of ubiquitinated  $^{Sp}$ PCNA. The rationale for choosing these particular experiments will be explained here.

In order to test the *S. pombe* strains deleted for specific DUB genes for potential involvement in PRR, it was decided to assay for sensitivity to UV irradiation. It was hypothesised that when a DUB with the ability to deubiquitinate  $^{Sp}$ PCNA is absent from the cell, PRR may be constitutively active or at least over-promoted. In such a situation where PRR is poorly controlled, the frequency of error-prone PRR of DNA damage may increase. This could lead to an increase in the number of cells dying as a result of high levels of mutation or chromosomal damage. Thus a strain deleted for a DUB that is involved in  $^{Sp}$ PCNA deubiquitination may show increased sensitivity to UV irradiation compared to wild-type.

It was hypothesised that when a deubiquitinating enzyme that can act on  $^{Sp}$ PCNA is not present in the cell, an increase in  $^{Sp}$ PCNA ubiquitination would be observed.

Increased levels of mono-ubiquitinated <sup>Hs</sup>PCNA was clearly observed in human cells when <sup>Hs</sup>USP1 was depleted by siRNA-mediated knockdown (Huang *et al.*, 2006). Hence, using the knockout strains utilised in this study, the levels of <sup>Sp</sup>PCNA ubiquitination were analysed in a variety of scenarios. The levels of <sup>Sp</sup>PCNA ubiquitination were measured in asynchronous, actively growing cells, in asynchronous cells treated with UV, and in cells treated with hydroxyurea. Levels found throughout the cell cycle were also measured by blocking the cells in S-phase and then releasing to allow progression into the subsequent G2 and beyond.

## 4.2. Screen for Sensitivity to UVC Radiation

A high throughput “drop test” assay for measuring sensitivity of mutant strains to UV radiation was used (see section 2.4.14). This qualitative assay was verified using a quantitative colony-forming assay. A known number of cells from each strain were spread evenly onto agar, which was subsequently subjected to a specific dose of UV. Surviving colonies were counted after three days growth, the percentage survival at that dose was calculated and a graph of percentage survival versus UV dose was plotted for each strain.

The results of the qualitative UV sensitivity assay for *S. pombe* strains deleted for the OTU superfamily DUBs are shown in Figure 4.1. The density of cells of strain *otu1Δ* following different doses of UV was similar to that shown by wild-type cells. The strain *otu2Δ* demonstrates a slightly reduced density of cells following UV irradiation compared to wild-type, which is particularly evident in the 0-200 Jm<sup>-2</sup> gradient. However, the *pcn1-K164R* strain demonstrates a dramatically more UV-sensitive phenotype in comparison. Hence, it is likely that the cell concentration in the *otu2Δ* culture used in this assay was slightly lower than that of the other strains and that this strain is not UV-sensitive at all. Furthermore, a double deletion strain resulting from a cross of the two aforementioned OTU DUB deleted strains, *otu1Δ otu2Δ*, showed the same UV-sensitivity as wild-type cells. These observations were verified by the quantitative assay, shown in Figure 4.8.

The results of the qualitative UV sensitivity assay for strains deleted for the UCH superfamily DUBs are shown in Figures 4.2 and 4.6. The strains *uch1Δ* (Figure 4.2) and *uch2Δ* (Figure 4.6) were not sensitive to UV. This observation was verified by the quantitative assay, shown in Figures 4.8 and 4.10, respectively.

When the gene encoding the PPPDE superfamily DUB *<sup>Sp</sup>Hag1* was deleted, the qualitative assay did not reveal any clear UV sensitivity (Figure 4.3). *S. pombe* cells deficient in *<sup>Sp</sup>Lub1*, *lub1Δ::kan*, also did not show any significant UV-sensitivity (Figure 4.3). A strain containing a point mutant in the *lub1<sup>+</sup>* gene, hereafter *lub1-1*, which was obtained from Tokayoshi Kuno and has already been described (Ogiso *et al.*, 2004), was also tested and found not to have any UV sensitivity (Figure 4.3). These findings were verified by UV-survival (Figure 4.11).

The qualitative UV sensitivity assay results for the strain deleted for the JAMM superfamily DUB, *<sup>Sp</sup>Amsh*, are shown in Figure 4.4. The strain *amshΔ* was not found to be sensitive to UV. This observation was verified by the quantitative assay, shown in Figure 4.11.

The results of the qualitative UV sensitivity assay for *S. pombe* strains deleted for the UBP/USP family DUBs are shown in Figures 4.1, 4.2, 4.3, 4.4, 4.5 and 4.6. Strains *ubp1Δ*, *ubp2Δ*, *ubp3Δ*, *ubp4Δ*, *ubp6Δ*, *ubp8Δ*, *ubp9Δ*, *ubp10Δ*, *ubp11Δ*, *ubp12Δ*, *ubp13Δ*, and *ubp14Δ* did not demonstrate any detectable sensitivity to UV. This observation was verified by the quantitative assay, shown in Figures 4.7, 4.9, 4.10 and 4.11. The doubly deleted strain, *ubp1Δ ubp12Δ*, was also not sensitive to UV (Figures 4.2 and 4.7). However, results for *ubp16Δ* strains are discussed in section 4.4. Furthermore, screen results for strains deficient in the MATH-domain containing UBP/USP superfamily DUBs *<sup>Sp</sup>Ubp21* and/or *<sup>Sp</sup>Ubp22* can be found in chapter 5.

### 4.3. Screen for an Increase in <sup>Sp</sup>PCNA Ubiquitination

It was expected that in a strain deficient in a DUB with an ability to deubiquitinate <sup>Sp</sup>PCNA, an increase in <sup>Sp</sup>PCNA ubiquitination beyond that seen in wild-type cells would be observed. It was not certain whether this expected increase would be found in untreated cells or those treated with agents that induced <sup>Sp</sup>PCNA ubiquitination or both, as observed in human cells (Huang *et al.*, 2006). Unfortunately, as the aim of the project is to find a DUB that can act on <sup>Sp</sup>PCNA, no positive control for this assay could be employed. However, <sup>Sp</sup>PCNA ubiquitination cannot occur in the *pcn1-K164R* strain, hence allowing differentiation between bands on a Western blot that demonstrate real ubiquitinated species of <sup>Sp</sup>PCNA, as opposed to other types of covalent modification of <sup>Sp</sup>PCNA or proteins that the anti-<sup>Sp</sup>PCNA antibodies cross react with in certain circumstances.

Figures 4.12 and 4.13 depict the levels of <sup>Sp</sup>PCNA ubiquitination prior to and following treatment with hydroxyurea. HU is an inhibitor of ribonucleotide reductase, an enzyme that processes ribonucleotides into deoxyribonucleotides (dNTPs). DNA is a polymer of dNTPs, and hence in the presence of a sufficient concentration of HU, the cell exhausts dNTPs before S-phase is complete. It is thought that HU induces <sup>Sp</sup>PCNA ubiquitination because replication forks stall when dNTP pools are drained, thus mimicking the effect of a DNA polymerase stalling as a result of a lesion. The cell tries to activate PRR, which is likely to be a futile event because both TLS and the proposed template switch pathways require DNA synthesis steps and hence dNTPs. After 2.5 h in the presence of HU, all *S. pombe* cells within a culture become synchronised in S-phase, and more slowly-migrating bands representing mono-, di-, and tri-ubiquitinated <sup>Sp</sup>PCNA are evident. As shown in Figure 4.12 and 4.13, the strains *otu1Δ*, *otu2Δ*, *otu1Δ otu2Δ*, *ubp1Δ*, *ubp2Δ*, *ubp3Δ*, *ubp12Δ*, *ubp1Δ ubp12Δ* and *uch1Δ* do not show significant or reproducibly increased levels of ubiquitinated <sup>Sp</sup>PCNA in asynchronous cells prior to treatment (-) or following 2.5 h in HU (+).

At this point there were concerns about bleed-through of ubiquitinated  $^{Sp}$ PCNA species from the samples where ubiquitination had been induced, into the neighbouring untreated samples. Due to very high levels of ubiquitination in the treated lane, even very small amount of contamination into an untreated lane may result in a greater level of  $^{Sp}$ PCNA ubiquitination compared to wild-type. Therefore treated and untreated samples were kept separate henceforth, as is demonstrated in Figure 4.14. Here, the same strains as described above were mock treated (Figure 4.14 A) or treated with  $100 \text{ Jm}^{-2}$  of UV (Figure 4.14 B) to induce  $^{Sp}$ PCNA ubiquitination. No increase in  $^{Sp}$ PCNA ubiquitination relative to wild-type was seen, consistent with the data obtained with HU.

Figure 4.15 shows the levels of  $^{Sp}$ PCNA ubiquitination in *ubp10 $\Delta$*  prior to and following treatment with 10 mM of HU. There were reports that 50 mM HU is quite a high dose for *S. pombe*, hence this lower dose is used henceforth. For some reason, high background levels of  $^{Sp}$ PCNA ubiquitination were seen in the wild-type and *ubp10 $\Delta$*  cells prior to treatment. Variability in the levels of  $^{Sp}$ PCNA ubiquitination is seen in unchallenged, asynchronous cells and seems to depend upon various factors, for example the exact state of the cells, type of experiment and the length of exposure to light-sensitive film. In repeat experiments, *ubp10 $\Delta$*  has only shown wild-type levels of  $^{Sp}$ PCNA ubiquitination. As expected, after the addition of HU, an increase in the levels of  $^{Sp}$ PCNA ubiquitination is seen, but once again, at wild-type levels.

Figure 4.16 shows the levels of  $^{Sp}$ PCNA ubiquitination in the strains *ubp8 $\Delta$*  and *ubp14 $\Delta$*  in untreated cells and following HU treatment. Here, the lower panel shows a lower exposure of the Western blot to more clearly demonstrate the relative levels of unmodified  $^{Sp}$ PCNA between lanes. This additional blot was added as a result of concerns that poorly normalised lanes will significantly impact on the interpretation of data. Normalisation between strains was performed by utilisation of the same number cells for each sample. However, often a few cells were lost in



the TCA extraction procedure, and the extracts could not be further normalised by protein amount due to the incompatibility of the sample buffer in which the extracted protein was finally resuspended, most notably the presence of sodium dodecyl sulfate. Furthermore, mutant cells with a large cell phenotype may contain more  $^{Sp}$ PCNA and possibly more ubiquitinated  $^{Sp}$ PCNA. The usefulness of this lower exposure of unmodified  $^{Sp}$ PCNA can be seen in Figure 4.16, with reference to the *ubp14Δ* lanes. At first glance, there appears to be an increase in  $^{Sp}$ PCNA ubiquitination following HU damage compared to wild-type. However, there is clearly more unmodified  $^{Sp}$ PCNA in this lane, compared to the *ubp8Δ* and wild-type lanes, and there is no increased  $^{Sp}$ PCNA ubiquitination seen in the untreated *ubp14Δ* lane compared to wild-type where the loading is more even. Certainly, there is no apparent increase in  $^{Sp}$ PCNA ubiquitination in the *ubp8Δ* samples compared to wild-type.

Another important observation from Figure 4.16 is that the ubiquitinated species of  $^{Sp}$ PCNA appear as doublets. This is very interesting because prior to this point, a supported nitrocellulose membrane had been utilised for Western blotting. This type of membrane is more robust than unsupported nitrocellulose, but provides less resolution. Certainly unsupported nitrocellulose was utilised in the study that previously characterised  $^{Sp}$ PCNA ubiquitination in *S. pombe* (Frampton *et al.*, 2006). Unsupported nitrocellulose was utilised for the first time in Figure 4.16, and hence this is the most likely reason for the resolution of the ubiquitinated species into doublets. There are reports in the literature that human  $^{Hs}$ PCNA is phosphorylated (Wang *et al.*, 2006) and acetylated (Naryzhny and Lee, 2004), hence these other types of modification of *S. pombe*  $^{Sp}$ PCNA seem most likely. Certainly, Nedd8 and SUMO, other important cellular ubiquitin-like proteins that contain the ubiquitin superfold and are known protein modifiers, are too large to cause such a subtle shift in molecular weight. In Figure 4.16, the upper band in each doublet appears approximately 50% less intense than the lower band of the pair. With the assumption that  $^{Sp}$ PCNA firstly exists as either an entirely unmodified protein, or as a phosphorylated or acetylated (or modified by some other small

modifier) version, the latter is ubiquitinated 50% less often than unmodified <sup>Sp</sup>PCNA. However, there is no difference between the relative levels of each band in the doublet between untreated and HU treated samples, implying that this other form of <sup>Sp</sup>PCNA modification does not occur in response to replication fork stall. Experiments undertaken to make native extracts of ubiquitinated <sup>Sp</sup>PCNA doublets failed. The TCA extraction procedure is optimal for retaining labile covalent bonds, such as ubiquitination, however treatment with alkaline phosphatase, for example, is incompatible with this type of extract. Ubiquitinated forms of <sup>Sp</sup>PCNA are not successfully retained in native extracts, particularly following incubation on ice, which is required for phosphatase or acetylase treatment. Hence, it was not possible to identify this other, smaller type of <sup>Sp</sup>PCNA modifier due to the instability of this modification.

Interestingly, human mono-ubiquitinated <sup>Hs</sup>PCNA cannot be resolved into a plurality of bands (Simone Sabbioneda, personal communication). This may imply that phosphorylated or acetylated human <sup>Hs</sup>PCNA cannot be ubiquitinated or that the phosphorylation or acetylation of <sup>Hs</sup>PCNA occurs at low levels such that it cannot be detected as a molecular weight shift on a Western blot.

In Figure 4.17, the strains *ubp4Δ*, *ubp7Δ*, *ubp8Δ*, *ubp11Δ*, *ubp13Δ*, *ubp14Δ* were tested for an increase in <sup>Sp</sup>PCNA ubiquitination compared to wild-type following UV irradiation, and these strains were found to be indistinguishable from wild-type. The strains *amshΔ*, *lub1Δ*, *lub1-1*, *hag1Δ*, *ubp6Δ* and *uch2Δ* were also tested for PCNA ubiquitination levels after UV in Figure 4.18. The strains entirely deficient in <sup>Sp</sup>Lub1 seemed to show slightly lower levels of <sup>Sp</sup>PCNA ubiquitination, which fits with the proposition that the <sup>Sp</sup>Lub1 homologue in *S. cerevisiae* provides ubiquitin required for <sup>Sp</sup>PCNA ubiquitination (Lis and Romesberg, 2006). However, this effect was not seen following HU treatment of the mutant *S. pombe* cells.

It has been previously shown that in *S. pombe*, <sup>Sp</sup>PCNA becomes ubiquitinated every S-phase in unchallenged cells synchronised by elutriation (Figure 4.19,

Frampton *et al.*, 2006). It is not known why this occurs. However, it was decided to utilise this effect for the identification of DUBs with the ability to deubiquitinate <sup>Sp</sup>PCNA. Very low levels of <sup>Sp</sup>PCNA ubiquitination are seen in the intervening cell cycle phases implying active deubiquitination of <sup>Sp</sup>PCNA in these phases. Hence, it could be hypothesised that when a DUB with the ability to deubiquitinate <sup>Sp</sup>PCNA is absent from the cell, ubiquitination of <sup>Sp</sup>PCNA may persist outside of S-phase. In this experiment, cells were blocked for 2.5 h in hydroxyurea, which is sufficient time for all cells to become synchronised in S-phase. The cells were then spun down gently, washed, and resuspended in fresh growth media. Samples to assay for the levels of <sup>Sp</sup>PCNA ubiquitination were taken immediately and every fifteen minutes following release. Figure 4.20 shows the profile of <sup>Sp</sup>PCNA ubiquitination seen for wild-type cells following HU block and release. High levels of ubiquitination are immediately evident after the HU treatment. On release, the cells are now able to synthesise dNTPs and finish replicating their DNA, the levels of ubiquitinated <sup>Sp</sup>PCNA soon decrease in the subsequent cell cycle phases. After 60-90 minutes, an increase in ubiquitination is seen again, which represents the following S-phase. These timings are significantly different from those that occur when the cells are synchronised by elutriation. This is because the cells are chemically blocked in S-phase when HU is utilised, but the cells are still alive and they can still grow but the S-phase checkpoint prevents cell division, hence they elongate. When released into fresh media, these elongated cells rush through the cell cycle more quickly, sometimes without dividing completely. The morphology of wild-type cells when released from HU block is depicted in Figure 4.21. At 0 and 15 minutes, the cells are elongated. The fuzzy nuclei indicative of DNA replication can be seen in cells after 75 minutes, and segregation of DNA can be seen in some cells after 90 minutes. After 210 minutes, the cells are clearly back to normal morphology. However, the variation in morphology between cells at each time point in this Figure shows that there is significant variation in each cell's ability to recover from this block.

When a population of cells is synchronised by elutriation, the cells are simply sorted into cell cycle phases by cell size. Although this would be a significantly less invasive method for synchronising cells, it is not appropriate and too time-consuming for this screening assay. The addition of HU strongly activates PRR, whereas it is not known if the complete PRR machinery is recruited in unperturbed cells every S-phase, and deubiquitination activities may be affected.

Figure 4.22 depicts the results of the HU block and release assay for *ubp13Δ::nat1* and *ubp8Δ::nat1*. Firstly, it is worth noting that a slightly different profile is displayed by the wild-type control in this Figure, the loading of protein across this gel is not highly uniform and there is smearing where the gel has been over-loaded. However, all three strains show an increase in <sup>Sp</sup>PCNA ubiquitination following HU treatment, and high levels of ubiquitination exist after 0 and 30 minutes (although the *ubp13Δ::nat1* 0 minutes sample is clearly erroneously under-loaded), these levels decrease after 45 minutes, and decrease further after 60 and 75 minutes. At 120 minutes, the levels of <sup>Sp</sup>PCNA ubiquitination are high again, which represents the following S-phase, although clearly there has been a gel running and transfer problem on the far right-hand side of this blot that has affected the clarity of the *ubp8Δ::nat1* 120 minute lane. In general though, it is concluded that all three strains behave similarly and neither <sup>Sp</sup>Ubp13- or <sup>Sp</sup>Ubp8-deficient cells demonstrate unusual levels of <sup>Sp</sup>PCNA ubiquitination.

The strains *lub1-1*, *lub1Δ::kan*, *hag1Δ::kan* and *ubp6Δ::kan* were compared with wild-type following HU block and release (Figure 4.23). This blot is difficult to interpret due to loading and transfer problems. However, the kinetics of the general trend where <sup>Sp</sup>PCNA ubiquitination levels are high, reduce and then increase again, is similar to that of wild-type cells. Figure 4.24 depicts samples taken from *amshΔ* cells following HU block and release. Here, in order to make the blot less smeary, less protein has been loaded, so the blot is much cleaner. Once again, *amshΔ* cells seem to exhibit wild-type kinetics of <sup>Sp</sup>PCNA ubiquitination. The strain *ubp3Δ*, shown in Figure 4.25, also shows wild-type levels of <sup>Sp</sup>PCNA ubiquitination

following HU block and release. Following 2.5 h after the addition of HU (lanes labelled “HU”), *ubp3Δ* cells appear to show increased <sup>Sp</sup>PCNA ubiquitination compared to wild-type, however the lower panel, which shows a low exposure of unmodified <sup>Sp</sup>PCNA, suggests that the wild-type lanes HU and 0 minutes are under-loaded.

#### 4.4. *ubp16<sup>+</sup>* Deleted *S. pombe* Cells

Two different *ubp16Δ* strains were utilised in this study. The first strain was constructed by integration of the *nat1<sup>+</sup>* gene into haploid wild-type cells as described in Chapter 3. The second was a gift from a colleague in the Genome Damage and Stability Centre, Edgar Hartsuiker. The latter was derived from the Bioneer deletion library (described in Chapter 3). Hence this strain was derived from an *h<sup>+</sup>/h<sup>+</sup>* diploid where one allele of *ubp16<sup>+</sup>* had been replaced with a kanamycin-resistance gene. However, the *ubp16Δ::kan* was not acquired from Bioneer directly. The entire Bioneer deletion library of heterozygous diploids was gifted to the laboratory of Prof. Paul Nurse and, as part of a global study, all of the diploids were transformed with the pON177 plasmid (which contains the *h<sup>-</sup>* genetic information) and sporulated into haploids in a high-throughput fashion. This resultant haploid deletion library was then obtained by Dr. Hartsuiker.

Figure 4.26 depicts the UV sensitivity of *ubp16Δ::kan* and *ubp16Δ::nat1* measured by qualitative assay. Confusingly, the *kan*-marked deletion strain shows a dramatic UV sensitivity, whereas the *nat1*-marked strain is significantly more UV-resistant – up to nearly wild-type levels. The *ubp16Δ::kan* strain was also highly growth defective (data not shown). The two strains were also tested in parallel for PCNA ubiquitination following HU block and release, which is shown in Figure 4.27. The *kan*-marked strain demonstrated an ubiquitination profile following release from HU that is very similar to that of wild-type cells. The *nat1*-marked strain showed considerably and consistently higher levels of both unmodified and ubiquitinated <sup>Sp</sup>PCNA. The levels do decrease after 60 and 75 minutes in this strain, and the

levels of ubiquitination are very low in the non-HU treated sample (NT). However, the reasons for the dramatic difference between these strains were not known, and therefore the status of the *ubp16* locus in these strains was investigated.

The source of the problem appears to be the size of the *ubp16*<sup>+</sup> gene. PCR amplification of the wild-type gene with flanking primers revealed a product that was almost exactly the same size as the product expected for either the *kan*- or *nat1*-marked deletion strain (Chapter 3, Figure 3.7). However, for *ubp16*Δ::*nat1* gDNA, the multiplex PCR amplification suggests that the *nat1* gene is positioned within the context of a *ubp16*Δ locus (Chapter 3, Figure 3.7). However, resolution of the PCR product from an amplification across the *ubp16* locus of *ubp16*Δ::*nat1* gDNA with flanking primers revealed a doublet (Figure 4.28), implying that two different types of *ubp16* locus are found in this strain.

To help elucidate this the PCR products from wild-type, *ubp16*Δ::*nat1*, and *ubp16*Δ::*kan* gDNA amplification depicted in Figure 4.28 were digested with either *Nco*I or *Bgl*II. The restriction endonuclease *Nco*I, which cuts at the sequence CCATGG, was expected to digest the start codon of the kanamycin- and nourseothricin-resistance genes. Whereas *Bgl*II was expected to cut within flanking DNA found at the *ubp16* locus in a *ubp16*Δ::*nat1* strain, but would not cut the product obtained from the wild-type *ubp16*<sup>+</sup> locus. However, Bioneer were not prepared to explain how their strains were originally created, so the sequences flanking the *kan*<sup>+</sup> gene at the *ubp16* locus were not known in the *ubp16*Δ::*kan* strain. Therefore, the expected sizes of DNA fragments resulting from digestion of the *kan*<sup>+</sup> product with *Nco*I were unknown and it was not known whether *Bgl*II would cut at all. However, for the *ubp16*Δ::*nat1* product, ~1100 bp and ~800 bp fragments were expected following *Nco*I digestion, and ~1500 bp and ~400 bp fragments following *Bgl*II digestion. The wild-type *ubp16* locus was expected to resist digestion. The results of the digests are shown in Figure 4.29. Both the wild-type and *ubp16*Δ::*kan* products resisted digestion. The DNA fragment sizes resulting from *Nco*I digestion of the *ubp16*Δ::*nat1* product were as expected,

although the ~400 bp fragment of *Bgl*II digestion was not detected, but it may be hidden under the bromophenol blue dye front. However, more notably, a large proportion of the *ubp16Δ::nat1* product was resistant to digestion. As a positive control digest was not performed in parallel, partial digestion may explain these results, but the likelihood is that the lower of the doublet bands seen from Figure 4.28 is *ubp16Δ::nat1* at the *ubp16* locus and was successfully digested with *Nco*I and *Bgl*II, whereas the upper band results from amplification of a *ubp16*<sup>+</sup> locus, which is resistant to digestion.

In addition to these experiments, the *ubp16Δ::nat1* strain was also found to exhibit a larger cell size that is associated with diploids. Hence, it is presumed that following transformation and the application of these cells onto nourseothricin-containing agar, the cells diploidised. This is presumably achieved by replicating both a wild-type copy of genomic DNA in addition to a mutant version, hence the cells become heterozygous h<sup>-</sup>/h<sup>-</sup> diploids for *ubp16Δ::nat1*. Interestingly, when the *ubp10Δ::kan* diploids purchased from Bioneer were sporulated, a high-percentage of the kanamycin-resistant ‘haploids’ isolated actually turned out to be diploids. Both the *ubp10*<sup>+</sup> and *ubp16*<sup>+</sup> genes are about 2 kb in size when amplified with flanking PCR primers, which is about the same size of the *kan*<sup>+</sup> and *nat1*<sup>+</sup> genes. Hence, it is possible that homologous recombination is more efficient when the homologous fragment to be recombined is a similar size to that found in the genome, and means that the probability of the cell retaining both a wild-type copy of the gene, plus an integrated copy of the antibiotic-resistance gene to be retained by the cell simultaneously, is much higher.

Amplification of the *ubp16* locus of genomic DNA from the *ubp16Δ::kan* strain using flanking primers revealed a 2 kb band that could not be resolved into doublets (Figure 4.28) and was resistant to digestion (Figure 4.29). The morphology of this strain was a haploid-like size. However, sequencing of this product revealed that this strain had a wild-type *ubp16*<sup>+</sup> copy at the *ubp16* locus. Hence, it is likely that the kanamycin-resistance of this strain is resultant from

integration of the *kan*<sup>+</sup> gene elsewhere in the genome. For this reason, the *ubp16Δ::kan* strain was discarded.

With hindsight, it may have been more appropriate to create the deletion strains by transforming DNA into a diploid wild-type strain, selecting for nourseothricin-resistance heterozygotes, and then dissecting tetrads to recover *ubp16Δ::nat1* haploids. Certainly this method is known to be more efficient in isolating haploid deletion mutants without error. However, it is much more time-consuming, which makes it less relevant when an important aim of the study was to allow time for investigating positive hits following screening.

However, not all of the isolated nourseothricin-resistant *ubp16Δ::nat1* colonies that showed a correct multiplex PCR doublet were found to be diploids, in the region of 50% were haploids, and six of these haploids were tested for UV-sensitivity. The qualitative result of this is shown in Figures 4.30 and 4.31. The haploids are numbered clone 26, 28, 34, 39, 42 and 43, and the diploid labelled as *ubp16Δ::nat1* in Figures 4.26 to 4.29, which is used as a comparison, is now labelled as “*ubp16Δ::nat1* diploid”. Haploids 39, 42 and 43 demonstrated very subtle UV-sensitive phenotype, as verified in the quantitative assay shown in Figure 4.33, whereas the other three haploids were not found to be UV-sensitive (Figure 4.32). The haploids were found to be correctly knocked out (Figure 4.34).

## 4.5. Discussion

It can be concluded from the experiments completed in this chapter that deletion of a gene encoding a deubiquitinating enzyme, in general, has little effect on *S. pombe* cells. A very slight growth defect was found in *ubp2Δ* cells, but otherwise the strains grew normally and no obvious cytological defects were observed. The double deletions *ubp1Δ ubp12Δ* and *otu1Δ otu2Δ* also showed no phenotypes.



It is important to note that the qualitative assay for measuring the sensitivity of strains to UV irradiation was verified in all cases by quantitative survival curves, hence this assay is reliable for further use as a high throughput method.

DUBs have multiple roles in the cell, from maintaining pools of free ubiquitin in the cell, removing ubiquitin modifications from ubiquitinated proteins, and removing inhibitory ubiquitin chains from the proteasome (Amerik and Hochstrasser, 2004). Numerous examples of DUBs working in concert with E3s exist in the literature and given that 46 E3s were found in the *S. pombe* genome, it is tempting to hypothesise that DUBs have more redundant roles than E3s. It is plausible that *Sp*PCNA may be deubiquitinated by different DUBs in different cell cycle phases. Furthermore, certain DUBs may be responsible for deubiquitinating the lysine-63-linked poly-ubiquitin chain from mono-ubiquitinated *Sp*PCNA, and another set may be responsible for removing the mono-ubiquitin from lysine-164 of *Sp*PCNA. Moreover, it is possible that different DUBs may be associated with deubiquitinating *Sp*PCNA following the bypass of different types of DNA lesions, or whether other DNA damage response pathways are activated concurrently, for example, other DNA repair pathways or cell cycle checkpoints.

Creation of double and triple DUB knockout strains may aid the elucidation of DUBs that have the ability to deubiquitinate *Sp*PCNA. However, one strain, *ubp21Δ ubp22Δ* displayed both UV sensitivity and increased *Sp*PCNA ubiquitination. As a result of this it was decided to prioritise investigations into the role of *Sp*Ubp21 and *Sp*Ubp22 in PRR over any further screening experiments of *S. pombe* DUBs. The screen results, plus further experiments performed on *ubp21Δ ubp22Δ*, are discussed in the following chapter.

## Chapter 5: Characterisation of *S. pombe* Strains Deficient in <sup>Sp</sup>Ubp21 and/or <sup>Sp</sup>Ubp22

### 5.1. Introduction

Chapter 4 explains the screening process utilised for detecting potential PRR phenotypes of *S. pombe* strains deficient in specific DUb genes. The majority of these strains did not display any interesting phenotypes and hence it was decided not to study these further. However, a double deletion strain with the genotype *ubp21Δ ubp22Δ* demonstrated positive results for both types of screen assay – it showed both UV sensitivity and increased <sup>Sp</sup>PCNA ubiquitination and the data for this immediately follows. <sup>Sp</sup>Ubp21 and <sup>Sp</sup>Ubp22 share 40% amino acid identity and are likely to be paralogous. In addition to a UBP/USP superfamily catalytic domain, they both also contain a little-studied meprin and tumour necrosis factor associated factor homology (MATH) domain. The potential function of the MATH domain is then discussed, followed by analysis of the literature with respect to DUBs from other species that contain the MATH domain. Finally, phenotypes of the singly deleted strains *ubp21Δ* and *ubp22Δ*, as well as the double delete *ubp21Δ ubp22Δ* are investigated more thoroughly.

### 5.2. Screening Results for the Strains *ubp21Δ::ura4*, *ubp22Δ::ura4* and *ubp21Δ::ura4 ubp22Δ::ura4*

Qualitative assays for UV sensitivity of the strains *ubp21Δ::ura4*, *ubp22Δ::ura4* and *ubp21Δ::ura4 ubp22Δ::ura4*, as shown in Figure 5.1, revealed a redundant relationship between <sup>Sp</sup>Ubp21 and <sup>Sp</sup>Ubp22 in *S. pombe*. The double delete, resultant from a cross between the two aforementioned singly deleted strains, was UV sensitive, but the two singles were not. This implies that in the absence of one, the other can efficiently restore UV resistance up to wild-type levels. Interestingly,

the double delete was found not to be as UV-sensitive as the *pcn1-K164R* strain where the entire PRR pathway is nullified. This is to be expected, however, as constitutively active PRR, such as may occur when a *Sp*PCNA DUB is absent from the cell, is unlikely to cause UV sensitivity beyond that of when PRR cannot be carried out at all.

Figure 5.2 shows *Sp*PCNA ubiquitination in the three aforementioned *ura4* disrupted strains prior to and following HU treatment. The double delete clearly shows *Sp*PCNA ubiquitination in unchallenged cells, and this level seems to increase further after exposure to HU for 2.5 h. This implies that a deficiency in both *Sp*Ubp21 and *Sp*Ubp22 results in high levels of *Sp*PCNA ubiquitination and this basal level increases further upon active ubiquitination of *Sp*PCNA to induce PRR, such as in the presence of HU. The *ubp22Δ::ura4* strain also seems to show higher levels of *Sp*PCNA ubiquitination after HU treatment. However, the panel depicting a low exposure of unmodified *Sp*PCNA shows more *Sp*PCNA loaded in this lane compared to wild-type, which may explain this observation.

However, it may be that only a sub-population of the cells demonstrate *Sp*PCNA ubiquitination – perhaps only cells in a particular cell cycle phase. Therefore the HU block and release experiment was performed, and *Sp*PCNA ubiquitination levels in various cell cycle phases analysed. This experiment is depicted in Figure 5.3. Very clearly, the doubly deleted strain shows a distinctly different *Sp*PCNA ubiquitination profile compared to that of wild-type cells. The untreated lane shows the background level of *Sp*PCNA ubiquitination characteristic of this strain. Following HU treatment, *Sp*PCNA ubiquitination levels are as bold and strong as seen in Figure 5.2. This high level decreases, but the ubiquitination seems to persist for a much greater length of time than in wild-type cells. Most interestingly, however, 75 minutes after release from HU, there is little or no *Sp*PCNA ubiquitination. There are a variety of plausible explanations for this. Given that the levels of *Sp*PCNA ubiquitination do not persist at a constant high level and there is some decrease, it is likely that another, unknown DUB can effect *Sp*PCNA

deubiquitination, and may even be upregulated in response to a deficiency in  $^{Sp}Ubp21$  and  $^{Sp}Ubp22$ . It is plausible that different DUBs control  $^{Sp}PCNA$  ubiquitination during different cell cycle phases.  $^{Sp}Ubp21$  and  $^{Sp}Ubp22$  may maintain pools of deubiquitinated  $^{Sp}PCNA$  during S-phase, whereas during G2, for example, a broader cohort of enzymes capable of deubiquitinating  $^{Sp}PCNA$  may be employed. Alternatively, the disappearance of ubiquitinated  $^{Sp}PCNA$  may be the result of degradation. However, it is important to note here that the lower exposure of unmodified  $^{Sp}PCNA$  suggests that there is less  $^{Sp}PCNA$  loaded into this lane.

The singly deleted strains show less easily interpretable  $^{Sp}PCNA$  ubiquitination levels following HU block and release. There appears to be a higher background level of  $^{Sp}PCNA$  ubiquitination than in the wild-type lanes, and the blot is generally less clean. One of the reasons for this is smearing, which can be most clearly seen in the *pcn1-K164R* lanes, and is thought to be the result of over-loading of the gel with protein. However, the general pattern seen for the *ubp21Δ::ura4* and *ubp22Δ::ura4* strains is most similar to that of the wild-type profile. There is little or no  $^{Sp}PCNA$  ubiquitination in the untreated lanes, ubiquitination increases dramatically following HU treatment and this is most evident after 30 minutes. However, this level of ubiquitination is significantly reduced after 45 minutes. These lanes alone, when contrasted with the  $^{Sp}PCNA$  ubiquitination levels demonstrated in the double delete, clarify the significance of the persistence and increased levels of  $^{Sp}PCNA$  ubiquitination seen in the double delete. They also agree with the UV sensitivity data that implies that  $^{Sp}Ubp21$  and  $^{Sp}Ubp22$  can act redundantly, in that there is little observable phenotype when either  $^{Sp}Ubp21$  or  $^{Sp}Ubp22$  is absent.

Upon reflection at this point in the project, it was decided to exclusively investigate further the potential involvement of  $^{Sp}Ubp21$  and  $^{Sp}Ubp22$  in PRR. Some very interesting data emerged from these experiments, which will be presented and discussed in this and the following chapters. Therefore, an analysis of what is already known about  $^{Sp}Ubp21$  and  $^{Sp}Ubp22$ , the human homologue of these DUBs

and the MATH domain will be provided at this point in order to properly introduce the remainder of this thesis.

### 5.3. Previous Studies, Homology and Domains of *Sp*Ubp21 and *Sp*Ubp22

*Sp*Ubp21 and *Sp*Ubp22 are discussed in one publication in the scientific literature (Richert *et al.*, 2002), which links these DUBs to pre-mRNA splicing, the process whereby intron sequences are removed and the remaining exons spliced together to generate mature mRNA. This process is carried out by a large complex called the spliceosome, which, in *S. pombe*, consists of RNA and more than 80 proteins (reviewed in Kuhn and Kaufer, 2003). Richert *et al* found that *Sp*Ubp21 is able to deubiquitinate a mutant version of an important kinase involved in pre-mRNA splicing, called *Sp*Prp4. The residues ALKHP in *Sp*Prp4 are conserved in cyclin-dependent and mitogen-activated protein kinases (MAPKs), and mutation of these residues to SSKLP resulted in loss of function of this kinase and sensitivity to growth at 36°C. Transformation with a plasmid containing *ubp21<sup>+</sup>* was found to suppress this. The deubiquitinating activity of *Sp*Ubp21 was found to stabilise the mutant version of *Sp*Prp4. It is thought that the growth defect of the *Sp*Prp4 mutant is caused by abnormally low levels of *Sp*Prp4, and that overexpression of *Sp*Ubp21 prevents proteasomal degradation of mutant *Sp*Prp4. Hence, they conclude that *Sp*Ubp21 is likely to stabilise wild-type *Sp*Prp4 *in vivo*. This implies that *Sp*Ubp21 has the capability for deubiquitinating lysine-48-linked poly-ubiquitin chains, but, of course, this does not preclude an ability to deubiquitinate poly-ubiquitin with different linkages. The authors also show that the double deletion, *ubp21Δ::ura4 ubp22Δ::ura4*, which is the same doubly deleted strain utilised in this study, is temperature sensitive (Richert *et al.*, 2002). Unfortunately, confusing wording in the text of this publication implies that deleting both *ubp21<sup>+</sup>* and *ubp22<sup>+</sup>* in *S. pombe* is lethal. However, it is clear that what the author actually meant is that the double delete cannot grow at 20°C and 36°C – the corresponding Figure clearly depicts

growth at the standard *S. pombe* growth temperature, 30°C. This misunderstanding has led to most public sequence databases stating that the double delete is lethal.

*Sp*Ubp21 and *Sp*Ubp22 are large DUB enzymes and are both UBP/USP superfamily members. They are also very occasionally referred to as *Sp*Ubp15 and *Sp*Ubp5 and are 1129 and 1108 amino acids in length, which corresponds to a molecular weight of approximately 130.8 and 128.6 kDa, respectively. They both contain two known protein domains in their N-terminal halves: a MATH domain, and a UBP/USP superfamily catalytic domain C-terminal to this. No clear protein domains have been assigned to the C-terminal half of these DUBs. The domains in *Sp*Ubp21 and *Sp*Ubp22 are positioned very similarly (Figure 5.4) and Ubp21 is only 1.9% bigger (21 amino acids). An alignment of the amino acid sequence of these two DUBs revealed 40% sequence identity (Figures 5.5 and 5.6), which is very high and, in agreement, most public sequence databases state that *Sp*Ubp21 and *Sp*Ubp22 are likely to be paralogues of each other.

The catalytic domain of *Sp*Ubp21 and *Sp*Ubp22 is boxed in red in Figures 5.5 and 5.6. UBP/USP DUBs are cysteine proteases wherein cysteine, histidine and aspartate residues form a catalytic triad, which are highlighted in blue in the alignment shown in Figures 5.5 and 5.6. The yellow highlighted residues in this Figure are other important amino acids for catalysis that are conserved in UBP/USP superfamily DUBs (Amerik and Hochstrasser, 2004).

The meprin and tumour necrosis factor receptor associated factor homology (MATH) domain, as its name suggests, was originally found in a class of mammalian metalloproteases called meprins, which are involved in development, as well as tumour necrosis factor receptor associated factors (TRAFs) that are involved in cellular signal transduction. Later, the MATH domain was also found in other protein classes, most of which contain domains that are involved in ubiquitination or deubiquitination. Bioinformatical analyses reveal that most

organisms contain one UBP/USP superfamily DUB with a MATH domain at the N-terminus, although a few organisms, like *S. pombe*, contain two. In published MATH domain structures, eight anti-parallel  $\beta$ -sheets come together to form a distinctive, partially twisted  $\beta$ -sandwich structure. The function of the MATH domain is not well understood, however in meprins and TRAFs it is proposed to be involved in oligomerisation – TRAFs and meprins are fundamentally dependent on oligomerisation for their activity. Having said this, it has been reported that the residues known to be interfacial in other MATH domain proteins are not conserved among MATH domain DUBs (Sunnarhagen *et al.*, 2002). The MATH domains of *Sp*Ubp21 and *Sp*Ubp22 are boxed in green in Figure 5.5. Interestingly, compared to *Sp*Ubp22, *Sp*Ubp21 has an extra 22 residues in the middle of the MATH domain sequence (Figure 5.5), whereas these DUBs align almost exactly throughout the rest of the amino acid sequence. Therefore this extra section accounts for the slightly bigger size of *Sp*Ubp21. The functional significance of this is not known, but will be discussed further in Chapter 7 when the structure of the MATH domains found in *Sp*Ubp21 and *Sp*Ubp22 are predicted. First, the MATH domain, and the proteins within which it is found, will be discussed more thoroughly.

#### **5.4. Meprin and Tumour Necrosis Factor Receptor Associated Factor (MATH) Domain**

The MATH (meprin and tumour necrosis factor [TNF] receptor [TNFR] associated factor [TRAF]) domain, was first coined in 1996 and is thought to be involved in protein-protein interactions between other MATH domain containing proteins (Uren and Vaux, 1996) to allow hetero- or homo-oligomerisation.

Meprins are zinc-dependent metalloendopeptidases comprising homo- or hetero-oligomers of  $\alpha$  and  $\beta$  subunits. Each subunit contains an astacin family metalloprotease domain, meprin/A5 protein/protein-tyrosine phosphatase  $\mu$  (MAM) domain, MATH domain and an “after MATH” (AM) domain (Bertenshaw *et al.*,

2003). Meprins are directed to the endoplasmic reticulum following biosynthesis, can either be in membrane-bound form or secreted extracellularly, cleave a wide variety of polypeptides such as growth factors and hormones, and are highly expressed in microvillar membranes of mammalian kidney and intestine (Johnson and Bond, 1997). The MAM and MATH domains are particularly important for oligomerisation and it has been demonstrated that rat  $\alpha$  and  $\beta$  subunits oligomerise quite differently, as shown in Figure 5.7 (Bertenshaw *et al.*, 2003).

TNFRs are membrane bound receptors that bind the extracellular growth factor TNF $\alpha$ . The majority of TNFRs transduce their signal to downstream signalling cascades via TRAF proteins and this results in activation of nuclear factor kappa B (NF- $\kappa$ B) transcription factors, mitogen-activated protein kinases (MAPKs) and pro-apoptotic death signalling. The interleukin-1 receptor and Toll-like receptors, which are important for the immune and inflammatory systems, also use TRAFs for signal transduction. In mammals, six TRAFs have been identified so far (reviewed in Arch *et al.*, 1998) and all TRAFs contain a MATH domain at their C-terminus. With the exception of TRAF1, all TRAFs contain a RING finger domain at their N-terminus and a stretch of zinc fingers that varies in length. TRAFs seem to function by recruiting other proteins, and each other, to signalling complexes (Arch *et al.*, 1998). TRAF oligomerisation via the MATH domain affects TRAF localisation and function, and many TRAF signalling functions are mediated through the RING domain (Au and Yeh, 2007). TRAF autoubiquitination has been reported (Petroski *et al.*, 2007), but how the ubiquitin-protein ligase activity of TRAF proteins effect TRAF function is not well understood.

## 5.5. Other MATH Domain Containing Proteins

In 1996 the MATH domain was first identified (Uren and Vaux, 1996). However, the MATH domain was only found in proteins **other than** TRAFs and meprins in 2001 (Zapata *et al.*, 2001). Using the position-specific iterative basic local alignment search tool (PSI-BLAST) bioinformatics program at the National Center for



Biotechnology Information, the Reed group and collaborators found novel MATH domain-containing proteins using the MATH domain of human <sup>Hs</sup>TRAF2 as a query. Three human cDNAs were selected as containing significant homology, which encoded the proteins <sup>Hs</sup>MUL, <sup>Hs</sup>SPOP and <sup>Hs</sup>HAUSP<sup>USP7</sup>.

The *MUL* gene was identified in 2000 as being mutant in mulibrey (muscle-liver-brain-eye) nanism, an autosomal recessive disorder with the typical characteristics; severe growth failure, hepatomegaly, muscle hypotonia, skull abnormality, yellow dots in the eyes, endocrine gland hypoplasia that results in hormone deficiency and, occasionally, kidney tumours (Avela *et al.*, 2000). It is thought that the <sup>Hs</sup>MUL protein has highly pleiotropic functions because several tissues of mesodermal origin are affected in mulibrey nanism (Perheentupa *et al.*, 1973). <sup>Hs</sup>MUL, more commonly known as tripartite motif-containing protein 37 (<sup>Hs</sup>TRIM37), contains three domains at the N-terminus that are known collectively as the RING-B-box-Coiled-coil (RBCC) domain, a MATH domain, and two Asp-Glu-Ser-rich sequences that have homology to several transcription factors (Avela *et al.*, 2000). Whilst the RING portion of the RBCC domain of <sup>Hs</sup>MUL has been shown to function as a *bona fide* E3 that is capable of auto-ubiquitination, substrates of MUL are yet to be identified (Kallijarvi *et al.*, 2002). The RBCC family of proteins have been reviewed (Meroni and Diez-Roux, 2005; Torok and Etkin, 2001).

The SKP1/CUL1/F-box (SCF) complex is the canonical RING finger E3, wherein CUL1 is utilised as a scaffold subunit to interact with the RING finger subunit, ROC1 (reviewed in Willems *et al.*, 2004). A variety of other cullins exist, including CUL3, which is thought to be involved in regulating cell cycle checkpoints, but the other subunits of this E3 complex are not yet well understood. Human speckle-type poxvirus and zinc finger (POZ) protein (<sup>Hs</sup>SPOP) contains an N-terminal MATH domain followed by a Bric-a-brac/Tramtrack/Broad complex (BTB) domain, which is also known as a POZ domain. The BTB domain is thought to inhibit DNA binding and aid specific protein-protein interactions (Bardwell and Treisman, 1994). <sup>Hs</sup>SPOP has been shown to promote the ubiquitination of the anti-apoptosis protein

<sup>Hs</sup>DAXX (death domain-associated protein) by recruiting <sup>Hs</sup>DAXX to <sup>Hs</sup>CUL3 (Kwon *et al.*, 2006). Poly-ubiquitinated <sup>Hs</sup>DAXX is directed to the proteasome for degradation, and low-levels of <sup>Hs</sup>DAXX trigger apoptosis and repressed <sup>Hs</sup>p53-dependent transcription (Kwon *et al.*, 2006). An N-terminally truncated <sup>Hs</sup>SPOP mutant with an intact BTB domain and C-terminus, but no MATH domain, could still interact with <sup>Hs</sup>CUL3 (Kwon *et al.*, 2006), but as <sup>Hs</sup>SPOP has been shown to interact with <sup>Hs</sup>DAXX via its MATH domain (La *et al.*, 2004), <sup>Hs</sup>DAXX degradation was abrogated (Kwon *et al.*, 2006). Hence, <sup>Hs</sup>SPOP acts as an adaptor protein – the BTB domain recruits the E3 functionality, and the MATH domain selects appropriate targets for degradation.

## 5.6. The Human Meprin and Tumour Necrosis Factor Receptor Associated Factor (MATH) Domain Deubiquitinating Enzyme

Herpes virus-associated ubiquitin-specific protease or ubiquitin-specific protease 7 (<sup>Hs</sup>HAUSP<sup>USP7</sup>) is a UBP/USP superfamily DUB with a MATH domain at the N-terminus and is the human orthologue of <sup>Sp</sup>Ubp21 and <sup>Sp</sup>Ubp22. It is 1102 amino acids in size, corresponding to a molecular weight of 128.3 kDa, and shares 31% identity to <sup>Sp</sup>Ubp21 and 29% identity to <sup>Sp</sup>Ubp22. An alignment of <sup>Hs</sup>HAUSP<sup>USP7</sup> with <sup>Sp</sup>Ubp21 and <sup>Sp</sup>Ubp22 is shown in Figure 5.8 and 5.9. <sup>Hs</sup>HAUSP<sup>USP7</sup> is the most highly characterised MATH domain DUB known and has been assigned to several interesting cellular functions related to cell cycle control, DNA damage responses and carcinogenesis.

The most characterised function of <sup>Hs</sup>HAUSP<sup>USP7</sup> is its ability to stabilise the key tumour suppressing gatekeeper protein, <sup>Hs</sup>p53, which was introduced in Chapter 1. Following DNA damage, <sup>Hs</sup>p53 becomes phosphorylated preventing interaction with a RING finger E3 called mouse double minute 2 (<sup>Hs</sup>MDM2), also known as <sup>Hs</sup>HDM2 in human cells, which poly-ubiquitinates <sup>Hs</sup>p53 directing it for proteasomal degradation. Stabilisation of <sup>Hs</sup>p53 has a fundamental impact on DNA damage signalling. After DNA damage, <sup>Hs</sup>p53 is able to effect cell cycle halt to enable repair

before the lesions are replicated into mutations, or damaged genetic material is transferred into daughter cells. However, in other cell types, DNA damage causes  $Hs$ p53 to direct the cell into apoptosis, which also avoids tumourigenesis. Clearly regulation of the activity of  $Hs$ p53 is fundamental, so the cell employs a variety of methods to control the levels of this tumour suppressor –  $Hs$ p53 levels are also modulated by its acetylation. Deubiquitination by  $Hs$ HAUSP<sup>USP7</sup> appears to be another method of stabilising  $Hs$ p53. However, confusingly,  $Hs$ HAUSP<sup>USP7</sup> has also been shown to stabilise  $Hs$ MDM2.

The potential role of  $Hs$ HAUSP<sup>USP7</sup> in the  $Hs$ p53 pathway was first noted by the Gu research group when  $Hs$ HAUSP<sup>USP7</sup> was found, by affinity-purification and mass spectrometry, to interact with  $Hs$ p53 (Li *et al.*, 2002). The overexpression of  $Hs$ HAUSP<sup>USP7</sup> was clearly found, both *in vitro* and *in vivo*, to abolish higher-molecular weight ladders of  $Hs$ p53 and to increase unmodified  $Hs$ p53 levels, even in the presence of cycloheximide. However,  $Hs$ p53 levels were unchanged when the catalytic cysteine of  $Hs$ HAUSP<sup>USP7</sup> was mutated to a serine. Due to the highly stable interaction between HAUSP<sup>USP7</sup> and  $Hs$ p53, the authors imply that HAUSP<sup>USP7</sup> not only deubiquitinates  $Hs$ p53, but maintains  $Hs$ p53 in deubiquitinated form. This hypothesis results from the finding that the expression of catalytically dead  $Hs$ HAUSP<sup>USP7</sup> in the presence of the wild-type, endogenous DUB, leads to increased  $Hs$ p53 ubiquitination. Hence, it was suggested that catalytically dead  $Hs$ HAUSP<sup>USP7</sup> prevents wild-type  $Hs$ HAUSP<sup>USP7</sup> from gaining access to the modified lysine on  $Hs$ p53. The group also found that the  $Hs$ p53– $Hs$ HAUSP<sup>USP7</sup> interaction is enhanced in response to DNA damage (Li *et al.*, 2002). Taken together, the Gu group proposed from this study that  $Hs$ HAUSP<sup>USP7</sup> acts *in vivo* as a tumour suppressor, and clearly this has important implications for clinical research in the treatment of tumours where  $Hs$ p53 levels have been compromised. However, a second study by the Gu group revealed that  $Hs$ MDM2 is also a  $Hs$ p53-independent substrate for the catalytic activity of  $Hs$ HAUSP<sup>USP7</sup> (Li *et al.*, 2004). RNAi-mediated knockdown of  $Hs$ HAUSP<sup>USP7</sup> in the presence of cycloheximide resulted in destabilisation of  $Hs$ MDM2 compared to a control knockdown. This reduction in the

levels of  $Hs$ MDM2 also correlated with an increase in  $Hs$ p53 levels, presumably due to a reduction in  $Hs$ MDM2-triggered proteolysis of  $Hs$ p53. The pathway is complicated because  $Hs$ MDM2 is known to constitutively auto-ubiquitinate itself, leading to its own degradation –  $Hs$ HAUSP<sup>USP7</sup> is thought to regulate this, which would of course have the knock-on effect of reducing  $Hs$ p53 levels. However, due to the pro-apoptotic and growth repressive effects of  $Hs$ HAUSP<sup>USP7</sup> expression demonstrated in the first study (Li *et al.*, 2002), the Gu group argue that  $Hs$ p53 is the preferential target of  $Hs$ HAUSP<sup>USP7</sup> *in vivo* (Li *et al.*, 2004). Interestingly, a second DUB,  $Hs$ USP2a, has been shown to stabilise  $Hs$ MDM2 but not  $Hs$ p53 (Stevenson *et al.*, 2007), revealing another player in this complex regulatory network. Furthermore, it has been proposed that a group of proteins linked by  $Hs$ DAXX regulate the switch of  $Hs$ MDM2 from self-ubiquitination to substrate ubiquitination mode (Ronai, 2006).  $Hs$ DAXX has been shown to be key in controlling the levels of  $Hs$ MDM2, and can bind  $Hs$ HAUSP<sup>USP7</sup> and  $Hs$ MDM2 concurrently. Furthermore, the DNA damage-inducing agent etoposide was shown to disrupt this association, which was partially dependent on  $Hs$ ATM (Tang *et al.*, 2006). From this it is proposed that  $Hs$ DAXX acts as a scaffold to bring together  $Hs$ HAUSP<sup>USP7</sup> and  $Hs$ MDM2, and possibly the  $Hs$ MDM2 E3  $Hs$ MDMX (Ronai, 2006), to act together to poly-ubiquitinate  $Hs$ p53.  $Hs$ DAXX allows  $Hs$ MDMX and  $Hs$ HAUSP<sup>USP7</sup> to work opposingly to regulate the levels of  $Hs$ MDM2, which is free to induce  $Hs$ p53 degradation. However, upon DNA damage,  $Hs$ ATM-mediated phosphorylation of  $Hs$ MDM2, and probably other components, cause this complex to fall apart, dissociated  $Hs$ MDM2 switches to auto-ubiquitination mode, and the levels of  $Hs$ p53 increase (Tang *et al.*, 2006). The model summarised by Ronai, 2006) is depicted in Figure 5.10. More recently, the tumour suppressor and cell cycle controller  $Hs$ RASSF1A has also been proposed to aid the dissociation of this complex (Song *et al.*, 2008b), and has also been shown to be ubiquitinated by  $Hs$ SKP2, the F-box protein in SCF E3s, by the same group (Song *et al.*, 2008a).

$Hs$ HAUSP<sup>USP7</sup> has also been shown to deubiquitinate mono-ubiquitinated Forkhead box O (FOXO) transcription factors, which affects their cellular localisation. FOXO

transcription factors are involved in a diverse range of cellular processes, for example cell cycle progression, stress responses and differentiation, and are described as acting within a genetic pathway “at the interface between ageing and cancer” (reviewed in Greer and Brunet, 2008). Like <sup>Hs</sup>p53, FOXO transcription factors are post-translationally regulated by phosphorylation, acetylation and ubiquitination. Lysine-48-linked poly-ubiquitination of FOXOs is thought to be effected by <sup>Hs</sup>SKP2 (Huang *et al.*, 2005). However, <sup>Hs</sup>FOXO3 and <sup>Hs</sup>FOXO4 mono-ubiquitination, as well as multi-ubiquitination with mono-ubiquitin, has also been found by the Burgering group and this modification seems to be induced by cellular stress, particularly oxidative stress induced by hydrogen peroxide (van der Horst *et al.*, 2006). Cells co-transfected with <sup>Hs</sup>FOXO4 tagged with the C-terminal half of YFP, and ubiquitin tagged with the N-terminal half of YFP, showed YFP staining in the nucleus indicating that ubiquitinated <sup>Hs</sup>FOXO4 occurs in this cellular compartment. This technique is known as bimolecular fluorescence complementation. Following further confirming experiments, this group concluded that mono-ubiquitination of <sup>Hs</sup>FOXO4 resulted in nuclear localisation, and mono-ubiquitinated <sup>Hs</sup>FOXO4 demonstrated a greater transcriptional activity than unmodified <sup>Hs</sup>FOXO4. The authors cite a yeast two-hybrid screen that had shown that amino acids 884-1065 of the C-terminus of <sup>Hs</sup>HAUSP<sup>USP7</sup> interacted with the C-terminus of <sup>Hs</sup>FOXO4 (Colland *et al.*, 2004). The Burgering group confirmed this interaction by immunoprecipitation and went on to show that <sup>Hs</sup>HAUSP<sup>USP7</sup> can deubiquitinate <sup>Hs</sup>FOXO4, which appears to reduce the amount of <sup>Hs</sup>FOXO4 present in the nucleus (van der Horst *et al.*, 2006). Certainly, knockdown of <sup>Hs</sup>HAUSP<sup>USP7</sup> significantly reduced the proportion of cells with cytosolic <sup>Hs</sup>FOXO4 staining. Furthermore, overexpression of wild-type, but not catalytically inactive <sup>Hs</sup>HAUSP<sup>USP7</sup>, reduced <sup>Hs</sup>FOXO-responsive gene transcription. From this study, this group draw parallels between <sup>Hs</sup>p53 and <sup>Hs</sup>FOXO functions, their functions in inducing cell cycle arrest and apoptosis, how they are regulated – by phosphorylation, acetylation and ubiquitination, and the proteins involved in these regulatory pathways (van der Horst *et al.*, 2006).

$HsHAUSP^{USP7}$  was first named as herpes virus-associated ubiquitin-specific protease because it was originally found to interact with the herpes simplex virus type 1 regulatory protein ICP0, which is an E3 of the RING finger variety (Everett *et al.*, 1997). Herpes infection in humans causes cold sores and skin lesions. ICP0 ubiquitinates the promyelocytic leukaemia protein,  $HsPML$ , and sumoylated  $HsSp100$ , targeting them for proteasome-mediated degradation (reviewed in Hagglund and Roizman, 2004).  $HsPML$  and  $HsSp100$  are major components of nuclear PML bodies, which are observed in a wide variety of neurodegenerative disorders such as Parkinson's and Alzheimer's diseases. Interestingly,  $HsPML$  is also known as  $HsTRIM19$  due to its RBCC motif. ICP0 also ubiquitinates the centromeric proteins  $HsCENP-A$  and  $-C$ , as well as  $HsDNA-PKcs$ , and also  $Hsp53$  at low levels. However, most interestingly, ICP0 can ubiquitinate itself (auto-ubiquitination) leading to its degradation, but its strong interaction with  $HsHAUSP^{USP7}$  prevents this (Canning *et al.*, 2004). Furthermore, ICP0 ubiquitinates  $HsHAUSP^{USP7}$  inducing its degradation, although it has been shown that the stabilising role of  $HsHAUSP^{USP7}$  is dominant over its ICP0-induced degradation during virus infection (Boutell *et al.*, 2005).

$HsHAUSP^{USP7}$  has also been shown to interact with Epstein-Barr nuclear antigen 1 (EBNA1; Holowaty *et al.*, 2003b) and  $HsATAXIN1$ . Epstein-Barr virus causes cellular immortalisation by manipulating a variety of host cell pathways, which predisposes infected individuals to carcinogenesis. EBNA1 affects cellular DNA replication, segregation and transcriptional activation. It has been proposed that as an EBNA1 peptide binds  $HsHAUSP^{USP7}$  with higher affinity than a  $Hsp53$  peptide (Holowaty *et al.*, 2003a), and can displace it, that EBNA1 promotes  $Hsp53$  degradation by preventing  $HsHAUSP^{USP7}$  from removing lysine-48 linked poly-ubiquitination of  $Hsp53$  (Saridakis *et al.*, 2005).

$HsATAXIN1$  is the protein product of *SCA1*, which is mutant in the disorder spinocerebellar ataxia type 1 (SCA1). SCA1 is a neurodegenerative disorder known to cause ataxia and progressive motor deterioration, and it is associated with the expansion of CAG repeats in the *SCA1* gene, which results in extended

poly-glutamine tracts in *Hs*ATAXIN1. The C-terminus of *Hs*ATAXIN1 was found to interact with the C-terminus (amino acids 705-1102) of *Hs*HAUSP<sup>USP7</sup> (Hong *et al.*, 2002). Interaction of *Hs*HAUSP<sup>USP7</sup> with full-length *Hs*ATAXIN1 was almost abrogated when the poly-glutamine tract length in the N-terminal region of *Hs*ATAXIN1 was increased significantly. The dominant negative function of mutant *Hs*ATAXIN1 is thought to manifest itself in the nucleus of neural Purkinje cells, and it has been shown to co-localise with *Hs*PML (Skinner *et al.*, 1997). Hence, it is thought that mutant *Hs*ATAXIN1 cannot be deubiquitinated by *Hs*HAUSP<sup>USP7</sup>, *Hs*ATAXIN1 degradation is accelerated (Hong *et al.*, 2002), and thus presumably a reduction in *Hs*ATAXIN1 levels causes the phenotypes observed in SCA1. However, it has not been shown whether *Hs*HAUSP<sup>USP7</sup> can stabilise the levels of *Hs*ATAXIN1, nor is any information given on the type of ubiquitination that *Hs*HAUSP<sup>USP7</sup> is supposed to deubiquitinate. Hence, HAUSP<sup>USP7</sup> may not provide a link between SCA1 and the ubiquitin-proteasome system at all. Co-incidentally, CAG repeat expansion is also associated with Machado-Joseph disease (MJD), from which the superfamily of MJD DUBs are named.

Checkpoint protein with Forkhead associated and RING domains (*Hs*CHFR) is an early mitotic checkpoint protein and important tumour suppressor that has been receiving considerable research interest recently (reviewed in Baker *et al.*, 2005). *Hs*HAUSP<sup>USP7</sup>, which was found by mass spectrometry to interact with *Hs*CHFR, has been shown to control the stability and activity of *Hs*CHFR by preventing its auto-ubiquitination (Oh *et al.*, 2007). Furthermore, an interesting link with PRR has also been revealed. *Hs*CHFR has been shown to catalyse the formation of lysine-63-linked poly-ubiquitin chains by functioning with an *Hs*UBC13-*Hs*MMS2 heterodimer (Bothos *et al.*, 2003). Studies with the *S. cerevisiae* homologues *Sc*Chf1 and *Sc*Chf2, also known as *Sc*Dma1 and *Sc*Dma2, suggest that *Sc*Ubc4-dependent ubiquitination results in *Sc*Chf protein auto-ubiquitination and subsequent degradation, which is involved in G1 cell cycle delay, and this activity is independent of the *Sc*Ubc13-*Sc*Mms2-dependent lysine-63-linked ubiquitination activity of *Sc*Chf proteins that affect G2/M cycle arrest (Loring *et al.*, 2008). The

involvement of  $HsHAUSP^{USP7}$  in these two processes is yet to be defined, but there is an *S. pombe*  $HsCHFR$  homologue called  $SpDma1$  that has been shown to be involved in the spindle checkpoint (Guertin *et al.*, 2002).

These elucidated roles have resulted in  $HsHAUSP^{USP7}$  receiving growing research interest from a clinical perspective. A clinical study on  $HsHAUSP^{USP7}$  expression in non-small cell lung carcinoma tumour cells revealed that 45% showed reduced  $HsHAUSP^{USP7}$  mRNA levels, and the levels were significantly more likely to be reduced in adenocarcinoma cells (Masuya *et al.*, 2006). The authors conclude that  $HsHAUSP^{USP7}$  may have a role in the transformation of these cells in particular (Masuya *et al.*, 2006), but it is not known whether a reduction in  $HsHAUSP^{USP7}$  levels induces transformation directly, or whether it is knock-on effect. However, to exploit the possible usefulness of targeting this deubiquitinating enzyme in the clinic, pharmaceutical companies have patented inhibitors of  $HsHAUSP^{USP7}$  binding and catalysis, which result in  $Hsp53$  stabilisation (presumably as a result of  $HsMDM2$  destabilisation) and the expected anti-carcinogenic effects of increased levels of  $Hsp53$  function (Guedat and Colland, 2007).

## 5.7. MATH Domain Containing DUBs in Other Species

Most eukaryotic organisms, for example *Mus musculus* (mouse), *Rattus norvegicus* (rat), *Xenopus laevis* (frog), *Anopheles gambiae* (mosquito) and *Dictyostelium discoideum* (slime mould), all contain one MATH domain DUB. However, in addition to *S. pombe*, *Arabidopsis thaliana* and *Neurospora crassa* also contain two paralogous MATH DUBs. Why these organisms have retained two MATH domain DUBs, whereas the majority of eukaryotes only utilise one, is not known. Unfortunately, very little is known about the MATH domain DUBs in these and other eukaryotes – the vast majority of research has focused on the human homologue. Although it is worth noting here that one  $HsHAUSP^{USP7}$  homologue,  $ScUbp15$ , is found in the commonly utilised yeast model organism *Saccharomyces cerevisiae*. More attention has been devoted to  $ScUbp15$  than its *S. pombe*



counterparts, but no definite functions for this enzyme have been elucidated. Analyses of this *S. cerevisiae* homologue will be discussed in Chapter 6. The considerable structural information available for  $^{Hs}HAUSP^{USP7}$ , and subsequently the implications for  $^{Sp}Ubp21$  and  $^{Sp}Ubp22$ , will now be analysed.

## 5.8. Structure of the Catalytic Core of $^{Hs}HAUSP^{USP7}$

In 2002, the Gu group and collaborators published the first crystal structure of a UBP/USP superfamily DUB,  $^{Hs}HAUSP^{USP7}$  (Hu *et al.*, 2002). Preparatory work revealed that  $^{Hs}HAUSP^{USP7}$  was monomeric, and limited proteolysis, DUB assays and bioinformatics concluded that residues 208-560 defined the catalytic domain. Only the structure of this 40 kDa catalytic core domain of  $^{Hs}HAUSP^{USP7}$  was solved, alone and when covalently linked to ubiquitin aldehyde (Figure 5.11). The structure is akin to an extended right hand comprising three domains, palm, fingers and thumb. A catalytic cleft, where the Cys and His boxes are located, is formed at the interface between the palm and thumb domains (Hu *et al.*, 2002). In the unbound  $^{Hs}HAUSP^{USP7}$  structure, the catalytic triad side chains of residues cysteine-223, histidine-464 and aspartate-481 were misaligned such that hydrogen bonding between them was implausible. However, upon binding to ubiquitin, the structure of  $^{Hs}HAUSP^{USP7}$  was found to switch into an active conformation with an effective catalytic triad. Ubiquitin was found to bind the concave pocket formed by the DUB 'hand-like' structure formed from its three domains. Ubiquitin is shaped like a "pear drop" – the bulkier N-terminus of ubiquitin was found to be held by the  $\beta$ -sheets in the finger domain of  $^{Hs}HAUSP^{USP7}$  and the tapered C-terminus lay in the DUB catalytic cleft. The mutant ubiquitin utilised in this study was modified such that the C-terminal carboxylate was replaced with an aldehyde moiety. This mutant ubiquitin acts as a suicide substrate for DUBs – the catalytic cysteine, cysteine-223 in the case of  $^{Hs}HAUSP^{USP7}$ , had been irreversibly reacted with the ubiquitin aldehyde group prior to crystallisation. Hence it is unsurprising that the C-terminus of ubiquitin lies in this cleft. However, it was also found that a layer of ordered water molecules was present at the interface between  $^{Hs}HAUSP^{USP7}$  and ubiquitin,

and these were thought to cause the reduced affinity of  $^{Hs}HAUSP^{USP7}$  for ubiquitin compared to other DUBs (Hu *et al.*, 2002). Therefore, perhaps a free complex of these two proteins, without a covalent linkage, would not be stable enough for crystallisation. Of course, if the orientation of ubiquitin binding by  $^{Hs}HAUSP^{USP7}$  shown in this study is physiological, it could be easily imagined how  $^{Hs}HAUSP^{USP7}$  would cleave the covalent bond between the C-terminal glycine-76 of ubiquitin and the lysine on the modified protein, hence effecting a deubiquitinating reaction. Interestingly, the authors also propose that by reducing the affinity for ubiquitin, these water molecules aid the selectivity of  $^{Hs}HAUSP^{USP7}$  for ubiquitinated  $^{Hs}p53$ , rather than a different ubiquitinated protein (Hu *et al.*, 2002). Presumably, it is meant here that in order for a deubiquitination event to be successful, a threshold of binding stability between DUB and ubiquitinated substrate must be achieved in order for the reaction to occur. The stability of protein-protein interactions is dependent upon affinity, which is modulated by the complementarities of charge and conformation shared by a pair of proteins. If a DUB has a high affinity for ubiquitin, then it may bind and deubiquitinate, sometimes fruitlessly, a variety of ubiquitinated proteins, in addition to free ubiquitin alone, whereas if a DUB has a modest affinity for ubiquitin and a modest affinity for particular ubiquitinated substrates, then both of these interactions must occur simultaneously in order for deubiquitination to be effected. Hence, it could be imagined that fewer futile interactions occur, and only cognate substrates are deubiquitinated.

In this same study, the *in vitro* DUB activity of  $^{Hs}HAUSP^{USP7}$  on lysine-48 linked di-ubiquitin was investigated (Hu *et al.*, 2002). Firstly, it was confirmed that the  $^{Hs}HAUSP^{USP7}$  catalytic domain and full-length  $^{Hs}HAUSP^{USP7}$  cleave this substrate with similar kinetics. Then mutagenesis of residues within the catalytic cleft revealed ten important amino acids, which when each mutated to alanine, abolished the ability of  $^{Hs}HAUSP^{USP7}$  to cleave di-ubiquitin (Hu *et al.*, 2002). All ten of these residues were completely conserved in *S. pombe*  $^{Sp}Ubp21$  and  $^{Sp}Ubp22$  (Figure 5.8 and 5.9). Furthermore, it was shown that these residues were totally conserved amongst other UBP/USP superfamily DUBs selected by the authors in

this study, with the exception of *S. cerevisiae* <sup>Sc</sup>Ubp8 where two residues were slightly divergent (Hu *et al.*, 2002). In this publication the authors also mapped the region of <sup>Hs</sup>HAUSP<sup>USP7</sup> that interacts with <sup>Hs</sup>p53 to within the MATH domain amino acids 53-208. The <sup>Hs</sup>p53 protein contains three main domains, the N-terminal DNA-binding domain, a central tetramerisation domain and a C-terminal regulatory domain. Eleven amino acids 357-367 within the regulatory domain of <sup>Hs</sup>p53 were shown to have a critical role in binding to <sup>Hs</sup>HAUSP<sup>USP7</sup> – removal of this section abrogated the interaction (Hu *et al.*, 2002).

Recently, the crystal structure of the catalytic domain of the human UBP/USP superfamily DUB <sup>Hs</sup>CYLD revealed some interesting information about <sup>Hs</sup>HAUSP<sup>USP7</sup> (Komander *et al.*, 2008). <sup>Hs</sup>CYLD seems to specifically deubiquitinate lysine-63 linked poly-ubiquitin chains formed by the E3s <sup>Hs</sup>TRAF2 and <sup>Hs</sup>TRAF6 to activate <sup>Hs</sup>NK-κB signalling pathways (reviewed in Courtois, 2008). These lysine-63 linked chains provide a “molecular scaffold for the coassembly of” <sup>Hs</sup>NK-κB pathway components (Komander *et al.*, 2008). Mutations in *CYLD* result in a type of skin cancer called cylindromatosis. In this paper, the catalytic domain of <sup>Hs</sup>HAUSP<sup>USP7</sup> was directly compared with that of <sup>Hs</sup>CYLD, and two major differences were identified. Firstly, in addition to the palm, thumb and finger domains, <sup>Hs</sup>CYLD was found to have an additional 60 amino acid zinc-binding domain, which was found to be most similar to a type 1 B-box domain. Deletion of this domain in <sup>Hs</sup>CYLD was not found to have any effect on the DUB activity nor <sup>Hs</sup>NK-κB suppression. This domain also could not function as an E3 and did not bind to ubiquitin or ubiquitin chains. This implies that the B-box does not confer the specificity of <sup>Hs</sup>CYLD for lysine-63-linked poly-ubiquitin chains. However, this domain did appear to play a role in excluding <sup>Hs</sup>CYLD from the nucleus (Komander *et al.*, 2008).

Secondly, <sup>Hs</sup>CYLD was found to have an extended loop between β-sheets 12 and 13 of the palm domain, which is near the vicinity of the catalytic cleft. If the N-terminus of ubiquitin sites in the concave pocket of the DUB “hand” and the tapered

C-terminus lies in the catalytic cleft, this extended loop points towards the likely location of the ubiquitinated substrate, or modified ubiquitin in the case of a poly-ubiquitin chain. In *in vitro* DUB assays where lysine-48 linked tetra-ubiquitin chains were used as a substrate, when the wild-type catalytic domain of <sup>Hs</sup>CYLD was utilised, only around 50% of the tetra-ubiquitin was cleaved into smaller fragments after 5 h. Hence, <sup>Hs</sup>CYLD certainly has some activity on lysine-48 linked poly-ubiquitin. When the <sup>Hs</sup>CYLD extended loop was decreased to the size of that found in the structure of <sup>Hs</sup>HAUSP<sup>USP7</sup>, even less tetra-ubiquitin was cleaved – less than 50% of the levels of mono-ubiquitin were seen after 5 h compared with the wild-type control. Furthermore, when a catalytically dead <sup>Hs</sup>CYLD was used dramatically less tetra-ubiquitin was cleaved – no mono-ubiquitin was seen at all. However, when lysine-63 linked tetra-ubiquitin was utilised with the wild-type catalytic domain of <sup>Hs</sup>CYLD, only mono-ubiquitin was seen after 5 h, hence deubiquitination had occurred to completion and when the truncated loop mutant of <sup>Hs</sup>CYLD was utilised, no mono-ubiquitin at all was seen after 5 h (Komander *et al.*, 2008).

From this it can be argued that there are two main factors that determine the kinetics of DUB activity of different poly-ubiquitin linkages. To clarify these points, the nomenclature utilised in Figure 5.12 will be additionally referred to in square parentheses. With reference to how <sup>Hs</sup>CYLD binds ubiquitin, position “a” of ubiquitin would indicate lysine-63 and position “b”, lysine-48. Firstly, the authors state that “modelling indicates that similar to <sup>Hs</sup>HAUSP..., the Lys48 side chain of the distal ubiquitin [Ub-3] would be occluded and that a Lys48-linked chain could not be extended from a ubiquitin molecule [Ub-2] bound to the distal ubiquitin binding site of CYLD”; hence preventing endo-deubiquitinating activity on lysine-48 linked chains because a more distal ubiquitin [Ub-3] cannot be attached by lysine-48. This must dramatically increase the kinetics for deubiquitination of lysine-63 linked poly-ubiquitin chains because only binding to the most proximal ubiquitin [Ub-1] would result in a futile cleavage attempt (where the poly-ubiquitin chain is not attached to a modified protein).

Secondly, the data implies that this extended loop dramatically increases the kinetics of the <sup>Hs</sup>CYLD DUB activity of lysine-63-linked chains specifically. Whether this loop has a stabilising effect on lysine-63-linked chains (a positive function), or whether it acts to exclude chains linked by a different lysine on the proximal ubiquitin [Ub-1] (a negative function), or both, is not discussed by Komander *et al.*, 2008. In the stabilising hypothesis, the extended loop somehow aids the binding of the proximal ubiquitin [Ub-1] if it is linked to the bound, distal ubiquitin [Ub-2] by lysine-63. The conformation of the proximal ubiquitin [Ub-1] in a lysine-63-linked mode could be not only complementary to the extended loop, but the extended loop amino acids (ADRGGQNGFNIP) could interact and bond non-covalently with ubiquitin [Ub-1] residues. Alternatively (or additionally), it could be imagined that <sup>Hs</sup>CYLD can only properly bind a distal ubiquitin [Ub-2] in its hand if it is attached via lysine-63 of the proximal ubiquitin [Ub-1], and this is controlled by the extended loop. Perhaps the extended loop sterically hinders the proximal ubiquitin [Ub-1] if it is attached via any lysine other than lysine-63, and the effect of this is that the distal ubiquitin [Ub-2] cannot bind the hand optimally and therefore the ubiquitin-ubiquitin bond can only be cleaved with slow kinetics. However, the negative, excluding hypothesis does not fit with the observation that truncation of the extended loop reduces the ability of <sup>Hs</sup>CYLD to deubiquitinate lysine-48-linked chains. Perhaps, also, the active site of <sup>Hs</sup>CYLD has evolved to require the extended loop for proper functionality as well as to select for lysine-63-linked ubiquitin-ubiquitin [Ub-2—Ub-1] bond. It is also worth noting that full length <sup>Hs</sup>CYLD has other domains that may interact with this extended loop modulating its function. The N-terminal residue of the catalytic domain used in this study is found in very close proximity to the extended loop, and the N-terminus of the full length protein accounts for a further 582 amino acids. At no point in Komander *et al.*, 2008 is the activity of the full length protein tested.

The impact of this data on the specificity of <sup>Hs</sup>HAUSP<sup>USP7</sup> for particular poly-ubiquitin linkages will now be explained. Komander *et al.*, 2008 argue that <sup>Hs</sup>CYLD is a DUB specific for lysine-63-linked chains and that other UBP/USP superfamily

DUBs that have published structures of their catalytic domains, are not. Contrary to what Komander *et al.*, 2008 incorrectly cite, in the seminal 2002 Cell paper by Hu *et al* that reported the structure of the catalytic domain of <sup>Hs</sup>HAUSP<sup>USP7</sup> in complex with ubiquitin-aldehyde (Ubal), the authors actually state:

“Both Lys29 and Lys63 are largely solvent accessible in the ubiquitin moiety of the HAUSP-Ubal complex, but the Lys48 side chain [of Ub-2] is involved in hydrogen bonds to residues in helix  $\alpha 5$  of HAUSP and is only partially exposed to solvent. Examination of the local structure indicates that the side chain of Lys48 can be linked to the C-terminal carboxylate of another ubiquitin [Ub-3] without disruption of the HAUSP-Ubal interface. Nevertheless, Lys48 is not as freely available as the other ubiquitin lysine residues. Moreover, the HAUSP residues Asp305 and Glu308 that coordinate ubiquitin [Ub-2] Lys48 are conserved as acidic amino acids in other UBPs...A possible function of these residues is to promote binding of a ubiquitin moiety [Ub-2] that contains a free Lys48 side chain. Thus, cleavage by HAUSP might be biased toward the ubiquitin at the distal end of a K48-linked chain [Ub-3] or toward conjugates with either monoubiquitin or non-K48-linked polyubiquitin.”

Therefore, this does not preclude <sup>Hs</sup>HAUSP<sup>USP7</sup> from deubiquitinating a lysine-63-linked poly-ubiquitin chain. Certainly, the data on <sup>Hs</sup>CYLD seem to imply that the extended loop is a gained function that has made the enzyme more able to deubiquitinate lysine-63-linked chains in particular, and less able to deubiquitinate a broader range of ubiquitin modifications. Hence, <sup>Hs</sup>CYLD is a more specialised DUB. Furthermore, <sup>Hs</sup>CYLD is known for deubiquitinating unattached (free) lysine-63-linked poly-ubiquitin chains, the extended loop may prevent <sup>Hs</sup>CYLD from deubiquitinating ubiquitinated substrates other than ubiquitin, for example removing the most proximal ubiquitin [Ub-1] from a lysine-63-linked poly-ubiquitinated protein.

## 5.9. Structure of the MATH Domain of *Hs*HAUSP<sup>USP7</sup>

The N-terminal MATH domain, sometimes referred to as the TRAF, TRAF-like, or simply N-terminal domain, of *Hs*HAUSP<sup>USP7</sup> has been demonstrated to be very important for the ascribed roles of this DUB. *Hs*HAUSP<sup>USP7</sup> was found to be nuclear, and although no nuclear localisation motif was found, the MATH domain was required for nuclear localisation (Fernandez-Montalvan *et al.*, 2007). The authors of this study propose that *Hs*HAUSP<sup>USP7</sup> utilises its MATH domain to bind unknown factors that are transported to the nucleus, allowing *Hs*HAUSP<sup>USP7</sup> to ‘piggy-back a ride’ to this cellular compartment (Fernandez-Montalvan *et al.*, 2007). Furthermore, it is the MATH domain that mediates interactions with *Hs*p53, *Hs*MDM2 and EBNA1, and crystal structures of the MATH domain in complex with peptides from each of these three proteins have been published (Hu *et al.*, 2006; Sheng *et al.*, 2006; Saridakis *et al.*, 2005).

The first *Hs*HAUSP<sup>USP7</sup> MATH domain structure published revealed an eight-stranded, partially twisted  $\beta$ -sandwich domain very similar to that seen in TRAFs. It was solved in complex with an EBNA1 peptide, which was found to bind laterally across the  $\beta$ -sheets and important residues in *Hs*HAUSP<sup>USP7</sup> for this interaction were defined (Saridakis *et al.*, 2005). Later structures of the *Hs*HAUSP<sup>USP7</sup> MATH domain in complex with *Hs*p53 and *Hs*MDM2 peptides were in agreement (Hu *et al.*, 2006; Sheng *et al.*, 2006). Due to the same binding position of these peptides, EBNA1, *Hs*p53, and *Hs*MDM2 must compete for the same binding site in the *Hs*HAUSP<sup>USP7</sup> MATH domain. The structure of the MATH domain in complex with a *Hs*p53 peptide elucidated in the Hu *et al.*, 2006 *PLoS Biology* paper is depicted in Figure 5.13.

## 5.10. Further Investigation of the Phenotypes of *S. pombe* Strains Deficient in MATH Domain DUBs

Based on analyses of the literature, mostly with respect to *Hs*HAUSP<sup>USP7</sup>, the experimental direction of further investigations into the role of *Sp*Ubp21 and *Sp*Ubp22 in responses to DNA damage were as follows. Firstly, the phenotypes demonstrated by the double delete seen in the screening assays were verified. The growth defect of this strain was analysed, in addition to verification of the temperature sensitivity previously reported. Due to the established involvement of *Hs*HAUSP<sup>USP7</sup> in responses to DNA damage in general, as well as to oxidative stress, spot test assays were utilised to measure the sensitivity of the doubly deleted strain to a wide variety of DNA damaging agents.

Firstly, the striking UV-sensitivity of the *ubp21Δ::ura4 ubp22Δ::ura4* was measured quantitatively by the colony-forming assay described in Chapter 4. As depicted in Figure 5.14, the two *ura4*-marked single deletes were found to demonstrate approximately the same UV-sensitivity as wild-type, and the double delete was found to have an intermediate sensitivity compared to these strains and the more sensitive *pcn1-K164R*. It is interesting to note here that double delete had a colony forming growth defect: when untreated cells were spread onto agar, colonies would form more slowly than wild-type, the singly deleted strains, or *pcn1-K164R*, which, incidentally, forms colonies slightly more quickly than wild-type. Where wild-type cells would take two days at 30°C, the double delete would take three days to reach approximately the same colony size. Furthermore, when *ubp21Δ::ura4 ubp22Δ::ura4* colonies were added to liquid media, they took significantly longer to recover from the stationary phase state within which cells in colonies exist. The reasons for these observations are unknown – it appears that these cells have difficulties exiting from G<sub>0</sub> or quiescence. These observations were tested by growth curve assays. Firstly, the exponential growth rates of the three *ura4*-marked strains, compared with wild-type and *pcn1-K164R*, was assayed, which is shown in



Figure 5.15. By observing the gradient of a graph measuring the absorbance of a culture versus time, the double delete was found to grow at a slightly slower rate. Absorbance at 600 nm measures the mass of cells present within a particular volume, hence a million cells doubling in size would result in the same change in optical density as a million cells dividing to make two million cells. Hence, this assay was verified by physically counting the cells over a time period, and the same result was obtained (data not shown). The growth defect was more evident when exponentially growing cultures were grown to stationary phase, and then re-diluted, to approximately the same density, in fresh, liquid media (Figure 5.16). The double delete was barely able to recover, grow and divide over a 10 h period. Although when a sample was taken the following day, after 20 h growth, it had clearly recovered from stationary phase during the night. Moreover, following irradiation the double delete was found to form colonies much more slowly, and this correlated with UV dose. This effect is seen in wild-type colonies at very high doses, but to a much lower extent. However, if *ubp21Δ::ura4 ubp22Δ::ura4* colonies were counted after six days at 30°C, the strain appeared more UV resistant than if they were counted after the usual 2-3 days. This is because some colonies were too small to be observed, and thus counted, after only a couple of day's growth. As this assay is designed to measure the percentage of cells that do not die after specified UV doses, the colonies were counted when they stopped increasing in number, and five days growth was deemed appropriate in this respect. Hence, Figure 5.14 shows data collected from all five strains following five days growth.

Before further studies of the phenotypes of the double delete were assayed, an important discrepancy between the UV sensitivity of two different *ubp22Δ* strains was investigated. Confusingly, Figure 5.17, which is an uncropped version of Figure 4.5 from Chapter 4, shows that the *ubp22Δ::nat1* strain has a subtle UV sensitive phenotype, whereas it was previously shown in Figure 5.1 that the *ubp22Δ::ura4* strain was not UV sensitive. The reason for this difference is unknown. PCR and sequencing results revealed the expected DNA sequences at

the *ubp22* locus, and there was no evidence of diploidisation. The *ubp21Δ::ura4 ubp22Δ::ura4* strain was created by a cross between the *ubp21Δ::ura4* and *ubp22Δ::ura4*. An important concern was that *ubp22Δ::ura4* may originally have been UV-sensitive, but subsequent to being crossed with the *ubp21Δ::ura4* strain, the single may have obtained suppressors of this phenotype. Furthermore, the UV-sensitivity and/or other interesting phenotypes of the *ubp21Δ::ura4 ubp22Δ::ura4* strain may, as a result, be entirely related to a lack of <sup>Sp</sup>Ubp22 in the cell. However, when an HU block and release experiment was performed on *ubp22Δ::nat1*, which is shown in Figure 5.18, an uncropped version of Figure 4.22 from Chapter 4, this strain demonstrated a similar profile to that of wild-type, and contrasts significantly with the profile of the *ubp21Δ::ura4 ubp22Δ::ura4* strain depicted in Figure 5.3. An alternative, less plausible explanation for the differences in UV-sensitivity between these strains is that the *ura4* marker somehow alleviates the phenotype of the strain, or that perhaps the *nat1* marker sensitises the strain. Certainly there is anecdotal evidence from the *S. pombe* research community that *ura4*-marked strains can behave differently to deletions marked with a different marker. Perhaps when placed within certain genomic DNA contexts, the *ura4* gene affects nucleotide pools. Alternatively, variation in UV-sensitivity may exist between different clones with an *ubp22Δ* genotype, irrespective of the marker utilised. To check for this, different clones of the *nat1* marked strain resultant from when this strain was originally made, and positive for multiplex PCR products, were checked for sensitivity to UV by qualitative assay. The results of this are shown in Figure 5.19. Clone number 19 is the *ubp22Δ::nat1* strain utilised previously in this study, and clones 20 and 21 are isogenic strains not previously tested for their sensitivity to UV. When these strains were compared with the *ubp22Δ::ura4* strain, wild-type and *pcn1-K164R*, all the *nat1*-marked strains demonstrated a very similar UV-sensitive phenotype. However, in the 0-200 Jm<sup>-2</sup> gradient, there is still evidence of smaller colonies in the arrays of the *nat1*-marked strains at the top of the agar plate, indicating that perhaps a more subtle UV-sensitive phenotype might be resultant if the colonies were left to grow for longer. To check for this, the quantitative assay was employed. A different *ubp22Δ* strain was created,

*ubp22Δ::hph* (verification shown in Figure 5.20), and a second *ubp21Δ* strain, this time marked with a kanamycin-resistance gene (verified in Chapter 3), was also tested. Figure 5.21 depicts the five different singly deleted strains compared to wild-type, *ubp21Δ::ura4* *ubp22Δ::ura4* and *pcn1-K164R*. After six days growth, the five singly deleted strains demonstrate a very similar phenotype to that of wild-type. Furthermore, the double delete is clearly far more sensitive than the singles, hence the redundancy between <sup>Sp</sup>Ubp21 and <sup>Sp</sup>Ubp22 can be confirmed. However, when the y-axis of this graph was altered in order to resolve the singly deleted strains (Figure 5.22) and the sensitivities of the strains are analysed at the 100 Jm<sup>-2</sup> dose in particular, the *ubp22Δ* strains are marginally more sensitive to UV compared to the *ubp21Δ* strains, and notably the *ubp22Δ::hph* strain appears intermediate. A *ubp22Δ::hph* strain was found to be UV sensitive to a similar level as *ubp22Δ::nat1*. It is important to note here that these conclusions are speculative without detailed statistical analysis. However, it is likely that either the *ura4* marked strain has picked up suppressors of its UV sensitivity or that somehow the *ura4* marker rescues the sensitivity of this strain. However, it is also possible that the strains marked with genes that confer antibiotic resistance function slightly differently from an auxotrophic marker, when placed at this locus. In general, it is concluded that there is little significant difference between *ubp22Δ* strains. However, it was decided to use the *ubp21Δ::ura4*, *ubp22Δ::ura4* and *ubp21Δ::ura4 ubp22Δ::ura4* strains for further investigations of the phenotypes of *ubp21Δ*, *ubp22Δ* and *ubp21Δ ubp22Δ*. This is because all three of these strains have the same genetic background in that they were made from the same wild-type strain.

In Figure 5.2, an increase in PCNA ubiquitination was seen in unchallenged *ubp21Δ::ura4 ubp22Δ::ura4* cells, and this basal level increased further when the cells were treated with HU. This experiment was repeated, except UV was utilised instead in order to analyse whether this effect was HU-specific. Furthermore, the kinetics of <sup>Sp</sup>PCNA ubiquitination following mock, or UV treatment was also analysed. This experiment is shown in Figure 5.23. As expected, the double delete shows an increase in <sup>Sp</sup>PCNA ubiquitination in the mock-treated samples. The lack

of  $^{Sp}$ PCNA ubiquitination after 180 minutes following mock treatment is the result of a Western transfer problem that also affected the *pcn1-K164R* unmodified  $^{Sp}$ PCNA bands. After UV treatment, the levels of  $^{Sp}$ PCNA ubiquitination increase, but beyond that seen in wild-type cells, and these levels persisted for 180 minutes after irradiation. Hence, this experiment verifies the finding of Figure 5.3.

In Chapter 4, when an unsupported nitrocellulose membrane was utilised and the ubiquitinated species of PCNA were run on a gel for a sufficiently long period of time, the ubiquitinated bands could be resolved into doublets. In case  $^{Sp}$ Ubp21 and/or  $^{Sp}$ Ubp22 are only involved in removing one variant of this ubiquitinated species, the levels of the doublets were checked in *ubp21Δ::ura4*, *ubp22Δ::ura4* and *ubp21Δ::ura4 ubp22Δ::ura4* after UV treatment, which is shown in Figure 5.24. An extra-long SDS-PAGE gel was utilised in order to resolve the ubiquitinated bands to a greater extent. This experiment shows that both bands in each doublet are present at approximately the same level in all strains used in this experiment, except for the *pcn1-K164R* strain where no ubiquitinated forms of  $^{Sp}$ PCNA at all were observed.

A possible explanation for the persistence of  $^{Sp}$ PCNA ubiquitination seen in the double delete following release from HU block, as shown in Figure 5.3, is that S-phase is delayed in this strain. This would be consistent with the slightly reduced exponential growth rate seen in Figure 5.15. In order to check this, the HU block and release was repeated, but with just wild-type cells and the double delete this time. The levels of  $^{Sp}$ PCNA ubiquitination observed at each time point, which were similar to that seen previously, are shown in Figure 5.25, but more importantly the DNA content of a duplicate set of samples was measured by DAPI staining and fluorescence activated cell sorting (FACS), which is shown in Figure 5.26. *S. pombe* cells spend 75% of their time in G2, and because cytokinesis occurs at almost the same time as DNA replication, *S. pombe* does not have a proper G1 phase and so when wild-type asynchronous cells are analysed by FACS, only one peak is seen, which represents 2C DNA content. Following block in HU for 2.5 h,

this peak moved dramatically to the left, indicating that all the cells were blocked in S-phase. This peak was denoted 1C DNA content. When the cells were released in to fresh media, the 1C peak gradually moved towards a 2C peak position as the cells quickly replicated their DNA and divided. After 210 minutes, the position of the peak was similar to that seen in the NT sample. The FACS profiles of wild-type and *ubp21Δ::ura4 ubp22Δ::ura4* cells were indistinguishable from each other. Hence, the persistence of <sup>Sp</sup>PCNA modification seen in the double delete cannot be explained by an elongated or delayed S-phase.

### **5.11. Sensitivity of *S. pombe* Strains Deficient in MATH Domain DUBs to Variety of Genotoxic Agents and Other Stresses**

In order to check for a role of MATH domain DUBs in a DNA damage responses in general, the double delete was exposed to wide variety of agents. For speed, it was decided to use an assay that was qualitative – spot tests are colony-forming assays that are more accurate than the UV drop tests assays employed previously because the effect of the agent on serial dilutions spotted onto agar containing the agent are assessed independently. Each set of experiments was repeated, and the most representative data are presented here.

Firstly, the sensitivity of *ubp21Δ::ura4*, *ubp22Δ::ura4*, and *ubp21Δ::ura4 ubp22Δ::ura4* cells to 4-nitroquinoline-1-oxide (4NQO) was compared with wild-type and *pcn1-K164R*. 4NQO is a UV-mimetic genotoxic agent in that it produces bulky DNA base adducts. As expected 4NQO treatment causes <sup>Sp</sup>PCNA poly-ubiquitination in *S. pombe* (Frampton *et al.*, 2006) and *pcn1-K164R* is sensitive to this agent (Figure 5.27). The double delete is less sensitive to this agent than expected from the UVC sensitivity data previously shown, but there still appears to be a subtle phenotype.

Many agents utilised in this study, including 4NQO, were dissolved in the organic solvent dimethylsulfoxide (DMSO). Whilst an appropriate DMSO control was

always used, it was deemed appropriate to check the sensitivity of the strains to higher doses of DMSO, which is shown in Figure 5.28. The double delete in particular was found to be sensitive to DMSO at doses above 4% (v/v). Previously, it had been shown that the double delete is sensitive to cold and hot temperatures – it did not grow at 20°C or 36°C (Richert *et al.*, 2002) and these data are reproduced in Figure 5.29 (although RT was used instead of 20°C). The sensitivity of this strain to DMSO correlates well with these findings. Strains sensitive to temperature also tend to be sensitive to DMSO because the solvent alters protein structure in the same way that temperature can.

The effect of HU on cells has been explained previously in this study. Interestingly, although it is well characterised that HU induces ubiquitination of <sup>Sp</sup>PCNA, the *pcn1-K164R* strain was not HU-sensitive (Figure 5.30). However, there is a simple explanation for this. Whilst the cell attempts to utilise PRR to bypass the replication fork block, it is futile. Without a dNTP pool, DNA cannot be replicated. In other words, PRR is not required by the cell to bypass ‘damage’ caused by HU, hence it is unsurprising that the *pcn1-K164R* strain was not found to be sensitive to this agent. However, the double delete was sensitive to HU.

The effect of the genotoxic agent methyl methanesulfonate (MMS) on colony formation was analysed and is shown in Figure 5.31. MMS is a methylating agent known to react with and methylate DNA bases, and indirectly this causes both SSBs and DSBs. NER and HR are thought to be the main processes in *S. pombe* that repair MMS damage (Memisoglu and Samson, 2000). However, MMS-induced PCNA ubiquitination in human cells (Niimi *et al.*, 2008) and *S. pombe* cells (Frampton *et al.*, 2006), and a role for PRR in repairing MMS damage has also been demonstrated in chicken DT40 cells – a *PCNA-K164R* mutant cell line was sensitive to MMS (Arakawa *et al.*, 2006) as well as in human cells (Niimi *et al.*, 2008). As expected from these studies, the *S. pombe pcn1-K164R* strain was very MMS-sensitive implying that <sup>Sp</sup>PCNA ubiquitination is required for bypass of this type of damage. However, for the *ubp21Δ::ura4 ubp22Δ::ura4* strain, only a subtle

sensitivity may exist if at all. The spot tests can be difficult to interpret due to the growth defect of the double delete, which is evident in the control plate (YEA).

Camptothecin (CPT) is a suicide substrate for DNA topoisomerase I (Hsiang *et al.*, 1985). Topoisomerase activity is required during S-phase to prevent supercoils from inhibiting DNA replication, hence treatment with camptothecin causes S-phases specific DSBs due to replication fork collapse. HR is thought to be the main process that repairs CPT damage in *S. pombe*, however mono-ubiquitination of *Sp*PCNA is seen in *S. pombe* cells following CPT treatment (Frampton *et al.*, 2006). Furthermore, a role for *Gg*RAD18, albeit independently of *Gg*PCNA, in controlling CPT repair has been elucidated in chicken DT40 cells (Saber *et al.*, 2007). However, a stable human cell line expressing exogenous *Hs*PCNA-K164R where endogenous *Hs*PCNA has been knocked down did not display any sensitivity to CPT (Niimi *et al.*, 2008). Interestingly, a subtle CPT-sensitivity may exist in the *pcn1-K164R S. pombe* strain, but the *ubp21Δ::ura4 ubp22Δ::ura4* strain was found to be more CPT sensitive (Figure 5.32).

The cross-linking agent *cis*-diamminedichloridoplatinum (II), also commonly known as *cisplatin*, can cause DNA inter- and intra-strand cross-links in addition to DNA-protein adducts. The *S. cerevisiae* strain *pol30-K164R* (*pol30* is the homologue of the *S. pombe pcn1<sup>+</sup>* gene) was found to be sensitive to nitrogen mustard (a different cross-linking agent) and subsequently a model of repair of DNA inter-strand cross-links has been proposed where the lesion is first ‘unhooked’ by the NER machinery, leaving a gap opposite the unhooked cross-link that is repaired by translesion synthesis (Sarkar *et al.*, 2006). PRR has also been demonstrated to be involved in the repair of *cisplatin* damage in chicken DT40 cells – a *PCNA-K164R* mutant cell line was sensitive to *cisplatin* (Arakawa *et al.*, 2006). In *S. pombe*, the *pcn1-K164R* strain was also found to be sensitive to *cisplatin*, and the double delete demonstrated the same, or slightly less sensitivity (Figure 5.33).

When the sensitivity of cells to *cisplatin* was assayed, a variety of diluents were utilised in order to dissolve the *cisplatin*. It was advised that dimethylsulfoxide (DMSO) should not be utilised as a *cisplatin* diluent because it is capable of chelating the platinum ion (Sigma). The stability of *cisplatin* in water is questionable, but *cisplatin* would not dissolve in the advised 0.9% saline solution. Dimethylformamide (DMF), which does not chelate platinum, was tried, but as *cisplatin* would only dissolve at low concentrations and DMF is a known carcinogenic agent in itself, the sensitivity of the five strains to DMF was assayed. Interestingly, there are also reports that hydrogen peroxide is released when DMF is broken down by cells (Midorikawa *et al.*, 2000). The results of these spot test assays are shown in Figure 5.34. In 2% DMF, the double delete did not appear to be more sensitive than the other strains and certainly *pcn1-K164R* was not sensitive. However, at 4% DMF, the strains exhibited some very strange resistances to DMF. The *ubp21Δ* and *pcn1-K164R* appeared more resistant than the other strains to DMF. The reasons for this are unknown and were not investigated. It is important to note here, however, that in the end no *cisplatin* diluent was utilised, appropriate masses of *cisplatin* powder was weighed out neat and then dissolved directly in the warm agar.

Hydrogen peroxide ( $H_2O_2$ ) causes oxidative damage to DNA, mostly to DNA bases. There are also reports that hydrogen peroxide has a similar effect on topoisomerase I as CPT (Daroui *et al.*, 2004). The main repair pathway that deals with oxidative damage is thought to be BER. It has been shown that hydrogen peroxide induces *Sp*PCNA ubiquitination (Montaner *et al.*, 2007). The *S. pombe pcn1-K164R* strain was not found to be sensitive to this type of oxidative damaging agent, but the *ubp21Δ::ura4 ubp22Δ::ura4* strain was (Figure 5.35).

Bleomycin is a large glycopeptide antibiotic that reacts with iron producing superoxide and hydroxyl radicals that subsequently react with DNA to produce SSB and DSBs. Approximately 10% of strand breaks are DSBs (Friedberg *et al.*, 2006). Furthermore, as bleomycin is an oxidising agent, base modifications are



also produced (Friedberg *et al.*, 2006). Bleomycin does not induce <sup>Hs</sup>PCNA ubiquitination in human cells, but it has been shown that  $\gamma$  radiation causes <sup>Sp</sup>PCNA poly-ubiquitination in *S. pombe* and *pcn1-K164R* cells were sensitive to irradiation (Frampton *et al.*, 2006). Bleomycin is thought to be an ionising radiation mimetic, so it would be expected that *pcn1-K164R* cells would be sensitive to this genotoxin. However, this was not found to be the case (Figure 5.36). Furthermore, a very similar glycopeptide antibiotic called phleomycin, which is often used instead of bleomycin because it is available more cheaply, also had no effect on the *pcn1-K164R* strain (Figure 5.37). Higher doses of bleomycin and phleomycin were used, and this also did not affect the ability of *pcn1-K164R* to grow. Moreover, because the effects of bleomycin and phleomycin are the result of the generation of oxygen free radicals, it would be expected that the *ubp21 $\Delta$ ::ura4 ubp22 $\Delta$ ::ura4* strain would also be sensitive to these agents, and this was found to be the case (Figures 5.36 and 5.37) – the double delete demonstrated a strong sensitivity to these agents.

As previously described (Frampton *et al.*, 2006), the *pcn1-K164R* strain was found to be sensitive to irradiation with  $\gamma$  radiation (Figure 5.38). Why this strain is sensitive to ionising radiation (IR), but not to bleomycin or phleomycin, which are often used as mimetics of this treatment, is not understood. It is plausible however, that IR causes non-specific, or “dirty” breaks in the DNA, which PRR is required to repair. Whereas the breaks caused by bleomycin and phleomycin are more specific to certain DNA bases, for example. Interestingly, the double delete was found to be sensitive to all types of DNA strand break inducing agents – bleomycin, phleomycin and IR. Interestingly, whilst the sensitivity of the double delete was evident at 800 Grays, the growth of this strain was not noticeably different at 1200 Grays, whereas there was a significant difference in the *pcn1-K164R* strain between these two doses. Why this occurs is not known, but perhaps there is a resistant fraction of cells e.g. those in a particular cell cycle stage.

The sensitivity of *ubp21 $\Delta$ ::ura4*, *ubp22 $\Delta$ ::ura4*, and *ubp21 $\Delta$ ::ura4 ubp22 $\Delta$ ::ura4* cells compared with wild-type and *pcn1-K164R* to microtubule poisons was also

assayed. Cells with a defective spindle checkpoint are sensitive to microtubule poisons. Spindles, which comprise filament-like microtubules, are used in chromosome segregation during mitosis, and the checkpoint blocks mitosis progression if not all chromosomes are properly attached to their respective spindles. Hence, cells with a defective spindle checkpoint are sensitive to microtubule poisons because either mitosis cannot occur properly, or resultant daughter cells do not have an adequate complement of genetic information. A homologue of *Hs*CHFR, which has been shown to be deubiquitinated by *Hs*HAUSP<sup>USP7</sup> (described above), called *Sp*Dma1 exists in *S. pombe*, hence it was worth investigating whether any of the MATH DUB deficient strains had spindle checkpoint defects. Nocodazole, which is typically used in mammalian and *S. cerevisiae* for this purpose, cannot traverse the cell wall of *S. pombe* cells, hence thiabendazole (TBZ) and the very similar drug carbendazim (CBZ), were utilised instead. The results of these experiments are depicted in Figure 5.39 and 5.40. The results for both TBZ and CBZ were consistent with each other, the double delete shows strong sensitivity to both of these microtubule destabilisers. A very subtle sensitivity was also seen reproducibly for the *ubp21Δ::ura4* strain.

In summary, the *ubp21Δ::ura4 ubp22Δ::ura4* strain demonstrated clear sensitivity to UVC, HU, DMSO, temperature, CPT, cisplatin, bleomycin and phleomycin, and thiabendazole and carbendazim. Intermediate sensitivity to 4NQO, IR and hydrogen peroxide, and very slight or no sensitivity to MMS and DMF was observed. The *pcn1-K164R* strain was found to be highly sensitive to UVC, 4NQO, MMS, cisplatin and IR, and was sensitive to high doses of CPT.

In order to eliminate any effect of the growth defect of the double delete, growth in the presence of some of these agents was observed after a week. Figure 5.41 depicts growth after one week in the presence of 4NQO; Figure 5.42, DMSO; Figure 5.43, cisplatin; Figure 5.44, DMF; Figure 5.45, bleomycin; Figure 5.46, phleomycin; and Figure 5.47, CBZ. All results were in agreement with the

observations described above except that a more subtle *cisplatin*-sensitive phenotype was also seen for *ubp21Δ::ura4* cells (Figure 5.43).

As a final summary, the sensitivities of the double delete relative to *pcn1-K164R* tested are depicted in Table 5.1.

## 5.12. Discussion

The MATH domain USP/UBP superfamily DUB <sup>Hs</sup>HAUSP<sup>USP7</sup> has a wide variety of roles in human cells, particularly in stabilising key signalling proteins and directing E3s towards non-self substrates. The MATH domain appears to be important for substrate binding in the case of <sup>Hs</sup>p53, <sup>Hs</sup>MDM2 and EBNA1. However, <sup>Hs</sup>FOXOs and ICP0 interact with the C-terminus of <sup>Hs</sup>HAUSP<sup>USP7</sup>. The important role of <sup>Hs</sup>HAUSP<sup>USP7</sup> in the DNA damage response is consistent with the observed role of Ubp21 and Ubp22 in the DNA damage response in *S. pombe*. Furthermore, the *ubp21Δ::ura4 ubp22Δ::ura4* strain was shown to be sensitive to hydrogen peroxide, and in human cells, <sup>Hs</sup>FOXO4 mono-ubiquitination in response to this stress is deubiquitinated by <sup>Hs</sup>HAUSP<sup>USP7</sup>. Confusingly however, many of the known substrates of <sup>Hs</sup>HAUSP<sup>USP7</sup> are not found in *S. pombe*, for example <sup>Hs</sup>p53, <sup>Hs</sup>MDM2, <sup>Hs</sup>FOXOs and <sup>Hs</sup>ATAXIN1.

Consistent with the known pleiotropic roles of <sup>Hs</sup>HAUSP<sup>USP7</sup>, *ubp21Δ::ura4 ubp22Δ::ura4* strain demonstrates sensitivity to a wide variety of stresses, genotoxic agents, microtubule poisons, and agents that alter protein structure. The sensitivity of the double delete overlaps with the sensitivity of a strain where all PRR has been abolished i.e. *pcn1-K164R*. However, where both aforementioned strains showed sensitivity, the double delete generally exhibited less extreme sensitivity than *pcn1-K164R*, with the exception of CPT treatment, (summarised in Table 5.1).

Although *Sp*Ubp21 can optimally take over the functions of *Sp*Ubp22 when the cell is deficient in *Sp*Ubp22, and *vice versa*, the subtle UV-sensitivity of *ubp22Δ* strains, and the subtle sensitivity of the *ubp21Δ* strain to spindle poisons may hint towards a segregation of roles of these DUBs in wild-type cells.

*Hs*HAUSP<sup>USP7</sup> has not been shown to have a role in PRR in human cells. However, there is emerging evidence that other human DUBs, in addition to *Hs*USP1, can deubiquitinate *Hs*PCNA (Martin Cohn, personal communication), but these data are yet to be published. Furthermore, PCNA ubiquitination occurs at much higher levels in *S. pombe* than in mammalian cells and *S. cerevisiae*, and *Hs*PCNA polyubiquitination is barely detectable in human cells. Moreover, there is no known *Hs*USP1 homologue in yeast (Kay Hoffmann, personal communication). Hence, it seems likely that *Sp*PCNA deubiquitination in *S. pombe* will be significantly different to that in other more highly characterised systems.

Based on these data, further work on *Sp*Ubp21 and *Sp*Ubp22 is justified and two main lines of experimental work were decided upon. Firstly, does overexpression of *Sp*Ubp21 or *Sp*Ubp22 result in a decrease in *Sp*PCNA ubiquitination? Secondly, how do *Sp*Ubp21 and *Sp*Ubp22 interact genetically with other PRR components? However, before these data are discussed, the *S. cerevisiae* orthologue *Sc*Ubp15 will be analysed along with the phenotypes of cells deficient in *Sc*Ubp15.

## Chapter 6: *S. cerevisiae* DUBs and the MATH Domain-Containing DUB <sup>Sc</sup>Ubp15

### 6.1. Introduction

*Saccharomyces cerevisiae* is a widely utilised species of budding yeast. As a result there is a much greater understanding of cell biochemistry in *S. cerevisiae* than in *S. pombe*. *S. cerevisiae* has been the yeast model organism of choice to date due to its easy availability as a result of its popular use in baking and brewing, hence a lot more is known about *S. cerevisiae* DNA repair mechanisms and, more importantly, there are more sophisticated experimental tools available. In fact, as detailed in the Introduction, the molecular details of PRR were first elucidated in *S. cerevisiae*. However, there are many aspects of *S. pombe* biochemistry that are more similar to that of human cells, for example cell cycle control. Taken together, study of the *S. cerevisiae* literature for researchers utilising *S. pombe* is very informative. Furthermore, demonstrating that a particular enzyme functions similarly or that a deletion strain is sensitive to the same genotoxin in both species of yeast is a powerful statement.

This chapter summarises DUBs in *S. cerevisiae* and their likely *S. pombe* and mammalian homologues. The representation of DUB superfamilies in these two species of yeast are compared and contrasted. As in human cells, only one MATH domain-containing DUB, <sup>Sc</sup>Ubp15, was found in this organism. Due to the fact that colleagues had assembled strains from a global deletion project of *S. cerevisiae* genes, and hence these strains were easily available, it was decided to assay for a DNA damage phenotype in <sup>Sc</sup>Ubp15-deficient cells. The results of this are presented.

## 6.2. Deubiquitinating Enzymes in *S. cerevisiae*

All the known DUb enzymes encoded in *S. cerevisiae* genome are displayed in Tables 6.1 to 6.3. Many of the *S. cerevisiae* DUBs that have orthologues in *S. pombe* have already been discussed in Chapter 3. However, the remainder and other differences will now be briefly outlined.

Unlike *S. pombe* only four out of the six known superfamilies of DUBs are represented in *S. cerevisiae*, no members of the MJD or PPPDE superfamilies have been identified. However, whilst there are three more members of the USP/UBP superfamily, the UCH and JAMM superfamilies are under-represented in *S. cerevisiae*.

The extra USP/UBP superfamily are accounted for as follows: Firstly, DUBs are represented differently in this organism. There are three rhodanese domain-containing DUBs, whereas the only likely orthologue in *S. pombe* has lost this domain. Also, there is only one DUSP domain DUB, one MATH domain DUB, but two *Sp*Ubp9 orthologues.

Secondly, there are three additional USP/UBP DUBs that do not have orthologues in *S. pombe*. *Sc*Ubp10<sup>Dot4</sup> also contains no additional domains and does not have any clear orthologues in humans or *S. pombe* (Kay Hofmann, personal communication). However, there are opinions within the research community that *Sp*Ubp16 is the orthologue of *Sc*Ubp10<sup>Dot4</sup> (Edgar Hartsuiker, personal communication), despite the fact that the domain structure is different (Kay Hofmann, personal communication). Hence, this is a contentious area in the research community. *Sc*Ubp10<sup>Dot4</sup> was originally shown to interact with various “Sir” proteins and be important in silencing (Kahana and Gottschling, 1999). Later, this DUB has been shown to deubiquitinate histones H2B and H3 and have some overlapping functions with *Sc*Ubp8 (Emre *et al.*, 2005).

<sup>Sc</sup>Ubp11 also does not have any obvious orthologues in humans or *S. pombe* (Kay Hofmann, personal communication). However, very weak orthology was found with <sup>Hs</sup>USP20<sup>VDU2</sup> and <sup>Hs</sup>USP33<sup>VDU1</sup> (Kay Hofmann, personal communication), but <sup>Sc</sup>Ubp11 lacks the UBP-type zinc finger and DUSP domains. Overexpression of <sup>Sc</sup>Ubp11 (in addition to <sup>Sc</sup>Ubp5) *in vivo* was found to confer growth resistance to treatment with an immunosuppressive drug fingolimod (Welsch *et al.*, 2003). Otherwise, very little is known about this 717 amino acid DUB.

<sup>Sc</sup>Ubp16 is an entirely membrane-associated DUB found to be localised to the outer mitochondrial membrane (Kinner and Kolling, 2003; Schmitz *et al.*, 2005). There is no clear orthologue of <sup>Sc</sup>Ubp16 in *S. pombe* or *H. sapiens* (Kay Hofmann, personal communication).

The remaining USP/UBP DUBs in *S. cerevisiae* seem to have similar counterparts in *S. pombe*.

Only one UCH DUB is present in *S. cerevisiae*, <sup>Sc</sup>Yuh1. A <sup>Hs</sup>UCH37/<sup>Sp</sup>Uch2 orthologue is not present, hence this organism appears to be missing this important proteasome subunit and DUB activity at the proteasome lid is thought to work differently in *S. cerevisiae* compared to *S. pombe* and human cells (Stone *et al.*, 2004).

A highly conserved orthologue of the <sup>Sp</sup>Rpn11<sup>Pad1</sup> and <sup>Hs</sup>RPN11 JAMM DUBs exists in *S. cerevisiae*. However, the likely <sup>Sp</sup>Amsh<sup>Sst2</sup>/<sup>Hs</sup>AMSH orthologue in baker's yeast, YLR073C, has lost its JAMM domain (reviewed in Clague and Urbé, 2006).

### 6.3. <sup>Sc</sup>Ubp15

As mentioned in Chapter 5, the <sup>Hs</sup>HAUSP<sup>USP7</sup>, <sup>Sp</sup>Ubp21 and <sup>Sp</sup>Ubp22 orthologue in budding yeast is <sup>Sc</sup>Ubp15. <sup>Sc</sup>Ubp15 is a 1230 amino acid protein with a very similar

domain structure to its *S. pombe* and human counterparts. Figure 6.1 to 6.3 depict an alignment between these four DUBs. This reveals that <sup>Sc</sup>Ubp15 appears to be a more divergent member of the MATH USP/UBP family. Whilst the catalytic triad residues (CHY, highlighted in blue), the residues found to be important for DUB activity (blue squares; Hu *et al.*, 2002), and the majority of Cys and His box residues (highlighted in yellow) are completely conserved in <sup>Sc</sup>Ubp15, the C-terminus contains inserts not found in any of the human or *S. pombe* proteins.

A previous study of DUBs in *S. cerevisiae* revealed that cells deficient in <sup>Sc</sup>Ubp15 were temperature sensitive (Amerik *et al.*, 2000). This study also found that the *ubp15Δ* strain was not sensitive to UV light, but only a very low dose of 1.3 Jm<sup>-2</sup> was utilised and the wavelength of UV used was not stated (Amerik *et al.*, 2000).

#### 6.4. Verification of the *ubp15Δ::kan* and *rad5Δ::kan* Strains

The *S. cerevisiae* strains *ubp15Δ::kan* and *rad5Δ::kan*, as well as an isogenic wild-type strain ("BY405") were a kind gift from Eva Hofmann. The deletion strains originated from the European S*accharo*ymces C*erevisiae* Archive for Functional Analysis (EUROSCARF) global deletion project (see Materials and Methods). The function of the <sup>Sc</sup>Rad5-deficient strain in this study was as a positive control for UV sensitivity – a *pol30-K164R* strain was not available (*pol30* encodes <sup>Sc</sup>PCNA). <sup>Sc</sup>Rad5 is the 1169 amino acid E3 and helicase found to poly-ubiquitinate <sup>Sc</sup>PCNA with lysine-63-linked poly-ubiquitin chains – <sup>Sc</sup>Rad5 and orthologues were discussed in section 1.18 of the Introduction. The UV sensitivity of *rad5Δ* is widely reported in the literature (Torres-Ramos *et al.*, 2002, for example). The status of the *ubp15* and *rad5* loci were checked by PCR amplification of genomic DNA, and were found to be correctly deleted (Figure 6.4) and both strains grew on rich media supplemented with G418, whereas wild-type cells did not.



## 6.5. Phenotypes of *ubp15Δ::kan* Cells

Firstly, the UVC sensitivity of *ubp15Δ* cells was considered. The UV drop test was utilised. The results are shown in Figure 6.5. The *ubp15Δ* cells were not found to be sensitive to UVC compared to wild-type. The *rad5Δ* cells were found to be very sensitive as expected – less than 10% survival has been reported following  $10 \text{ Jm}^{-2}$  UV (Torres-Ramos *et al.*, 2002) – indicating that the experiment was successful. Furthermore, using the spot test assay, the *ubp15Δ* cells were not found to be sensitive to hydrogen peroxide (Figure 6.6), phleomycin (Figure 6.7), or DMSO (Figure 6.8). However, modest sensitivity to thiabendazole was detected (Figures 6.9 and 6.10).

## 6.6. Discussion

Assuming that there are 99 DUBs in human cells, the proportional representations of each superfamily are thus 61% UBP/USP, 4% UCH, 5% MJD, 14% OTU, 2% PPPDE and 14% JAMM. Whilst both species of yeast lack the MJD superfamily, the *S. pombe* DUBs present appear more similar to those found in human cells. Most significantly, there is no <sup>Hs</sup>PNAS4/<sup>Sp</sup>Hag1 orthologue in *S. cerevisiae* and the <sup>Sp</sup>Amsh/<sup>Hs</sup>AMSH orthologue, YLR073C, is missing its JAMM domain altogether. The proportional representations of each superfamily in *S. cerevisiae* are thus: 78% UBP/USP, 4% UCH, 9% OTU, and 9% JAMM. The proportional representations of each superfamily in *S. pombe* are thus: 67% UBP/USP, 8% UCH, 8% OTU, 4% PPPDE, and 13% JAMM. Hence, the representations of each superfamily are more similar to human cells in *S. pombe* than in baker's yeast. Most notably, there are three *S. cerevisiae* DUBs, <sup>Sc</sup>Ubp11, <sup>Sc</sup>Ubp11 and <sup>Sc</sup>Ubp16, which do not contain any clear human or *S. pombe* orthologues (Kay Hofmann, personal communication). Furthermore, there is only one known DUB that contains a rhodanese domain in humans, <sup>Hs</sup>USP8<sup>UBPY</sup>, but three in *S. cerevisiae*.

The lack of a sensitivity of baker's yeast cells deficient in <sup>Sc</sup>Ubp15 to genotoxic agents does not preclude a role of <sup>Sp</sup>Ubp21 and <sup>Sp</sup>Ubp22 in deubiquitinating <sup>Sp</sup>PCNA. Recent work on PCNA modification in other organisms has revealed distinct differences between species (see, for example, Frampton *et al.*, 2006; Andersen *et al.*, 2008; Ulrich, 2009). Following exposure genotoxic agents, a higher proportion of PCNA is mono-ubiquitinated in *S. pombe* than in human cells. Furthermore, PCNA poly-ubiquitination has only recently been detected in human cells, whereas it occurs strongly in *S. pombe*. Unlike in *S. pombe*,  $\alpha$ -PCNA antibodies are not sufficient to detect PCNA ubiquitination in *S. cerevisiae* on a Western blot – immunoprecipitation and the utilisation of tagged ubiquitin is normal procedure. Despite extensive investigation by the group of Felicity Watts, who performed lysine codon mutagenesis of *pcn1*, sumoylation of <sup>Sp</sup>PCNA was very difficult to detect, and there are no reports of <sup>Hs</sup>PCNA sumoylation. Clearly, due to the lack of an obvious <sup>Hs</sup>USP1 homologue in yeast, deubiquitination of PCNA occurs differently in yeast compared to humans. Therefore, it would not be surprising if <sup>Sp</sup>PCNA deubiquitination occurred differently in *S. pombe* compared to *S. cerevisiae*. The thiabendazole data may indicate that <sup>Sc</sup>Ubp15 is more involved in regulating the mitotic checkpoint in baker's yeast? Or perhaps more than one DUB can deubiquitinate <sup>Sc</sup>PCNA in *S. cerevisiae*, and hence no phenotype is seen in <sup>Sc</sup>Ubp15-deficient cells due to redundancy.

The above considered, it was decided not to investigate the role of <sup>Sc</sup>Ubp15 further, but to concentrate on further characterising the *S. pombe* orthologues.

## Chapter 7: Expression of *Sp*Ubp21 and *Sp*Ubp22

### 7.1. Introduction

If *Sp*Ubp21 and *Sp*Ubp22 can deubiquitinate *Sp*PCNA one might predict that a reduction in *Sp*PCNA ubiquitination levels would be seen when *Sp*Ubp21 or *Sp*Ubp22 were overexpressed in wild-type cells. *Hs*USP1 knockdown was shown to increase *Hs*PCNA mono-ubiquitination in human cells, and *Hs*PCNA mono-ubiquitination levels decreased when *Hs*USP1 was overexpressed (Huang *et al.*, 2006). Hence, verification of the whether *Sp*Ubp21 and *Sp*Ubp22 can deubiquitinate *Sp*PCNA specifically could be achieved by overexpressing each of these DUBs in wild-type cells. Unfortunately, no antibody against either DUB was available therefore the endogenous levels of the proteins are not known. Hence, it is not known whether the exogenous expression, as described below, constitutes overexpression. In this Chapter, investigations were carried out to ask whether exogenously expressed *Sp*Ubp21 and *Sp*Ubp22 were functional by expressing the proteins in *ubp21Δ::kan ubp22Δ::nat1* strain and analysing the rescue of UV sensitivity of this strain. Furthermore, a conserved DWGF motif was found in the MATH domain – the importance of this was investigated, in addition to the relevance of two potential PIP boxes.

### 7.2. Construction of Gateway System-Based Plasmids for the Expression of *Sp*Ubp21 and *Sp*Ubp22

The Gateway System (Invitrogen) was utilised in order to clone *Sp*Ubp21 and *Sp*Ubp22 into a suitable expression vector. All *S. pombe* DUB genes already cloned into the pDONR201 entry vector were purchased from RIKEN Bioresource Center, Japan (Matsuyama *et al.*, 2006). Unfortunately, a large proportion of the DUB genes, including *ubp21* and *ubp22*, contained missense mutations. Furthermore, in all genes the last base of the stop codon had been mutated, which would have

resulted in an additional C-terminal amino acid tail on all non-C-terminally tagged expressed protein. Hence, it was necessary to create four plasmids pDONR201-*ubp21*<sup>+</sup>, pDONR201-*ubp21*<sup>+</sup>-STOP, pDONR201-*ubp22*<sup>+</sup>, pDONR201-*ubp22*<sup>+</sup>-STOP by site-directed mutagenesis. Then each DUB gene was transferred via the “LR” reaction into Gateway System compatible pDUAL destination vectors, which were a kind gift from Ken Sawin (Matsuyama *et al.*, 2004). These vectors allowed His<sub>6</sub>FLAG<sub>2</sub> tagging of *S. pombe* proteins where protein expression was under the control of the *nmt1* (no message in thiamine 1) promoter. A summary of the protein constructs resulting from this cloning strategy to be expressed *in vivo* are depicted in Figure 7.1.

### 7.3. Exogenous Expression of *Sp*Ubp21 and *Sp*Ubp22 in Wild-Type Cells

For each DUB, the four different pDUAL constructs were transformed into wild-type *S. pombe* cells and positive clones selected by plating onto minimal media without uracil. Growth in the absence of uracil is required in order to force the cells to keep the plasmid. The *nmt1* is the strongest promoter of its type and is not 100% repressable. This is useful. Repression of the promoter via the addition of thiamine results in low protein expression levels, whereas growth in the absence of thiamine results in very high expression levels.

Figure 7.2 depicts the ubiquitination status of *Sp*PCNA in cells expressing *Sp*Ubp21 following HU treatment. No reproducible reduction in ubiquitinated forms were observed relative to the vector only control. The αFLAG Western shows FLAG-tagged species that correspond with the molecular weight of *Sp*Ubp21. As expected, greater quantities of FLAG-tagged *Sp*Ubp21 were detected in the absence of thiamine. Interestingly, higher levels of C-terminally tagged *Sp*Ubp21 were found compared to the N-terminally tagged version. Tubulin proteins were detected as a loading control. Two forms of tubulin alpha are detected in *S. pombe* – *Sp*Atb2<sup>Tub1</sup> and *Sp*Nda2, which are 50.5 kDa and 51.1 kDa, respectively. The

loading is relatively equal across the gel, except at the edges where presumably the  $\alpha$ -tubulin antibody appears not to have bound properly. However, the amount of unmodified  $^{Sp}$ PCNA in the far left lanes does not appear significantly lower than the others.

Figure 7.3 depicts the ubiquitination status of  $^{Sp}$ PCNA in cells expressing  $^{Sp}$ Ubp22 following HU treatment. Similar to the previous figure, no reproducible reduction in ubiquitinated forms were observed relative to the vector only control. As with  $^{Sp}$ Ubp21, higher levels of C-terminally tagged  $^{Sp}$ Ubp22 were found compared to the N-terminally tagged version.

Using the same samples as depicted in Figure 7.3, in Figure 7.4 the Western blot was probed with  $\alpha$ -Ubiquitin antibodies. The question asked by this experiment was: Does  $^{Sp}$ Ubp22 have a promiscuous role in its deubiquitination of cellular proteins? Whilst this is not a very precise experiment, this experiment is routinely utilised in the study of DUBs. However, no significant, reproducible reduction in ubiquitinated forms of cellular proteins was detected when  $^{Sp}$ Ubp22 was expressed. Having said this, no antibody raised against *S. pombe* ubiquitin is commercially available. This experiment was carried out using a commercial antibody raised against human ubiquitin, which is only 3 amino acids different from *S. pombe* and *S. cerevisiae* versions. However, this antibody was found to be very sensitive to immunodetection conditions and Figure 7.4 was the cleanest, most reliable blot generated using this antibody.

#### 7.4. Expression of <sup>Sp</sup>Ubp21 and <sup>Sp</sup>Ubp22 in *ubp21Δ::kan ubp22Δ::nat1* Cells

Was the lack of reduction in <sup>Sp</sup>PCNA ubiquitination when either <sup>Sp</sup>Ubp21 or <sup>Sp</sup>Ubp22 are expressed because the expressed forms of the DUBs are non-functional? To test this, each DUB was expressed in the doubly deleted strain and assessed for rescue of UVC sensitivity.

In order to express <sup>Sp</sup>Ubp21 and <sup>Sp</sup>Ubp22 in cells deficient in both of these DUBs, which is required for assessment of the functionality of these expressed DUBs, the construction of a doubly deleted, but *ura4<sup>-</sup>* strain was necessary. This is because the expression plasmids were marked with *ura4<sup>+</sup>* and hence this marker is necessary for retention of the expression plasmids by growth on/in media deficient in uracil. Therefore, the strains *ubp21Δ::kan* and *ubp22Δ::nat1* previously characterised in this thesis were crossed and the *ubp21* and *ubp22* loci in the resulting G418 and NAT resistant haploids were verified by PCR. Figure 7.5 shows the successful verification of this new double delete.

Furthermore, the UVC sensitivity of this new strain was found to be the same as that of the *ubp21Δ::ura4 ubp22Δ::ura4* strain. These data are depicted in Figure 7.6, where three different clones (both mating types) of *ubp21Δ::kan ubp22Δ::nat1* were tested for UVC sensitivity by drop test and compared with controls. Moreover, the *ubp21Δ::kan ubp22Δ::nat1* strain was also found to be temperature sensitive (Figure 7.7). Thus the phenotype of the double delete was similar irrespective of the marker used to generate the deletions.

Next, the ability of expressed <sup>Sp</sup>Ubp21 and <sup>Sp</sup>Ubp22 to rescue the UV sensitivity of the double delete was checked. These experiments are shown in Figure 7.8 and 7.9, respectively. Figure 7.8 shows that <sup>Sp</sup>Ubp21 cannot rescue the UVC sensitivity

of *ubp21Δ::kan ubp22Δ::nat1* strain up to wild-type levels. This result was confirmed by spot test (data not shown). This was not entirely unexpected given that *ubp22Δ::nat1* was shown in previous Chapters to be UVC sensitive compared to the *ura4*-marked version. Rescue was better in the absence of thiamine and above that of the vector only control. Hence, it can be concluded that expressed <sup>Sp</sup>Ubp21 can, to some extent, rescue the UVC sensitivity and hence at least a proportion of expressed <sup>Sp</sup>Ubp21 must be functional in terms of negating the effects of UV.

Figure 7.9 shows that expressed <sup>Sp</sup>Ubp22 can fully rescue the UVC sensitivity of the double delete up to wild-type levels. This indicates that expressed <sup>Sp</sup>Ubp22 is functional in terms of negating the effects of UV. However, rescue was only complete in the presence of thiamine i.e. low-level expression – only partial rescue was observed in the absence of thiamine. This suggests that high levels of <sup>Sp</sup>Ubp22 were deleterious in its role in negating UVC sensitivity.

## 7.5. An Important DWGF Motif in the MATH domain

In Chapter 5, the literature surrounding the MATH domain was discussed. In <sup>Hs</sup>HAUSP<sup>USP7</sup>, it appears to act as a binding module and a nuclear locator. An alignment of the primary sequence of the MATH domain of MATH domain-containing UBP/USP DUBs from a wide variety of eukaryotic organisms (including *S. pombe*) is depicted in Figure 7.10. Strikingly, four adjacent residues, DWGF, were 100% conserved in all organisms, even in the most divergent slime mould DUB. An upstream phenylalanine was also found to be 100% conserved.

Analyses of the structure of <sup>Hs</sup>HAUSP<sup>USP7</sup>, revealed that this DWGF motif is the binding site for the EBNA1, <sup>Hs</sup>p53, and <sup>Hs</sup>MDM2 peptides (Hu *et al.*, 2006; Sheng *et al.*, 2006; Saridakis *et al.*, 2005). Figure 7.11 shows the structure of the MATH domain of <sup>Hs</sup>HAUSP<sup>USP7</sup> in complex with the <sup>Hs</sup>MDM2 peptide (Sheng *et al.*, 2006). Using Protein Explorer (website link in Chapter 2), all aspartate, tryptophan, glycine

and phenylalanine residues were shaded (see legend for the colours). Important residues are labelled with their one-letter code and residue number. DWGF represents residues 164 to 167. The <sup>Hs</sup>MDM2 peptide is shown in this Figure to sit neatly on top of this motif. The conserved upstream phenylalanine previously alluded to is F158, which is positioned higher and presumably interacts with a different part of the <sup>Hs</sup>HAUSP<sup>USP7</sup> interacting proteins. Some other phenylalanines were also found to be in the vicinity of the DWGF motif: F117 and F150 are only conserved in higher eukaryotes (the first six from the top of the alignment); and F169 is conserved in all organisms except *S. cerevisiae*.

In order to assess the importance of the DWGF motif in <sup>Sp</sup>Ubp22, it was mutated to AAAA. The mutant protein was expressed as before in the double delete cells and assayed for its ability to rescue the UVC sensitivity phenotype of this strain. The results are shown in Figure 7.12. In the furthest lefthand lane (lane 1), the *ubp21Δ::kan ubp22Δ::nat1* cells have been transformed with the vector only as a control. The rescue of the UVC sensitivity of the double delete is shown in lane 2 with the expression of untagged wild-type <sup>Sp</sup>Ubp22. Lane 2 shows the ability of mutant <sup>Sp</sup>Ubp22 to rescue when untagged. No live colonies resulted when N- or C-terminally tagged mutant <sup>Sp</sup>Ubp22 was transformed into *S. pombe ubp21Δ::kan ubp22Δ::nat1* cells. Under thiamine repression, mutant <sup>Sp</sup>Ubp22 is not able to rescue. Without thiamine repression, the mutant of <sup>Sp</sup>Ubp22 is able to rescue a little more, but this rescue is not complete. Therefore, the DWGF motif is important in <sup>Sp</sup>Ubp22 function to protect the cell from UVC. Furthermore, the difference between rescue with and without thiamine implies that mutant <sup>Sp</sup>Ubp22 can carry out some of its UV protective function, but with very low efficiency. However, perhaps when there is a high abundance of mutant <sup>Sp</sup>Ubp22 in the cell, random collisions with interaction partners occur sufficiently often to suppress the mutation.



## 7.6. Structure of Prediction of <sup>Sp</sup>Ubp21 and <sup>Sp</sup>Ubp22

Two potential PIP boxes were found in <sup>Sp</sup>Ubp21 and <sup>Sp</sup>Ubp22. As introduced, the PIP box comprises KAxQxxψxxθθ, wherein x is any residue, ψ is L, M or I, and θ is F or Y (Xu *et al.*, 2001). Figure 7.13 shows their conservation in the budding yeast and human counterparts. In <sup>Sp</sup>Ubp22, the motif KVQLITPEFY was found a few amino acids downstream of the catalytic domain (PIP box A). In <sup>Sp</sup>Ubp21 the motif SHNQNVVMFY was found in the middle of the C-terminus (PIP box B).

Recent work with <sup>Hs</sup>MSH6 showed that for a PIP to function as such, it must occur in an unstructured region of a protein (Shell *et al.*, 2007). Hence, in order to elucidate whether these motifs have the potential to be functioning PIP boxes, the structures of <sup>Sp</sup>Ubp21 and <sup>Sp</sup>Ubp22 were predicted using the protein homology/analogy recognition engine (PHYRE) program (Kelley and Sternberg, 2009; see also section 2.6 for the website address). This program works by comparing a query amino acid sequence to a known structure, aligning with that structure and matching them with algorithms.

As expected, the structures were very similar to that of <sup>Hs</sup>HAUSP<sup>USP7</sup>. As depicted in Figure 7.14, the two potential PIP boxes were found to occur in ordered regions of the proteins. Furthermore, the poor conservation of these sequences between organisms implies that they are unlikely to be functionally important.

## 7.7. Discussion

Expression of <sup>Sp</sup>Ubp21 and <sup>Sp</sup>Ubp22 does not result in reduced <sup>Sp</sup>PCNA ubiquitination. The result does not appear to be explained by non-functionality of these proteins when expressed or tagging. As a result of this, the following chapter uses a different approach in order to clarify the involvement of these DUBs in PRR.

Given the 100% conservation of the DWGF motif in the aligned species in Figure 7.10 and the fact that the reported crystal structures of *Hs*HAUSP<sup>USP7</sup> in combination with peptides from its binding partners show the peptides binding across the DWGF motif, it is not surprising that this motif is important for *Sp*Ubp22 function. It seems likely, therefore, for the DWGF motif to act as a binding interface, or important part thereof, with *Sp*Ubp22 targets or cofactors. With a mutant MATH domain, *Sp*Ubp22 cannot bind these partners so efficiently, and therefore cannot deubiquitinate its targets so efficiently.

The amino acid sequences of both DUBs were checked for PIP boxes and any potentials were checked for likelihood of functionality. *Sp*Ubp21 and *Sp*Ubp22 do not contain any likely PIP boxes. However, no PIP box has been found in *Hs*USP1 either.

## Chapter 8: Epistasis Analysis

### 8.1. Introduction

A method of attributing a protein to a cellular pathway can be deduced in yeast by epistasis analysis. This method involves crossing a knockout strain where the product of the disrupted gene(s) have known function(s) with a second knockout strain in order to test the involvement of the protein encoded by the latter disrupted gene in the pathway of the former. A dramatic increase in the UV sensitivity of strain  $x\Delta y\Delta$  compared to  $x\Delta$  and  $y\Delta$  singles implies protein X and protein Y function in different, parallel UV repair pathways – this effect is known as synergy. If the UV sensitivity of the  $x\Delta y\Delta$  is the same as to  $y\Delta$ , then this implies that Y is involved in the same pathway – an epistatic effect is observed. The paradigm for this effect in the DNA repair field is experiments with *E. coli* mutants of HR and NER components – a cross between two NER mutants, for example, would be epistatic to UV relative to its parental strains, whereas a cross between a HR and an NER deficient strain would show synergistic UV sensitivity. There is also an intermediate effect known as additivity where the sensitivity of  $x\Delta y\Delta$  is approximately the sum of the sensitivity of  $x\Delta$  and  $y\Delta$ .

The aim of this Chapter, therefore, is to perform epistasis analysis with cells deficient in  $^{Sp}Ubp21$  and  $^{Sp}Ubp22$  and crosses thereof with cells deficient in components of PRR. The aim is to further elucidate potential functions of these two DUBs, in particular, to confirm or exclude a role in PRR.

### 8.2. Creation of Strains

*ubp21 $\Delta$ ::kan ubp22 $\Delta$ ::nat1* cells were crossed with the *pcn1-K164R::ura4* strain, plus also *rad8 $\Delta$ ::ura4* (Doe *et al.*, 1993) and *rhp18 $\Delta$ ::ura4* strains (Verkade *et al.*, 2001). Isolated triple mutants, which were NAT and G418 resistant and able to

grow with uracil independence, were verified by PCR (Figures 8.1-8.3). In Figure 8.1 one primer was designed to anneal to the *ura4* locus and the other within or flanking the PRR gene. Hence, no fragments result when wild-type genomic DNA is utilised.

### 8.3. Epistasis with *pcn1-K164R*, *rad8Δ* and *rhp18Δ*

*ubp21Δ::kan ubp22Δ::nat1* appears epistatic with *pcn1-K164R::ura4* (Figure 8.4). An epistatic relationship of the triple with *pcn1-K164R* suggests that these two DUBs and ubiquitination of *Sp*PCNA at lysine-164 participate in the same pathway when it comes to protecting from cell death due to UV. Possible explanations for this include: (1) the DUBs directly deubiquitinate *Sp*PCNA at lysine-63, thereby preventing PRR and hence resulting in UV sensitivity due to replication fork breakage and so forth; (2) the DUBs stabilise a protein involved in promoting, protecting or stabilising *Sp*PCNA ubiquitination. The identity of this protein is not known.

It seems unlikely that the DUBs could stabilise *Sp*PCNA itself i.e. deubiquitinate lysine-48-linked poly-ubiquitin chains from *Sp*PCNA, because this could result in decreased cellular levels of *Sp*PCNA in the double DUB delete, which is not seen in the Westerns in Chapter 4 and 5. Furthermore, if the DUBs stabilised the levels of e.g. *Sp*Rhp6, *Sp*Rhp18, *Sp*Ubc13, *Sc*Mms2, or *Sp*Rad8 such that UV sensitivity was the result when the DUBs were absent, then in the double DUB delete a reduction in *Sp*PCNA ubiquitination would also be expected. Of course, the DUBs could stabilise a different or yet to be identified PRR protein.

Figure 8.5 shows the analysis with *rad8Δ::ura4*. Comparing the red and purple lines, whilst the error bars are not very tight they do overlap at all doses, which suggests an epistatic relationship. However, epistasis cannot be clearly concluded. *Sp*Rad8, E3 an orthologue of *Sc*Rad5, extends the mono-ubiquitination of *Sp*PCNA into a lysine-63-linked poly-ubiquitin chain (Frampton *et al.*, 2006). However,

epistasis of these DUBs with *SpRad8* and lysine-164 of *SpPCNA* points towards a role of *SpUbp21/SpUbp22* in *SpPCNA* deubiquitination. The genetic relationship of *SpUbp21/SpUbp22* with *SpRad8* could be verified by performing epistasis with strains deficient in *SpUbc13* or *ScMms2*.

The relationship between *ubp21Δ::kan ubp22Δ::nat1* and *rhp18Δ::ura4* is not clear (Figure 8.6). The error bars of the red and purple lines slightly overlap at 100 J/m<sup>-2</sup> and are very close at 40 J/m<sup>-2</sup>, but are clearly different at 60 J/m<sup>-2</sup>. The rescue of the UV sensitivity of a strain deficient in *SpRhp18* by removing *SpUbp21* and *SpUbp22* was unexpected. If a lack of *SpRhp18*-mediated mono-ubiquitination of *SpPCNA* results in UV sensitivity, it is not obvious how also removing *SpUbp21* and *SpUbp22* could relieve the cell of the effects of UV. An explanation could be that *SpUbp21/SpUbp22* action generates a toxic product that requires processing by *SpRhp18*. For example, the DUBs could over-deubiquitinate a target and require *SpRhp18* to re-ubiquitinate it. In the absence of *SpRhp18* the toxic product accumulates, but in the concurrent absence of *SpUbp21/SpUbp22*, it does not exist.

Another explanation could be that somehow the presence of *SpUbp21/SpUbp22* stabilises a PRR promoter that commits the cell to bypass the damage via PRR. Therefore, when *SpUbp21* and *SpUbp22* are present, the cellular effects are worse than in the absence of *SpRhp18* than in the presence of *SpRhp18*. An epistatic relationship would corroborate a role of *SpUbp21/SpUbp22* in *SpPCNA* deubiquitination, but this cannot be concluded from Figure 8.6. A method to verify the genetic relationship of *SpUbp21/SpUbp22* with *SpRhp18* is to perform epistasis with strains deficient in *SpRhp6*, the E2 that participates in *SpPCNA* mono-ubiquitination.

It was attempted to create an *ubp21Δ ubp22Δ rad13Δ uvdeΔ* strain. *SpRad13* is fundamental to NER in fission yeast and *uvdeΔ* strains are deficient in a CPD and 64-PP exonuclease that effects the UV damage repair (UVDR) pathway. It would be expected that *SpUbp21/SpUbp22* might be synergistic with *SpRad13* and *SpUvdE*.

However, this strain could not be constructed. Tetrad analysis would elucidate clearly as to whether this quadruple delete is viable.

#### 8.4. Mutation Frequency Analysis

In section 1.27 of Chapter 1, the phenotypes of <sup>Hs</sup>USP1 knockdown in human cells is discussed -- one of these was an increased mutation frequency (Huang *et al.*, 2006). To assay for an increased mutation frequency in the *ubp21Δ ubp22Δ*, due to e.g. increased error-prone PRR or defective error-free PRR, a canavanine-resistance assay was performed. Canavanine is a toxic arginine analogue because it is incorporated into proteins in the place of arginine – the chemistry of canavanine versus arginine is sufficiently different such that proteins do not fold and function normally. However, canavanine is taken up into the cell via an arginine permease and canavanine resistance results when the gene encoding this permease is mutant. Hence, mutation frequency following DNA damage e.g. by UVC, can be quantified by counting the number of cells that developed into canavanine-resistant colonies out of a known number of cells.

Whilst the UV-induced mutation frequency for wild-type and the *pcn1-K164R* strain was as expected, the double DUB delete did not grow on media comprising canavanine. The reasons for this are unknown, but it is not an unusual finding for *S. pombe* mutant strains.

#### 8.5. Discussion

This chapter described a genetic analysis of the role of <sup>Sp</sup>Ubp21 and <sup>Sp</sup>Ubp22 in PRR. <sup>Sp</sup>Ubp21/<sup>Sp</sup>Ubp22 seems to be epistatic with <sup>Sp</sup>*pcn1-K164R*. The relationship with <sup>Sp</sup>Rad8 and <sup>Sp</sup>Rhp18 was less clear, however and the genetic relationship with these DUBs were rather complex, with suggestions of some suppression of the UV sensitivity of *rad8Δ* and *rhp18Δ*. A shortcoming of the work was that there was no positive control with which synergistic effects have been demonstrated. Future

work, therefore, should be carried out using triple deletes with *rad13Δ* or *uvdeΔ* alone, since quadruple may not be viable.

## Chapter 9: Discussion

### 9.1. Introduction

This study has revealed that the *S. pombe* orthologue of one of the most highly-characterised DUBs in *H. sapiens* has a role in the DNA damage response. This finding has significance because of the fundamental role of <sup>Hs</sup>p53 in mammalian cells in responding to DNA damage and yet there is no orthologue of <sup>Hs</sup>p53 in yeast. In this chapter the data elucidated in this study will be brought together, conclusions drawn, and important future research directions discussed.

### 9.2. Deubiquitination of <sup>Sp</sup>PCNA and Functions of <sup>Sp</sup>Ubp21 and <sup>Sp</sup>Ubp22

Chapter 3 of this thesis discussed what is known about *S. pombe* DUBs and provided the basis for a strategy to elucidate potential DUB involvement in *S. pombe* PRR. Promisingly, DUBs with known roles in DNA repair have orthologues in *S. pombe*, for example <sup>Hs</sup>USP11, which functions in the <sup>Hs</sup>BRCA2 pathway and in sensitivity to MMC. However, none of these DUBs have previously been implicated in PRR. It was very exciting, therefore, to discover that two paralogous DUBs with an orthologue in humans that has a fundamental role in the DNA damage response, were indirectly implicated in *S. pombe* PRR and were required for an efficient response to UV irradiation.

In Chapter 4 and 5, an increase in <sup>Sp</sup>PCNA ubiquitination was seen in the absence of both <sup>Sp</sup>Ubp21 and <sup>Sp</sup>Ubp22. It seems most likely that these are lysine-63-linked forms of ubiquitin, although this has not been directly proven and should be demonstrated in future experimentation. From this it was hypothesised that <sup>Sp</sup>Ubp21/<sup>Sp</sup>Ubp22 can remove mono- and lysine-63-linked ubiquitin from lysine-164 of <sup>Sp</sup>PCNA, which had the effect of sensitising the cells to UV due to lack of PRR.



However the data in Chapter 7 show that expression of either of these DUBs did not, as predicted from the above hypothesis, reduce the level of  $^{Sp}$ PCNA ubiquitination. Thus the nature of the role played by these DUBs in PRR remains unclear.

Chapter 8 linked the UV-sensitivity of the double DUB delete with lysine-164 of  $^{Sp}$ PCNA. However, in Chapter 5, the *pcn1-K164R* strain was found to be highly IR sensitive, whereas the double DUB delete showed only intermediate sensitivity to this genotoxin. Furthermore, the *pcn1-K164R* strain was sensitive to MMS, but *ubp21Δ ubp22Δ* cells were not. Hence, the link between  $^{Sp}$ Ubp21/ $^{Sp}$ Ubp22 and lysine-164 of  $^{Sp}$ PCNA appears to be dependent upon the nature of the damage. Furthermore, the sensitivity of the double DUB delete to spindle poisons suggests roles for  $^{Sp}$ Ubp21/ $^{Sp}$ Ubp22 outside of DNA repair.

Given what is known about  $^{Hs}$ HAUSP<sup>USP7</sup>, it seems more likely that  $^{Sp}$ Ubp21/ $^{Sp}$ Ubp22 stabilise target(s) by disassembling lysine-48-linked poly-ubiquitin chains. Equally, for such a role on  $^{Sp}$ PCNA, a reduction in cellular  $^{Sp}$ PCNA could be expected in the double DUB delete, which is not observed. However, perhaps the proteasome is not able to degrade  $^{Sp}$ PCNA sufficiently quickly enough, which results in a build up of lysine-48-linked poly-ubiquitinated  $^{Sp}$ PCNA.

Another explanation could be that  $^{Sp}$ Ubp21/ $^{Sp}$ Ubp22 stabilise the levels of a protein that specifically protects  $^{Sp}$ PCNA ubiquitination on lysine-164 or stabilises such forms of ubiquitinated  $^{Sp}$ PCNA. In *ubp21Δ ubp22Δ* cells, UV sensitivity is seen because this protein (protein X) is degraded more rapidly, lysine-164 ubiquitinated forms of  $^{Sp}$ PCNA are less prevalent, and therefore PRR is inhibited. In fact,  $^{Sp}$ Ubp21/ $^{Sp}$ Ubp22 could be said 'protein X'.  $^{Sp}$ Ubp21/ $^{Sp}$ Ubp22 could bind lysine-164 ubiquitinated  $^{Sp}$ PCNA and protect it from lysine-48-linked poly-ubiquitination. However, this does not explain why an increase in ubiquitinated  $^{Sp}$ PCNA is seen when the DUBs are absent.

Based on the findings of Chapter 7, it would be useful if an antibody against  $^{Sp}Ubp21/^{Sp}Ubp22$  could be created in order to detect the endogenous levels of these proteins, which would enable true overexpression, and also to allow for expression experiments without the use of tags. Alternatively or additionally, the *ubp21* and *ubp22* genes could be tagged *in situ* in order to detect the endogenous levels of the protein products.

Furthermore, purification of  $^{Sp}Ubp21/^{Sp}Ubp22$  protein would also be very useful. It would enable *in vitro* deubiquitination experiments to be carried out e.g. to check for specificity for lysine-48- or lysine-63-linked polyubiquitin chains, as has been previously described (Frampton *et al.*, 2006). However, this would take considerable time to be completed and commitment to such a direction should only occur once the importance of  $^{Sp}Ubp21/^{Sp}Ubp22$  has been clarified with less time-consuming methods. Also, as discussed below, these DUBs may require accessory proteins for catalytic function.

The obvious direction from Chapter 8 is to repeat the epistasis experiments with other DNA damaging agents, for example 4-NQO. As discussed in Chapter 8, epistasis analysis with cells deficient in  $^{Sp}Rhp6$  and also  $^{Sp}Ubc13$  and/or  $^{Sp}Mms2$ , would also be suitable directions. Furthermore, synergy with NER, UVDR and HR mutants would exclude roles in these pathways.

### 9.3. *S. cerevisiae* $^{Sc}PCNA$ Deubiquitination

No  $^{Sc}PCNA$ -specific DUBs have been identified in budding yeast, despite research effort. The case in point, it has been stated: “In [budding] yeast, the reaction is clearly reversible, and although a dedicated isopeptidase has not been identified, the modification disappears after removal of the damaging agent within the time it takes the cells to recover from the damage and complete S phase (A.A. Davies and H.D. Ulrich, unpublished observations)” (Ulrich, 2009). These findings are commensurate with the findings described in section 3.2 of Chapter 3 and Figure

3.1, plus the findings in Chapter 6 wherein no DNA repair defects were found in cells deficient in *Sc*Ubp15. As has been already discussed, there are interesting differences between budding and fission yeast PRR. For example, *Sp*PCNA sumoylation cannot be detected and ubiquitinated forms of *Sp*PCNA are more abundant (Frampton *et al.*, 2006). Different PRR regulation pathways may be supported or facilitated by duplication of the MATH domain DUB gene in fission yeast i.e. *Sp*Ubp21 and *Sp*Ubp22.

#### 9.4. *Hs*HAUSP<sup>USP7</sup>, *Hs*USP1 and *Hs*UAF1<sup>WDR48</sup>

Given the extensive characterisation of the roles of *Hs*HAUSP<sup>USP7</sup>, it seems unlikely that it could have a role in deubiquitination of *Hs*PCNA in addition to *Hs*USP1. Certainly such a role would likely be less significant than in *S. pombe*. It is not known if *Hs*HAUSP<sup>USP7</sup> knockdown results in UV sensitivity, for example.

However, there is room for non-*Hs*USP1 DUBs in human PRR – whether deubiquitinating *Hs*PCNA directly or another PRR component such as a *Hs*PCNA E2 or E3. *Hs*USP1 was discussed in section 1.27 of Chapter 1 where it was explained that the *Hs*USP1 protein auto-cleaves following UV irradiation, which correlates with an increase in ubiquitinated forms of *Sp*PCNA. However, no such correlation has been elucidated following other types of genetic insult, such as HU, MMS or MMC treatment (Huang *et al.*, 2006; Niimi *et al.*, 2008). Hence, other DUBs may be involved in modulating PRR in human cells.

Also, it has been shown that *Hs*USP1 mRNA levels are decreased following UV irradiation – the authors compared this with the inhibition of RNA polymerase II using actinomycin D and found a similar result, and subsequently concluded that transcription of *USP1* is inhibited in response to UV (Cohn *et al.*, 2007). Given that *Sp*Ubp21/*Sp*Ubp22 have been shown to play a role in splicing (Richert *et al.*, 2002), it is possible that PRR is controlled by these enzymes at the RNA level in *S. pombe*.

At the time this project was being completed, there were rumours within the research community that other DUBs capable of deubiquitinating <sup>Hs</sup>PCNA were in the process of being identified. So far, however, the identity of these DUBs has been concealed by referring to them as “DUB-X” and “DUB-Y”. It is assumed that this does not refer to <sup>Hs</sup>USP9X and <sup>Hs</sup>USP9Y, which are thought to control <sup>Hs</sup>SMAD4 levels in <sup>Hs</sup>TGFβ signalling pathways (Dupont *et al.*, 2009).

It has been shown by the D’Andrea laboratory that the activity of <sup>Hs</sup>USP1 is greatly enhanced in the presence of <sup>Hs</sup>USP1 associated factor 1 (<sup>Hs</sup>UAF1; Cohn *et al.*, 2007), which is also known as WD repeat-containing protein 48 (<sup>Hs</sup>WDR48). WD repeats form a β-propeller structure that is thought to create a rigid scaffold suitable for facilitating the assembly of protein complexes i.e. it is a stabilising interaction domain. Each repeat often ends in a tryptophan-aspartate dipeptide, hence the name. <sup>Hs</sup>UAF1<sup>WDR48</sup> comprises eight WD repeats, each of which are about 40 residues long, and hence are known as WD40 repeats. WD40 repeats are a very commonly found motif in cellular proteins. In this study, the authors analysed the literature concerning 19 budding yeast DUBs and found that 11 had been reported to interact with WD40 repeat proteins, which included <sup>Sc</sup>Ubp15 (Cohn *et al.*, 2007). However, the *Saccharomyces* Genome Database lists 73 genetic and physical interactors of <sup>Sc</sup>Ubp15, hence it is not so surprising that some comprise WD40 repeats.

In a recent follow-up study, the D’Andrea laboratory found that <sup>Hs</sup>UAF1<sup>WDR48</sup> also interacted with the paralogous <sup>Hs</sup>USP12 and <sup>Hs</sup>USP46 (Cohn *et al.*, 2009). Neither the <sup>Hs</sup>USP12–<sup>Hs</sup>UAF1<sup>WDR48</sup> nor the <sup>Hs</sup>USP46–<sup>Hs</sup>UAF1<sup>WDR48</sup> complex are thought to deubiquitinate the <sup>Hs</sup>USP1 substrate <sup>Hs</sup>Ub-FANCD2. Any function in deubiquitinating <sup>Hs</sup>PCNA was not discussed. As reported in the tables in Chapters 3 and 6, the *S. pombe* and *S. cerevisiae* orthologues are <sup>Sp</sup>Ubp9 and the paralogous <sup>Sc</sup>Ubp9 and <sup>Sc</sup>Ubp13, respectively. The authors submit that the likely <sup>Hs</sup>UAF1<sup>WDR48</sup> orthologue in *S. cerevisiae* is YOL087C. The *S. pombe* orthologue of

YOL087C is the uncharacterised protein SPAC31A2.14, which, according to the Pfam database, comprise two and three WD40 repeats, respectively. It is also concluded in this study that perhaps a WD40 cofactor is required for optimal activity of *Hs*HAUSP<sup>USP7</sup> due to its low catalytic activity when expressed recombinantly. Furthermore, the authors speculate that complexes “USPX–UAF2” and “USPY–UAF2” may exist (Cohn *et al.*, 2009). It is not known if USPX and USPY are capable of deubiquitinating *Hs*PCNA, but it is assumed that they are the “DUB-X” and “DUB-Y” referred to above.

## 9.5. Functions of the MATH Domain

The importance of the MATH domain in *Sp*Ubp22 function was demonstrated in Chapter 7. Here it was proposed that the highly conserved DWGF motif acts as a binding interface with targets of these DUBs. A suitable follow-on experiment would be to utilise the *Sp*Ubp22 MATH domain as bait in a yeast-2-hybrid experiment on the *S. pombe* proteome in order to search for potential *Sp*Ubp22 substrates and interactors.

In some MATH domain-containing proteins, such as meprins, the MATH domain acts as an oligomerisation interface. Therefore, it is plausible that homo- or hetero-oligomers of *Sp*Ubp21/*Sp*Ubp22 exist *in vitro*. For example, it is possible that the inability of DWGF-mutated *Sp*Ubp22 to rescue the UV sensitivity of the double delete is due to abrogated homo-oligomerisation, rather than binding its substrate. However, there is no evidence that *Hs*HAUSP<sup>USP7</sup> forms homo-oligomers. Furthermore, given that only very mild phenotypes were observed in the single deletes, it is clear that hetero-oligomers are not a required or major species in the cell. However, it would be interesting to see in such a yeast-2-hybrid experiment, whether e.g. the *Sp*Ubp22 MATH domain interacts with *Sp*Ubp22 or *Sp*Ubp21.

Site-directed mutations could be carried out on the primary sequence of *Sp*Ubp21/*Sp*Ubp22. For example, rather than deleting the genes in their entirety, the

catalytic site in the USP/UBP domain could be disrupted e.g. by mutating the catalytic cysteine. The inability of such a mutant to rescue the UV sensitivity of the double delete would confirm that the DUB activity is responsible for the role in the response to UV. *Sp*Ubp21/*Sp*Ubp22 may merely act as scaffolding components. It would also be interesting to see the effects of further mutations in the MATH domain i.e. in addition to the DWGF/AAAA mutation, for example, mutation of other residues highly conserved in yeast or removing the MATH domain completely. Furthermore, mutation of potential ubiquitin domains in the C-terminus may also affect the catalytic activity of these DUBs and may provide pointers as to whether the DUBs bind poly-ubiquitin chains e.g. in the C-terminus, or whether binding to a single ubiquitin in the active site is sufficient.

## 9.6. *Sp*PCNA Deubiquitination in *S. pombe*

The importance of *Hs*PCNA deubiquitination is not well understood. In the model proposed by Niimi *et al.*, 2008, which is discussed in section 1.19 of Chapter 1, it was suggested that a persistence of ubiquitinated *Hs*PCNA is not inhibitory to the cell because it is the combined effect of: (1) the inability for normal replicative polymerases to bypass damage DNA, and (2) promotion of PRR e.g. by ubiquitinating *Hs*PCNA, that results in PRR. Hence, ubiquitinated *Hs*PCNA species in the absence of damage i.e. in the absence of (1), does not necessarily result in PRR. Having promoted PRR e.g. an abundance of ubiquitinated *Hs*PCNA, is not likely to cause (1) to occur. Therefore, minimising *Hs*PCNA ubiquitination in the absence of damage may not be as important as previously thought.

It is also not known whether ubiquitinated PCNA is deposited on the DNA at every lesion, or whether deposition only occurs when the TLS machinery does not effect bypass sufficiently quickly. Hence PCNA ubiquitination may not be necessary/required for PRR to occur, but simply a PRR promoter. Afterall, *Hs*RAD18 binds ssDNA and *Hs*Pol $\eta$  via different domains, hence a TLS polymerase could be recruited to a stalled fork in the absence of an ubiquitinated *Hs*PCNA.

The Niimi *et al* model also implies that *in situ* deubiquitination of <sup>Hs</sup>PCNA is less important for the switch back to the normal replicative polymerase because the replicative machinery is simply reloaded. The pool of deubiquitinated <sup>Hs</sup>PCNA may be maintained by (1) deubiquitination by one or more DUBs with particular specificity towards <sup>Hs</sup>PCNA, and/or (2) deubiquitination events by numerous non-<sup>Hs</sup>PCNA-dedicated DUBs, and/or (3) degradation of ubiquitinated <sup>Hs</sup>PCNA and synthesis of new <sup>Hs</sup>PCNA. Whilst there is no hint of <sup>Sp</sup>PCNA degradation (e.g. in Figure 5.3), which suggests that pathway (3) is not major in *S. pombe*, it is possible that pathway (1) is simply not found in yeast.

### 9.7. A Role of <sup>Sp</sup>Ubp21 and <sup>Sp</sup>Ubp22 in the Spindle Checkpoint

As discussed in Chapter 5, <sup>Hs</sup>HAUSP<sup>USP7</sup> has been shown to control the stability and activity of <sup>Hs</sup>CHFR by preventing its auto-ubiquitination (Oh *et al.*, 2007). It would be interesting to investigate whether <sup>Sp</sup>Ubp21/<sup>Sp</sup>Ubp22 are capable of affecting the levels of <sup>Sp</sup>Dma1, the orthologue of <sup>Hs</sup>CHFR. For example, whether exogenous expression of <sup>Sp</sup>Ubp21/<sup>Sp</sup>Ubp22 results in an increase in <sup>Sp</sup>Dma1 levels, whether there is a decrease in the double DUB delete and whether these DUBs act redundantly in this function. Further experiments with thiabendazole/carbendazim treatment could also be carried out to check for a functioning spindle checkpoint.

### 9.8. Final Conclusions

This study has shown that <sup>Sp</sup>Ubp21 and <sup>Sp</sup>Ubp22 are important in DNA damage responses in *S. pombe*. This is an entirely novel finding, and hence is an important contribution for the understanding of DNA damage responses in fission yeast. Whilst a role for them in PRR has not been clearly demonstrated, the ground has been prepared for further research into this.

## Chapter 10: Bibliography

Aasland, R., Gibson, T. J. and Stewart, A. F. **(1995)**. The PHD finger: implications for chromatin-mediated transcriptional regulation. *Trends Biochem Sci* **20**, 56-59.

Al-Hakim, A. K., Zagorska, A., Chapman, L., Deak, M., Pegg, M. and Alessi, D. R. **(2008)**. Control of AMPK-related kinases by USP9X and atypical Lys(29)/Lys(33)-linked polyubiquitin chains. *Biochem J* **411**, 249-260.

Albrecht, M. and Lengauer, T. **(2004)**. Survey on the PABC recognition motif PAM2. *Biochem Biophys Res Commun* **316**, 129-138.

Allen, M. D. and Bycroft, M. **(2007)**. The solution structure of the ZnF UBP domain of USP33/VDU1. *Protein Sci* **16**, 2072-2075.

Almeida, K. H. and Sobol, R. W. **(2007)**. A unified view of base excision repair: Lesion-dependent protein complexes regulated by post-translational modification. *DNA Repair (Amst)* **6**, 695-711.

Alpi, A. F. and Patel, K. J. **(2009)**. Monoubiquitylation in the Fanconi anemia DNA damage response pathway. *DNA Repair (Amst)* **8**, 430-435.

Amerik, A., Swaminathan, S., Krantz, B. A., Wilkinson, K. D. and Hochstrasser, M. **(1997)**. In vivo disassembly of free polyubiquitin chains by yeast Ubp14 modulates rates of protein degradation by the proteasome. *Embo J* **16**, 4826-4838.

Amerik, A. Y. and Hochstrasser, M. **(2004)**. Mechanism and function of deubiquitinating enzymes. *Biochim Biophys Acta* **1695**, 189-207.

Amerik, A. Y., Li, S. J. and Hochstrasser, M. **(2000)**. Analysis of the deubiquitinating enzymes of the yeast *Saccharomyces cerevisiae*. *Biol Chem* **381**, 981-992.



Andersen, P. L., Xu, F. and Xiao, W. **(2008)**. Eukaryotic DNA damage tolerance and translesion synthesis through covalent modifications of PCNA. *Cell Res* **18**, 162-173.

Arakawa, H., Moldovan, G. L., Saribasak, H., Saribasak, N. N., Jentsch, S. and Buerstedde, J. M. **(2006)**. A role for PCNA ubiquitination in immunoglobulin hypermutation. *PLoS Biol* **4**, e366.

Arch, R. H., Gedrich, R. W. and Thompson, C. B. **(1998)**. Tumor necrosis factor receptor-associated factors (TRAFs)--a family of adapter proteins that regulates life and death. *Genes Dev* **12**, 2821-2830.

Atkinson, J. and McGlynn, P. **(2009)**. Replication fork reversal and the maintenance of genome stability. *Nucleic Acids Res* **37**, 3475-3492.

Au, P. Y. and Yeh, W. C. **(2007)**. Physiological roles and mechanisms of signaling by TRAF2 and TRAF5. *Adv Exp Med Biol* **597**, 32-47.

Avela, K., Lipsanen-Nyman, M., Idanheimo, N., Seemanova, E., Rosengren, S., Makela, T. P., Perheentupa, J., Chapelle, A. D. and Lehesjoki, A. E. **(2000)**. Gene encoding a new RING-B-box-Coiled-coil protein is mutated in mulibrey nanism. *Nat Genet* **25**, 298-301.

Avvakumov, G. V., Walker, J. R., Xue, S., Finerty, P. J., Jr., Mackenzie, F., Newman, E. M. and Dhe-Paganon, S. **(2006)**. Amino-terminal dimerization, NRDP1-rhodanese interaction, and inhibited catalytic domain conformation of the ubiquitin-specific protease 8 (USP8). *J Biol Chem* **281**, 38061-38070.

Baehler, J., Wu, J. Q., Longtine, M. S., Shah, N. G., McKenzie, A., 3rd, Steever, A. B., Wach, A., Philippsen, P. and Pringle, J. R. **(1998)**. Heterologous modules for efficient and versatile PCR-based gene targeting in *Schizosaccharomyces pombe*. *Yeast* **14**, 943-951.

Baker, D. J., Chen, J. and van Deursen, J. M. **(2005)**. The mitotic checkpoint in cancer and aging: what have mice taught us? *Curr Opin Cell Biol* **17**, 583-589.

- Baker, S. P. and Grant, P. A. **(2007)**. The SAGA continues: expanding the cellular role of a transcriptional co-activator complex. *Oncogene* **26**, 5329-5340.
- Bardwell, V. J. and Treisman, R. **(1994)**. The POZ domain: a conserved protein-protein interaction motif. *Genes Dev* **8**, 1664-1677.
- Barnes, D. E. **(2001)**. Non-homologous end joining as a mechanism of DNA repair. *Curr Biol* **11**, R455-457.
- Bayer, P., Arndt, A., Metzger, S., Mahajan, R., Melchior, F., Jaenicke, R. and Becker, J. **(1998)**. Structure determination of the small ubiquitin-related modifier SUMO-1. *J Mol Biol* **280**, 275-286.
- Bellare, P., Kutach, A. K., Rines, A. K., Guthrie, C. and Sontheimer, E. J. **(2006)**. Ubiquitin binding by a variant Jab1/MPN domain in the essential pre-mRNA splicing factor Prp8p. *Rna* **12**, 292-302.
- Bertenshaw, G. P., Norcum, M. T. and Bond, J. S. **(2003)**. Structure of homo- and hetero-oligomeric meprin metalloproteases. Dimers, tetramers, and high molecular mass multimers. *J Biol Chem* **278**, 2522-2532.
- Bertolaet, B. L., Clarke, D. J., Wolff, M., Watson, M. H., Henze, M., Divita, G. and Reed, S. I. **(2001)**. UBA domains of DNA damage-inducible proteins interact with ubiquitin. *Nat Struct Biol* **8**, 417-422.
- Bi, X., Barkley, L. R., Slater, D. M., Tateishi, S., Yamaizumi, M., Ohmori, H. and Vaziri, C. **(2006)**. Rad18 regulates DNA polymerase kappa and is required for recovery from S-phase checkpoint-mediated arrest. *Mol Cell Biol* **26**, 3527-3540.
- Bienko, M., Green, C. M., Crosetto, N., Rudolf, F., Zapart, G., Coull, B., Kannouche, P., Wider, G., Peter, M., Lehmann, A. R., Hofmann, K. and Dikic, I. **(2005)**. Ubiquitin-binding domains in Y-family polymerases regulate translesion synthesis. *Science* **310**, 1821-1824.

- Bilsland, E., Hult, M., Bell, S. D., Sunnerhagen, P. and Downs, J. A. **(2007)**. The Bre5/Ubp3 ubiquitin protease complex from budding yeast contributes to the cellular response to DNA damage. *DNA Repair (Amst)* **6**, 1471-1484.
- Blastyak, A., Pinter, L., Unk, I., Prakash, L., Prakash, S. and Haracska, L. **(2007)**. Yeast Rad5 protein required for postreplication repair has a DNA helicase activity specific for replication fork regression. *Mol Cell* **28**, 167-175.
- Boeck, R., Tarun, S., Jr., Rieger, M., Deardorff, J. A., Muller-Auer, S. and Sachs, A. B. **(1996)**. The yeast Pan2 protein is required for poly(A)-binding protein-stimulated poly(A)-nuclease activity. *J Biol Chem* **271**, 432-438.
- Bohm, S., Frishman, D. and Mewes, H. W. **(1997)**. Variations of the C2H2 zinc finger motif in the yeast genome and classification of yeast zinc finger proteins. *Nucleic Acids Res* **25**, 2464-2469.
- Bonnet, J., Romier, C., Tora, L. and Devys, D. **(2008)**. Zinc-finger UBPs: regulators of deubiquitylation. *Trends Biochem Sci* **33**, 369-375.
- Bothos, J., Summers, M. K., Venere, M., Scolnick, D. M. and Halazonetis, T. D. **(2003)**. The Chfr mitotic checkpoint protein functions with Ubc13-Mms2 to form Lys63-linked polyubiquitin chains. *Oncogene* **22**, 7101-7107.
- Bourdon, J. C. **(2007)**. p53 and its isoforms in cancer. *Br J Cancer* **97**, 277-282.
- Boutell, C., Canning, M., Orr, A. and Everett, R. D. **(2005)**. Reciprocal activities between herpes simplex virus type 1 regulatory protein ICP0, a ubiquitin E3 ligase, and ubiquitin-specific protease USP7. *J Virol* **79**, 12342-12354.
- Brachmann, C. B., Davies, A., Cost, G. J., Caputo, E., Li, J., Hieter, P. and Boeke, J. D. **(1998)**. Designer deletion strains derived from *Saccharomyces cerevisiae* S288C: a useful set of strains and plasmids for PCR-mediated gene disruption and other applications. *Yeast* **14**, 115-132.

- Bridges, B. A. **(2005)**. Error-prone DNA repair and translesion synthesis: focus on the replication fork. *DNA Repair (Amst)* **4**, 618-619, 634.
- Brooks, C. L. and Gu, W. **(2006)**. p53 ubiquitination: Mdm2 and beyond. *Mol Cell* **21**, 307-315.
- Brun, J., Chiu, R., Lockhart, K., Xiao, W., Wouters, B. G. and Gray, D. A. **(2008)**. hMMS2 serves a redundant role in human PCNA polyubiquitination. *BMC Mol Biol* **9**, 24.
- Buchberger, A., Howard, M. J., Proctor, M. and Bycroft, M. **(2001)**. The UBX domain: a widespread ubiquitin-like module. *J Mol Biol* **307**, 17-24.
- Burhans, W. C. and Weinberger, M. **(2007)**. DNA replication stress, genome instability and aging. *Nucleic Acids Res* **35**, 7545-7556.
- Burrows, J. F., Kelvin, A. A., McFarlane, C., Burden, R. E., McGrattan, M. J., De la Vega, M., Govender, U., Quinn, D. J., Dib, K., Gadina, M., Scott, C. J. and Johnston, J. A. **(2009)**. USP17 Regulates Ras Activation and Cell Proliferation by Blocking RCE1 Activity. *J Biol Chem* **284**, 9587-9595.
- Burrows, J. F., McGrattan, M. J. and Johnston, J. A. **(2005)**. The DUB/USP17 deubiquitinating enzymes, a multigene family within a tandemly repeated sequence. *Genomics* **85**, 524-529.
- Canning, M., Boutell, C., Parkinson, J. and Everett, R. D. **(2004)**. A RING finger ubiquitin ligase is protected from autocatalyzed ubiquitination and degradation by binding to ubiquitin-specific protease USP7. *J Biol Chem* **279**, 38160-38168.
- Catic, A., Fiebigler, E., Korbel, G. A., Blom, D., Galardy, P. J. and Ploegh, H. L. **(2007)**. Screen for ISG15-crossreactive deubiquitinases. *PLoS ONE* **2**, e679.
- Chiu, R. K., Brun, J., Ramaekers, C., Theys, J., Weng, L., Lambin, P., Gray, D. A. and Wouters, B. G. **(2006)**. Lysine 63-polyubiquitination guards against translesion synthesis-induced mutations. *PLoS Genet* **2**, e116.

Chung, C. H. and Baek, S. H. **(1999)**. Deubiquitinating enzymes: their diversity and emerging roles. *Biochem Biophys Res Commun* **266**, 633-640.

Ciechanover, A. **(2005)**. Intracellular protein degradation: from a vague idea, through the lysosome and the ubiquitin-proteasome system, and onto human diseases and drug targeting (Nobel lecture). *Angew Chem Int Ed Engl* **44**, 5944-5967.

Clague, M. J. and Urbé, S. **(2006)**. Endocytosis: the DUB version. *Trends Cell Biol* **16**, 551-559.

Cohen, M., Stutz, F., Belgareh, N., Haguenauer-Tsapis, R. and Dargemont, C. **(2003a)**. Ubp3 requires a cofactor, Bre5, to specifically de-ubiquitinate the COPII protein, Sec23. *Nat Cell Biol* **5**, 661-667.

Cohen, M., Stutz, F. and Dargemont, C. **(2003b)**. Deubiquitination, a new player in Golgi to endoplasmic reticulum retrograde transport. *J Biol Chem* **278**, 51989-51992.

Cohn, M. A., Kee, Y., Haas, W., Gygi, S. P. and D'Andrea, A. D. **(2009)**. UAF1 is a subunit of multiple deubiquitinating enzyme complexes. *J Biol Chem* **284**, 5343-5351.

Cohn, M. A., Kowal, P., Yang, K., Haas, W., Huang, T. T., Gygi, S. P. and D'Andrea, A. D. **(2007)**. A UAF1-containing multisubunit protein complex regulates the Fanconi anemia pathway. *Mol Cell* **28**, 786-797.

Colland, F., Jacq, X., Trouplin, V., Mouglin, C., Groizeleau, C., Hamburger, A., Meil, A., Wojcik, J., Legrain, P. and Gauthier, J. M. **(2004)**. Functional proteomics mapping of a human signaling pathway. *Genome Res* **14**, 1324-1332.

Coornaert, B., Carpentier, I. and Beyaert, R. **(2009)**. A20: central gatekeeper in inflammation and immunity. *J Biol Chem* **284**, 8217-8221.

Costa, R. M., Chigancas, V., Galhardo Rda, S., Carvalho, H. and Menck, C. F. **(2003)**. The eukaryotic nucleotide excision repair pathway. *Biochimie* **85**, 1083-1099.

Courtois, G. **(2008)**. Tumor suppressor CYLD: negative regulation of NF-kappaB signaling and more. *Cell Mol Life Sci* **65**, 1123-1132.

Crimmins, S., Jin, Y., Wheeler, C., Huffman, A. K., Chapman, C., Dobrunz, L. E., Levey, A., Roth, K. A., Wilson, J. A. and Wilson, S. M. **(2006)**. Transgenic rescue of ataxia mice with neuronal-specific expression of ubiquitin-specific protease 14. *J Neurosci* **26**, 11423-11431.

de Jong, R. N., Ab, E., Diercks, T., Truffault, V., Daniels, M., Kaptein, R. and Folkers, G. E. **(2006)**. Solution structure of the human ubiquitin-specific protease 15 DUSP domain. *J Biol Chem* **281**, 5026-5031.

DeSalle, L. M., Latres, E., Lin, D., Graner, E., Montagnoli, A., Baker, R. T., Pagano, M. and Loda, M. **(2001)**. The de-ubiquitinating enzyme Unp interacts with the retinoblastoma protein. *Oncogene* **20**, 5538-5542.

Doe, C. L., Murray, J. M., Shayeghi, M., Hoskins, M., Lehmann, A. R., Carr, A. M. and Watts, F. Z. **(1993)**. Cloning and characterisation of the *Schizosaccharomyces pombe* rad8 gene, a member of the SNF2 helicase family. *Nucleic Acids Res* **21**, 5964-5971.

Doherty, A. J. and Jackson, S. P. **(2001)**. DNA repair: how Ku makes ends meet. *Curr Biol* **11**, R920-924.

Dong, Y., Hakimi, M. A., Chen, X., Kumaraswamy, E., Cooch, N. S., Godwin, A. K. and Shiekhhattar, R. **(2003)**. Regulation of BRCC, a holoenzyme complex containing BRCA1 and BRCA2, by a signalosome-like subunit and its role in DNA repair. *Mol Cell* **12**, 1087-1099.

Dupont, S., Mamidi, A., Cordenonsi, M., Montagner, M., Zacchigna, L., Adorno, M., Martello, G., Stinchfield, M. J., Soligo, S., Morsut, L., Inui, M., Moro, S., Modena,

N., Argenton, F., Newfeld, S. J. and Piccolo, S. **(2009)**. FAM/USP9x, a deubiquitinating enzyme essential for TGF $\beta$  signaling, controls Smad4 monoubiquitination. *Cell* **136**, 123-135.

Emre, N. C., Ingvarsdottir, K., Wyce, A., Wood, A., Krogan, N. J., Henry, K. W., Li, K., Marmorstein, R., Greenblatt, J. F., Shilatifard, A. and Berger, S. L. **(2005)**. Maintenance of low histone ubiquitylation by Ubp10 correlates with telomere-proximal Sir2 association and gene silencing. *Mol Cell* **17**, 585-594.

Endo, A., Matsumoto, M., Inada, T., Yamamoto, A., Nakayama, K. I., Kitamura, N. and Komada, M. **(2009)**. Nucleolar structure and function are regulated by the deubiquitylating enzyme USP36. *J Cell Sci* **122**, 678-686.

Enesa, K., Zakkar, M., Chaudhury, H., Luong le, A., Rawlinson, L., Mason, J. C., Haskard, D. O., Dean, J. L. and Evans, P. C. **(2008)**. NF-kappaB suppression by the deubiquitinating enzyme Cezanne: a novel negative feedback loop in pro-inflammatory signaling. *J Biol Chem* **283**, 7036-7045.

Everett, R. D., Meredith, M., Orr, A., Cross, A., Kathoria, M. and Parkinson, J. **(1997)**. A novel ubiquitin-specific protease is dynamically associated with the PML nuclear domain and binds to a herpesvirus regulatory protein. *Embo J* **16**, 1519-1530.

Fischhaber, P. L. and Friedberg, E. C. **(2005)**. How are specialized (low-fidelity) eukaryotic polymerases selected and switched with high-fidelity polymerases during translesion DNA synthesis? *DNA Repair (Amst)* **4**, 279-283.

Fleischer, T. C., Weaver, C. M., McAfee, K. J., Jennings, J. L. and Link, A. J. **(2006)**. Systematic identification and functional screens of uncharacterized proteins associated with eukaryotic ribosomal complexes. *Genes Dev* **20**, 1294-1307.

Forsburg, S. L. and Rhind, N. **(2006)**. Basic methods for fission yeast. *Yeast* **23**, 173-183.

Frampton, J., Irmisch, A., Green, C. M., Neiss, A., Trickey, M., Ulrich, H. D., Furuya, K., Watts, F. Z., Carr, A. M. and Lehmann, A. R. **(2006)**. Postreplication Repair and PCNA Modification in *Schizosaccharomyces pombe*. *Mol Biol Cell* **17**, 2976-2985.

Frederick, A., Rolfe, M. and Chiu, M. I. **(1998)**. The human UNP locus at 3p21.31 encodes two tissue-selective, cytoplasmic isoforms with deubiquitinating activity that have reduced expression in small cell lung carcinoma cell lines. *Oncogene* **16**, 153-165.

Friedberg, E. C. **(2001)**. How nucleotide excision repair protects against cancer. *Nat Rev Cancer* **1**, 22-33.

Friedberg, E. C. **(2003)**. DNA damage and repair. *Nature* **421**, 436-440.

Friedberg, E. C. **(2005)**. Suffering in silence: the tolerance of DNA damage. *Nat Rev Mol Cell Biol* **6**, 943-953.

Friedberg, E. C. **(2006)**. Reversible monoubiquitination of PCNA: A novel slant on regulating translesion DNA synthesis. *Mol Cell* **22**, 150-152.

Friedberg, E. C., Lehmann, A. R. and Fuchs, R. P. **(2005)**. Trading places: how do DNA polymerases switch during translesion DNA synthesis? *Mol Cell* **18**, 499-505.

Friedberg, E. C., McDaniel, L. D. and Schultz, R. A. **(2004)**. The role of endogenous and exogenous DNA damage and mutagenesis. *Curr Opin Genet Dev* **14**, 5-10.

Friedberg, E. C., Wagner, R. and Radman, M. **(2002)**. Specialized DNA polymerases, cellular survival, and the genesis of mutations. *Science* **296**, 1627-1630.

Friedberg, E. C., Walker, G. C., Siede, W., Wood, R. D., Schultz, R. A. and Ellenberger, T. (2006). *DNA Repair and Mutagenesis*, 2nd edn (Washington, American Society for Microbiology).



Gabriely, G., Kama, R., Gelin-Licht, R. and Gerst, J. E. **(2008)**. Different Domains of the UBL-UBA Ubiquitin Receptor, Ddi1/Vsm1, Are Involved in Its Multiple Cellular Roles. *Mol Biol Cell* **19**, 3625-3637.

Game, J. C. and Chernikova, S. B. **(2009)**. The role of RAD6 in recombinational repair, checkpoints and meiosis via histone modification. *DNA Repair (Amst)* **8**, 470-482.

Ganesan, A. K. **(1974)**. Persistence of pyrimidine dimers during post-replication repair in ultraviolet light-irradiated Escherichia coli K12. *J Mol Biol* **87**, 103-119.

Giaever, G., Chu, A. M., Ni, L., Connelly, C., Riles, L., Veronneau, S., Dow, S., Lucau-Danila, A., Anderson, K., Andre, B., Arkin, A. P., Astromoff, A., El-Bakkoury, M., Bangham, R., Benito, R., Brachat, S., Campanaro, S., Curtiss, M., Davis, K., Deutschbauer, A., Entian, K. D., Flaherty, P., Foury, F., Garfinkel, D. J., Gerstein, M., Gotte, D., Guldener, U., Hegemann, J. H., Hempel, S., Herman, Z., Jaramillo, D. F., Kelly, D. E., Kelly, S. L., Kotter, P., LaBonte, D., Lamb, D. C., Lan, N., Liang, H., Liao, H., Liu, L., Luo, C., Lussier, M., Mao, R., Menard, P., Ooi, S. L., Revuelta, J. L., Roberts, C. J., Rose, M., Ross-Macdonald, P., Scherens, B., Schimmack, G., Shafer, B., Shoemaker, D. D., Sookhai-Mahadeo, S., Storms, R. K., Strathern, J. N., Valle, G., Voet, M., Volckaert, G., Wang, C. Y., Ward, T. R., Wilhelmy, J., Winzeler, E. A., Yang, Y., Yen, G., Youngman, E., Yu, K., Bussey, H., Boeke, J. D., Snyder, M., Philippsen, P., Davis, R. W. and Johnston, M. **(2002)**. Functional profiling of the *Saccharomyces cerevisiae* genome. *Nature* **418**, 387-391.

Goehler, T., Munoz, I. M., Rouse, J. and Blow, J. J. **(2008)**. PTIP/Swift is required for efficient PCNA ubiquitination in response to DNA damage. *DNA Repair (Amst)* **7**, 775-787.

Goodman, M. F. **(2002)**. Error-prone repair DNA polymerases in prokaryotes and eukaryotes. *Annu Rev Biochem* **71**, 17-50.

Grabbe, C. and Dikic, I. **(2009a)**. Functional roles of ubiquitin-like domain (ULD) and ubiquitin-binding domain (UBD) containing proteins. *Chem Rev* **109**, 1481-1494.

Grabbe, C. and Dikic, I. **(2009b)**. Functional Roles of Ubiquitin-Like Domain (ULD) and Ubiquitin-Binding Domain (UBD) Containing Proteins. *Chem Rev* **109**, 1481-1494.

Gratchev, A., Strein, P., Utikal, J. and Sergij, G. **(2003)**. Molecular genetics of Xeroderma pigmentosum variant. *Exp Dermatol* **12**, 529-536.

Gray, D. A., Inazawa, J., Gupta, K., Wong, A., Ueda, R. and Takahashi, T. **(1995)**. Elevated expression of Unph, a proto-oncogene at 3p21.3, in human lung tumors. *Oncogene* **10**, 2179-2183.

Green, C. M. **(2006)**. One ring to rule them all? Another cellular responsibility for PCNA. *Trends Mol Med* **12**, 455-458.

Greer, E. L. and Brunet, A. **(2008)**. FOXO transcription factors in ageing and cancer. *Acta Physiol (Oxf)* **192**, 19-28.

Guedat, P. and Colland, F. **(2007)**. Patented small molecule inhibitors in the ubiquitin proteasome system. *BMC Biochem* **8 Suppl 1**, S14.

Guertin, D. A., Venkatram, S., Gould, K. L. and McCollum, D. **(2002)**. Dma1 prevents mitotic exit and cytokinesis by inhibiting the septation initiation network (SIN). *Dev Cell* **3**, 779-790.

Gulbis, J. M., Kelman, Z., Hurwitz, J., O'Donnell, M. and Kuriyan, J. **(1996)**. Structure of the C-terminal region of p21(WAF1/CIP1) complexed with human PCNA. *Cell* **87**, 297-306.

Guo, C., Kosarek-Stancel, J. N., Tang, T. S. and Friedberg, E. C. **(2009)**. Y-family DNA polymerases in mammalian cells. *Cell Mol Life Sci* **66**, 2363-2381.

Ha, B. H. and Kim, E. E. **(2008)**. Structures of proteases for ubiquitin and ubiquitin-like modifiers. *BMB Rep* **41**, 435-443.

Haber, J. E., Ira, G., Malkova, A. and Sugawara, N. **(2004)**. Repairing a double-strand chromosome break by homologous recombination: revisiting Robin Holliday's model. *Philos Trans R Soc Lond B Biol Sci* **359**, 79-86.

Hagglund, R. and Roizman, B. **(2004)**. Role of ICP0 in the strategy of conquest of the host cell by herpes simplex virus 1. *J Virol* **78**, 2169-2178.

Halawani, D. and Latterich, M. **(2006)**. p97: The cell's molecular purgatory? *Mol Cell* **22**, 713-717.

Halliwell, B. and Aruoma, O. I. **(1991)**. DNA damage by oxygen-derived species. Its mechanism and measurement in mammalian systems. *FEBS Lett* **281**, 9-19.

Hammet, A., Pike, B. L. and Heierhorst, J. **(2002)**. Posttranscriptional regulation of the RAD5 DNA repair gene by the Dun1 kinase and the Pan2-Pan3 poly(A)-nuclease complex contributes to survival of replication blocks. *J Biol Chem* **277**, 22469-22474.

Helleday, T., Petermann, E., Lundin, C., Hodgson, B. and Sharma, R. A. **(2008)**. DNA repair pathways as targets for cancer therapy. *Nat Rev Cancer* **8**, 193-204.

Heller, R. C. and Marians, K. J. **(2006)**. Replication fork reactivation downstream of a blocked nascent leading strand. *Nature* **439**, 557-562.

Henry, K. W., Wyce, A., Lo, W. S., Duggan, L. J., Emre, N. C., Kao, C. F., Pillus, L., Shilatifard, A., Osley, M. A. and Berger, S. L. **(2003)**. Transcriptional activation via sequential histone H2B ubiquitylation and deubiquitylation, mediated by SAGA-associated Ubp8. *Genes Dev* **17**, 2648-2663.

Hentges, P., Van Driessche, B., Tafforeau, L., Vandenhaute, J. and Carr, A. M. **(2005)**. Three novel antibiotic marker cassettes for gene disruption and marker switching in *Schizosaccharomyces pombe*. *Yeast* **22**, 1013-1019.

- Hetfeld, B. K., Helfrich, A., Kapelari, B., Scheel, H., Hofmann, K., Guterman, A., Glickman, M., Schade, R., Kloetzel, P. M. and Dubiel, W. **(2005)**. The zinc finger of the CSN-associated deubiquitinating enzyme USP15 is essential to rescue the E3 ligase Rbx1. *Curr Biol* **15**, 1217-1221.
- Heyer, W. D. **(2004)**. Recombination: Holliday junction resolution and crossover formation. *Curr Biol* **14**, R56-58.
- Higgins, N. P., Kato, K. and Strauss, B. **(1976)**. A model for replication repair in mammalian cells. *J Mol Biol* **101**, 417-425.
- Hillis, D. M. **(1996)**. Life in the hot zone around Chernobyl. *Nature* **380**, 665-666.
- Hochstrasser, M. **(1996)**. Ubiquitin-dependent protein degradation. *Annu Rev Genet* **30**, 405-439.
- Hochstrasser, M. **(2002)**. Molecular biology. New proteases in a ubiquitin stew. *Science* **298**, 549-552.
- Hoegel, C., Pfander, B., Moldovan, G. L., Pyrowolakis, G. and Jentsch, S. **(2002)**. RAD6-dependent DNA repair is linked to modification of PCNA by ubiquitin and SUMO. *Nature* **419**, 135-141.
- Hoeijmakers, J. H. **(2001a)**. DNA repair mechanisms. *Maturitas* **38**, 17-22.
- Hoeijmakers, J. H. **(2001b)**. Genome maintenance mechanisms for preventing cancer. *Nature* **411**, 366-374.
- Hofmann, K. **(2009)**. Ubiquitin-binding domains and their role in the DNA damage response. *DNA Repair (Amst)* **8**, 544-556.
- Holowaty, M. N., Sheng, Y., Nguyen, T., Arrowsmith, C. and Frappier, L. **(2003a)**. Protein interaction domains of the ubiquitin-specific protease, USP7/HAUSP. *J Biol Chem* **278**, 47753-47761.

- Holowaty, M. N., Zeghouf, M., Wu, H., Tellam, J., Athanasopoulos, V., Greenblatt, J. and Frappier, L. **(2003b)**. Protein profiling with Epstein-Barr nuclear antigen-1 reveals an interaction with the herpesvirus-associated ubiquitin-specific protease HAUSP/USP7. *J Biol Chem* **278**, 29987-29994.
- Hong, S., Kim, S. J., Ka, S., Choi, I. and Kang, S. **(2002)**. USP7, a ubiquitin-specific protease, interacts with ataxin-1, the SCA1 gene product. *Mol Cell Neurosci* **20**, 298-306.
- Hsiang, Y. H., Hertzberg, R., Hecht, S. and Liu, L. F. **(1985)**. Camptothecin induces protein-linked DNA breaks via mammalian DNA topoisomerase I. *J Biol Chem* **260**, 14873-14878.
- Hu, M., Gu, L., Li, M., Jeffrey, P. D., Gu, W. and Shi, Y. **(2006)**. Structural basis of competitive recognition of p53 and MDM2 by HAUSP/USP7: implications for the regulation of the p53-MDM2 pathway. *PLoS Biol* **4**, e27.
- Hu, M., Li, P., Li, M., Li, W., Yao, T., Wu, J. W., Gu, W., Cohen, R. E. and Shi, Y. **(2002)**. Crystal structure of a UBP-family deubiquitinating enzyme in isolation and in complex with ubiquitin aldehyde. *Cell* **111**, 1041-1054.
- Hu, M., Li, P., Song, L., Jeffrey, P. D., Chenova, T. A., Wilkinson, K. D., Cohen, R. E. and Shi, Y. **(2005)**. Structure and mechanisms of the proteasome-associated deubiquitinating enzyme USP14. *Embo J* **24**, 3747-3756.
- Huang, H., Regan, K. M., Wang, F., Wang, D., Smith, D. I., van Deursen, J. M. and Tindall, D. J. **(2005)**. Skp2 inhibits FOXO1 in tumor suppression through ubiquitin-mediated degradation. *Proc Natl Acad Sci U S A* **102**, 1649-1654.
- Huang, T. T., Nijman, S. M., Mirchandani, K. D., Galardy, P. J., Cohn, M. A., Haas, W., Gygi, S. P., Ploegh, H. L., Bernards, R. and D'Andrea, A. D. **(2006)**. Regulation of monoubiquitinated PCNA by DUB autocleavage. *Nat Cell Biol* **8**, 339-347.
- Hubscher, U., Maga, G. and Spadari, S. **(2002)**. Eukaryotic DNA polymerases. *Annu Rev Biochem* **71**, 133-163.

Huibregtse, J. M., Yang, J. C. and Beaudenon, S. L. **(1997)**. The large subunit of RNA polymerase II is a substrate of the Rsp5 ubiquitin-protein ligase. *Proc Natl Acad Sci U S A* **94**, 3656-3661.

Hurley, J. H., Lee, S. and Prag, G. **(2006)**. Ubiquitin-binding domains. *Biochem J* **399**, 361-372.

Huttner, D. and Ulrich, H. D. **(2008)**. Cooperation of replication protein A with the ubiquitin ligase Rad18 in DNA damage bypass. *Cell Cycle* **7**, 3629-3633.

Ikeda, F. and Dikic, I. **(2008)**. Atypical ubiquitin chains: new molecular signals. 'Protein Modifications: Beyond the Usual Suspects' review series. *EMBO Rep* **9**, 536-542.

Iwaki, T., Onishi, M., Ikeuchi, M., Kita, A., Sugiura, R., Giga-Hama, Y., Fukui, Y. and Takegawa, K. **(2007)**. Essential roles of class E Vps proteins for sorting into multivesicular bodies in *Schizosaccharomyces pombe*. *Microbiology* **153**, 2753-2764.

Iyer, L. M., Babu, M. M. and Aravind, L. **(2006)**. The HIRAN domain and recruitment of chromatin remodeling and repair activities to damaged DNA. *Cell Cycle* **5**, 775-782.

Iyer, L. M., Koonin, E. V. and Aravind, L. **(2004)**. Novel predicted peptidases with a potential role in the ubiquitin signaling pathway. *Cell Cycle* **3**, 1440-1450.

Jacquemont, C. and Taniguchi, T. **(2007)**. The Fanconi anemia pathway and ubiquitin. *BMC Biochem* **8 Suppl 1**, S10.

Jentsch, S. and Rumpf, S. **(2006)**. Cdc48 (p97): a 'molecular gearbox' in the ubiquitin pathway? *Trends Biochem Sci* **32**, 6-11.

Johnson, A. and O'Donnell, M. **(2005)**. Cellular DNA replicases: components and dynamics at the replication fork. *Annu Rev Biochem* **74**, 283-315.

Johnson, E. S. **(2004)**. Protein modification by SUMO. *Annu Rev Biochem* **73**, 355-382.

Johnson, E. S., Ma, P. C., Ota, I. M. and Varshavsky, A. **(1995)**. A proteolytic pathway that recognizes ubiquitin as a degradation signal. *J Biol Chem* **270**, 17442-17456.

Johnson, G. D. and Bond, J. S. **(1997)**. Activation mechanism of meprins, members of the astacin metalloendopeptidase family. *J Biol Chem* **272**, 28126-28132.

Johnson, R. E., Prakash, S. and Prakash, L. **(1999)**. Efficient bypass of a thymine-thymine dimer by yeast DNA polymerase, Poleta. *Science* **283**, 1001-1004.

Johnston, J. A. and Burrows, J. F. **(2006)**. De-ubiquitinating enzymes: intracellular signalling and disease. *Biochem Soc Trans* **34**, 764-769.

Johnston, S. C., Larsen, C. N., Cook, W. J., Wilkinson, K. D. and Hill, C. P. **(1997)**. Crystal structure of a deubiquitinating enzyme (human UCH-L3) at 1.8 Å resolution. *Embo J* **16**, 3787-3796.

Joo, H. Y., Zhai, L., Yang, C., Nie, S., Erdjument-Bromage, H., Tempst, P., Chang, C. and Wang, H. **(2007)**. Regulation of cell cycle progression and gene expression by H2A deubiquitination. *Nature* **449**, 1068-1072.

Kaliszewski, P. and Zoladek, T. **(2008)**. The role of Rsp5 ubiquitin ligase in regulation of diverse processes in yeast cells. *Acta Biochim Pol* **55**, 649-662.

Kallijarvi, J., Avela, K., Lipsanen-Nyman, M., Ulmanen, I. and Lehesjoki, A. E. **(2002)**. The TRIM37 gene encodes a peroxisomal RING-B-box-coiled-coil protein: classification of mulibrey nanism as a new peroxisomal disorder. *Am J Hum Genet* **70**, 1215-1228.

Kannouche, P. L., Wing, J. and Lehmann, A. R. **(2004)**. Interaction of human DNA polymerase eta with monoubiquitinated PCNA: a possible mechanism for the polymerase switch in response to DNA damage. *Mol Cell* **14**, 491-500.

Karran, P. **(2000)**. DNA double strand break repair in mammalian cells. *Curr Opin Genet Dev* **10**, 144-150.

Kato, M., Miyazawa, K. and Kitamura, N. **(2000)**. A deubiquitinating enzyme UBPY interacts with the Src homology 3 domain of Hrs-binding protein via a novel binding motif PX(V/I)(D/N)RXXKP. *J Biol Chem* **275**, 37481-37487.

Kawakami, T., Chiba, T., Suzuki, T., Iwai, K., Yamanaka, K., Minato, N., Suzuki, H., Shimbara, N., Hidaka, Y., Osaka, F., Omata, M. and Tanaka, K. **(2001)**. NEDD8 recruits E2-ubiquitin to SCF E3 ligase. *EMBO J* **20**, 4003-4012.

Kayagaki, N., Phung, Q., Chan, S., Chaudhari, R., Quan, C., O'Rourke, K. M., Eby, M., Pietras, E., Cheng, G., Bazan, J. F., Zhang, Z., Arnott, D. and Dixit, V. M. **(2007)**. DUBA: a deubiquitinase that regulates type I interferon production. *Science* **318**, 1628-1632.

Kee, Y., Lyon, N. and Huibregtse, J. M. **(2005)**. The Rsp5 ubiquitin ligase is coupled to and antagonized by the Ubp2 deubiquitinating enzyme. *Embo J* **24**, 2414-2424.

Kelley, L. A. and Sternberg, M. J. **(2009)**. Protein structure prediction on the Web: a case study using the Phyre server. *Nat Protoc* **4**, 363-371.

Kerscher, O., Felberbaum, R. and Hochstrasser, M. **(2006)**. Modification of proteins by ubiquitin and ubiquitin-like proteins. *Annu Rev Cell Dev Biol* **22**, 159-180.

Kikuchi, K., Ishii, N., Asao, H. and Sugamura, K. **(2003)**. Identification of AMSH-LP containing a Jab1/MPN domain metalloenzyme motif. *Biochem Biophys Res Commun* **306**, 637-643.



- Kim, J. H., Park, K. C., Chung, S. S., Bang, O. and Chung, C. H. **(2003)**. Deubiquitinating enzymes as cellular regulators. *J Biochem* **134**, 9-18.
- Kim, J. M., Parmar, K., Huang, M., Weinstock, D. M., Ruit, C. A., Kutok, J. L. and D'Andrea, A. D. **(2009)**. Inactivation of murine Usp1 results in genomic instability and a Fanconi anemia phenotype. *Dev Cell* **16**, 314-320.
- Kinner, A. and Kolling, R. **(2003)**. The yeast deubiquitinating enzyme Ubp16 is anchored to the outer mitochondrial membrane. *FEBS Lett* **549**, 135-140.
- Kleijer, W. J., Laugel, V., Berneburg, M., Nardo, T., Fawcett, H., Gratchev, A., Jaspers, N. G., Sarasin, A., Stefanini, M. and Lehmann, A. R. **(2008)**. Incidence of DNA repair deficiency disorders in western Europe: Xeroderma pigmentosum, Cockayne syndrome and trichothiodystrophy. *DNA Repair (Amst)* **7**, 744-750.
- Kolas, N. K. and Durocher, D. **(2006)**. DNA repair: DNA polymerase zeta and Rev1 break in. *Curr Biol* **16**, R296-299.
- Komander, D., Lord, C. J., Scheel, H., Swift, S., Hofmann, K., Ashworth, A. and Barford, D. **(2008)**. The structure of the CYLD USP domain explains its specificity for Lys63-linked polyubiquitin and reveals a B box module. *Mol Cell* **29**, 451-464.
- Kraemer, K. H., Lee, M. M. and Scotto, J. **(1987)**. Xeroderma pigmentosum. Cutaneous, ocular, and neurologic abnormalities in 830 published cases. *Arch Dermatol* **123**, 241-250.
- Krishna, S. S. and Grishin, N. V. **(2004)**. The finger domain of the human deubiquitinating enzyme HAUSP is a zinc ribbon. *Cell Cycle* **3**, 1046-1049.
- Krylov, D. M. and Koonin, E. V. **(2001)**. A novel family of predicted retroviral-like aspartyl proteases with a possible key role in eukaryotic cell cycle control. *Curr Biol* **11**, R584-587.

Kuhn, A. N. and Kaufer, N. F. **(2003)**. Pre-mRNA splicing in *Schizosaccharomyces pombe*: regulatory role of a kinase conserved from fission yeast to mammals. *Curr Genet* **42**, 241-251.

Kunkel, T. A. **(2004)**. DNA replication fidelity. *J Biol Chem* **279**, 16895-16898.

Kwon, J. E., La, M., Oh, K. H., Oh, Y. M., Kim, G. R., Seol, J. H., Baek, S. H., Chiba, T., Tanaka, K., Bang, O. S., Joe, C. O. and Chung, C. H. **(2006)**. BTB domain-containing speckle-type POZ protein (SPOP) serves as an adaptor of Daxx for ubiquitination by Cul3-based ubiquitin ligase. *J Biol Chem* **281**, 12664-12672.

La, M., Kim, K., Park, J., Won, J., Lee, J. H., Fu, Y. M., Meadows, G. G. and Joe, C. O. **(2004)**. Daxx-mediated transcriptional repression of MMP1 gene is reversed by SPOP. *Biochem Biophys Res Commun* **320**, 760-765.

Lam, M. H., Urban-Grimal, D., Bugnicourt, A., Greenblatt, J. F., Haguenaer-Tsapis, R. and Emili, A. **(2009)**. Interaction of the deubiquitinating enzyme Ubp2 and the e3 ligase Rsp5 is required for transporter/receptor sorting in the multivesicular body pathway. *PLoS ONE* **4**, e4259.

Langston, L. D. and O'Donnell, M. **(2006)**. DNA replication: keep moving and don't mind the gap. *Mol Cell* **23**, 155-160.

Lee, K. Y. and Myung, K. **(2008)**. PCNA modifications for regulation of post-replication repair pathways. *Mol Cells* **26**, 5-11.

Leggett, D. S., Hanna, J., Borodovsky, A., Crosas, B., Schmidt, M., Baker, R. T., Walz, T., Ploegh, H. and Finley, D. **(2002)**. Multiple associated proteins regulate proteasome structure and function. *Mol Cell* **10**, 495-507.

Lehmann, A. R. **(1972)**. Postreplication repair of DNA in ultraviolet-irradiated mammalian cells. *J Mol Biol* **66**, 319-337.

Lehmann, A. R. **(2006)**. New functions for Y family polymerases. *Mol Cell* **24**, 493-495.

Lehmann, A. R. and Fuchs, R. P. **(2006)**. Gaps and forks in DNA replication: Rediscovering old models. *DNA Repair (Amst)* **5**, 1495-1498.

Lehmann, A. R., Kirk-Bell, S., Arlett, C. F., Paterson, M. C., Lohman, P. H., de Weerd-Kastelein, E. A. and Bootsma, D. **(1975)**. Xeroderma pigmentosum cells with normal levels of excision repair have a defect in DNA synthesis after UV-irradiation. *Proc Natl Acad Sci U S A* **72**, 219-223.

Lehmann, A. R., Niimi, A., Ogi, T., Brown, S., Sabbioneda, S., Wing, J. F., Kannouche, P. L. and Green, C. M. **(2007)**. Translesion synthesis: Y-family polymerases and the polymerase switch. *DNA Repair (Amst)* **6**, 891-899.

Li, M., Brooks, C. L., Kon, N. and Gu, W. **(2004)**. A dynamic role of HAUSP in the p53-Mdm2 pathway. *Mol Cell* **13**, 879-886.

Li, M., Chen, D., Shiloh, A., Luo, J., Nikolaev, A. Y., Qin, J. and Gu, W. **(2002)**. Deubiquitination of p53 by HAUSP is an important pathway for p53 stabilization. *Nature* **416**, 648-653.

Li, T., Naqvi, N. I., Yang, H. and Teo, T. S. **(2000)**. Identification of a 26S proteasome-associated UCH in fission yeast. *Biochem Biophys Res Commun* **272**, 270-275.

Li, X. and Heyer, W. D. **(2008)**. Homologous recombination in DNA repair and DNA damage tolerance. *Cell Res* **18**, 99-113.

Lindahl, T. **(1993)**. Instability and decay of the primary structure of DNA. *Nature* **362**, 709-715.

Lindahl, T. and Wood, R. D. **(1999)**. Quality control by DNA repair. *Science* **286**, 1897-1905.

Lindner, H. A. **(2007)**. Deubiquitination in virus infection. *Virology* **362**, 245-256.

Lis, E. T. and Romesberg, F. E. **(2006)**. Role of Doa1 in the *Saccharomyces cerevisiae* DNA damage response. *Mol Cell Biol* **26**, 4122-4133.

Liu, Y., Fallon, L., Lashuel, H. A., Liu, Z. and Lansbury, P. T., Jr. **(2002)**. The UCH-L1 gene encodes two opposing enzymatic activities that affect alpha-synuclein degradation and Parkinson's disease susceptibility. *Cell* **111**, 209-218.

Liu, Y. and West, S. C. **(2004)**. Happy Hollidays: 40th anniversary of the Holliday junction. *Nat Rev Mol Cell Biol* **5**, 937-944.

Liu, Y. and Xiao, W. **(1997)**. Bidirectional regulation of two DNA-damage-inducible genes, MAG1 and DDI1, from *Saccharomyces cerevisiae*. *Mol Microbiol* **23**, 777-789.

Lodish, H., Berk, A., Matsudaira, P., Kaiser, C. A., Krieger, M., Scott, M. P., Zipursky, S. L. and Darnell, J. (2004). *Molecular cell biology*, 5th edn (New York, W. H. Freeman and Company).

Lopes, M., Foiani, M. and Sogo, J. M. **(2006)**. Multiple mechanisms control chromosome integrity after replication fork uncoupling and restart at irreparable UV lesions. *Mol Cell* **21**, 15-27.

Loring, G. L., Christensen, K. C., Gerber, S. A. and Brenner, C. **(2008)**. Yeast Chfr homologs retard cell cycle at G1 and G2/M via Ubc4 and Ubc13/Mms2-dependent ubiquitination. *Cell Cycle* **7**, 96-105.

Lu, J. Y., Lin, Y. Y., Qian, J., Tao, S. C., Zhu, J., Pickart, C. and Zhu, H. **(2008)**. Functional dissection of a HECT ubiquitin E3 ligase. *Mol Cell Proteomics* **7**, 35-45.

Lygerou, Z., Christophides, G. and Seraphin, B. **(1999)**. A novel genetic screen for snRNP assembly factors in yeast identifies a conserved protein, Sad1p, also required for pre-mRNA splicing. *Mol Cell Biol* **19**, 2008-2020.

Maga, G. and Hubscher, U. **(2003)**. Proliferating cell nuclear antigen (PCNA): a dancer with many partners. *J Cell Sci* **116**, 3051-3060.

Maga, G. and Huebscher, U. **(2003)**. Proliferating cell nuclear antigen (PCNA): a dancer with many partners. *J Cell Sci* **116**, 3051-3060.

Makarova, K. S., Aravind, L. and Koonin, E. V. **(2000)**. A novel superfamily of predicted cysteine proteases from eukaryotes, viruses and Chlamydia pneumoniae. *Trends Biochem Sci* **25**, 50-52.

Makarova, O. V., Makarov, E. M. and Luhrmann, R. **(2001)**. The 65 and 110 kDa SR-related proteins of the U4/U6.U5 tri-snRNP are essential for the assembly of mature spliceosomes. *Embo J* **20**, 2553-2563.

Masutani, C., Kusumoto, R., Yamada, A., Dohmae, N., Yokoi, M., Yuasa, M., Araki, M., Iwai, S., Takio, K. and Hanaoka, F. **(1999)**. The XPV (xeroderma pigmentosum variant) gene encodes human DNA polymerase eta. *Nature* **399**, 700-704.

Masuya, D., Huang, C., Liu, D., Nakashima, T., Yokomise, H., Ueno, M., Nakashima, N. and Sumitomo, S. **(2006)**. The HAUSP gene plays an important role in non-small cell lung carcinogenesis through p53-dependent pathways. *J Pathol* **208**, 724-732.

Matsuoka, S., Ballif, B. A., Smogorzewska, A., McDonald, E. R., 3rd, Hurov, K. E., Luo, J., Bakalarski, C. E., Zhao, Z., Solimini, N., Lerenthal, Y., Shiloh, Y., Gygi, S. P. and Elledge, S. J. **(2007)**. ATM and ATR substrate analysis reveals extensive protein networks responsive to DNA damage. *Science* **316**, 1160-1166.

Matsuyama, A., Arai, R., Yashiroda, Y., Shirai, A., Kamata, A., Sekido, S., Kobayashi, Y., Hashimoto, A., Hamamoto, M., Hiraoka, Y., Horinouchi, S. and Yoshida, M. **(2006)**. ORFeome cloning and global analysis of protein localization in the fission yeast *Schizosaccharomyces pombe*. *Nat Biotechnol* **24**, 841-847.

Matsuyama, A., Shirai, A., Yashiroda, Y., Kamata, A., Horinouchi, S. and Yoshida, M. **(2004)**. pDUAL, a multipurpose, multicopy vector capable of chromosomal integration in fission yeast. *Yeast* **21**, 1289-1305.

Matunis, M. J. **(2002)**. On the road to repair: PCNA encounters SUMO and ubiquitin modifications. *Mol Cell* **10**, 441-442.

Maytal-Kivity, V., Reis, N., Hofmann, K. and Glickman, M. H. **(2002)**. MPN+, a putative catalytic motif found in a subset of MPN domain proteins from eukaryotes and prokaryotes, is critical for Rpn11 function. *BMC Biochem* **3**, 28.

McCullough, J., Clague, M. J. and Urbe, S. **(2004)**. AMSH is an endosome-associated ubiquitin isopeptidase. *J Cell Biol* **166**, 487-492.

McCullough, J., Row, P. E., Lorenzo, O., Doherty, M., Beynon, R., Clague, M. J. and Urbe, S. **(2006)**. Activation of the endosome-associated ubiquitin isopeptidase AMSH by STAM, a component of the multivesicular body-sorting machinery. *Curr Biol* **16**, 160-165.

McGlynn, P. and Lloyd, R. G. **(2002a)**. Genome stability and the processing of damaged replication forks by RecG. *Trends Genet* **18**, 413-419.

McGlynn, P. and Lloyd, R. G. **(2002b)**. Recombinational repair and restart of damaged replication forks. *Nat Rev Mol Cell Biol* **3**, 859-870.

Memisoglu, A. and Samson, L. **(2000)**. Contribution of base excision repair, nucleotide excision repair, and DNA recombination to alkylation resistance of the fission yeast *Schizosaccharomyces pombe*. *J Bacteriol* **182**, 2104-2112.

Meray, R. K. and Lansbury, P. T., Jr. **(2007)**. Reversible monoubiquitination regulates the Parkinson disease-associated ubiquitin hydrolase UCH-L1. *J Biol Chem* **282**, 10567-10575.

Meroni, G. and Diez-Roux, G. **(2005)**. TRIM/RBCC, a novel class of 'single protein RING finger' E3 ubiquitin ligases. *Bioessays* **27**, 1147-1157.

Messick, T. E., Russell, N. S., Iwata, A. J., Sarachan, K. L., Shiekhhattar, R., Shanks, J. R., Reyes-Turcu, F. E., Wilkinson, K. D. and Marmorstein, R. **(2008)**.

Structural basis for ubiquitin recognition by the Otu1 ovarian tumor domain protein. *J Biol Chem* **283**, 11038-11049.

Meulmeester, E., Kunze, M., Hsiao, H. H., Urlaub, H. and Melchior, F. **(2008)**. Mechanism and consequences for paralog-specific sumoylation of ubiquitin-specific protease 25. *Mol Cell* **30**, 610-619.

Midorikawa, K., Murata, M., Oikawa, S., Tada-Oikawa, S. and Kawanishi, S. **(2000)**. DNA damage by dimethylformamide: role of hydrogen peroxide generated during degradation. *Chem Res Toxicol* **13**, 309-315.

Mimnaugh, E. G., Kayastha, G., McGovern, N. B., Hwang, S. G., Marcu, M. G., Trepel, J., Cai, S. Y., Marchesi, V. T. and Neckers, L. **(2001)**. Caspase-dependent deubiquitination of monoubiquitinated nucleosomal histone H2A induced by diverse apoptogenic stimuli. *Cell Death Differ* **8**, 1182-1196.

Mitchell, J. R., Hoeijmakers, J. H. and Niedernhofer, L. J. **(2003)**. Divide and conquer: nucleotide excision repair battles cancer and ageing. *Curr Opin Cell Biol* **15**, 232-240.

Miyase, S., Tateishi, S., Watanabe, K., Tomita, K., Suzuki, K., Inoue, H. and Yamaizumi, M. **(2005)**. Differential regulation of Rad18 through Rad6-dependent mono- and polyubiquitination. *J Biol Chem* **280**, 515-524.

Mizuno, E., Iura, T., Mukai, A., Yoshimori, T., Kitamura, N. and Komada, M. **(2005)**. Regulation of epidermal growth factor receptor down-regulation by UBPY-mediated deubiquitination at endosomes. *Mol Biol Cell* **16**, 5163-5174.

Moazed, D. and Johnson, D. **(1996)**. A deubiquitinating enzyme interacts with SIR4 and regulates silencing in *S. cerevisiae*. *Cell* **86**, 667-677.

Moldovan, G. L., Pfander, B. and Jentsch, S. **(2007)**. PCNA, the maestro of the replication fork. *Cell* **129**, 665-679.

- Moore, C. W. **(1991)**. Further characterizations of bleomycin-sensitive (blm) mutants of *Saccharomyces cerevisiae* with implications for a radiomimetic model. *J Bacteriol* **173**, 3605-3608.
- Motegi, A., Liaw, H. J., Lee, K. Y., Roest, H. P., Maas, A., Wu, X., Moinova, H., Markowitz, S. D., Ding, H., Hoeijmakers, J. H. and Myung, K. **(2008)**. Polyubiquitination of proliferating cell nuclear antigen by HLTF and SHPRH prevents genomic instability from stalled replication forks. *Proc Natl Acad Sci U S A* **105**, 12411-12416.
- Motegi, A., Sood, R., Moinova, H., Markowitz, S. D., Liu, P. P. and Myung, K. **(2006)**. Human SHPRH suppresses genomic instability through proliferating cell nuclear antigen polyubiquitination. *J Cell Biol* **175**, 703-708.
- Mullally, J. E., Chernova, T. and Wilkinson, K. D. **(2006)**. Doa1 is a Cdc48 adapter that possesses a novel ubiquitin binding domain. *Mol Cell Biol* **26**, 822-830.
- Mundt, K. E., Liu, C. and Carr, A. M. **(2002)**. Deletion mutants in COP9/signalosome subunits in fission yeast *Schizosaccharomyces pombe* display distinct phenotypes. *Mol Biol Cell* **13**, 493-502.
- Nakamura, M., Tanaka, N., Kitamura, N. and Komada, M. **(2006)**. Clathrin anchors deubiquitinating enzymes, AMSH and AMSH-like protein, on early endosomes. *Genes Cells* **11**, 593-606.
- Nanao, M. H., Tcherniuk, S. O., Chroboczek, J., Dideberg, O., Dessen, A. and Balakirev, M. Y. **(2004)**. Crystal structure of human otubain 2. *EMBO Rep* **5**, 783-788.
- Nicassio, F., Corrado, N., Vissers, J. H., Areces, L. B., Bergink, S., Marteijn, J. A., Geverts, B., Houtsmuller, A. B., Vermeulen, W., Di Fiore, P. P. and Citterio, E. **(2007)**. Human USP3 is a chromatin modifier required for S phase progression and genome stability. *Curr Biol* **17**, 1972-1977.



- Niimi, A., Brown, S., Sabbioneda, S., Kannouche, P. L., Scott, A., Yasui, A., Green, C. M. and Lehmann, A. R. **(2008)**. Regulation of proliferating cell nuclear antigen ubiquitination in mammalian cells. *Proc Natl Acad Sci U S A* **105**, 16125-16130.
- Nijman, S. M., Huang, T. T., Dirac, A. M., Brummelkamp, T. R., Kerkhoven, R. M., D'Andrea, A. D. and Bernards, R. **(2005a)**. The deubiquitinating enzyme USP1 regulates the Fanconi anemia pathway. *Mol Cell* **17**, 331-339.
- Nijman, S. M., Luna-Vargas, M. P., Velds, A., Brummelkamp, T. R., Dirac, A. M., Sixma, T. K. and Bernards, R. **(2005b)**. A genomic and functional inventory of deubiquitinating enzymes. *Cell* **123**, 773-786.
- Nishikawa, H., Wu, W., Koike, A., Kojima, R., Gomi, H., Fukuda, M. and Ohta, T. **(2009)**. BRCA1-associated protein 1 interferes with BRCA1/BARD1 RING heterodimer activity. *Cancer Res* **69**, 111-119.
- Notenboom, V., Hibbert, R. G., van Rossum-Fikkert, S. E., Olsen, J. V., Mann, M. and Sixma, T. K. **(2007)**. Functional characterization of Rad18 domains for Rad6, ubiquitin, DNA binding and PCNA modification. *Nucleic Acids Res* **35**, 5819-5830.
- Nurse, P. M. **(2002)**. Nobel Lecture. Cyclin dependent kinases and cell cycle control. *Biosci Rep* **22**, 487-499.
- O'Neill, B. M., Hanway, D., Winzeler, E. A. and Romesberg, F. E. **(2004)**. Coordinated functions of WSS1, PSY2 and TOF1 in the DNA damage response. *Nucleic Acids Res* **32**, 6519-6530.
- Oakley, T. J. and Hickson, I. D. **(2002)**. Defending genome integrity during S-phase: putative roles for RecQ helicases and topoisomerase III. *DNA Repair (Amst)* **1**, 175-207.
- Ogi, T. and Lehmann, A. R. **(2006)**. The Y-family DNA polymerase kappa (pol kappa) functions in mammalian nucleotide-excision repair. *Nat Cell Biol* **8**, 640-642.

Ogiso, Y., Sugiura, R., Kamo, T., Yanagiya, S., Lu, Y., Okazaki, K., Shuntoh, H. and Kuno, T. **(2004)**. Lub1 participates in ubiquitin homeostasis and stress response via maintenance of cellular ubiquitin contents in fission yeast. *Mol Cell Biol* **24**, 2324-2331.

Oh, Y. M., Yoo, S. J. and Seol, J. H. **(2007)**. Deubiquitination of Chfr, a checkpoint protein, by USP7/HAUSP regulates its stability and activity. *Biochem Biophys Res Commun* **357**, 615-619.

Ohmori, H., Friedberg, E. C., Fuchs, R. P., Goodman, M. F., Hanaoka, F., Hinkle, D., Kunkel, T. A., Lawrence, C. W., Livneh, Z., Nohmi, T., Prakash, L., Prakash, S., Todo, T., Walker, G. C., Wang, Z. and Woodgate, R. **(2001)**. The Y-family of DNA polymerases. *Mol Cell* **8**, 7-8.

Osley, M. A. **(2006)**. Regulation of histone H2A and H2B ubiquitylation. *Brief Funct Genomic Proteomic* **5**, 179-189.

Pai, M. T., Tzeng, S. R., Kovacs, J. J., Keaton, M. A., Li, S. S., Yao, T. P. and Zhou, P. **(2007)**. Solution structure of the Ubp-M BUZ domain, a highly specific protein module that recognizes the C-terminal tail of free ubiquitin. *J Mol Biol* **370**, 290-302.

Papouli, E., Chen, S., Davies, A. A., Huttner, D., Krejci, L., Sung, P. and Ulrich, H. D. **(2005)**. Crosstalk between SUMO and ubiquitin on PCNA is mediated by recruitment of the helicase Srs2p. *Mol Cell* **19**, 123-133.

Parker, F., Maurier, F., Delumeau, I., Duchesne, M., Faucher, D., Debussche, L., Dugue, A., Schweighoffer, F. and Tocque, B. **(1996)**. A Ras-GTPase-activating protein SH3-domain-binding protein. *Mol Cell Biol* **16**, 2561-2569.

Pastink, A., Eeken, J. C. and Lohman, P. H. **(2001)**. Genomic integrity and the repair of double-strand DNA breaks. *Mutat Res* **480-481**, 37-50.

Paulsson, K., Bekassy, A. N., Olofsson, T., Mitelman, F., Johansson, B. and Panagopoulos, I. **(2006)**. A novel and cytogenetically cryptic t(7;21)(p22;q22) in

acute myeloid leukemia results in fusion of RUNX1 with the ubiquitin-specific protease gene USP42. *Leukemia* **20**, 224-229.

Perheentupa, J., Autio, S., Leisti, S., Tuuteri, L. and Raitta, C. **(1973)**. Letter: Mulibrey nanism v. hereditary congenital dwarfism with pericardial constriction. *Lancet* **2**, 1095.

Petroski, M. D., Zhou, X., Dong, G., Daniel-Issakani, S., Payan, D. G. and Huang, J. **(2007)**. Substrate modification with lysine 63-linked ubiquitin chains through the UBC13-UEV1A ubiquitin-conjugating enzyme. *J Biol Chem* **282**, 29936-29945.

Pfander, B., Moldovan, G. L., Sacher, M., Hoege, C. and Jentsch, S. **(2005)**. SUMO-modified PCNA recruits Srs2 to prevent recombination during S phase. *Nature* **436**, 428-433.

Pijnappel, W. W. and Timmers, H. T. **(2008)**. Dubbing SAGA unveils new epigenetic crosstalk. *Mol Cell* **29**, 152-154.

Plosky, B. S., Vidal, A. E., Fernandez de Henestrosa, A. R., McLenigan, M. P., McDonald, J. P., Mead, S. and Woodgate, R. **(2006)**. Controlling the subcellular localization of DNA polymerases  $\iota$  and  $\eta$  via interactions with ubiquitin. *Embo J* **25**, 2847-2855.

Popov, N., Wanzel, M., Madiredjo, M., Zhang, D., Beijersbergen, R., Bernards, R., Moll, R., Elledge, S. J. and Eilers, M. **(2007)**. The ubiquitin-specific protease USP28 is required for MYC stability. *Nat Cell Biol* **9**, 765-774.

Potter, J. L., Narasimhan, J., Mende-Mueller, L. and Haas, A. L. **(1999)**. Precursor processing of pro-ISG15/UCRP, an interferon-beta-induced ubiquitin-like protein. *J Biol Chem* **274**, 25061-25068.

Prakash, L. **(1981)**. Characterization of postreplication repair in *Saccharomyces cerevisiae* and effects of rad6, rad18, rev3 and rad52 mutations. *Mol Gen Genet* **184**, 471-478.

- Prakash, S., Johnson, R. E. and Prakash, L. **(2005)**. Eukaryotic translesion synthesis DNA polymerases: specificity of structure and function. *Annu Rev Biochem* **74**, 317-353.
- Raymond, M., Gros, P., Whiteway, M. and Thomas, D. Y. **(1992)**. Functional complementation of yeast *ste6* by a mammalian multidrug resistance *mdr* gene. *Science* **256**, 232-234.
- Reyes-Turcu, F. E., Horton, J. R., Mullally, J. E., Heroux, A., Cheng, X. and Wilkinson, K. D. **(2006)**. The ubiquitin binding domain ZnF UBP recognizes the C-terminal diglycine motif of unanchored ubiquitin. *Cell* **124**, 1197-1208.
- Reyes-Turcu, F. E., Shanks, J. R., Komander, D. and Wilkinson, K. D. **(2008)**. Recognition of polyubiquitin isoforms by the multiple ubiquitin binding modules of isopeptidase T. *J Biol Chem* **283**, 19581-19592.
- Reyes-Turcu, F. E., Ventii, K. H. and Wilkinson, K. D. **(2009)**. Regulation and Cellular Roles of Ubiquitin-Specific Deubiquitinating Enzymes. *Annual Review of Biochemistry* **78**, 363-397.
- Reyes-Turcu, F. E. and Wilkinson, K. D. **(2009)**. Polyubiquitin binding and disassembly by deubiquitinating enzymes. *Chem Rev* **109**, 1495-1508.
- Richert, K., Schmidt, H., Gross, T. and Kaeufer, F. **(2002)**. The deubiquitinating enzyme Ubp21p of fission yeast stabilizes a mutant form of protein kinase Prp4p. *Mol Genet Genomics* **267**, 88-95.
- Riley, T., Sontag, E., Chen, P. and Levine, A. **(2008)**. Transcriptional control of human p53-regulated genes. *Nat Rev Mol Cell Biol* **9**, 402-412.
- Ronai, Z. **(2006)**. Balancing Mdm2 - a Daxx-HAUSP matter. *Nat Cell Biol* **8**, 790-791.
- Row, P. E., Liu, H., Hayes, S., Welchman, R., Charalabous, P., Hofmann, K., Clague, M. J., Sanderson, C. M. and Urbe, S. **(2007)**. The MIT domain of UBPY

constitutes a CHMP binding and endosomal localization signal required for efficient epidermal growth factor receptor degradation. *J Biol Chem* **282**, 30929-30937.

Row, P. E., Prior, I. A., McCullough, J., Clague, M. J. and Urbe, S. **(2006)**. The ubiquitin isopeptidase UBPY regulates endosomal ubiquitin dynamics and is essential for receptor down-regulation. *J Biol Chem* **281**, 12618-12624.

Rumpf, S. and Jentsch, S. **(2006)**. Functional division of substrate processing cofactors of the ubiquitin-selective Cdc48 chaperone. *Mol Cell* **21**, 261-269.

Rupp, W. D. and Howard-Flanders, P. **(1968)**. Discontinuities in the DNA synthesized in an excision-defective strain of *Escherichia coli* following ultraviolet irradiation. *J Mol Biol* **31**, 291-304.

Rytönen, A. and Holden, D. W. **(2007)**. Bacterial interference of ubiquitination and deubiquitination. *Cell Host Microbe* **1**, 13-22.

Sambrook, J., Fritsch, E. F. and Maniatis, T., eds. (1989). *Molecular Cloning: A Laboratory Manual*, 2nd edn (Cold Spring Harbor: Cold Spring Harbor Laboratory Press).

San Filippo, J., Sung, P. and Klein, H. **(2008)**. Mechanism of eukaryotic homologous recombination. *Annu Rev Biochem* **77**, 229-257.

Sancar, A. **(1996)**. DNA excision repair. *Annu Rev Biochem* **65**, 43-81.

Sancar, A., Lindsey-Boltz, L. A., Unsal-Kacmaz, K. and Linn, S. **(2004)**. Molecular mechanisms of mammalian DNA repair and the DNA damage checkpoints. *Annu Rev Biochem* **73**, 39-85.

Saridakis, V., Sheng, Y., Sarkari, F., Holowaty, M. N., Shire, K., Nguyen, T., Zhang, R. G., Liao, J., Lee, W., Edwards, A. M., Arrowsmith, C. H. and Frappier, L. **(2005)**. Structure of the p53 binding domain of HAUSP/USP7 bound to Epstein-Barr nuclear antigen 1 implications for EBV-mediated immortalization. *Mol Cell* **18**, 25-36.

Sarkar, S., Davies, A. A., Ulrich, H. D. and McHugh, P. J. **(2006)**. DNA interstrand crosslink repair during G1 involves nucleotide excision repair and DNA polymerase zeta. *Embo J* **25**, 1285-1294.

Sato, Y., Yoshikawa, A., Yamagata, A., Mimura, H., Yamashita, M., Ookata, K., Nureki, O., Iwai, K., Komada, M. and Fukai, S. **(2008)**. Structural basis for specific cleavage of Lys 63-linked polyubiquitin chains. *Nature* **455**, 358-362.

Schmitz, C., Kinner, A. and Kolling, R. **(2005)**. The deubiquitinating enzyme Ubp1 affects sorting of the ATP-binding cassette-transporter Ste6 in the endocytic pathway. *Mol Biol Cell* **16**, 1319-1329.

Schoenfeld, A. R., Apgar, S., Dolios, G., Wang, R. and Aaronson, S. A. **(2004)**. BRCA2 is ubiquitinated in vivo and interacts with USP11, a deubiquitinating enzyme that exhibits prosurvival function in the cellular response to DNA damage. *Mol Cell Biol* **24**, 7444-7455.

Schwechheimer, C. **(2004)**. The COP9 signalosome (CSN): an evolutionary conserved proteolysis regulator in eukaryotic development. *Biochim Biophys Acta* **1695**, 45-54.

Seeberg, E., Eide, L. and Bjoras, M. **(1995)**. The base excision repair pathway. *Trends Biochem Sci* **20**, 391-397.

Setsuie, R. and Wada, K. **(2007)**. The functions of UCH-L1 and its relation to neurodegenerative diseases. *Neurochem Int* **51**, 105-111.

Shell, S. S., Putnam, C. D. and Kolodner, R. D. **(2007)**. The N terminus of *Saccharomyces cerevisiae* Msh6 is an unstructured tether to PCNA. *Mol Cell* **26**, 565-578.

Sheng, Y., Saridakis, V., Sarkari, F., Duan, S., Wu, T., Arrowsmith, C. H. and Frappier, L. **(2006)**. Molecular recognition of p53 and MDM2 by USP7/HAUSP. *Nat Struct Mol Biol* **13**, 285-291.

Sipiczki, M. **(2000)**. Where does fission yeast sit on the tree of life? *Genome Biol* **1**, REVIEWS1011.

Sirkis, R., Gerst, J. E. and Fass, D. **(2006)**. Ddi1, a eukaryotic protein with the retroviral protease fold. *J Mol Biol* **364**, 376-387.

Skinner, P. J., Koshy, B. T., Cummings, C. J., Klement, I. A., Helin, K., Servadio, A., Zoghbi, H. Y. and Orr, H. T. **(1997)**. Ataxin-1 with an expanded glutamine tract alters nuclear matrix-associated structures. *Nature* **389**, 971-974.

Smogorzewska, A., Matsuoka, S., Vinciguerra, P., McDonald, E. R., 3rd, Hurov, K. E., Luo, J., Ballif, B. A., Gygi, S. P., Hofmann, K., D'Andrea, A. D. and Elledge, S. J. **(2007)**. Identification of the FANCI protein, a monoubiquitinated FANCD2 paralog required for DNA repair. *Cell* **129**, 289-301.

Soboleva, T. A., Jans, D. A., Johnson-Saliba, M. and Baker, R. T. **(2005)**. Nuclear-cytoplasmic shuttling of the oncogenic mouse UNP/USP4 deubiquitylating enzyme. *J Biol Chem* **280**, 745-752.

Soncini, C., Berdo, I. and Draetta, G. **(2001)**. Ras-GAP SH3 domain binding protein (G3BP) is a modulator of USP10, a novel human ubiquitin specific protease. *Oncogene* **20**, 3869-3879.

Song, L. and Rape, M. **(2008)**. Reverse the curse--the role of deubiquitination in cell cycle control. *Curr Opin Cell Biol* **20**, 156-163.

Song, M. S., Song, S. J., Kim, S. J., Nakayama, K., Nakayama, K. I. and Lim, D. S. **(2008a)**. Skp2 regulates the antiproliferative function of the tumor suppressor RASSF1A via ubiquitin-mediated degradation at the G1-S transition. *Oncogene* **27**, 3176-3185.

Song, M. S., Song, S. J., Kim, S. Y., Oh, H. J. and Lim, D. S. **(2008b)**. The tumour suppressor RASSF1A promotes MDM2 self-ubiquitination by disrupting the MDM2-DAXX-HAUSP complex. *Embo J* **27**, 1863-1874.

- Stahl, F. W. **(1994)**. The Holliday junction on its thirtieth anniversary. *Genetics* **138**, 241-246.
- Stevenson, L. F., Sparks, A., Allende-Vega, N., Xirodimas, D. P., Lane, D. P. and Saville, M. K. **(2007)**. The deubiquitinating enzyme USP2a regulates the p53 pathway by targeting Mdm2. *Embo J* **26**, 976-986.
- Stone, M., Hartmann-Petersen, R., Seeger, M., Bech-Otschir, D., Wallace, M. and Gordon, C. **(2004)**. Uch2/Uch37 is the major deubiquitinating enzyme associated with the 26S proteasome in fission yeast. *J Mol Biol* **344**, 697-706.
- Styrkarsdottir, U., Egel, R. and Nielsen, O. **(1993)**. The *smt-0* mutation which abolishes mating-type switching in fission yeast is a deletion. *Curr Genet* **23**, 184-186.
- Sunnerhagen, M., Pursglove, S. and Fladvad, M. **(2002)**. The new MATH: homology suggests shared binding surfaces in meprin tetramers and TRAF trimers. *FEBS Lett* **530**, 1-3.
- Symington, L. S. **(2002)**. Role of RAD52 epistasis group genes in homologous recombination and double-strand break repair. *Microbiol Mol Biol Rev* **66**, 630-670.
- Takebe, H., Nishigori, C. and Satoh, Y. **(1987)**. Genetics and skin cancer of xeroderma pigmentosum in Japan. *Jpn J Cancer Res* **78**, 1135-1143.
- Tang, J., Qu, L. K., Zhang, J., Wang, W., Michaelson, J. S., Degenhardt, Y. Y., El-Deiry, W. S. and Yang, X. **(2006)**. Critical role for Daxx in regulating Mdm2. *Nat Cell Biol* **8**, 855-862.
- Taylor, D. L., Ho, J. C., Oliver, A. and Watts, F. Z. **(2002)**. Cell-cycle-dependent localisation of Ulp1, a *Schizosaccharomyces pombe* Pmt3 (SUMO)-specific protease. *J Cell Sci* **115**, 1113-1122.
- Tenno, T., Fujiwara, K., Tochio, H., Iwai, K., Morita, E. H., Hayashi, H., Murata, S., Hiroaki, H., Sato, M., Tanaka, K. and Shirakawa, M. **(2004)**. Structural basis for



distinct roles of Lys63- and Lys48-linked polyubiquitin chains. *Genes Cells* **9**, 865-875.

Timms, K. M., Ansari-Lari, M. A., Morris, W., Brown, S. N. and Gibbs, R. A. **(1998)**. The genomic organization of Isopeptidase T-3 (ISOT-3), a new member of the ubiquitin specific protease family (UBP). *Gene* **217**, 101-106.

Torok, M. and Etkin, L. D. **(2001)**. Two B or not two B? Overview of the rapidly expanding B-box family of proteins. *Differentiation* **67**, 63-71.

Torres-Ramos, C. A., Prakash, S. and Prakash, L. **(2002)**. Requirement of RAD5 and MMS2 for postreplication repair of UV-damaged DNA in *Saccharomyces cerevisiae*. *Mol Cell Biol* **22**, 2419-2426.

Tran, H. J., Allen, M. D., Lowe, J. and Bycroft, M. **(2003)**. Structure of the Jab1/MPN domain and its implications for proteasome function. *Biochemistry* **42**, 11460-11465.

Tsuji, Y., Watanabe, K., Araki, K., Shinohara, M., Yamagata, Y., Tsurimoto, T., Hanaoka, F., Yamamura, K., Yamaizumi, M. and Tateishi, S. **(2008)**. Recognition of forked and single-stranded DNA structures by human RAD18 complexed with RAD6B protein triggers its recruitment to stalled replication forks. *Genes Cells* **13**, 343-354.

Ulrich, H. D. **(2001)**. The srs2 suppressor of UV sensitivity acts specifically on the RAD5- and MMS2-dependent branch of the RAD6 pathway. *Nucleic Acids Res* **29**, 3487-3494.

Ulrich, H. D. **(2005)**. Mutual interactions between the SUMO and ubiquitin systems: a plea of no contest. *Trends Cell Biol* **15**, 525-532.

Ulrich, H. D. **(2006)**. Deubiquitinating PCNA: a downside to DNA damage tolerance. *Nat Cell Biol* **8**, 303-305.

Ulrich, H. D. **(2009)**. Regulating post-translational modifications of the eukaryotic replication clamp PCNA. *DNA Repair (Amst)* **8**, 461-469.

Unk, I., Hajdu, I., Fatyol, K., Szakal, B., Blastyak, A., Bermudez, V., Hurwitz, J., Prakash, L., Prakash, S. and Haracska, L. **(2006)**. Human SHPRH is a ubiquitin ligase for Mms2-Ubc13-dependent polyubiquitylation of proliferating cell nuclear antigen. *Proc Natl Acad Sci U S A* **103**, 18107-18112.

Uren, A. G. and Vaux, D. L. **(1996)**. TRAF proteins and meprins share a conserved domain. *Trends Biochem Sci* **21**, 244-245.

van der Horst, A., de Vries-Smits, A. M., Brenkman, A. B., van Triest, M. H., van den Broek, N., Colland, F., Maurice, M. M. and Burgering, B. M. **(2006)**. FOXO4 transcriptional activity is regulated by monoubiquitination and USP7/HAUSP. *Nat Cell Biol* **8**, 1064-1073.

van Hoffen, A., Balajee, A. S., van Zeeland, A. A. and Mullenders, L. H. **(2003)**. Nucleotide excision repair and its interplay with transcription. *Toxicology* **193**, 79-90.

van Leuken, R. J., Luna-Vargas, M. P., Sixma, T. K., Wolthuis, R. M. and Medema, R. H. **(2008)**. Usp39 is essential for mitotic spindle checkpoint integrity and controls mRNA-levels of aurora B. *Cell Cycle* **7**, 2710-2719.

Varadan, R., Assfalg, M., Haririnia, A., Raasi, S., Pickart, C. and Fushman, D. **(2004)**. Solution conformation of Lys63-linked di-ubiquitin chain provides clues to functional diversity of polyubiquitin signaling. *J Biol Chem* **279**, 7055-7063.

Veaute, X., Jeusset, J., Soustelle, C., Kowalczykowski, S. C., Le Cam, E. and Fabre, F. **(2003)**. The Srs2 helicase prevents recombination by disrupting Rad51 nucleoprotein filaments. *Nature* **423**, 309-312.

Verkade, H. M., Teli, T., Laursen, L. V., Murray, J. M. and O'Connell, M. J. **(2001)**. A homologue of the Rad18 postreplication repair gene is required for DNA damage

responses throughout the fission yeast cell cycle. *Mol Genet Genomics* **265**, 993-1003.

Verma, R., Aravind, L., Oania, R., McDonald, W. H., Yates, J. R., 3rd, Koonin, E. V. and Deshaies, R. J. **(2002)**. Role of Rpn11 metalloprotease in deubiquitination and degradation by the 26S proteasome. *Science* **298**, 611-615.

Vertegaal, A. C. **(2007)**. Small ubiquitin-related modifiers in chains. *Biochem Soc Trans* **35**, 1422-1423.

Vijay-Kumar, S., Bugg, C. E. and Cook, W. J. **(1987)**. Structure of ubiquitin refined at 1.8 Å resolution. *J Mol Biol* **194**, 531-544.

Voges, D., Zwickl, P. and Baumeister, W. **(1999)**. The 26S proteasome: a molecular machine designed for controlled proteolysis. *Annu Rev Biochem* **68**, 1015-1068.

Wada, K. and Kamitani, T. **(2006)**. UnpEL/Usp4 is ubiquitinated by Ro52 and deubiquitinated by itself. *Biochem Biophys Res Commun* **342**, 253-258.

Wada, K., Tanji, K. and Kamitani, T. **(2006)**. Oncogenic protein UnpEL/Usp4 deubiquitinates Ro52 by its isopeptidase activity. *Biochem Biophys Res Commun* **339**, 731-736.

Wang, L., Huang, G., Zhao, X., Hatlen, M. A., Vu, L., Liu, F. and Nimer, S. D. **(2009)**. Post-translational modifications of Runx1 regulate its activity in the cell. *Blood Cells Mol Dis* **43**, 30-34.

Wang, S. C., Nakajima, Y., Yu, Y. L., Xia, W., Chen, C. T., Yang, C. C., McIntush, E. W., Li, L. Y., Hawke, D. H., Kobayashi, R. and Hung, M. C. **(2006)**. Tyrosine phosphorylation controls PCNA function through protein stability. *Nat Cell Biol* **8**, 1359-1368.

Warbrick, E. **(2000)**. The puzzle of PCNA's many partners. *Bioessays* **22**, 997-1006.

Watanabe, K., Tateishi, S., Kawasuji, M., Tsurimoto, T., Inoue, H. and Yamaizumi, M. **(2004)**. Rad18 guides poleta to replication stalling sites through physical interaction and PCNA monoubiquitination. *Embo J* **23**, 3886-3896.

Waters, L. S. and Walker, G. C. **(2006)**. The critical mutagenic translesion DNA polymerase Rev1 is highly expressed during G(2)/M phase rather than S phase. *Proc Natl Acad Sci U S A* **103**, 8971-8976.

Watts, F. Z., Skilton, A., Ho, J. C., Boyd, L. K., Trickey, M. A., Gardner, L., Ogi, F. X. and Outwin, E. A. **(2007)**. The role of Schizosaccharomyces pombe SUMO ligases in genome stability. *Biochem Soc Trans* **35**, 1379-1384.

Weake, V. M. and Workman, J. L. **(2008)**. Histone ubiquitination: triggering gene activity. *Mol Cell* **29**, 653-663.

Wee, S., Geyer, R. K., Toda, T. and Wolf, D. A. **(2005)**. CSN facilitates Cullin-RING ubiquitin ligase function by counteracting autocatalytic adapter instability. *Nat Cell Biol* **7**, 387-391.

Welchman, R. L., Gordon, C. and Mayer, R. J. **(2005)**. Ubiquitin and ubiquitin-like proteins as multifunctional signals. *Nat Rev Mol Cell Biol* **6**, 599-609.

West, S. C. **(2003)**. Molecular views of recombination proteins and their control. *Nat Rev Mol Cell Biol* **4**, 435-445.

Whitby, M. C. **(2004)**. Junctions on the road to cancer. *Nat Struct Mol Biol* **11**, 693-695.

Wilkinson, K. D. **(2002)**. Cell biology: unchaining the condemned. *Nature* **419**, 351-353.

Wilkinson, K. D. **(2005)**. The discovery of ubiquitin-dependent proteolysis. *Proc Natl Acad Sci U S A* **102**, 15280-15282.

Willems, A. R., Schwab, M. and Tyers, M. **(2004)**. A hitchhiker's guide to the cullin ubiquitin ligases: SCF and its kin. *Biochim Biophys Acta* **1695**, 133-170.

Wilson, P. O., Barber, P. C., Hamid, Q. A., Power, B. F., Dhillon, A. P., Rode, J., Day, I. N., Thompson, R. J. and Polak, J. M. **(1988)**. The immunolocalization of protein gene product 9.5 using rabbit polyclonal and mouse monoclonal antibodies. *Br J Exp Pathol* **69**, 91-104.

Winborn, B. J., Travis, S. M., Todi, S. V., Scaglione, K. M., Xu, P., Williams, A. J., Cohen, R. E., Peng, J. and Paulson, H. L. **(2008)**. The deubiquitinating enzyme ataxin-3, a polyglutamine disease protein, edits Lys63 linkages in mixed linkage ubiquitin chains. *J Biol Chem* **283**, 26436-26443.

Wing, S. S. **(2003)**. Deubiquitinating enzymes--the importance of driving in reverse along the ubiquitin-proteasome pathway. *Int J Biochem Cell Biol* **35**, 590-605.

Wood, R. D. **(1997)**. Nucleotide excision repair in mammalian cells. *J Biol Chem* **272**, 23465-23468.

Wood, V., Gwilliam, R., Rajandream, M. A., Lyne, M., Lyne, R., Stewart, A., Sgouros, J., Peat, N., Hayles, J., Baker, S., Basham, D., Bowman, S., Brooks, K., Brown, D., Brown, S., Chillingworth, T., Churcher, C., Collins, M., Connor, R., Cronin, A., Davis, P., Feltwell, T., Fraser, A., Gentles, S., Goble, A., Hamlin, N., Harris, D., Hidalgo, J., Hodgson, G., Holroyd, S., Hornsby, T., Howarth, S., Huckle, E. J., Hunt, S., Jagels, K., James, K., Jones, L., Jones, M., Leather, S., McDonald, S., McLean, J., Mooney, P., Moule, S., Mungall, K., Murphy, L., Niblett, D., Odell, C., Oliver, K., O'Neil, S., Pearson, D., Quail, M. A., Rabinowitsch, E., Rutherford, K., Rutter, S., Saunders, D., Seeger, K., Sharp, S., Skelton, J., Simmonds, M., Squares, R., Squares, S., Stevens, K., Taylor, K., Taylor, R. G., Tivey, A., Walsh, S., Warren, T., Whitehead, S., Woodward, J., Volckaert, G., Aert, R., Robben, J., Grymonprez, B., Weltjens, I., Vanstreels, E., Rieger, M., Schafer, M., Muller-Auer, S., Gabel, C., Fuchs, M., Dusterhoft, A., Fritz, C., Holzer, E., Moestl, D., Hilbert, H., Borzym, K., Langer, I., Beck, A., Lehrach, H., Reinhardt, R., Pohl, T. M., Eger,

P., Zimmermann, W., Wedler, H., Wambutt, R., Purnelle, B., Goffeau, A., Cadieu, E., Dreano, S., Gloux, S., Lelaure, V., Mottier, S., Galibert, F., Aves, S. J., Xiang, Z., Hunt, C., Moore, K., Hurst, S. M., Lucas, M., Rochet, M., Gaillardin, C., Tallada, V. A., Garzon, A., Thode, G., Daga, R. R., Cruzado, L., Jimenez, J., Sanchez, M., del Rey, F., Benito, J., Dominguez, A., Revuelta, J. L., Moreno, S., Armstrong, J., Forsburg, S. L., Cerutti, L., Lowe, T., McCombie, W. R., Paulsen, I., Potashkin, J., Shpakovski, G. V., Ussery, D., Barrell, B. G. and Nurse, P. **(2002)**. The genome sequence of *Schizosaccharomyces pombe*. *Nature* **415**, 871-880.

Xiao, W., Chow, B. L., Broomfield, S. and Hanna, M. **(2000)**. The *Saccharomyces cerevisiae* RAD6 group is composed of an error-prone and two error-free postreplication repair pathways. *Genetics* **155**, 1633-1641.

Xu, H., Zhang, P., Liu, L. and Lee, M. Y. **(2001)**. A novel PCNA-binding motif identified by the panning of a random peptide display library. *Biochemistry* **40**, 4512-4520.

Yamaguchi, T., Kimura, J., Miki, Y. and Yoshida, K. **(2007a)**. The deubiquitinating enzyme USP11 controls an I $\kappa$ B kinase  $\alpha$  (IKK $\alpha$ )-p53 signaling pathway in response to tumor necrosis factor  $\alpha$  (TNF $\alpha$ ). *J Biol Chem* **282**, 33943-33948.

Yamaguchi, T., Miki, Y. and Yoshida, K. **(2007b)**. Protein kinase C  $\delta$  activates I $\kappa$ B-kinase  $\alpha$  to induce the p53 tumor suppressor in response to oxidative stress. *Cell Signal* **19**, 2088-2097.

Yao, S., Xie, L., Qian, M., Yang, H., Zhou, L., Zhou, Q., Yan, F., Gou, L., Wei, Y., Zhao, X. and Mo, X. **(2008a)**. Pnas4 is a novel regulator for convergence and extension during vertebrate gastrulation. *FEBS Lett* **582**, 2325-2332.

Yao, T. and Cohen, R. E. **(2002)**. A cryptic protease couples deubiquitination and degradation by the proteasome. *Nature* **419**, 403-407.

Yao, T., Song, L., Jin, J., Cai, Y., Takahashi, H., Swanson, S. K., Washburn, M. P., Florens, L., Conaway, R. C., Cohen, R. E. and Conaway, J. W. **(2008b)**. Distinct modes of regulation of the Uch37 deubiquitinating enzyme in the proteasome and in the Ino80 chromatin-remodeling complex. *Mol Cell* **31**, 909-917.

Zapata, J. M., Pawlowski, K., Haas, E., Ware, C. F., Godzik, A. and Reed, J. C. **(2001)**. A diverse family of proteins containing tumor necrosis factor receptor-associated factor domains. *J Biol Chem* **276**, 24242-24252.

Zhang, D., Zaugg, K., Mak, T. W. and Elledge, S. J. **(2006)**. A role for the deubiquitinating enzyme USP28 in control of the DNA-damage response. *Cell* **126**, 529-542.

Zhang, P., Wang, C. T., Yan, F., Gou, L., Tong, A. P., Cai, F., Li, Q., Deng, H. X. and Wei, Y. Q. **(2008a)**. Prokaryotic expression of a novel mouse pro-apoptosis protein PNAS-4 and application of its polyclonal antibodies. *Braz J Med Biol Res* **41**, 504-511.

Zhang, X. Y., Pfeiffer, H. K., Thorne, A. W. and McMahon, S. B. **(2008b)**. USP22, an hSAGA subunit and potential cancer stem cell marker, reverses the polycomb-catalyzed ubiquitylation of histone H2A. *Cell Cycle* **7**, 1522-1524.

Zhang, X. Y., Varthi, M., Sykes, S. M., Phillips, C., Warzecha, C., Zhu, W., Wyce, A., Thorne, A. W., Berger, S. L. and McMahon, S. B. **(2008c)**. The putative cancer stem cell marker USP22 is a subunit of the human SAGA complex required for activated transcription and cell-cycle progression. *Mol Cell* **29**, 102-111.

Zhao, J. **(2007)**. Sumoylation regulates diverse biological processes. *Cell Mol Life Sci* **64**, 3017-3033.

Zhou, C., Seibert, V., Geyer, R., Rhee, E., Lyapina, S., Cope, G., Deshaies, R. J. and Wolf, D. A. **(2001)**. The fission yeast COP9/signalosome is involved in cullin modification by ubiquitin-related Ned8p. *BMC Biochem* **2**, 7.

- Zhou, C., Wee, S., Rhee, E., Naumann, M., Dubiel, W. and Wolf, D. A. **(2003)**. Fission yeast COP9/signalosome suppresses cullin activity through recruitment of the deubiquitylating enzyme Ubp12p. *Mol Cell* **11**, 927-938.
- Zhou, L. and Watts, F. Z. **(2005)**. Nep1, a *Schizosaccharomyces pombe* deneddylating enzyme. *Biochem J* **389**, 307-314.
- Zhu, X., Menard, R. and Sulea, T. **(2007)**. High incidence of ubiquitin-like domains in human ubiquitin-specific proteases. *Proteins* **69**, 1-7.
- Zhu, Y., Carroll, M., Papa, F. R., Hochstrasser, M. and D'Andrea, A. D. **(1996a)**. DUB-1, a deubiquitinating enzyme with growth-suppressing activity. *Proc Natl Acad Sci U S A* **93**, 3275-3279.
- Zhu, Y., Pless, M., Inhorn, R., Mathey-Prevot, B. and D'Andrea, A. D. **(1996b)**. The murine DUB-1 gene is specifically induced by the betac subunit of interleukin-3 receptor. *Mol Cell Biol* **16**, 4808-4817.
- Zofall, M. and Grewal, S. I. **(2007)**. HULC, a histone H2B ubiquitinating complex, modulates heterochromatin independent of histone methylation in fission yeast. *J Biol Chem* **282**, 14065-14072.



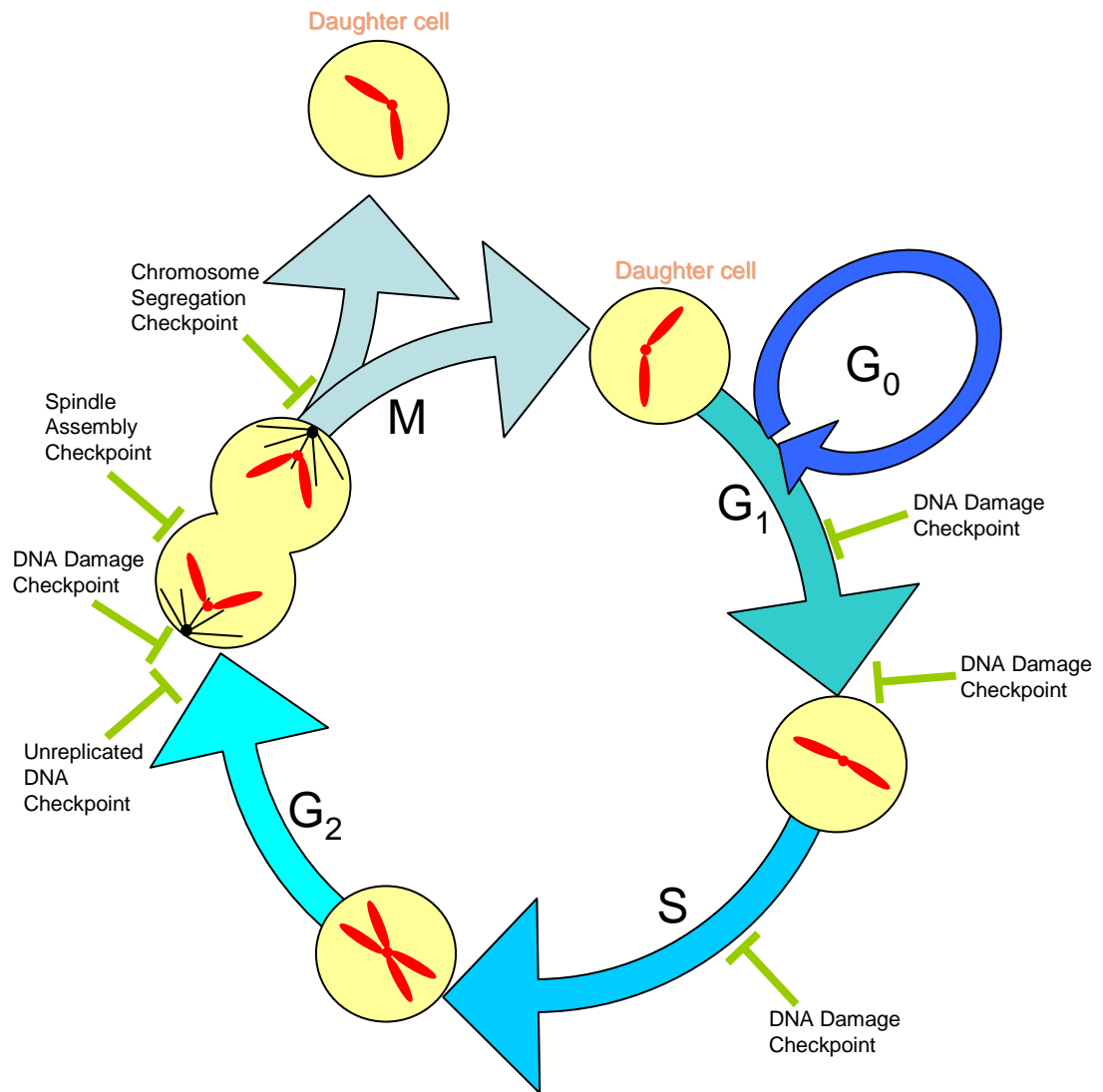


**Figure 1.1. Summary of the Mammalian Cell Cycle and its Checkpoints.** Following growth or gap phase 1 ( $G_1$ ), the cell duplicates its genome in the synthesis phase (S). Afterwards the cell contains two identical copies of each chromosome (only one chromosome is shown here for brevity). During mitosis (M), one copy of an identical pair is separated by the spindle network. Eventually, two identical daughter cells are resultant, whereupon the cycle starts again. However, most cells in the mammalian body are not cycling, but in a quiescent state known as  $G_0$ . Cell cycle checkpoints act as quality control mechanisms throughout the process, and are explained in the text. Figure adapted from Lodish *et al.*, 2004.

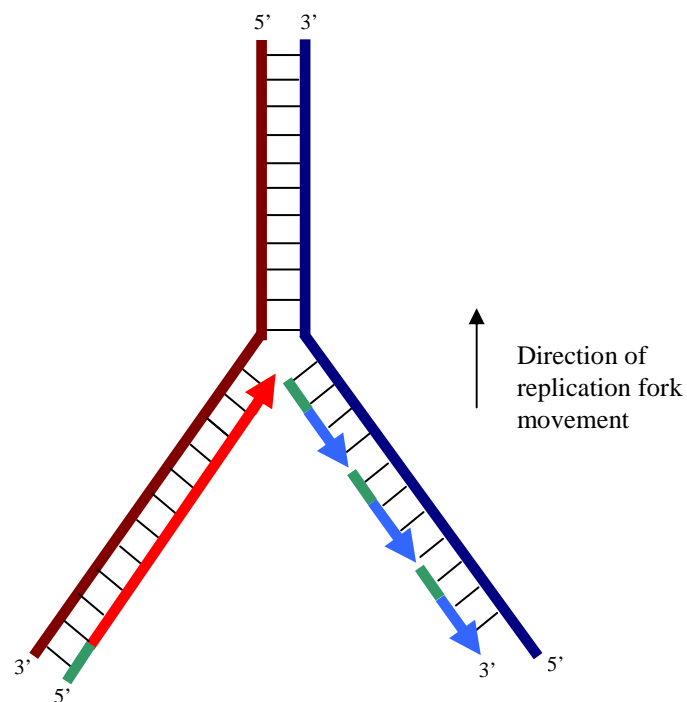


**Figure 1.2. The Semi-Discontinuous Model of DNA Replication: Leading and Lagging Strand DNA Synthesis.** The DNA polymerase can only synthesise DNA in the 5' to 3' direction. The parental leading and lagging template strands are shown in burgundy and navy, respectively. Newly synthesised DNA from continuous replication is shown in red and Okazaki fragments are shown blue. RNA primers are shown in green.

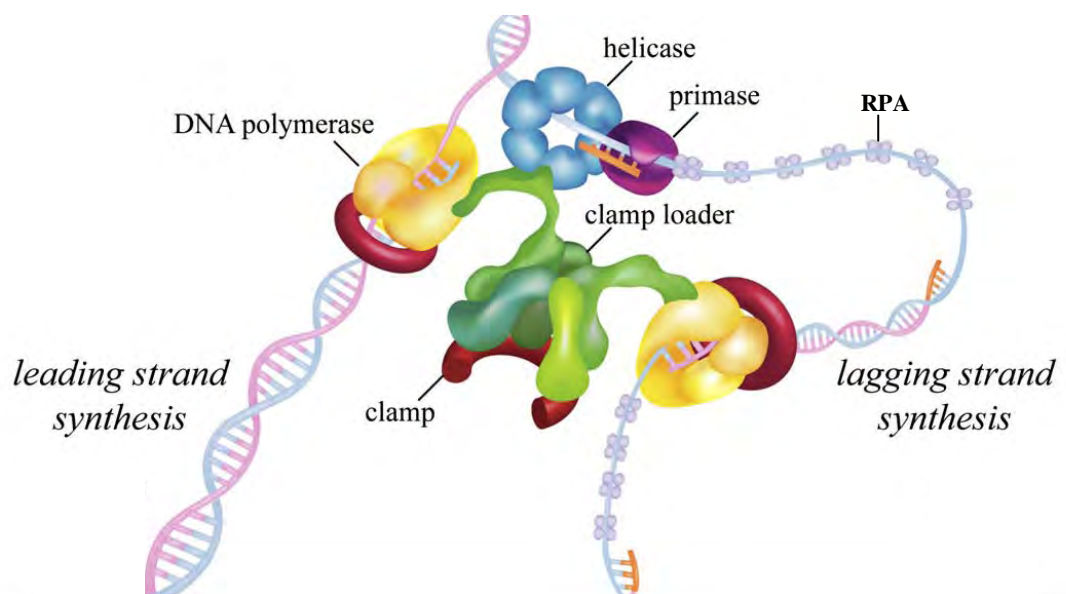


**Figure 1.3. Core Components of the Replication Factory.** This figure is oriented as in Figure 1.2 – the replication fork is proceeding towards the top of the page. dsDNA is unwound by the helicase, and a complementary daughter strand is synthesised by the DNA polymerases using the unwound ssDNA as a template. Replication protein A (RPA) protects and stabilises the ssDNA. The sliding clamp confers processivity to the DNA polymerase, and is loaded periodically onto newly unwound lagging strand by the clamp-loader complex. The primase synthesises a short RNA primer to allow the lagging strand polymerase to synthesise DNA *de novo*. Figure adapted from Langston and O'Donnell, 2006.

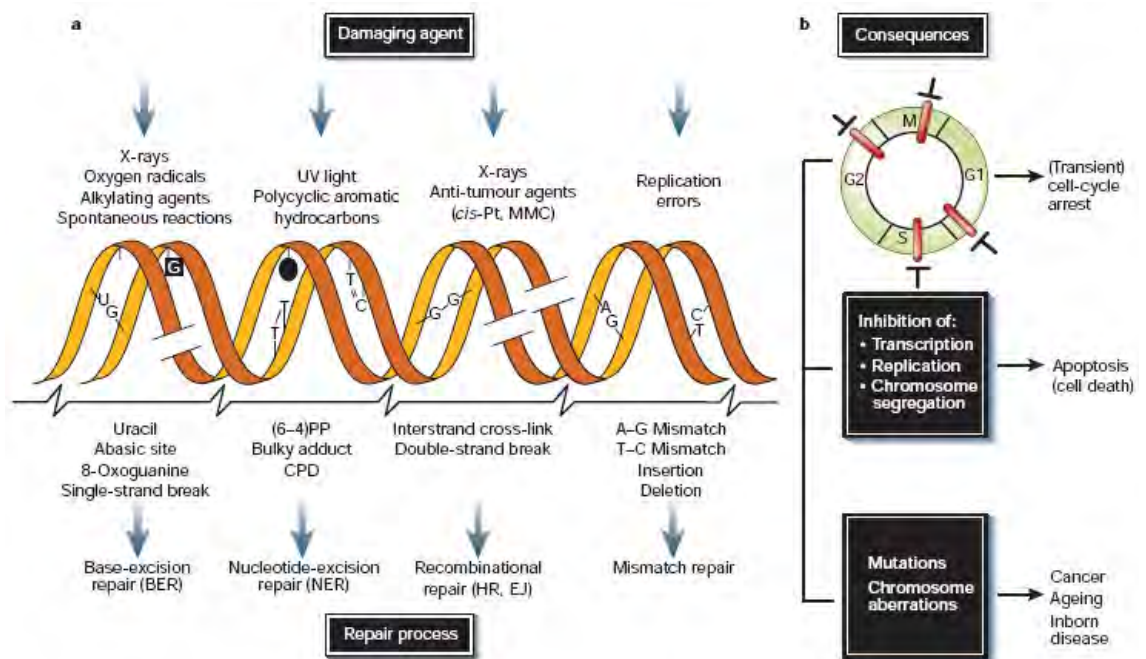


**Figure 1.4. DNA Damage and its Consequences.** **a)** Common DNA damaging agents (top); examples of DNA lesions induced by these agents (middle); and most the relevant DNA repair mechanism responsible for the removal of the lesions (bottom). **b)** The effects of DNA damage on cell-cycle progression, leading to transient arrest in G1, S, G2 and M phases (top), and on DNA metabolism (middle). Long-term consequences of DNA injury (bottom) include permanent changes in the DNA sequence and their biological effects. Abbreviations: *cis*-Pt and MMC, *cis*platin and mitomycin C, respectively (both DNA crosslinking agents); (6-4)PP and CPD, 6-4 photoproduct and cyclobutane pyrimidine dimer, respectively (both induced by UV light); HR, homologous recombination; EJ, end joining. Figure and legend from Hoeijmakers, 2001.

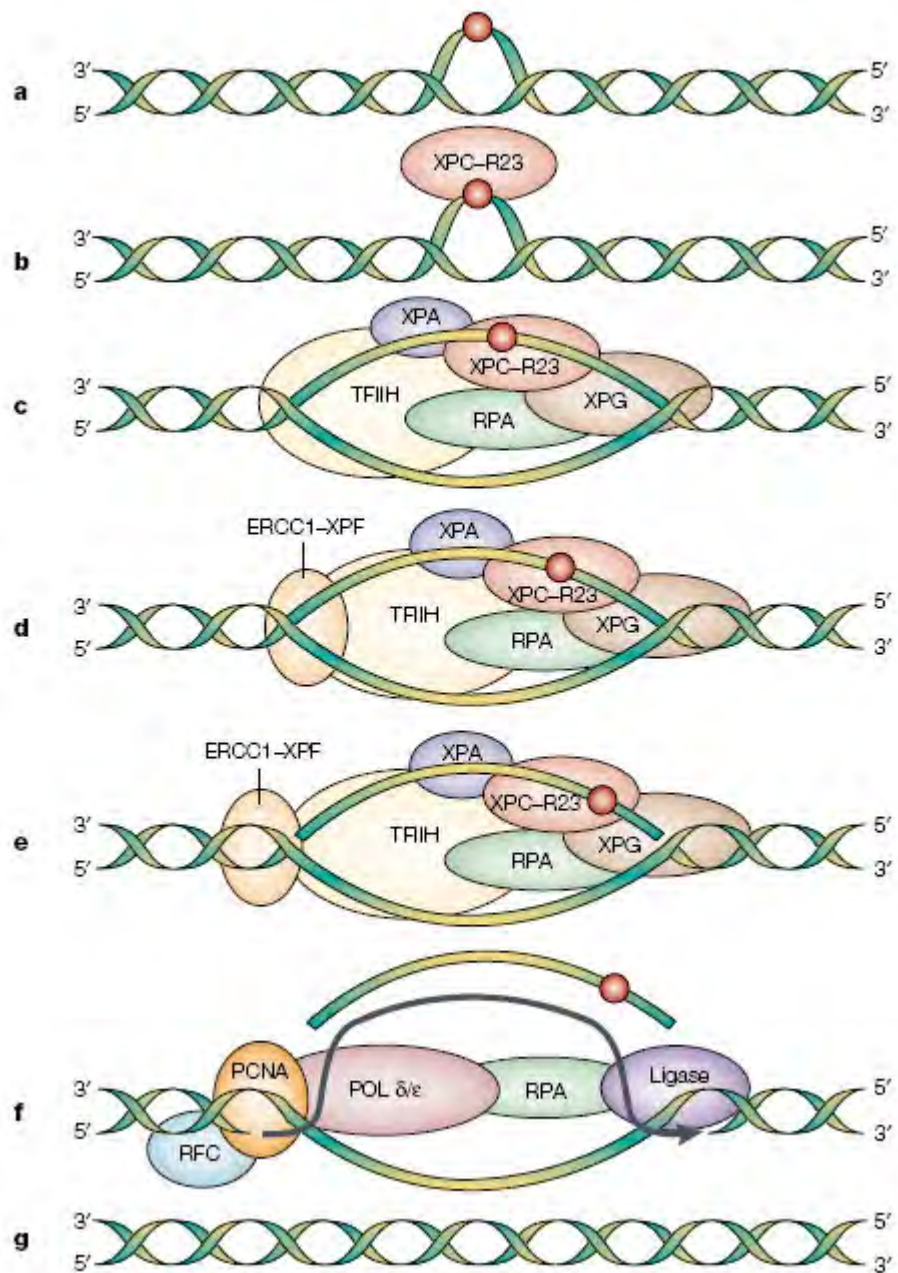


**Figure 1.5. Nucleotide Excision Repair (NER).** **a)** Damage (red circle) that alters the secondary structure of the duplex, is, as shown in **b)**, is detected and bound by a heterodimer of XPC and RAD23 (XPC-R23). **c)** and **d)** XPA, RPA, XPG, and TFIIH follow. TFIIH comprises the DNA helicases XPD and XPB, which unwind the DNA to form a bubble around the damage. ERCC1-XPF also binds. **e)** XPG cleaves the damaged strand at the 3' end, and ERCC1-XPF cuts at the 5' end. **f)** The damaged portion is excised and with the aid of clamp-loader RFC, PCNA, a DNA polymerase, healthy DNA is synthesised across the gap, and sealed in place with a DNA ligase. **g)** Undamaged dsDNA is restored. Figure and legend adapted from Friedberg, 2001.

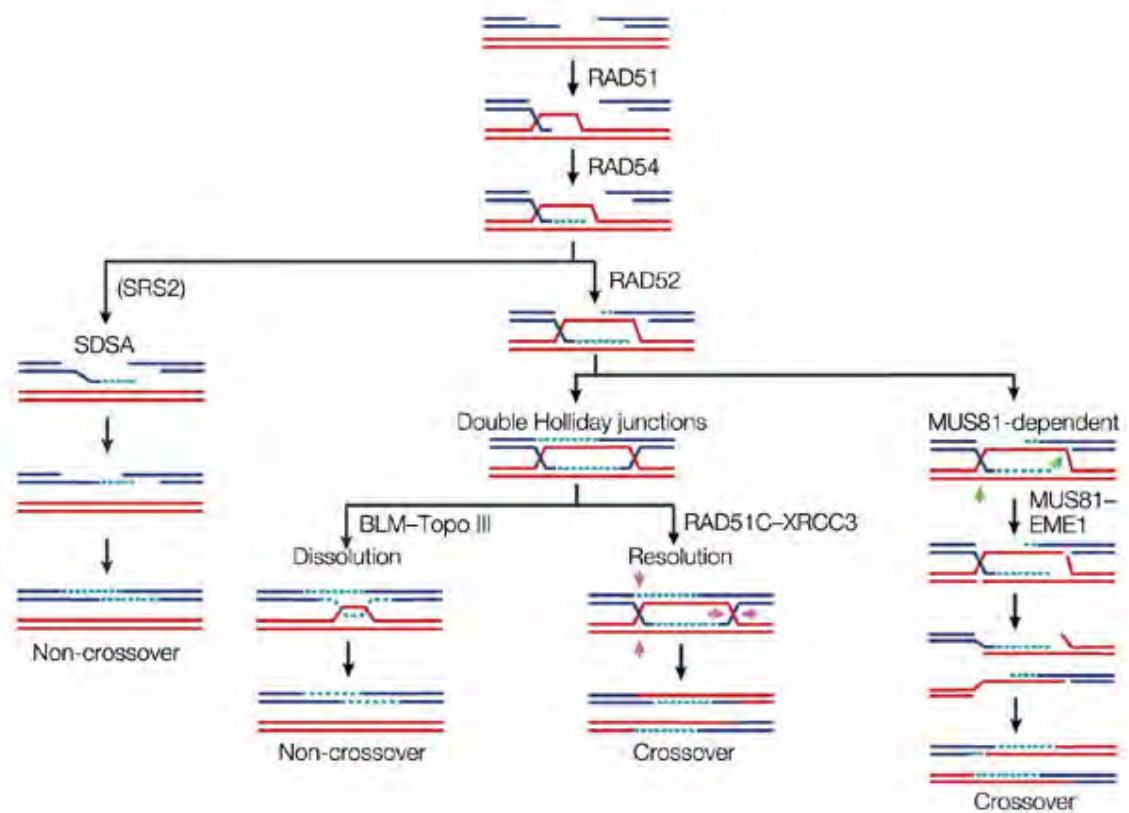


**Figure 1.6. A Summary of Homologous Recombination (HR) Pathways** initiated by a DNA double-strand break (DSB) and which lead to gene conversion with or without crossover. First, the ends of the DSB are resected to produce single-stranded DNA that recruits the recombination protein RAD51. The RAD51 nucleoprotein filament leads to interactions with homologous duplex DNA and strand invasion. Intermediate structures might be stabilized by RAD54. In the central pathway, strand invasion is followed by capture of the second DNA end in reactions that are likely to involve RAD52. This intermediate can proceed to form double Holliday junctions, and any remaining gaps might be filled by new DNA synthesis. The resulting Holliday junctions might then serve as the substrate for classical Holliday-junction-resolution reaction, involving RAD51C, XRCC3, or be dissociated by the combined actions of BLM (Bloom's syndrome protein) and topoisomerase III (Topo III). The BLM–Topo-III reaction primarily leads to the formation of non-crossover products. Recombinants can also form by a MUS81-dependent pathway (right) that does not involve Holliday-junction formation. Similarly, DSBs can be repaired by synthesis-dependent strand annealing (SDSA), a pathway that is dependent on the SRS2 helicase (left). Figure and legend adapted from Liu and West, 2004.



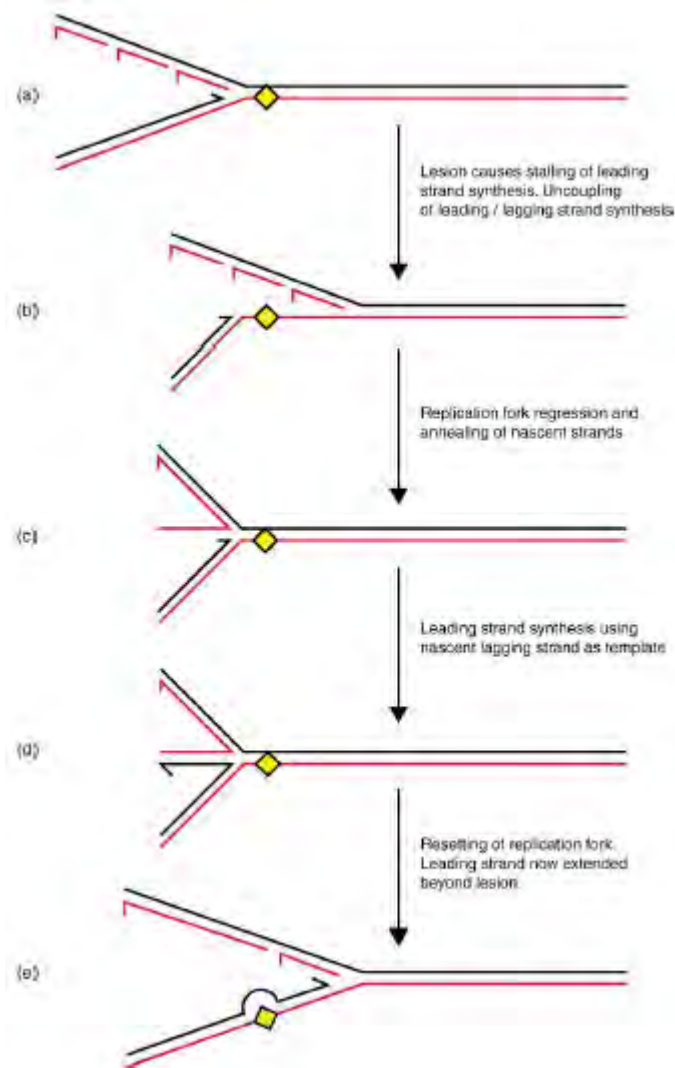


**Figure 1.7. The “Chicken Foot” Model – Homologous Recombination at Replication Forks.** (a) A lesion (yellow diamond) in the leading strand template blocks leading strand synthesis, (b) but lagging strand synthesis can continue for a short distance. (c) The fork regresses due to helical tension ahead of the fork, or it is thought that this reaction could be promoted by a specialised enzyme e.g. RecG in *E. coli*. (d) The nascent strands anneal, permitting leading strand synthesis using the nascent lagging strand as a template. The ‘chicken-foot’ structure (a Holliday junction) can be branch migrated to reset the fork. (e) The leading strand has been extended beyond the lesion. Figure and legend adapted from Oakley and Hickson, 2002.

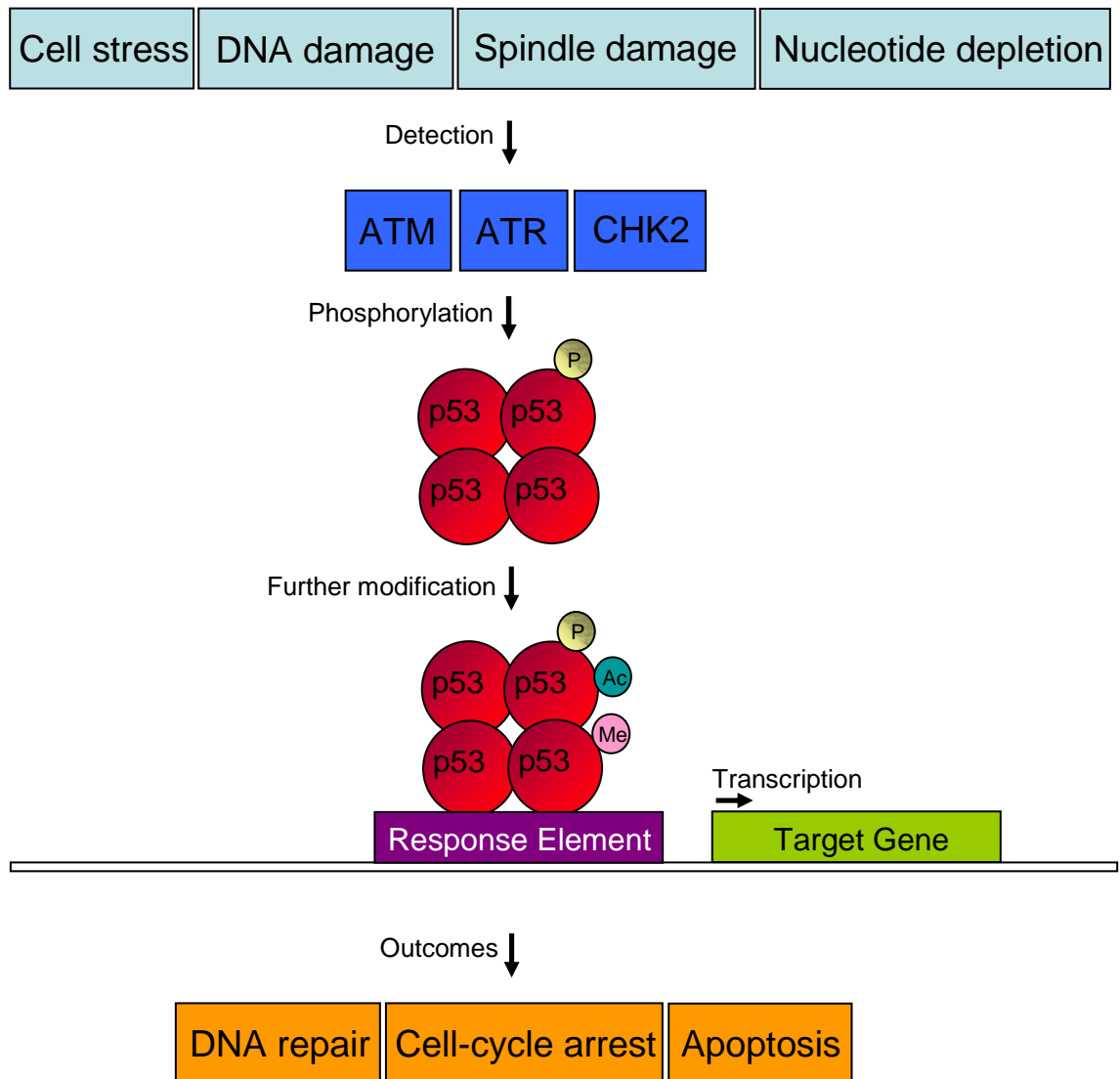


**Figure 1.8. Summary of p53 Activation and the Resultant Downstream Effects.** Adapted from Riley *et al*, 2008.



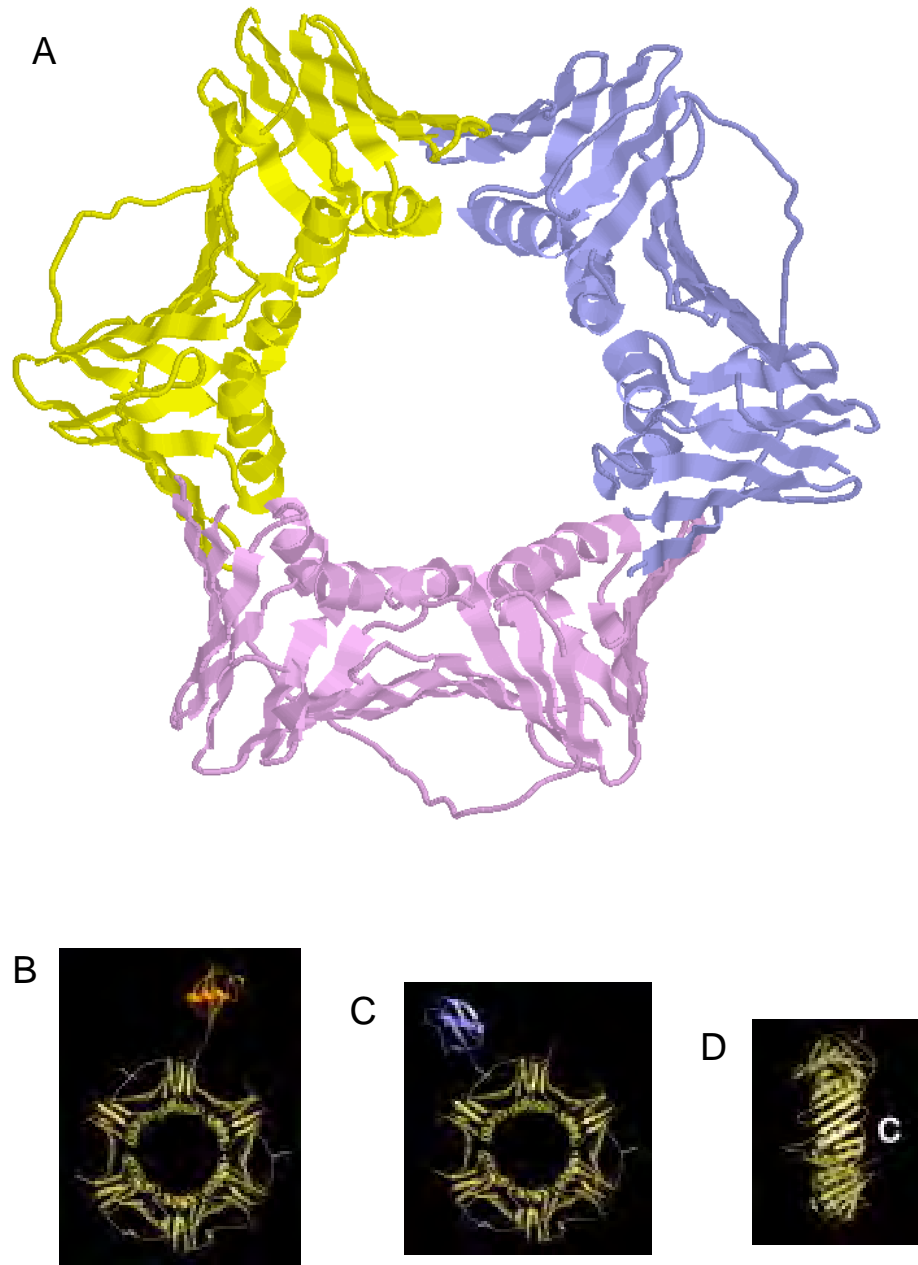


**Figure 1.9. Structure of PCNA in Cartoon Format.** (A) Each subunit of the homotrimer is in yellow, pink and light purple. (B) PCNA (yellow) modified on lysine 164 with ubiquitin (orange). (C) PCNA (yellow) modified on lysine 127 with small ubiquitin-like modifier (SUMO, blue). (D) PCNA (yellow) side-view. The symbol 'C' is found on the side of PCNA where the C-terminus protrudes. Structure (A) was prepared using Protein Explorer (see Chapter 2) using PDB ID: 1AXC (PCNA, Gulbis *et al.* 1996). B to D are modified from Moldovan *et al.*, 2007.

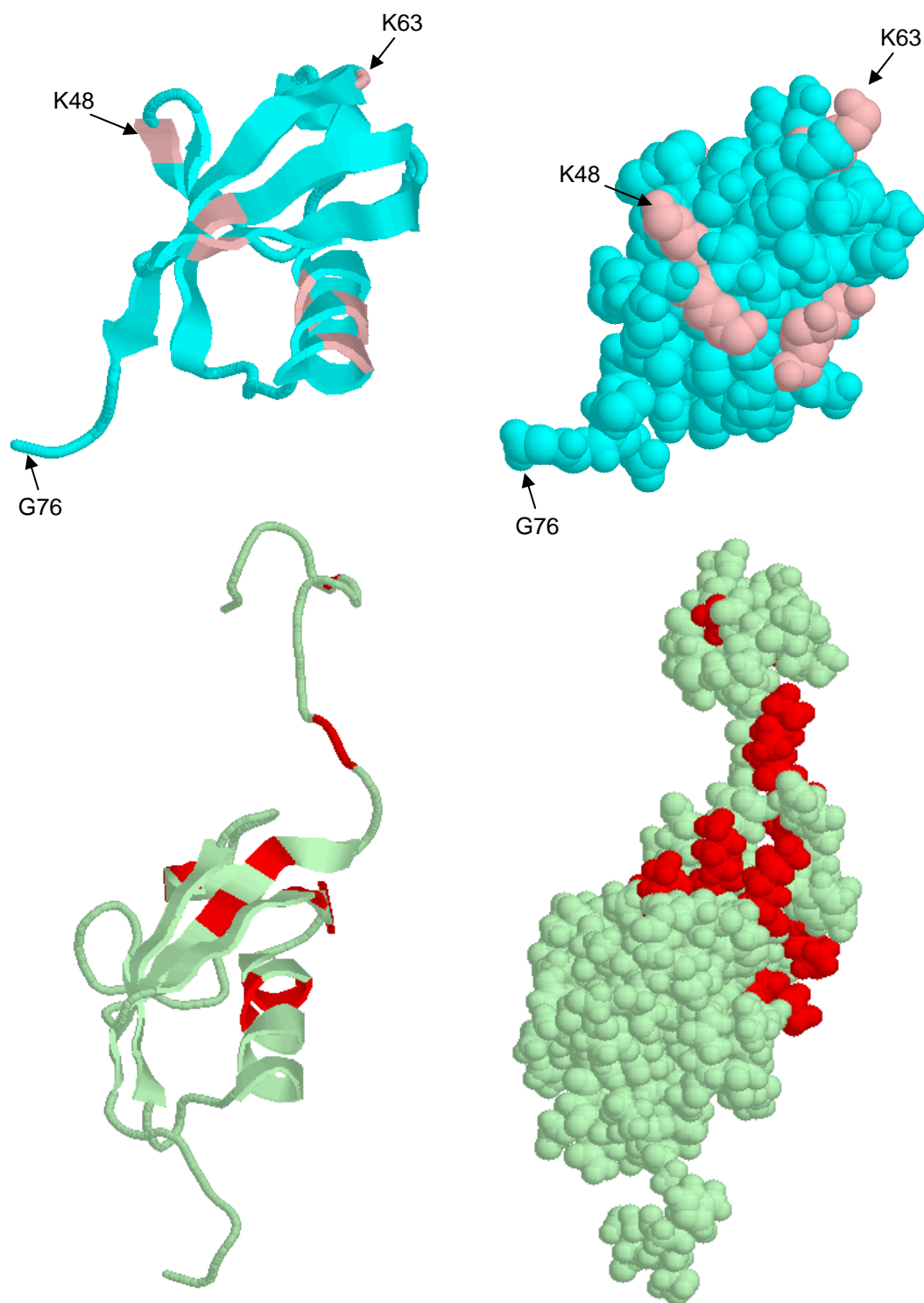


**Figure 1.10. Structures of Ubiquitin (light blue) and SUMO-1 (light green)** in cartoon format (left) to show the secondary structure elements, and in spacefill format (right). Lysine residues of ubiquitin and SUMO-1 are shown in pink and red, respectively. Structures were prepared using Protein Explorer (see Chapter 2) using PDB ID: 1UBQ (ubiquitin, Vijay-Kumar *et al*, 1987) and 1A5R (SUMO-1, Bayer *et al*, 1998).

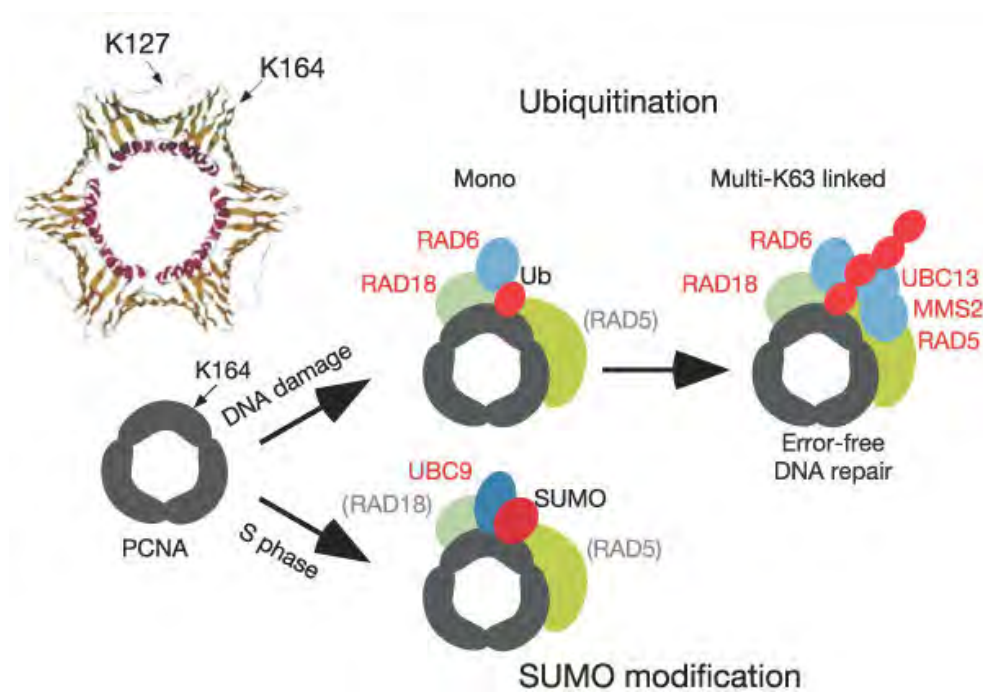


**Figure 1.11. Post-replication Repair in *S. cerevisiae*.** Modified from Hoege *et al*, 2002.

<b>Name of DUb Superfamily</b>	<b>Peptidase Domain</b>
Ubiquitin-specific proteases (USP/UBPs)	Cysteine-type peptidase, clan CA, C19 family
Ubiquitin C-terminal hydrolases (UCHs)	Cysteine-type peptidase, clan CA, C12 family
Ovarian tumour-like proteases (OTUs)	Cysteine-type peptidase, clan CA, C64 and C65 families
Machado-Joseph/Jakob disease protein/Josephin domain proteases (MJDs)	Cysteine-type peptidase, classification not known
Permutated papain fold peptidases of dsDNA viruses and eukaryotes (PPPDEs)	Cysteine-type peptidase, classification not known
Jab1/Pad1/MPN/Mov34 domain metalloenzymes (JAMMs)	Metallopeptidase, clan MP, family C67 A, B and C

**Table 1.1. Superfamilies of Deubiquitinating enzymes and their Peptidase Domains.**

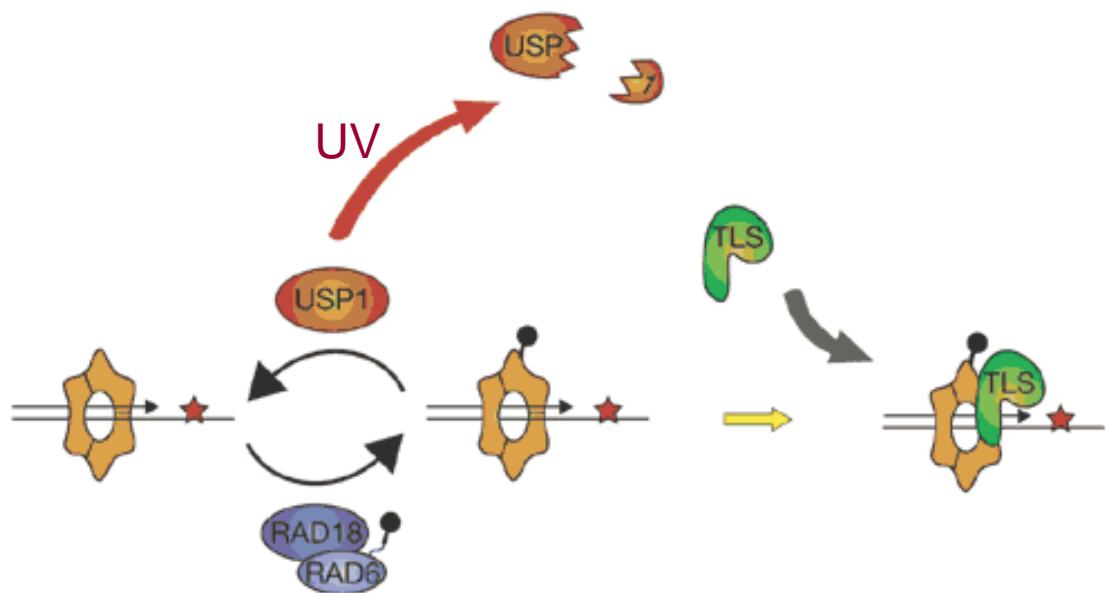




**Figure 1.12. Function of *Hs*USP1 in the Deubiquitination of *Hs*PCNA.** The replication machinery encounters stalling damage on the DNA template (red star). *Hs*RAD6 (light blue), aided by *Hs*RAD18 (dark blue), mono-ubiquitinates the *Hs*PCNA homotrimer (beige). At this point, a TLS polymerase (green) may bind to mono-ubiquitinated *Hs*PCNA and bypass the damage. Alternatively, *Hs*USP1 may deubiquitinate *Hs*PCNA. *Hs*USP1 autocleavage is induced by UV irradiation. Figure adapted from Ulrich, 2006.

<b>Gel</b>	<b>8%</b>	<b>10%</b>	<b>12%</b>	<b>Stack</b>
Water	4.6	4.0	3.3	6.8
30% acrylamide mix*	2.7	3.3	4.0	1.7
1.5 M tris pH 8.8	2.5	2.5	2.5	1.25**
10% SDS	0.1	0.1	0.1	0.1
10% AMPS	0.1	0.1	0.1	0.1
TEMED	0.006	0.004	0.004	0.01
Total	10	10	10	10

**Table 2.1. SDS-PAGE Gel Preparation.** Recipes for 8%, 10% and 12% resolving gels are shown for illustration. Quantities are in ml. \* Protogel (National Diagnostics) contains 30% acrylamide, 0.8% bisacrylamide. \*\* For the stacking gel, 0.5 M tris pH 6.8 was used.

Protocol	Block	1° Antibody Incubation	Washes	2° Antibody Incubation	Washes
Immunodection using rabbit $\alpha$ - $\text{SpPCNA}$	5% milk in 0.5% PBST for 1 h	1 in 10000 in 5% milk in 0.5% PBST for 1 hour	(a) 15 mins in water. (b) 3x 15 mins in 0.5% PBST.	Goat $\alpha$ -Rabbit HRP 1 in 10000 in 5% milk in 0.5% PBST for 1 h	(a) 1x 15 mins in water. (b) 3x 15 mins in 0.5% PBST. (c) 1x 15 mins in 1x PBS.
Improved immunodection using affinity purified rabbit $\alpha$ - $\text{SpPCNA}$	5% milk in 0.1% PBST at RT for 30 min	1 in 5000 in 5% milk in 0.1% PBST overnight	(a) 5 mins in water. (b) 3x 5 mins in 0.1% PBST.	Goat $\alpha$ -Rabbit HRP 1 in 5000 in 5% milk in 0.1% PBST for 1 h	(a) 1x 5 mins in water. (b) 3x 5 mins in 0.1% PBST. (c) 1x 5 mins in 1x PBS.
Immunodection using mouse $\alpha$ -His <sub>6</sub> (Amersham Pharmacia Biotech)	5% milk in 0.1% PBST for 1 h	1 in 3000 in 5% milk in 0.1% PBST for 1 hour	(a) 1x 3 mins in water. (b) 3x 3 mins in 0.1% PBST	Rabbit $\alpha$ -Mouse HRP 1 in 10 000 in 5% milk in 0.1% PBST for 1 h	(a) 1x 5 mins in water. (b) 3x 5 mins in 0.1% PBST. (c) 1x 5 min in 1x PBS.
Immunodection using mouse $\alpha$ -tubulin (Sigma)	5% milk in 0.1% PBST for 30 min	1 in 2000 in 5% milk in 0.1% PBST for 1 h	(a) 1x 3 mins in water. (b) 3x 3 mins in 0.1% PBST	Rabbit $\alpha$ -Mouse HRP 1 in 5000 in 5% milk in 0.1% PBST for 1 h	(a) 1x 5 mins in water. (b) 3x 5 mins in 0.1% PBST. (c) 1x 5 min in 1x PBS.
Immunodection using mouse $\alpha$ -FLAG (Sigma)	5% milk in 0.1% PBST for 30 min	1 in 500 in 5% milk in 0.1% PBST for 1 h	(a) 1x 3 mins in water. (b) 3x 3 mins in 0.1% PBST	Rabbit $\alpha$ -Mouse HRP 1 in 5000 in 5% milk in 0.1% PBST for 1 h	(a) 1x 5 mins in water. (b) 3x 5 mins in 0.1% PBST. (c) 1x 5 min in 1x PBS.
Immunodection using rabbit $\alpha$ -ubiquitin (DAKO)	5% milk in 0.1% PBST for 30 min	1 in 500 in 5% milk in 0.1% PBST overnight at RT	(a) 1x 3 mins in water. (b) 3x 3 mins in 0.1% PBST	Rabbit $\alpha$ -Mouse HRP 1 in 5000 in 5% milk in 0.1% PBST for 1 h	(a) 1x 5 mins in water. (b) 3x 5 mins in 0.1% PBST. (c) 1x 5 min in 1x PBS.

**Table 2.2. Immunodetection Methods.** Milk powder was Marvel or a supermarket own-branded version and percentages are w/v. All other percentages are v/v. Room temperature (RT) was about 22°C. Water was double distilled. Secondary antibodies were from DAKO.

Time	Temperature	Repetitions
30 s	95 °C	
40 s	95 °C	 x 5
30 s	50 °C	
2.5 min	72 °C	
40 s	95 °C	 x 25
30 s	60 °C	
2.5 min	72 °C	
10 min	72 °C	
Hold	6 °C	

**Table 2.3. PCR Cycling Conditions for Amplification of Transforming DNA.**



Genotoxic Agent	Bench Stock Concentration	Diluent	Source
Camptothecin (CPT)	5 mM	DMSO	Sigma
Methylmethano sulfonate (MMS)	1% (v/v)	Water	Sigma
Hydroxyurea (HU)	1-2 M	Water	Sigma
Hydrogen peroxide (H <sub>2</sub> O <sub>2</sub> )	9.8M	Water	Sigma
4-nitroquinoline-1-oxide (4-NQO)	5 mM	DMSO	Sigma
Phleomycin	10 µg/ml	Water	Melford
Bleomycin	10 µg/ml	Water	Melford
<i>cis</i> -platin	neat powder	None	Sigma
Thiabendazole (TBZ)	33.3 mg/ml	DMSO	Sigma
Carbendazim (CBZ)	2.5 mg/ml	DMSO	Sigma

**Table 2.4. Genotoxic Agent Stocks and Diluents.**

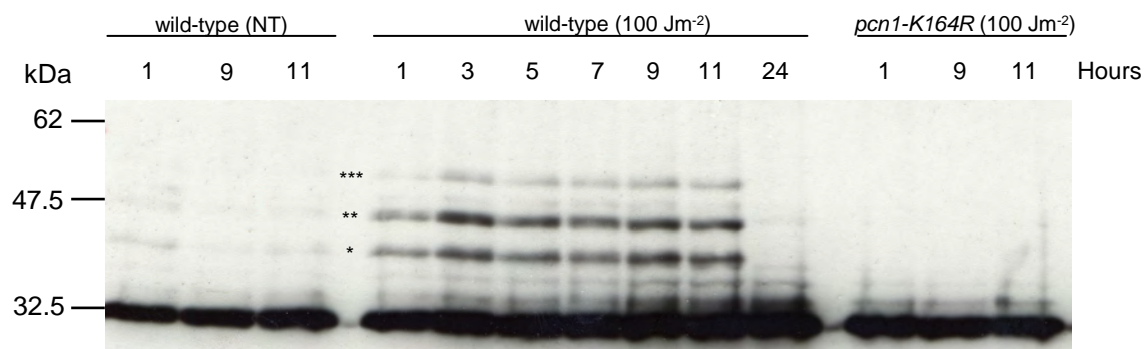


**Figure 3.1. Persistence of *Sp*PCNA Ubiquitination after UVC Irradiation in wild-type and *pcn1-K164R* cells.** The same number of cells of exponentially growing cultures were irradiated or mock irradiated (NT) with 100 J/m<sup>2</sup> UVC and samples were taken at the indicated times. Size fractionated whole cell extracts were probed with anti-*Sp*PCNA antibodies. Mono-ubiquitinated (\*), di-ubiquitinated (\*\*) and tri-ubiquitinated (\*\*\*) forms of *Sp*PCNA are labelled.

<i>S. pombe</i>	<i>S. cerevisiae</i>	<i>H. sapiens</i>
<i>SpUbp1</i>	<i>ScUbp12</i>	<i>HsUSP4</i> , <i>HsUSP11</i> , <i>HsUSP15</i>
<i>SpUbp12</i>	<i>SpUbp12</i>	<i>HsUSP4</i> , <i>HsUSP11</i> , <i>HsUSP15</i>
<i>SpUbp7</i>	-	<i>HsUSP16</i> <sup>UBP-M</sup> , <i>HsUSP45</i>
<i>SpUbp8</i>	<i>ScUbp8</i>	<i>HsUSP22</i> , <i>HsUSP27*</i> , <i>HsUSP51*</i>
<i>SpUbp10</i>	<i>ScSad1</i>	<i>HsUSP39</i> <sup>SNUT2*</sup>
<i>SpUbp14</i> <sup>Ucp2</sup>	<i>ScUbp14</i>	<i>HsUSP5</i> <sup>IsoT1</sup> , <i>HsUSP13</i> <sup>IsoT2</sup>
<i>SpUbp6</i>	<i>ScUbp6</i>	<i>HsUSP14</i>
<i>SpUbp11</i>	<i>ScUbp1</i>	-
<i>SpUbp13</i> <sup>Pan2</sup>	<i>ScPan2</i>	<i>HsUSP52</i>
<i>SpUbp21</i> <sup>Ubp15</sup>	<i>ScUbp15</i>	<i>HsUSP7</i>
<i>SpUbp22</i> <sup>Ubp5</sup>	<i>ScUbp15</i>	<i>HsUSP7</i>
<i>SpUbp4</i>	<i>ScUbp5</i> , <i>ScUbp7</i> , <i>ScDoa4</i>	<i>HsUSP8</i> <sup>UBPY</sup>
<i>SpUbp3</i>	<i>ScUbp3</i>	<i>HsUSP10</i>
<i>SpUbp9</i>	<i>ScUbp9</i> , <i>ScUbp13</i>	<i>HsUSP12</i> , <i>HsUSP46</i>
<i>SpUbp2</i>	<i>ScUbp2</i>	<i>HsUSP25</i> , <i>HsUSP28</i>
<i>SpUbp16</i>	-	<i>HsUSP36</i> , <i>HsUSP42</i> , <i>HsUSP17</i>
<i>SpUch1</i>	<i>ScYuh1</i>	<i>HsUCH-L1</i> , <i>HsUCH-L3</i>
<i>SpUch2</i>	-	<i>HsUCH37</i> <sup>UCH-L5</sup>
<i>SpOtu1</i> <sup>Mug141</sup>	<i>ScOtu1</i>	<i>HsOTU1</i> <sup>YOD1</sup>
<i>SpOtu2</i>	<i>ScOtu2</i>	<i>HsOTUD6B</i> and <i>HsOTUD6A</i>
<i>SpHag1</i> <sup>Mug67</sup>	-	<i>HsPNAS4</i> <sup>FAM152A</sup>
<i>SpAmsh</i> <sup>Sst2</sup>	-	<i>HsAMSH</i> , <i>HsAMSH-L1</i>
<i>**SpRpn11</i> <sup>Pad1</sup>	<i>ScRpn11</i>	<i>HsRPN11</i>
<i>**SpCsn5</i>	<i>ScRri1</i> <sup>Csn5/Jab1</sup>	<i>HsCSN5</i> .

**Table 3.1. DUBs in Three Species.** Table of DUBs in *S. pombe* and their likely orthologues in *S. cerevisiae* and *H. sapiens*. USP/UBP DUBs are shown in green, UCHs in blue, OTUs in pink, PPPDEs in yellow, and JAMMs in beige. A single asterisk indicates that the enzyme is unlikely to possess DUB activity. A double asterisk adjacent to a *S. pombe* DUB indicates it is not included in this study.

Additional Domains		S. <i>pombe</i> Deubiquitinating Enzyme
	UBP/USP Superfamily DUBs	
DUSP domain	<i>SpUbp1</i> -849 a.a. -DUSP domain -SPCC16A11.12c -Paralogue is <i>SpUbp12</i> -Likely orthologues are <i>ScUbp12</i> , <i>HsUSP4</i> , <i>HsUSP11</i> , <i>HsUSP15</i>	
	<i>SpUbp12</i> -979 a.a. -DUSP domain -SPCC1494.05c -Paralogue is <i>SpUbp1</i> -Likely orthologues are <i>ScUbp12</i> , <i>HsUSP4</i> , <i>HsUSP11</i> , <i>HsUSP15</i>	
UBP-type Zinc Finger Domain	<i>SpUbp7</i> -875 a.a. -UBP-type zinc finger domain -SPAC23G3.08c -Likely orthologues are <i>HsUSP16</i> <sup>UBP-M</sup> , <i>HsUSP45</i>	
	<i>SpUbp8</i> -449 a.a. -UBP-type zinc finger domain -SPAC13A11.04c -Likely orthologues are <i>ScUbp8</i> , <i>HsUSP22</i> , <i>HsUSP27*</i> , <i>HsUSP51*</i>	
	<i>SpUbp10</i> -502 a.a. -UBP-type zinc finger domain -SPBC577.07 -Likely orthologues are <i>ScSad1</i> , <i>HsUSP39</i> <sup>SNUT2*</sup>	
	<i>SpUbp14</i> <sup>Ucp2</sup> -775 a.a. -Two UBP-type zinc finger domains. -Two UBA domains within UBP/USP domain. -SPBC6B1.06c -Likely orthologues are <i>ScUbp14</i> , <i>HsUSP5</i> <sup>IsoT1</sup> , <i>HsUSP13</i> <sup>IsoT2</sup>	
Ubiquitin-like Domain	<i>SpUbp6</i> -467 a.a. -Ubiquitin-like domain. -SPAC6G9.08 -Likely orthologues are <i>ScUbp6</i> , <i>HsUSP14</i>	

**Table 3.2. DUBs in *S. pombe*.** Important facts for each *S. pombe* DUB is provided. USP/UBP DUBs are shown in green, UCHs in blue, OTUs in pink, PPPDEs in yellow, and JAMMs in beige. USP/UBPs are further divided by additional domains. A single asterisk indicates that the enzyme is unlikely to possess DUB activity. A double asterisk adjacent to a *S. pombe* DUB indicates it is not included in this study.

Trans-membrane Helix	<p><i>SpUbp11</i></p> <p>-350 a.a.</p> <p>-Probable transmembrane helix</p> <p>-SPBC19C2.04c</p> <p>-Likely orthologues are <i>ScUbp1</i></p>
Exonuclease Domain	<p><i>SpUbp13<sup>Pan2</sup></i></p> <p>-1115 a.a.</p> <p>-WD-40 repeat.</p> <p>-Exonuclease domain.</p> <p>-Ribonuclease H fold</p> <p>-SPAC22G7.04</p> <p>-Likely orthologues are <i>ScPan2</i>, <i>HsUSP52</i></p>
MATH domain	<p><i>SpUbp21<sup>Ubp15</sup></i></p> <p>-1129 a.a.</p> <p>-MATH domain.</p> <p>-SPBC713.02c</p> <p>-Paralogue is <i>SpUbp22</i></p> <p>-Likely orthologues are <i>ScUbp15</i>, <i>HsHAUSP<sup>USP7</sup></i></p>
	<p><i>SpUbp22<sup>Ubp5</sup></i></p> <p>-1108 a.a.</p> <p>-MATH domain.</p> <p>-SPCC188.08c</p> <p>-Paralogue is <i>SpUbp21</i></p> <p>-Likely orthologues are <i>ScUbp15</i>, <i>HsHAUSP<sup>USP7</sup></i></p>
No extra domains	<p><i>SpUbp4</i></p> <p>-438 a.a.</p> <p>-SPBC18H10.08c</p> <p>-Likely orthologues are <i>ScUbp5</i>, <i>ScUbp7</i>, <i>ScDoa4</i>, <i>HsUSP8<sup>UBPY</sup></i></p>
	<p><i>SpUbp3</i></p> <p>-512 a.a.</p> <p>-SPBP8B7.21</p> <p>-Likely orthologues are <i>ScUbp3</i>, <i>HsUSP10</i></p>
	<p><i>SpUbp9</i></p> <p>-585 a.a.</p> <p>-SPBC1703.12</p> <p>-Likely orthologues are <i>ScUbp9</i>, <i>ScUbp13</i>, <i>HsUSP12</i>, <i>HsUSP46</i></p>
	<p><i>SpUbp2</i></p> <p>-1141 a.a.</p> <p>-SPAC328.06</p> <p>-Likely orthologues are <i>ScUbp2</i>, <i>HsUSP25</i>, <i>HsUSP28</i></p>
	<p><i>SpUbp16</i></p> <p>-457 a.a.</p> <p>-SPCC1682.12c</p> <p>-Likely orthologues are <i>HsUSP36</i>, <i>HsUSP42</i>, <i>HsUSP17</i></p>

**Table 3.3. DUBs in *S. pombe*.** Legend as Table 3.1.

	UCH Superfamily DUBs	
	<p><i>SpUch1</i>  -222 a.a.  -SPAC27F1.03c  -Likely orthologues are <i>ScYuh1</i>, <i>HsUCH-L1</i>, <i>HsUCH-L3</i>.</p>	
	<p><i>SpUch2</i>  -300 a.a.  -SPBC409.06  -Likely orthologue is <i>HsUCH37</i><sup>UCH-L5</sup>.</p>	
	OTU Superfamily DUBs	
	<p><i>SpOtu1</i><sup>Mug141</sup>  -329 a.a.  -C2H2 zinc finger  -SPAC24C9.14  -Likely orthologues are <i>ScOtu1</i>, <i>HsOTU1</i><sup>YOD1</sup>.</p>	
	<p><i>SpOtu2</i>  -324 a.a.  -SPAC1952.03  -Likely orthologues are <i>ScOtu2</i>, <i>HsOTUD6B</i> and <i>HsOTUD6A</i>.</p>	
	PPPDE Superfamily DUBs	
	<p><i>SpHag1</i><sup>Mug67</sup>  -201 a.a.  -PPPDE domain.  -SPAPYUG7.06  -Likely orthologue is <i>HsPNAS4</i><sup>FAM152A</sup>.</p>	
	JAMM Superfamily DUBs	
	<p><i>SpAmsh</i><sup>Sst2</sup>  -435 a.a.  -SPAC19B12.10  -Likely orthologues are <i>HsAMSH</i>, <i>HsAMSH-L1</i>.</p>	
	<p><b>**</b><i>SpRpn11</i><sup>Pad1</sup>  -308 a.a.  -SPAC31G5.13  -Likely orthologues are <i>ScRpn11</i>, <i>HsRPN11</i>.</p>	
	<p><b>**</b><i>SpCsn5</i>  -299 a.a.  -SPAC1687.13c  -Likely orthologues are <i>ScRri1</i><sup>Csn5/Jab1</sup>, <i>HsCSN5</i>.</p>	

**Table 3.4. DUBs in *S. pombe*.** Legend as Table 3.1.

```

ScOtu1      -----MKLKVTGAGINQVVTLKQDATLNDLIEHINVDVKT-----MR 37
SpOTU1      -----MSSLRLRLKYENQSAVETVEANATVGSFLDLVAAKFSLPNSIALK 46
HsOTU1      MFGPAKGRHFGVHPAPGFPGGVSQAAAGTKAGPAGAWPVGSRDTDMURLRCKAKDGTHVL 60
              :  : .  .  .  .  .  .  :  :  :

ScOtu1      FGYPQR--INLQGEDASLG-----QTQLDELGINSGEKITIESSDSNESFSL 83
SpOTU1      FGFPQD--IPLVNSDVPLSTLVSSGQILVLKNAATSFSSTNEPAKPPIPNAATKPTFFP 104
HsOTU1      QQLSSRTVRRELQGGIAAITGIAPEGGRILVGYPPPECLDLSNGDTILEDLPQSGDMLII 120
              *  . . :  *  . . . :  *  :  :

ScOtu1      PPPQPKPKRVLKSTEMSIG-----GSGENVLSVHPVLDDNSCLFHAIAYGIFK-----QDS 134
SpOTU1      QTEISNPPAVSHQSKNTSQDPPYVSTPIGDIALRVMPDDNSCLFRALSKPLG-----FS 158
HsOTU1      EEDQTRPRSSPAFTKRGASS--YVRETLPVLTTRTVVPADNSCLFTSVYYVVEGGVLNPAC 178
              . . *  :  :  :  :  :  :  :  :  :

ScOtu1      VRDLREMVSKEVLNMPVKFNDAILDKPNKDYAQWILKMESUGGAIEIGIISDALAVAIYV 194
SpOTU1      PYELREIVANQVLSNPDISTAILGKPSIEYASWIRKETSUGGYIELSSHFGEVICS 218
HsOTU1      APEMRRLIAQIVASDPDFYSEAILGKTNQEYCDWIKRDDTWGGAIEISILSKFYQCEICV 238
              :  * . :  :  :  :  :  :  :  :  :

ScOtu1      VDIDAVKIEKFN-EDKFDNYILILFNGIHYDSLTMNEFKTVFNKNQPSDD----VLTA 249
SpOTU1      VDVKTGRVDSYNPQATGQRTYIVYSGIHYDLAALA AVLWDVDVVLFDASDVITITPV 278
HsOTU1      VDTQTVRIDRFGEDAGYTKRVLLIYDGIHYDPLQNFDPDTP-PLTIFSSNDIVLVQA 297
              ** . : :  :  :  :  :  :  :  :

ScOtu1      LQLASNLKQTGYSFNTHKAQIKCNTCQMTFVGEREVARHAEESTGHVDFGQNR 301
SpOTU1      QQLASLLKNMHYYTDTASFSSIRCTICGTGLVGEKDATAHALATGHTQFGEY- 329
HsOTU1      LELADEARRRRQFTDVNRFTLCMVCQKGLTGQAEAREHAKETGHTNFGEV- 348
              :  * . :  :  :  :  :  :  :  :  :

```

DUb 1	DUb 2	Score
<i>Hs</i> OTU1YOD1	<i>Sc</i> Otu1	28
<i>Hs</i> OTU1YOD1	<i>Sp</i> Otu1	27
<i>Sc</i> Otu1	<i>Sp</i> Otu1	29

**Figure 3.2. Alignment of Otu1 DUBs in Three Eukaryotic Species.** The catalytic Cys and His boxes are boxed in red, the C2H2 in blue. Residue letters are coloured according to type. Acidic residues, Asp and Glu, are typed in blue; basic residues, Arg and Lys, pink; green residues, His, Asn, Gly, Tyr, Ser, Gln, Thr, are hydrophilic; and hydrophobic residues, Phe, Met, Ala, Leu, Iso, Pro, Trp, are typed in red. An asterisk indicates homologous residues; a colon indicates conservation with a highly similar residue; a dot, conservation with less similar residues; and no symbol indicates no conservation. The table underneath shows the percentage identity (score) of pairwise comparisons.

```

HsOTUD6B      -----MEAVLTEELDEEEQLLRHRKEKKELQAKIQGMKNVAPKNDKKRRKQ 47
HsOTUD6A      -----MDDPKSEQQRILRRHQREFQELQAQIRSLKNSVPKTDKTKRKQ 43
SpOtu2        MRCPLAYYYTQTITPTQQKRKSKKMEELLSKQREECKELQSKITNLRKQLKEGNKKQKRA 60
ScOtu2        -----MTGMESGENLENMEDILARHRKENKDLQNKITGMKKQATKSKRKE--- 45
                . : : * : : : * : : * : * : : : : : : . : . . .

HsOTUD6B      LTEDVAKLEKEMEOKHREELEQLKLT-----KENKIDSVAVNISM 88
HsOTUD6A      LLQDVARMEAEQAQKHQLEKFQ-----DDSSIESVVEDLAK 81
SpOtu2        LQQKISQMEADLSQKHATERQKLDKGDEETNETQQEDLLNTLLQQMEDTKITTAEKSSVQ 120
ScOtu2        VNSKCLDLQDKLTKQENEIRDWKIANNEVFDAEQEDEV-TPEKLEQLSISRDEKE--Q 102
                : . . : : : : * : * . . . : : . * . : :

HsOTUD6B      LVLENQPPRISKAQKRREKKAALKEKEREERIAEAEI-ENLTG-----ARHMESEKLAQIL 142
HsOTUD6A      MNLENRPPRSSKAHRRKERMESEERERQESIFQAEMSEHLAG-----FKREEEEKLAAIL 136
SpOtu2        SSLNTKENTPQQPKKSNNRQKERLERRKAEMKKMSEQAELESEKMDLKNEEKKKFSKIL 180
ScOtu2        QNVVPVQQQQGQTKKRRNRQKERLAKRDAIAKMKEEAALASQKQPDLLKMEQESIDQLC 162
                : : : : : * : : . * . : : . * . : : * : : :

HsOTUD6B      AARQLEIKQIPSDGHCMYKAIEDQLKEKD-----CALTVVALRSQTAEYMQSHVEDFLP 196
HsOTUD6A      GARGLEMKAIPADGHCMYRAIQDQLV-----FSVSVEMLCRTASYMKKHVDEFLP 187
SpOtu2        EEAGLVAVDIPADGNCLFASISHQLNYHHN-----VKLNSQALFNKSADYVLKHCEQFEG 235
ScOtu2        ELKRLKQFDIQPDGHCFLFASILDQLKLRHDPKKLDQDMVLMKRLWLSKNYVQEHRRDDFIP 222
                * . * : * : : : : * . : : * : : . : : * : : *

HsOTUD6B      FLTNPNTGDMYTPPEFQKYCEDIVNTAAWGGQLELRALSHILQTPIEIIQADSPPIIVGE 256
HsOTUD6A      FFSNPETSDSFGYDDFMIYCDNIVRTTAWGGQLELRALSHVLKTPIEVIQADSPTLIIGE 247
SpOtu2        FLLDEESGEVL---PVSDYCNIEIRNNSKWGSDIEIQALANSLEVPHVYNTGEPVLKFNFP 292
ScOtu2        YLFDEETMKMK---DIDEYTKEMEHTAQWGGIEILALSHVFDCPISILMSGRPIQVYNE 279
                : : : : . . * . : : . : * : : : : * : : : : * .

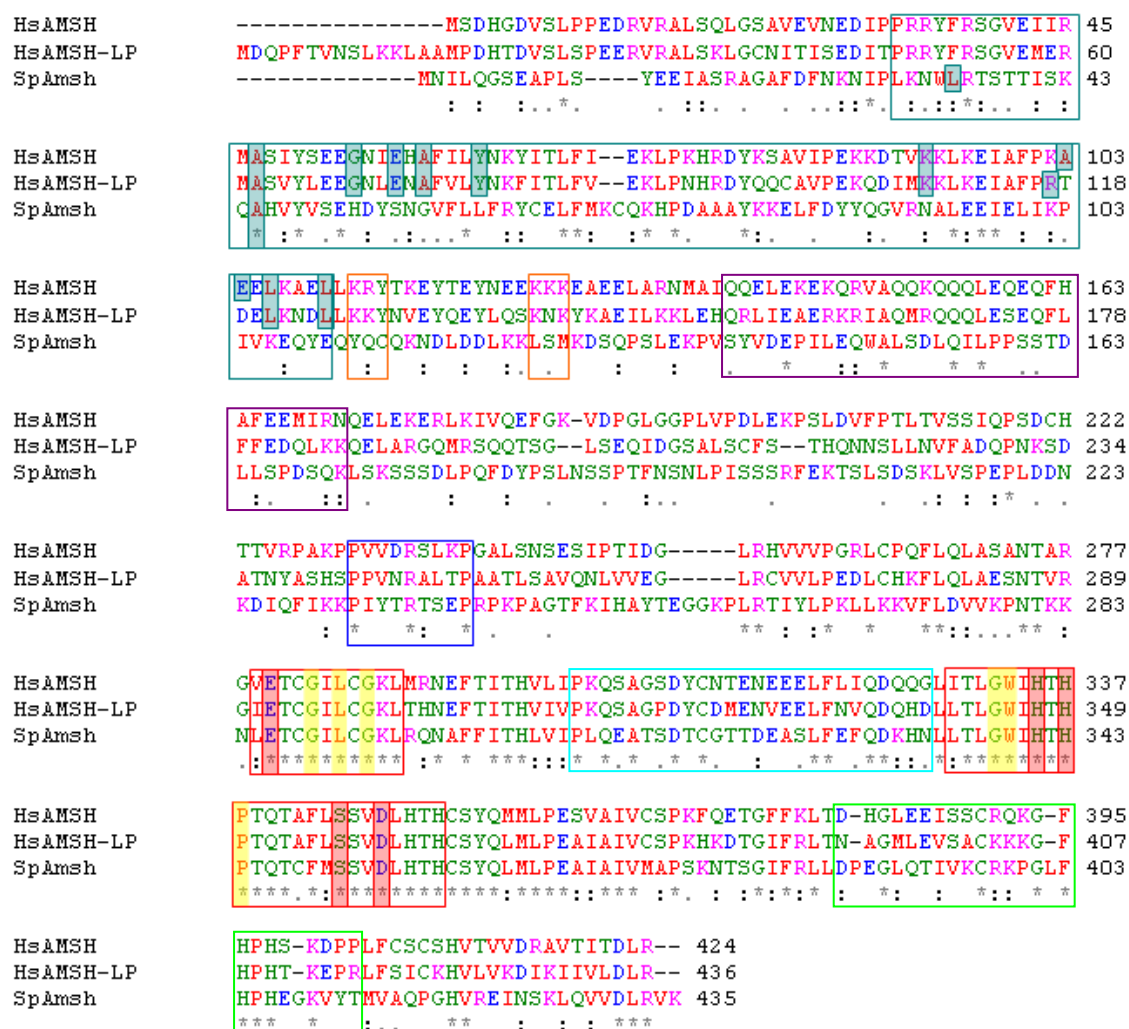
HsOTUD6B      EYSKKP--LILVYMRHAYGLGEHYNSTRLVNIVTENC----- 293
HsOTUD6A      EYVKKP--IILVYLRAYSLGEHYNSTPLEAGAAGGVLPRL 288
SpOtu2        STVKFEKFLCIAYYQHFLGLGAHYNSTLYLDN----- 324
ScOtu2        CGKNPE--LKLVYYKHSYALGEHYNSTHDS----- 307
                : : : * : : : * : * : * :

```

DUb 1	DUb 2	Score
<i>Hs</i> OTUD6B	<i>Sp</i> Otu2	27
<i>Hs</i> OTUD6B	<i>Sc</i> Otu2	32
<i>Hs</i> OTUD6B	<i>Hs</i> OTUD6A	54
<i>Sp</i> Otu2	<i>Sc</i> Otu2	31
<i>Sp</i> Otu2	<i>Hs</i> OTUD6A	27
<i>Sc</i> Otu2	<i>Hs</i> OTUD6A	25

**Figure 3.3. Alignment of Otu2 DUBs in Three Eukaryotic Species.** Colour coding as previous figure. The table underneath shows the percentage identity (score) of pairwise comparisons.





DUb 1	DUb 2	Score
<i>Hs</i> AMSH	<i>Hs</i> AMSH-LP	56
<i>Hs</i> AMSH	<i>Sp</i> Amsh	28
<i>Hs</i> AMSH-LP	<i>Sp</i> Amsh	25

**Figure 3.4. Alignment of AMSH DUBs in *S. pombe* and *H. sapiens*.** The MIT domain is boxed in green. Important MIT domain residues are highlighted in green. The bi-partite NLS is boxed in orange. The CBS is boxed in violet. The SBM domain is boxed in dark blue. The JAMM domain residues are boxed in red. MPN+ residues are highlighted in red. Residues that are invariant in over 50% of JAMM domain proteins are highlighted in yellow (Maytal-Kivity *et al*, 2002). The inserts conferring ubiquitin chain specificity are shown in light blue and light green (Sato *et al*, 2008). Other colour coding as Figure 3.1. The table underneath shows the percentage identity (score) of pairwise comparisons.

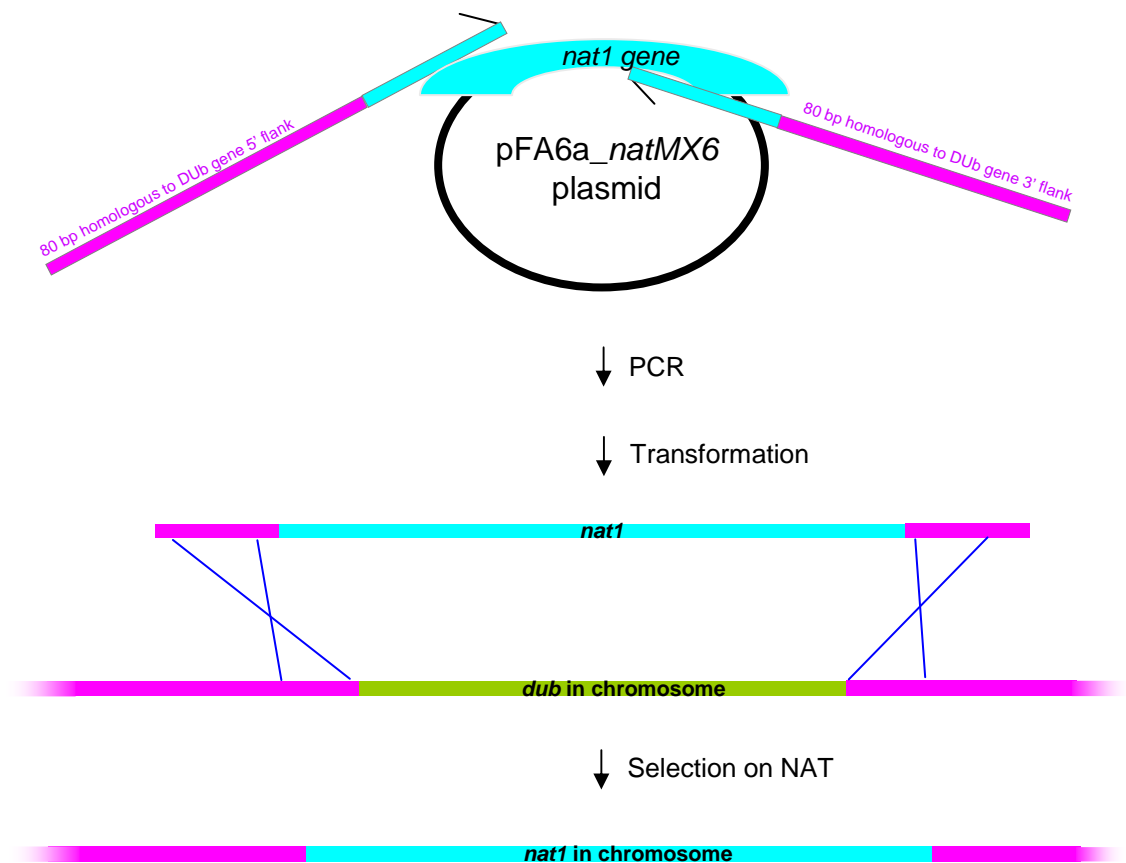


**Figure 3.5. DUB Gene Deletion-Insertion Approach Using the *nat1* Integration.** Firstly, transforming DNA was synthesised by one-step PCR using long (100 bp) primers. The pFA6a\_*natMX6* plasmid comprises the NAT resistance gene. The *nat1* gene is represented in turquoise, a *dub* gene in green, flanking sequences of the *dub* gene in pink, and an HR reaction is represented by a blue cross.

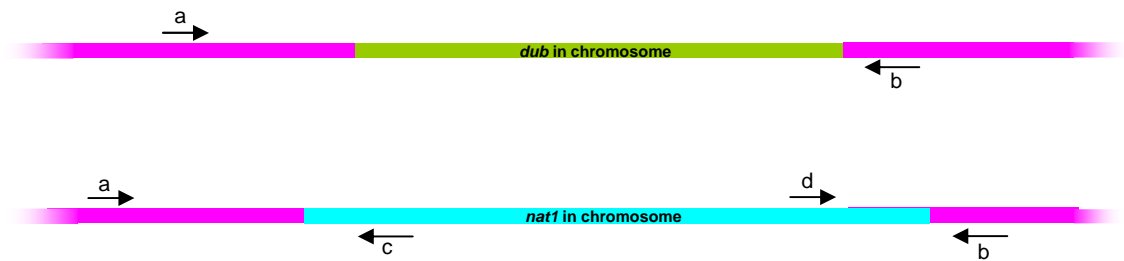


**Figure 3.6. PCR Primer Positions for Checking *dub* Knockout Status.**

PCR was performed on genomic DNA preparations of nourseothricin (NAT) resistant strains. The gene encoding NAT resistance (*nat1*) is represented in turquoise, a *dub* gene in green, flanking sequences of the *dub* gene in pink.

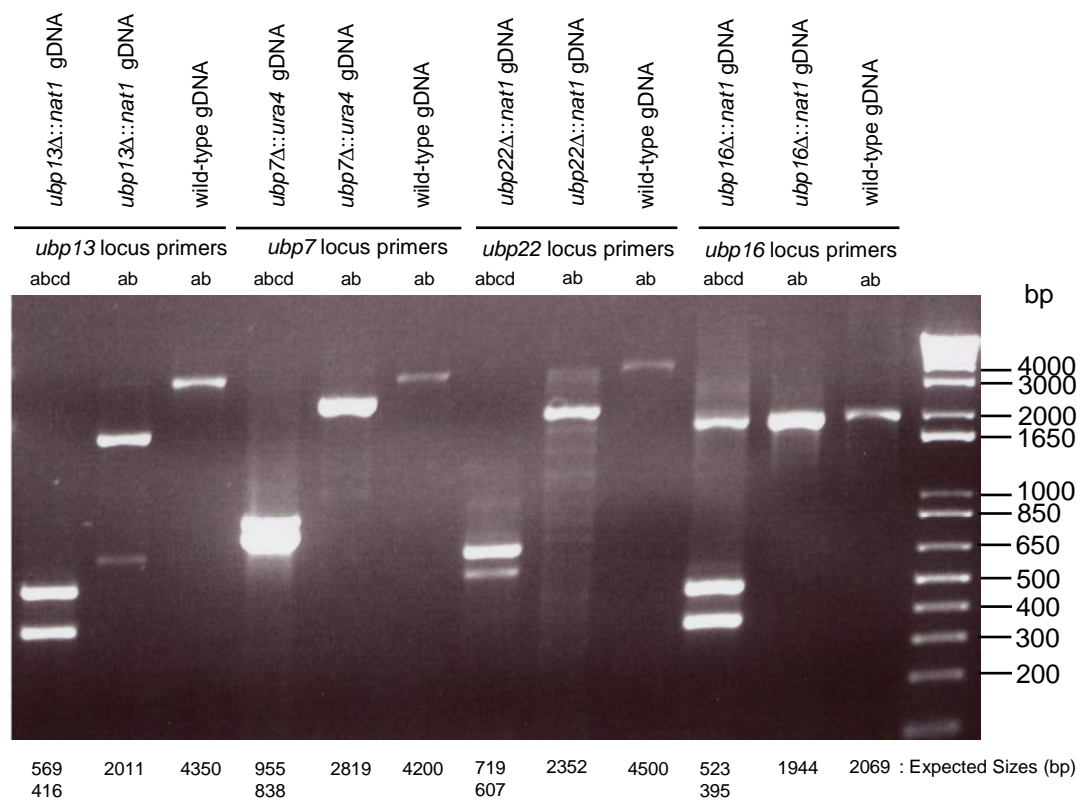


**Figure 3.7. PCR Amplification of the *ubp13*, *ubp7*, *ubp22*, and *ubp16* Loci Utilising Primers that Anneal to Flanking DNA and the *nat1* marker.** Using genomic DNA from of the *S. pombe* strains wild-type, *ubp13Δ::nat1*, *ubp7Δ::nat1*, *ubp22Δ::nat1*, and *ubp16Δ::nat1*. Lanes are marked with the primers utilised (as per figure 3.6).

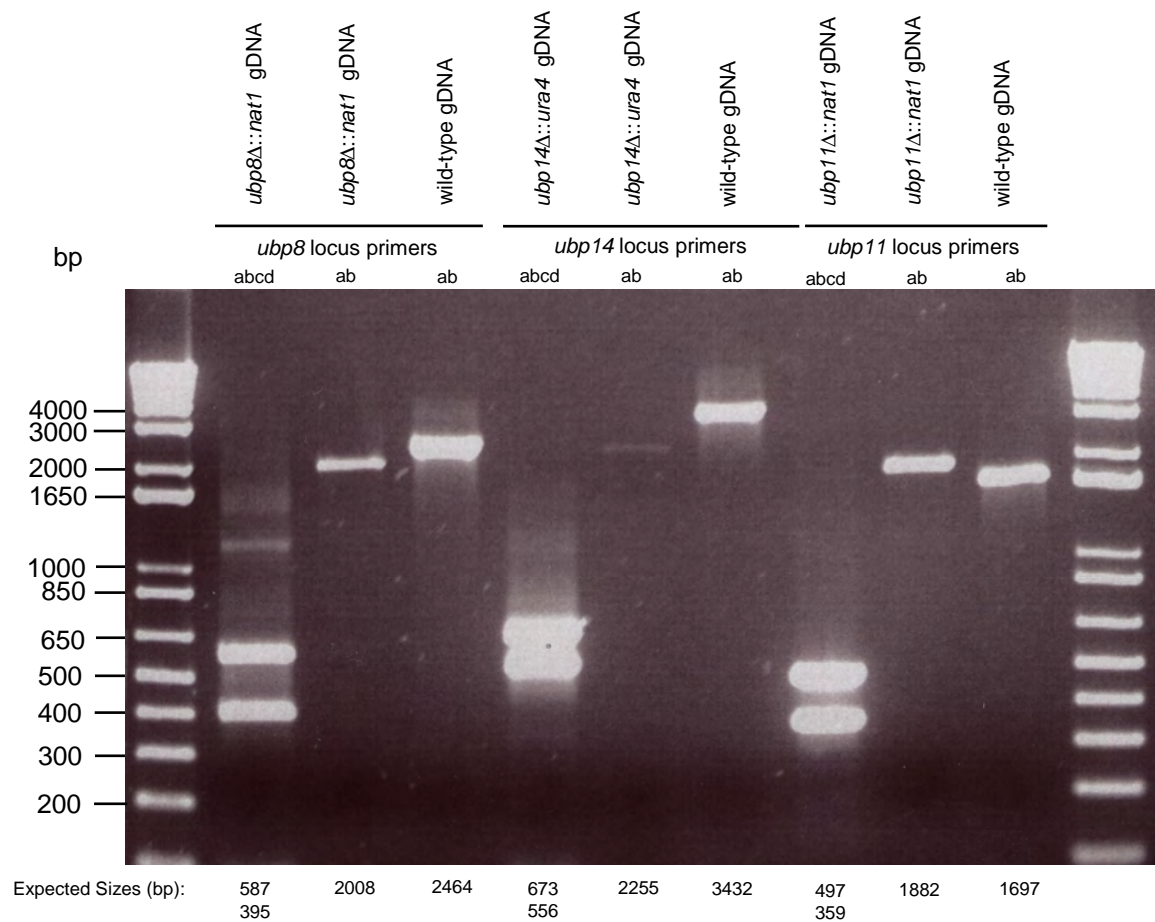


**Figure 3.8. PCR Amplification of the *ubp8*, *ubp14*, and *ubp11* Loci Utilising Primers that Anneal to Flanking DNA and the *nat1* Marker.** Using Genomic DNA from of the *S. pombe* Strains wild-type, *ubp8Δ::nat1*, *ubp14Δ::nat1*, and *ubp11Δ::nat1*. Lanes are marked with the primers utilised (as per figure 3.6).

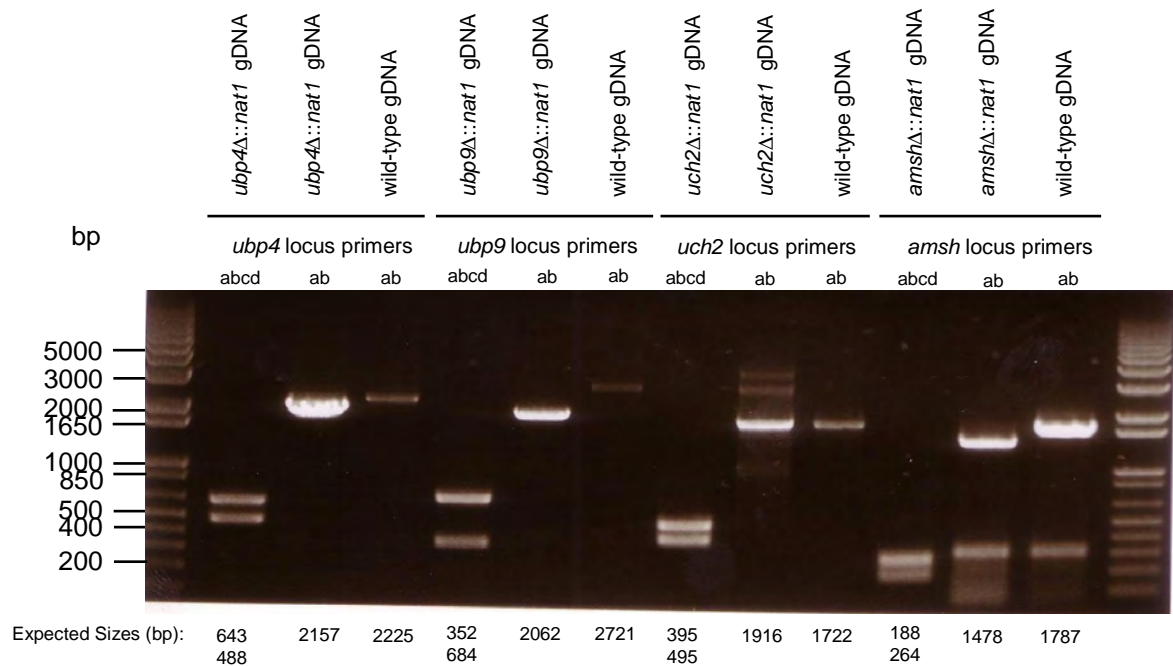


**Figure 3.9. PCR Amplification of the *ubp4*, *ubp9*, *uch2*, and *amsh* Loci Utilising Primers that Anneal to Flanking DNA and the *nat1* Marker.** Using Genomic DNA from of the *S. pombe* Strains wild-type, *ubp4*Δ::*nat1*, *ubp9*Δ::*nat1*, *uch2*Δ::*nat1*, and *amsh*Δ::*nat1*. Lanes are marked with the primers utilised (as per figure 3.6).

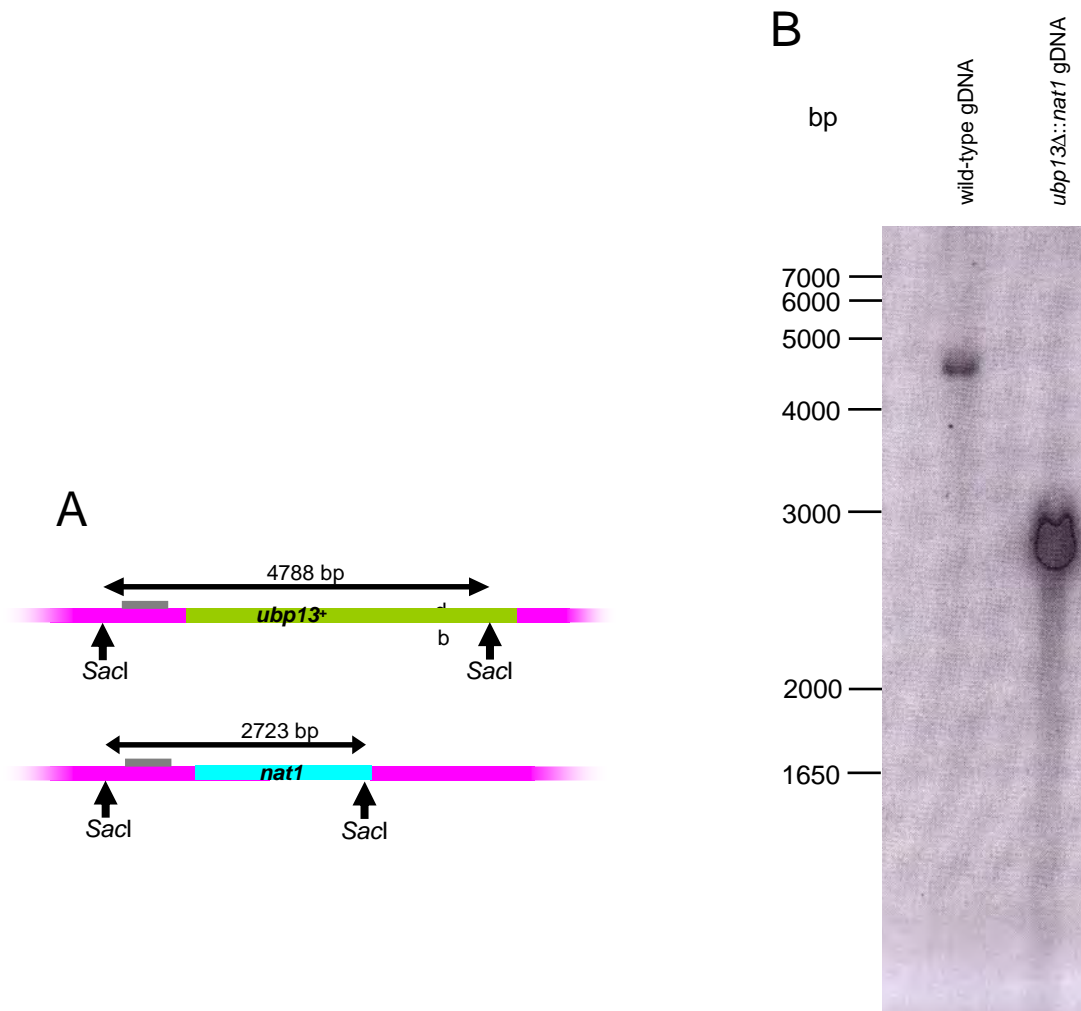


**Figure 3.10. Verification of *ubp13*Δ::*nat1* Genotype via Southern Analysis.** (A) Genomic DNA from wild-type and a candidate *ubp13*Δ::*nat1* strain was digested overnight with the indicated endonucleases. Subsequently, the digested DNA was fractionated on an agarose gel and transferred onto a membrane, which was then probed with a small piece of radiolabelled dsDNA (grey) designed to anneal just downstream of the *ubp13* locus. The expected sizes detected are shown. (B) The DNA fragments detected on the Southern blot.

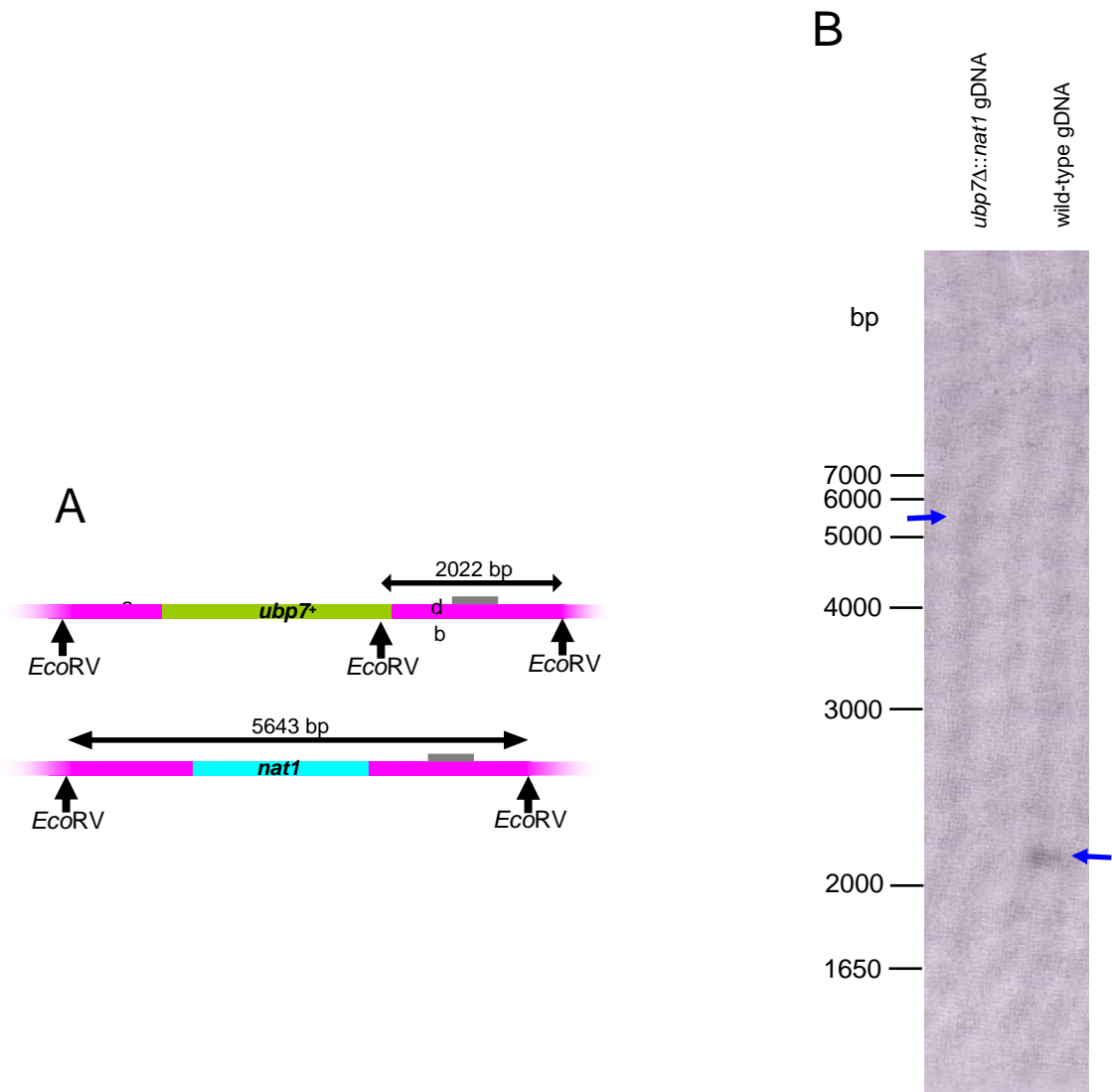


**Figure 3.11. Verification of *ubp7Δ::nat1* Genotype via Southern Analysis.** As figure 3.10. Blue arrows indicate the position of the bands on the Southern.



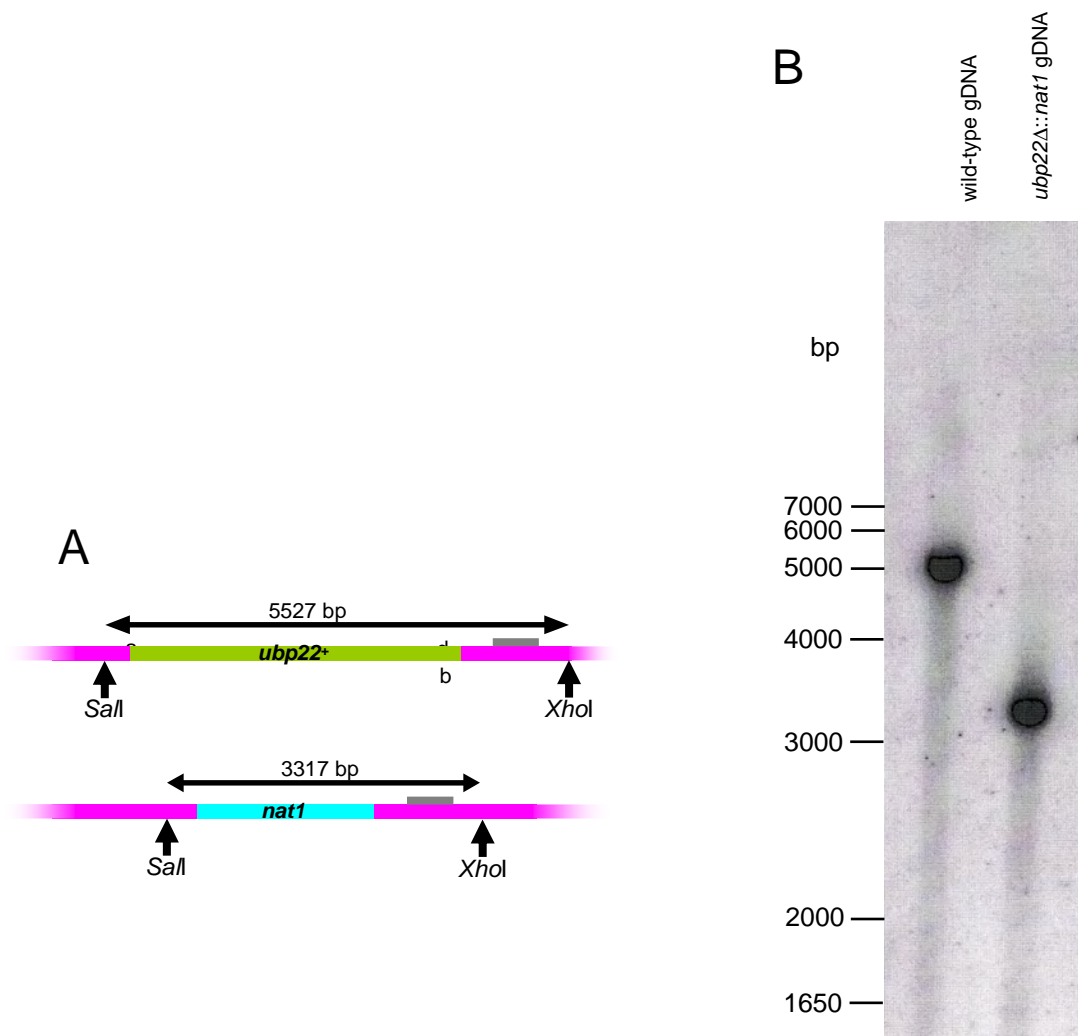


**Figure 3.12. Verification of *ubp22Δ::nat1* Genotype via Southern Analysis.** As figure 3.10

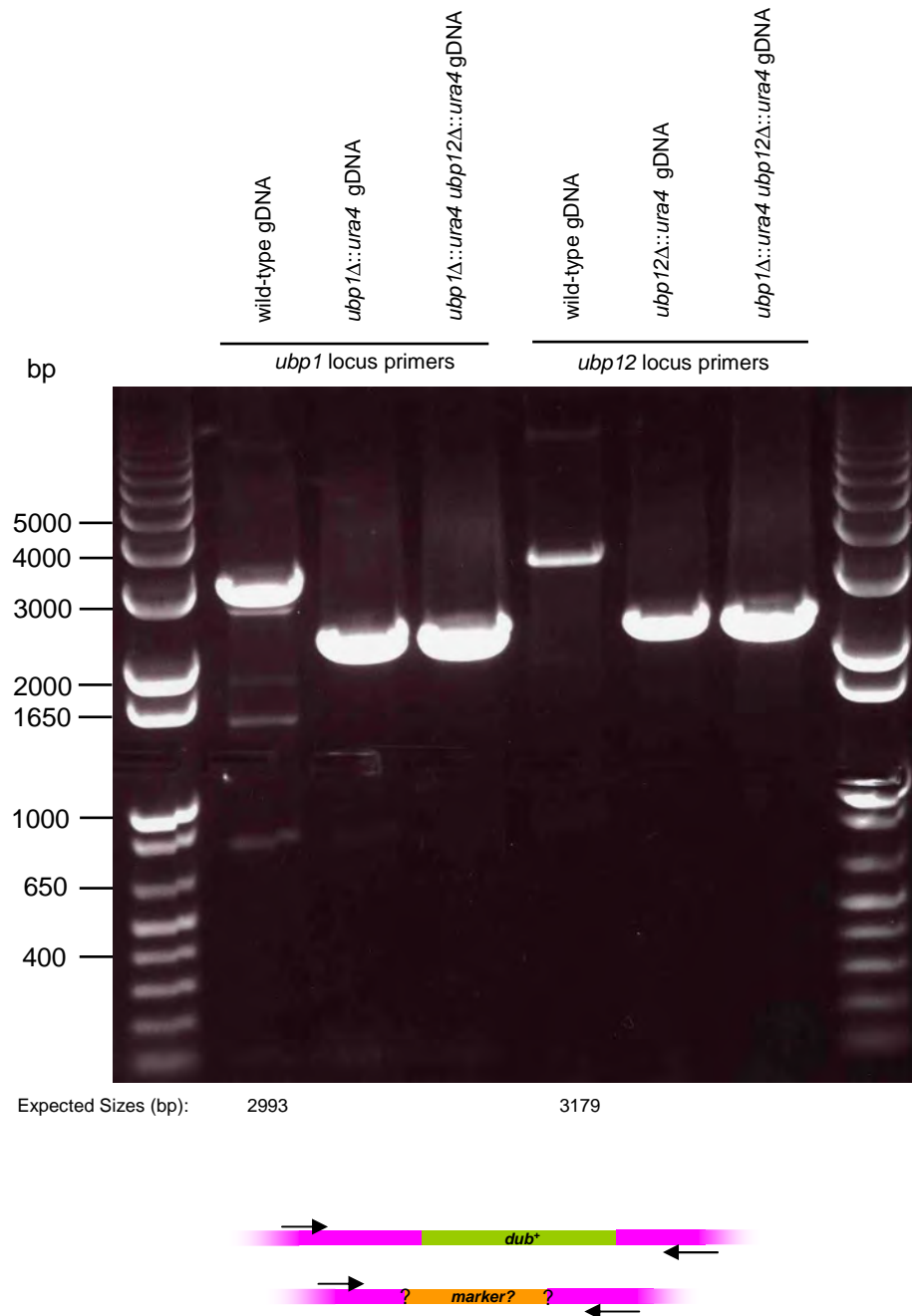


**Figure 3.13. PCR Amplification of the *ubp1* and *ubp12* Loci Utilising Primers that Anneal to Flanking DNA.** Using Genomic DNA from of the *S. pombe* Strains wild-type, *ubp1*Δ::*ura4*, *ubp12*Δ::*ura4*, and *ubp1*Δ::*ura4 ubp12*Δ::*ura4*. Expected size of deletions was not known because these strains were made by collaborators – the locus was checked by sequencing. The lower diagram shows the PCR strategy in wild-type gDNA and potentially *dub*-deleted gDNA. Primers that flank the DUB gene locus are depicted by arrows.

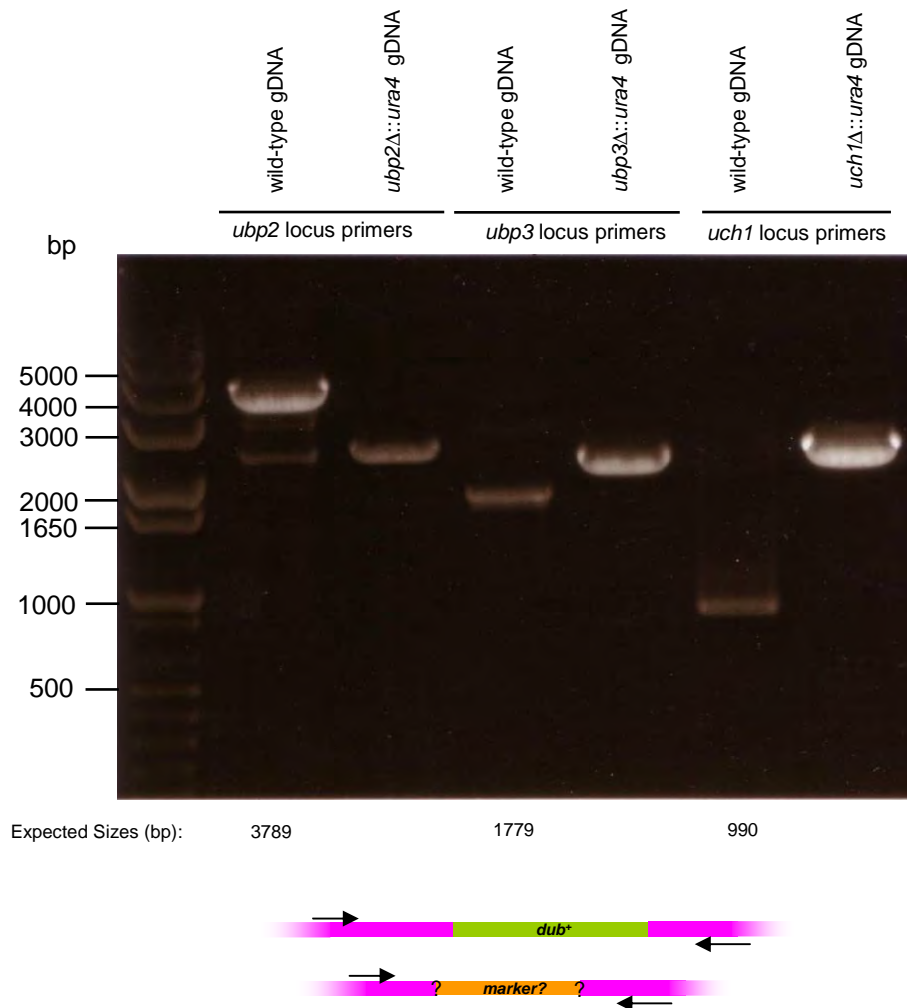


**Figure 3.14. PCR Amplification of the *ubp2*, *ubp3*, and *uch1* Loci Utilising Primers that Anneal to Flanking DNA.** Using Genomic DNA from of the *S. pombe* Strains wild-type, *ubp2Δ::ura4*, *ubp3Δ::ura4* and *uch1Δ::ura4*. Expected size of deletions was not known because these strains were made by collaborators – the locus was checked by sequencing. The lower diagram shows the PCR strategy in wild-type gDNA and potentially *dub*-deleted gDNA. Primers that flank the DUB gene locus are depicted by arrows.

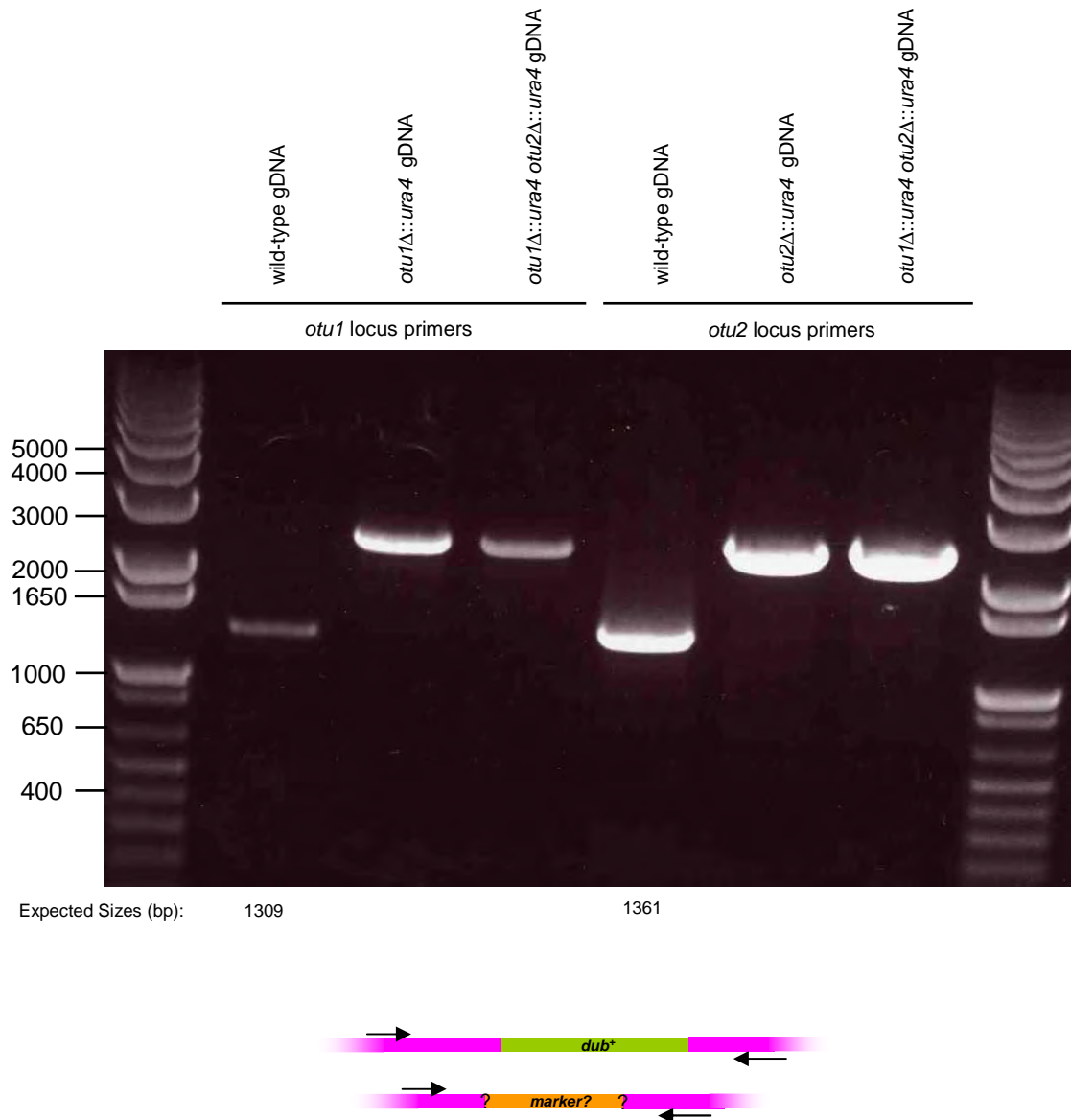


**Figure 3.15. PCR Amplification of the *otu1* and *otu2* Loci Utilising Primers that Anneal to Flanking DNA.** Using Genomic DNA from of the *S. pombe* Strains wild-type, *otu1*Δ::ura4, *otu2*Δ::ura4, and *otu1*Δ::ura4 *otu2*Δ::ura4. Expected size of deletions was not known because these strains were made by collaborators – the locus was checked by sequencing. The lower diagram shows the PCR strategy in wild-type gDNA and potentially *dub*-deleted gDNA. Primers that flank the DUB gene locus are depicted by arrows.

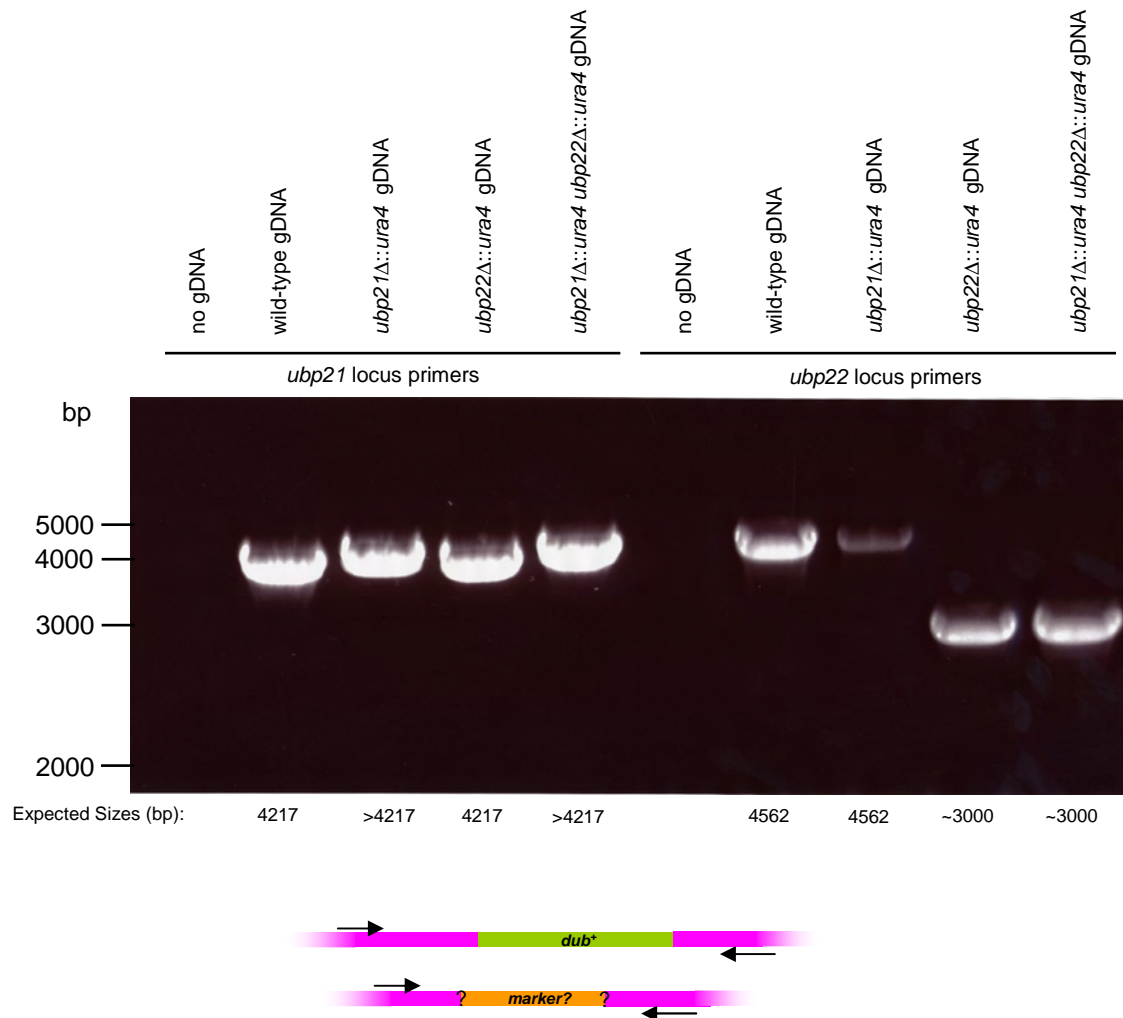


**Figure 3.16. PCR Amplification of the *ubp21* and *ubp22* Loci Utilising Primers that Anneal to Flanking DNA.** Using Genomic DNA from of the *S. pombe* Strains wild-type, *ubp21*Δ::*ura4*, *ubp22*Δ::*ura4* and *ubp21*Δ::*ura4* *ubp22*Δ::*ura4*. Sizes of PCR products from deletion strains was estimated from what was described of their knockout strategy (Richert *et al.*, 2002). The locus was further checked by sequencing. The lower diagram shows the PCR strategy in wild-type gDNA and potentially *dub*-deleted gDNA. Primers that flank the DUB gene locus are depicted by arrows.

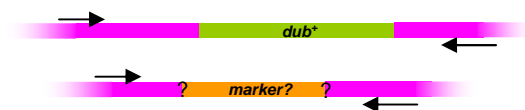
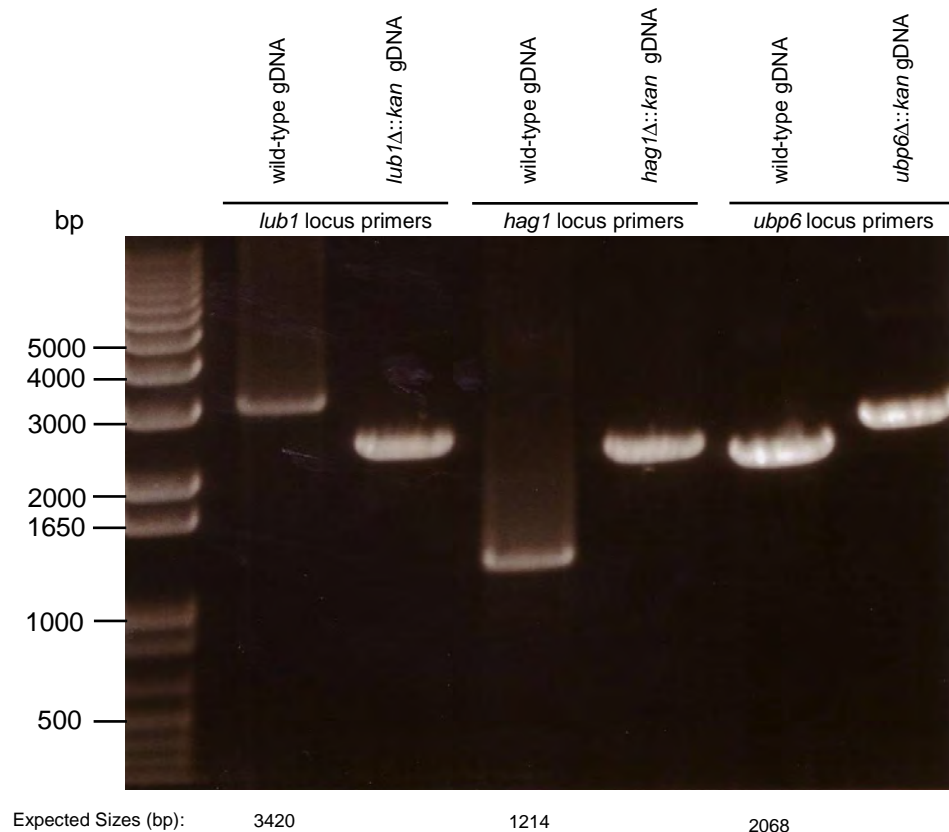


**Figure 3.17. PCR Amplification of the *lub1*, *hag1* and *ubp6* Loci Utilising Primers that Anneal to Flanking DNA.** Using genomic DNA from of the *S. pombe* Strains wild-type, *lub1*Δ::kan, *hag1*Δ::kan and *ubp6*Δ::kan. Expected size of deletions was not known because these strains were purchased from Bioneer who refused to disclose the sequence information – the locus was checked later by sequencing. The lower diagram shows the PCR strategy in wild-type gDNA and potentially *dub*-deleted gDNA. Primers that flank the DUB gene locus are depicted by arrows.

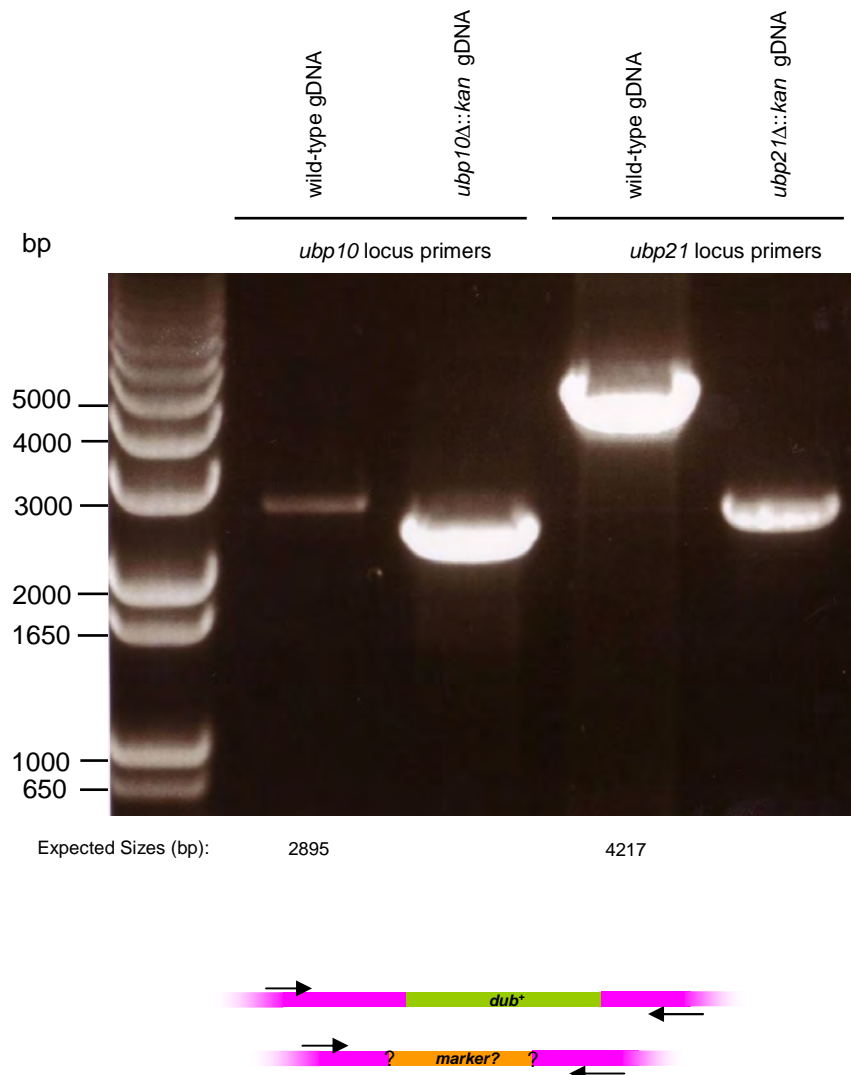


**Figure 3.18. PCR Amplification of the *ubp10* and *ubp21* Loci Utilising Primers that Anneal to Flanking DNA.** Using Genomic DNA from of the *S. pombe* Strains wild-type, *ubp10*Δ::*kan*, and *ubp21*Δ::*kan*. Expected size of deletions was not known because these strains were purchased from Bioneer who refused to disclose the sequence information – the locus was checked later by sequencing. The lower diagram shows the PCR strategy in wild-type gDNA and potentially *dub*-deleted gDNA. Primers that flank the DUB gene locus are depicted by arrows.



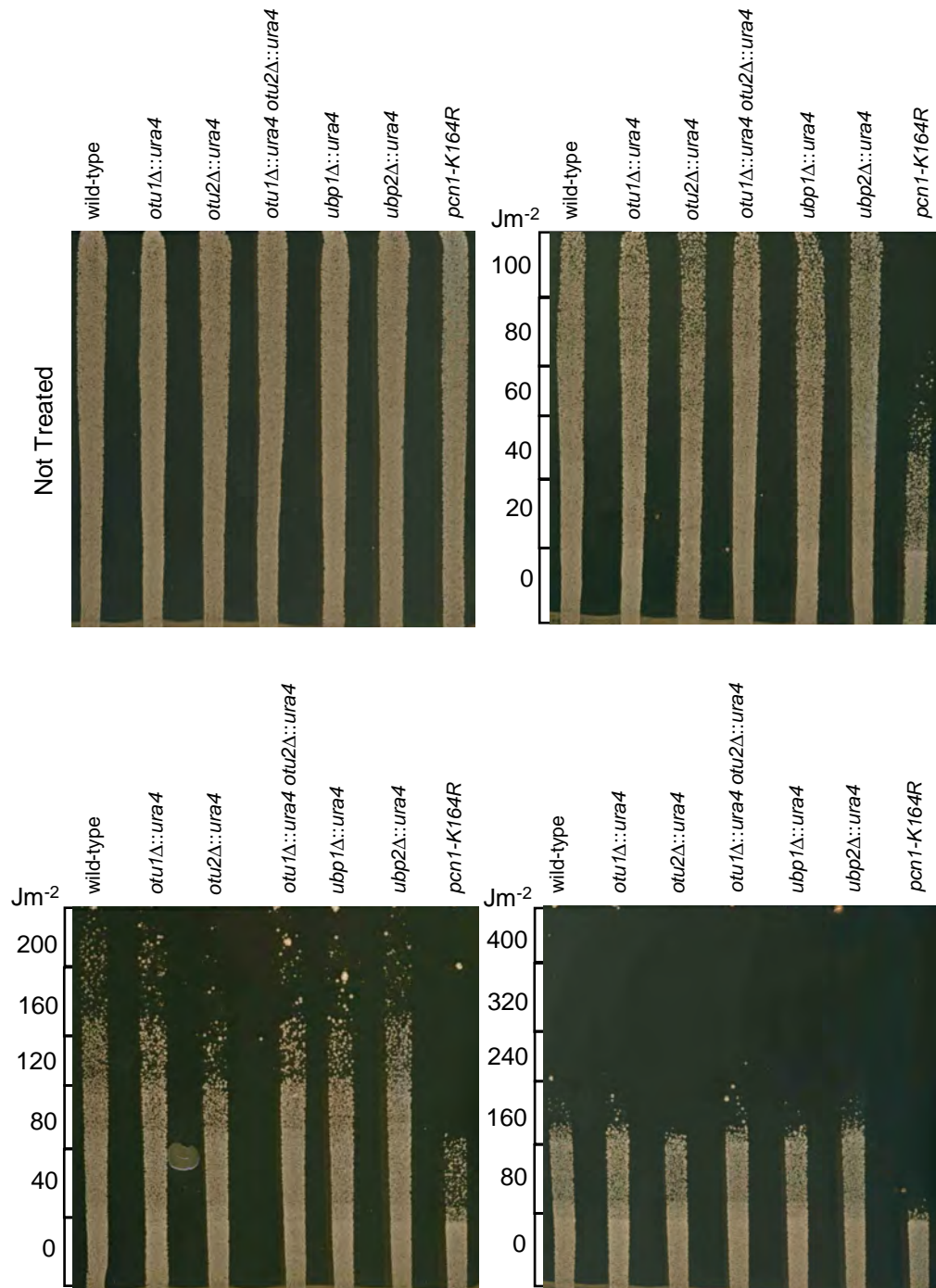


**Figure 4.1. Drop Test Assays Measuring the Relative Sensitivities of *S. pombe* Strains wild-type, *otu1Δ*, *otu2Δ*, *otu1Δ otu2Δ*, *ubp1Δ*, *ubp2Δ* and *pcn1-K164R* to Different Doses of UVC.** Exponentially growing cultures were normalised by cell concentration and dropped down YEA agar plates, which were subsequently exposed to a UVC dose gradient as indicated. Plates were grown for three days at 30°C before photographing.



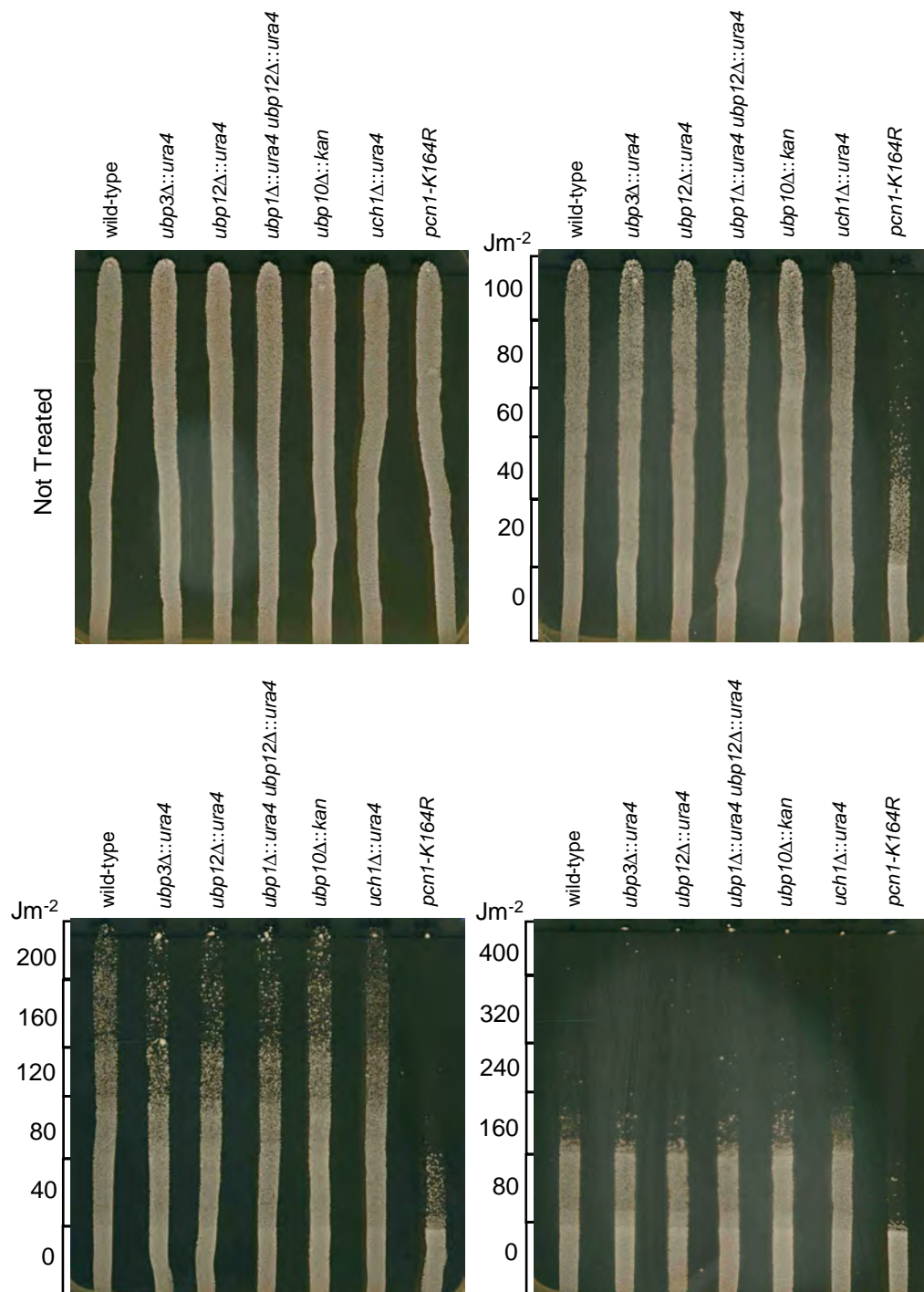


**Figure 4.2. Drop Test Assays Measuring the Relative Sensitivities of *S. pombe* Strains wild-type, *ubp3Δ*, *ubp12Δ*, *ubp1Δ ubp12Δ*, *ubp10Δ*, *uch1Δ* and *pcn1-K164R* to Different Doses of UVC.** This experiment was performed as described in figure 4.1.

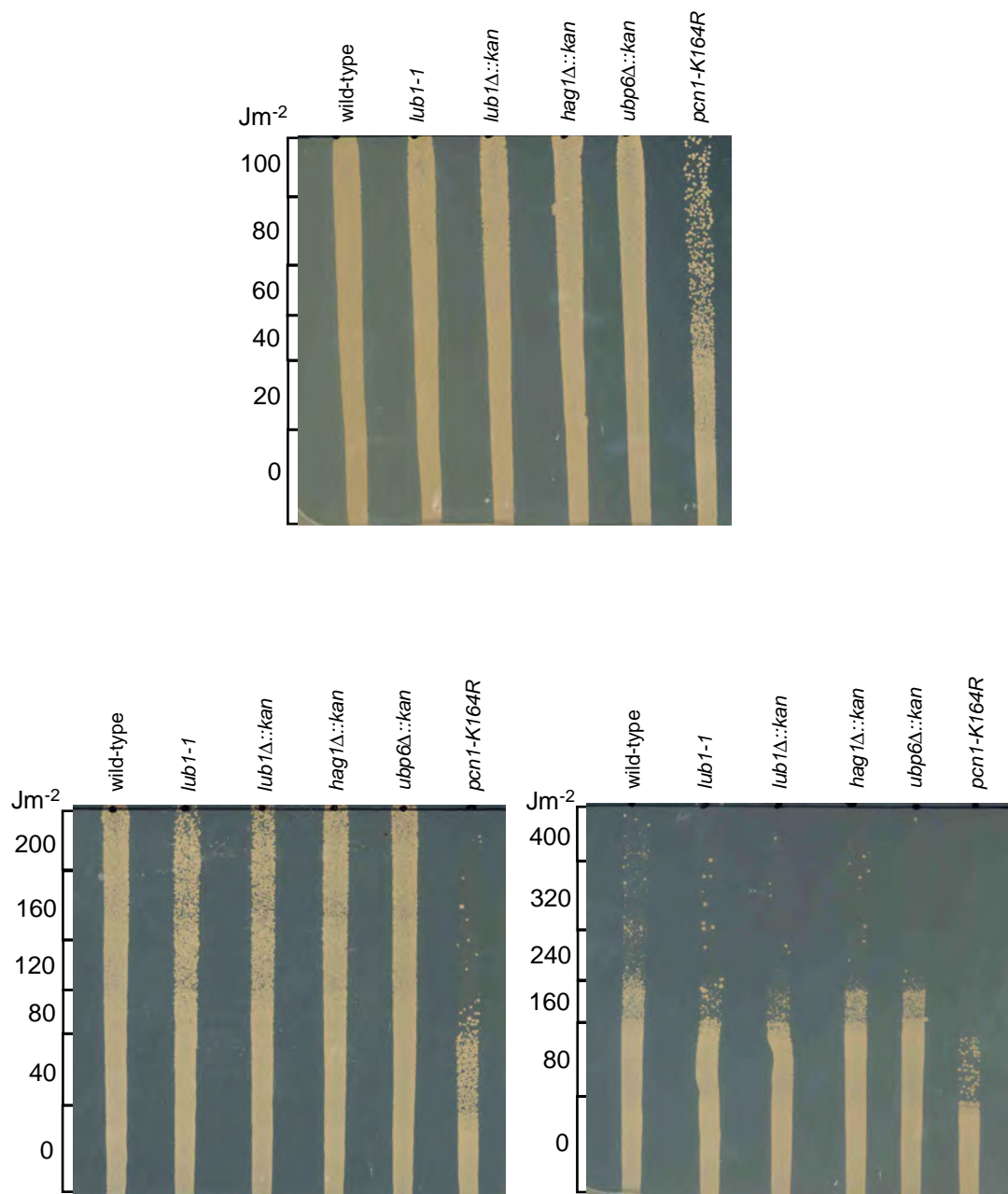


**Figure 4.3. Drop Test Assays Measuring the Relative Sensitivities of *S. pombe* Strains wild-type, *lub1-1*, *lub1Δ*, *hag1Δ*, *ubp6Δ*, and *pcn1-K164R* to Different Doses of UVC.** This experiment was performed as described in figure 4.1.

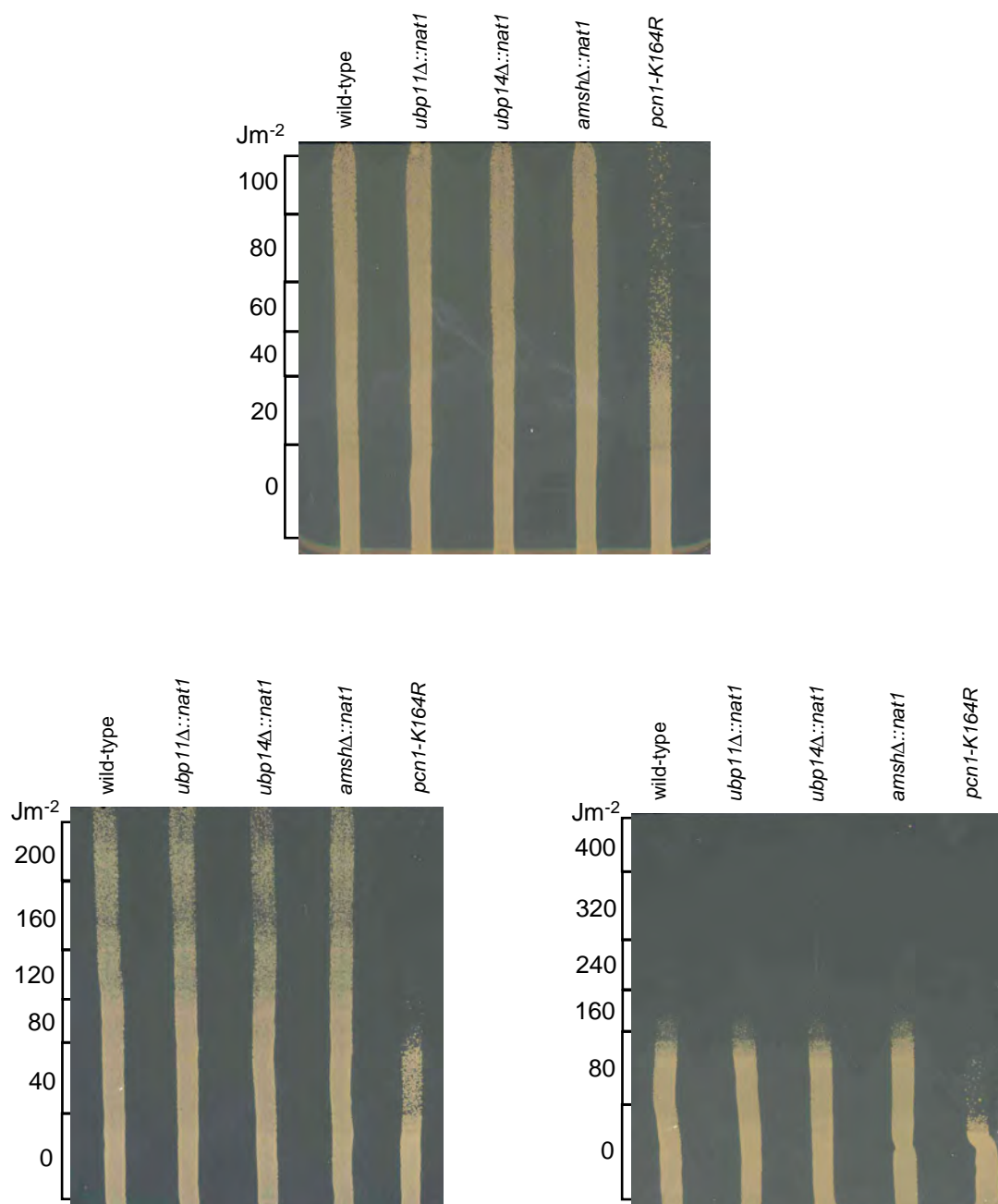


**Figure 4.4. Drop Test Assays Measuring the Relative Sensitivities of *S. pombe* Strains wild-type, *ubp11Δ*, *ubp14Δ*, *amshΔ*, and *pcn1-K164R* to Different Doses of UVC.** This experiment was performed as described in figure 4.1.

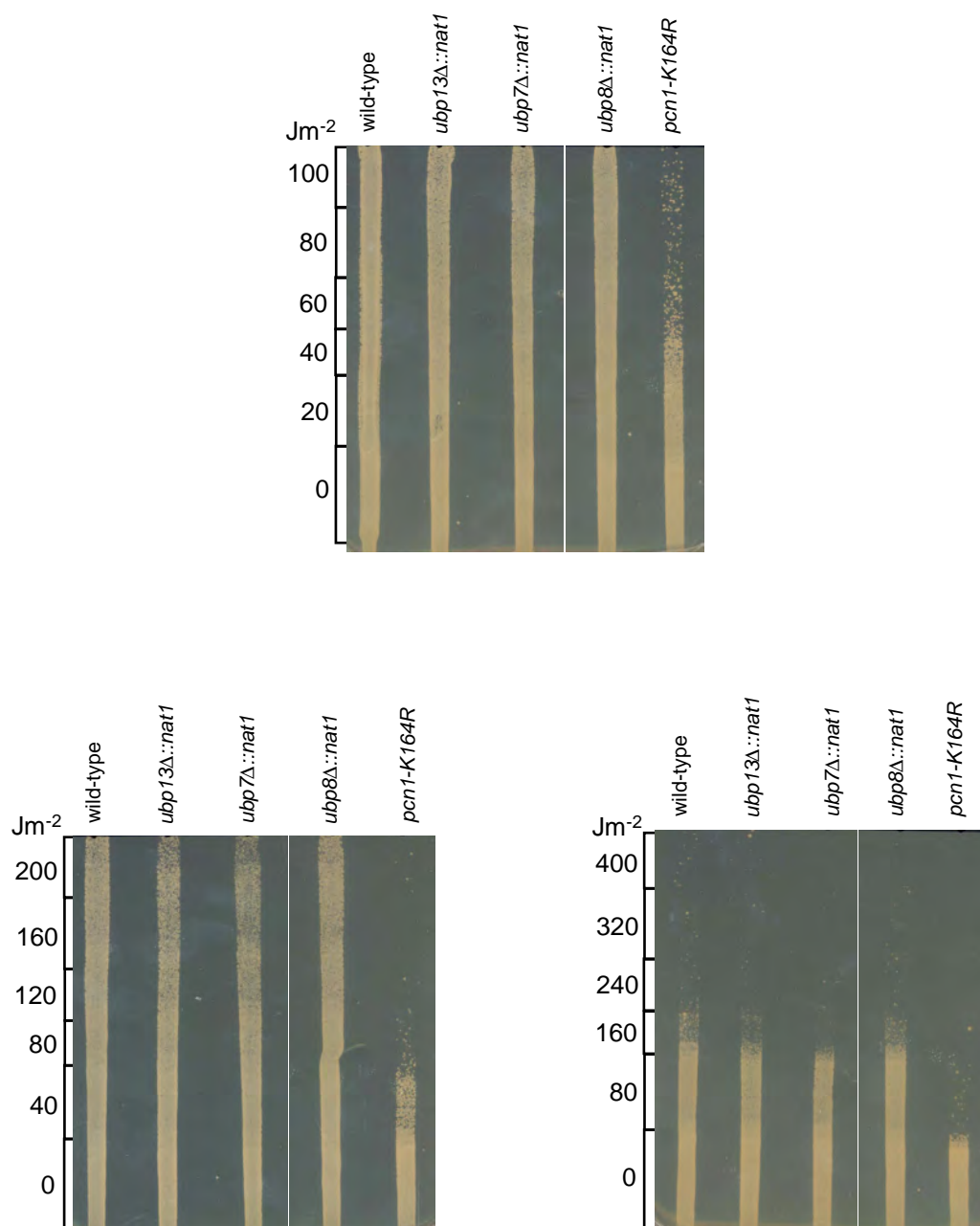


**Figure 4.5. Drop Test Assays Measuring the Relative Sensitivities of *S. pombe* Strains wild-type, *ubp13Δ*, *ubp7Δ*, *ubp8Δ*, and *pcn1-K164R* to Different Doses of UVC.** This experiment was performed as described in figure 4.1. The complete agar plates can be found in figure 5.17.

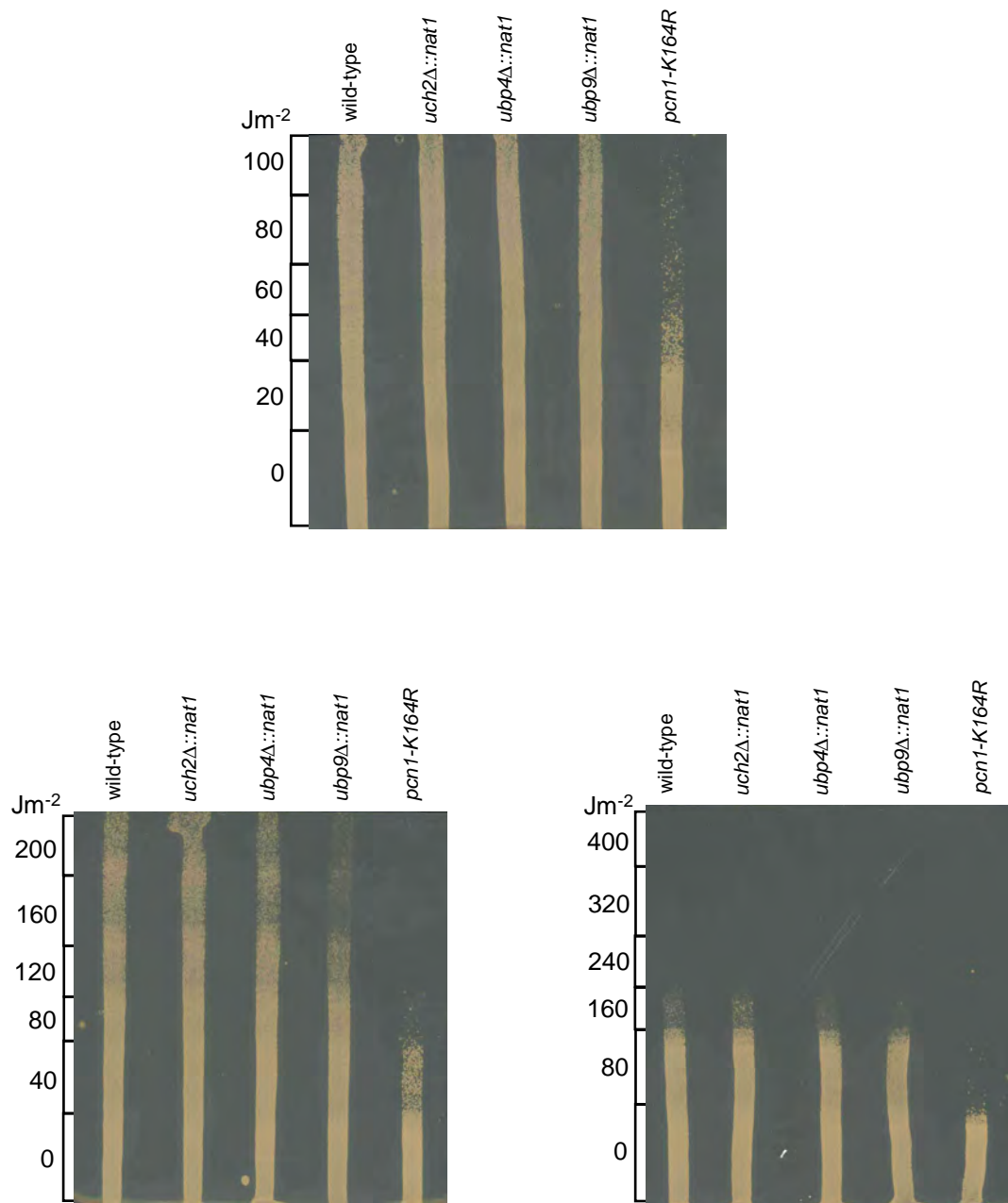


**Figure 4.6. Drop Test Assays Measuring the Relative Sensitivities of *S. pombe* Strains wild-type, *uch2Δ*, *ubp4Δ*, *ubp9Δ*, and *pcn1-K164R* to Different Doses of UVC.** This experiment was performed as described in figure 4.1.

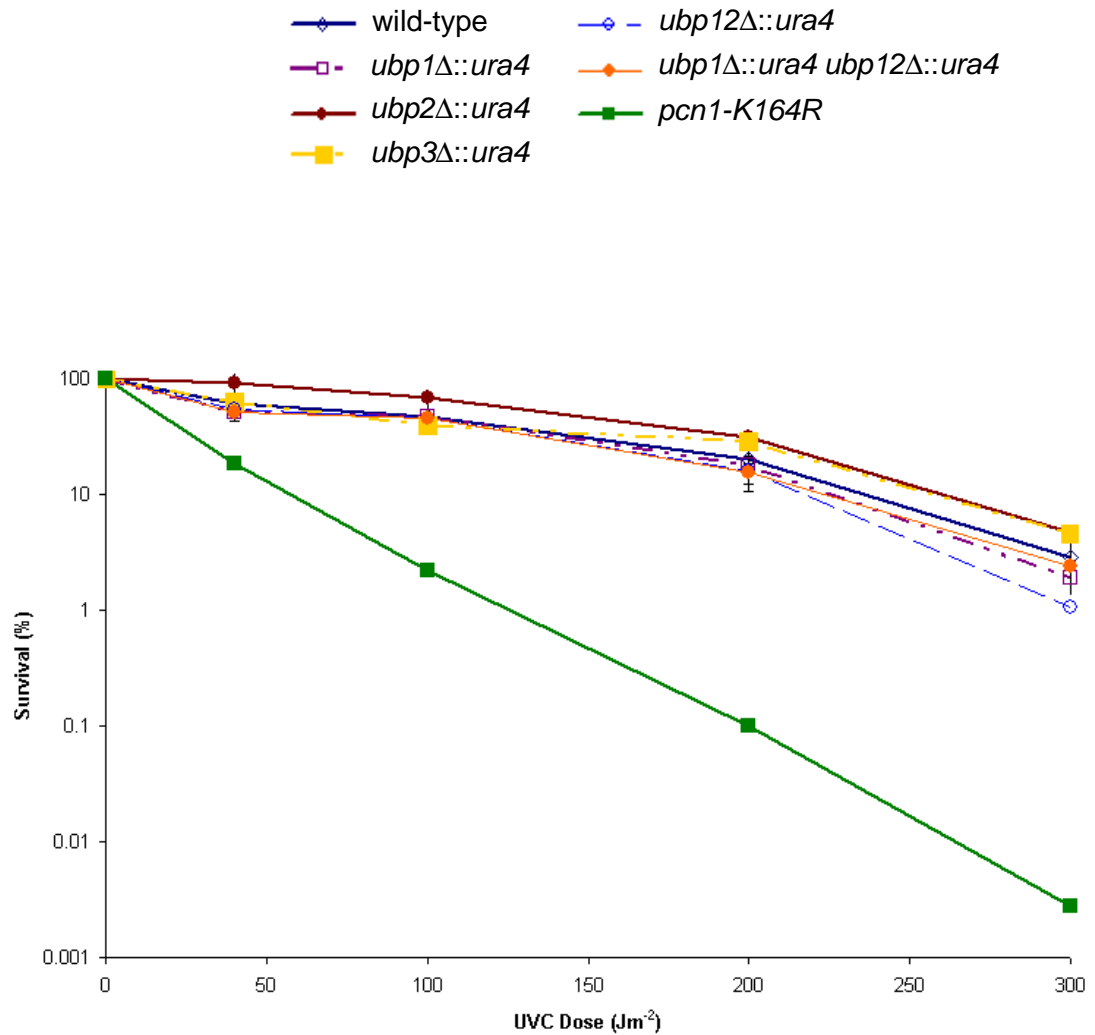


**Figure 4.7. Colony Forming Assay Measuring the Percentage Survival Following UVC Irradiation.** Strains *ubp1Δ*, *ubp2Δ*, *ubp3Δ*, *ubp12Δ*, and *ubp1Δ ubp12Δ* were compared with wild-type and *pcn1-K164R*. Exponentially growing cultures were plated onto YEA agar, which were exposed to the UVC doses indicated. Plates were grown for three days at 30°C before counting. The results represent the mean of two independent experiments and the error bars represent the standard deviation.

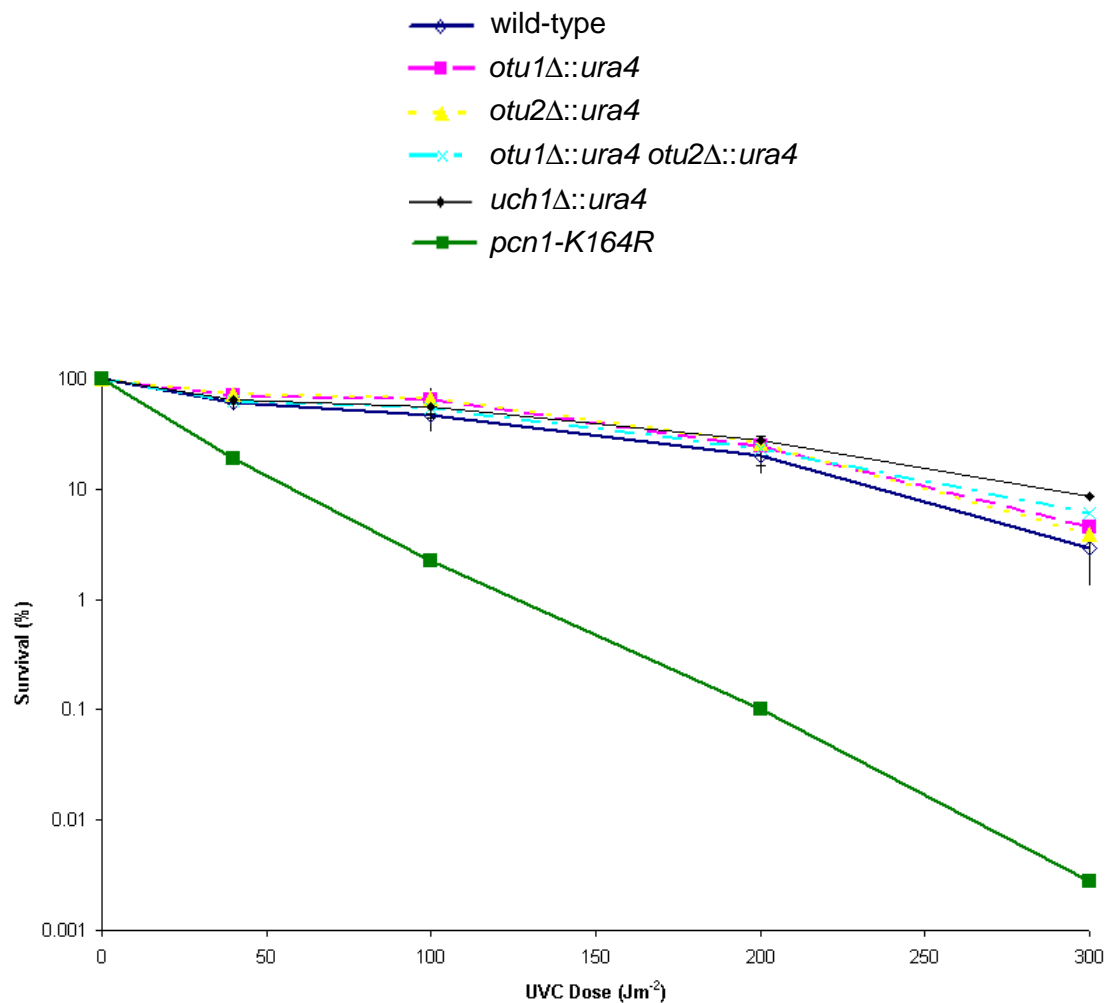


**Figure 4.8. Colony Forming Assay Measuring the Percentage Survival Following UVC Irradiation.** Strains *otu1*Δ, *otu2*Δ, *otu1*Δ *otu2*Δ, *uch1*Δ were compared with wild-type and *pcn1*-K164R. This experiment was performed as described in figure 4.7.

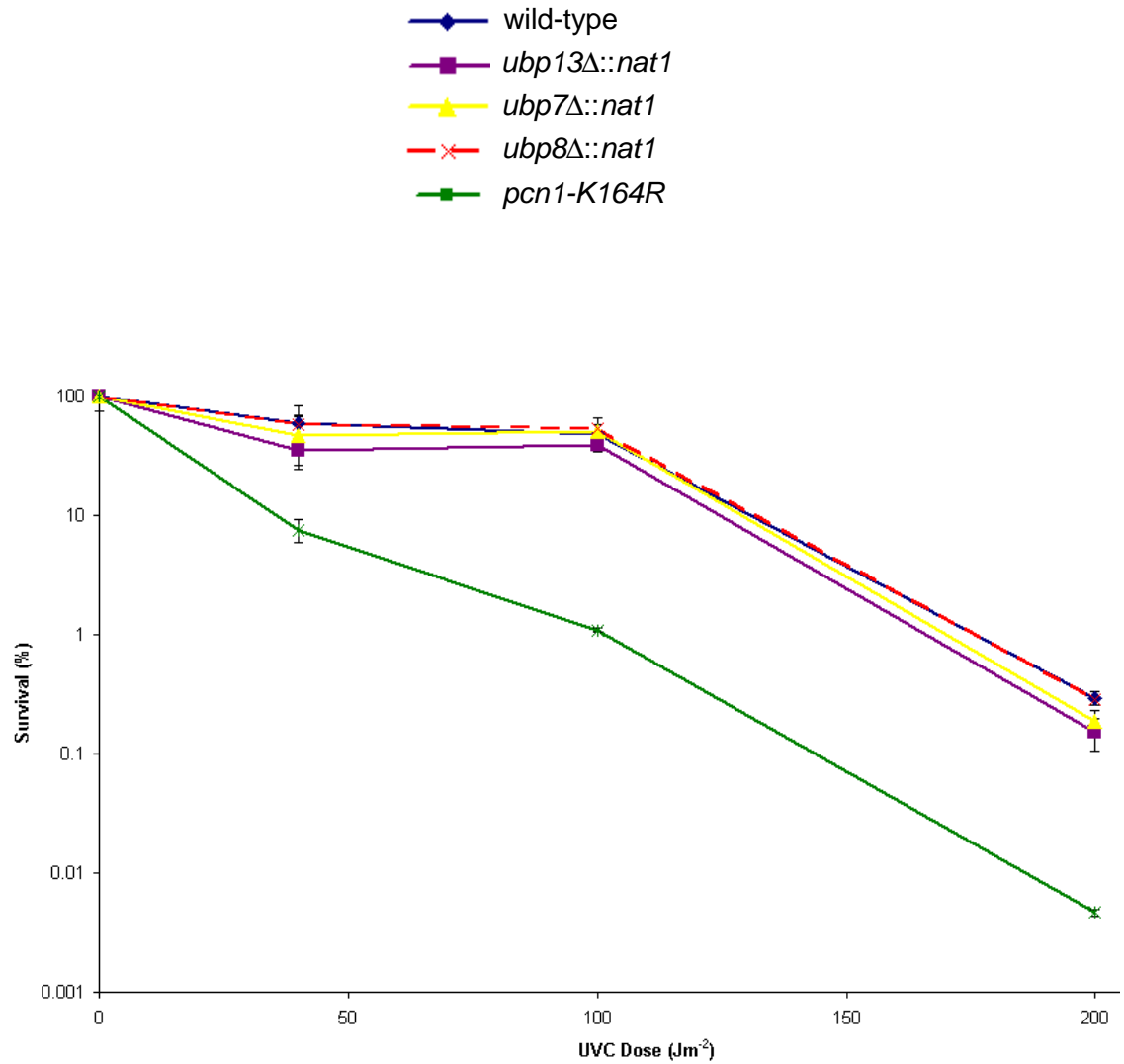


**Figure 4.9. Colony Forming Assay Measuring the Percentage Survival Following UVC Irradiation.** Strains *ubp13Δ*, *ubp7Δ*, *ubp8Δ* were compared with wild-type and *pcn1-K164R*. This experiment was performed as described in figure 4.7.



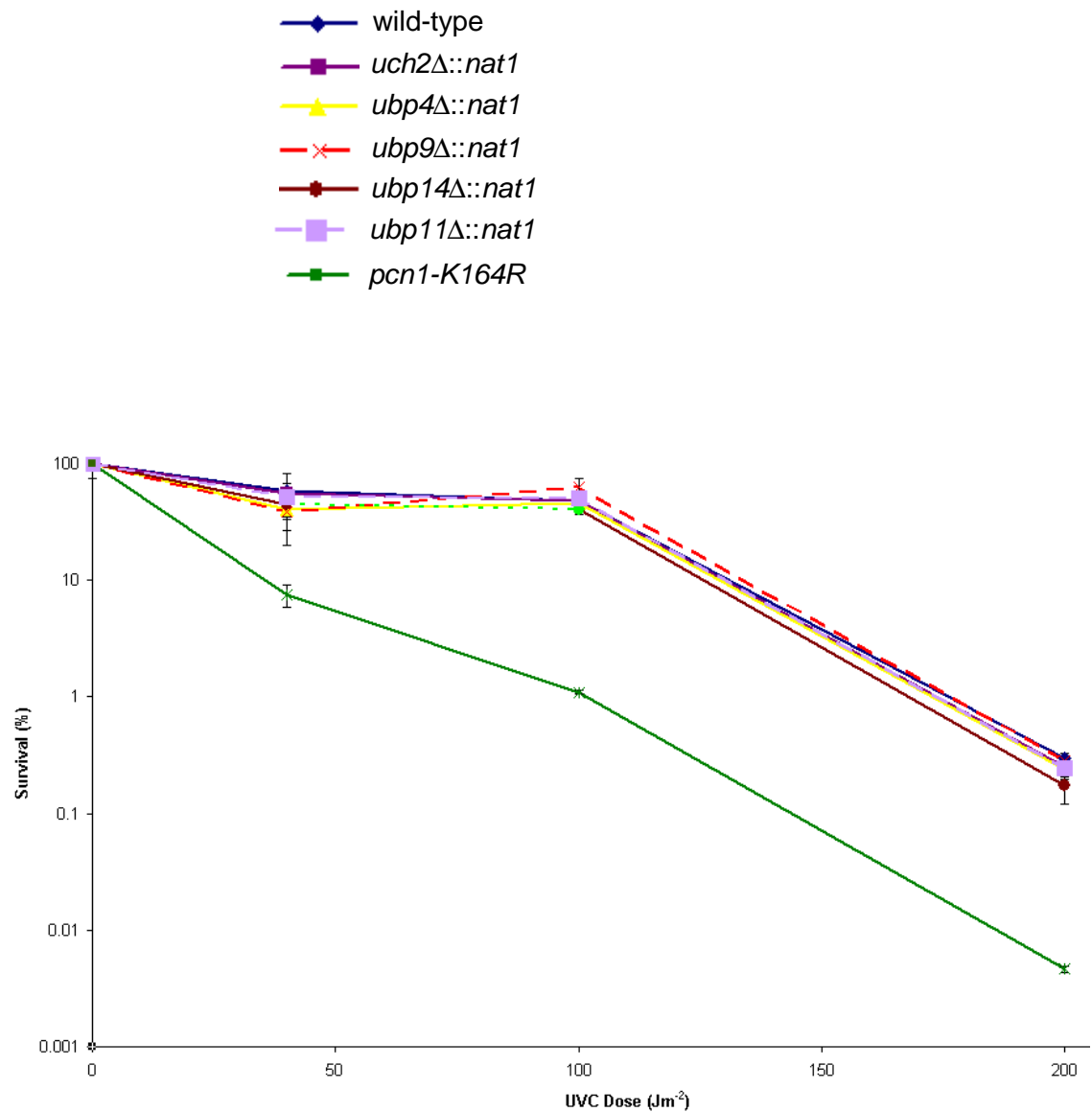


**Figure 4.10. Colony Forming Assay Measuring the Percentage Survival Following UVC Irradiation.** Strains *uch2Δ*, *ubp4Δ*, *ubp9Δ*, *ubp14Δ*, *ubp11Δ* were compared with wild-type and *pcn1-K164R*. This experiment was performed as described in figure 4.7.

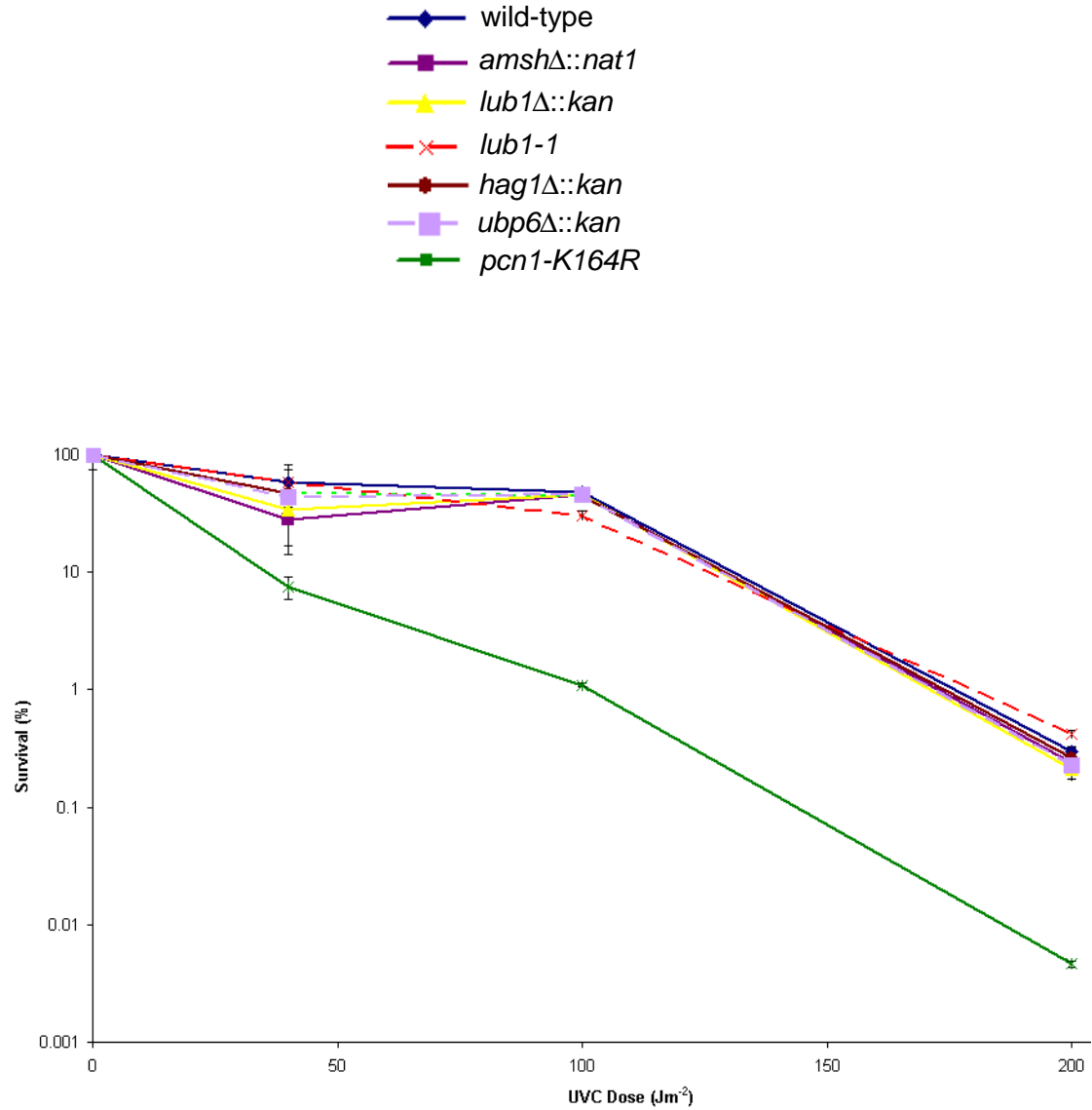


**Figure 4.11. Colony Forming Assay Measuring the Percentage Survival Following UVC Irradiation.** Strains *amsh*Δ, *lub1*Δ, *lub1-1*, *hag1*Δ, *ubp6*Δ were compared with wild-type and *pcn1-K164R*. This experiment was performed as described in figure 4.7.

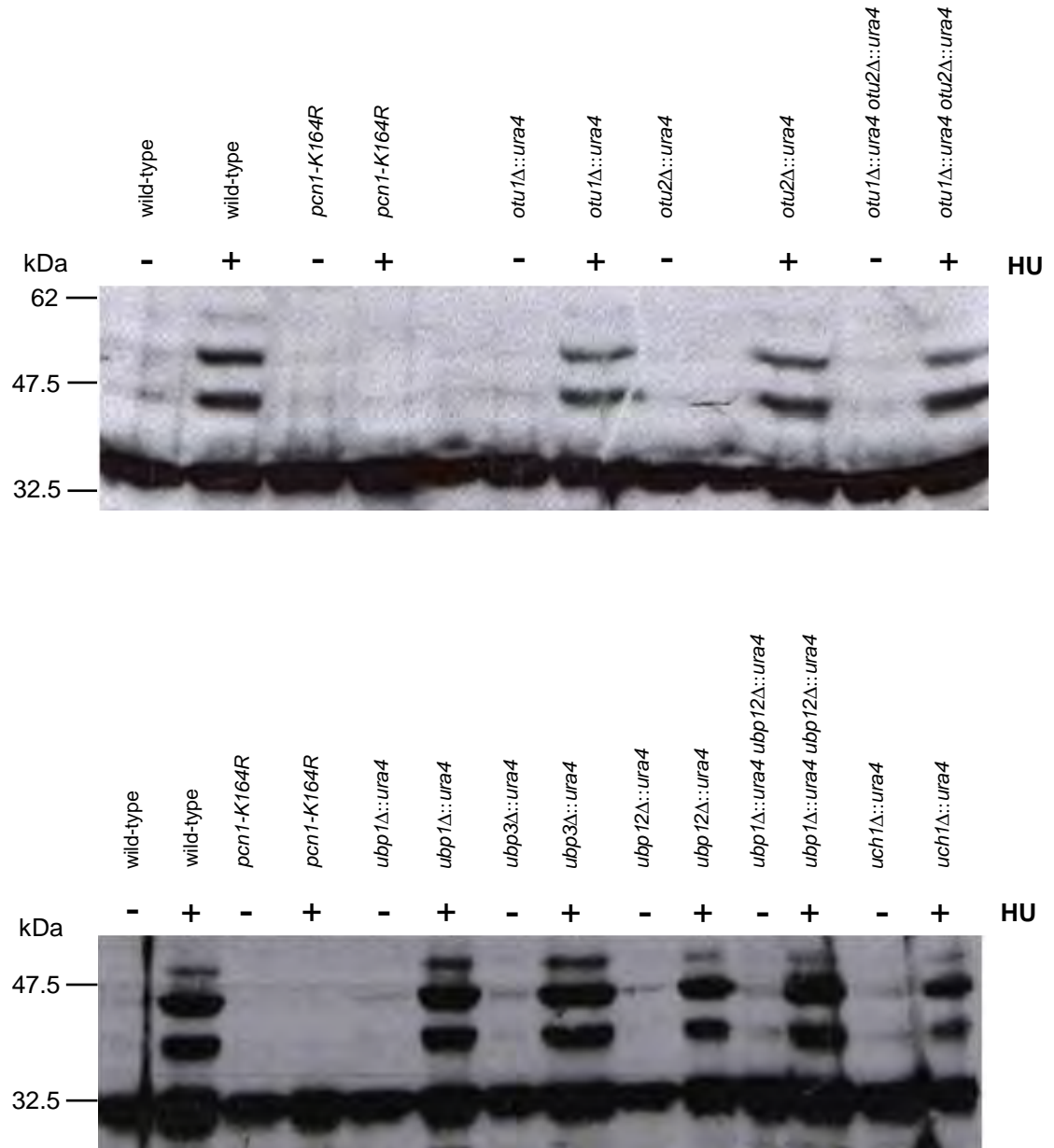


**Figure 4.12. Levels of *Sp*PCNA Ubiquitination in the *S. pombe* Strains wild-type, *pcn1-K164R*, *otu1Δ*, *otu1Δ otu2Δ*, *ubp1Δ*, *ubp3Δ*, *ubp12Δ*, *ubp1Δ ubp12Δ* and *uch1Δ* Without Treatment (-) or Following 50 mM Hydroxyurea Treatment (+).** The same number of cells of exponentially growing cultures were left untreated or treated with hydroxyurea, then size-fractionated whole cell extracts were probed with anti-*Sp*PCNA antibodies.

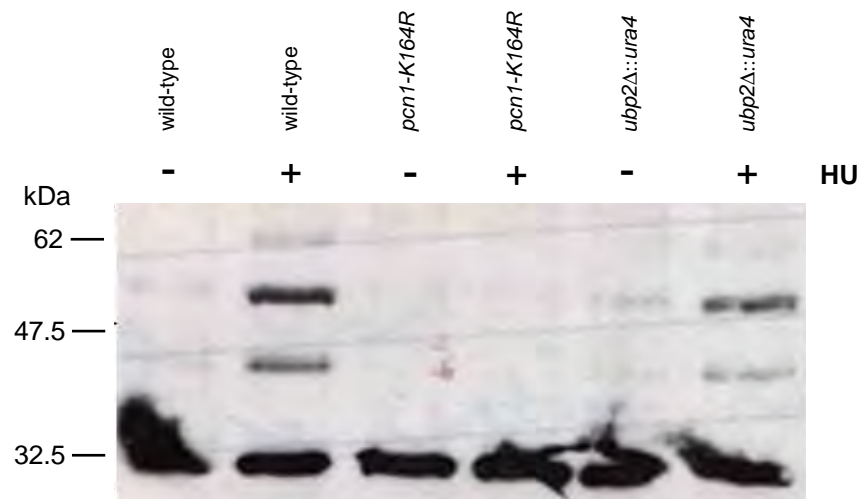


**Figure 4.13. Levels of *Sp*PCNA Ubiquitination in the *S. pombe* Strains wild-type, *pcn1-K164R*, and *ubp2Δ* Without Treatment (-) or Following 50 mM Hydroxyurea (+). This experiment was performed as described in figure 4.12.**

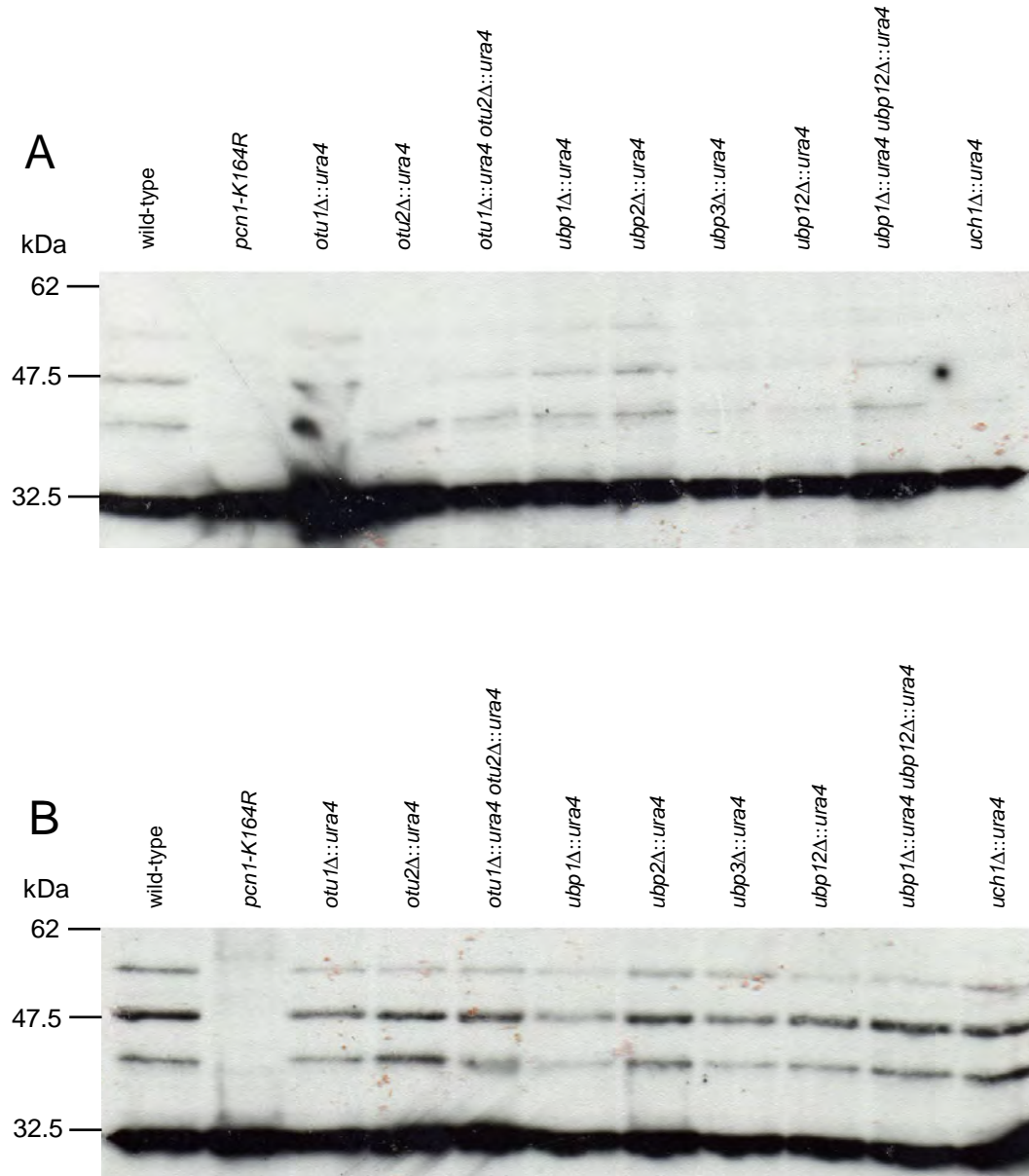


**Figure 4.14. Levels of *Sp*PCNA Ubiquitination in the *S. pombe* Strains wild-type, *pcn1-K164R*, *otu1Δ*, *otu1Δ*, *otu1Δ otu2Δ*, *ubp1Δ*, *ubp2Δ*, *ubp3Δ*, *ubp12Δ*, *ubp1Δ ubp12Δ* and *uch1Δ* Following Mock Treatment (A) or 100 Jm<sup>-2</sup> UVC (B).** The same number of cells of exponentially growing cultures were irradiated or mock irradiated with UVC, then size fractionated whole cell extracts were probed with anti-*Sp*PCNA antibodies.

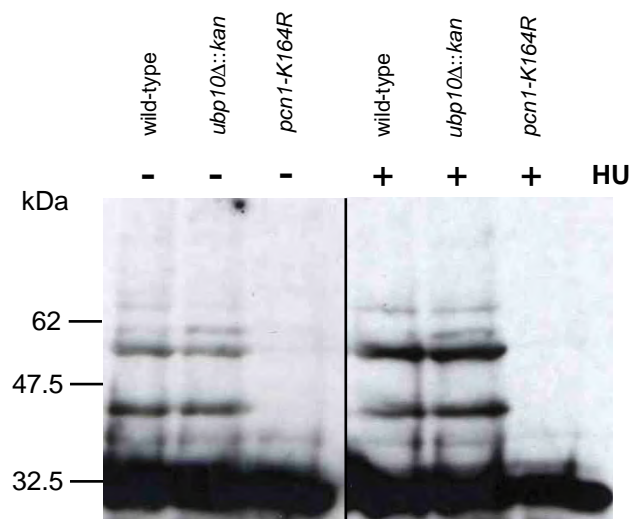


**Figure 4.15. Levels of *Sp*PCNA Ubiquitination in the *S. pombe* Strains wild-type, *ubp10Δ* and *pcn1-K164R* Without Treatment (-) or Following 10 mM Hydroxyurea (+). This experiment was performed as described in figure 4.12.**

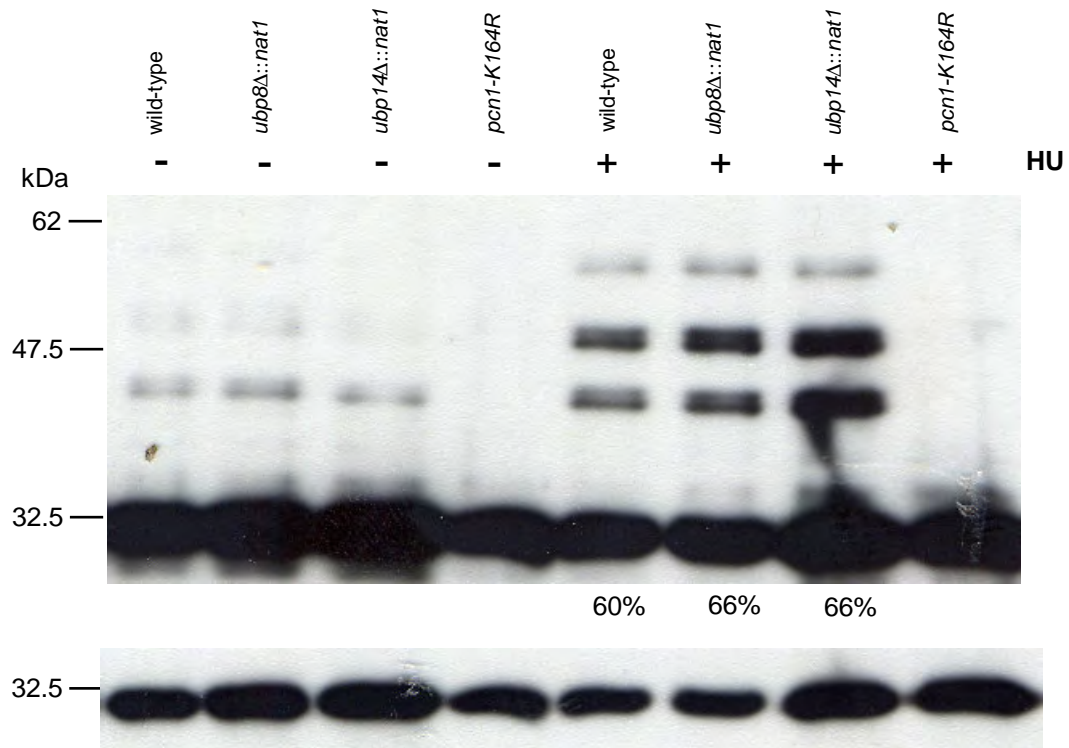


**Figure 4.16. Levels of *Sp*PCNA Ubiquitination in the *S. pombe* Strains wild-type, *ubp8Δ*, *ubp14Δ* and *pcn1-K164R* Without Treatment (-) or Following 10 mM Hydroxyurea Treatment (+).** This experiment was performed as described in figure 4.12. A percentage value under a lane indicates the relative level of ubiquitinated *Sp*PCNA when unmodified PCNA is set to 100%, which was measured by quantification of bands on a low exposure using ImageJ (<http://rsb.info.nih.gov/ij/>). The lower panel indicates a lower exposure of the unmodified *Sp*PCNA band to indicate relative gel loading levels between lanes.

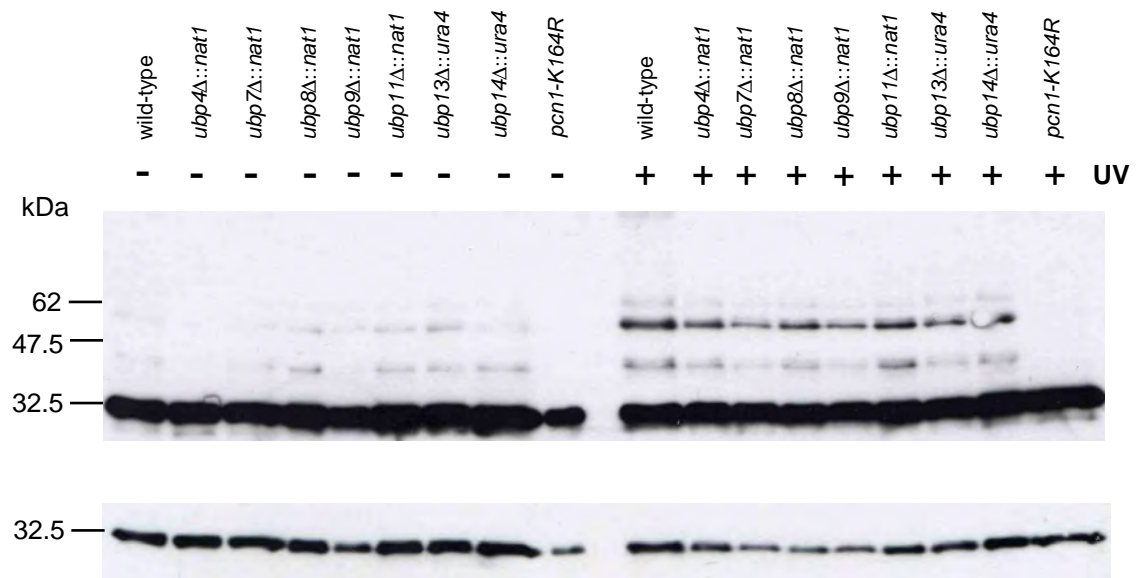


**Figure 4.17. Levels of *Sp*PCNA Ubiquitination in the *S. pombe* Strains wild-type, *ubp4Δ*, *ubp7Δ*, *ubp8Δ*, *ubp11Δ*, *ubp13Δ*, *ubp14Δ* and *pcn1-K164R* Following Mock Treatment (-) or UVC Treatment (+). As Figure 4.16.**



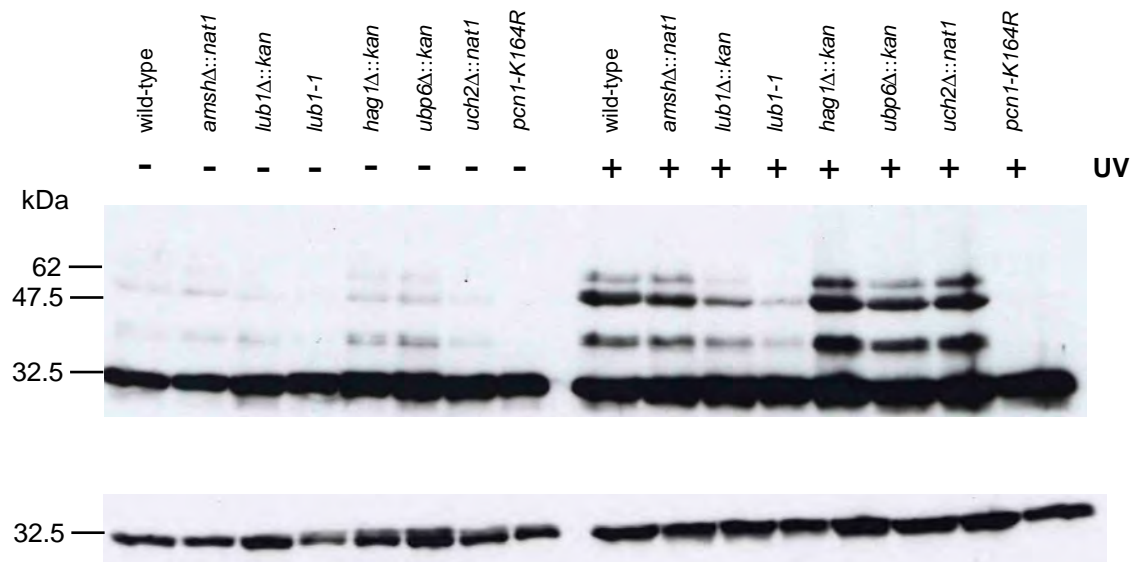


**Figure 4.18. Levels of *Sp*PCNA Ubiquitination in the *S. pombe* Strains wild-type, *amshΔ*, *lub1Δ*, *lub1-1*, *hag1Δ*, *ubp6Δ*, *uch2Δ* and *pcn1-K164R* Following Mock Treatment (-) or UVC Treatment (+).** The same number of cells of exponentially growing cultures were irradiated or mock irradiated with 50 Jm<sup>-2</sup> UVC, then size fractionated whole cell extracts were probed with anti-*Sp*PCNA antibodies. The lower panel indicates a lower exposure of the unmodified *Sp*PCNA band to indicate relative gel loading levels between lanes.

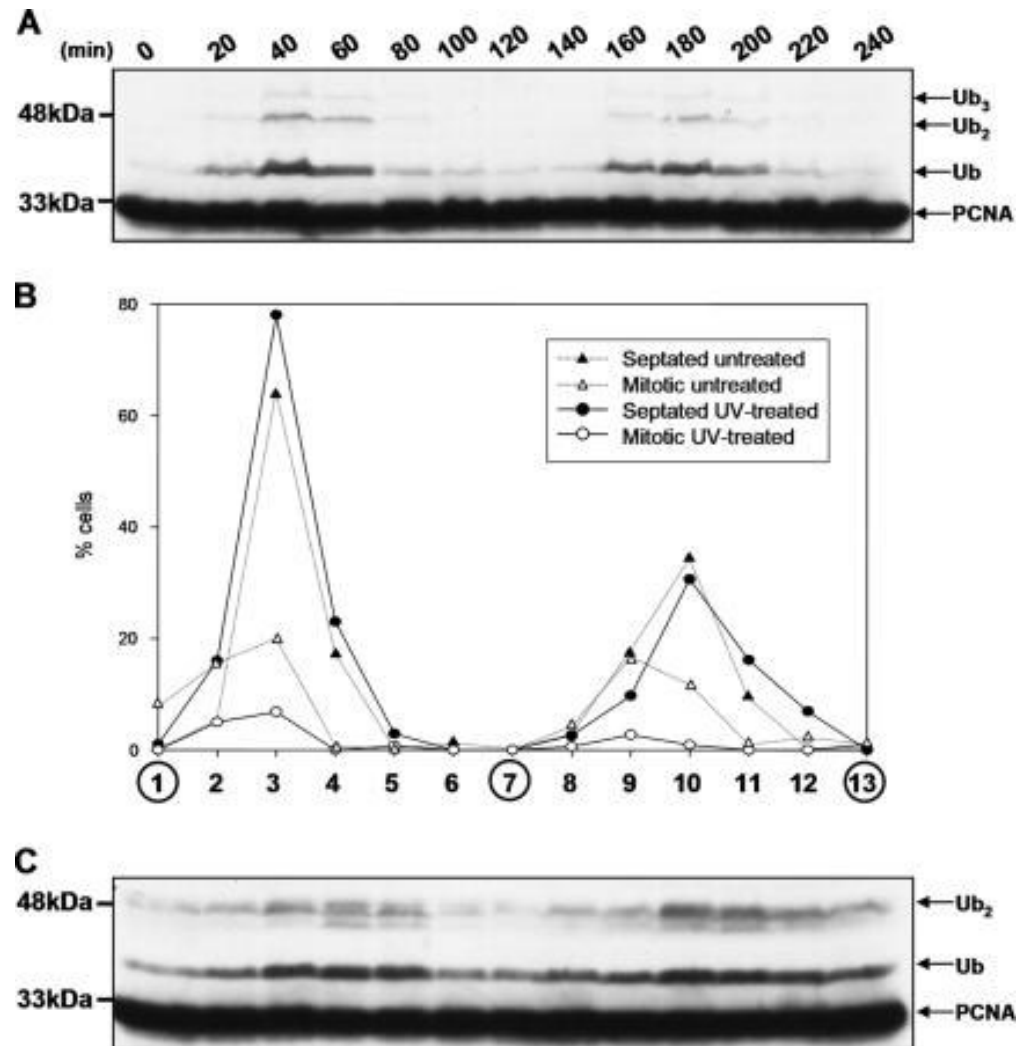


**Figure 4.19. Levels of *Sp*PCNA Ubiquitination in Wild-type *S. pombe* Cells During the Cell Cycle.** (A) shows samples from mock treated cells and (C) from UV irradiated cells (50 Jm<sup>-2</sup>). Cell cycle position was measured by mitotic or septation index. Septation occurs in early S-phase. Figure from Frampton *et al*, 2006.

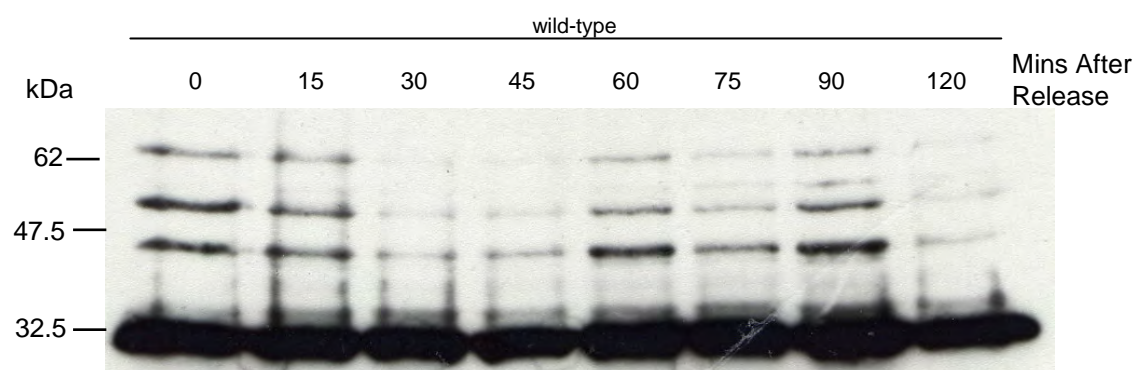


**Figure 4.20. Levels of *Sp*PCNA Ubiquitination Prior to and Following Cell Cycle Block in S-phase in wild-type *S. pombe* cells.** Exponentially growing cultures were treated with 10 mM hydroxyurea for 2.5 hrs and then released into fresh media. Samples were taken every 15 mins following release from HU. Size fractionated whole cell extracts were probed with anti-*Sp*PCNA antibodies.

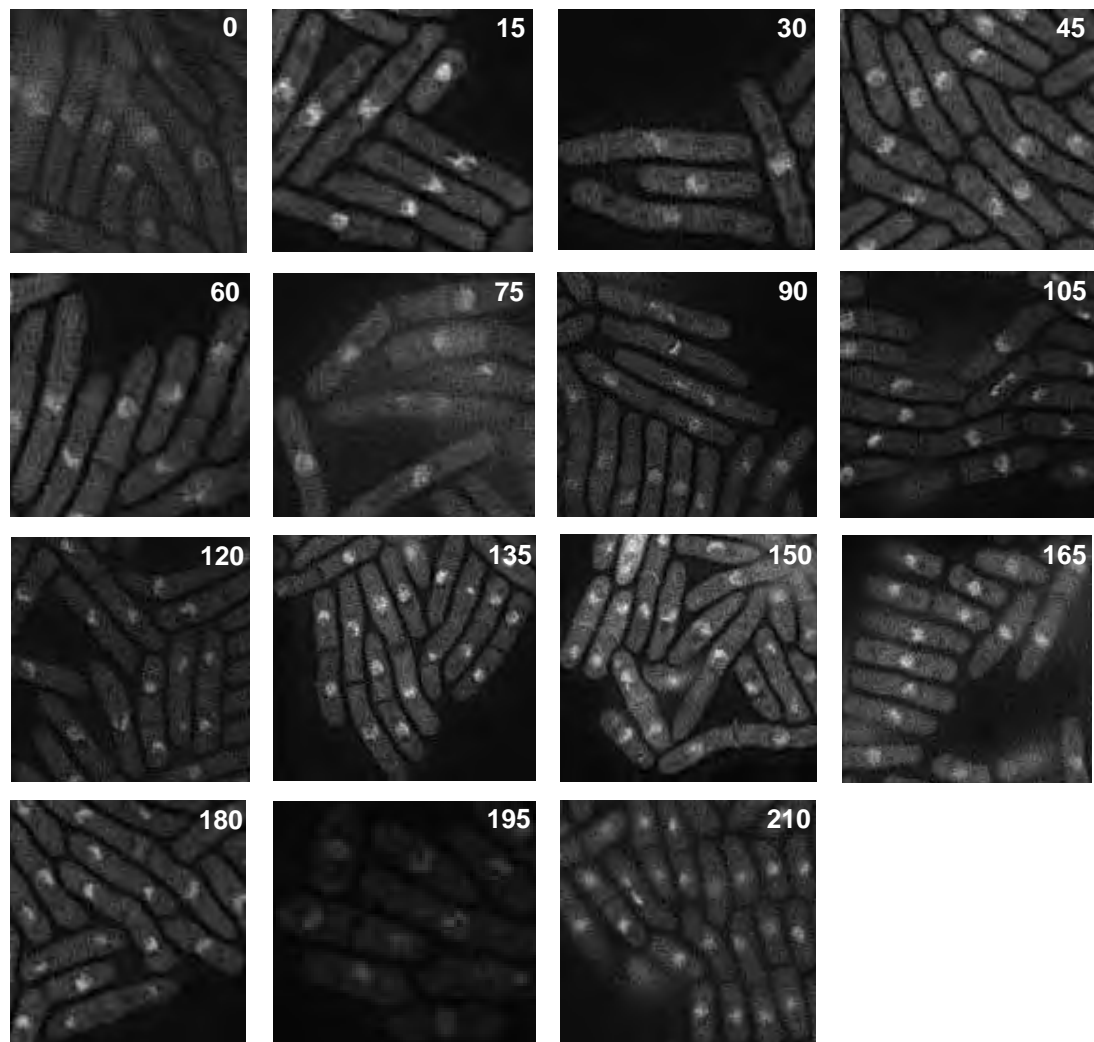


**Figure 4.21. Cell Cytology Following Cell Cycle Block in S-phase in Wild-type *S. pombe* Cells.** Exponentially growing cultures were treated with 10 mM hydroxyurea for 2.5 hrs and then released into fresh media. Samples were taken every 15 mins following release from HU as labels indicate. Cells were stained with DAPI and calcofluor and photographs taken under the fluorescent microscope.

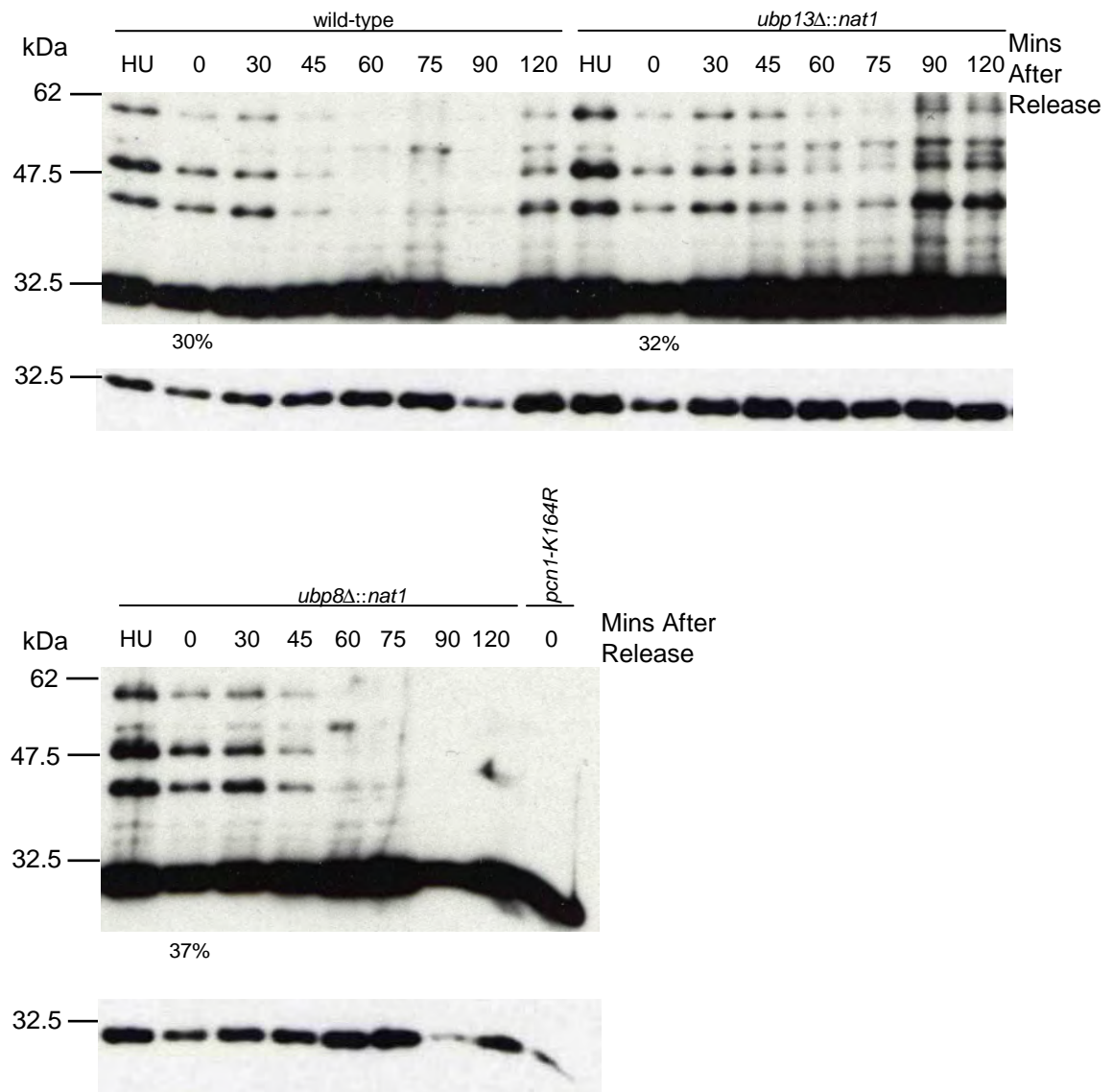


**Figure 4.22. Levels of *Sp*PCNA Ubiquitination Following Cell Cycle Block in S-phase in the *S. pombe* Strains Wild-type, *ubp13Δ::nat1*, *ubp8Δ::nat1*, and *pcn1-K164R*.** The same number of cells of exponentially growing cultures were treated with 10 mM hydroxyurea for 2.5 hrs and then released into fresh media. Samples were taken after treatment (HU) and then approximately every 15 mins following release from HU. Size fractionated whole cell extracts were probed with anti-*Sp*PCNA antibodies. A percentage value under a lane indicates the relative level of ubiquitinated *Sp*PCNA when unmodified PCNA is set to 100%, which was measured by quantification of bands on a low exposure using ImageJ (<http://rsb.info.nih.gov/ij/>). The lower panel indicates a lower exposure of the unmodified *Sp*PCNA band to indicate relative gel loading levels between lanes. The complete version of this gel is shown in Figure 5.18.

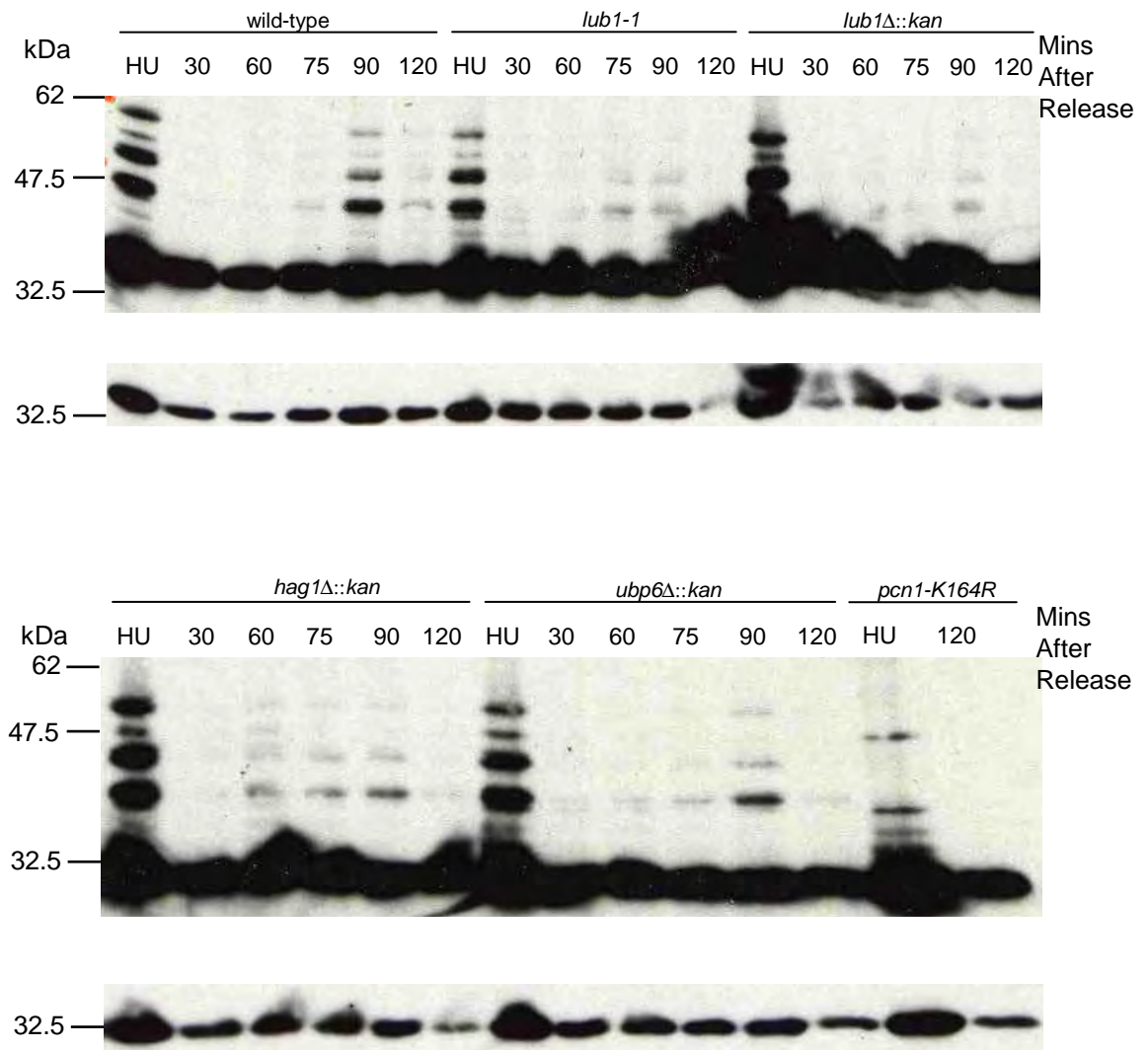


**Figure 4.23. Levels of *Sp*PCNA Ubiquitination Following Cell Cycle Block in S-phase in the *S. pombe* Strains wild-type, *lub1-1*, *lub1Δ::kan*, *hag1Δ::kan*, *ubp6Δ::kan* and *pcn1-K164R*.** This experiment was carried out as described in figure 4.22.

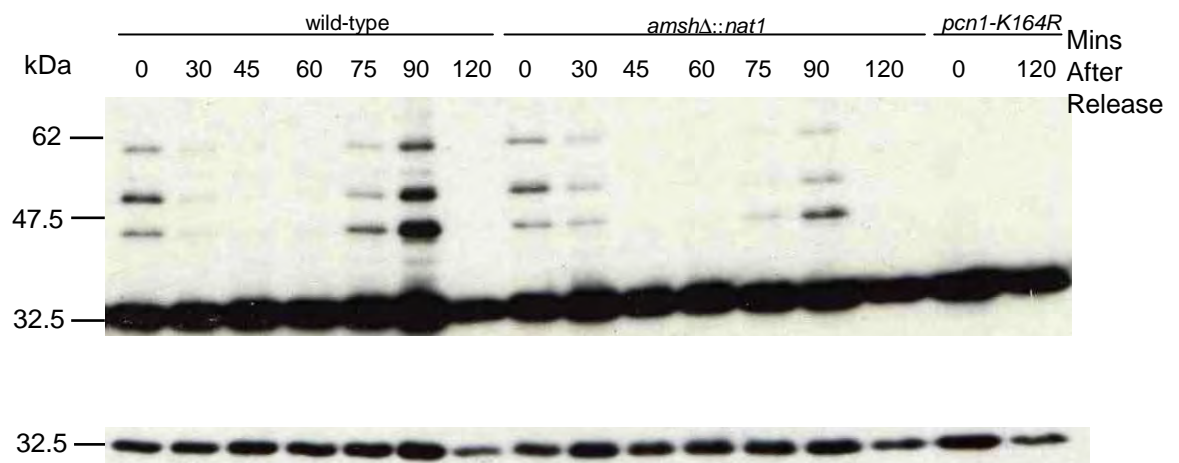


**Figure 4.24. Levels of *Sp*PCNA Ubiquitination Prior to and Following Cell Cycle Block in S-phase in the *S. pombe* Strains wild-type, *amshΔ::nat1*, and *pcn1-K164R*.** This experiment was carried out as described in figure 4.22.

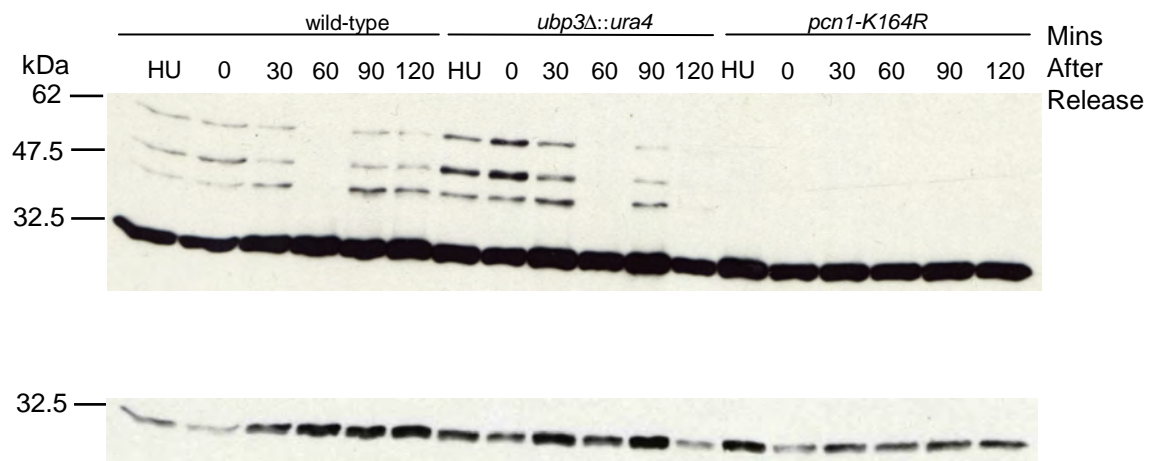


**Figure 4.25. Levels of *Sp*PCNA Ubiquitination Prior to and Following Cell Cycle Block in S-phase in the *S. pombe* Strains wild-type, *ubp3Δ::ura4*, and *pcn1-K164R*.** This experiment was carried out as described in figure 4.22.



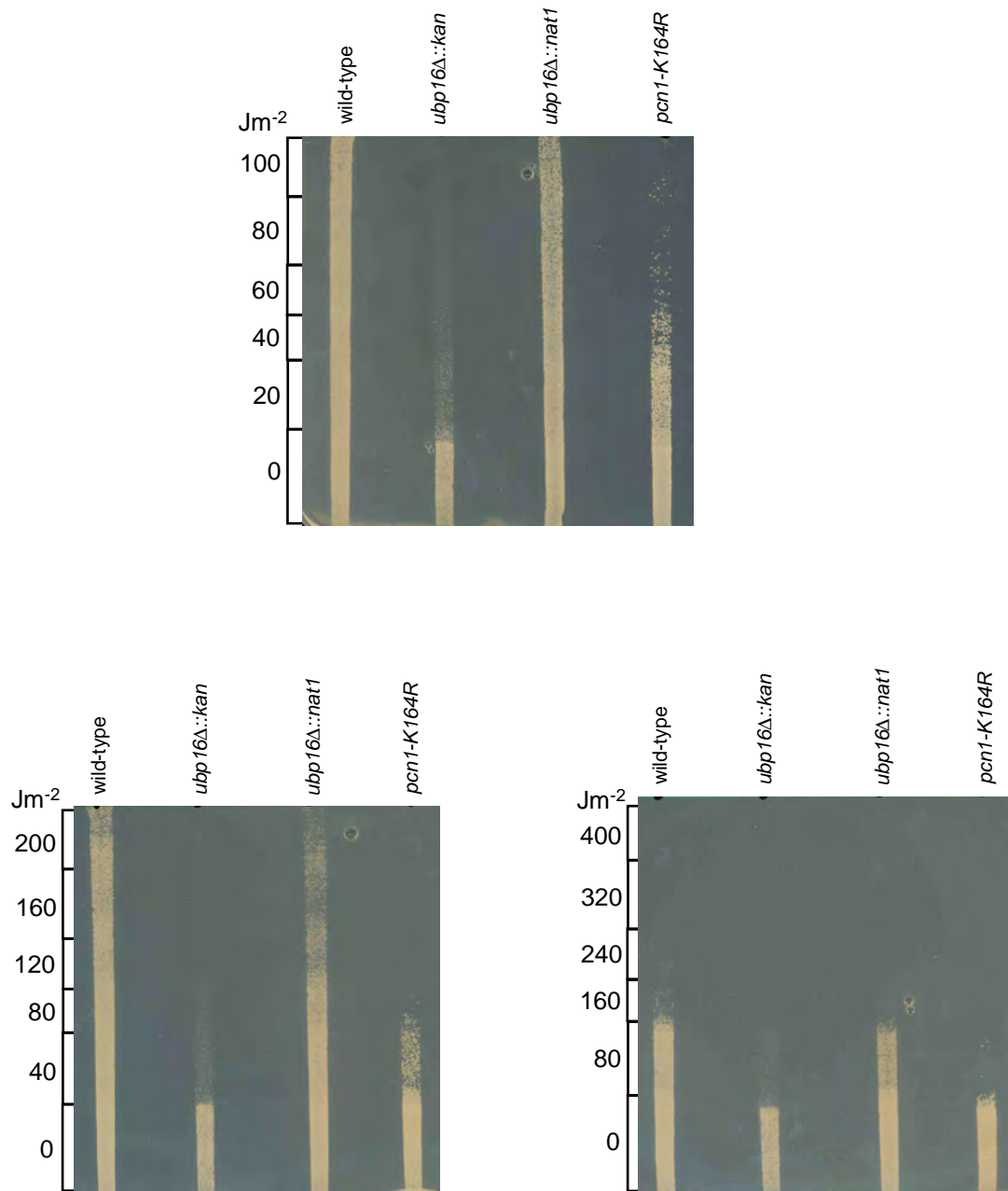


**Figure 4.26. Drop Test Assays Measuring the Relative Sensitivities of *S. pombe* Strains wild-type, *ubp16Δ::kan*, *ubp16Δ::nat1*, and *pcn1-K164R* to Different Doses of UVC.** Exponentially growing cultures were normalised by cell concentration and dropped down YEA agar plates, which were subsequently exposed to a UVC gradient as indicated. Plates were grown for three days at 30°C before photographing.

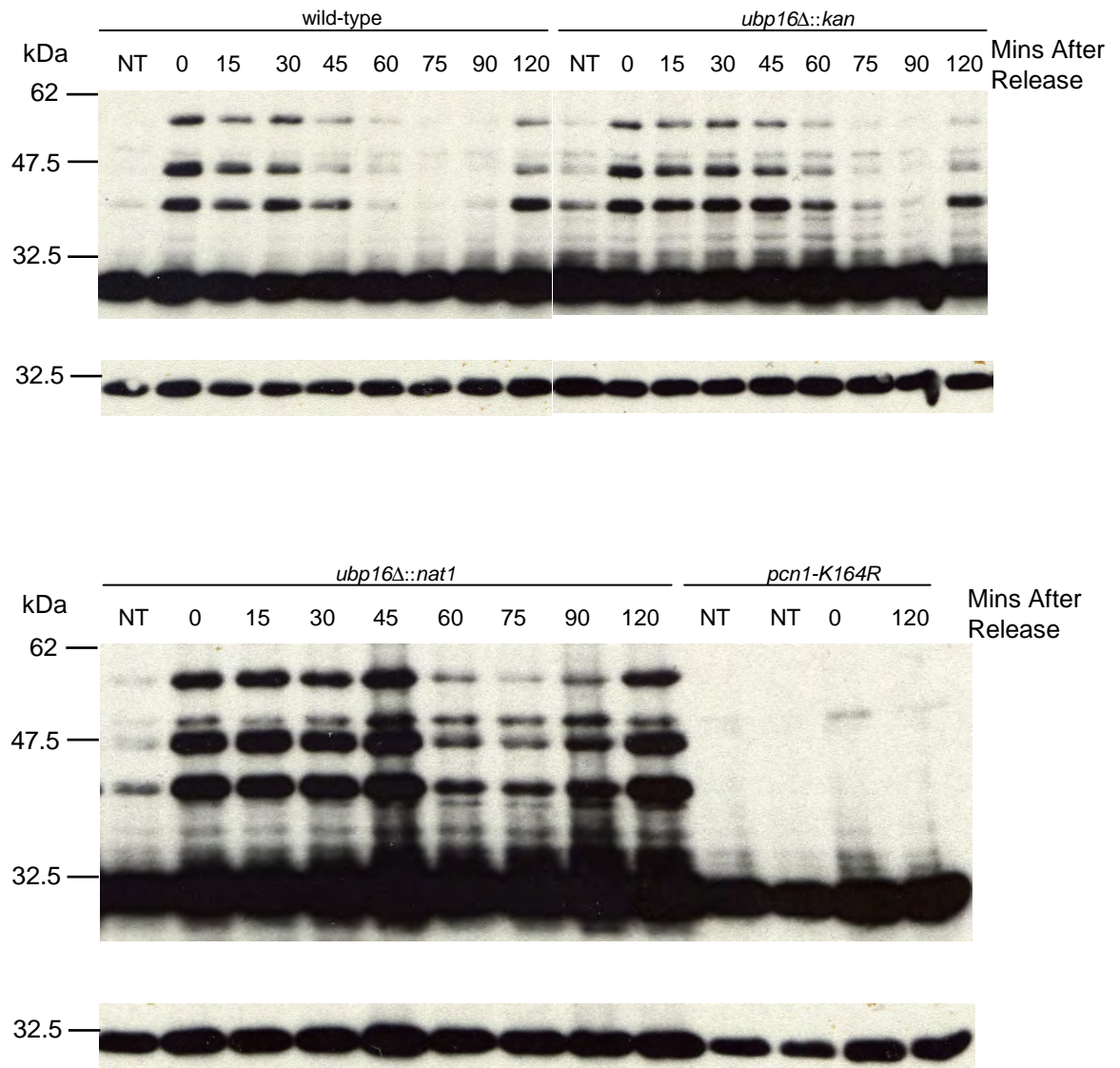


**Figure 4.27. Levels of *Sp*PCNA Ubiquitination Prior to and Following Cell Cycle Block in S-phase in the *S. pombe* Strains wild-type, *ubp16Δ::kan*, *ubp16Δ::nat1*, and *pcn1-K164R*.** This experiment was carried out as described in figure 4.22.

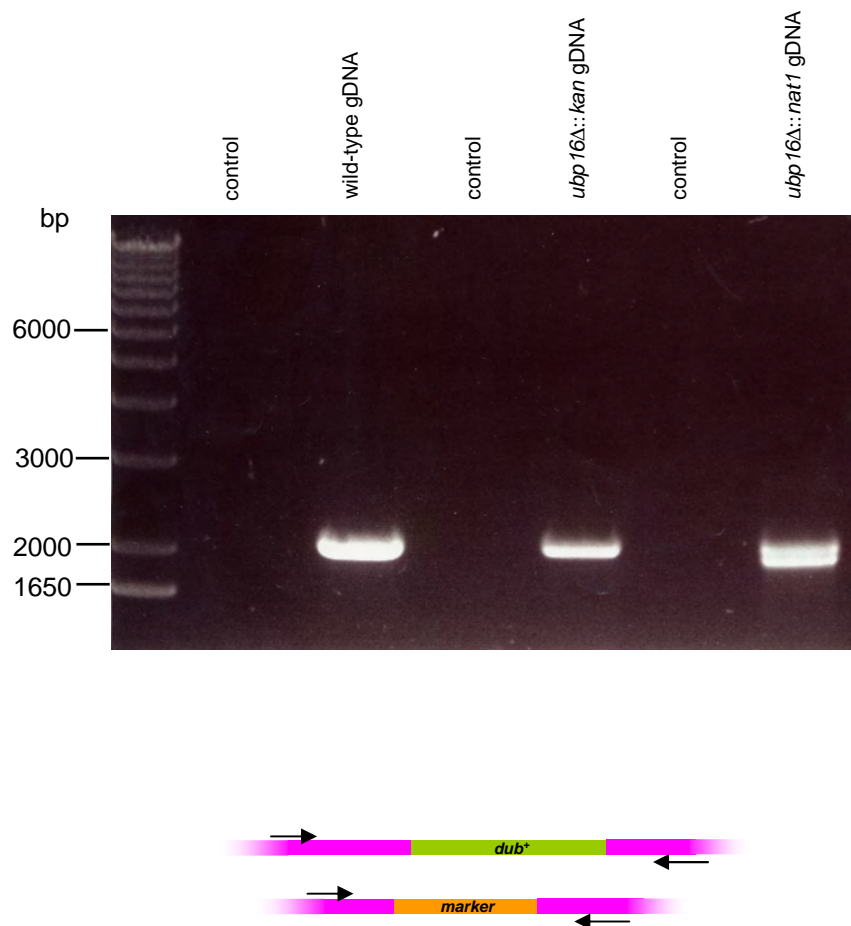


**Figure 4.28. PCR Amplification of the *ubp16* Locus Utilising Primers that Anneal to Flanking DNA.** Using genomic DNA from of the *S. pombe* strains wild-type, *ubp16*Δ::*kan* and *ubp16*Δ::*nat1*. The control lanes indicate PCR reactions where water was added in place of genomic DNA. The lower diagram shows the PCR strategy in wild-type gDNA and *dub*-deleted gDNA. Primers that flank the DUB gene locus are depicted by arrows.

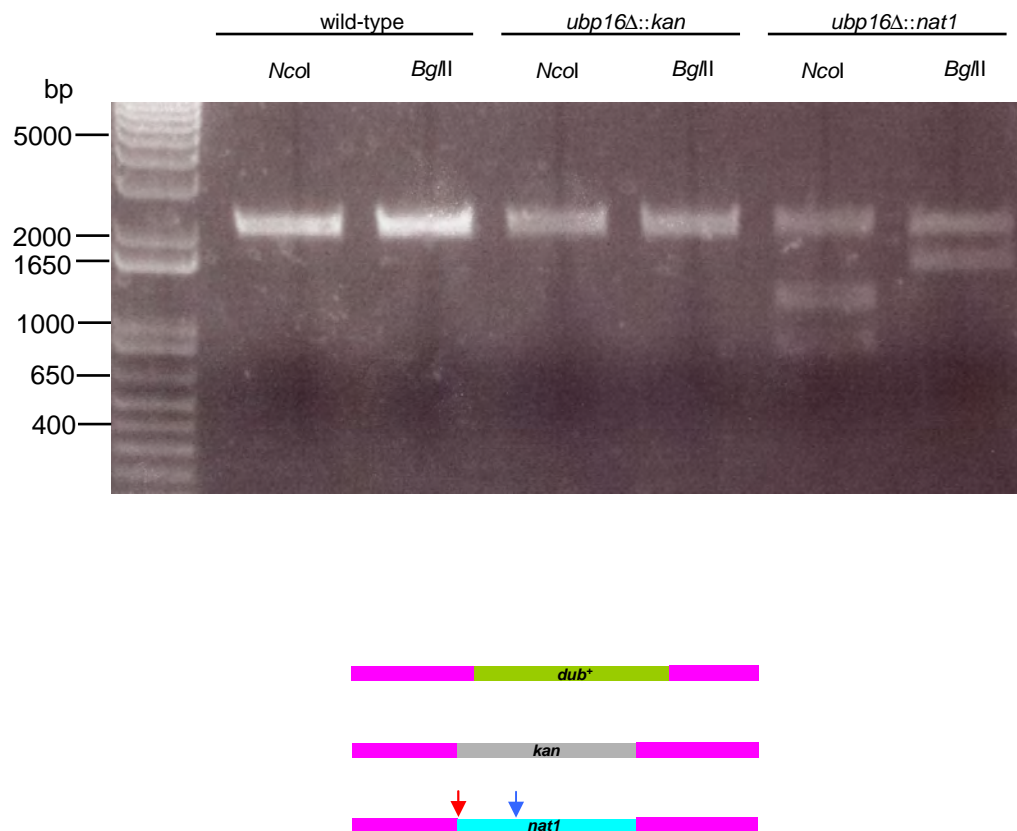


**Figure 4.29. Digestion of PCR Products Obtained from Amplification of the *ubp16* Locus.** Using genomic DNA from of the *S. pombe* strains wild-type, *ubp16Δ::kan* and *ubp16Δ::nat1*. Digestion of PCR products shown in figure 4.28 with *NcoI* and *BglII*, the location of the restriction sites of which are shown in the lower diagram with blue and red arrows, respectively.

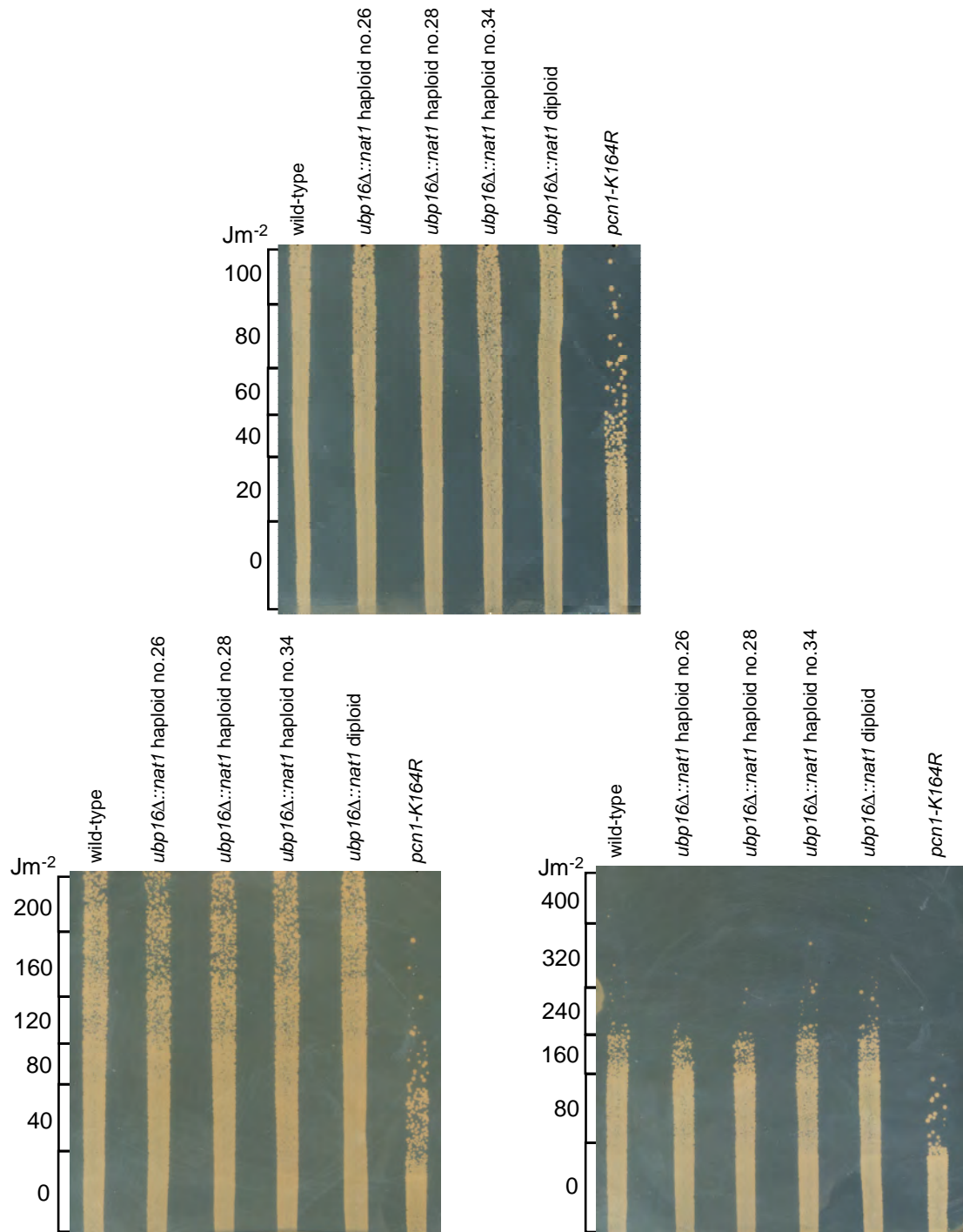


**Figure 4.30. Drop Test Assays Measuring the Relative Sensitivities to Different Doses of UVC of Different *S. pombe* *ubp16Δ::nat1* Haploid Clones Compared to wild-type, *ubp16Δ::nat1* Diploid and *pcn1-K164R*.** Exponentially growing cultures were normalised by cell concentration and dropped down YEA agar plates, which were subsequently exposed to a UVC dose gradient as indicated. Plates were grown for three days at 30°C before photographing.

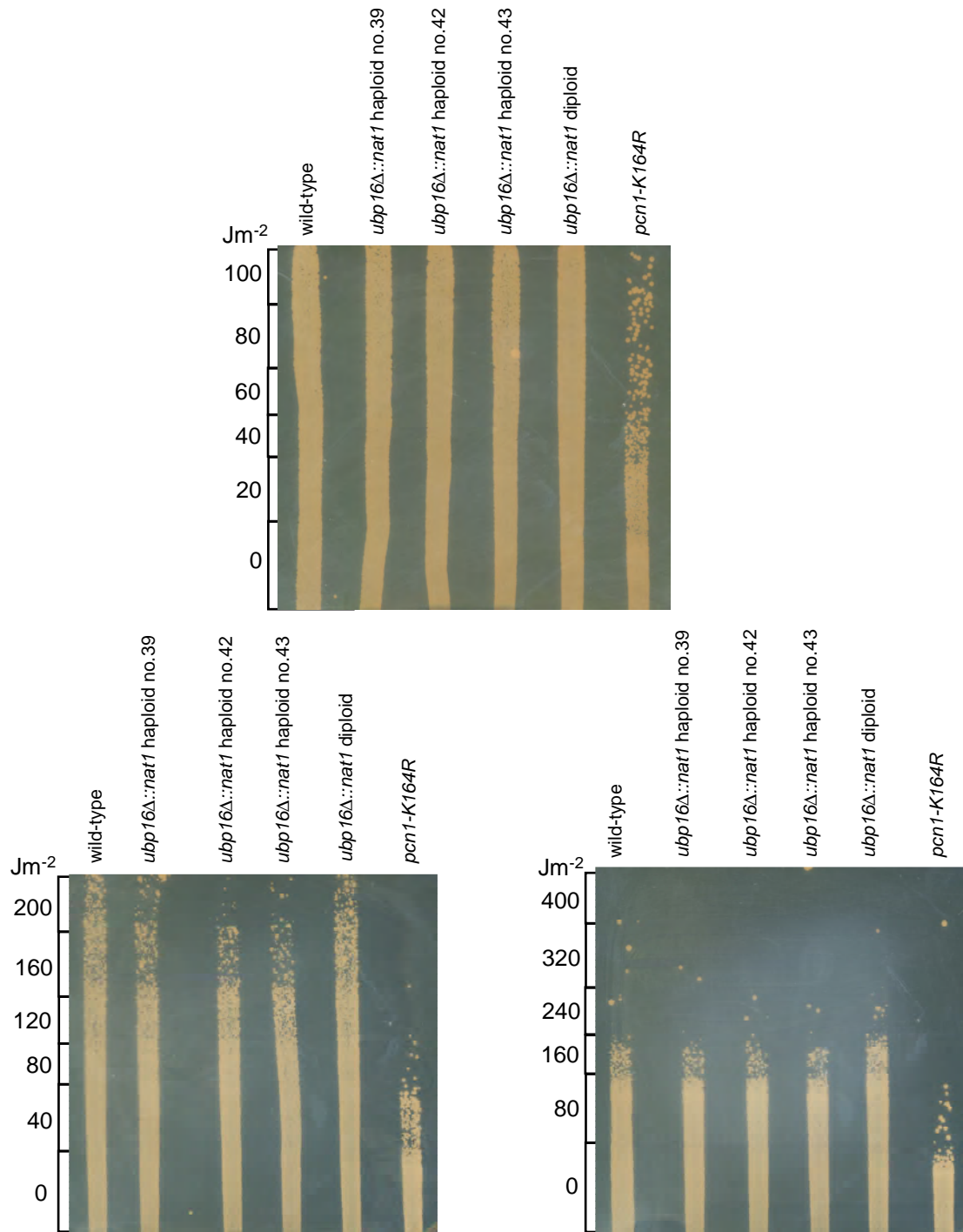


**Figure 4.31. Drop Test Assays Measuring the Relative Sensitivities to Different Doses of UVC of Different *S. pombe* *ubp16Δ::nat1* Haploid Clones Compared to wild-type, *ubp16Δ::nat1* Diploid and *pcn1-K164R*.** This experiment was carried out as described in figure 4.30.

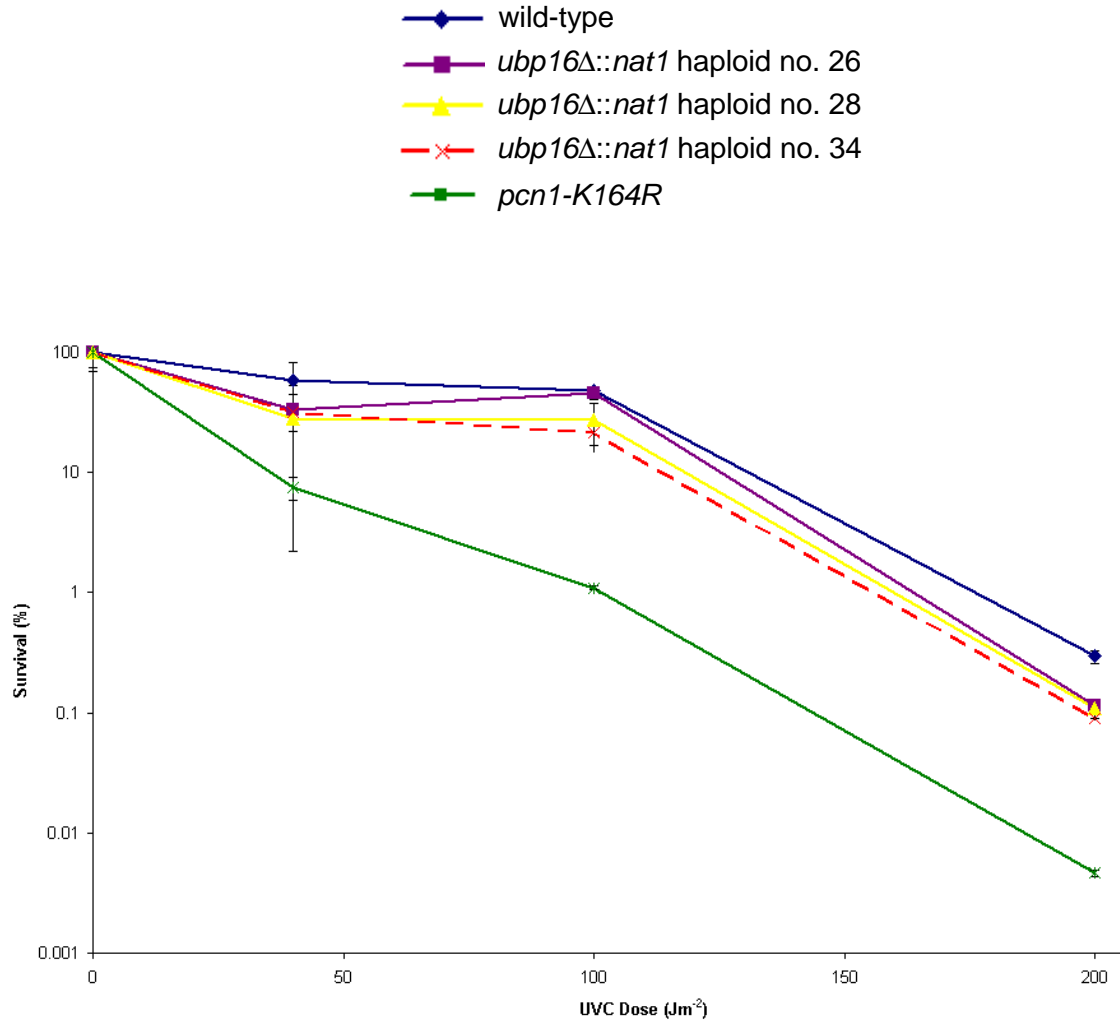


**Figure 4.32. Colony Forming Assay Measuring the Percentage Survival Following UVC Irradiation.** Haploids 26, 28 and 34 with the genotype *ubp16Δ::nat1* were compared with wild-type and *pcn1-K164R*. Exponentially growing cultures were plated onto YEA agar, which were exposed to the UVC doses indicated. Plates were grown for three days at 30°C before counting. The results represent the mean of replicates and the error bars represent the standard deviation.

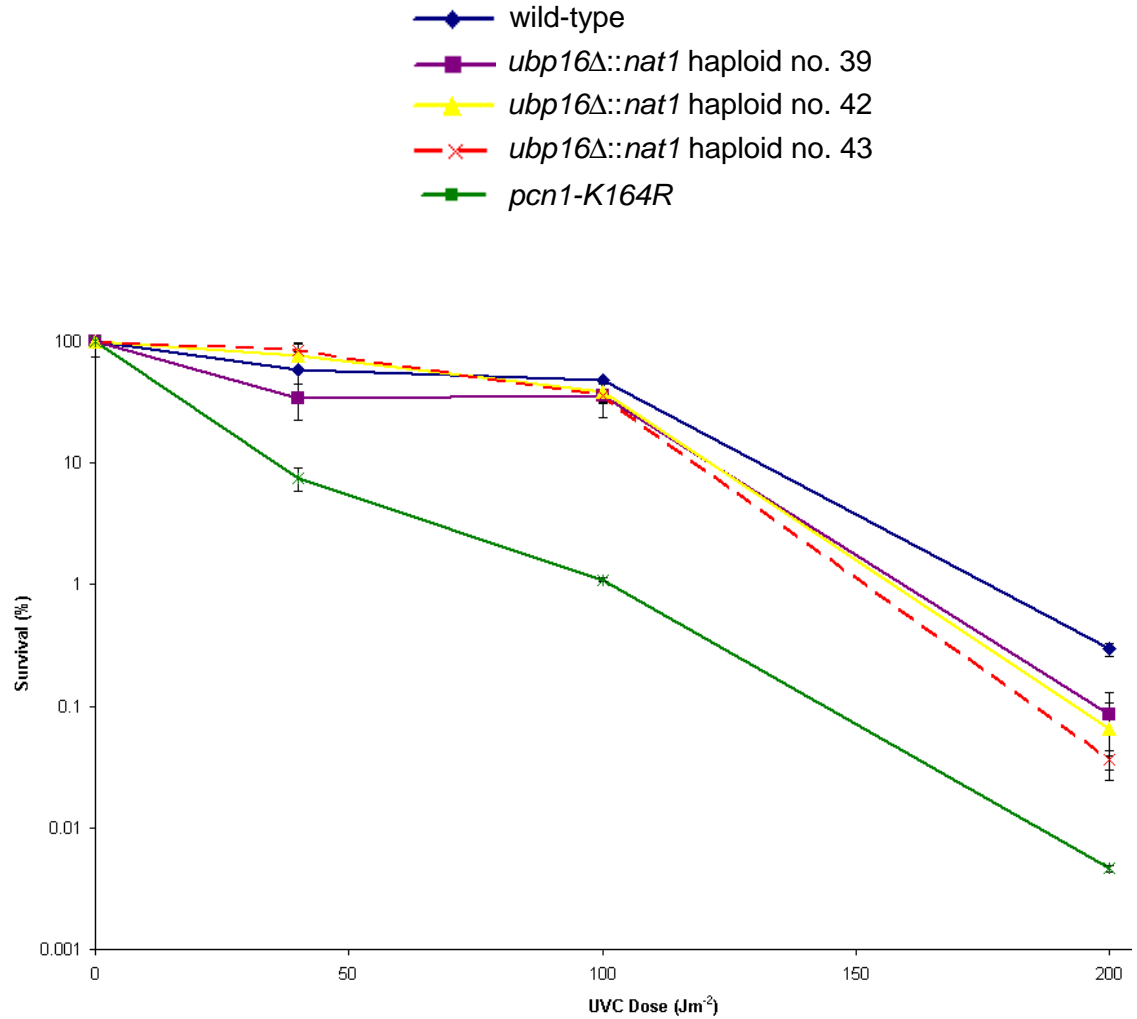


**Figure 4.33. Colony Forming Assay Measuring the Percentage Survival Following UVC Irradiation.** Haploids 39, 42 and 43 with the genotype *ubp16Δ::nat1* were compared with wild-type and *pcn1-K164R*. This experiment was carried out as described in figure 4.32.



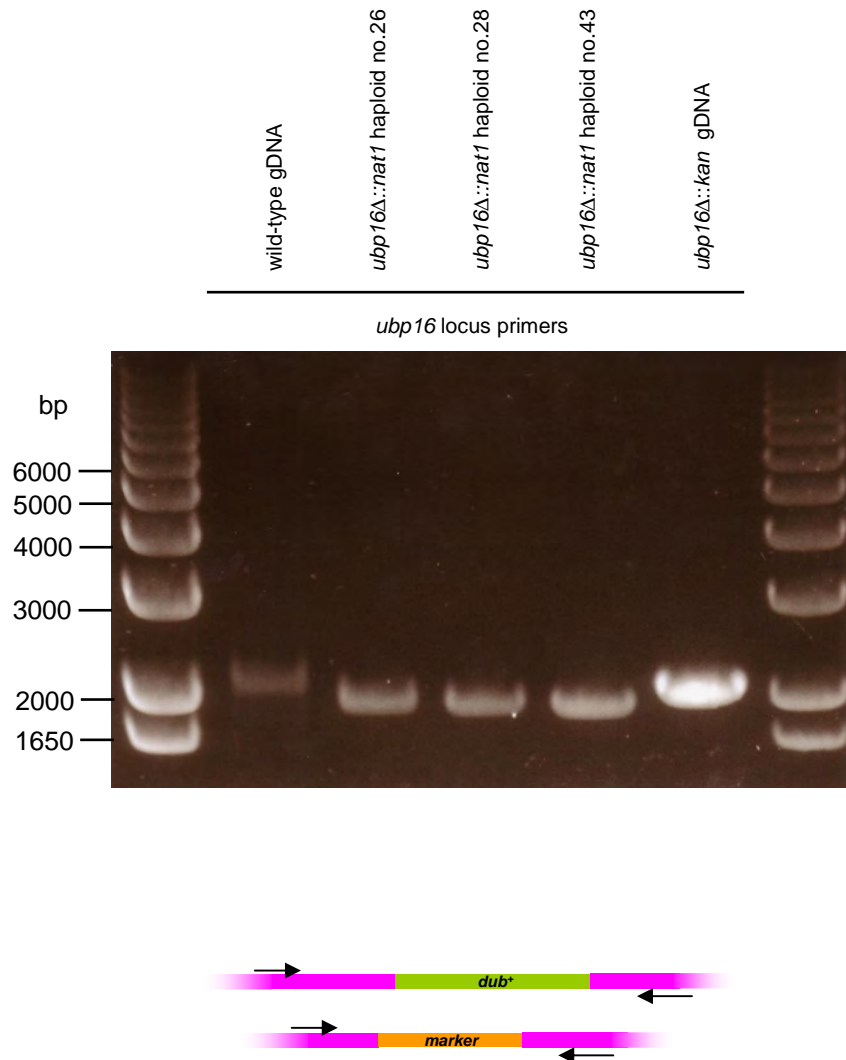


**Figure 4.34. PCR Amplification of the *ubp16* Locus Utilising Primers that Anneal to Flanking DNA.** Using genomic DNA from of the *S. pombe* strains wild-type, *ubp16Δ::nat1* diploid, *ubp16Δ::nat1* haploid clones 26, 28 and 43, and *ubp16Δ::kan*. Amplification of the *ubp16* locus in clones 26, 28 and 43 results in DNA with higher mobility than wild-type and *ubp16Δ::kan*. The lower diagram shows the PCR strategy in wild-type gDNA and *dub*-deleted gDNA. Primers that flank the *DUb* gene locus are depicted by arrows.

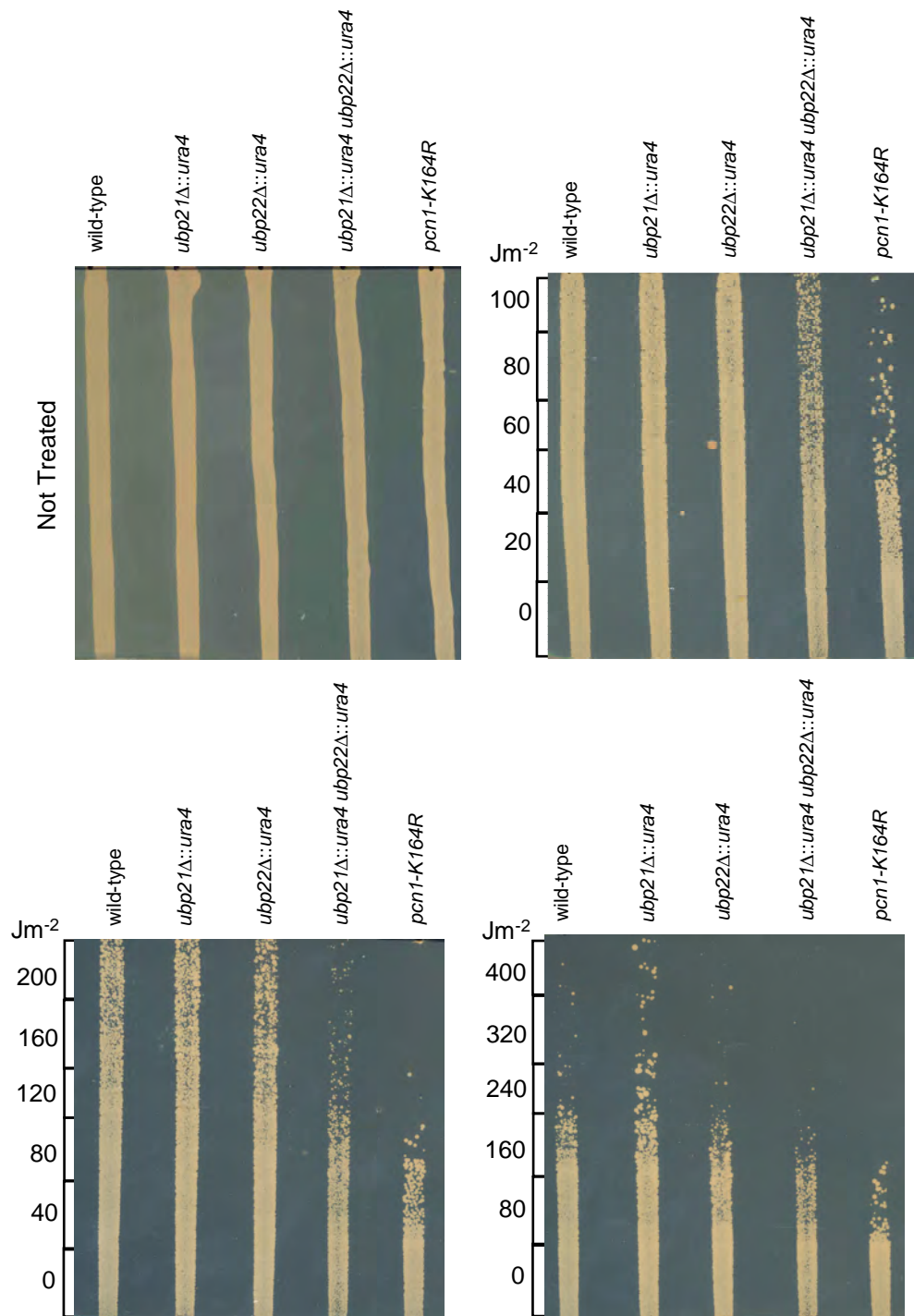


**Figure 5.1. Drop Test Assays Measuring the Relative Sensitivities of *S. pombe* Strains wild-type, *ubp21Δ*, *ubp22Δ*, *ubp21Δ ubp22Δ*, and *pcn1-K164R* to Different Doses of UVC.** Exponentially growing cultures were normalised by cell concentration and dropped down YEA plates, which were subsequently exposed to a UVC dose gradient as indicated. Plates were grown for three days at 30°C before photographing. The “Not Treated” experiment was performed by a summer research student Sonoko Oshima.

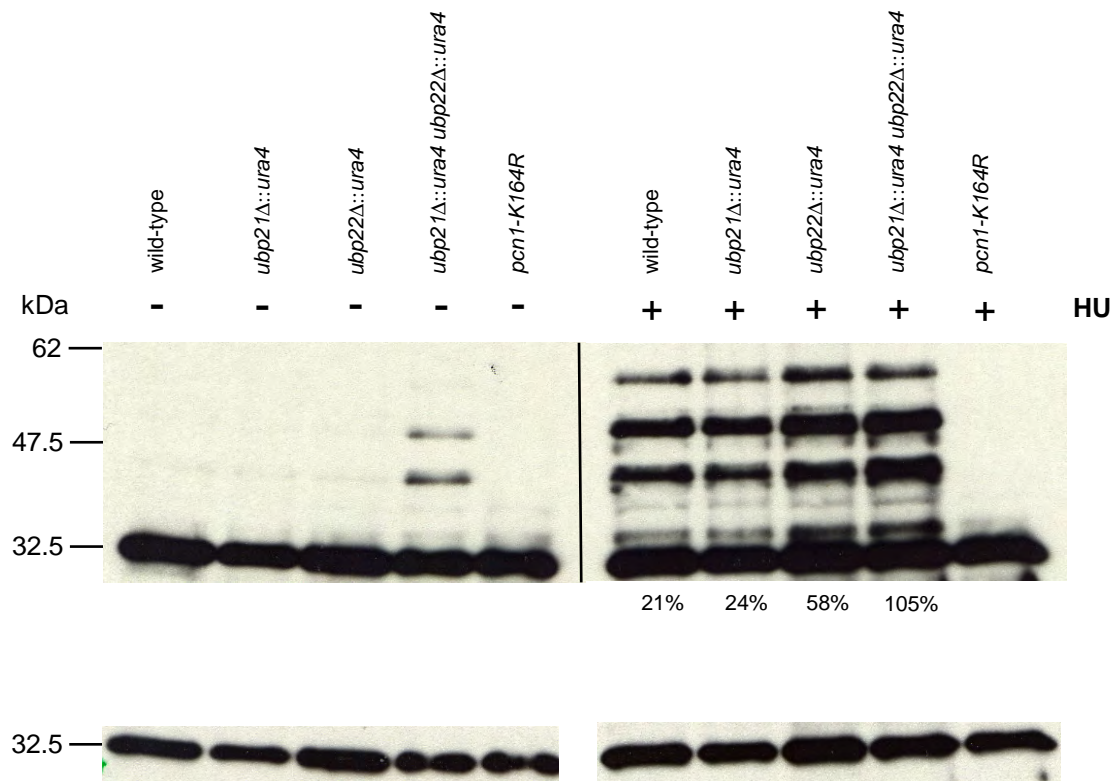


**Figure 5.2. Levels of *Sp*PCNA Ubiquitination in the *S. pombe* Strains wild-type, *ubp21Δ::ura4*, *ubp22Δ::ura4*, *ubp21Δ::ura4 ubp22Δ::ura4* and *pcn1-K164R* Without Treatment (-) or Following Hydroxyurea Treatment (+).** The same number of cells of exponentially growing cultures were left untreated or treated with 10 mM HU, then size fractionated whole cell extracts were probed with anti-*Sp*PCNA antibodies. A percentage value under a lane indicates the relative level of ubiquitinated *Sp*PCNA when unmodified PCNA is set to 100%, which was measured by quantification of bands on a low exposure using ImageJ (<http://rsb.info.nih.gov/ij/>). The lower panel indicates a lower exposure of the unmodified *Sp*PCNA band to indicate relative sample loading levels between lanes.

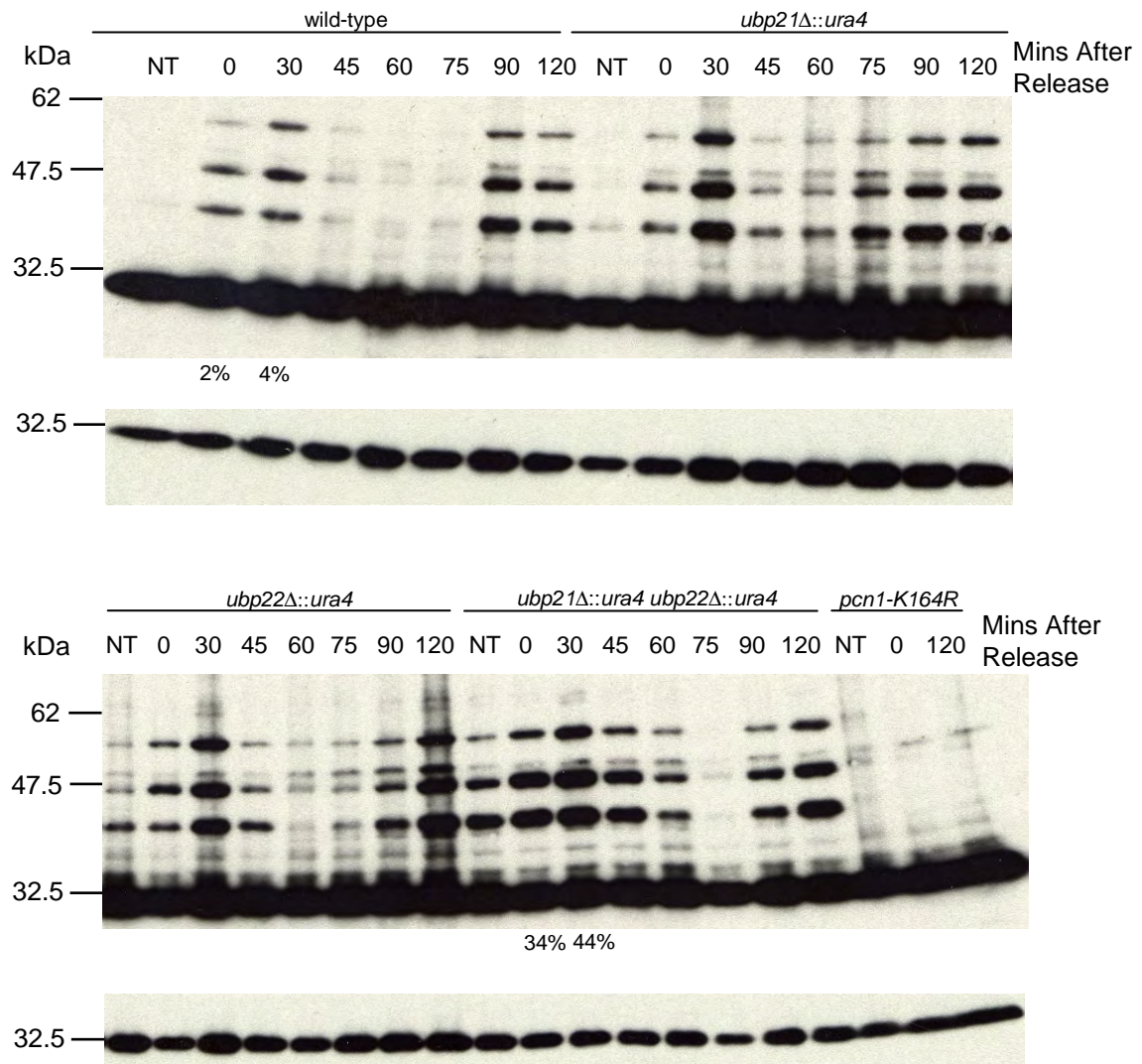


**Figure 5.3. Levels of *Sp*PCNA Ubiquitination Prior to and Following Cell Cycle Block in S-phase in the *S. pombe* Strains wild-type, *ubp21Δ::ura4*, *ubp22Δ::ura4*, *ubp21Δ::ura4 ubp22Δ::ura4*, and *pcn1-K164R*.** The same number of cells of exponentially growing cultures were treated with 10 mM hydroxyurea for 2.5 hrs and then released into fresh media. Samples were taken prior to treatment (NT) and every 15 mins following release from HU. Size fractionated whole cell extracts were probed with anti-*Sp*PCNA antibodies. A percentage value under a lane indicates the relative level of ubiquitinated *Sp*PCNA when unmodified PCNA is set to 100%, which was measured by quantification of bands on a low exposure using ImageJ (<http://rsb.info.nih.gov/ij/>). The lower panel indicates a lower exposure of the unmodified *Sp*PCNA band to indicate relative sample loading levels between lanes.

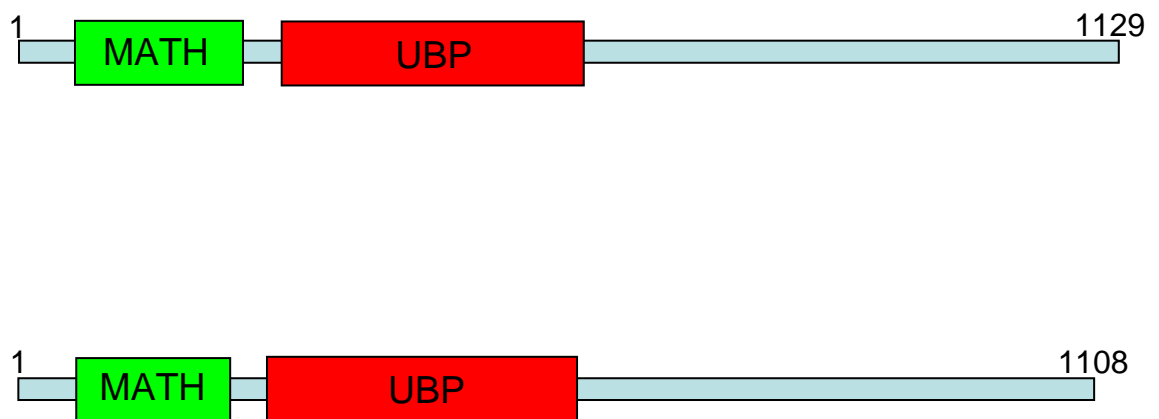


**Figure 5.4. Domain Structures of the *S. pombe* DUBs (A) *SpUbp21* and (B) *SpUbp22*.** The green box depicts the position of the MATH domain and the red box shows the UBP/USP catalytic domain.



**Figure 5.5. EBI-CLUSTALW Alignment of the Amino Acid Sequence S.**

***pombe* DUBs *SpUbp22* and *SpUbp21*.** Amino acids 1-518 of *SpUbp22* and 1-535 of *SpUbp21* are shown. The second half of this alignment, depicting the C-terminal amino acids are shown in figure 5.6. The region boxed in light green shows the MATH domain and the region boxed in red shows the UBP/USP catalytic domain. Residues highlighted in yellow are conserved in the catalytic Cys and His boxes of UBP/USP DUBs, and those that function in the catalytic triad, in blue. Residues letters are coloured according to type. Acidic residues, Asp and Glu, are typed in blue; basic residues, Arg and Lys, pink; green residues, His, Asn, Gly, Tyr, Ser, Gln, Thr, are hydrophilic; and hydrophobic residues, Phe, Met, Ala, Leu, Iso, Pro, Trp, are typed in red. An asterisk indicates homologous residues; a colon indicates conservation with a highly similar residue; a dot, conservation with less similar residues; and no symbol indicates no conservation.





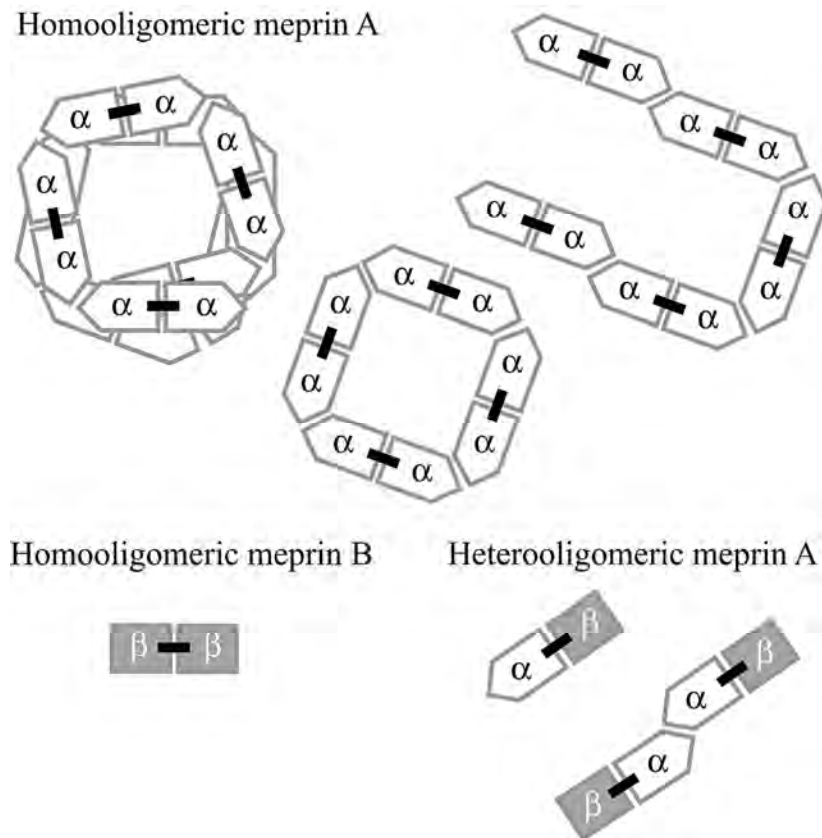


**Figure 5.7. Oligomerisation of  $\alpha$  and  $\beta$  Subunits to Form Rat Meprins.**  
 The MATH and MAM domains of meprin subunits are important for oligomerisation. Adapted from Bertenshaw *et al*, 2003.



```

ubp22      ----MVTGETLVDSQKSLINNDTLNEKLKED-----FEENVSIDVKIHEELRRAL 47
ubp21      ----MVLN--VDAEEVNMDSSMELEESSQEP-----LRADN--YEEIYNLSLVHHE 43
USP7_HUMAN MNHQQQQQQKAGEQQLSEPEDMEMEAGDTDDPPRITQNPVINGNVALSDGHMTAEEDME 60
           :  . . : :  . . : :  :  :  :  :  :

ubp22      PDYEE SCFQRFTWHIKSWHELDRAVSPQFAVGSRQFKITYFPQGTLSAGFTSIFLEYI 107
ubp21      PDLEEAAHASYWVVKNFSTLEDKTYSPLFKAGHTTWRIVLFPKGCNQTE-YASVFLEYL 102
USP7_HUMAN DDTSWRSEATFQFTVERFSRLSESVLSPPCFVRNLPWKIMVMRPFYPDRPHQKSVGFFLQ 120
           * . . : : : : * . ** . : : * : : : * : :

ubp22      PSEEEKLSN-----KYGCCQFAFVISNPRKPSLSVANSACHCR 145
ubp21      PQCKVEAIRKYEAEALAGKTPTIDPEIVNDETYSCCAQFALSLSNVQDPTVMQINTSHHR 162
USP7_HUMAN CNAESDSTS-----WSCHAQAVLKIINYRDDEKSFSSRRISHL 157
           . : . : : : : : : : : : : :

ubp22      FSPEIVDWGFTQFAELKKLLCRQAPDVPIVEDGALLLTAYVRLLKDP TGVLWHSFNDYD 205
ubp21      FRSEVKDWGFTRFVDLRKIAVPTPEFPVPFLENDEICISVTVRVLQDPTGVLWHSFVNYN 222
USP7_HUMAN FFHKENDWGFSNFMAWSEVTDPE---KGFIDDDKVTFEV FVQADAPHG-----VAWD 206
           * : * : : : * : : : : : : : : : : : :

ubp22      SKIATGYVGLKNQCATCYMNSLLQSLYIIHAFRRIVYQIPTDSPQCKDSIAYALQRCFYN 265
ubp21      SKKETGYVGLKNQCATCYMNSLLQSLFFTNIFRKT VYKIPTDNDSDS VAYALQRVFYN 282
USP7_HUMAN SKKHTGYVGLKNQCATCYMNSLLQTLFFTNQLRKAVYMMPTGDDSSKSVPLALQRVFYE 266
           ** * : : : : : : : : : : : : : : : : : : : : : :

ubp22      LQFMNEPVSTTELTKSFGWDSLDSFMQHDVQEFNRVLQDNLEKSMRDTKVENALTNLFVG 325
ubp21      LEKQREPVSTTELTRSGFWSFDSFMQHDIQEFNRVLQDNLEKMKGTVEENALNDIFVG 342
USP7_HUMAN LQHSDEKPVGTRKLTKSFGWETLDSFMQHDVQELCRVLLDNVENKMKGTCEGTIPKLFRG 326
           * : : : : * : : : : : : : : : : : : : : : : :

ubp22      KMKSYIACVNVNFESARSEDYWDIQLNVKGMKNLEDSFRSYIQVETLEGDNCFADTYGF 385
ubp21      KMKSYVKCIDVNYESSRVEDFWDIQLNVKGMDTLEDSEFRDAIQVETLTGDNKYAEGHGL 402
USP7_HUMAN KMVSYIQCKEVDYRSRRREDYYDIQLSIRGKKNIFSFVDYVAVEQLDGDNKYDAGEHGL 386
           ** * : : * : : : * : : : : : : : : : : : : : : : : :

ubp22      QEAKGVIFESFPPIHLHLQLKRFYDFERDMMIKINDRYEFPLEFDAKAFLSPEADQSQN 445
ubp21      QDAHKGIFESLPNVLQLQLKRFDYDMLRDMVKINDRHEFPLEIDLEPYLSETADKSES 462
USP7_HUMAN QEAEKGVKFLTLPPVLHLQLMRFYDPQTDQNIKINDRFEFPEQLPLDEFLQKTDPK-DP 445
           * : : * : : : : : : : * : : : : : : : : : : : : : : :

```

DUb 1	DUb 2	Score
<i>Hs</i> HAUSP <sup>USP7</sup>	<i>Sp</i> Ubp22	29
<i>Hs</i> HAUSP <sup>USP7</sup>	<i>Sp</i> Ubp21	31
<i>Sp</i> Ubp22	<i>Sp</i> Ubp21	40

**Figure 5.8. EBI-CLUSTALW Alignment of the Amino Acid Sequence *Sp*Ubp22 and *Sp*Ubp21 with *Hs*HAUSP<sup>USP7</sup>.** Amino acids 1-445 of *Sp*Ubp22, 1-462 of *Sp*Ubp21, and 1-445 of HAUSP<sup>USP7</sup> are shown. The second portion of this alignment, depicting the C-terminal amino acids, is shown in figure 5.9. The residue colouring, boxed regions and conservation symbols utilised in this alignment are described in figure 5.4. In addition, blue squares indicate residues that, when mutated, were shown to abolish DUb activity on K48-linked di-ubiquitin (Hu *et al*, 2002). The table underneath shows the percentage identity (score) of pairwise comparisons.



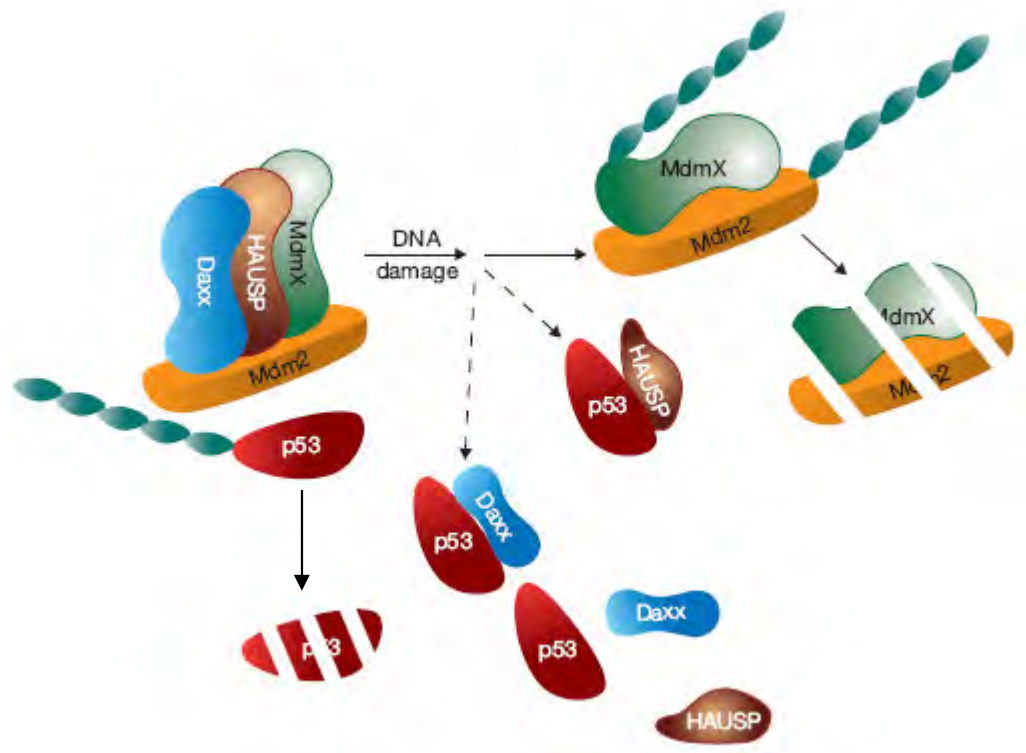


**Figure 5.10. Association of *Hs*MDM2 with *Hs*DAXX, *Hs*HAUSP<sup>USP7</sup> and *Hs*MDMX to induce *Hs*MDM2 destabilisation of *Hs*p53.** In unstressed cells, *Hs*DAXX, *Hs*HAUSP<sup>USP7</sup> and *Hs*MDMX prevent *Hs*MDM2 from ubiquitinating itself and direct it to ubiquitinate *Hs*p53 instead, which results in *Hs*p53 degradation. Following DNA damage and possibly *Hs*ATM-mediated phosphorylation, the complex breaks apart. *Hs*MDM2 and *Hs*MDMX switch to auto-ubiquitination mode. *Hs*p53 may or may not associate with *Hs*DAXX or may be stabilised by the deubiquitinating activity of *Hs*HAUSP<sup>USP7</sup>. Adapted from Ronai, 2006.

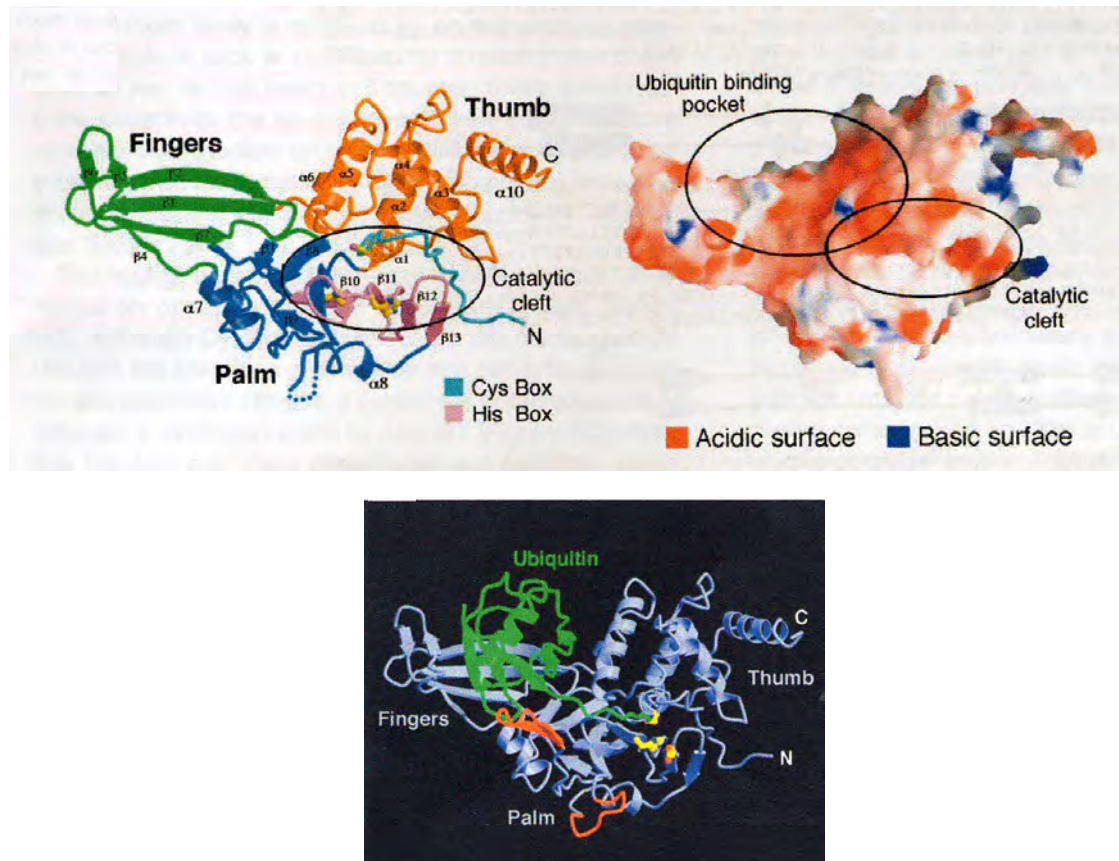


**Figure 5.11. Crystal Structure of *HsHAUSP*<sup>USP7</sup> Catalytic Core.** Overall structure shown as a ribbon diagram (top left) and space-filling diagram with the surface coloured according to electrostatic potential (top right). In the ribbon diagram, the thumb domain is shown in orange, the fingers in green and palm in blue. The active site found in the catalytic cleft is made from Cys box residues (the secondary structure is shaded in cyan) and His box residues (the secondary structure is shaded in pink). In the space-filling diagram, the concave site made by the 'hand' of this DUB binds ubiquitin, and the tapered C-terminus of ubiquitin falls into the catalytic cleft. The lower diagram shaded in black depicts the structure of the catalytic core of this DUB in complex with ubiquitin (green). Adapted from Hu *et al.*, 2002.

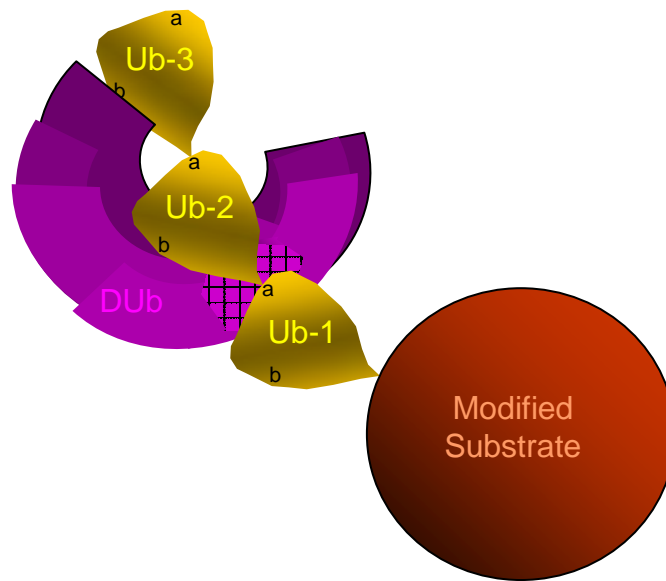


**Figure 5.12. Ubiquitin Binding by DUBs.** The DUB (purple) deubiquitinates a poly-ubiquitinated “modified protein” (burgundy) by binding a ubiquitin monomer (gold) in its concave “hand”. The poly-ubiquitin linkage is via lysines on ubiquitin found at positions “a”. The diagram depicts the DUB binding Ub-2, wherein the C-terminus is covalently linked to another ubiquitin monomer, Ub-1. The DUB active site is highlighted with hatching. If the poly-ubiquitin linkage was via lysines at position “b”, then the DUB pictured would only be able to bind Ub-3, not Ub-2 or -1. For example, if Ub-3 was linked to Ub-2 via position “b” on Ub-2, then Ub-3 would be sterically hindered by the DUB “fingers”, hence Ub-2 would not be bound properly in the DUB active site and the Ub-2—Ub-1 linkage would not be cleaved. However, the most distal ubiquitin (Ub-3 in this case) in a lysine “b”-linked poly-ubiquitin chain could be accommodated in the DUB active site. Hence it could be concluded that this DUB can deubiquitinate lysine “a” linked poly-ubiquitin chains with exo- or endo-deubiquitinating functionality, and lysine “b” linked poly-ubiquitin in only an exo-deubiquitinating manner.

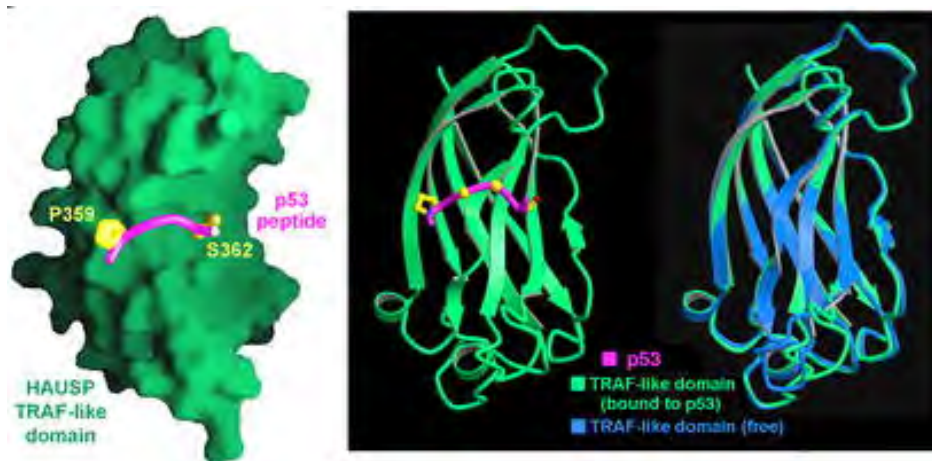


**Figure 5.13. Crystal Structure of the MATH domain of *Hs*HAUSP<sup>USP7</sup> in Complex with a *Hs*p53 Peptide.** Left, space-filling surface representation of the MATH domain – the *Hs*p53 peptide (pink) binding position is also shown. Centre and right, ribbon diagram of the MATH domain. Right, binding to *Hs*p53 does not induce any significant conformational change in the domain. Adapted from Hu *et al.*, 2006.



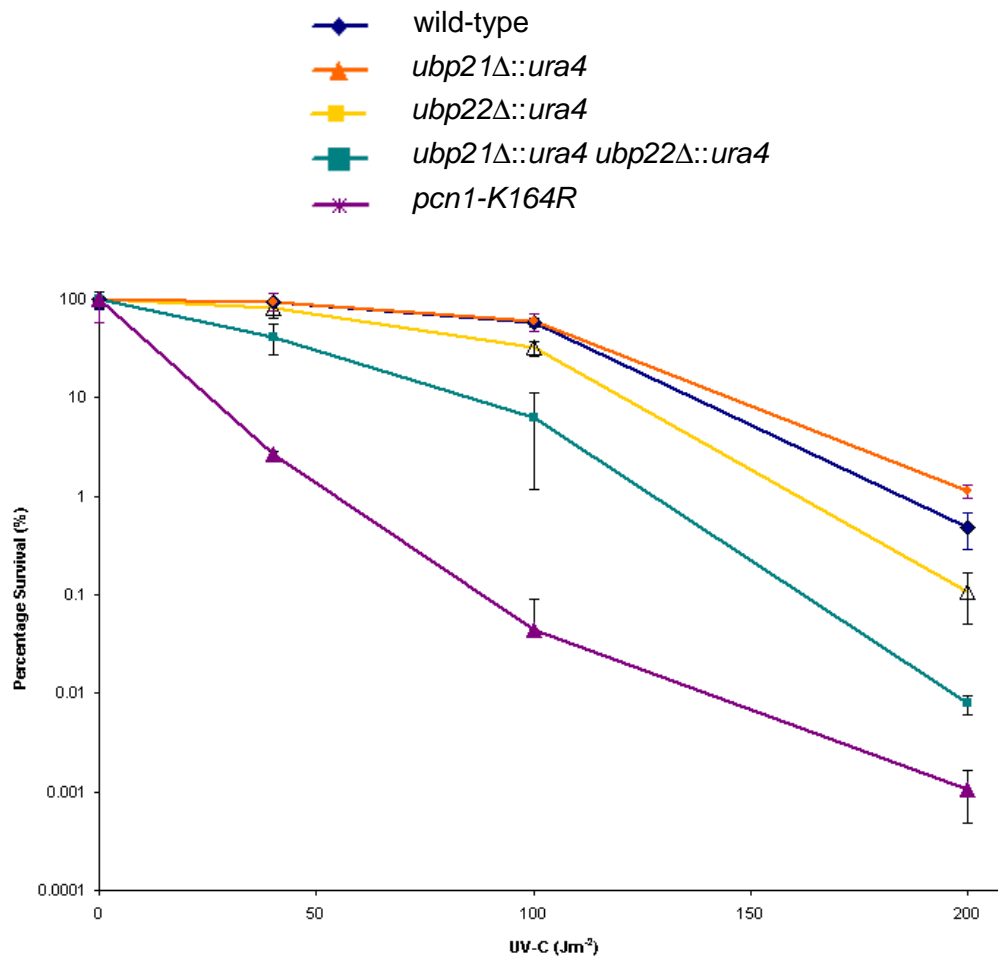


**Figure 5.14. Colony Forming Assay Measuring the Percentage Survival Following UVC Irradiation.** Strains *ubp21Δ*, *ubp22Δ* and *ubp21Δ ubp22Δ* were compared with wild-type and *pcn1-K164R*. Exponentially growing cultures were plated onto agar, which were exposed to the UVC doses indicated. Plates were grown for five days at 30°C before counting. The results represent the mean of two independent experiments and the error bars represent the standard deviation.

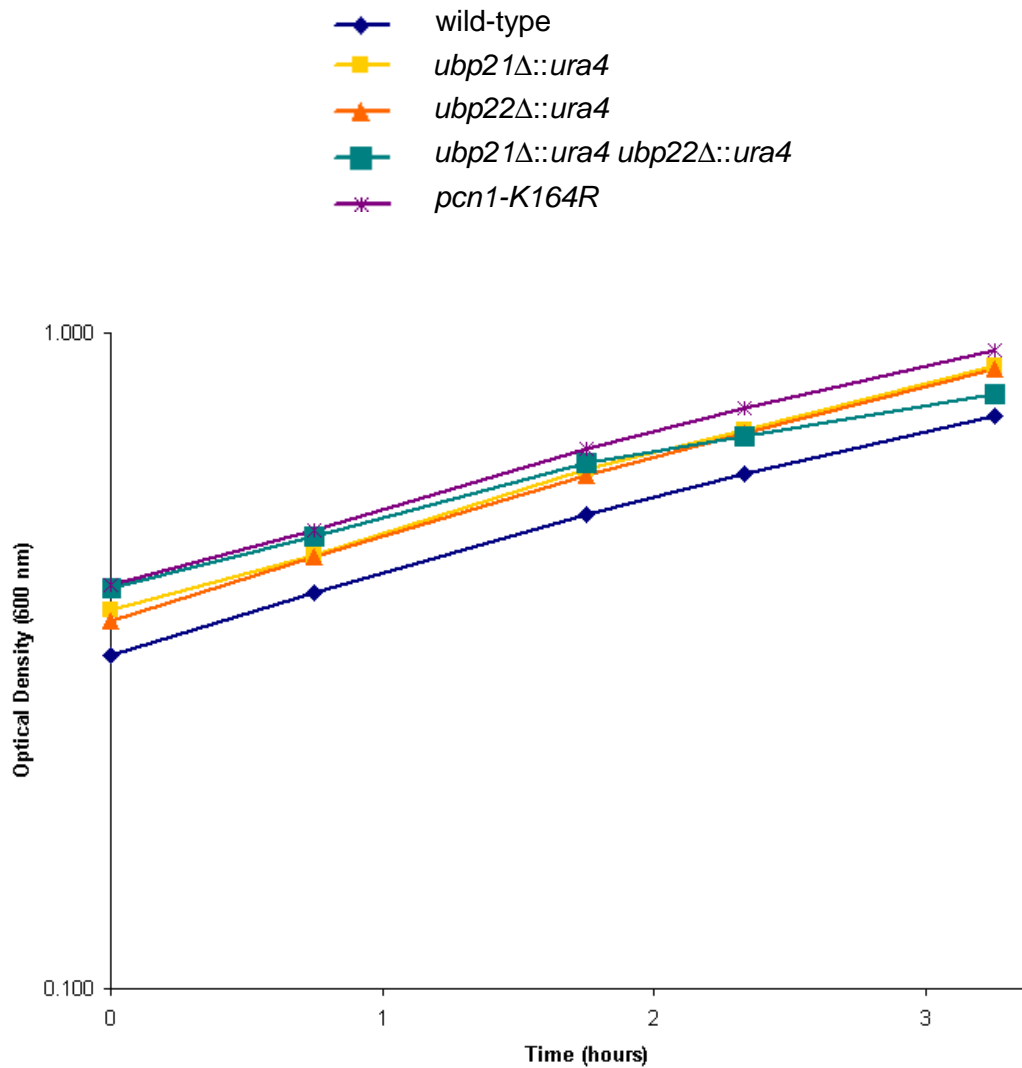


**Figure 5.15. Growth Curve Comparing Mid-log Growth Rates Between Strains.** Strains *ubp21Δ*, *ubp22Δ* and *ubp21Δ ubp22Δ* were compared with wild-type and *pcn1-K164R*. Exponentially growing cultures were grown at 30°C. Samples were taken at the indicated times and the absorbance was measured at 600 nm.



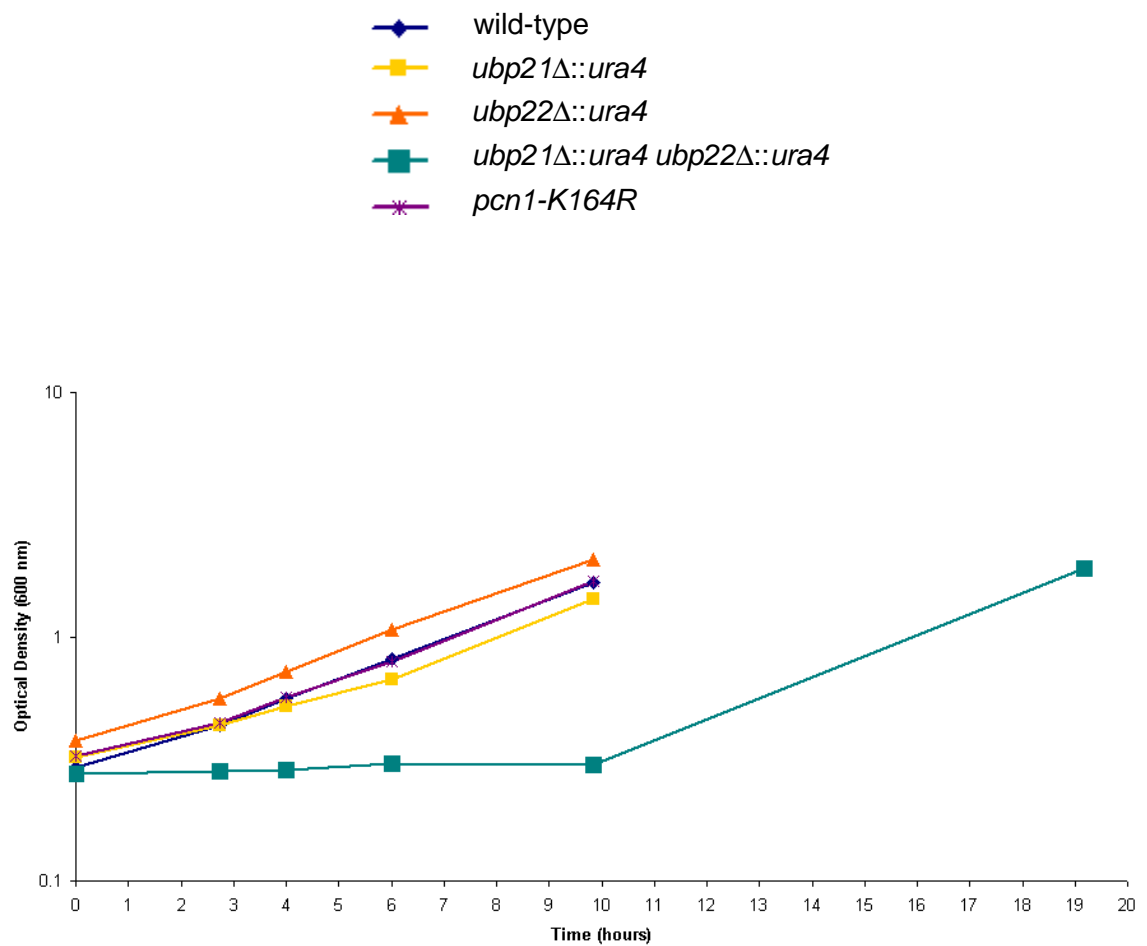


**Figure 5.16. Growth Curve Comparing Recovery of Strains Following Release From Stationary Phase.** Strains *ubp21Δ*, *ubp22Δ* and *ubp21Δ ubp22Δ* were compared with wild-type and *pcn1-K164R*. Cultures were grown to stationary phase and then released into fresh media normalising to approximately the same absorbance. Samples were taken at the indicated times and the optical density measured at 600 nm.

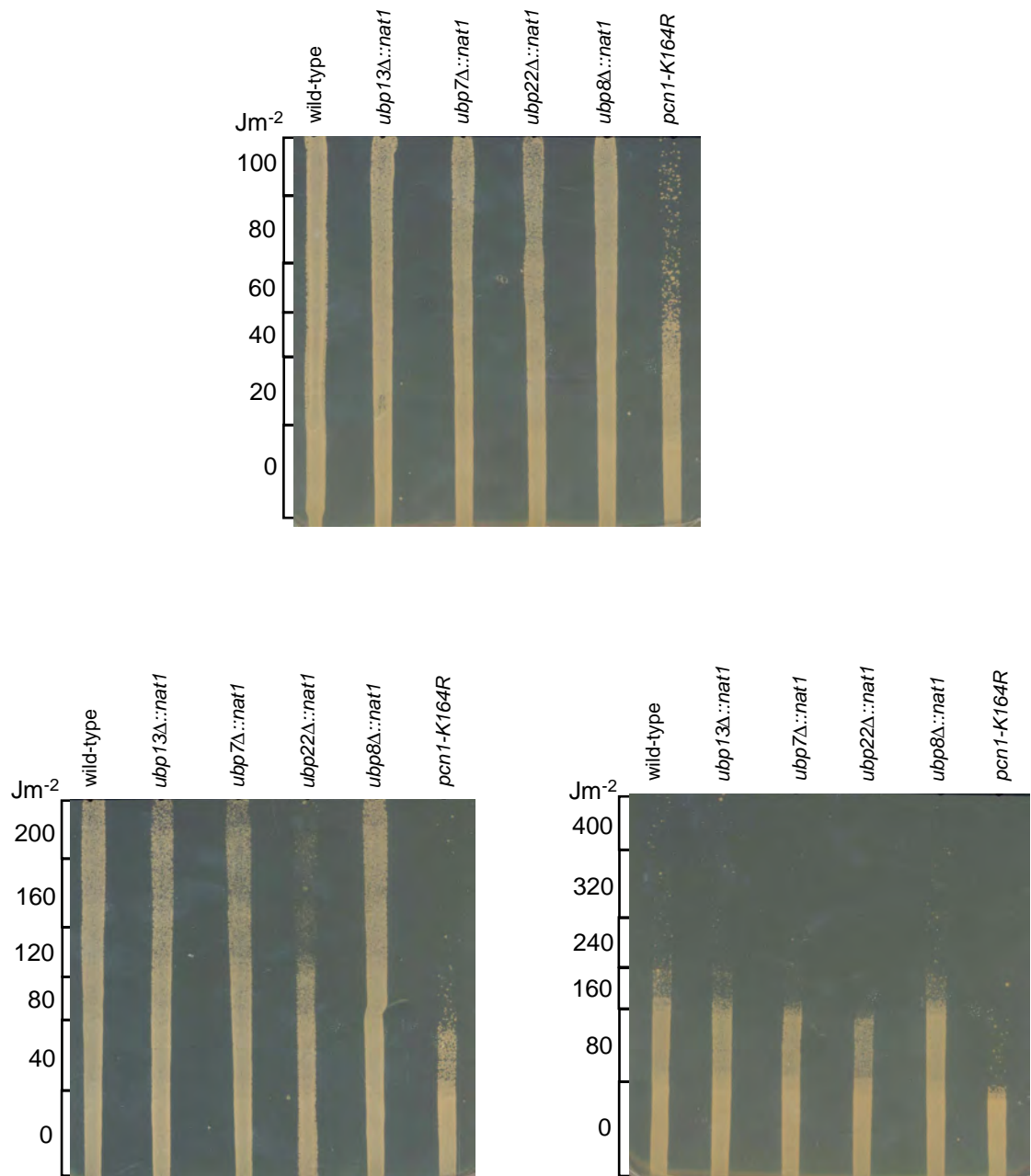


**Figure 5.17. Drop Test Assays Measuring the Relative Sensitivities of *S. pombe* Strains wild-type, *ubp13Δ*, *ubp7Δ*, *ubp22Δ*, *ubp8Δ*, and *pcn1-K164R* to Different Doses of UVC.** Exponentially growing cultures were normalised by cell concentration and dropped down YEA plates, which were subsequently exposed to a UVC dose gradient as indicated. Plates were grown for three days at 30°C before photographing.

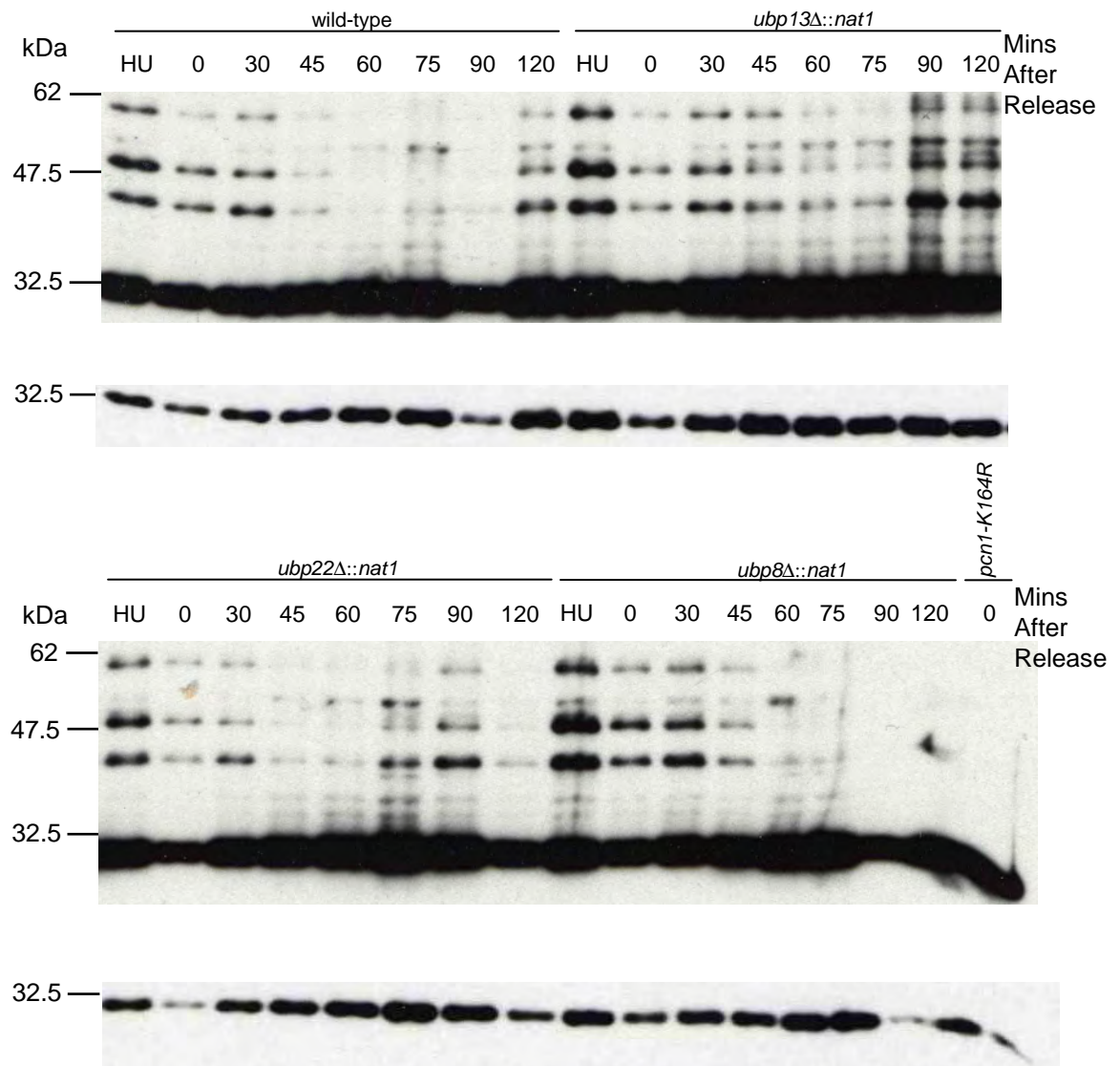


**Figure 5.18. Levels of *Sp*PCNA Ubiquitination Following Cell Cycle Block in S-phase in the *S. pombe* Strains Wild-type, *ubp13Δ::nat1*, *ubp22Δ::nat1*, *ubp8Δ::nat1*, and *pcn1-K164R*.** The same number of cells of exponentially growing cultures were treated with 10 mM HU for 2.5 hrs and then released into fresh media. Samples were taken after treatment (HU) and every 15 mins following release from HU. Size fractionated whole cell extracts were probed with anti-*Sp*PCNA antibodies.

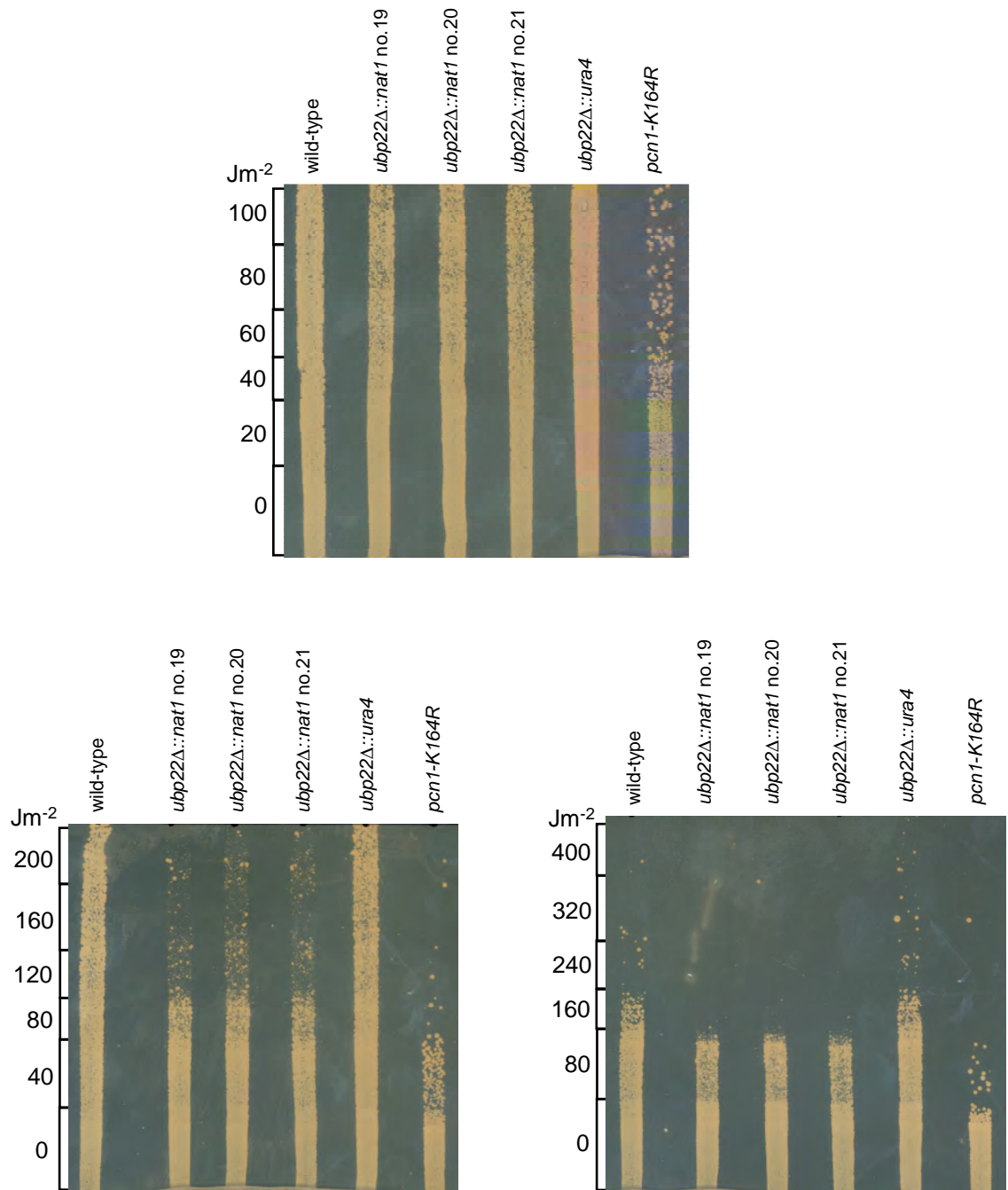


**Figure 5.19. Drop Test Assays Measuring the Relative Sensitivities to Different Doses of UVC of Different *S. pombe* *ubp22Δ::nat1* Clones Compared to wild-type, *ubp22Δ::ura4* and *pcn1-K164R*.** Exponentially growing cultures were normalised by cell concentration and dropped down YEA plates, which were subsequently exposed to a UVC dose gradient as indicated. Plates were grown for three days at 30°C before photographing. Clone number 21 is that utilised previously.

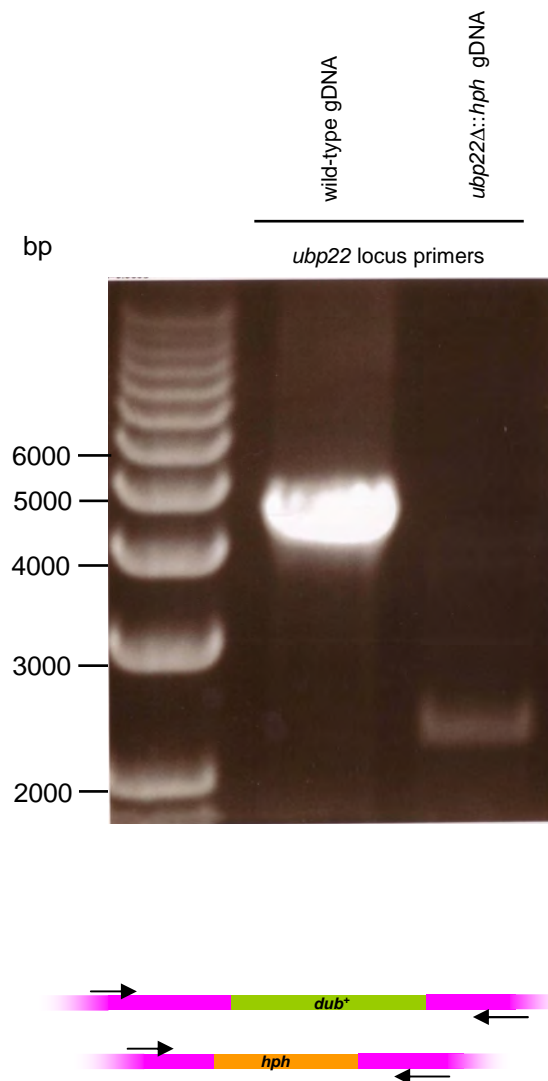


**Figure 5.20. PCR Amplification of the *ubp22* Locus Utilising Primers that Anneal to Flanking DNA and Genomic DNA from the *S. pombe* Strains wild-type, and *ubp22Δ::hph*.** The lower diagram shows the PCR strategy in wild-type gDNA and *dub*-deleted gDNA. Primers that flank the DUB gene locus are depicted by arrows.

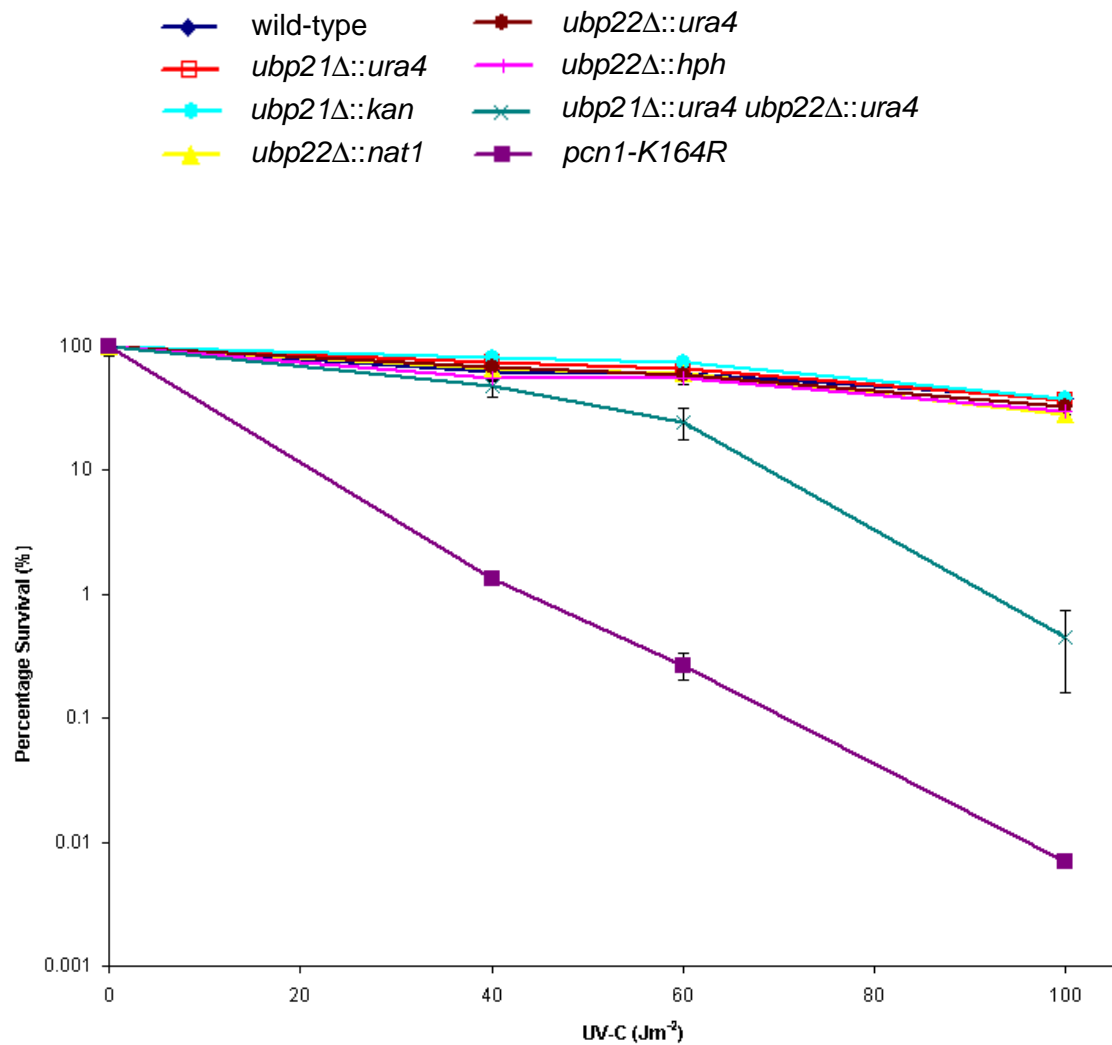


**Figure 5.21. Colony Forming Assay Measuring the Percentage Survival Following UVC Irradiation.** Strains *ubp21Δ*, *ubp22Δ* and *ubp21Δ ubp22Δ* were compared with wild-type and *pcn1-K164R*. Exponentially growing cultures were plated onto agar, which were exposed to the UVC doses indicated. Plates were grown for six days at 30°C before counting. The results represent the mean of two independent experiments and the error bars represent the standard error of the mean.

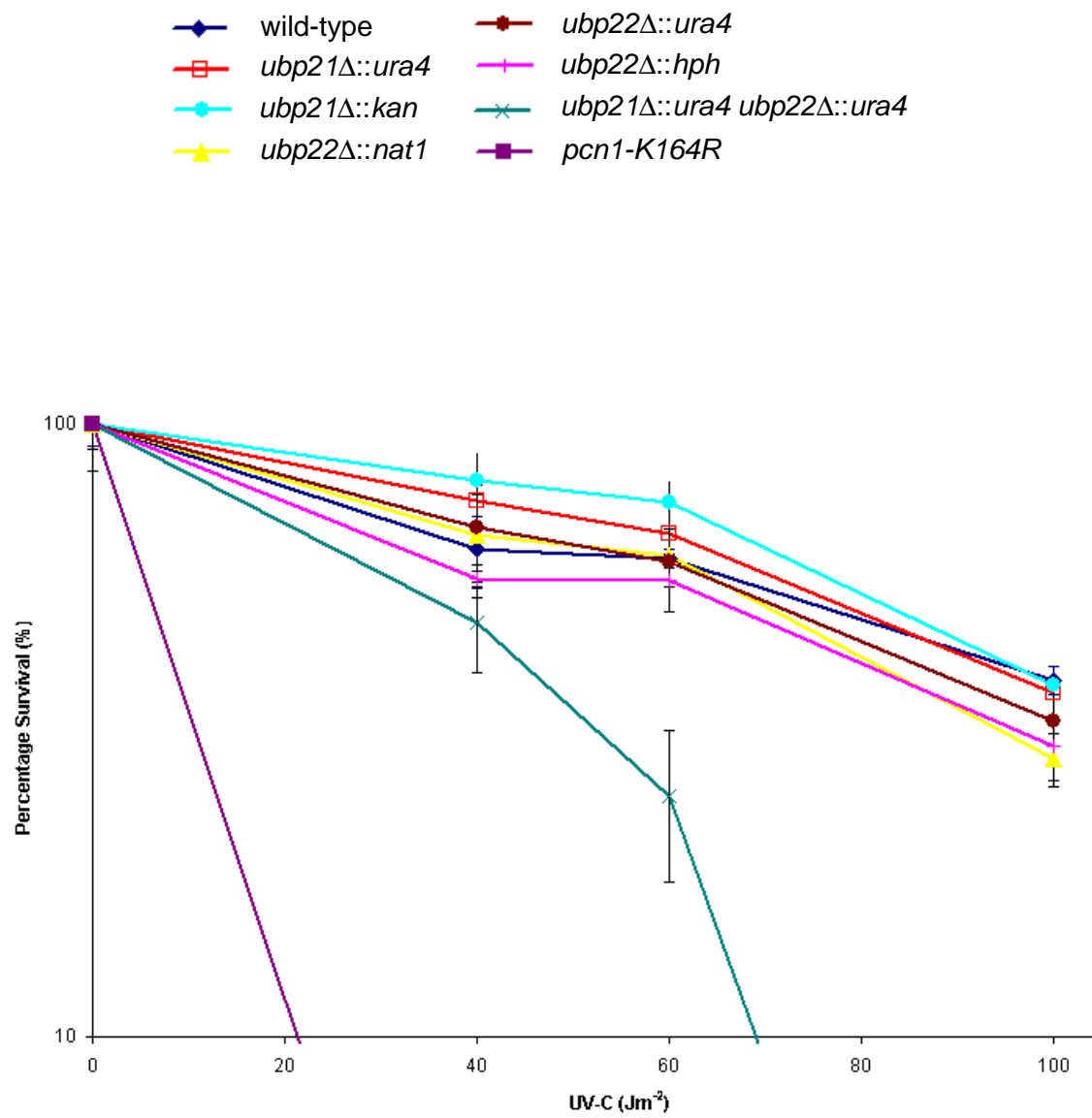


**Figure 5.22. Colony Forming Assay Measuring the Percentage Survival Following UVC Irradiation.** As Figure 5.21.

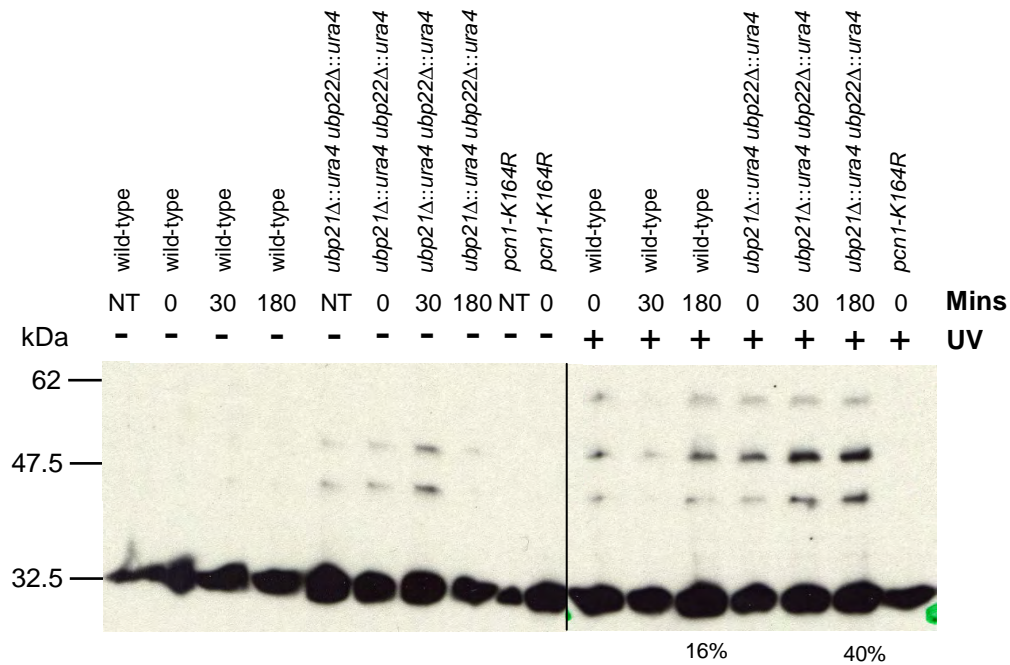


**Figure 5.23. Levels of *Sp*PCNA Ubiquitination in the *S. pombe* Strains wild-type, *ubp21Δ::ura4 ubp22Δ::ura4* and *pcn1-K164R* Following Mock (-) or UVC Treatment (+).** The same number of cells of exponentially growing cultures were mock treated or treated with UVC. Samples were taken before treatment (NT) and at the indicated times following mock or UVC treatment. Size fractionated whole cell extracts were probed with anti-*Sp*PCNA antibodies. A percentage value under a lane indicates the relative level of ubiquitinated *Sp*PCNA when unmodified PCNA is set to 100%, which was measured by quantification of bands on a low exposure using ImageJ (<http://rsb.info.nih.gov/ij/>).



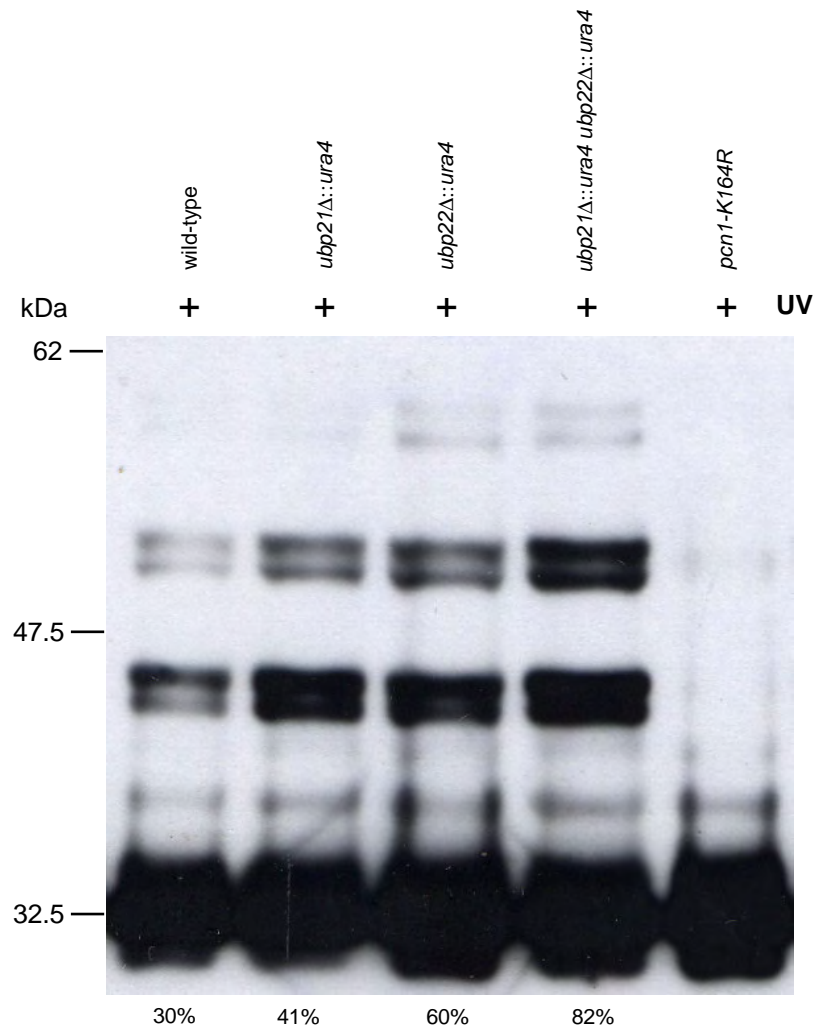


**Figure 5.24. Levels of *Sp*PCNA Ubiquitination in the *S. pombe* Strains wild-type, *ubp21Δ::ura4* *ubp22Δ::ura4* and *pcn1-K164R* Following Mock (-) or UVC Treatment (+).** The same number of cells of exponentially growing cultures were mock treated or treated with UVC. Samples were taken before treatment (NT) and at the indicated times following mock or UVC treatment. Size fractionated whole cell extracts were probed with anti-*Sp*PCNA antibodies. A percentage value under a lane indicates the relative level of ubiquitinated *Sp*PCNA when unmodified PCNA is set to 100%, which was measured by quantification of bands on a low exposure using ImageJ (<http://rsb.info.nih.gov/ij/>).

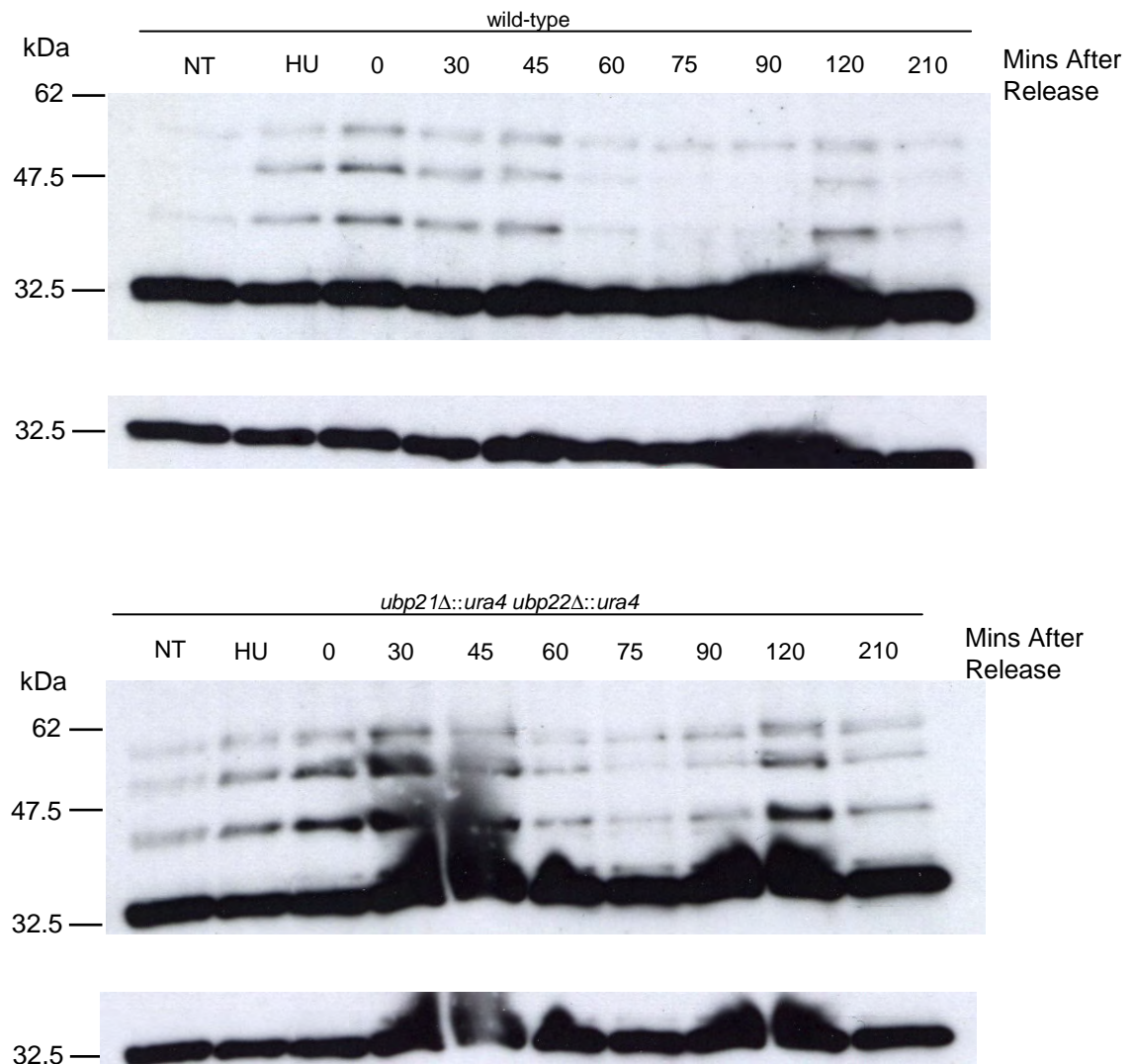


**Figure 5.25. Levels of *Sp*PCNA Ubiquitination Following Cell Cycle Block in S-phase in the *S. pombe* Strains wild-type and *ubp21Δ::ura4, ubp22Δ::ura4*.** The same number of cells of exponentially growing cultures were treated with 10 mM hydroxyurea for 2.5 hrs and then released into fresh media. Samples were taken before (NT) and after treatment (HU), in addition to every 15 mins following release from HU. Size fractionated whole cell extracts were probed with anti-*Sp*PCNA antibodies. Samples at the aforementioned times were taken concurrently for analysis of DNA content, the results of which are shown in figure 5.25.

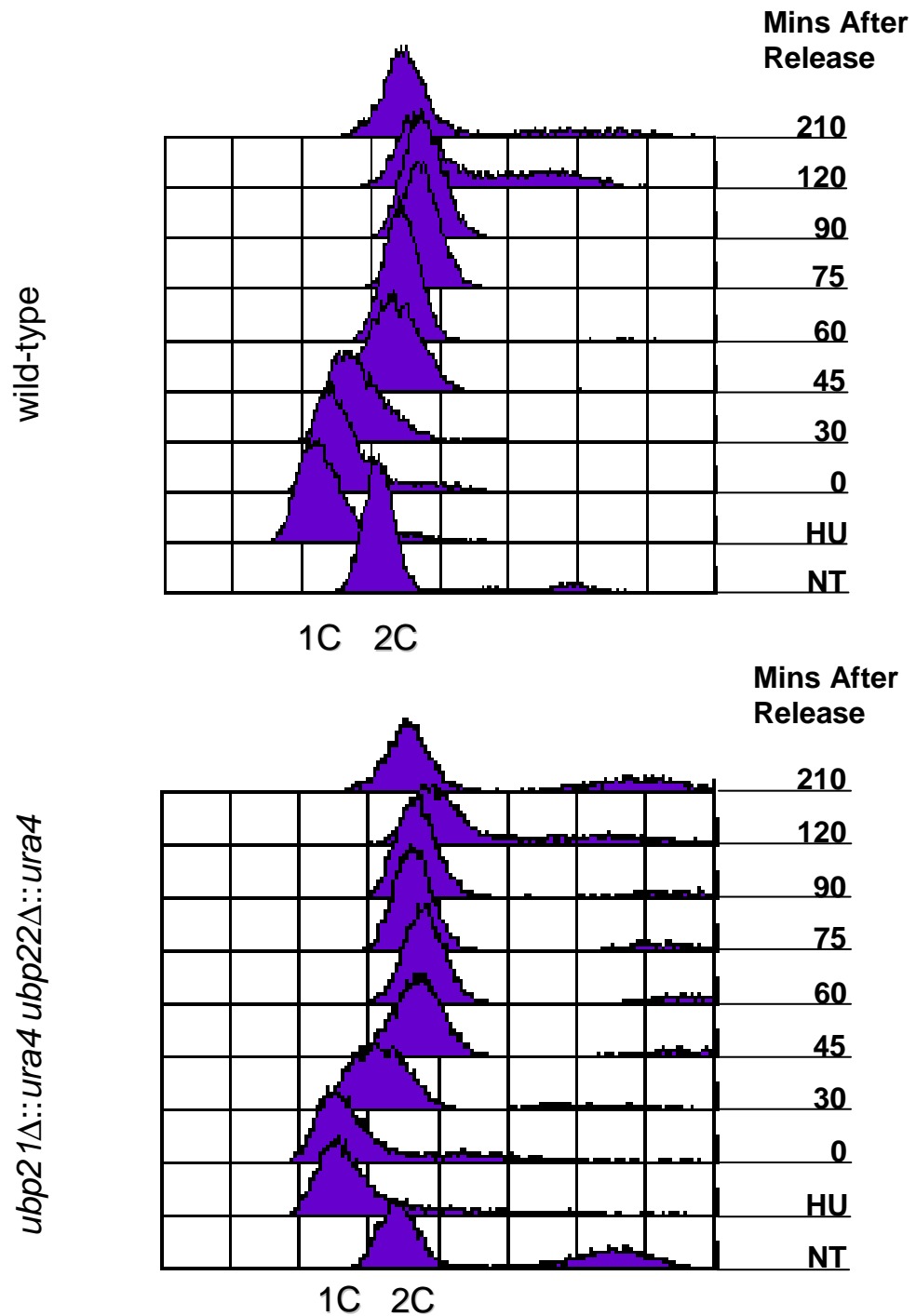


**Figure 5.26. DNA Content Analysis Following Cell Cycle Block in S-phase in the *S. pombe* Strains wild-type and *ubp21Δ::ura4 ubp22Δ::ura4*.** The same number of cells of exponentially growing cultures were treated with 10 mM hydroxyurea for 2.5 hrs and then released into fresh media. Samples were taken before (NT) and after treatment (HU), in addition to every 15 mins following release from hydroxyurea. DNA content was assayed using DAPI staining followed by analysis by FACS. Additional samples were taken concurrently at the aforementioned times for analysis of PCNA ubiquitination, the results of which are shown in Figure 5.25.

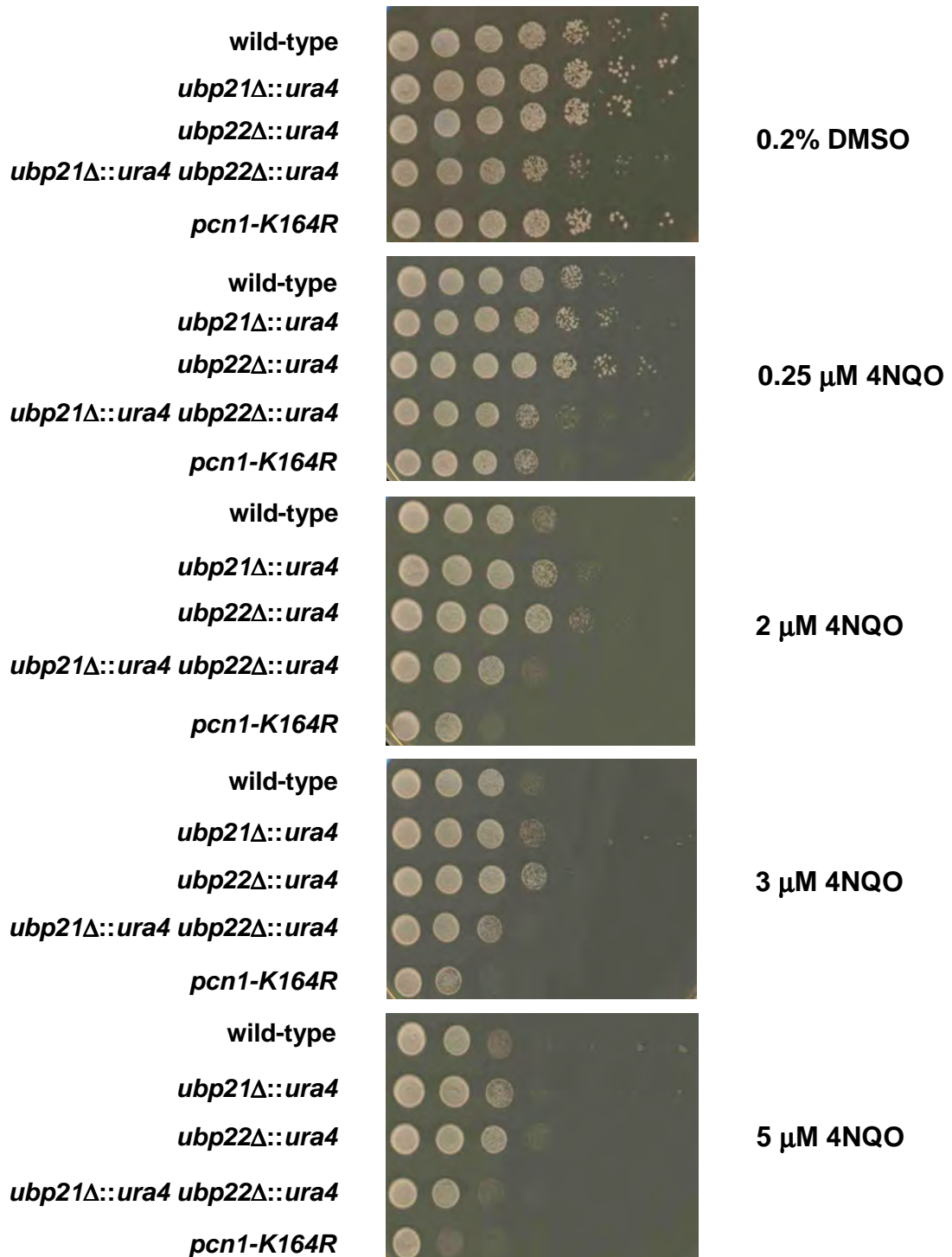


**Figure 5.27. Growth Analysis on Agar Containing 4-Nitroquinoline-1-oxide (4NQO) of the *S. pombe* Strains wild-type, *ubp21Δ::ura4*, *ubp22Δ::ura4*, *ubp21Δ::ura4 ubp22Δ::ura4* and *pcn1-K164R*.** The same number of cells of exponentially growing cultures were normalised by cell number, and six 1 in 6 serial dilutions were carried out. Cells were spotted onto agar containing 4NQO diluted in  $\leq 0.2\%$  DMSO and colonies were grown for two days at 30°C.

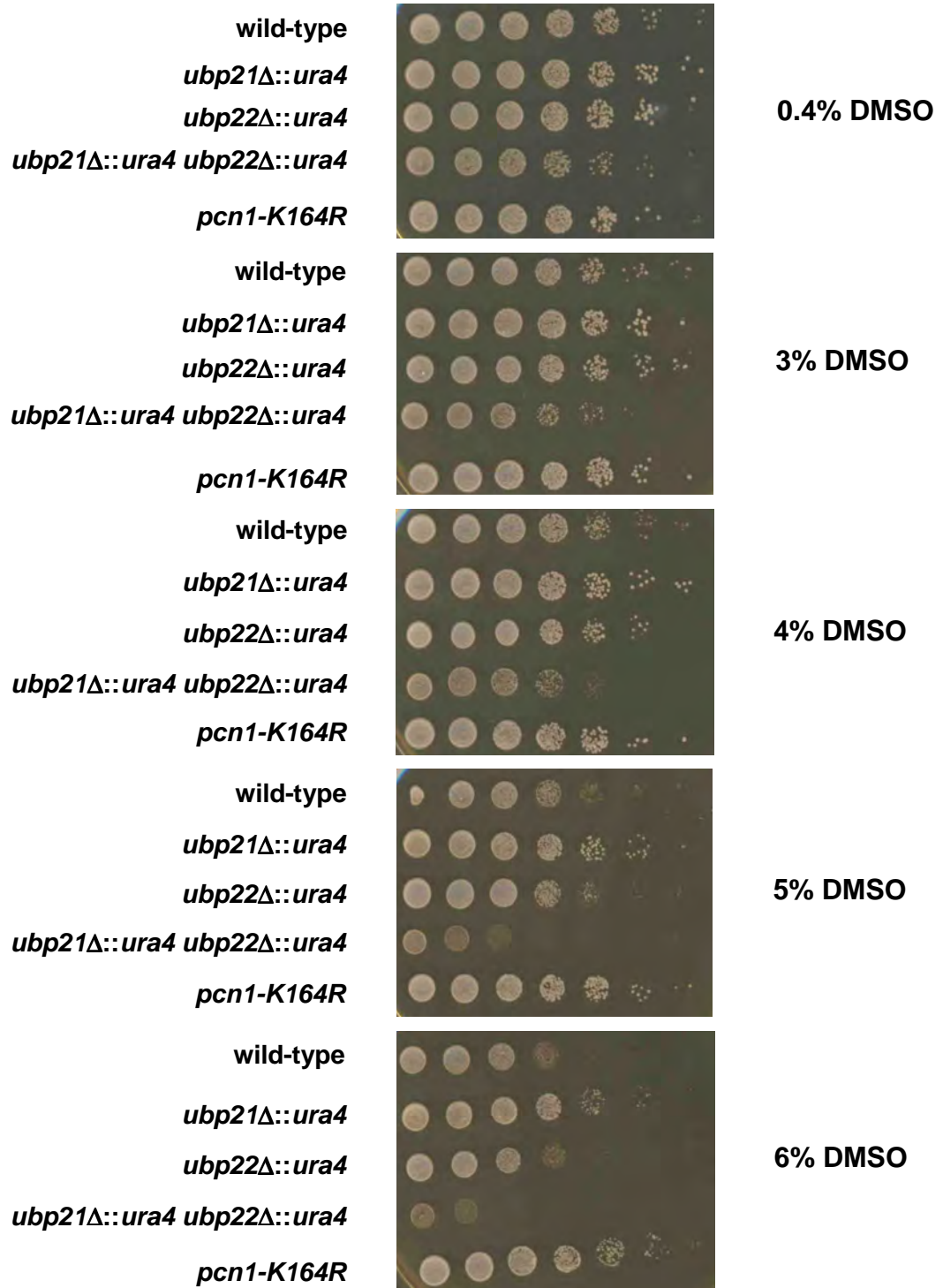


**Figure 5.28. Growth Analysis on Agar Containing Dimethylsulfoxide (DMSO) of the *S. pombe* Strains wild-type, *ubp21Δ::ura4*, *ubp22Δ::ura4*, *ubp21Δ::ura4 ubp22Δ::ura4* and *pcn1-K164R*.** The experiment was carried as described in figure 5.26.



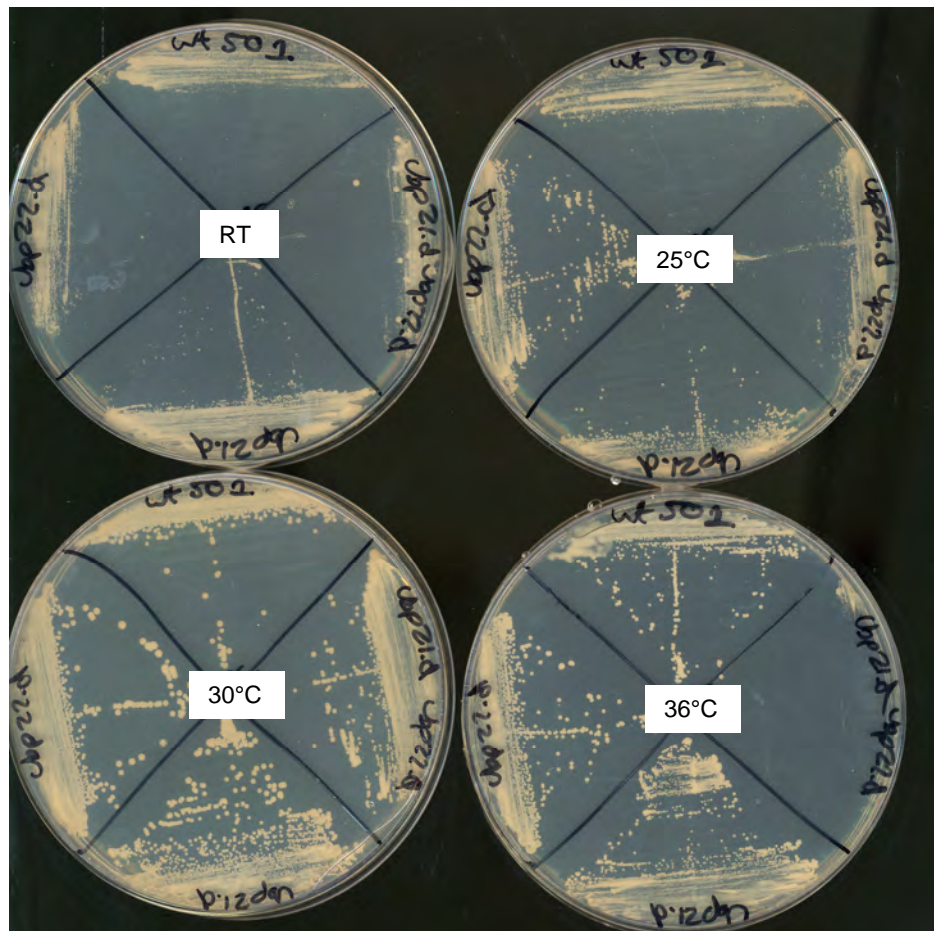


**Figure 5.29. Temperature Sensitivity of Strains *ubp21Δ*, *ubp22Δ* and *ubp21Δ ubp22Δ*.** Each plate was streaked with the strains *ubp21Δ ::ura4* (lower quadrant), *ubp22Δ ::ura4* (left quadrant) and *ubp21Δ::ura4 ubp22Δ ::ura4* (right quadrant). Growth of these strains were compared with wild-type (top quadrant) after three days at the temperatures depicted. RT stands for room temperature, which was about 23°C.

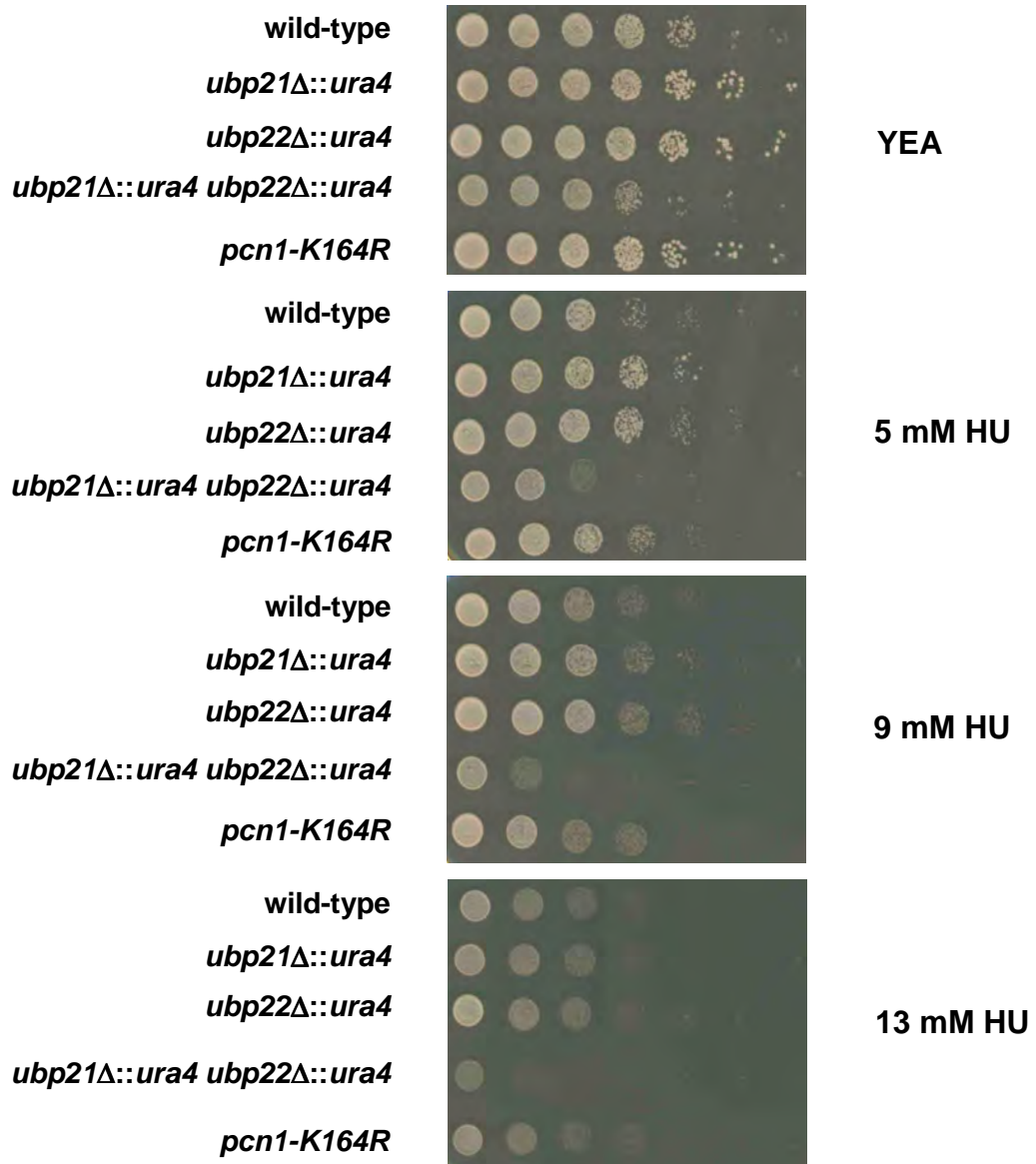


**Figure 5.30. Growth Analysis on Agar Containing Hydroxyurea (HU) of the *S. pombe* Strains wild-type, *ubp21Δ::ura4*, *ubp22Δ::ura4*, *ubp21Δ::ura4 ubp22Δ::ura4* and *pcn1-K164R*.** The experiment was carried as described in figure 5.26 except the HU was dissolved in water.

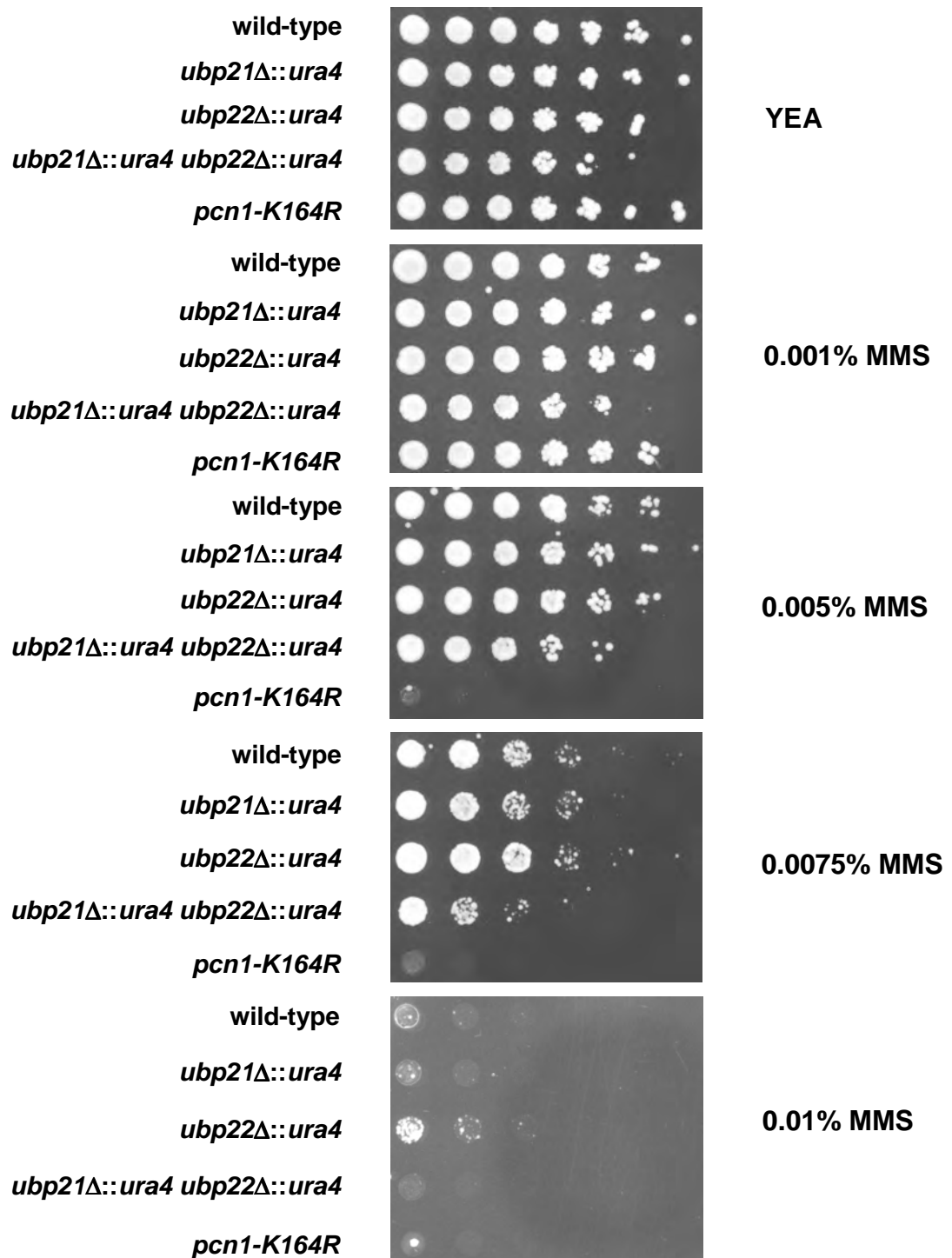


**Figure 5.31. Growth Analysis on Agar Containing Methyl Methanesulfonate (MMS) of the *S. pombe* Strains wild-type, *ubp21Δ::ura4*, *ubp22Δ::ura4*, *ubp21Δ::ura4 ubp22Δ::ura4* and *pcn1-K164R*. The experiment was carried as described in figure 5.26 except the MMS was dissolved in water.**



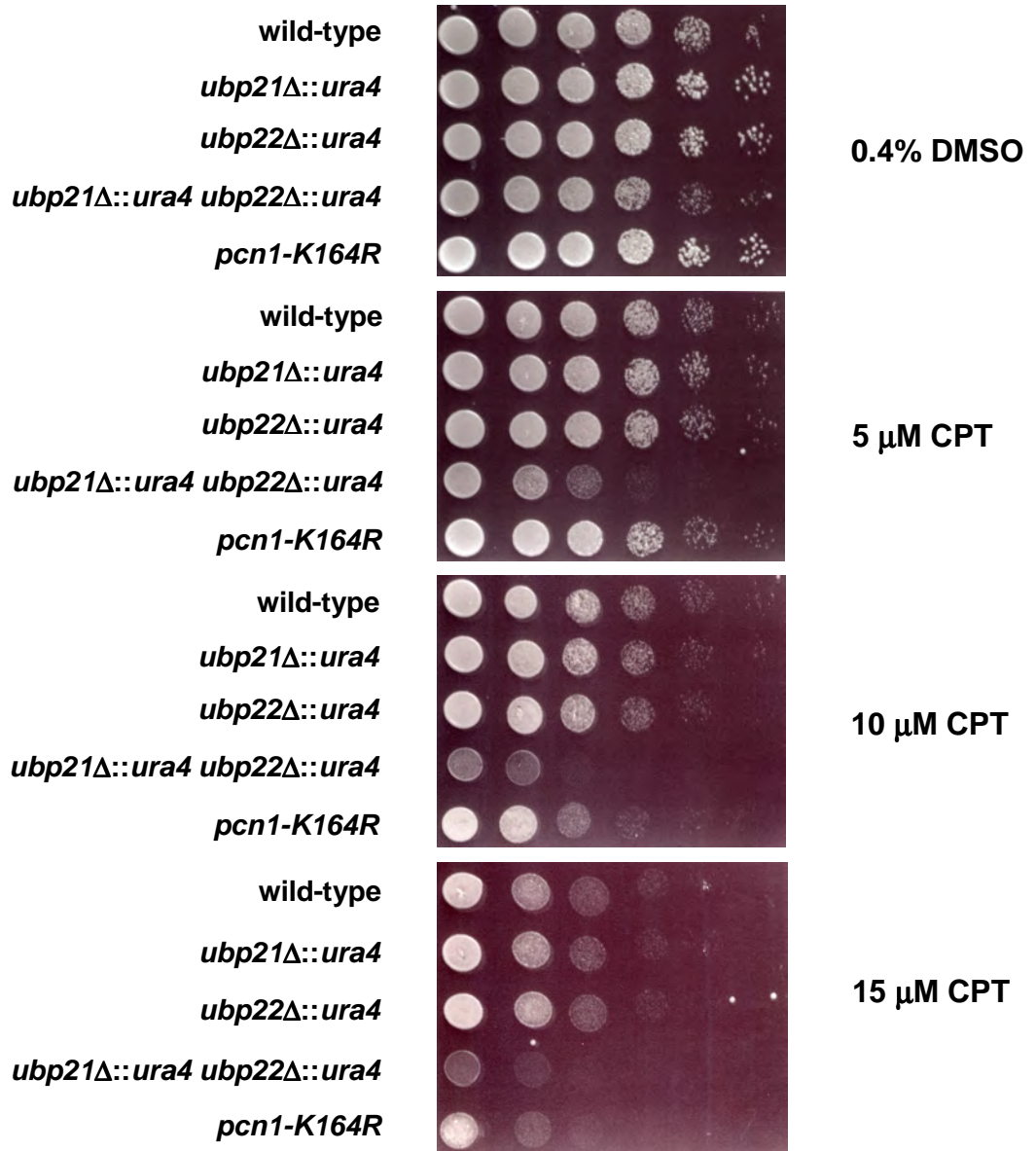


**Figure 5.32. Growth Analysis on Agar Containing Camptothecin (CPT) of the *S. pombe* Strains wild-type, *ubp21Δ::ura4*, *ubp22Δ::ura4*, *ubp21Δ::ura4 ubp22Δ::ura4* and *pcn1-K164R*.** The experiment was carried as described in figure 5.26.

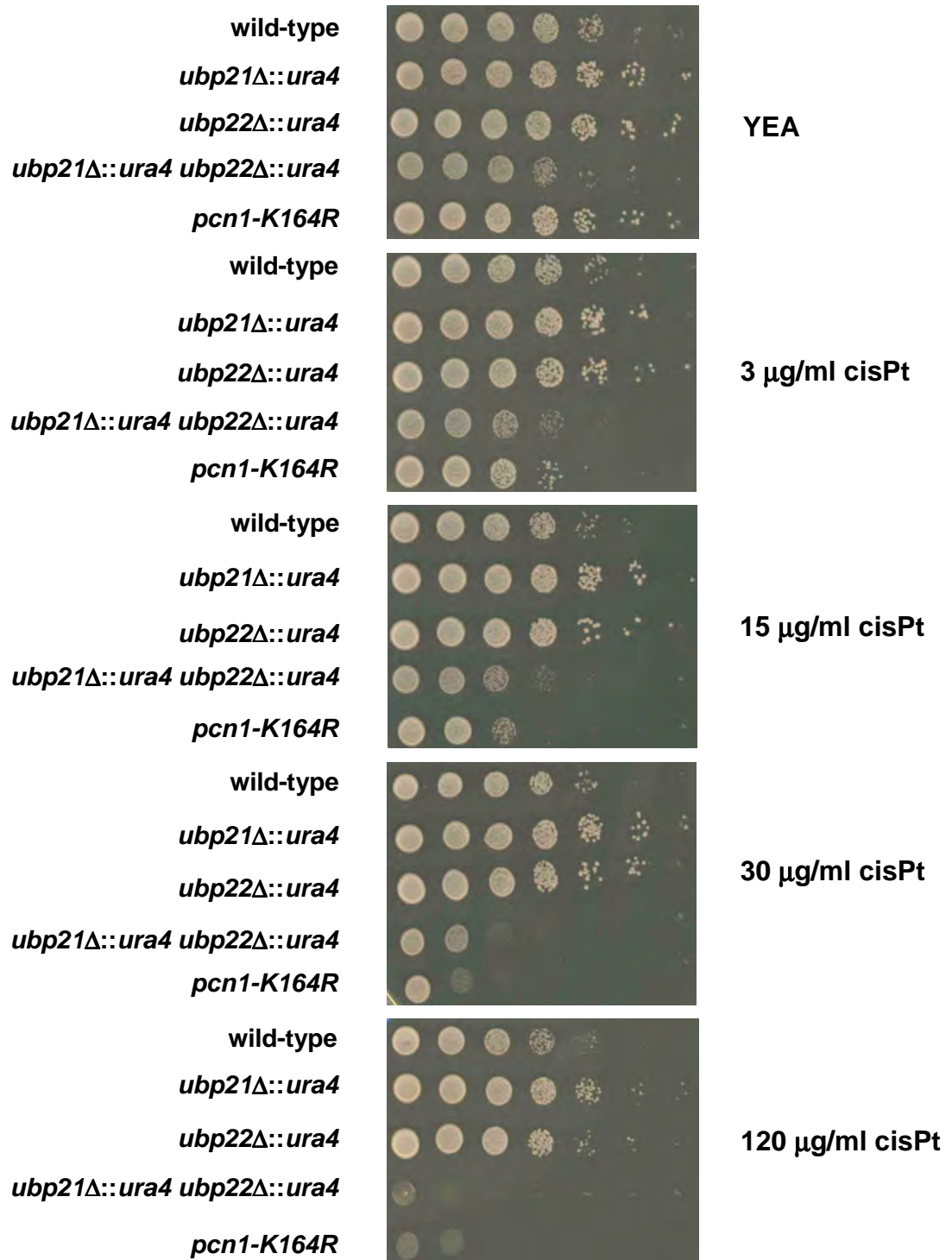


**Figure 5.33. Growth Analysis on Agar Containing *cis*platin (*cis*Pt) of the *S. pombe* Strains wild-type, *ubp21Δ::ura4*, *ubp22Δ::ura4*, *ubp21Δ::ura4 ubp22Δ::ura4* and *pcn1-K164R*.** The experiment was carried as described in figure 5.26 except *cis*Pt was added to the agar as neat powder.

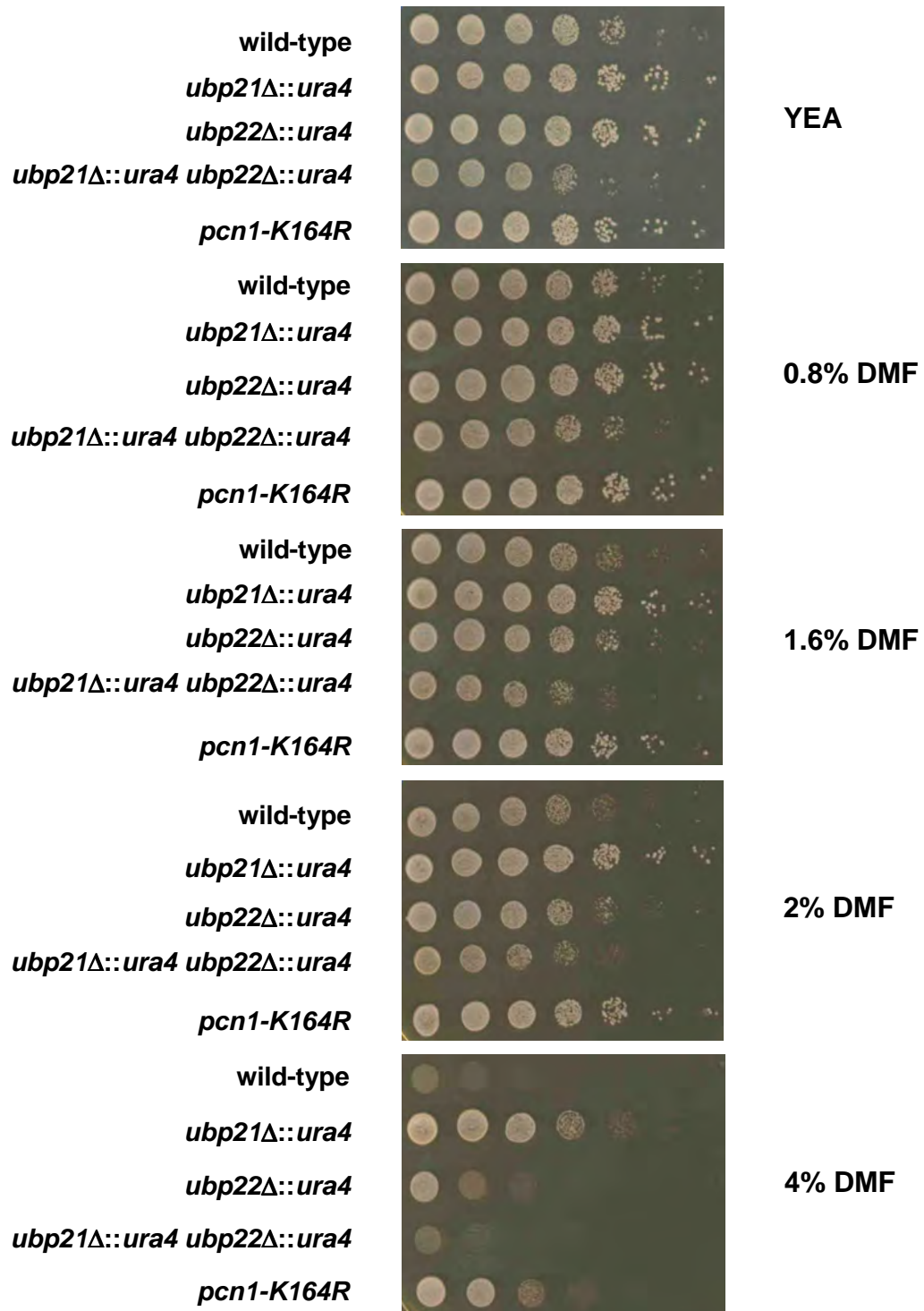


**Figure 5.34. Growth Analysis on Agar Containing Dimethylformamide (DMF) of the *S. pombe* Strains wild-type, *ubp21Δ::ura4*, *ubp22Δ::ura4*, *ubp21Δ::ura4 ubp22Δ::ura4* and *pcn1-K164R*.** The experiment was carried as described in figure 5.26.

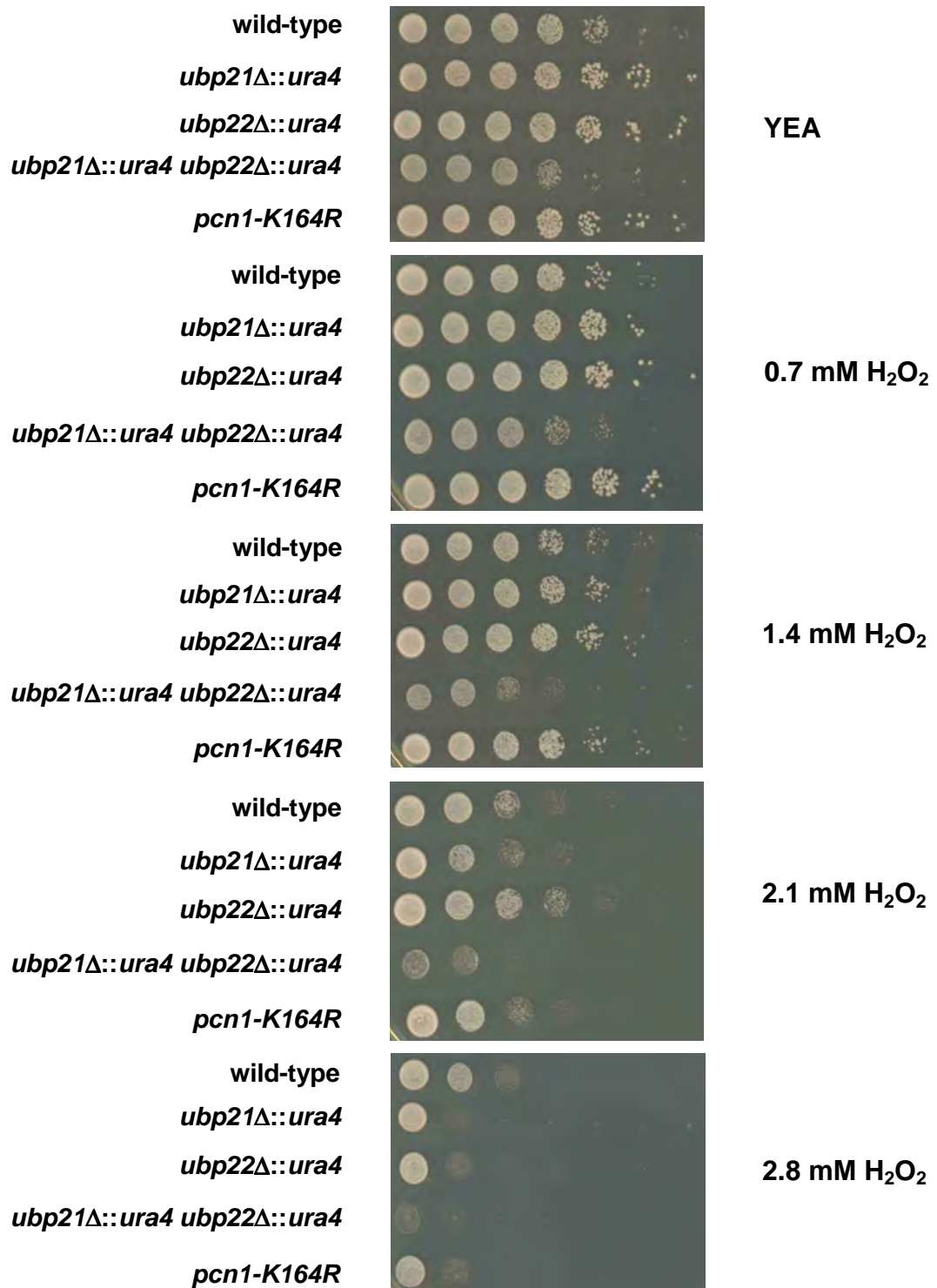


**Figure 5.35. Growth Analysis on Agar Containing Hydrogen Peroxide (H<sub>2</sub>O<sub>2</sub>) of the *S. pombe* Strains wild-type, *ubp21Δ::ura4*, *ubp22Δ::ura4*, *ubp21Δ::ura4 ubp22Δ::ura4* and *pcn1-K164R*. The experiment was carried as described in figure 5.26 except the H<sub>2</sub>O<sub>2</sub> was dissolved in water.**

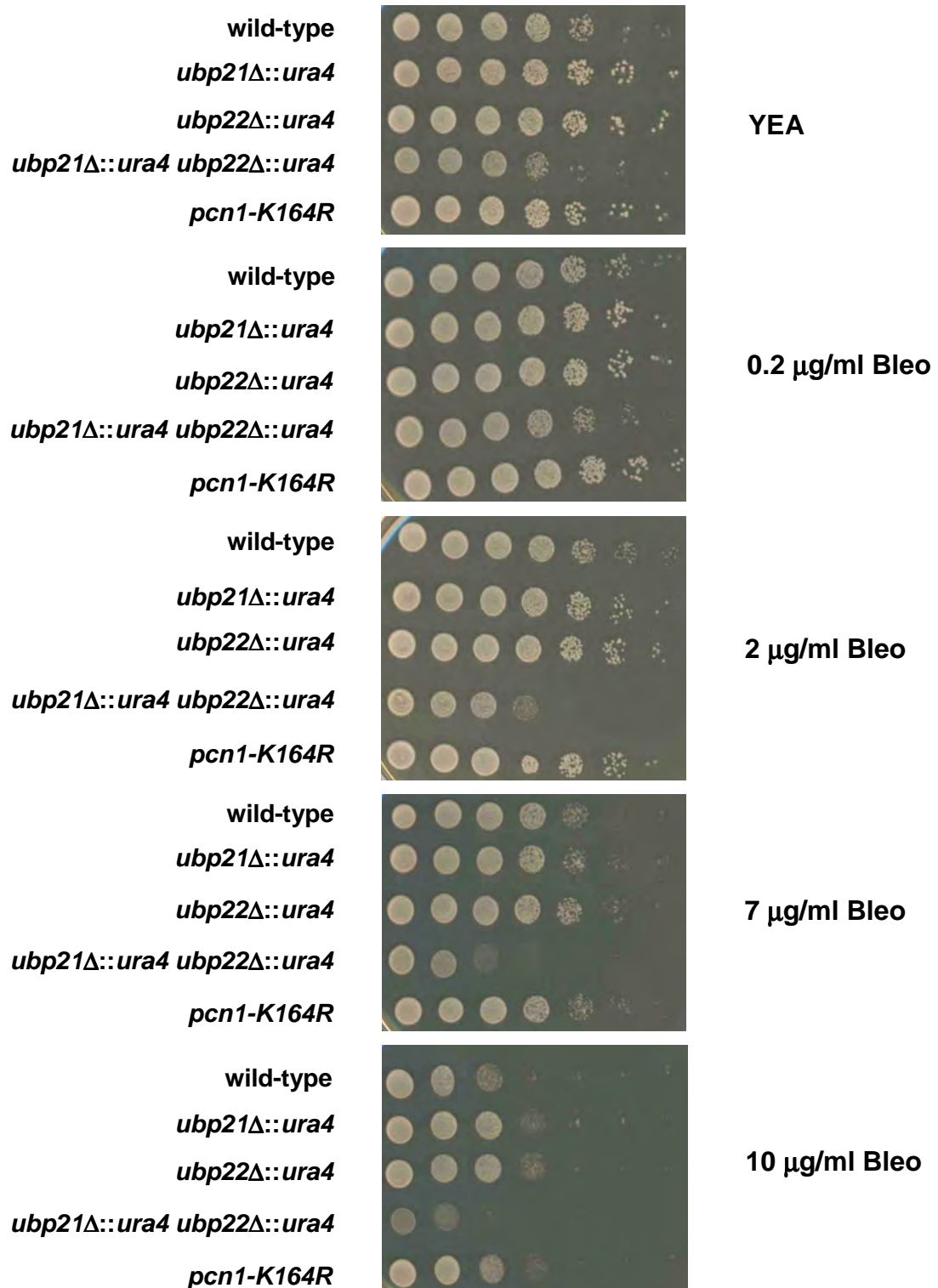


**Figure 5.36. Growth Analysis on Agar Containing Bleomycin (Bleo) of the *S. pombe* Strains wild-type, *ubp21Δ::ura4*, *ubp22Δ::ura4*, *ubp21Δ::ura4 ubp22Δ::ura4* and *pcn1-K164R*.** The experiment was carried as described in figure 5.26 except the diluant was water.



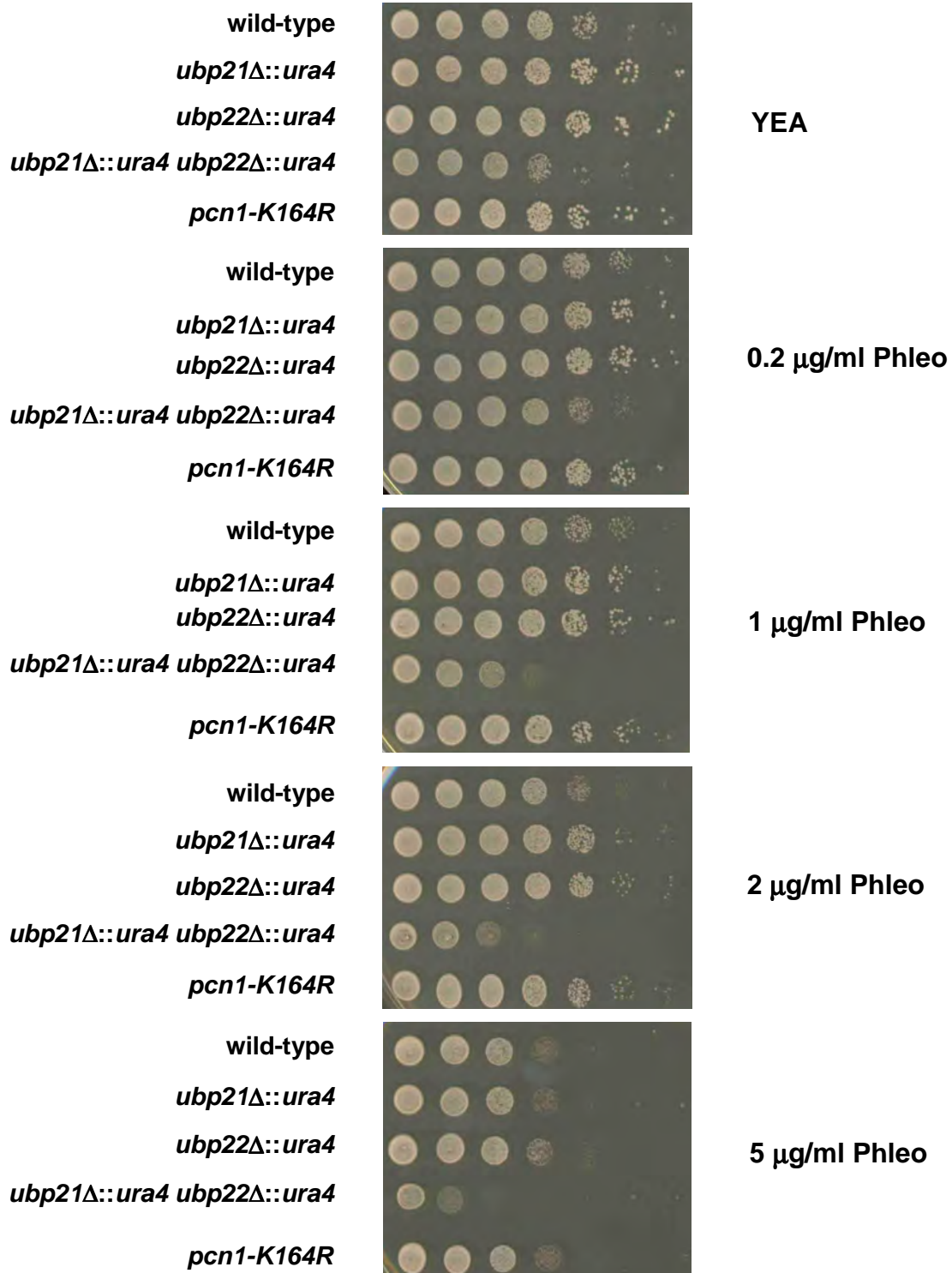


**Figure 5.37. Growth Analysis on Agar Containing Phleomycin (Phleo) of the *S. pombe* Strains wild-type, *ubp21Δ::ura4*, *ubp22Δ::ura4*, *ubp21Δ::ura4 ubp22Δ::ura4* and *pcn1-K164R*.** The experiment was carried as described in figure 5.26 except the diluant was water.

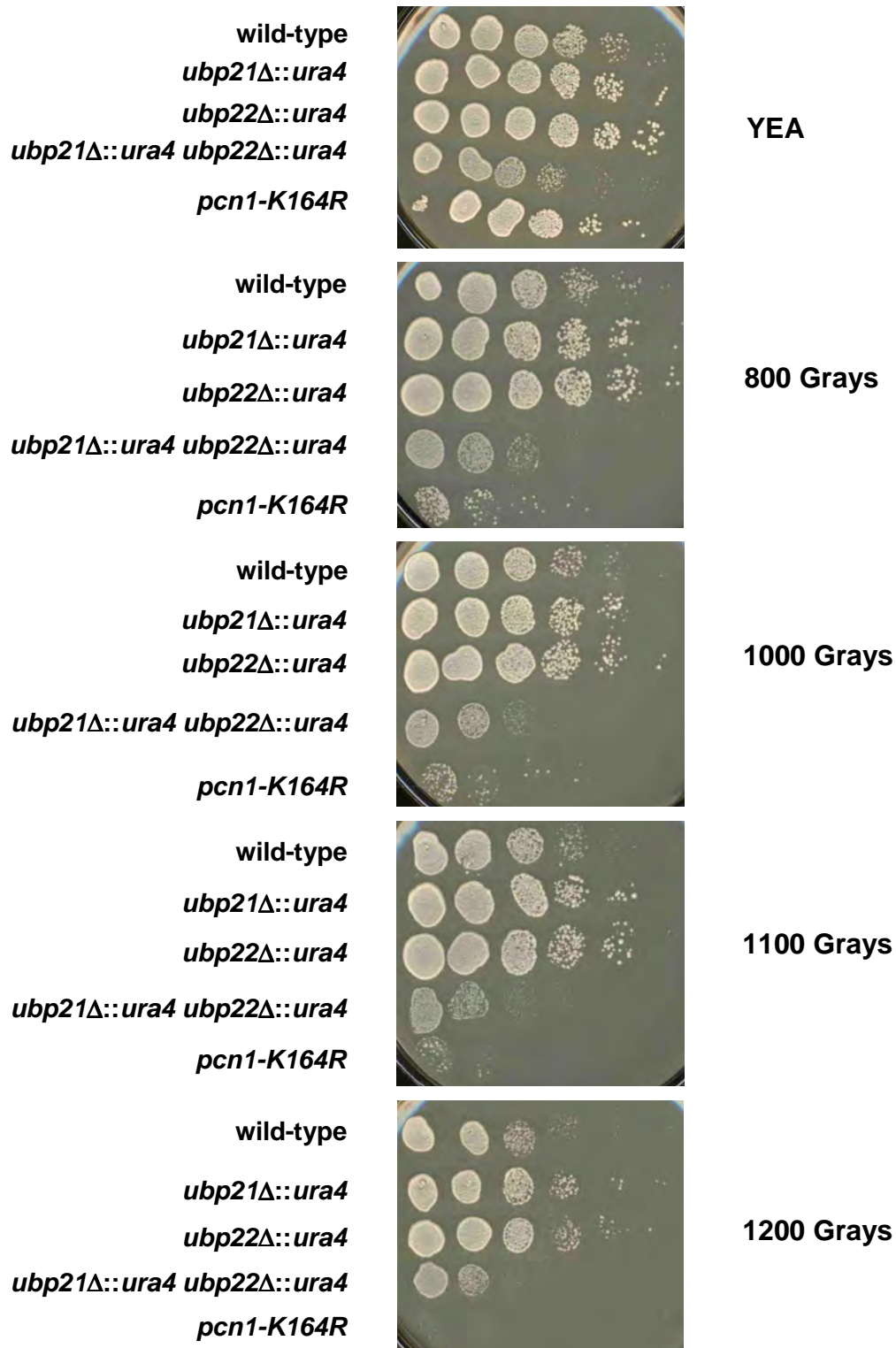


**Figure 5.38. Growth Analysis Following  $\gamma$  Irradiation of the *S. pombe* Strains wild-type, *ubp21Δ::ura4*, *ubp22Δ::ura4*, *ubp21Δ::ura4 ubp22Δ::ura4* and *pcn1-K164R*.** The same number of cells of exponentially growing cultures were normalised by cell number, and six 1 in 6 serial dilutions were carried out. Cells were spotted onto agar, irradiated at different doses and colonies were grown for two days at 30°C.

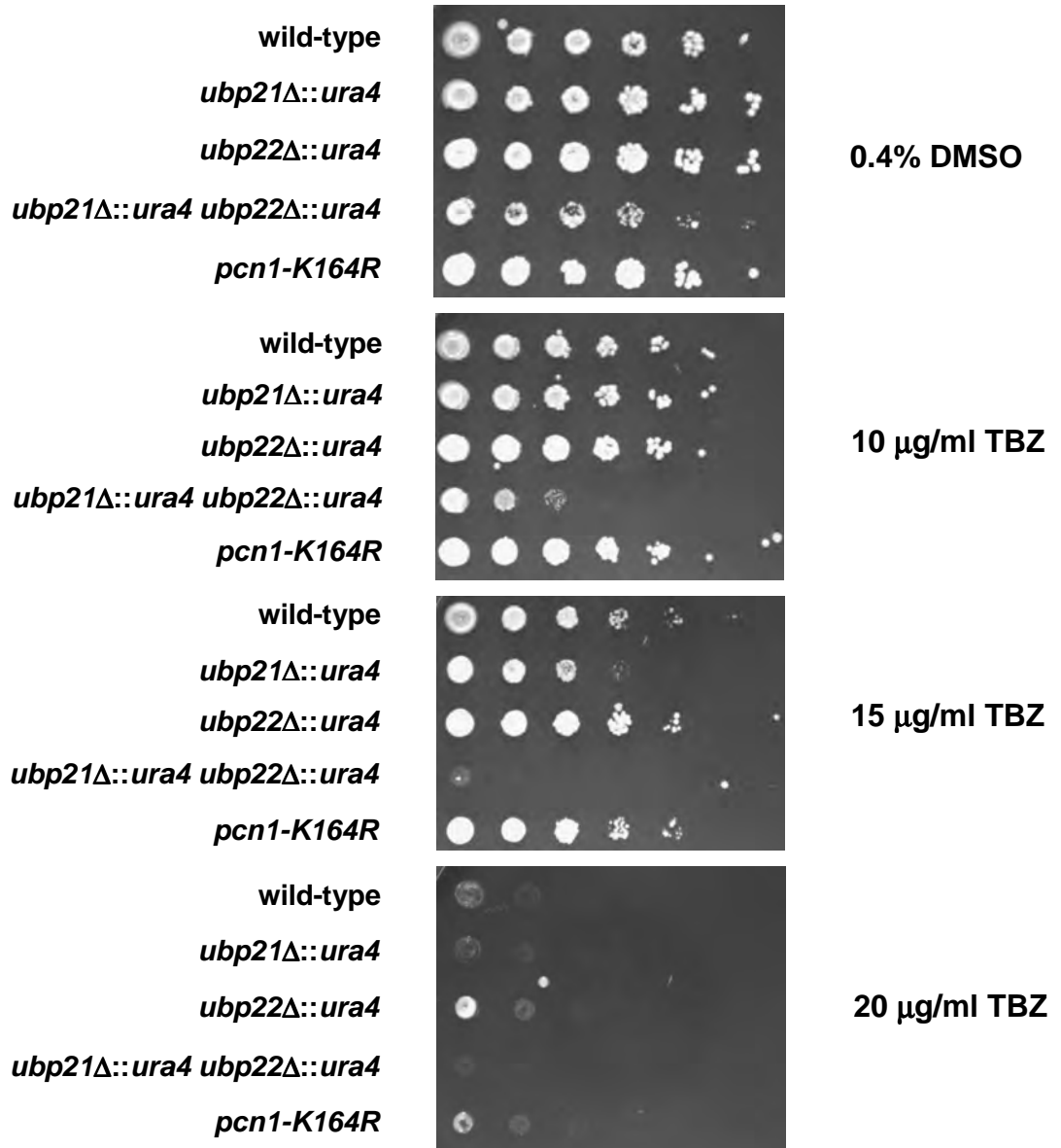


**Figure 5.39. Growth Analysis on Agar Containing Thiabendazole (TBZ) of the *S. pombe* Strains wild-type, *ubp21Δ::ura4*, *ubp22Δ::ura4*, *ubp21Δ::ura4 ubp22Δ::ura4* and *pcn1-K164R*.** The experiment was carried out as described in figure 5.26.



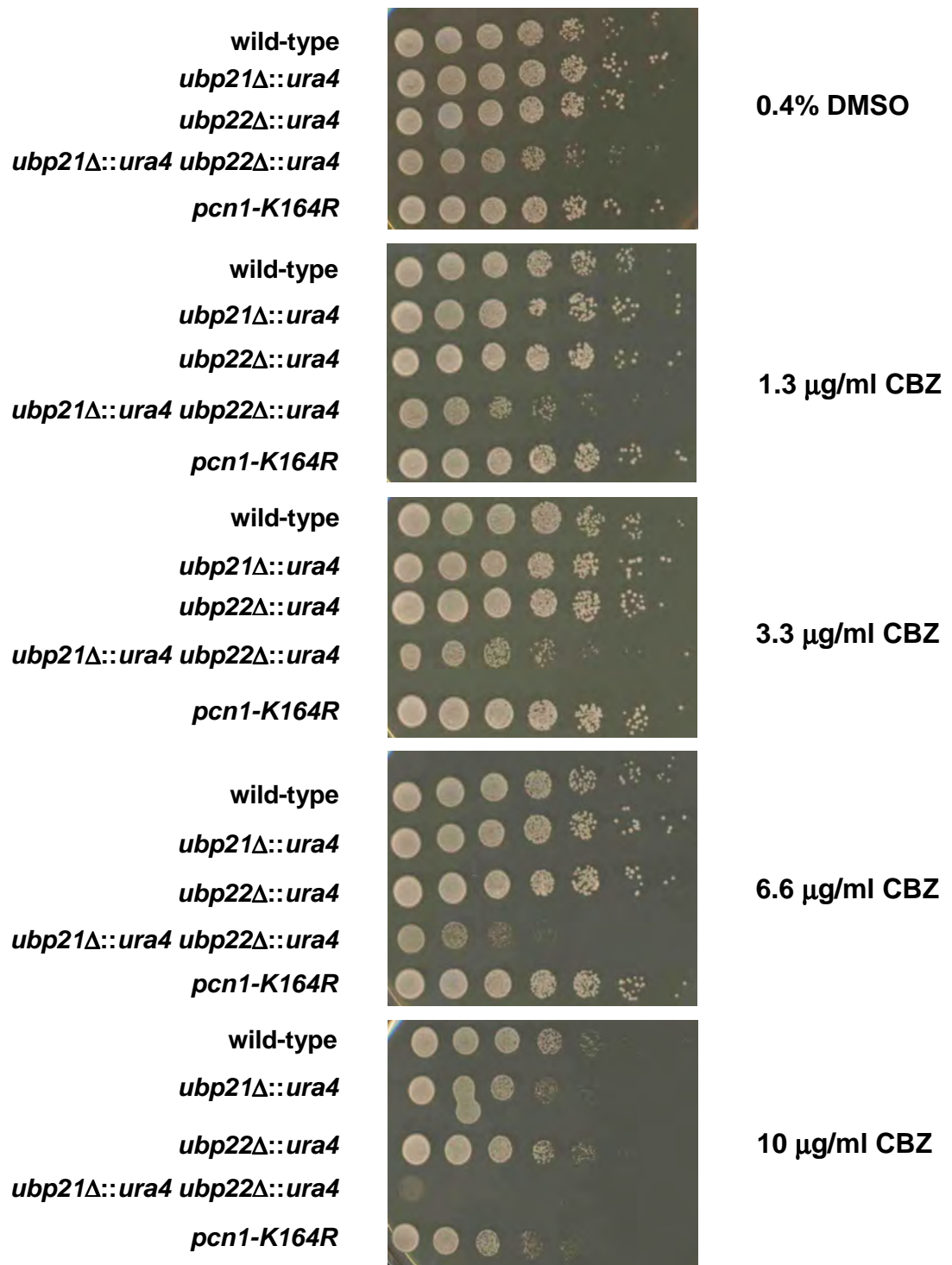


**Figure 5.40. Growth Analysis on Agar Containing Carbendazim (CBZ) of the *S. pombe* Strains wild-type, *ubp21Δ::ura4*, *ubp22Δ::ura4*, *ubp21Δ::ura4 ubp22Δ::ura4* and *pcn1-K164R*.** The experiment was carried as described in figure 5.26. .

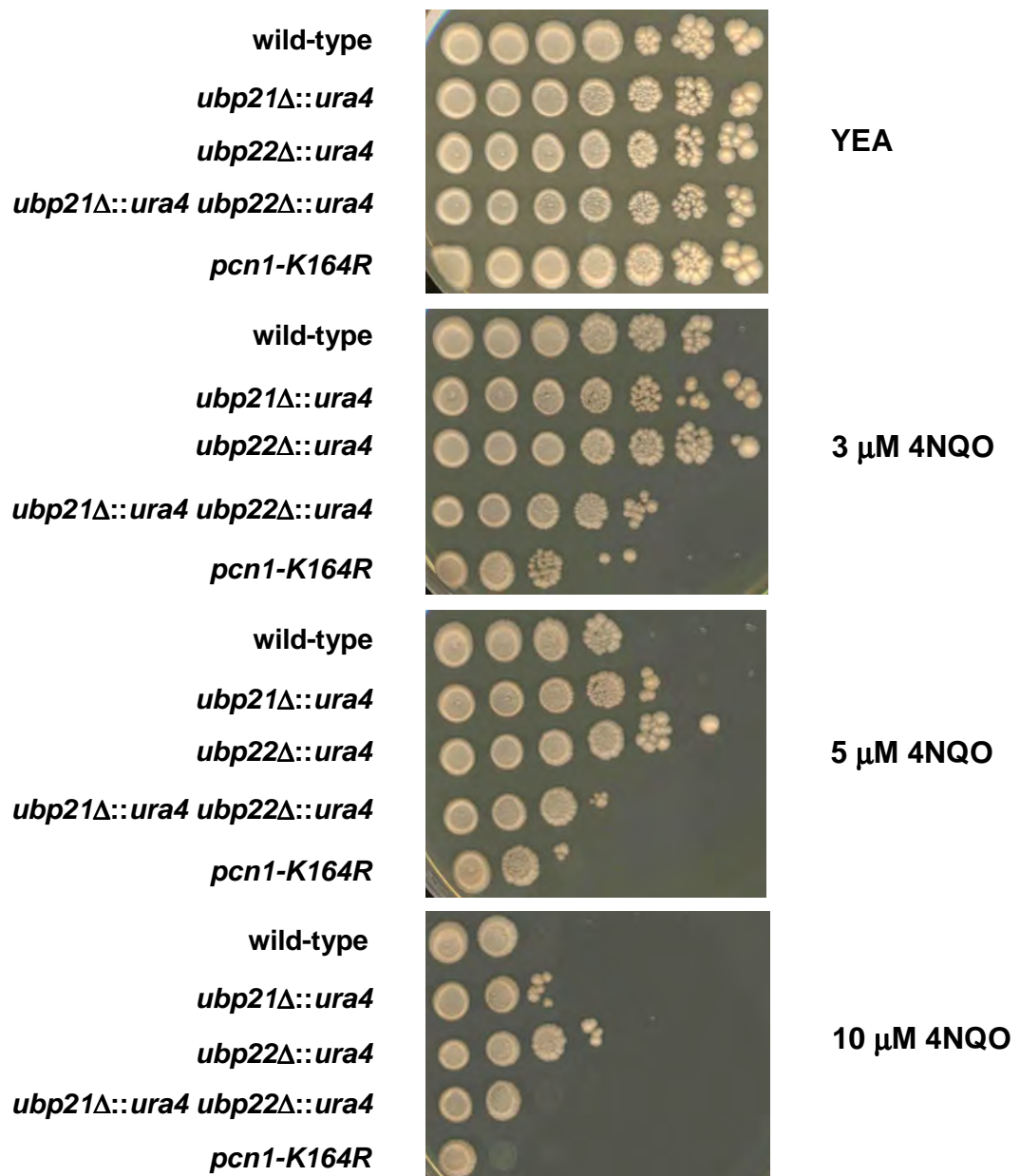


**Figure 5.41. Growth Analysis on Agar Containing 4-Nitroquinoline-1-oxide (4NQO) of the *S. pombe* Strains wild-type, *ubp21Δ::ura4*, *ubp22Δ::ura4*, *ubp21Δ::ura4 ubp22Δ::ura4* and *pcn1-K164R*.** The same number of cells of exponentially growing cultures were normalised by cell number, and six 1 in 6 serial dilutions were carried out. Cells were spotted onto agar containing different concentrations of 4NQO and colonies were grown for one week at 30°C.

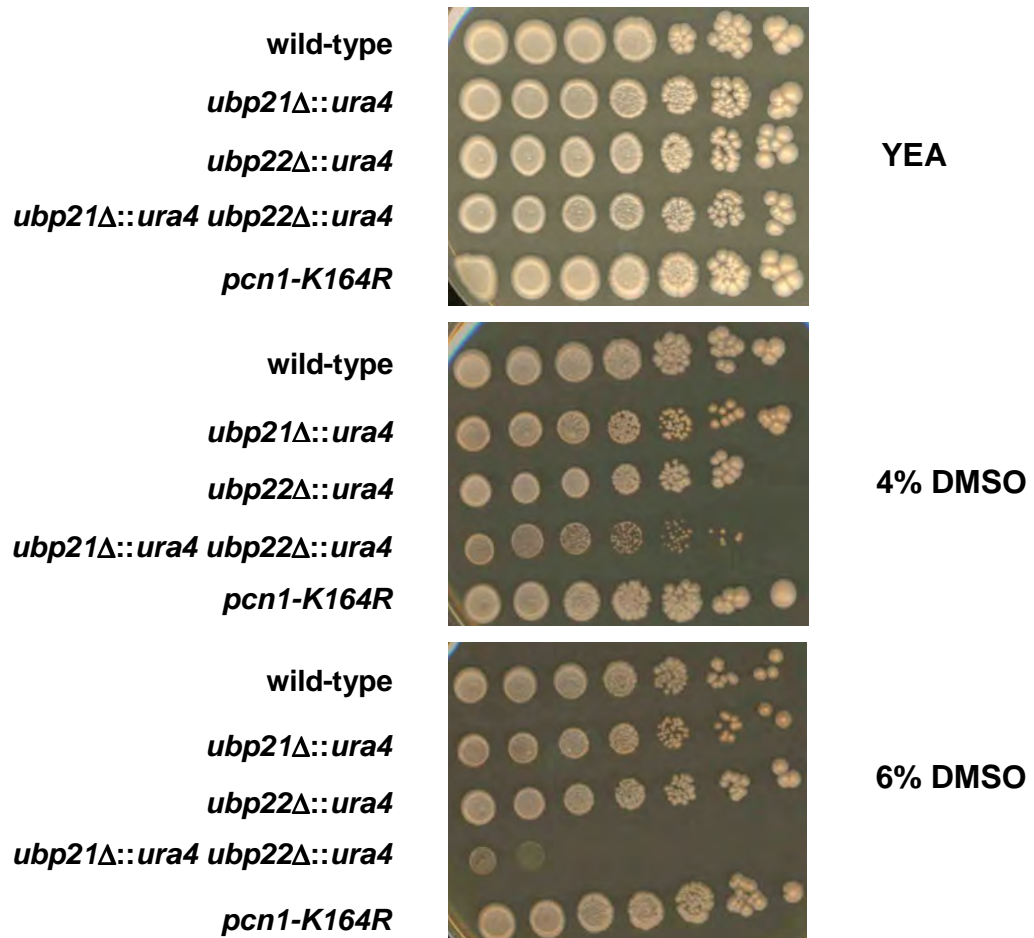


**Figure 5.42. Growth Analysis on Agar Containing Dimethylsulfoxide (DMSO) of the *S. pombe* Strains wild-type, *ubp21Δ::ura4*, *ubp22Δ::ura4*, *ubp21Δ::ura4 ubp22Δ::ura4* and *pcn1-K164R*.** The experiment was performed as in figure 5.41.

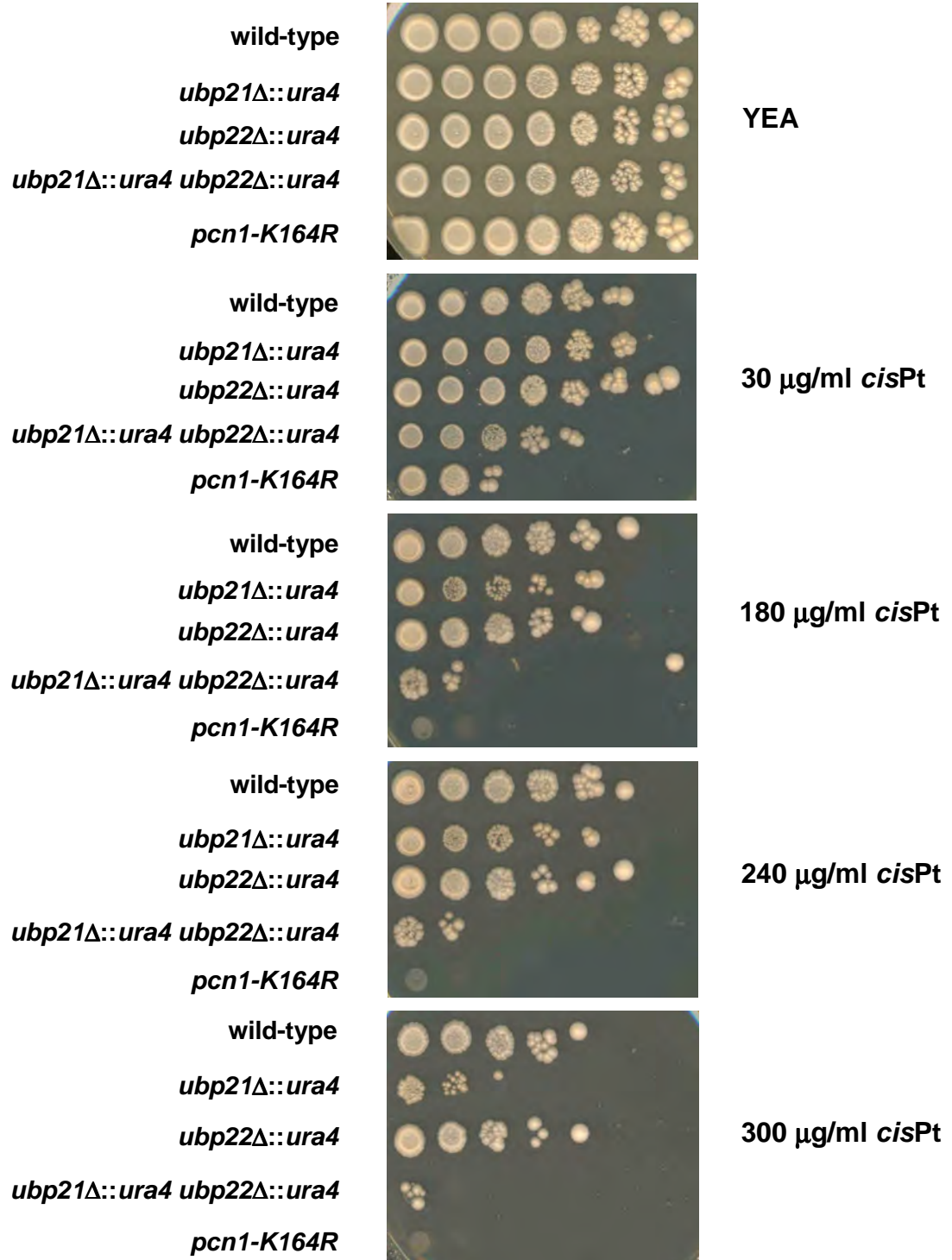
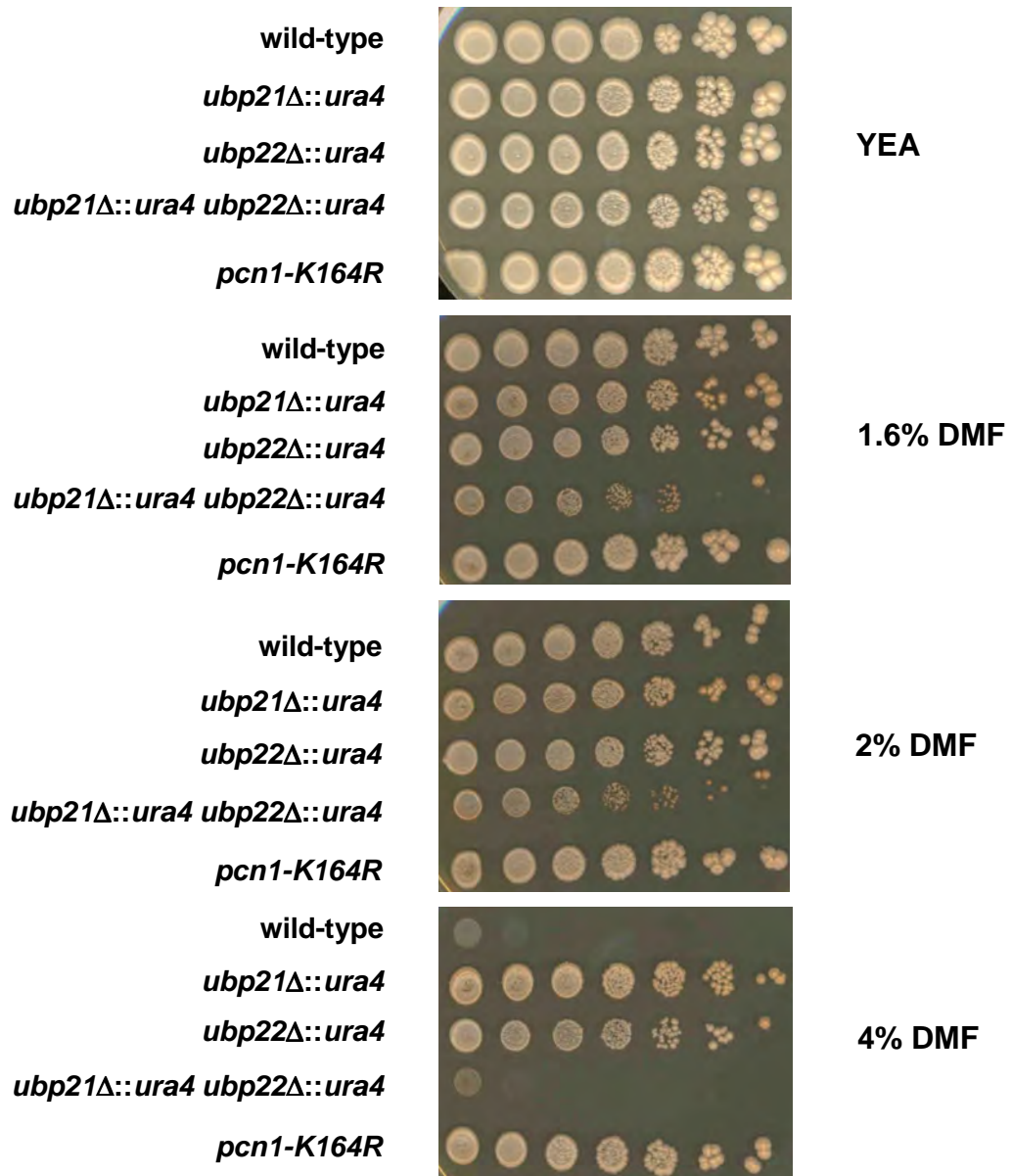
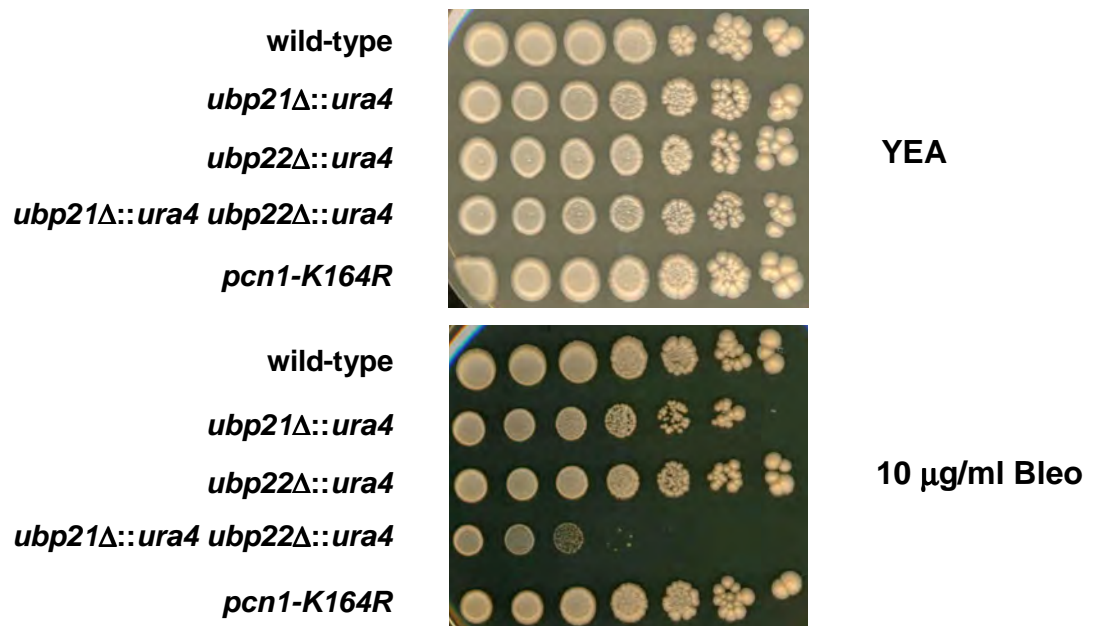


Figure 5.43. Growth Analysis on Agar Containing *cis*platin (*cisPt*) of the *S. pombe* Strains wild-type, *ubp21Δ::ura4*, *ubp22Δ::ura4*, *ubp21Δ::ura4 ubp22Δ::ura4* and *pcn1-K164R*. The experiment was performed as in figure 5.41.



**Figure 5.44. Growth Analysis on Agar Containing Dimethylformamide (DMF) of the *S. pombe* Strains wild-type, *ubp21Δ::ura4*, *ubp22Δ::ura4*, *ubp21Δ::ura4 ubp22Δ::ura4* and *pcn1-K164R*. The experiment was performed as in figure 5.41.**



**Figure 5.45. Growth Analysis on Agar Containing Bleomycin (Bleo) of the *S. pombe* Strains wild-type, *ubp21Δ::ura4*, *ubp22Δ::ura4*, *ubp21Δ::ura4 ubp22Δ::ura4* and *pcn1-K164R*. The experiment was performed as in figure 5.41.**



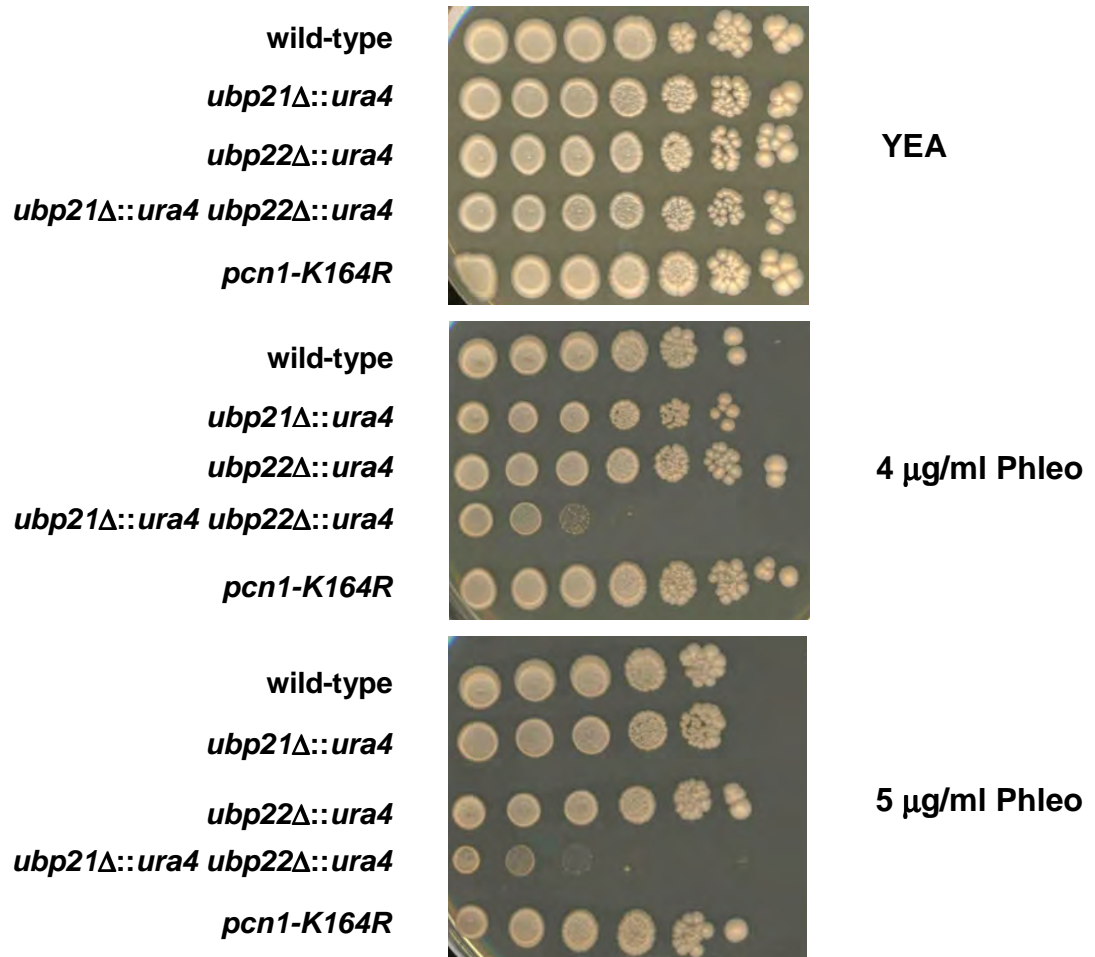


**Figure 5.46. Growth Analysis on Agar Containing Phleomycin (Phleo) of the *S. pombe* Strains wild-type, *ubp21Δ::ura4*, *ubp22Δ::ura4*, *ubp21Δ::ura4 ubp22Δ::ura4* and *pcn1-K164R*.** The experiment was performed as in figure 5.41.

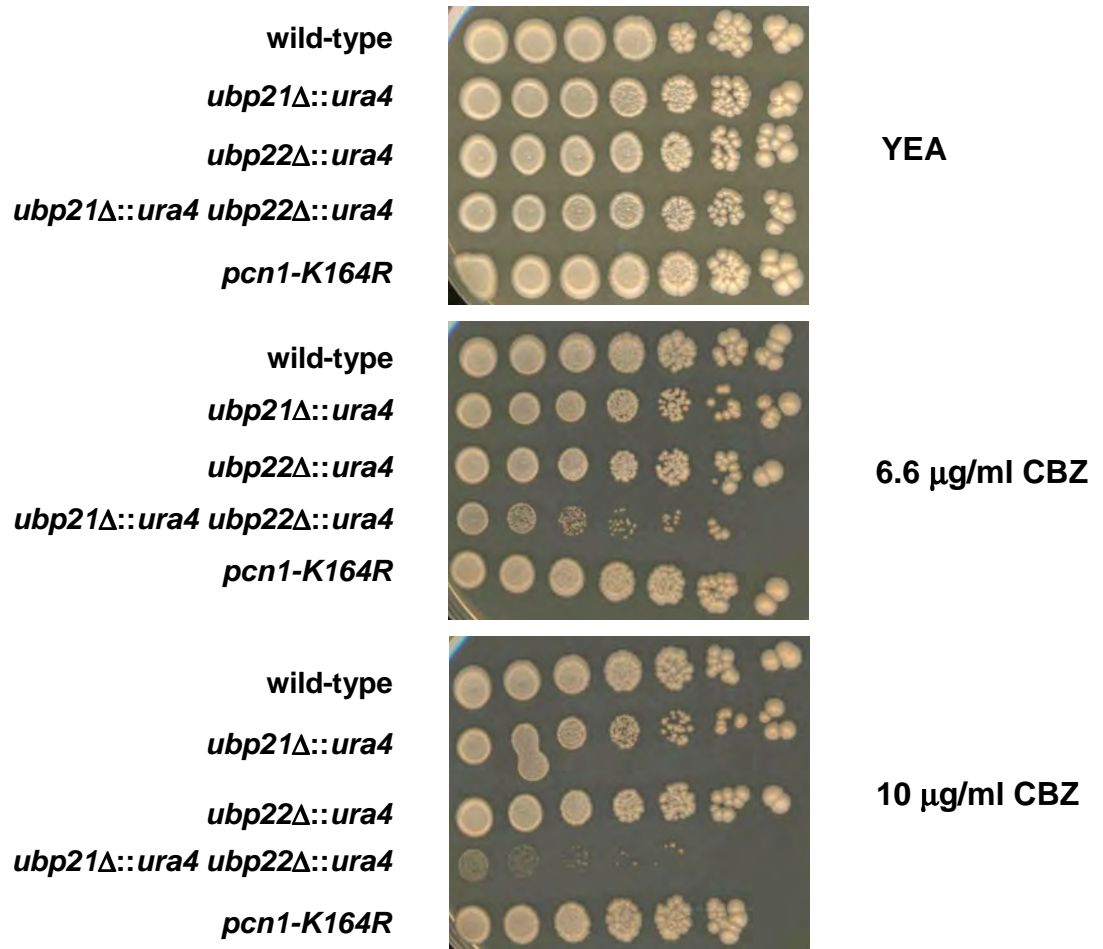


**Figure 5.47. Growth Analysis on Agar Containing Carbendazim (CBZ) of the *S. pombe* Strains wild-type, *ubp21Δ::ura4*, *ubp22Δ::ura4*, *ubp21Δ::ura4 ubp22Δ::ura4* and *pcn1-K164R*.** The experiment was performed as in figure 5.41.



<b>Genotoxin</b>	<b><i>ubp21Δ::ura4 ubp22Δ::ura4</i></b>	<b><i>pcn1-K164R</i></b>
UVC	+++	++++
HU	+++	0
DMSO	+++	0
Temperature	+++	-
CPT	+++	++
<i>cisplatin</i>	+++	++++
Bleomycin	+++	0
Phleomycin	+++	0
Thiabendazole	+++	0
Carbendazim	+++	0
4NQO	++	+++
IR	++	++++
H <sub>2</sub> O <sub>2</sub>	++	0
MMS	+/0	++++
DMF	+/0	0

**Table 5.1. Sensitivity of *ubp21Δ::ura4 ubp22Δ::ura4* and *pcn1-K164R* To Genotoxins.** Table summarises the relative sensitivities of these strains to the genotoxins tested. Key: ++++ extremely high sensitivity; +++ relatively high sensitivity; ++ intermediate; + low; 0 none; - not tested.

Additional Domains		<i>S. cerevisiae</i> Deubiquitinating Enzyme
	UBP/USP Superfamily DUBs	
DUSP domain	<i>ScUbp12</i> -1254 a.a. -DUSP domain -YJL197W -Likely orthologues are <i>SpUbp1</i> , <i>SpUbp12</i> , <i>HsUSP4</i> , <i>HsUSP11</i> , <i>HsUSP15</i> .	
Zinc Finger Domain	<i>ScUbp8</i> -471 a.a. -UBP-type zinc finger domain -YMR223W -Likely orthologues are <i>SpUbp8</i> , <i>HsUSP22</i> , <i>HsUSP27*</i> , <i>HsUSP51*</i> .	
	<i>ScSad1</i> -448 a.a. -UBP-type zinc finger domain -YFR005C -Likely orthologues are <i>SpUbp10</i> , <i>HsUSP39</i> <sup>SNUT2*</sup> .	
	<i>ScUbp14</i> -803 a.a. -UBP-type zinc finger domain -PHD-type zinc finger domain -Two UBA domains within UBP/USP domain. -YBR058C -Likely orthologues are <i>SpUbp14</i> <sup>Ucp2</sup> , <i>HsUSP5</i> <sup>IsoT1</sup> , <i>HsUSP13</i> <sup>IsoT2</sup> .	
Ubiquitin Domain	<i>ScUbp6</i> -499 a.a. -Ubiquitin domain. -YFR010W -Likely orthologues are <i>SpUbp6</i> , <i>HsUSP14</i> .	
Trans-membrane Helix	<i>ScUbp1</i> -809 a.a. -Probable trans-membrane helix. -YDL122W -Likely orthologue is <i>SpUbp11</i> .	
Exonuclease Domain	<i>ScPan2</i> -1115 a.a. -WD-40 repeat. -Exonuclease domain. -Ribonuclease H fold -YGL094C -Likely orthologues are <i>SpUbp13</i> <sup>Pan2</sup> , <i>HsUSP52</i> .	

**Table 6.1. DUBs in *S. cerevisiae*.** Important facts for each *S. cerevisiae* DUB is provided. USP/UBP DUBs are shown in green, UCHs in blue, OTUs in pink, and JAMMs in beige. USP/UBPs are further divided by additional domains. A single asterisk indicates that the enzyme is unlikely to possess DUB activity.

MATH domain	<p>ScUbp15</p> <p>-1230 a.a.</p> <p>-MATH domain.</p> <p>-YMR304W</p> <p>-Likely orthologues are <i>SpUbp21</i>, <i>SpUbp22</i>, <i>HsHAUSP</i><sup>USP7</sup>.</p>
Rhodanese domain	<p>ScDoa4<sup>Ubp4</sup></p> <p>-926 a.a.</p> <p>-Rhodanese domain.</p> <p>-YDR069C</p> <p>-Paralogues are <i>ScUbp5</i> and <i>ScUbp7</i></p> <p>-Likely orthologues are <i>SpDoa4</i>, <i>HsUSP8</i><sup>UBPY</sup>.</p>
	<p>ScUbp5</p> <p>-805 a.a.</p> <p>-Rhodanese domain.</p> <p>-YER144C</p> <p>-Paralogues are <i>ScDoa4</i><sup>Ubp4</sup> and <i>ScUbp7</i></p> <p>-Likely orthologues are <i>SpDoa4</i>, <i>HsUSP8</i><sup>UBPY</sup>.</p>
	<p>ScUbp7</p> <p>-1071 a.a.</p> <p>-Rhodanese domain.</p> <p>-YIL156W</p> <p>-Paralogues are <i>ScDoa4</i><sup>Ubp4</sup> and <i>ScUbp7</i></p> <p>-Likely orthologues are <i>SpDoa4</i>, <i>HsUSP8</i><sup>UBPY</sup>.</p>
No additional domains	<p>ScUbp2</p> <p>-1272 a.a</p> <p>-YOR124C</p> <p>-Likely orthologues are <i>ScUbp2</i>, <i>HsUSP25</i>, <i>HsUSP28</i>.</p>
	<p>ScUbp3</p> <p>-912 a.a.</p> <p>-YER151C</p> <p>-Likely orthologues are <i>ScUbp3</i>, <i>HsUSP10</i>.</p>
	<p>ScUbp9</p> <p>-754 a.a.</p> <p>-YER098W</p> <p>-Paralogue is <i>ScUbp13</i></p> <p>-Likely orthologues are <i>SpUbp9</i>, <i>HsUSP12</i>, <i>HsUSP46</i>.</p>
	<p>ScUbp13</p> <p>-688 a.a.</p> <p>-YBL067C</p> <p>-Paralogue is <i>ScUbp9</i></p> <p>-Likely orthologues are <i>SpUbp9</i>, <i>HsUSP12</i>, <i>HsUSP46</i>.</p>
	<p>ScUbp11</p> <p>-717 a.a.</p> <p>-YKR098C</p>

**Table 6.2. DUBs in *S. cerevisiae*.** Legend as Table 6.1.

	ScUbp10Dot4 -792 a.a. -Three poly-Glu tracts -Two poly-Ser tracts -YNL186W	
	ScUbp16 -499 a.a. -YPL072W	
	UCH Superfamily DUBs	
	ScYuh1 -236 a.a. -YJR099W -Likely orthologues are <i>SpUch1</i> , <i>HsUCH-L1</i> , <i>HstUCH-L3</i> .	
	OTU Superfamily DUBs	
	ScOtu1 -301 a.a. -C2H2 zinc finger -YFL044C -Likely orthologues are <i>SpOtu1</i> , <i>HsOTU1</i> <sup>YOD1</sup> .	
	ScOtu2 -307 a.a. -YHL013C -Likely orthologues are <i>ScOtu2</i> , <i>HsOTUD6B</i> and <i>HsOTUD6A</i> .	
	JAMM Superfamily DUBs	
	ScRpn11 -306 a.a. -YFR004W -Likely orthologues are <i>SpRpn11</i> <sup>Pad1</sup> , <i>HsRPN11</i> .	
	ScRri1Csn5/Jab1 -455 a.a. -YDL216C -Likely orthologues are <i>SpCsn5</i> , <i>HsCSN5</i> .	

**Table 6.3. DUBs in *S. cerevisiae*.** Legend as Table 6.1.

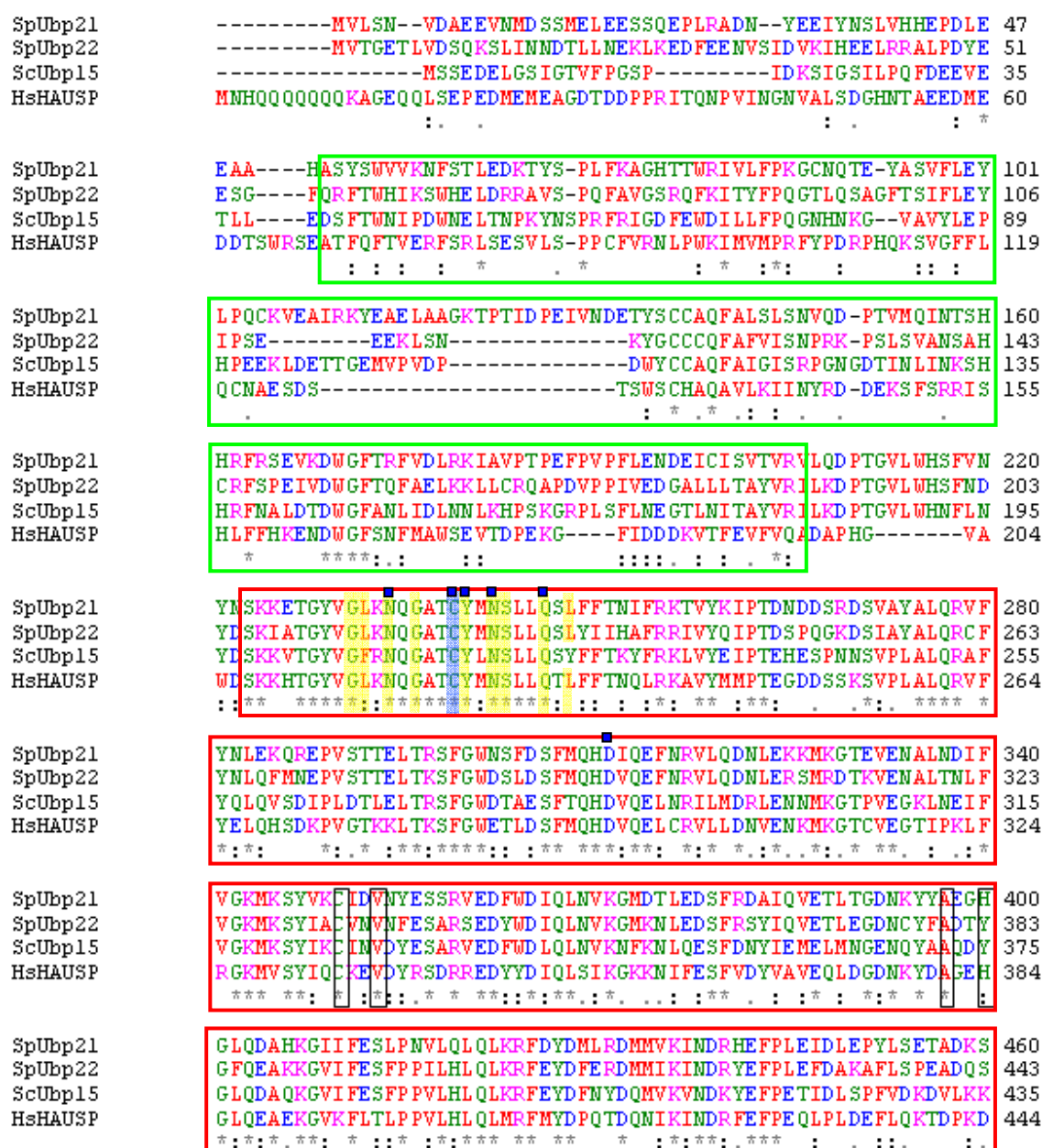


**Figure 6.1. EBI-CLUSTALW Alignment of the Amino Acid Sequence *SpUbp21*, *SpUbp22*, *ScUbp15* and *HsHAUSP*<sup>USP7</sup>.** N-terminal amino acids are shown. The second portion of this alignment, depicting the central amino acids, is shown in figure 6.2 and the third portion, depicting the C-terminal amino acids, is shown in figure 6.3. The residue colouring, boxed regions and conservation symbols utilised in this alignment are as described in Figures 5.5 and 5.8. Additionally, the circularly permuted zinc finger residues are boxed in black (Krishna and Grishin, 2004).



**Figure 6.2. EBI-CLUSTALW Alignment of the Amino Acid Sequence *SpUbp21*, *SpUbp22*, *ScUbp15* and *HsHAUSP*<sup>7</sup>.** Central amino acids are shown. The first portion of this alignment, depicting the N-terminal amino acids, is shown in figure 6.1 and the third portion, depicting the C-terminal amino acids, is shown in figure 6.3. The residue colouring, boxed regions and conservation symbols utilised in this alignment are as described in Figures 5.5 and 5.8.



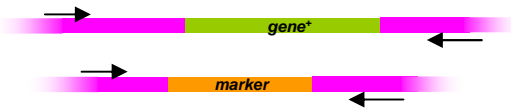
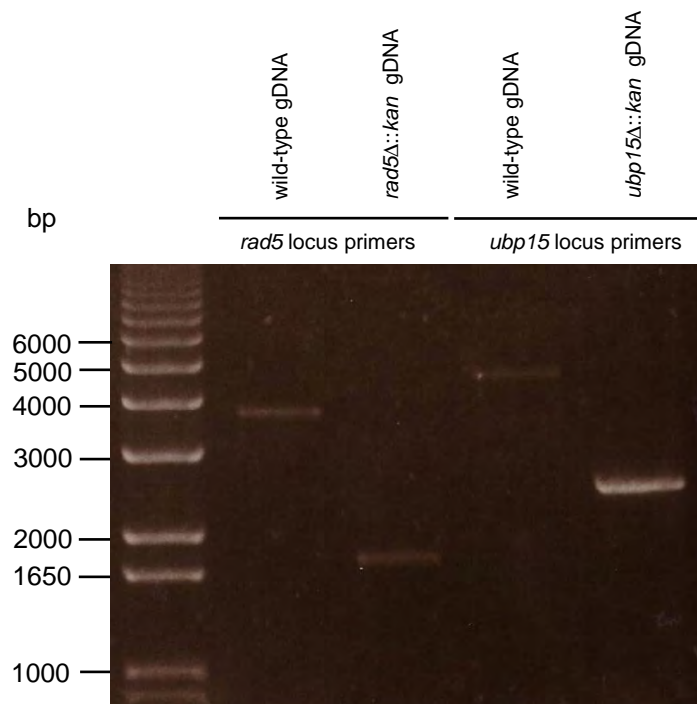


**Figure 6.4. PCR Amplification of the *rad5* and *ubp15* Loci Utilising Primers that Anneal to Flanking DNA and Genomic DNA.** From of the *S. cerevisiae* Strains wild-type, *rad5* $\Delta$ ::*kan*, and *ubp15* $\Delta$ ::*kan*. The lower diagram shows the PCR strategy in wild-type gDNA and deleted gDNA. Primers that flank the gene locus are depicted by arrows.



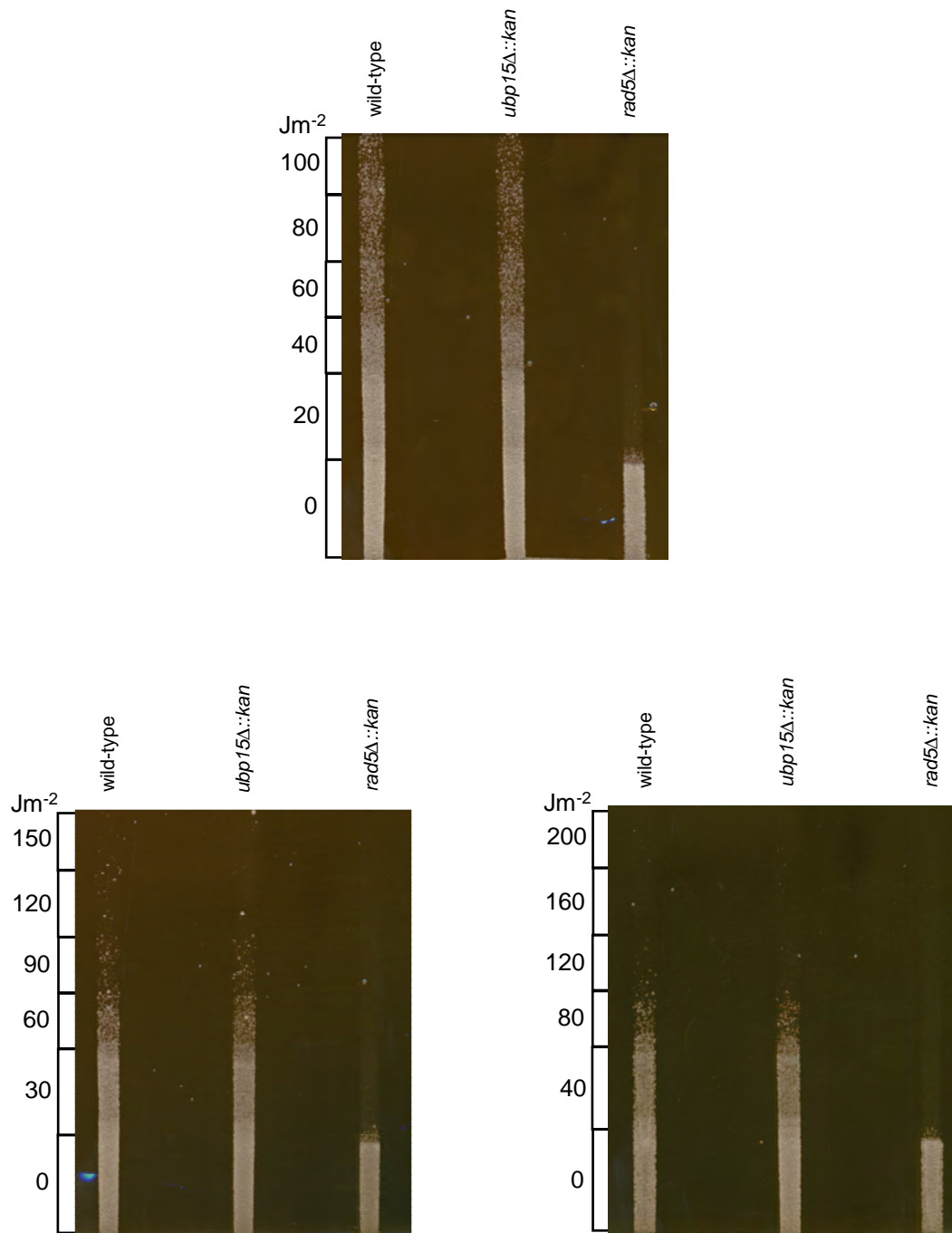


**Figure 6.5. Drop Test Assays Measuring the Relative Sensitivities of *S. cerevisiae* Strains wild-type, *ubp15Δ* and *rad5Δ* to Different Doses of UVC.** Exponentially growing cultures were normalised by cell concentration and dropped down YPD agar plates, which were subsequently exposed to a UVC dose gradient as indicated. Plates were grown for three days at 25°C before photographing.

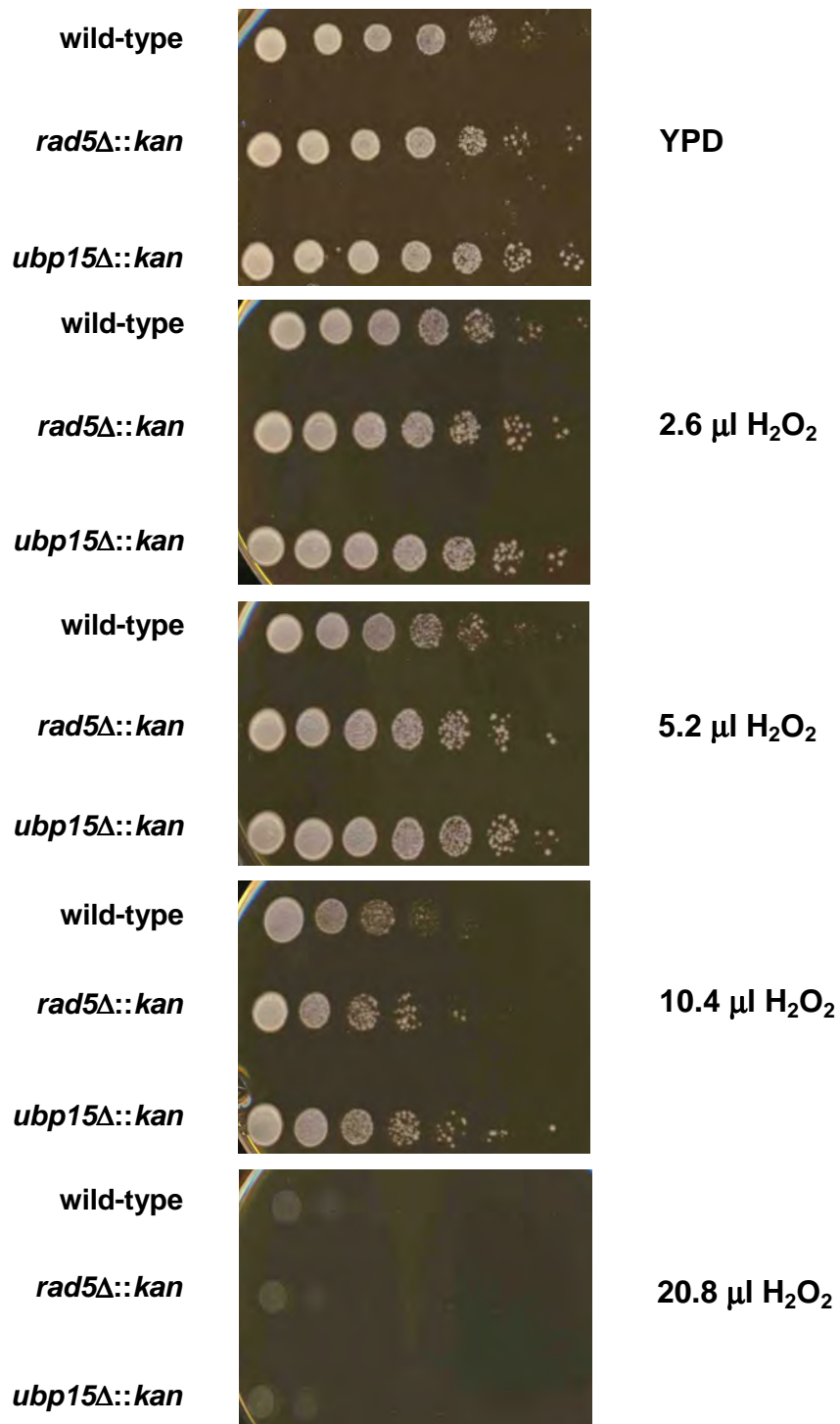


**Figure 6.6. Growth Analysis on Agar Containing Hydrogen Peroxide of the *S. cerevisiae* Strains wild-type, *ubp15Δ* and *rad5Δ*.** The same number of cells of exponentially growing cultures were normalised by cell number, and six 1 in 6 serial dilutions were carried out. Cells were spotted onto agar containing H<sub>2</sub>O<sub>2</sub> and colonies were grown for two days at 25°C.

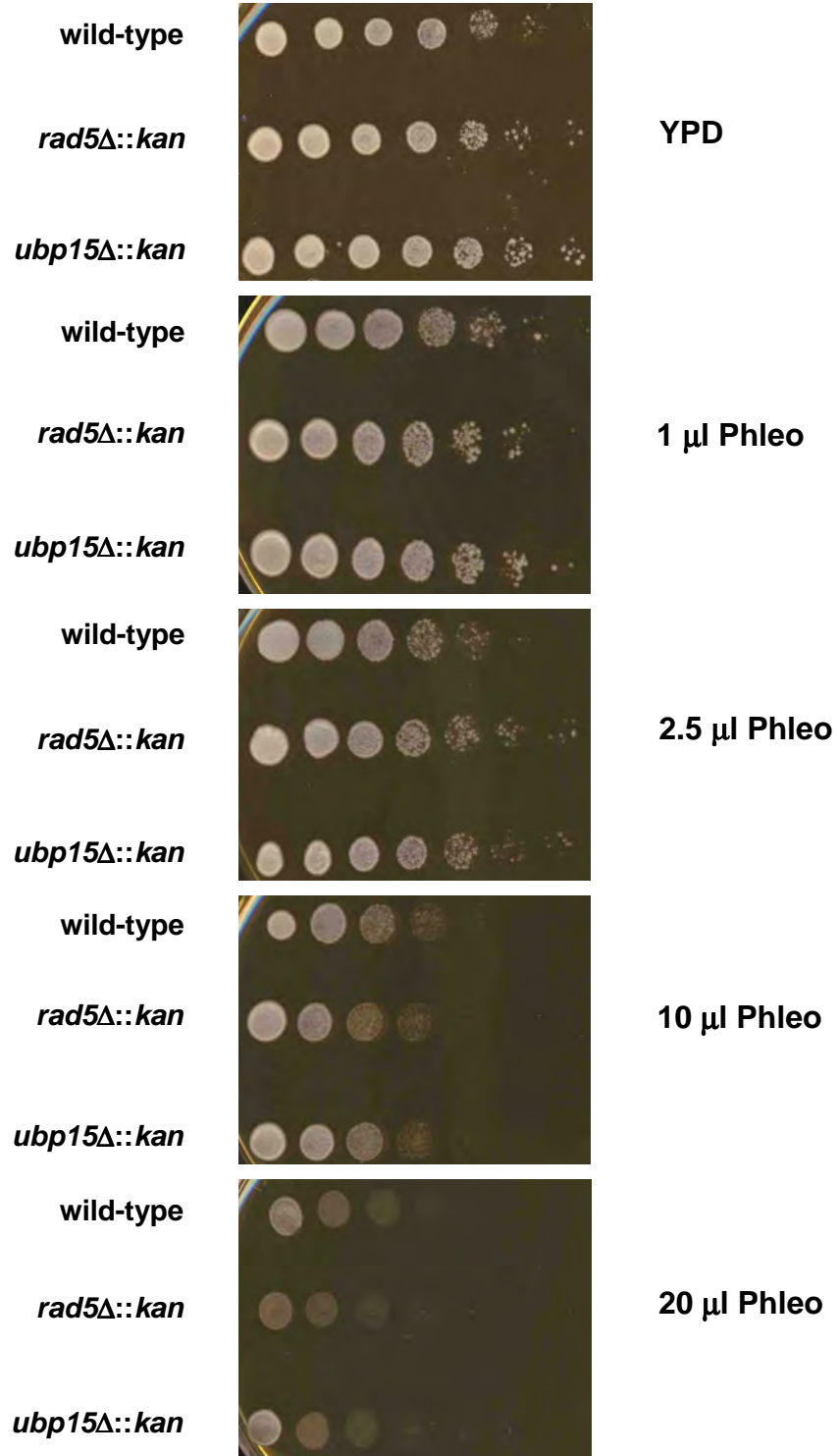


**Figure 6.7. Growth Analysis on Agar Containing Phleomycin of the *S. cerevisiae* Strains wild-type, *ubp15Δ* and *rad5Δ*. As Figure 6.6.**

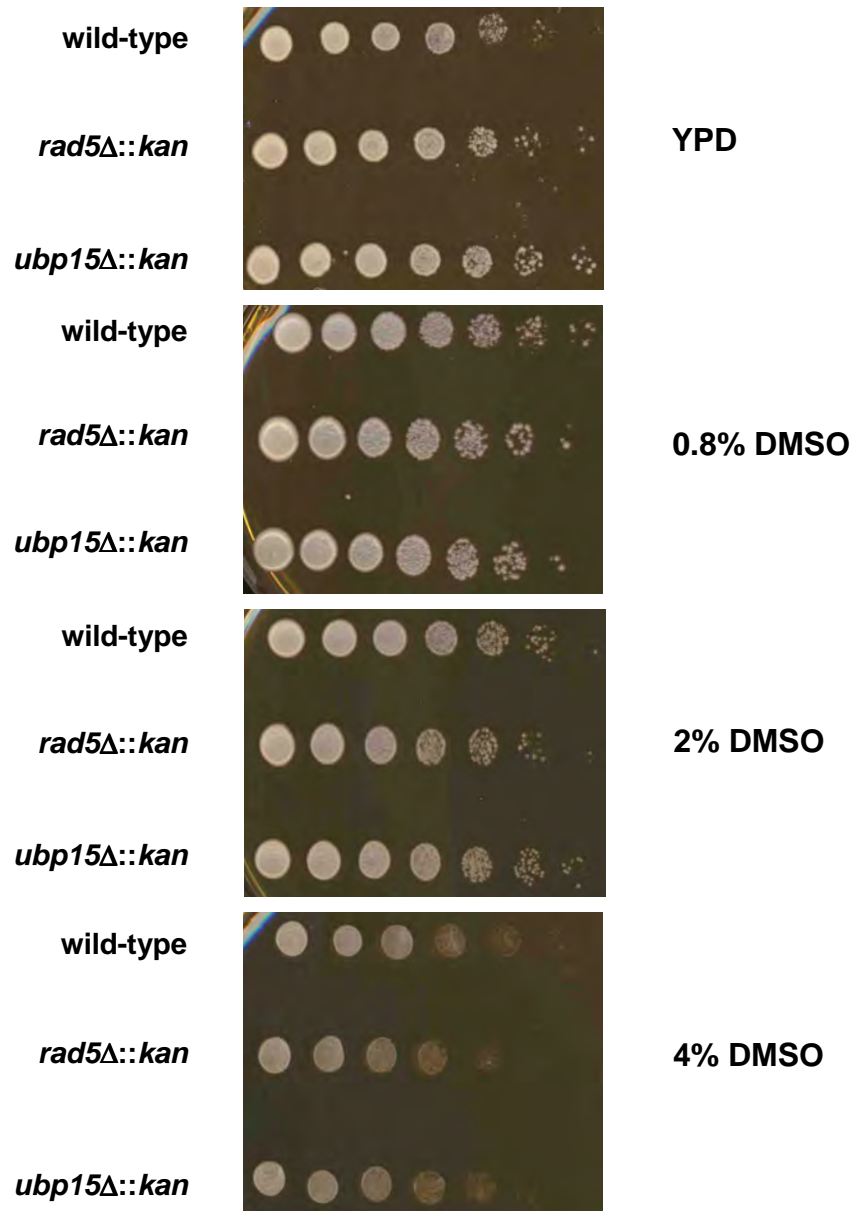


**Figure 6.8. Growth Analysis on Agar Containing Hydrogen Peroxide of the *S. cerevisiae* Strains wild-type, *ubp15Δ::kan* and *rad5Δ::kan*. As Figure 6.6..**

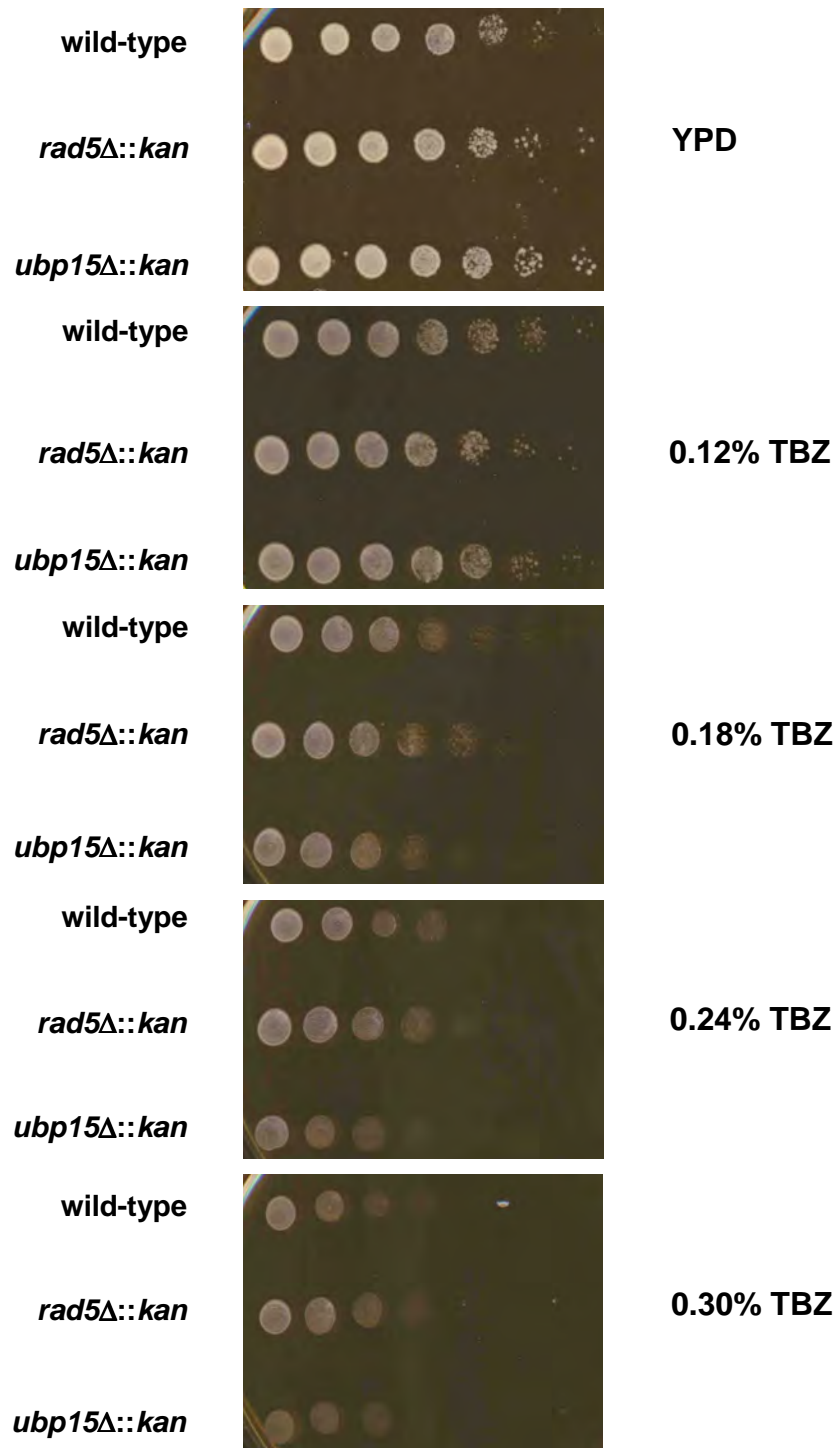


**Figure 6.9. Growth Analysis on Agar Containing Thiabendazole (TBZ) of the *S. cerevisiae* Strains wild-type, *ubp15Δ* and *rad5Δ*. As Figure 6.6.**

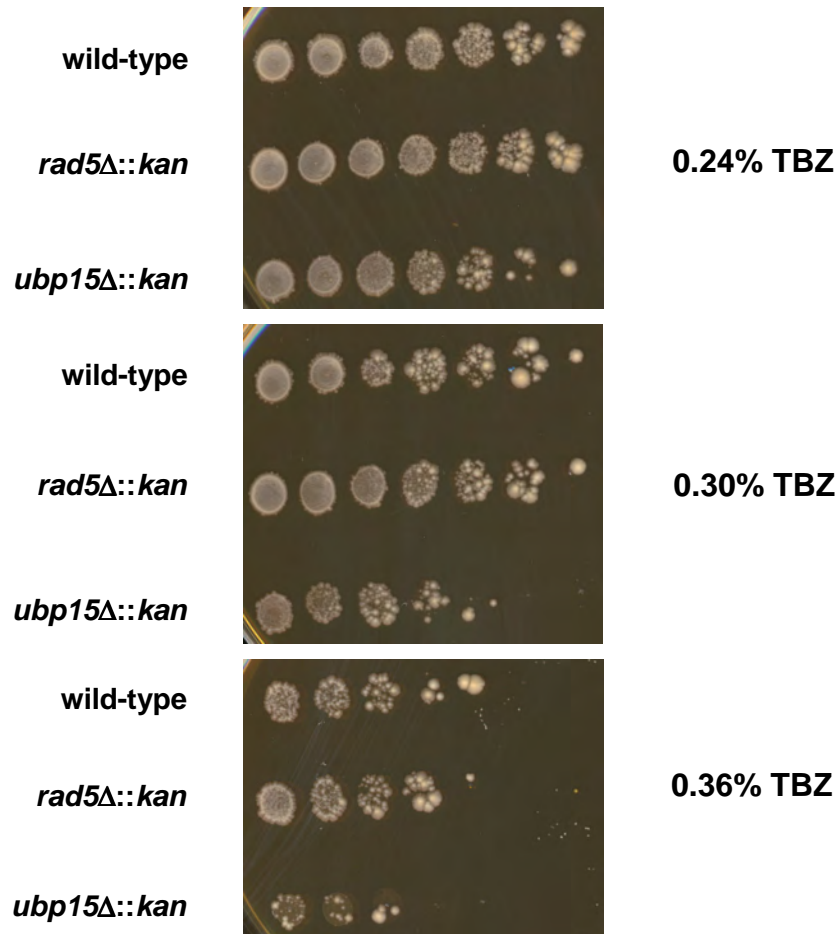


**Figure 6.10. Growth Analysis on Agar Containing Thiabendazole of the *S. cerevisiae* Strains wild-type, *ubp15Δ::kan* and *rad5Δ::kan*.** The same number of cells of exponentially growing cultures were normalised by cell number, and six 1 in 6 serial dilutions were carried out. Cells were spotted onto agar containing TBZ and colonies were grown for one week at 25°C.

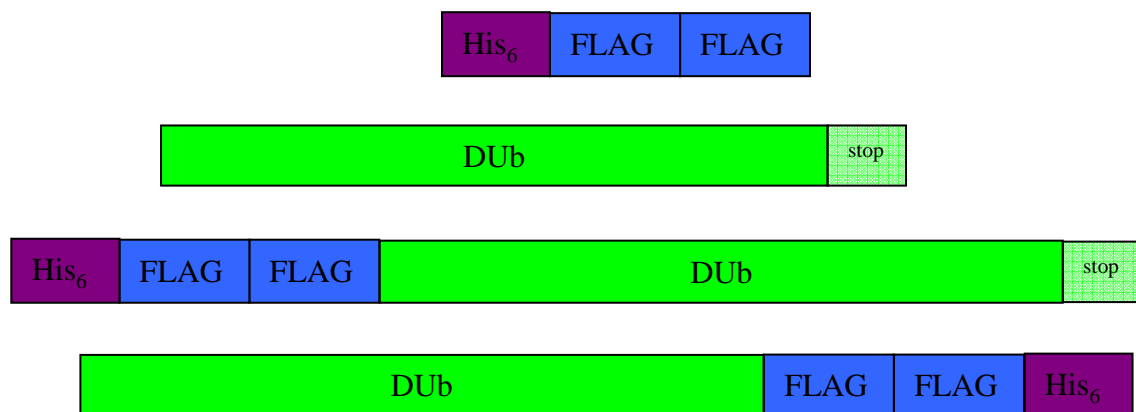


**Figure 7.1. Exogenously Expressed *Sp*Ubp21 and *Sp*Ubp22 Protein Constructs.**  
From top to bottom: vector only control, untagged, N-terminally tagged, C-terminally tagged.

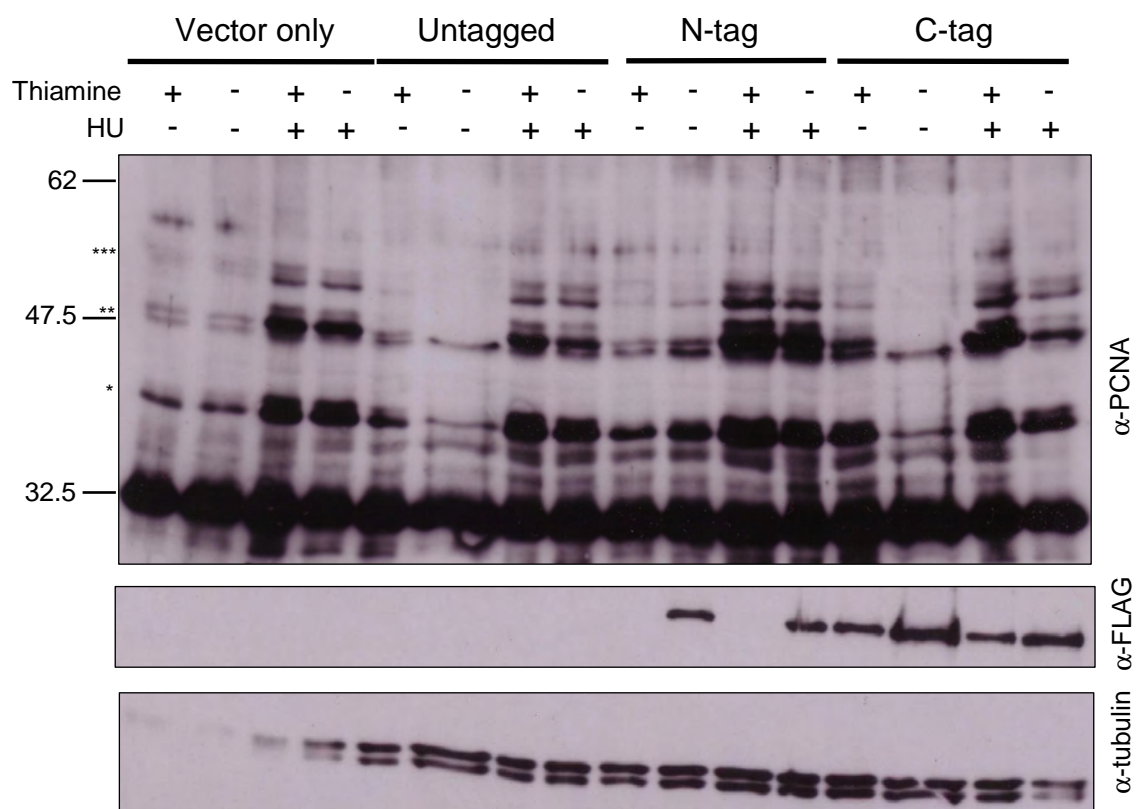


**Figure 7.2. *Sp*PCNA Ubiquitination Following Exogenous Expression of *Sp*Ubp21.** Wild-type cells transformed with the *ubp21* constructs (as indicated) maintained on minimal media with or without thiamine (as indicated) were treated with 10 mM HU or left untreated (as indicated) for 3 hours. Whole cell extracts were then fractionated and probed with the indicated antibodies. Sizes of mono-ubiquitinated (\*), di-ubiquitinated (\*\*) and tri-ubiquitinated (\*\*\*) forms of *Sp*PCNA are labelled.



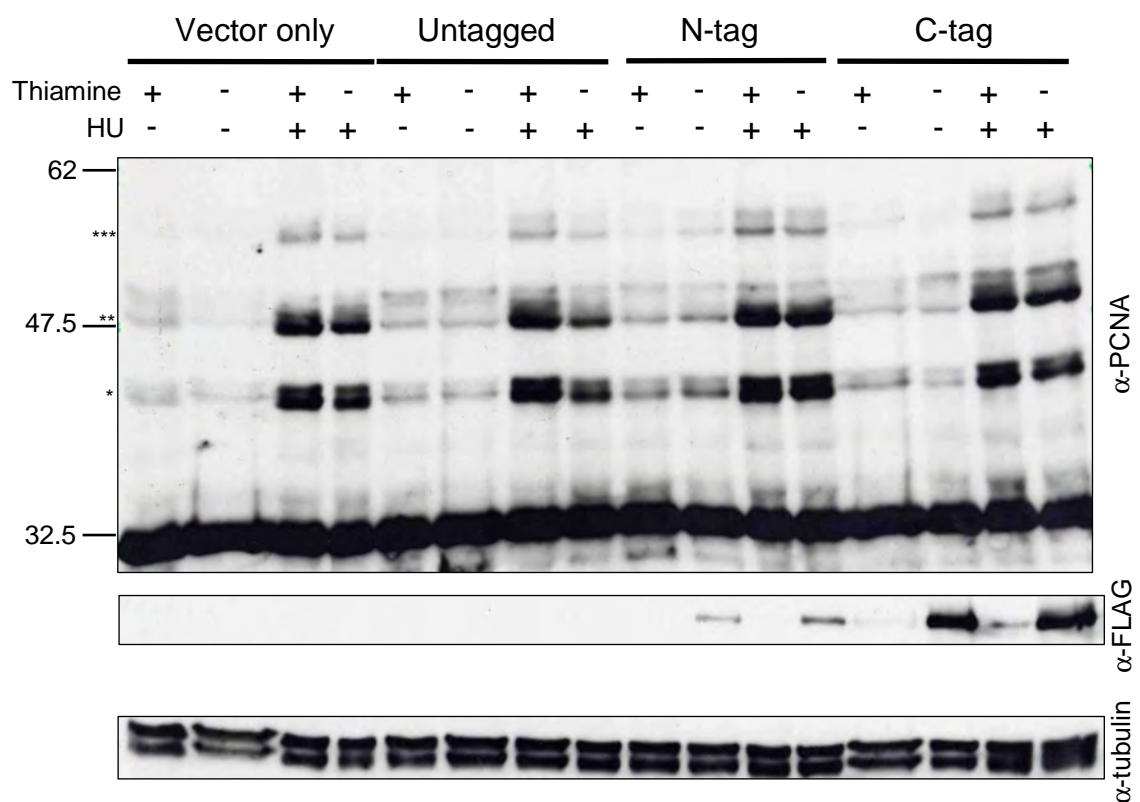


**Figure 7.3. *Sp*PCNA Ubiquitination Following Exogenous Expression of *Sp*Ubp22.** Wild-type cells transformed with the *ubp22* constructs (as indicated) maintained on minimal media with or without thiamine (as indicated) were treated with 10 mM HU or left untreated (as indicated) for 3 hours. Whole cell extracts were then fractionated and probed with the indicated antibodies. Sizes of mono-ubiquitinated (\*), di-ubiquitinated (\*\*) and tri-ubiquitinated (\*\*\*) forms of *Sp*PCNA are labelled.

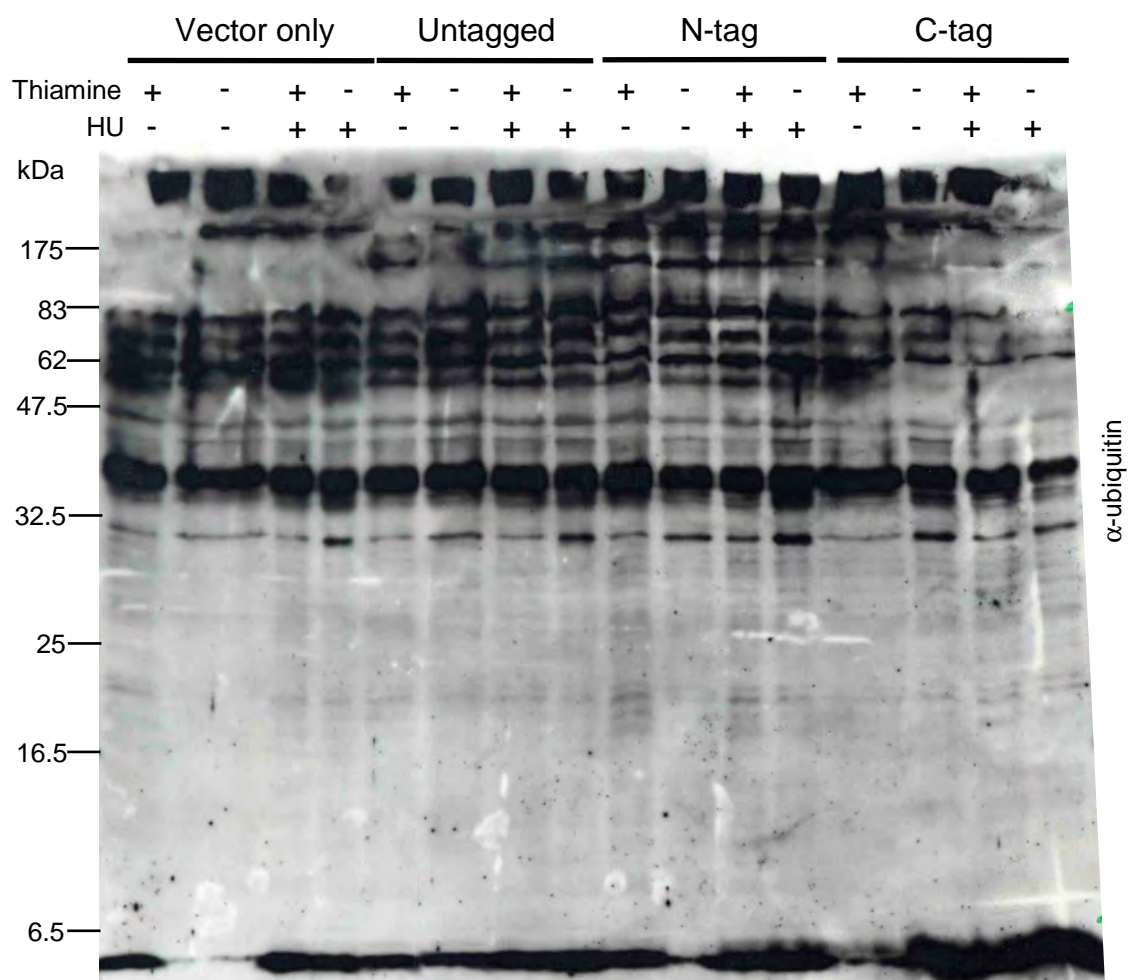


**Figure 7.4. Status of Ubiquitinated Species of Cellular Proteins Following the Exogenous Expression of *Sp*Ubp22.** Legend as previous figure.

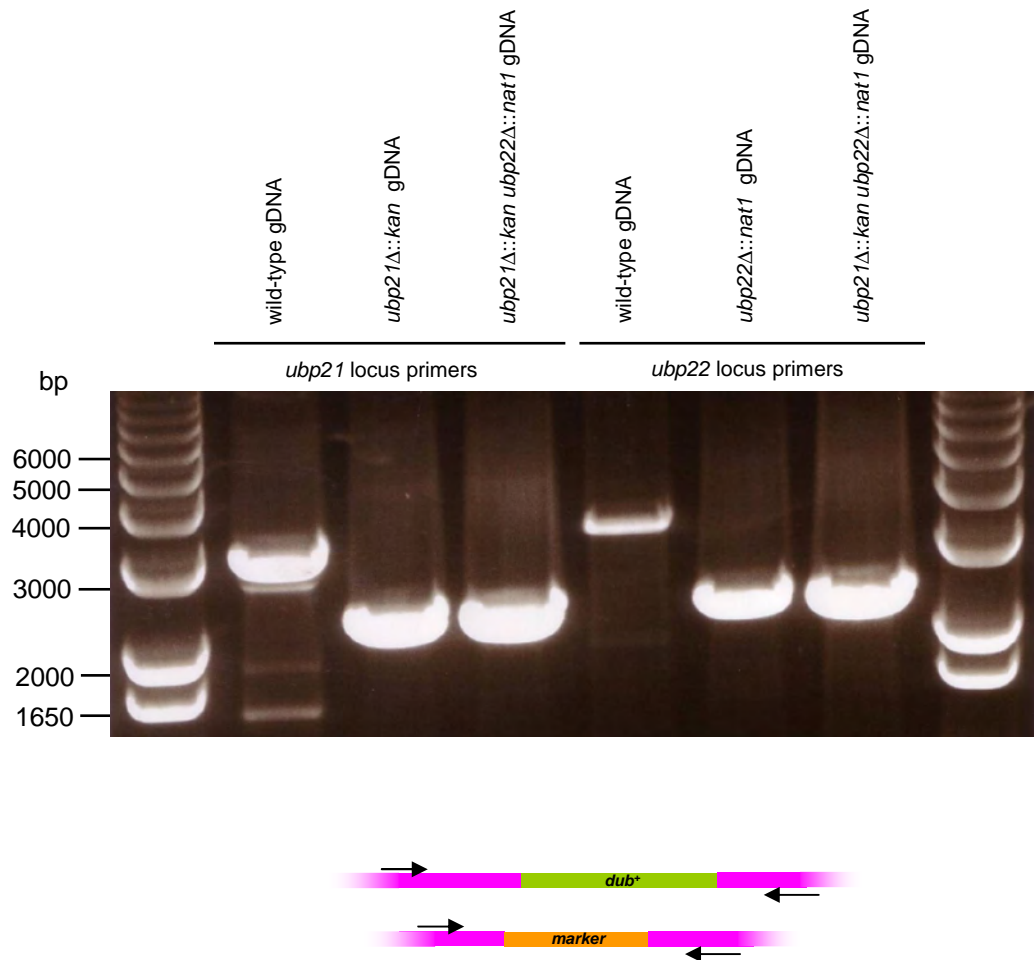


**Figure 7.5. PCR Amplification of the *ubp21* and *ubp22* Loci Utilising Primers that Anneal to Flanking DNA and Genomic DNA.** From of the *S. pombe* Strains: Wild-type, *ubp21*Δ::kan, *ubp22*Δ::nat1 and *ubp21*Δ::kan *ubp22*Δ::nat1. The lower diagram shows the PCR strategy in wild-type gDNA and *dub*-deleted gDNA. Primers that flank the DUB gene locus are depicted by arrows.

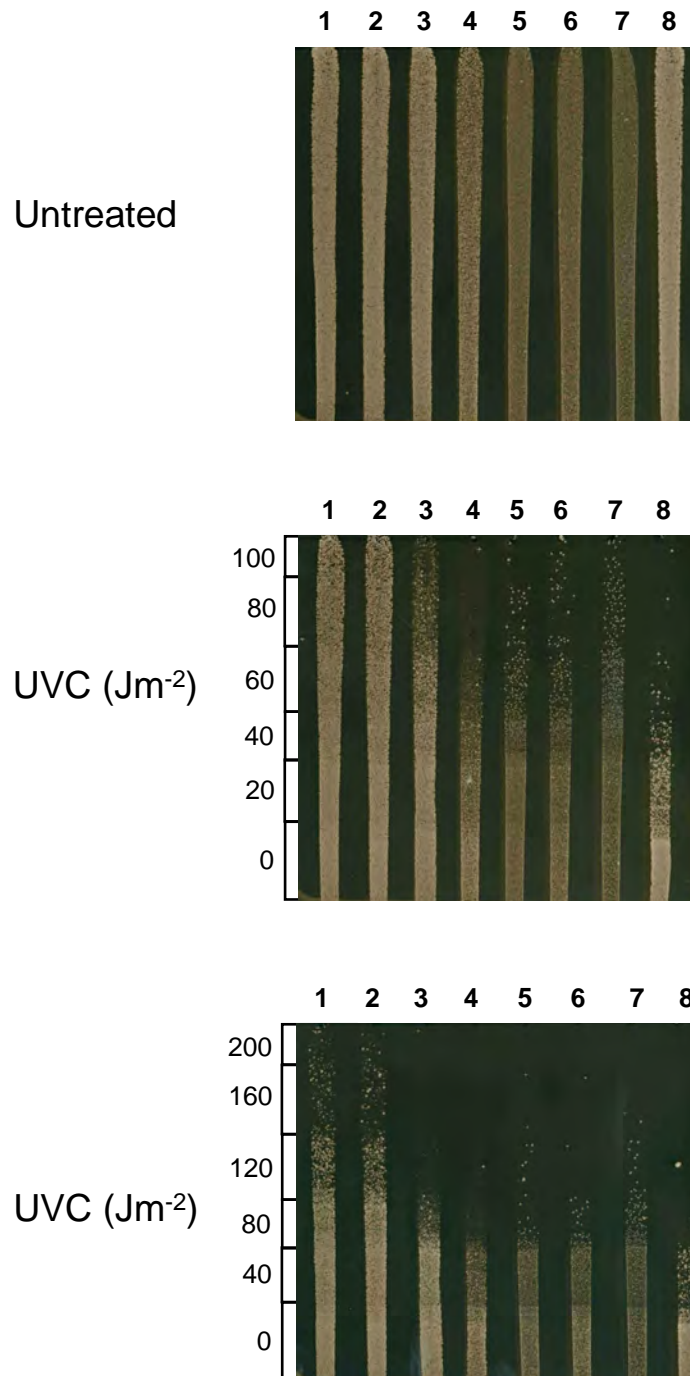


**Figure 7.6. *ubp21Δ::kan ubp22Δ::nat1* Cells have the Same Sensitivity to UVC as *ubp21Δ::ura4 ubp22Δ::ura4* Cells.** Lanes: (1) Wild-type, (2) *ubp21Δ::kan*, (3) *ubp22Δ::nat1*, (4-6) three different clones of *ubp21Δ::kan ubp22Δ::nat1*, (7) *ubp21Δ::ura4 ubp22Δ::ura4*, (8) *pcn1-K164R::ura4*. Plates were photographed after 6 days growth at 30°C.

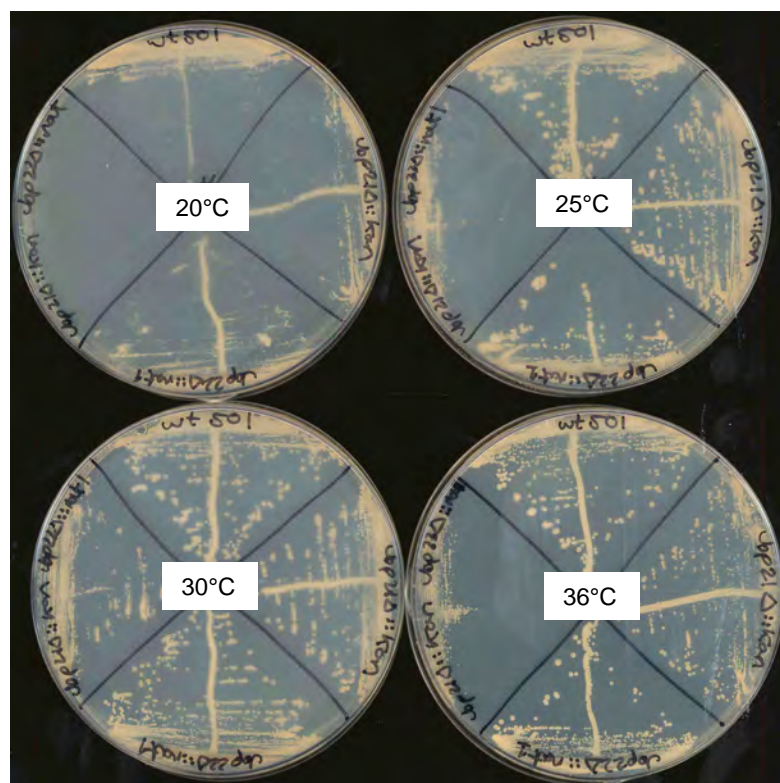


**Figure 7.7. *ubp21Δ::kan ubp22Δ::nat1* Cells are Temperature Sensitive.** Each plate was streaked with the strains *ubp22Δ::nat1* (lower quadrant), *ubp21Δ::kan ubp22Δ::nat1* (left quadrant) and *ubp21Δ::kan* (right quadrant). Growth of these strains were compared with wild-type (top quadrant) after six days at the temperatures indicated.

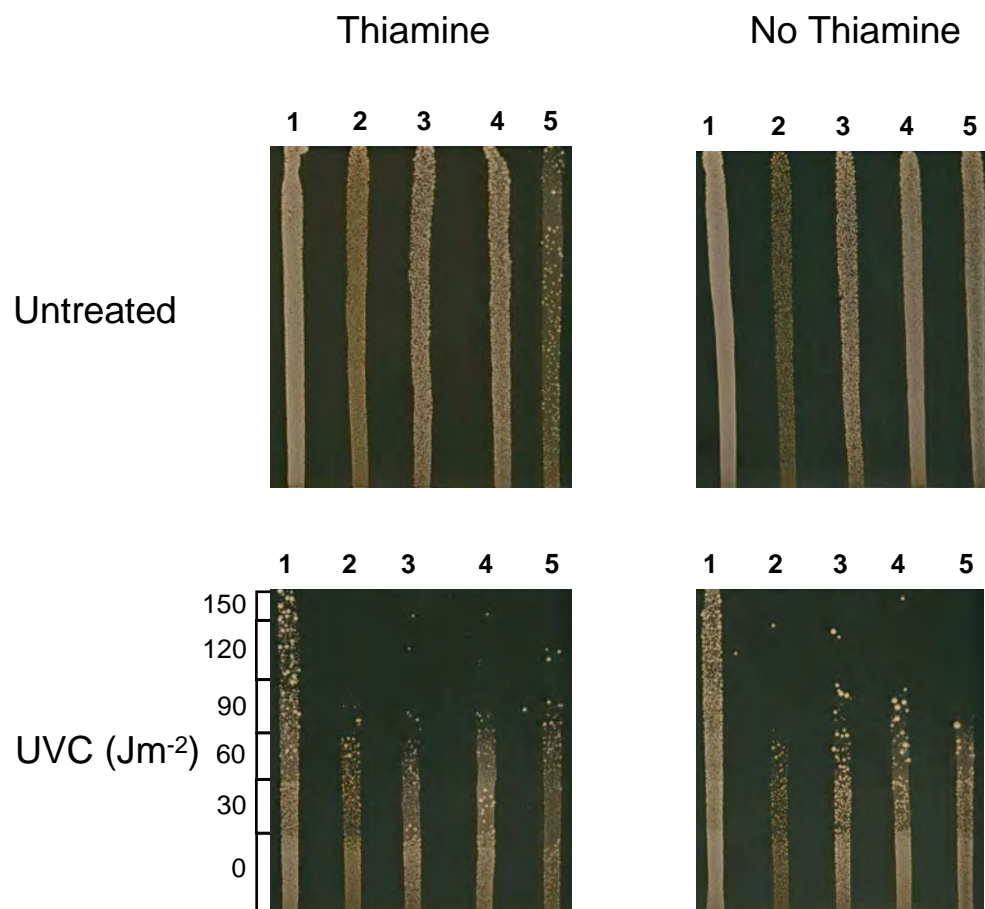


**Figure 7.8. Rescue of UVC sensitivity by the Exogenous Expression of *SpUbp21* Protein Constructs in *ubp21Δ::kan ubp22Δ::nat1* Cells.** Lanes: (1) Wild-type cells + vector only, (2) double delete cells + vector only, (3) double delete cells + untagged *SpUbp21*, (4) double delete cells + N-terminally tagged *SpUbp21*, (5) double delete cells + C-terminally tagged *SpUbp21*. Plates were photographed after 6 days growth at 30°C.



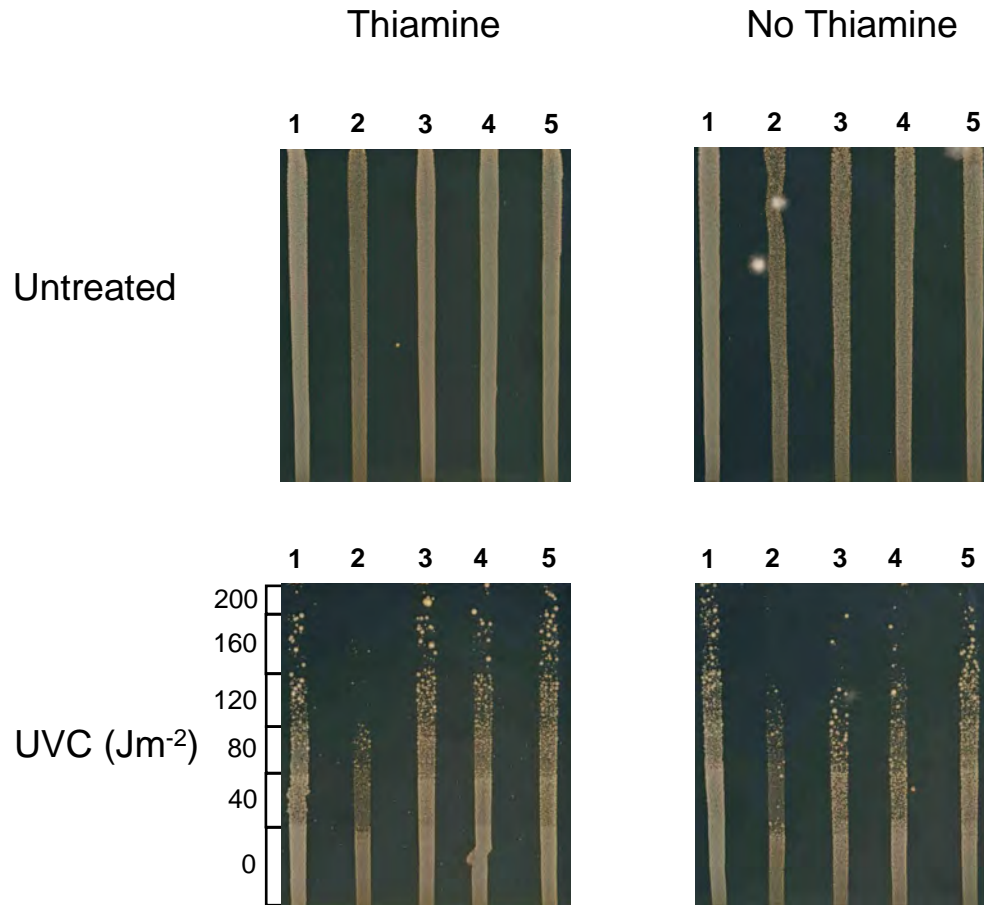


**Figure 7.9. Rescue of UVC sensitivity by the Exogenous Expression of *SpUbp22* Protein Constructs in *ubp21Δ::kan ubp22Δ::nat1* Cells.** Lanes: (1) Wild-type cells + vector only, (2) double delete cells + vector only, (3) double delete cells + untagged *SpUbp22*, (4) double delete cells + N-terminally tagged *SpUbp22*, (5) double delete cells + C-terminally tagged *SpUbp22*. Plates were photographed after 6 days growth at 30°C.

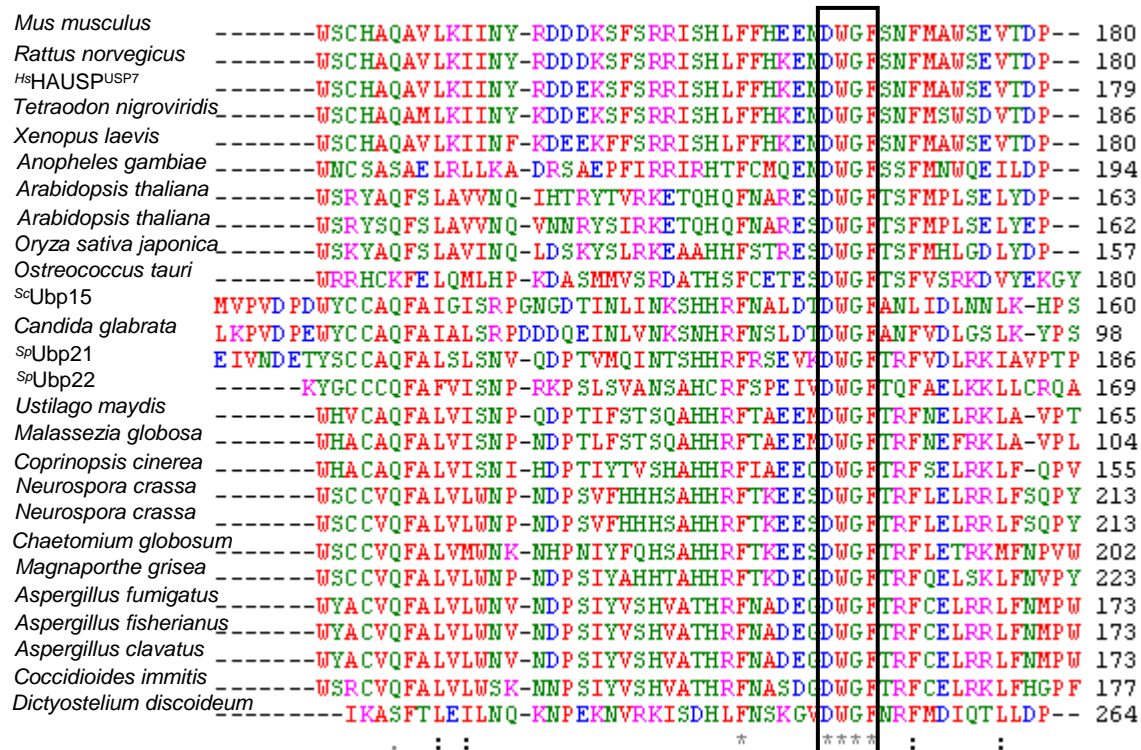


**Figure 7.10. Alignment of the MATH Domain in MATH-USP/UBP DUBs from 23 Different Species.** The entirely conserved DWGF motif is boxed.



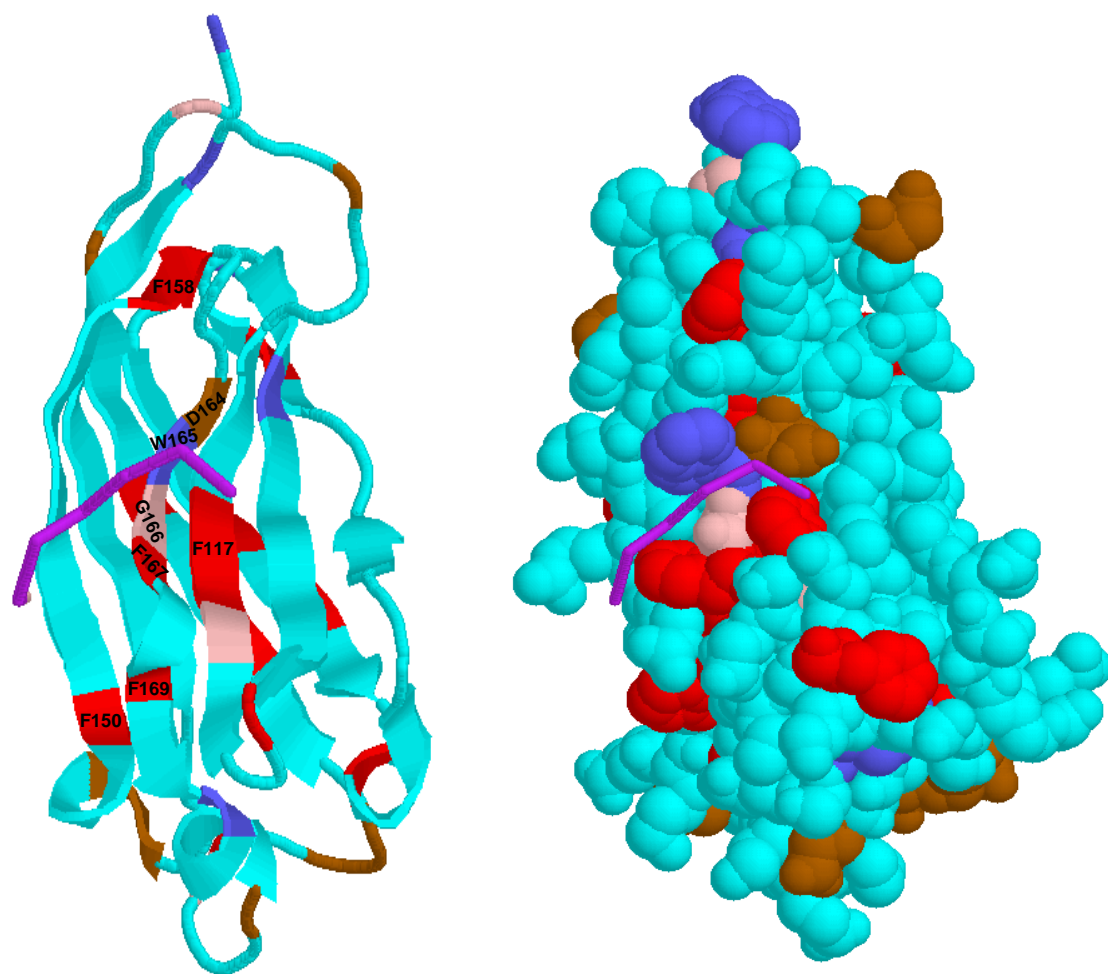


**Figure 7.11. Structure of the MATH Domain of *HsHAUSP*<sup>USP7</sup> in Complex with an *HsMDM2* peptide.** Left: Ribbon structure in turquoise. Phenylalanines (F) highlighted in red, aspartic acids (D) in brown, tryptophans (W) in purple, and glycines (G) in pink. Highly conserved residues labelled with the *HsHAUSP*<sup>USP</sup> amino acid number. *HsMDM2* peptide shown stick form in magenta. Right: Space fill model. Structures from PDB ID: 2FOJ (Sheng *et al*, 2006).

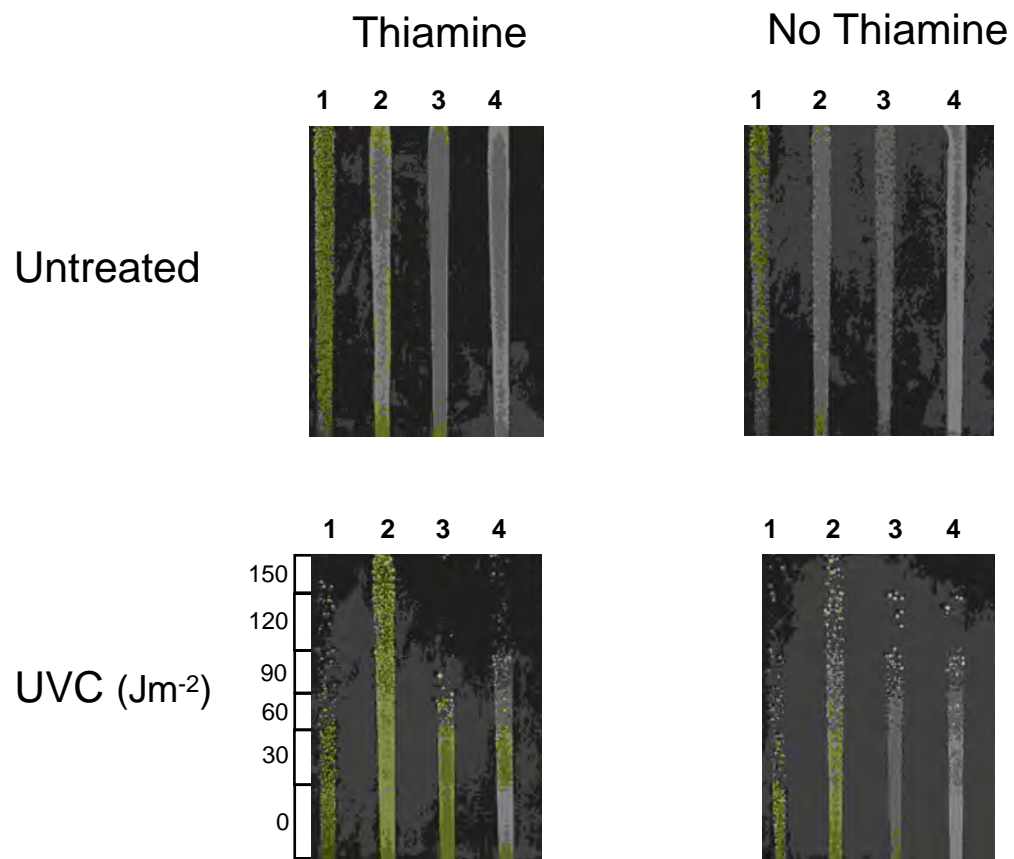


**Figure 7.12. Rescue of UV Sensitivity of Double Delete Via Exogenous Expression of *Sp*Ubp22-DWGF-AAAA.** Lanes: (1) Vector only, (2) untagged Ubp22, (3) untagged Ubp22-DWGF-AAAA, (4) *pcn1-K164R::ura4*. Plates were photographed after 4 days growth at 30°C.

A

SpUbp21	RNTLDEEHRVVERKLLEREE	QQIYR	RVRVL	TIDGF	KYHG	FDMTD	FS	-----	ASDDD	616
SpUbp22	KEALNPSIQLAELRRKERLE	SHLYT	KVQLIT	PEFY	SEHHE	FDIAD	FG	-----	NAYKE	599
ScUbp15	ITRVREEIKERETKEKEIRE	AHLYV	TLRLHS	IKF	IHYEG	FDYFA	HDGFRLFAEELND	SG	615	
HsHAUSP	VERLQEEKRIEAKRKERQE	AHLYM	QVQIVA	AEDQF	CGHQGN	DMYDEE	-----	K	588	
	:	:	:	*	*	:	:	:	*	

B

SpUbp21	TYSHNQNVVMFY	EVLDITLSE	LERKQLIR	VHFLS	NGISHE	TQMEFYVDKE	GTVEDILRQVTQK	963
SpUbp22	SEEMPSNVIFY	ETMDVSLSD	DRKRLVRL	RWLVD	GLANIELVEAY	INKSGDINDLFGAVCER	946	
ScUbp15	DINCDQIPPFAR	EVLSVPLKE	LERLRPIKLY	WLKNSYIHY	QCFF	FEVANDYTESQFLEKVVQHK	1019	
HsHAUSP	FTKPRQPKLY	YQQLKMKITD	FENRRSFKC	IWLN-	SQFREEITLY	PDKHGCVRDLL	EECKKA	928
	.	:	:	:	:	:	:	:

**Figure 7.13. EBI-CLUSTALW Alignment of the Amino Acid Sequence *SpUbp21*, *SpUbp22*, *ScUbp15* and *HsHAUSP*<sup>USP7</sup>.** The residue colouring and conservation symbols utilised in this alignment are as described in Figures 5.5. Potential PIP boxes, designated (A) and (B), are boxed in dark red.

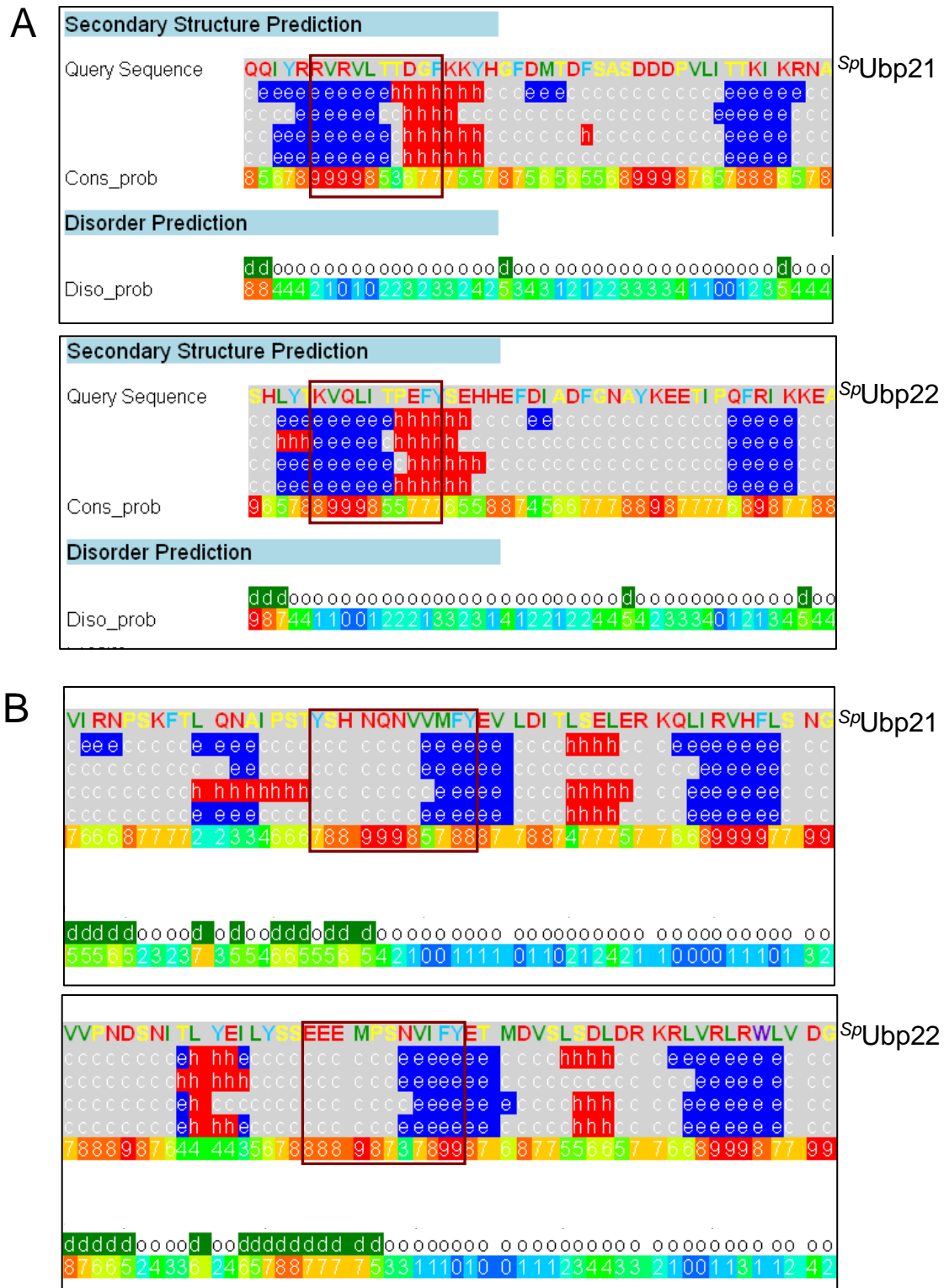


**Figure 7.14. Secondary Structure Prediction of the Potential PIP Boxes of *SpUbp21* and *SpUbp22* Using the PHYRE Program.** (A) and (B) as previous figure and in the text. For each query amino acid sequence, the program predicted the likelihood of an  $\alpha$ -helix (h) or  $\beta$ -sheet (e), using different algorithms. The consensus probability (Cons\_prob) rates the likelihood of secondary structure being present – high rating equates to high likelihood. The potential for disorder (d) and order (o) is also predicted and rated (Diso\_prob).

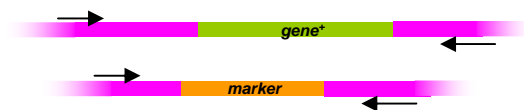
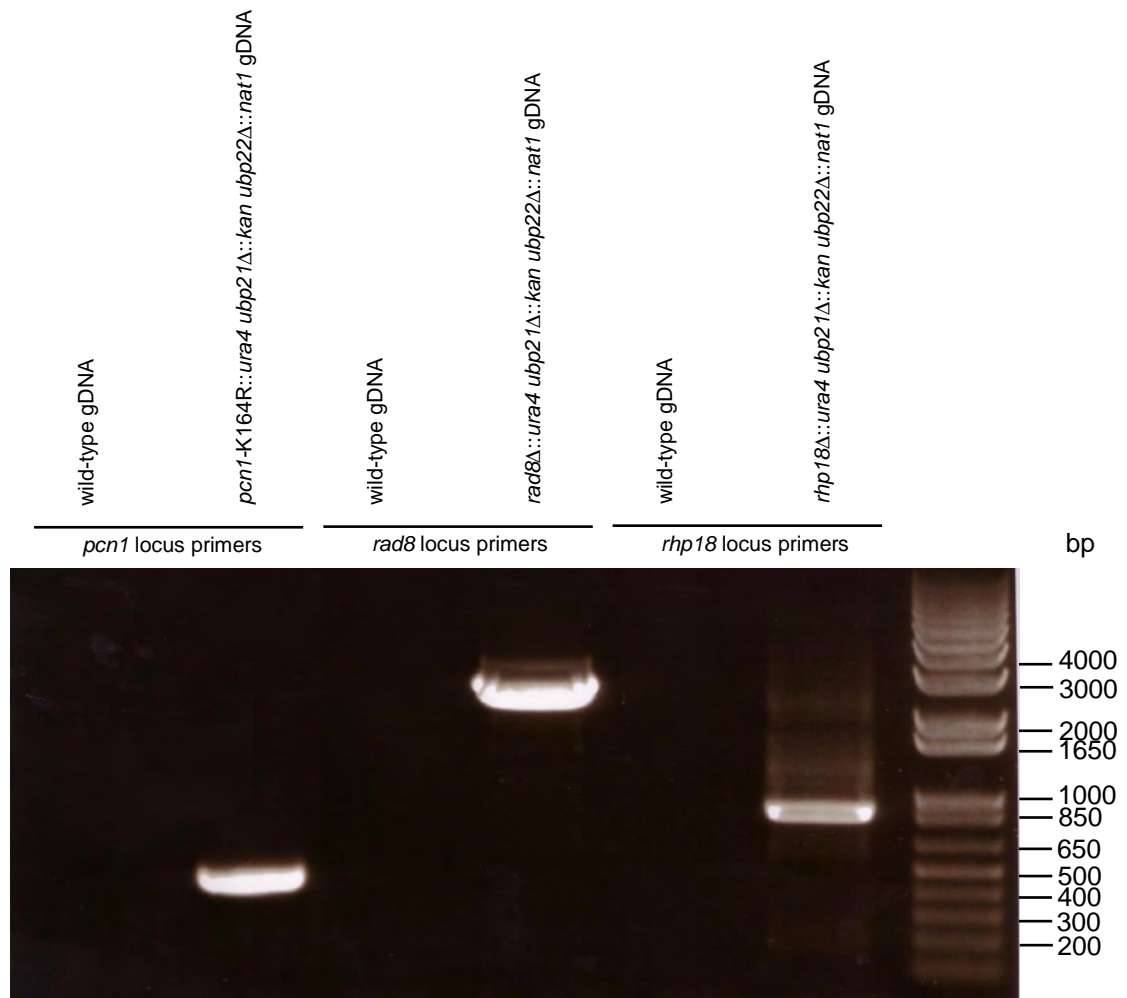


**Figure 8.1. PCR Amplification of the *pcn1*, *rad8* and *rhp18* Loci Utilising *ura4* Gene Primers, and Genomic DNA.** From of the *S. pombe* Strains wild-type, *pcn1*-K164R::*ura4 ubp21Δ::kan ubp22Δ::nat1*, *rad8Δ::ura4 ubp21Δ::kan ubp22Δ::nat1*, and *rhp18Δ::ura4 ubp21Δ::kan ubp22Δ::nat1*. For the *rad8* and *rhp18* PCRs, the *ura4* primer was coupled with a primer that anneals to flanking DNA. The lower diagram shows the PCR strategy in wild-type gDNA and deleted gDNA. Primers that flank the gene locus are depicted by arrows. For the *pcn1* PCRs, the *ura4* primer was coupled with a primer that anneals within the *pcn1* gene (diagram not shown).

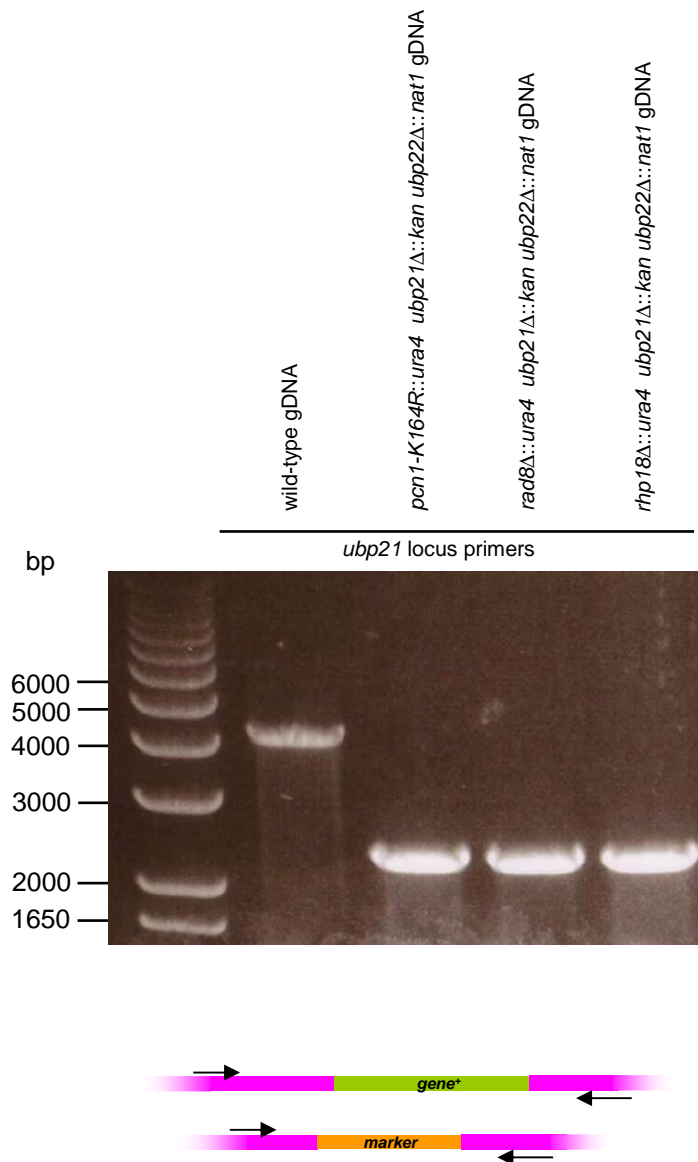


**Figure 8.2. PCR Amplification of the *ubp21* Locus Utilising Primers that Anneal to Flanking DNA and Genomic DNA.** From of the *S. pombe* Strains wild-type, *pcn1-K164R::ura4 ubp21Δ::kan ubp22Δ::nat1*, *rad8Δ::ura4 ubp21Δ::kan ubp22Δ::nat1*, and *rhp18Δ::ura4 ubp21Δ::kan ubp22Δ::nat1*. Diagram as previous figure.

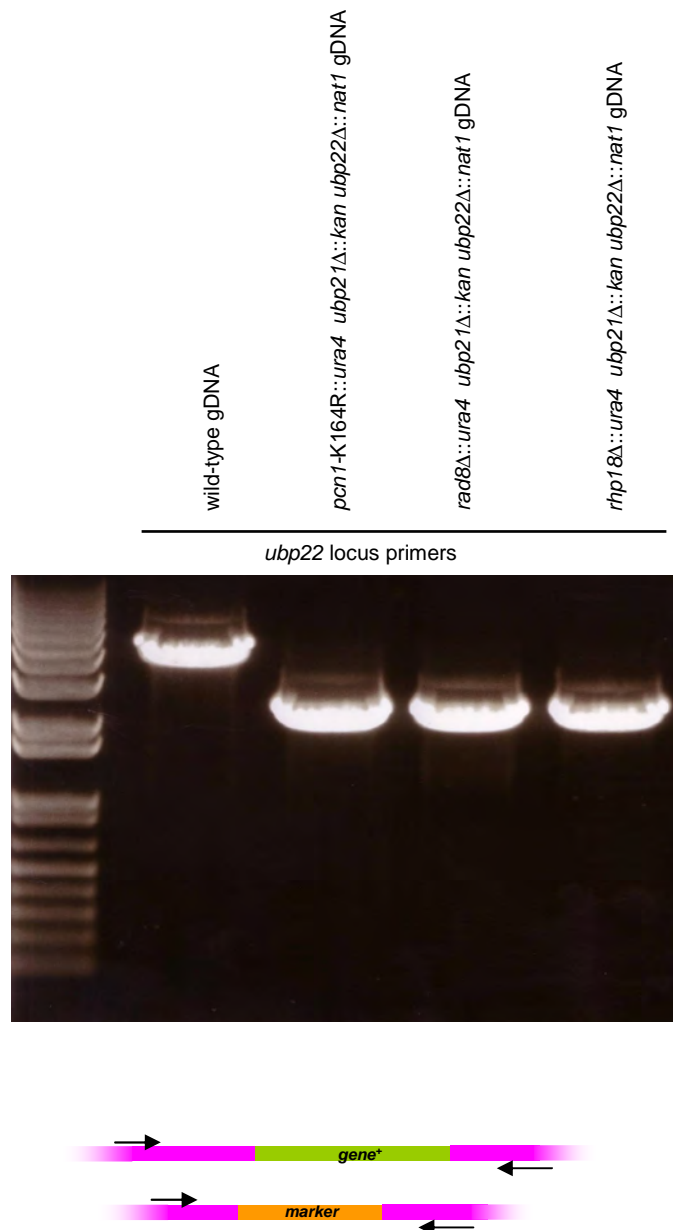


**Figure 8.3. PCR Amplification of the *ubp21* Locus Utilising Primers that Anneal to Flanking DNA and Genomic DNA.** From the *S. pombe* Strains wild-type, *pcn1-K164R::ura4 ubp21Δ::kan ubp22Δ::nat1*, *rad8Δ::ura4 ubp21Δ::kan ubp22Δ::nat1*, and *rhp18Δ::ura4 ubp21Δ::kan ubp22Δ::nat1*. Diagram as Figure 8.1.

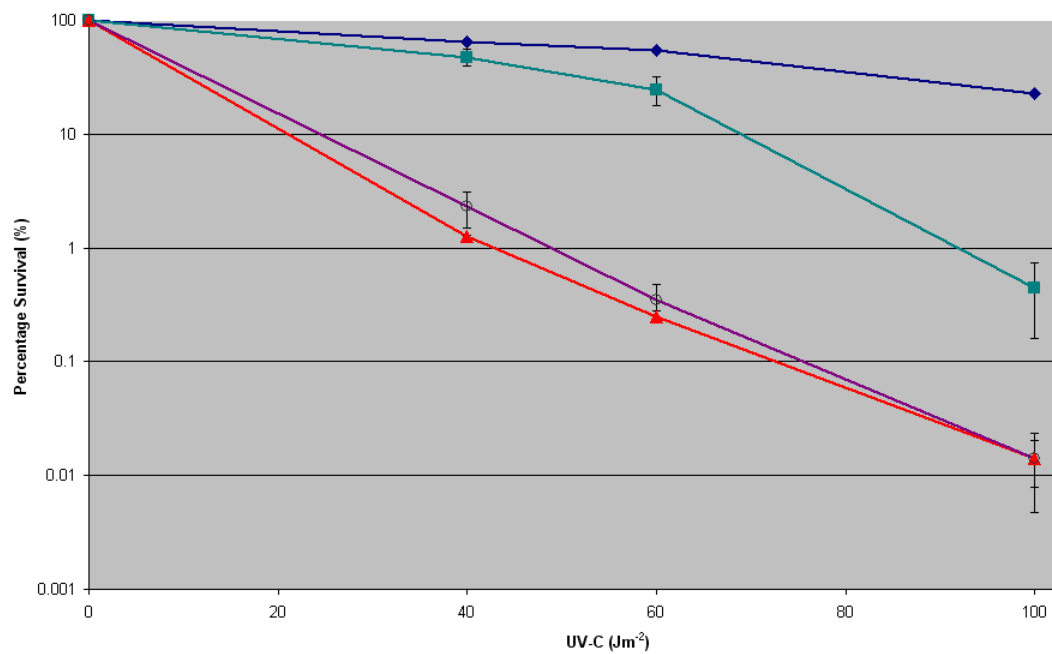


**Figure 8.4. UV Epistasis Analysis with *pcn1-K164R*.** *S. pombe* strains wild-type (blue diamonds), *ubp21Δ::kan ubp22Δ::nat1* (teal squares), *ubp21Δ::kan ubp22Δ::nat1 pcn1-K164R::ura4* (red triangles) and *pcn1-K164R::ura4* (purple, open circles). Colonies were counted following 6 days growth at 30°C. Error bars indicate the standard error of the mean of three independent experiments.



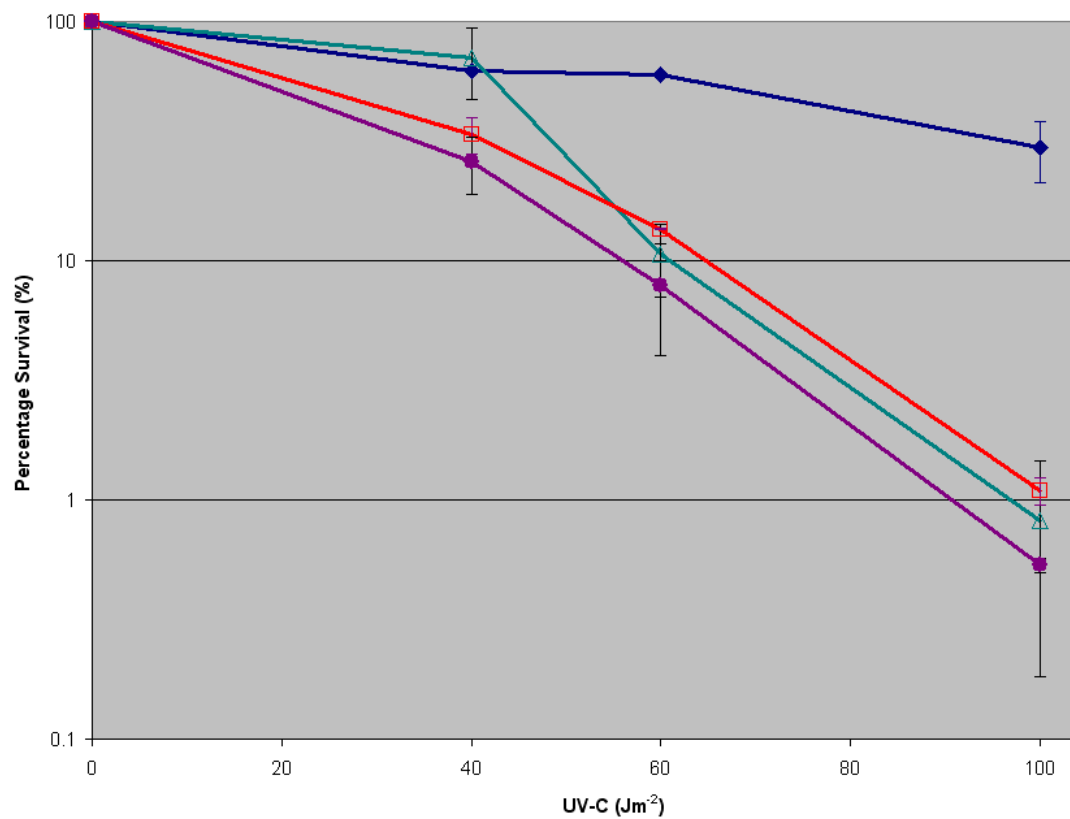


**Figure 8.5. UV Epistasis Analysis with *rad8Δ*.** *S. pombe* strains wild-type (blue diamonds), *ubp21Δ::kan ubp22Δ::nat1* (teal, open triangles), *ubp21Δ::kan ubp22Δ::nat1 rad8Δ::ura4* (red, open squares) and *rad8Δ::ura4* (purple circles). Colonies were counted following 6 days growth at 30°C. Error bars indicate the standard deviation of two independent experiments.

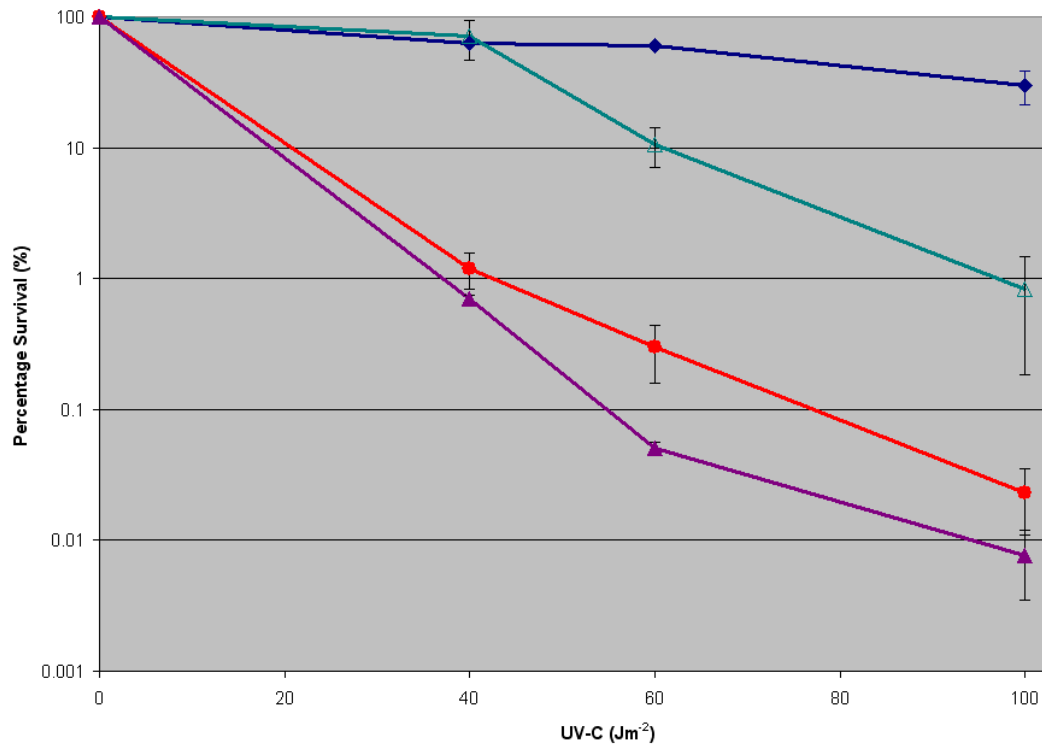


**Figure 8.6. UV Epistasis Analysis with *rhp18Δ*.** *S. pombe* strains wild-type (blue diamonds), *ubp21Δ::kan ubp22Δ::nat1* (teal, open triangles), *ubp21Δ::kan ubp22Δ::nat1 rhp18Δ::ura4* (red circles) and *rhp18Δ::ura4* (purple triangles). Colonies were counted following 6 days growth at 30°C. Error bars indicate the standard deviation of two independent experiments.